NASA CR-134617
BCAC D6-41805

727/JT8D-100 SERIES ENGINE EXHAUST SYSTEM PROPULSION PERFORMANCE MODEL TEST

by W. J. Haugan
P. R. A. Kern

BOEING COMMERCIAL AIRPLANE COMPANY
A DIVISION OF
THE BOEING COMPANY

Prepared for

NATIONAL AERONAUTICS AND SPACE ADMINISTRATION

NASA Lewis Research Center

CONTRACT NAS3-17842

1. Report No.
CR 134617

2. Government Accession No.

3. Recipient's Catalog No.

4. Title and Subtitle
727/JT8D-100 Series Engine Exhaust System Propulsion Performance Model Test

5. Report Date
May 1974

6. Performing Organization Code

7. Author(s)
W. J. Haugan, P.R A. Kern

8. Performing Organization Report No.
D6-41805

9. Performing Organization Name and Address
The Boeing Commercial Airplane Company
P. O. Box 3707
Seattle, Washington 98124

10. Work Unit No.

11. Contract or Grant No.
NAS3-17842

12. Sponsoring Agency Name and Address
National Aeronautics and Space Administration
Washington, D. C. 20546

13. Type of Report and Period Covered
Contractor Report

14. Sponsoring Agency Code

15. Supplementary Notes
Project Manager, A. A. Medeiros, V/STOL and Noise Division
NASA Lewis Research Center, Cleveland, Ohio

16. Abstract

This report presents the results from testing one-eighth scale models of the Pratt and Whitney Aircraft Reference and Boeing nozzles for the JT8D-100 series mixed flow engines (-109, -115, -117). The objective of the test was to obtain the nozzle velocity and flow coefficients for the Reference configurations and compare these with the Boeing configurations which incorporated a longer splitter between the fan and primary flows. A further comparison was made between the JT8D-100 series nozzles and the Boeing JT8D-9/727 production nozzle performance. A statistical analysis was used to compare configurations. This showed the performance (velocity coefficient) of the P&WA Reference and the Boeing configuration was the same for the JT8D-109. It also showed no difference between P&WA Reference and the Boeing configuration for the JT8D-115 and no difference for the JT8D-117 nozzles. Bypass ratio (match) was shown to be equally dependent on splitter position as on nozzle area within the range investigated. The nozzles were very similar in flow coefficient within an engine family. Excellent profile data was recorded. The effects of swirl on the nozzle performance was examined and found to degrade the velocity and flow coefficients.

17. Key Words (Suggested by Author(s))
727 Airplane
Nozzle
Statistical Comparison
Mixing
JT8D-100 Engines
Velocity Coefficient
Flow Coefficient

18. Distribution Statement
Unclassified - Unlimited

19. Security Classif. (of this report)	20. Security Classif. (of this page)	21. No. of Pages	22. Price*
Unclassified	Unclassified	416	

* For sale by the National Technical Information Service, Springfield, Virginia 22151

FOREWORD

The exhaust system propulsion model test described in this report was performed by the Propulsion Technology Staff of the Boeing Commercial Airplane Company, A Division of The Boeing Company, Seattle, Washington. The work, sponsored by NASA Lewis Research Center and reported herein, was performed between July 1973 and May 1974.

This report has been reviewed and is approved by:

L. J. Winslow — 21 OCTOBER 1974

L. J. Winslow, Group Engineer
Propulsion Technology Staff
Date

J. A. Ferrell — 23 OCTOBER 1974

J. A. Ferrell
Chief, Technology Staff
JT8D Refan Porgram
Date

K. P. Rice — 10/28/74

K. P. Rice
Program Manager
JT8D Refan Program
Date

PRECEDING PAGE BLANK NOT FILMED

TABLE OF CONTENTS

PRECEDING PAGE BLANK NOT FILMED

Page

Page

1.0 SUMMARY

This test was conducted to determine the performance (nozzle velocity and flow coefficient) of Boeing nozzles for the mixed flow JT8D-100 series, refanned JT8D, engines and to compare these with Pratt and Whitney Aircraft (P&WA) Reference nozzles, and with the JT8D-9/727 airplane production exhaust system. The test evaluated Boeing and P&WA nozzles for satisfying the hot rematch requirements of the JT8D-100 series engines (-109, -115, and -117). This necessitated a change of fan-to-primary mixing plane area ratio and small changes in nozzle exit area for each of the different engine cycles. Changes in mixing plane area were accomplished by varying the splitter position, or varying the plug size with a common splitter.

The P&WA Reference nozzles were designed with a short splitter dividing the fan and primary flows upstream of the point where the two flows mix. The Boeing configurations were designed with a longer splitter for acoustic treatment. The Boeing configurations, which are designated Config. No. 2, and the P&WA Reference configurations fall in the category of free mixing nozzles as opposed to forced mixing nozzles. The Reference nozzles were considered to adequately represent Boeing designs for Config. No. 1 (short splitter) where the only difference is a slight contour change in the nozzle tailpipe.

The effects of splitter position and nozzle area variation on mixing plane match as indicated by the bypass ratio and surface static pressure measurements on the splitters were examined. Mixing plane total pressure and exit plane total pressure and temperature profiles were taken. The effects of primary swirl on nozzle performance were determined. The mixing efficiencies of the best JT8D-109, -115 and -117 nozzles relative to the theoretical mixing potential for the hardware and stream conditions tested were also evaluated.

The testing was conducted with both the primary and fan flows cold, and also with the primary flow heated to the correct total temperature ratio relative to the fan. The fan-to-primary pressure ratio was set according to the typical 727 airplane with the JT8D-100 series engine operating schedule, from idle to cruise, for the respective engines.

A statistical analysis of variance computer program was used to compare the performance of the respective Boeing and P&WA Reference nozzles to determine whether real differences existed between the configurations. This computer program examines the variance about a data run and between data runs for each configuration tested and, using the nozzle pressure ratio distribution to weight the data at any particular point of comparison, computes the data required for a statistical "F test". This tests the hypothesis that two configurations are the same. The use of statistics necessitated careful choice of the number of data points per run to support the order of curve fit expected through the data and of three runs per configuration as a desirable minimum to make comparisons statistically valid. The nozzle pressure ratio distribution was chosen to support statistically consistent samples of data from run to run and configuration to configuration.

Rig quality was maintained by daily checks, and by a rig calibration before and after the test nozzle program with a 4-inch standard long radius ASME nozzle. Rig repeatability was excellent throughout the test.

During the testing of the third configuration a failure occurred in the n duct instrumentation section. The decision was made to compare configurations using only runs made following the repair. The comparison of configurations became more definitive using this procedure than when all the data recorded for some

configurations (pre- and post- instrumentation section repair) was used. Whereas comparisons are considered in this way to be free of any instrumentation bias, it is at the expense of reduced confidence in the estimates of the levels of the nozzle velocity coefficients. Exclusion of the pre-failure data has the effect of lowering the estimates of the true level of the velocity coefficients on these configurations where the data showed two levels. The amount of reduction is approximately 0.1% at takeoff and about half this at cruise.

The 95% confidence limits for the estimate of the velocity coefficient at any pressure ratio for the P&WA Reference and Boeing nozzles is ± 0.0010.

The best performing Boeing nozzles were determined to be those which used a common small plug and varied the splitter position to satisfy the hot rematch cycle requirements at the mixing plane for the respective JT8D-100 engines. Figures 1 through 4 show the various comparisons made in this test between P&WA Reference nozzles and Boeing Config. No. 2 nozzles. Options for the Boeing Config. No. 2 were also tested and comparisons made. The results of the statistical analysis at two pressure ratios are shown in the bar charts. Where the statistical analysis showed nozzle equality there is no difference shown by the statistical symbol.

Figures 5 through 10 show the velocity coefficient as a function of mixed nozzle pressure ratio for the JT8D-109, -115 and -117 nozzles combined in accordance with the results of the statistical analysis. Symbols are not used on these curves to distinguish the nozzles constituting the combinations, as the mathematical analysis precludes that distinction and declares the data common. Figures 11 and 12 show the mixed flow hot and cold velocity coefficients for the JT8D/727 airplane production nozzle.

The Boeing Config. No. 2 and P&WA Reference nozzles for the JT8D-109 engine have the same performance which is slightly lower than the current performance for the JT8D-9 Boeing production nozzle without the thrust reverser effects.

The Boeing Config. No. 2 and P&WA Reference nozzles for the JT8D-115 engine have the same performance which is just slightly better than the current performance for the JT8D-9 Boeing production nozzle without the thrust reverser effects.

The Boeing Config. No. 2 and P&WA Reference nozzles for the JT8D-117 engine have the same performance which is better than the current performance for the JT8D-9 Boeing production nozzle without the thrust reverser effects.

Larger plug options for the Boeing Config. No. 2 nozzles which employed a common splitter, resulted in reduced takeoff performance but in general suffer no losses at cruise. The losses associated with these designs and the inevitable weight increase was sufficient to discourage their use as an economic expedient on the JT8D-100 series engines.

The effect of the introduction of primary flow swirl was shown to be the same on both the P&WA and Boeing JT8D-109 nozzle. Figure 13 shows the hot mixed velocity coefficient of the combined data. Comparison of Figure 13 with 5 shows a loss due to the swirl. Part of this loss is due to the losses introduced by the swirl vanes, which when accounted for, results in mixed velocity coefficient reductions due to swirl alone of 0.5% at takeoff and 0.25% at cruise.

The nozzle flow coefficients indicated that the P&WA Reference and Boeing Config. No. 2 nozzles for the JT8D-109 engine were identically matched at all pressure ratios and that the desired decrease in nozzle coefficient relative to the JT8D-9/727 airplane production nozzle to aid the idle thrust condition was

accomplished, Figure 14. The P&WA Reference and Boeing Config. No. 2 for the JT8D-115 and -117 engines respectively show differences of the order of 1% at takeoff and are the same at cruise, Figures 15 and 16.

Bypass ratio was shown to be sensitive to splitter position, and to exhaust nozzle area variation. The sensitivity of bypass ratio to splitter position was the only useful measure of match on this model test due to the inability to place the splitter static pressures in the correct places. Splitter position and nozzle exit area will be the controlling influences to obtain match at the mixing plane on the full scale engine. The exit area will be used to control the total mass flow. The exit plane surveys indicated that total temperature profiles and non-dimensionalized velocity profiles are insensitive to pressure ratio. Good agreement was obtained between the profiles obtained for the JT8D-9/727 airplane production nozzle and the full scale data obtained from a JT8D-9 engine. The mixing plane total pressure surveys showed no surprises. The introduction of swirl on the P&WA Reference and Boeing Config. No. 2 nozzles for the JT8D-109 engine showed a marked defect in the core of the flow, indicating a vortex was present at the center of the exit flow.

Mixing efficiency of the JT8D-100 series nozzles was better than had been expected, attaining approximately 45% of the theoretical thrust gains available at takeoff pressure ratio and 35% at cruise.

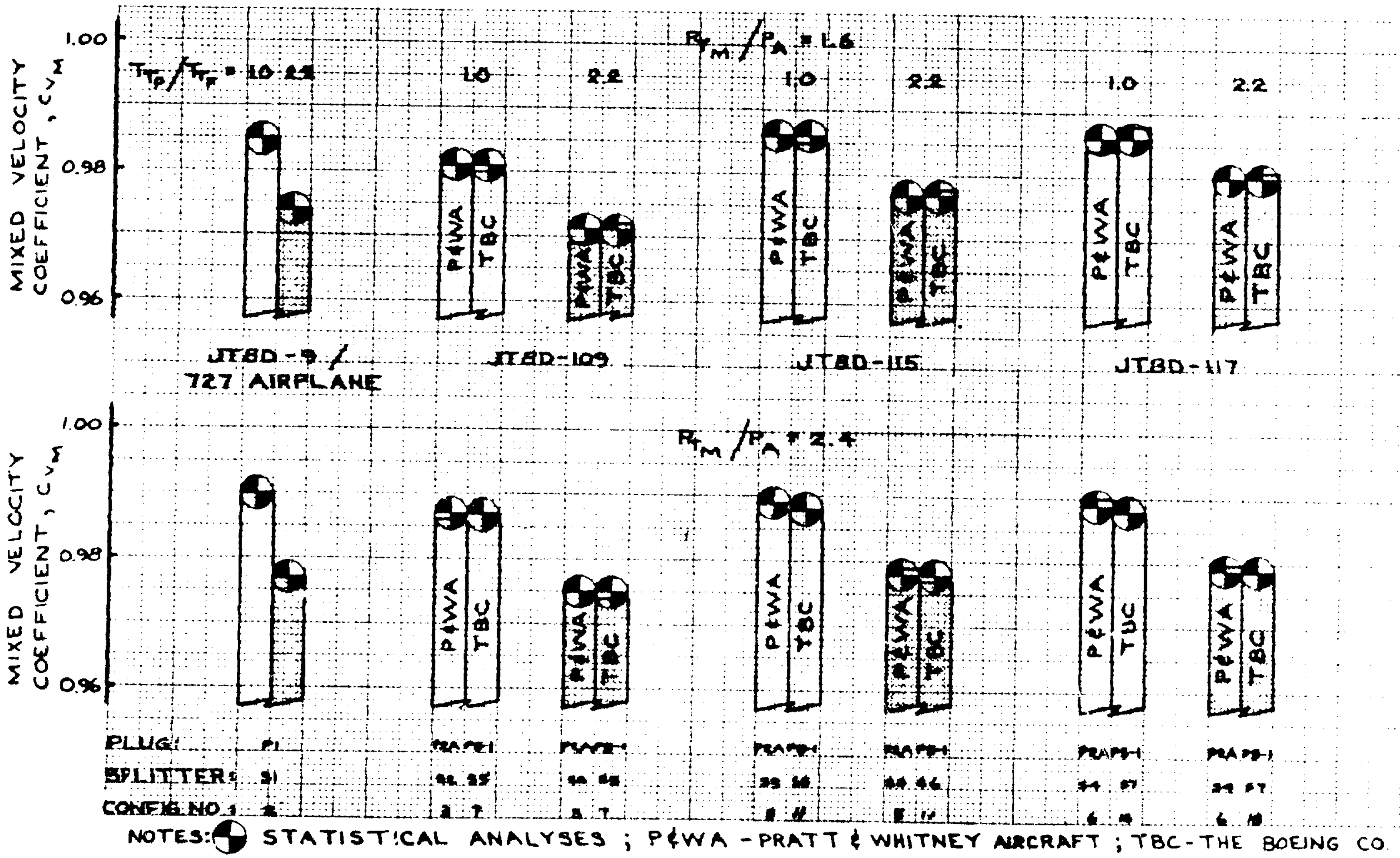

FIGURE 1 - SUMMARY OF P&WA REF. NOZZLE AND BOEING CONFIG. NO. 2 COMMON PLUG/VARIABLE SPLITTER COMPARISONS

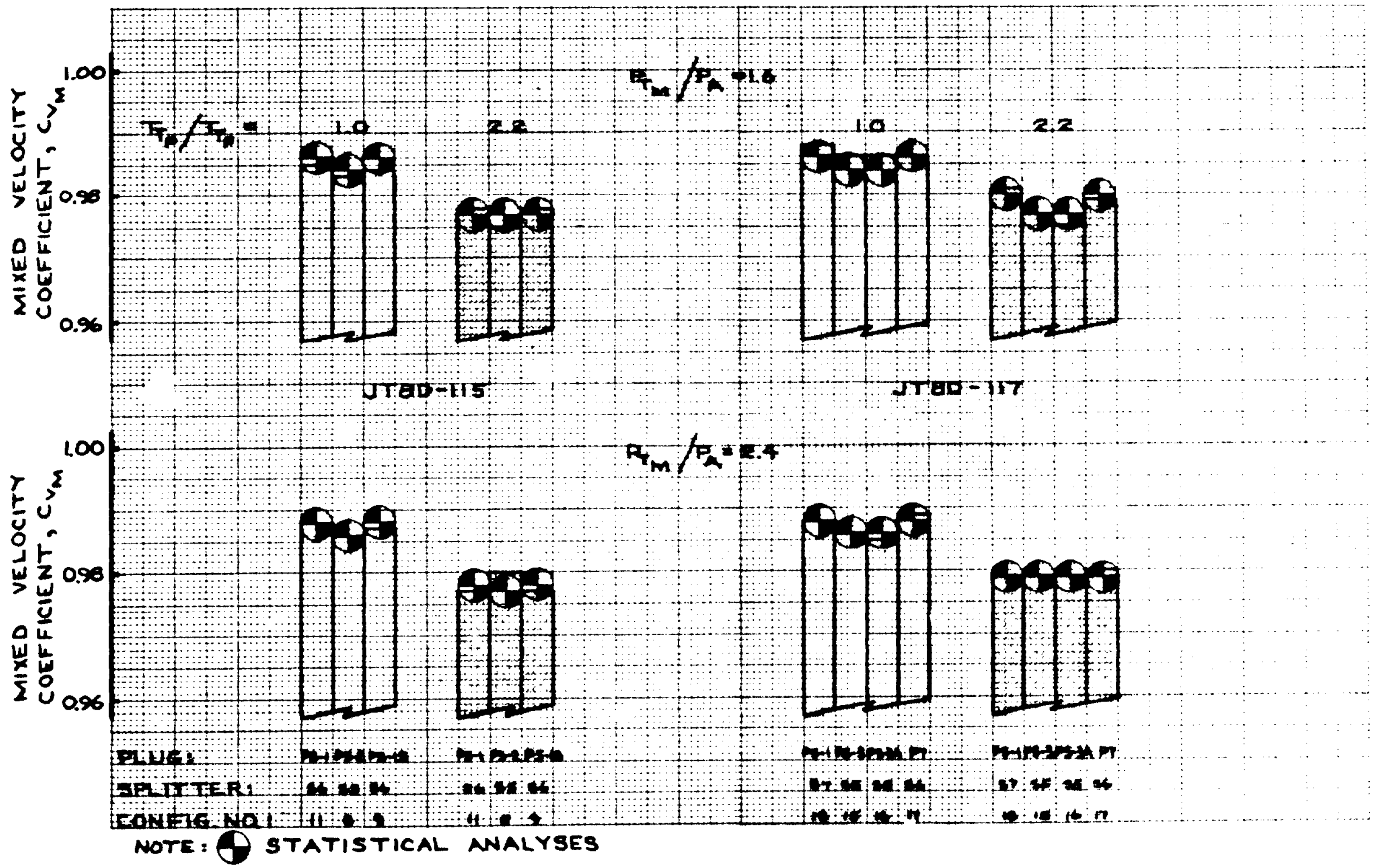

FIGURE 2 - SUMMARY OF BOEING CONFIG. NO. 2 PLUG/SPLITTER COMPARISONS

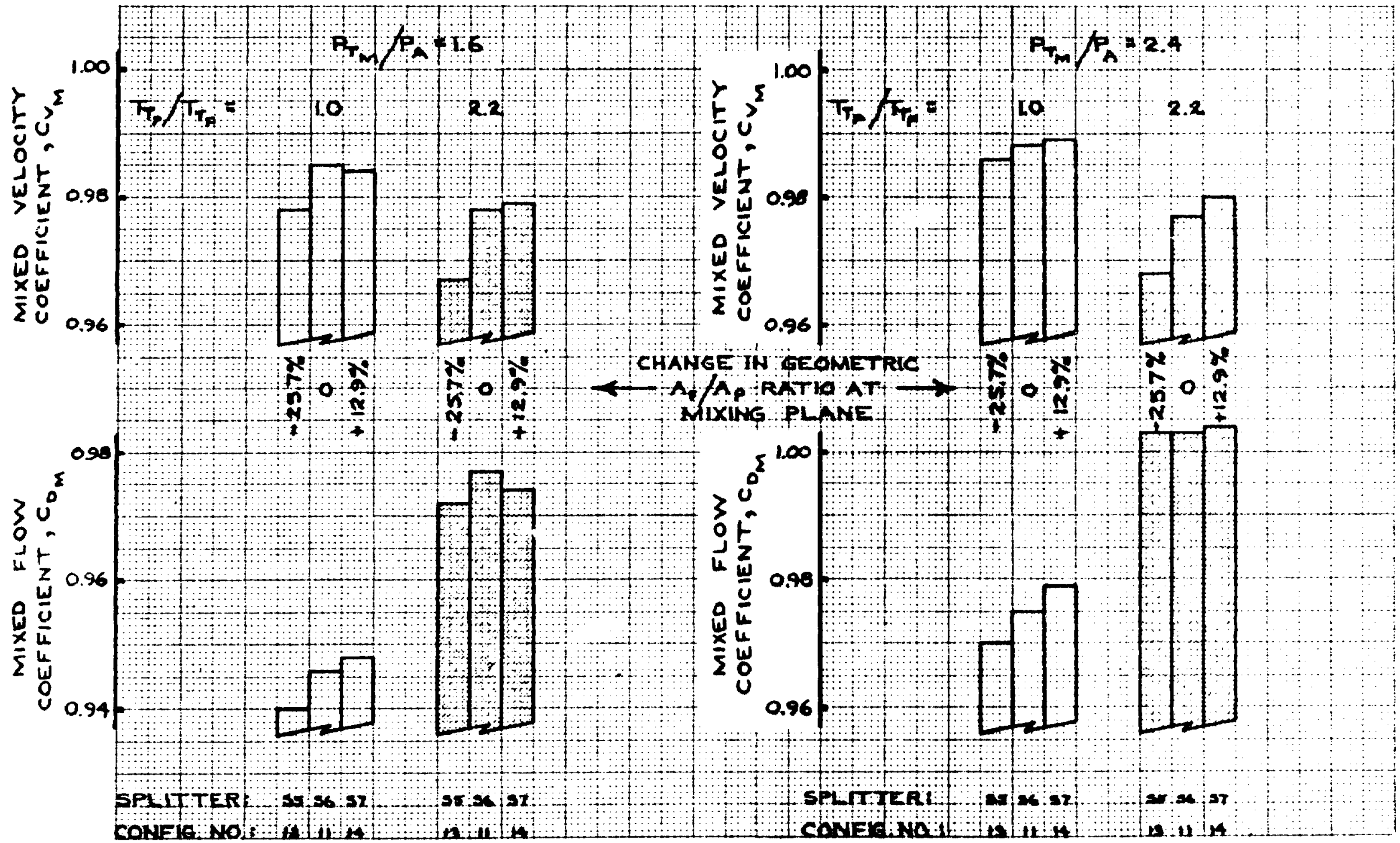

FIGURE 3 - SUMMARY OF JT8D-115 BOEING CONFIG. NO. 2 SPLITTER LOCATION VARIATIONS

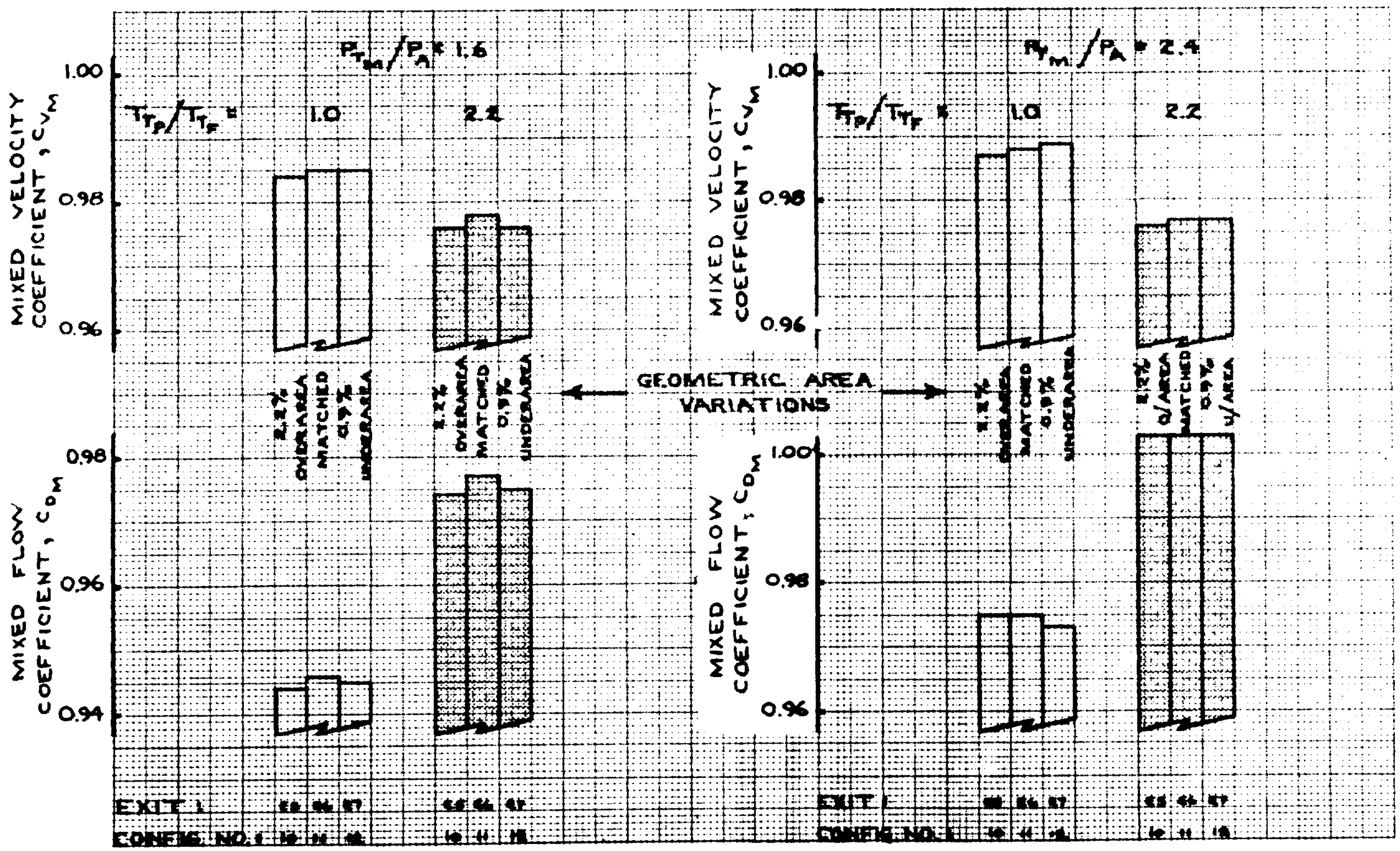

FIGURE 4 - SUMMARY OF JT8D-115 BOEING CONFIG. NO. 2 EXIT AREA VARIATIONS

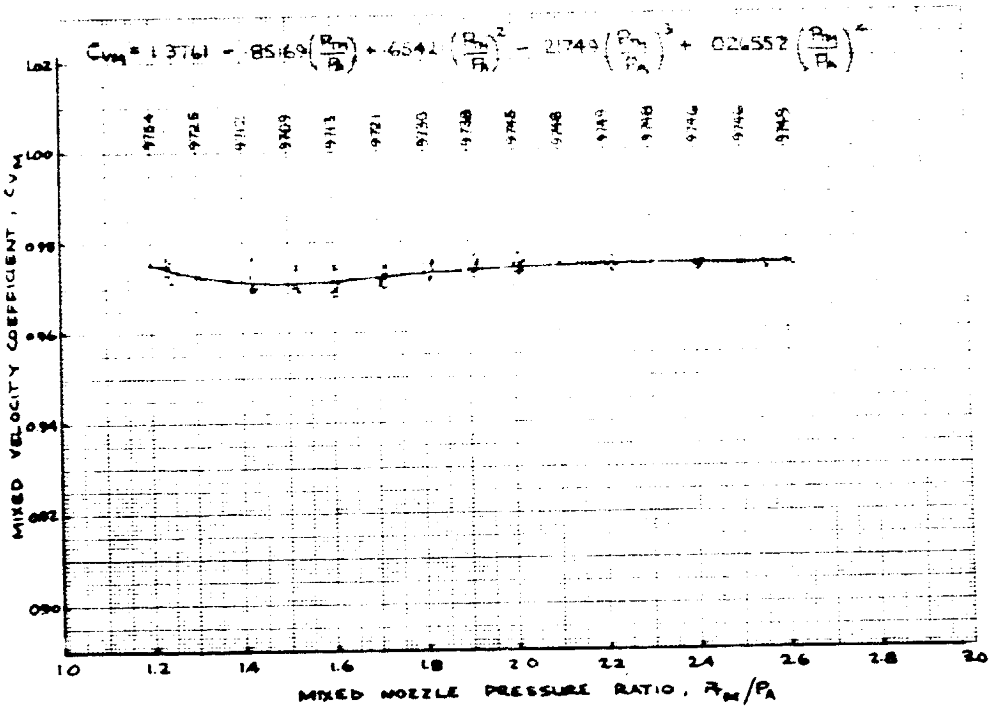

FIGURE 5 - MIXED VELOCITY COEFFICIENT FOR P&WA REF. AND BOEING CONFIG. NO. 2 NOZZLES INSTALLED ON JT8D-109 ENGINE (T_{T_P}/T_{T_F} = 2.2).

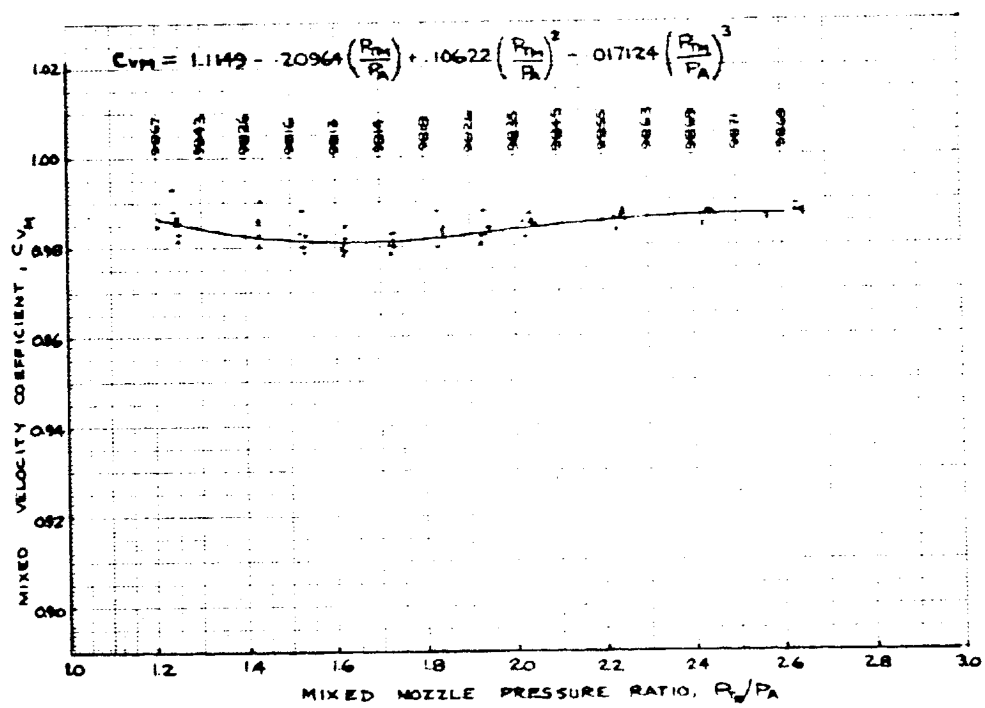

FIGURE 6 - MIXED VELOCITY COEFFICIENT FOR P&WA REF. AND BOEING CONFIG. NO. 2 NOZZLES INSTALLED ON JT8D-109 ENGINE (T_{T_P}/T_{T_F} = 1.0).

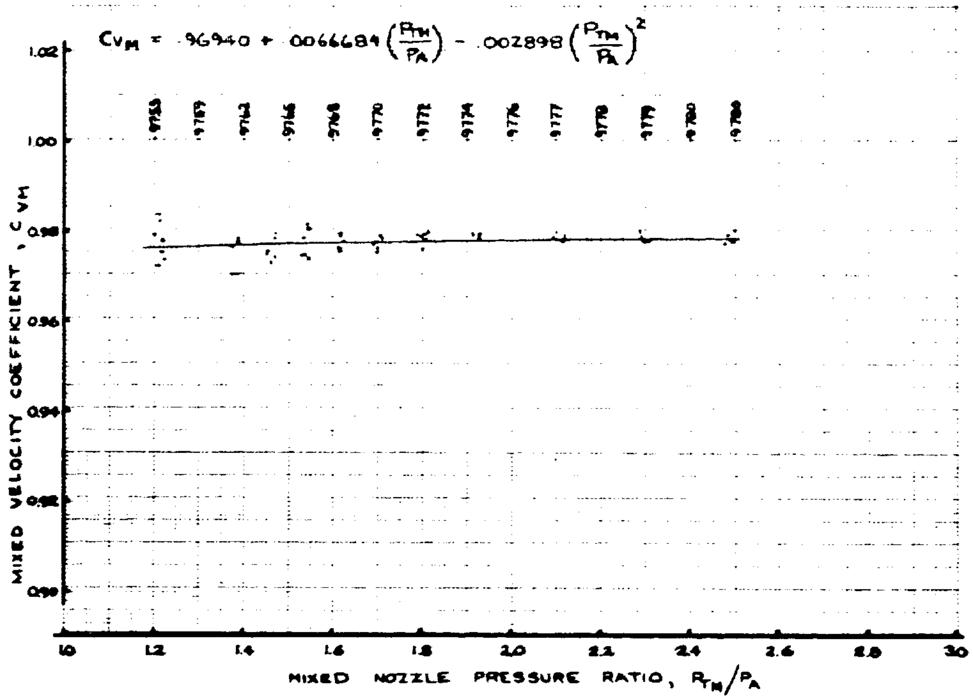

FIGURE 7 - MIXED VELOCITY COEFFICIENT FOR P&WA REF. AND BOEING CONFIG. NO. 2 NOZZLES INSTALLED ON JT8D-115 ENGINE ($T_{T_P}/T_{T_F} = 2.2$).

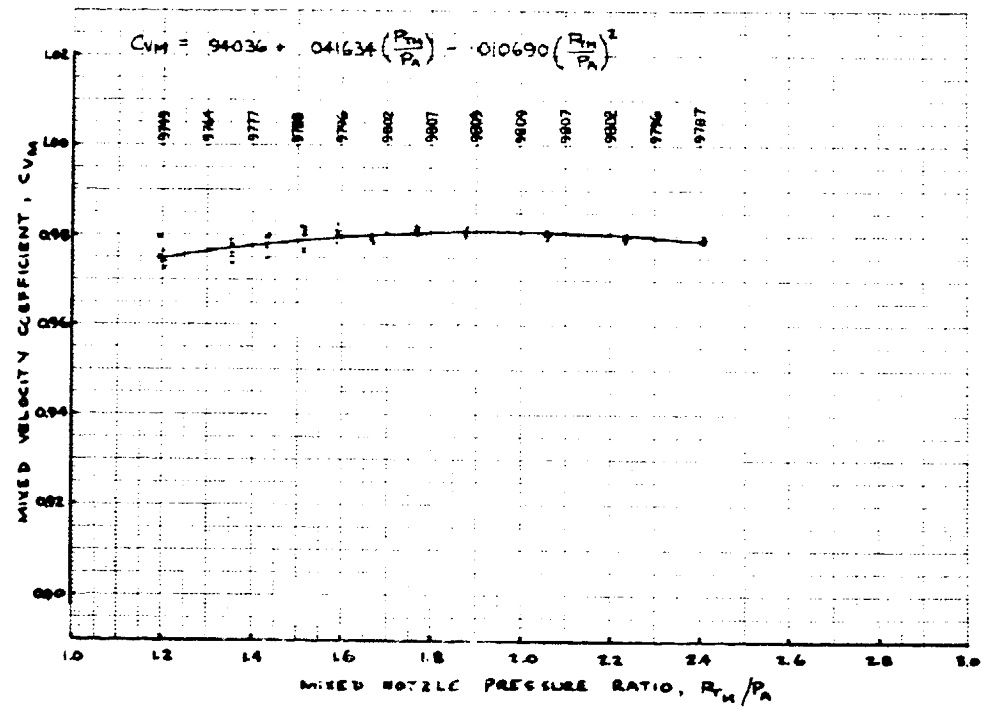

FIGURE 8 - MIXED VELOCITY COEFFICIENT FOR P&WA REF. AND BOEING CONFIG. NO. 2 NOZZLES INSTALLED ON JT8D-117 ENGINE ($T_{T_P}/T_{T_F} = 2.2$).

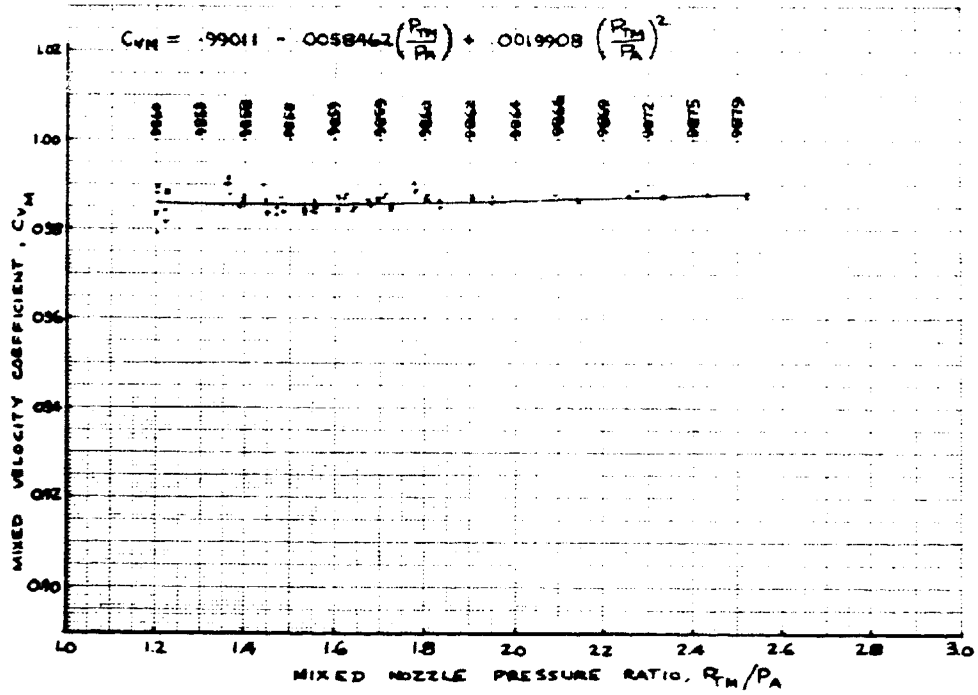

FIGURE 9 - MIXED VELOCITY COEFFICIENT FOR BOEING CONFIG. NO. 2 NOZZLES INSTALLED ON JT8D-115 AND JT8D-117 ENGINES ($T_{T_P}/T_{T_F} = 1.0$).

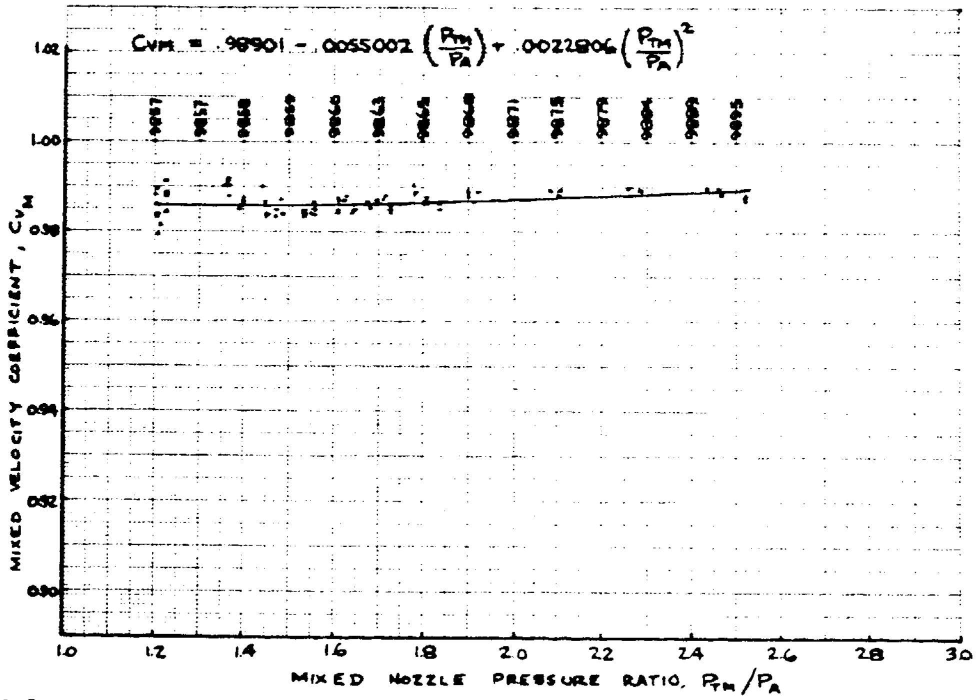

FIGURE 10 - MIXED VELOCITY COEFFICIENT FOR P&WA REF. NOZZLES INSTALLED ON JT8D-115 AND JT8D-117 ENGINES ($T_{T_P}/T_{T_F} = 1.0$).

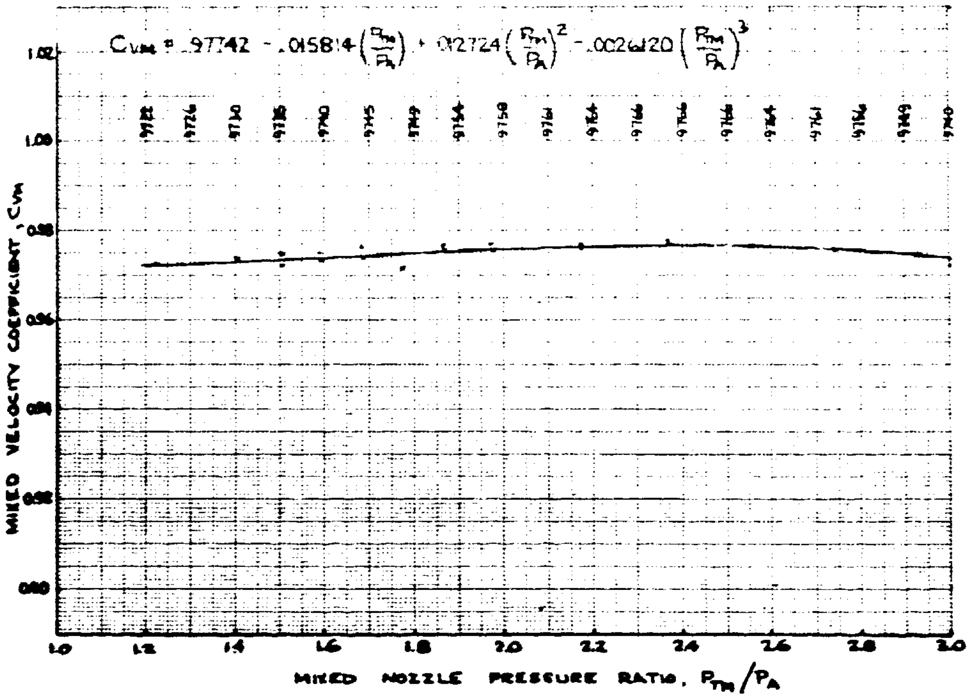

FIGURE 11 - MIXED VELOCITY COEFFICIENT FOR JT8D-9/727 AIRPLANE PRODUCTION NOZZLE (T_{T_P}/T_{T_F} = 2.2).

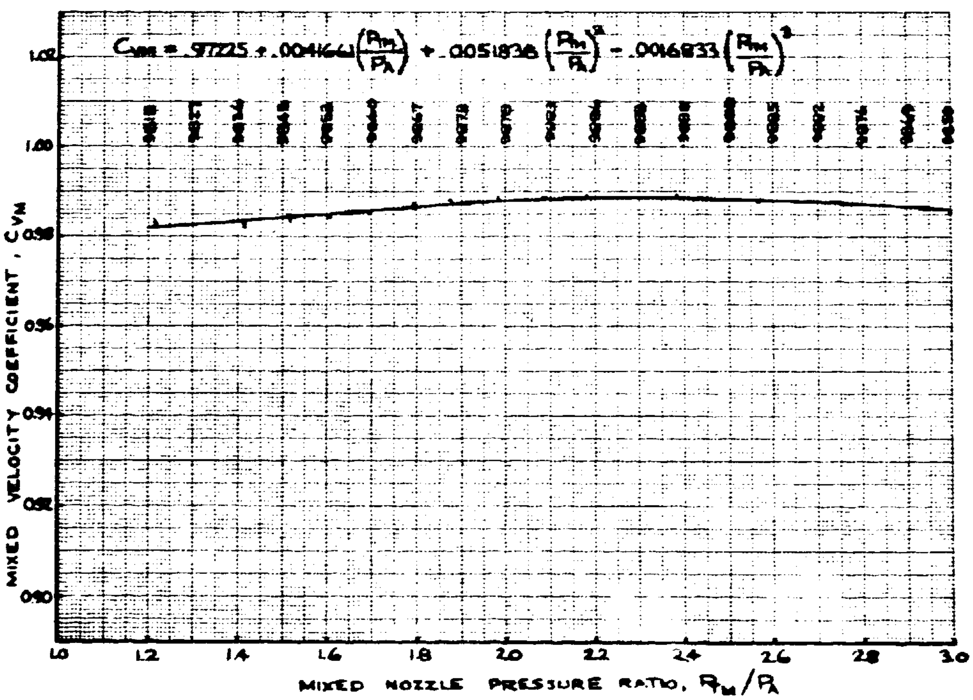

FIGURE 12 - MIXED VELOCITY COEFFICIENT FOR JT8D-9/727 AIRPLANE PRODUCTION NOZZLE (T_{T_P}/T_{T_F} = 1.0).

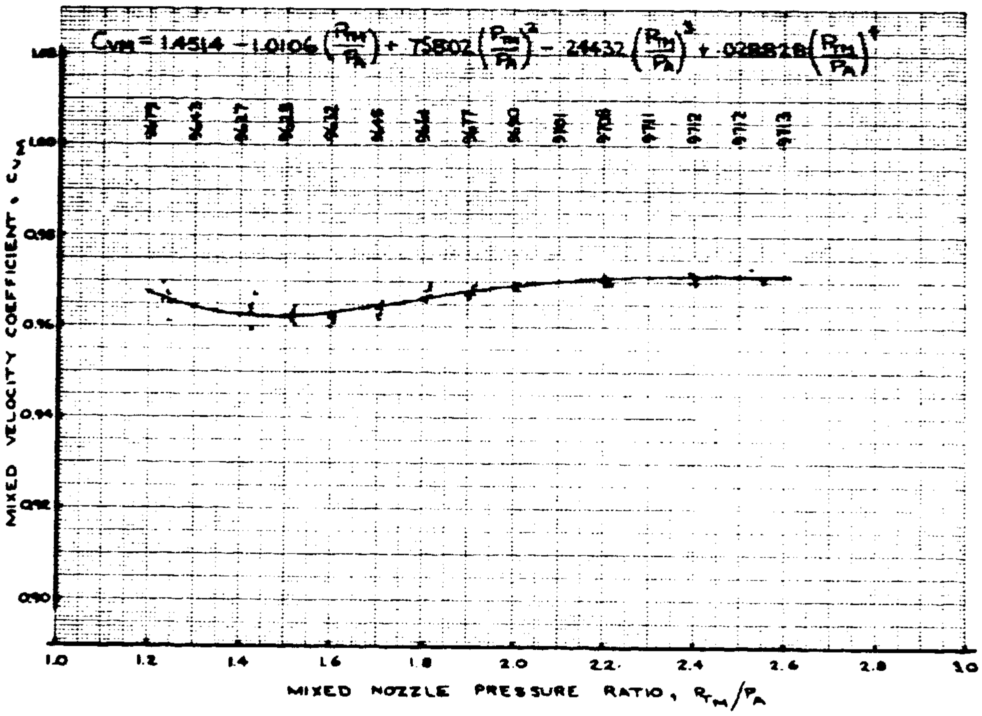

FIGURE 13 - MIXED VELOCITY COEFFICIENT FOR P&WA REF. AND BOEING CONFIG. NO. 2 NOZZLES WITH PRI. SWIRL VANES INSTALLED ON JT8D-109 ENGINE (T_{T_P}/T_{T_F} = 2.2).

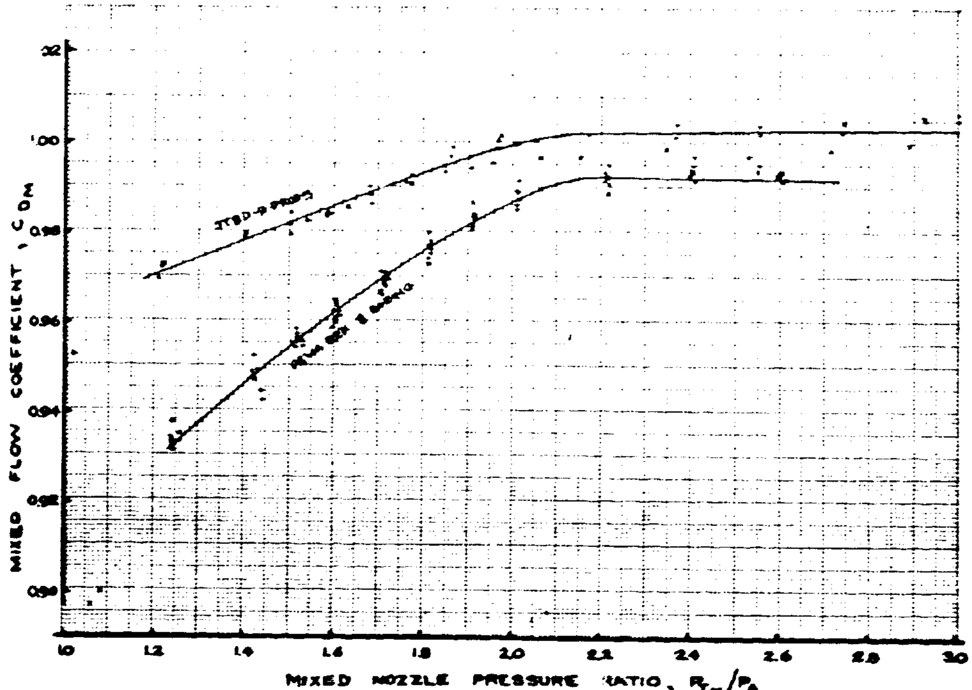

FIGURE 14 - MIXED FLOW COEFFICIENT FOR JT8D-9/727 PRODUCTION NOZZLE; P&WA REF. AND BOEING CONFIG. NO. 2 NOZZLES INSTALLED ON JT8D-109 ENGINES (T_{T_P}/T_{T_F} = 2.2).

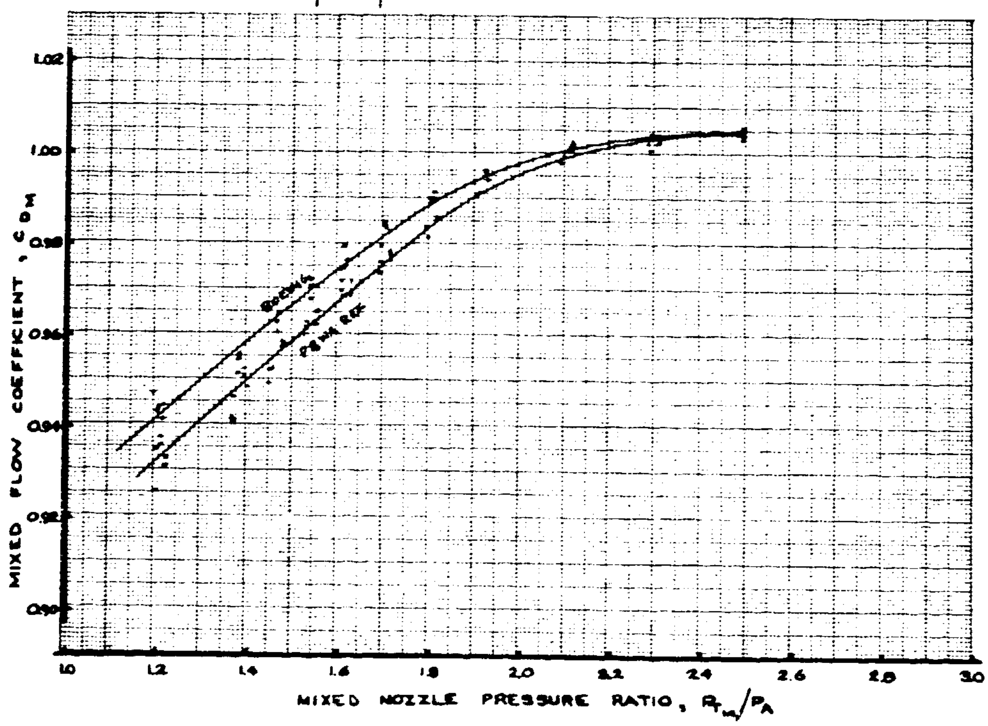

FIGURE 15 - MIXED FLOW COEFFICIENT FOR P&WA REF. AND BOEING CONFIG. NO. 2 NOZZLES INSTALLED ON JT8D-115 ENGINES (T_{T_P}/T_{T_F} = 2.2).

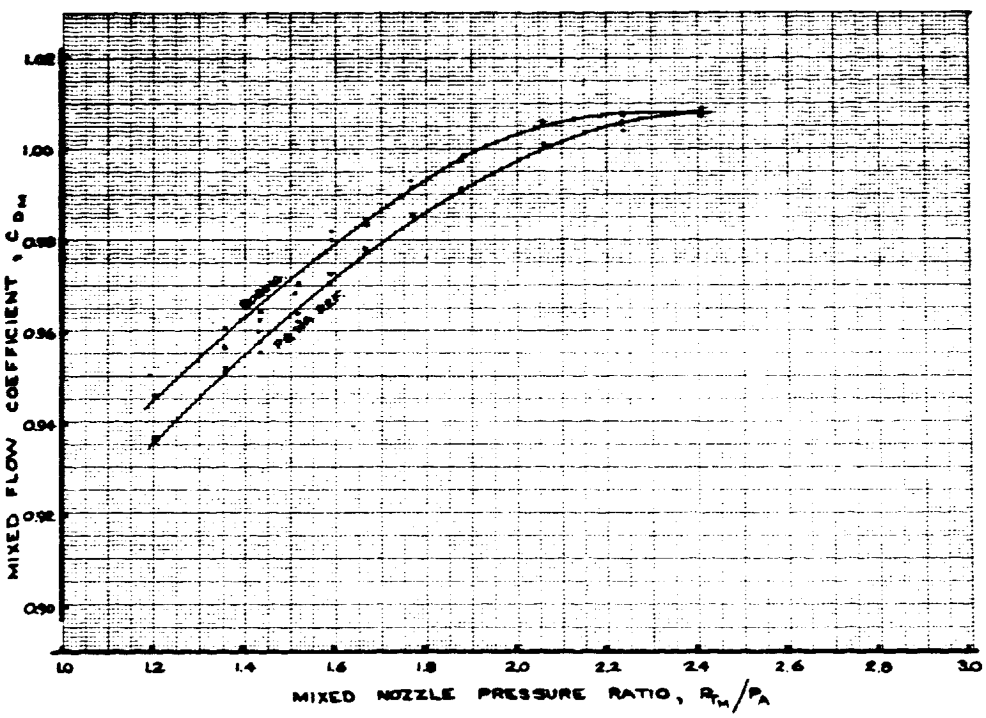

FIGURE 16 - MIXED FLOW COEFFICIENT FOR P&WA REF. AND BOEING CONFIG. NO. 2 NOZZLES INSTALLED ON JT8D-117 ENGINES (T_{T_P}/T_{T_F} = 2.2).

2.0 INTRODUCTION

The Pratt & Whitney Aircraft refanned JT8D-100 engines are derivatives of the basic JT8D engines used to power the 727 airplane. The JT8D-100 engines use a single stage fan of larger diameter than the two fan stages on the basic engine to achieve higher thrust, lower specific fuel consumption and reduced jet noise. These higher thrust versions require changes in the area distribution between fan and primary flows at the mixing plane to satisfy the hot rematch requirements of these engines. In addition, small changes in the exhaust nozzle areas are required for each engine version. The following table shows the estimated uninstalled thrusts and specific fuel consumptions for the basic JT8D and refanned JT8D-100 engines:

P&WA ESTIMATED UNINSTALLED TAKEOFF PERFORMANCE (STATIC SEA-LEVEL CONDITIONS)

ENGINE	THRUST (LB.)	SPECIFIC FUEL CONSUMPTION, TSFC (LB/HR LB)
Basic JT8D-9	14,500	.57
Refanned JT8D-109	16,600	.50
Basic JT8D-15	15,500	.60
Refanned JT8D-115	17,500	.52
Basic JT8D-17	16,000	.62
Refanned JT8D-117	17,900	.53

The purpose of this 1/8-scale model test was to evaluate the performance of various free mixing nozzle options for the refanned JT8D (i.e., JT8D-100 series engines). A report entitled "Scale Model Testing of the Jet Noise Characteristics of the JT8D Refan Engine Nozzle System" CR 134618, BCAC D6-41529 was issued concurrently with this document to report the noise characteristics of these nozzles.

The mixed flow configurations covered three engine variants, the JT8D-109, -115, -117, the corresponding Pratt and Whitney Aircraft (P&WA) Reference nozzles and two Boeing configuration designs, designated Config. No. 1 and Config. No. 2. Simply stated the differences between nozzle configurations concern the axial location and shape of the splitter dividing the fan and primary flow and the internal plug. Design effort by P&WA for their Reference nozzles resulted in nozzle contours which Boeing felt represented a suitable solution for a short splitter design. Boeing considered that the replacement of the P&WA outer wall contour with the Boeing contour, designed to accommodate a thrust reverser, would not invalidate that conclusion. Boeing designs, therefore, concentrated on Config. No. 2 options. The Config. No. 2 geometries reflect alternative designs for the JT8D-100 series engine variations based on the concepts of either a common plug and a variable splitter position (to accommodate the required variation in primary and fan area split at the mixing plane) or, a common splitter and variations in the plug. Geometries of the P&WA and Boeing configurations are described in Section 4.2.

The following is a list of the major objectives of the test:

- Obtain the relative performance levels of various Boeing options in exhaust configurations to suit the JT8D-100 series engines.
- Compare the performance (velocity coefficients) of the P&WA Reference nozzle configurations with short splitters (similar to a Boeing Config. No. 1) with the Boeing configurations with long splitters (designated Config. No. 2) for the various JT8D-100 series engine configurations.
- To obtain an estimate of the absolute performance levels of the various configurations using an ASME standard.

- To examine the effects on performance of other Boeing Config. No. 2 designs which could have merit from a cost effective parts commonality point of view in production configurations for the three engine cycles.

- To investigate the effects of the P&WA predicted primary flow swirl for the JT8D-109 engine on the performance of the P&WA and Boeing nozzles.

- To determine within the constraints imposed by model tests, the influence of exhaust area variation and splitter radial position on the required match (bypass ratio) of the JT8D-100 engines.

- To obtain nozzle exit total temperature and total pressure surveys to determine exit velocities for noise analysis and to qualitatively assess mixing efficiency, and to obtain mixing plane total pressure surveys to assess mixing plane behavior.

- To determine the differences between the Boeing and P&WA Reference nozzle discharge coefficients.

The test was designed recognizing the requirements to compare configurations using mathematically valid statistical techniques for determining differences between configurations, if any. This was the first comprehensive application of these statistical techniques to model nozzle testing in The Boeing Company. For this reason, the statistical analysis is dealt with at some length in Section 5.9 in order to acquaint the reader with the principles involved. The complex mathematics involved is not included as it has been assumed that anyone interested in the standard statistical techniques employed can avail themselves of the various sources of information on the subject.

3.0 NOMENCLATURE

A	Area.
A_E	Nozzle geometric exit area.
A_{e_F}	Fan effective flow area at nozzle exit plane.
A_{e_p}	Primary effective flow area at nozzle exit plane.
A_F	Fan effective flow area at mixing plane.
A_M	Total effective flow area at mixing plane.
A_P	Primary effective flow area at mixing plane.
C_D	Flow coefficient based on single or separate flow relations, see Appendix A.1.
C_{D_M}	Flow coefficient based on fully mixed flow relations, see Appendix A.2.
C_{PR}	Specific heat at constant pressure.
C_{PR_F}	Specific heat at constant pressure based on fan stream properties.
C_{PR_M}	Specific heat at constant pressure based on fully mixed stream properties.
C_{PR_P}	Specific heat at constant pressure based on primary stream properties.
C_{VOL}	Specific heat at constant volume.
C_V	Velocity coefficient based on single or separate flow relations, see Appendix A.3.
C_{V_M}	Velocity coefficient based on fully mixed flow relations, see Appendix A.4.
Fg	Gross thrust or resultant measured force.
F_x	Measured force in X-direction.
F_y	Measured force in Y-direction.
F_z	Measured force in Z-direction.
g	Gravitation constant, 32.174 ft/sec^2

PRECEDING PAGE BLANK NOT FILMED

M	Mach number.
M_F	Fan stream Mach number at mixing plane.
M_M	Fully mixed stream Mach number.
M_P	Primary stream Mach number at mixing plane.
P	Pressure.
P_A	Ambient Pressure.
P_O	Standard sea level ambient pressure, 14.696 psia.
P_S	Static pressure.
P_{S_F}	Fan stream static pressure at mixing plane.
P_{S_P}	Primary stream static pressure at mixing plane.
P_T	Total pressure.
P_{T_F}	Fan stream total pressure.
P_{T_M}	Fully mixed total pressure
P_{T_P}	Primary stream total pressure.
T	Temperature.
T_A	Ambient temperature.
T_O	Standard sea level ambient temperature, 518.69^{O}R.
T_T	Total temperature.
T_{T_F}	Fan stream total temperature.
T_{T_M}	Fully mixed total temperature.
T_{T_P}	Primary stream total temperature.
R	Radius.
R_C	Gas constant, 53.35 ft-lb/lb-^{O}R.

R_{EXIT}	Outer wall radius at nozzle exit plane.
R_I	Inner radius.
R_O	Outer radius.
R_{OW}	Outer wall radius.
R_{PL}	Plug radius.
R_{SPL}	Splitter trailing edge radius at mixing plane.
V_{i_F}	Ideal fully expanded fan jet velocity.
V_{i_M}	Ideal fully expanded jet veolicty based on fully mixed flow conditions.
V_{i_P}	Ideal fully expanded primary jet velocity.
V_{JET}	Fully expanded jet velocity at nozzle exit plane.
$(V_{JET})_{\text{℄}}$	Fully expanded jet velocity on the geometric center-line at the nozzle exit plane.
$(V_{JET})_{MAX}$	Maximum fully expanded jet velocity at the nozzle exit plane.
W_a	Air flow rate.
W_{a_F};W_{FAN}	Measured fan stream flow rate.
W_{a_p};W_{PRI}	Measured primary stream flow rate, including burner fuel flow rate.
δ_A	P_A/P_0
θ_A	T_A/T_o
γ	Ratio of specific heats, $\gamma = C_{PR}/C_{VOL}$

4.0 TEST DESCRIPTION

4.1 TEST FACILITY

The test was conducted on the Boeing Thrust-Vectoring Rig No. 2, Figure 17, which is located at Boeing Field, Seattle, Washington. This rig has a single air supply which is divided upstream of the balance, and each flow is thereafter individually controlled and measured by critical flow venturis. The primary flow can be heated by a propane burner up to a temperature of about 1500^{0}F maximum. The air flow rate capability is 10 lb/sec primary flow and 15 lb/sec fan flow at a nozzle pressure ratio of approximately 4.0. With choke plates in the line to provide a uniform total pressure profile entering the model, the total flow capability is reduced and the maximum pressure ratio which can be accomplished depends on the bypass ratio being simulated. For the subject test, a maximum pressure ratio of 2.6 (about the normal cruise thrust level of the JT8D-100 Series Engines) was accomplished for bypass ratio 2.0 conditions. Four strain gauge load cells are used to measure the three components of force F_x, F_y, F_z. The pressure and temperature ratios between primary and fan passages can be varied at will.

The exhaust from the rig is collected by an axial silencer and discharged to the atmosphere. The rig itself is surrounded by a wooden "dog house" for acoustic suppression. Static pressure measurements have shown that no change in the static pressure from ambient around the rig is caused by either of these two pieces of noise abatement equipment, and that the rig is a true free jet facility.

PRECEDING PAGE BLANK NOT FILMED

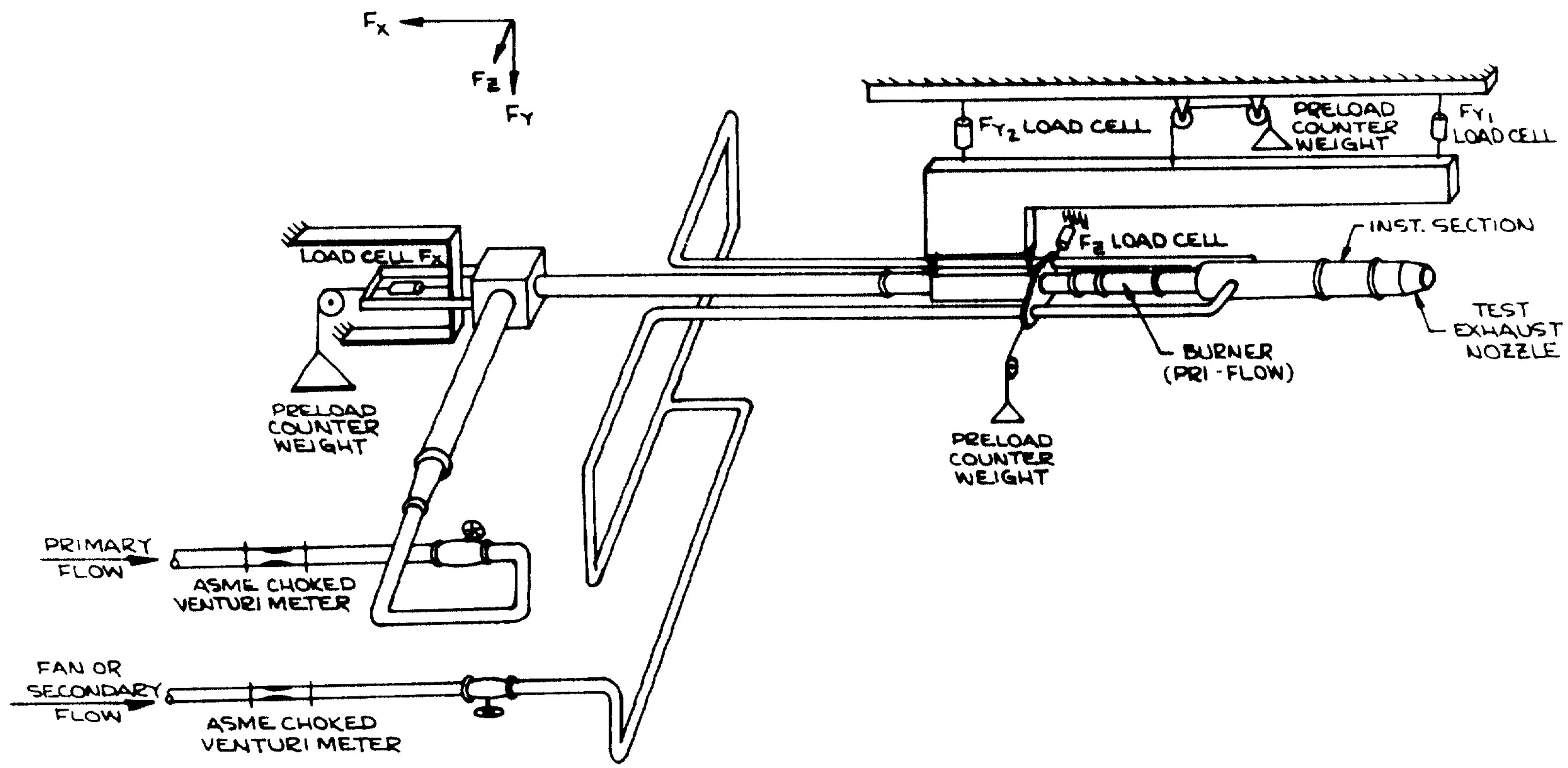

FIGURE 17- THRUST VECTORING RIG SCHEMATIC

4.2 INSTRUMENTATION

Photographs of the Instrumentation Section and Nozzle Test Parts are in Section 7.4.

4.2.1 INSTRUMENTATION SECTION

A 1/8 scale model of the JT8D-100 engine duct exists was constructed. This constituted the part referred to as the instrumentation section which incorporated constant area primary and fan passages with choke plates to provide flat pressure profiles in both ducts. (See Figure 299, Section 7.4)

The model did not expressly simulate the engine rear bearing support struts and the fan case support structure of tie rods etc. However, the model primary duct had four struts and the fan duct had six struts in the stream downstream of the pressure and temperature measurement station and therefore incorporates a system of comparable losses. It is worthy of comment that swirl was not present in the primary stream as it is in the full scale engine. When swirl was introduced, it was produced downstream of all the struts. Therefore, any additional loss of the rear bearing support structure occasioned by the presence of swirl was not included in the performance measurements made with swirl in this model test.

The fan and primary total pressure and total temperature measurement station was 29.1 inches (full scale) upstream of exhaust station 0.0. Full scale engine instrumentation is approximately 17.5 inches (full scale) upstream of this exhaust station.

The fan duct contains three, nine probe, area weighted, total pressure probes on three struts, 120° apart. On one other strut, four thermocouples are mounted to monitor fan air flow temperature. The primary duct contains three, ten probe, area

weighted, total pressure probes on three struts, 120° apart, and between two of these struts, a fourth strut is located with four thermocouples to monitor primary gas stream temperature.

The instrumentation section accepted different nozzles for the P&WA JT8D-100 and Boeing JT8D-100 and JT8D-9 configurations. Variations in the splitter between the fan and primary flow passages could be incorporated and different plugs could be attached to the center of the section.

4.2.2 NOZZLE

Figure 18 shows line drawings of the various P&WA Reference nozzles, (. r all intents and purposes, Boeing Config. No. 1 also). Fiugre 19 shows line drawing definitions of the Boeing Config. No. 2 options for the various JT8D-100 engine variants.

The following tables list the model parts associated with the P&WA Reference and Boeing Config. No. 2 designs.

Boeing 727 Airplane Production & P&WA Reference Nozzles

Engine	Plug	Splitter	Nozzle Outer Wall	Nozzle Exit
JT8D-9	P1	S1	C2	E1
JT8D-109	P2A	S2	C3	E2
JT8D-115	P2A	S3	C3	E3
JT8D-117	P2A	S4	C3	E4

Boeing Config. No. 2 Nozzles

ENGINE	PLUG	SPLITTER	NOZZLE OUTER WALL	NOZZLE EXIT
JT8D-109	P5-1	S5	C4	E5
JT8D-115	P5-1	S6	C4	E6
JT8D-115	P5-1S	S6	C4	E6
JT8D-115	P5-2	S5	C4	E6
JT8D-117	P5-1	S7	C4	E7
JT8D-117	P5-3	S5	C4	E7
JT8D-117	P5-3A	S5	C4	E7
JT8D-117	P7	S6	C4	E7

The exit areas of each of the nozzles, except the JT8D-9, were capable of being varied to suit the various JT8D-100 series engine nozzle exit requirements. The nozzles incorporated bosses to which exit survey rakes or mixing plane survey rakes could be attached. The JT8D-100 nozzle outer walls were capable of circumferential rotation about the attachment plane to facilitate rake surveys at any position.

The model contours were designed in accordance with P&WA mixing plane area match and nozzle exit requirements for the respective JT8D-100 series engine configurations, taking into account design requirements for the incorporation of thrust reversers on the Boeing configuration, length restrictions for the 727 airplane, aerodynamic convergence or diffusion where applicable, and flow smoothness for minimum loss.

The P&WA Reference nozzle configurations have a total mixing plane area of 1562 sq.in.(full scale) compared to the Boeing Config. No. 2 designs which for the common plug versions (P5-1 and P5-1S) have a mixing plane area of 1534 sq. in. Efforts to use a common splitter (S5) for the JT8D-109, -115, and -117 using plugs P5-1, P5-2 and P5-3 or -3A respectively, or a

common splitter S6 for the -115 and -117 only, using plugs P5-1 and P7 respectively, result in decreased mixing plane areas for the -115 and -117 (see Figure 19 and Table IV). Reduced mixing plane area increases the respective mixing plane Mach numbers in the fan and primary ducts. Inherently this is undesirable as regards mixing efficiency and nozzle losses, but in certain instances, it can improve the aerodynamic conditions upstream of the mixing plane by reducing flow turning and/or diffusion.

Each model was equipped with eight coplanar static pressures on the splitter trailing edge, four on the fan side and four on the primary side located at 90° intervals around the circumference of the splitters. The thinness of the model scale splitters prevented the placement of the static pressures as close to the trailing edge as was really desirable. On the P&WA Reference nozzles they were placed the equivalent of 4.16 inches, full scale, upstream of the splitter trailing edge, and on the Boeing Config. No. 2 nozzles, the equivalent of 2.32 inches upstream.

EXH STA	NOZZLE OUTER WALL CONFIGURATION NO. C2 *RADIUS~IN.	C3 *RADIUS~IN.
0	20.5	24.5
6.0	18.0	----
21.0	----	22.1
27.08	17.18	22.1
46.76	17.18	22.1
52.03	-----	22.1

EXH STA	NO E1 *RADIUS~IN
60.64	14.92(D) 14.96(A)
70.0	
NOTE: D	

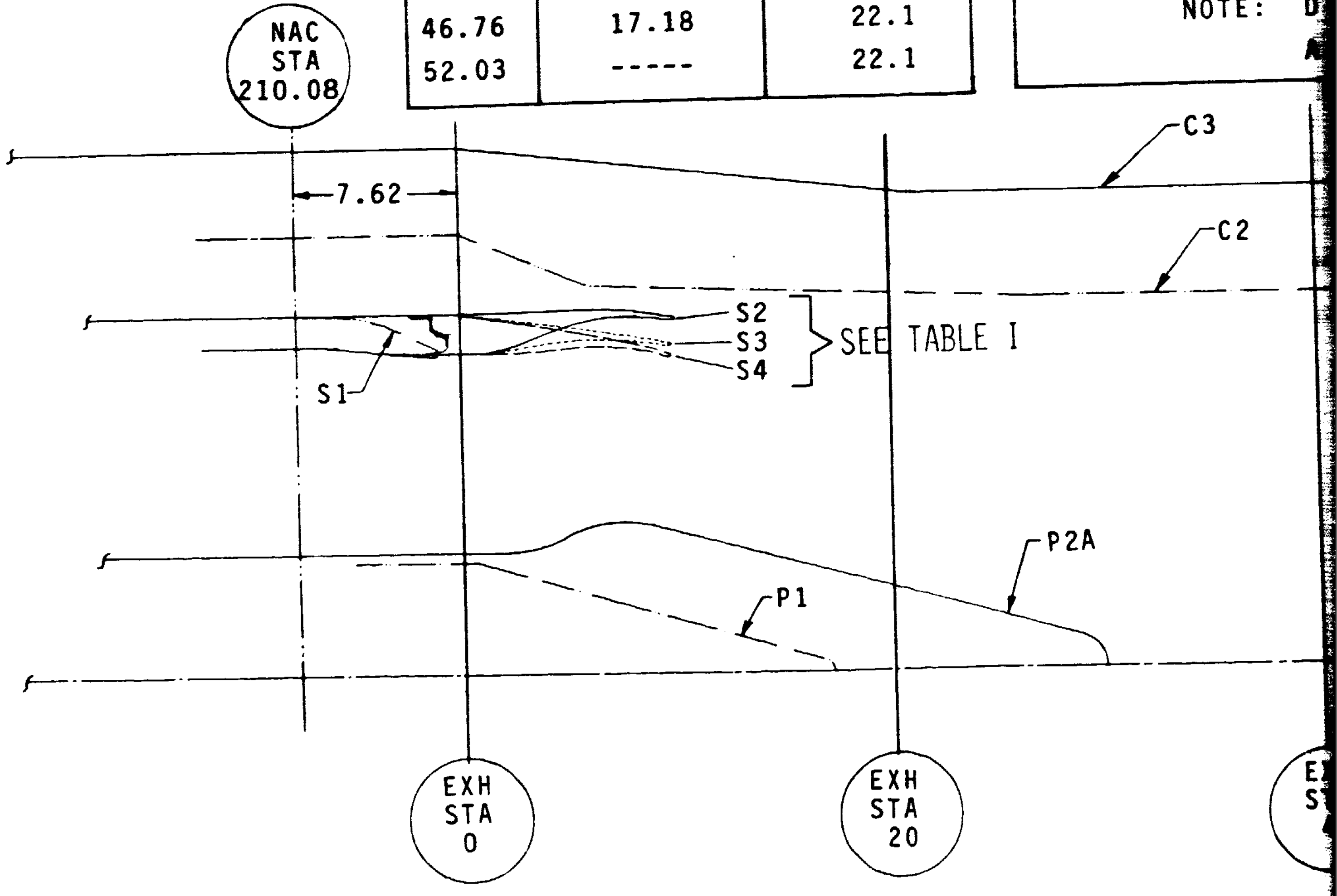

FIGURE 18 - JT8D-9/727 & P&WA JT8D-100 REFERENCE NOZZLE TE

FOLDOUT FRAME

FOLDOUT FRA

EXH STA	NOZZLE EXIT CONFIGURATION NO. E1 *RADIUS~IN.	E2 *RADIUS~IN.	E3 *RADIUS~IN.	E4 *RADIUS~IN.
60.64	14.92(D) 14.96(A)			
70.0		19.24(D) 19.22(A)	19.01(D) 18.99(A)	18.93(D) 18.92(A)

NOTE: D - DESIGN DIMENSIONS
A - ACTUAL HARDWARE DIMENSIONS

*FULL SCALE DIMENSIONS

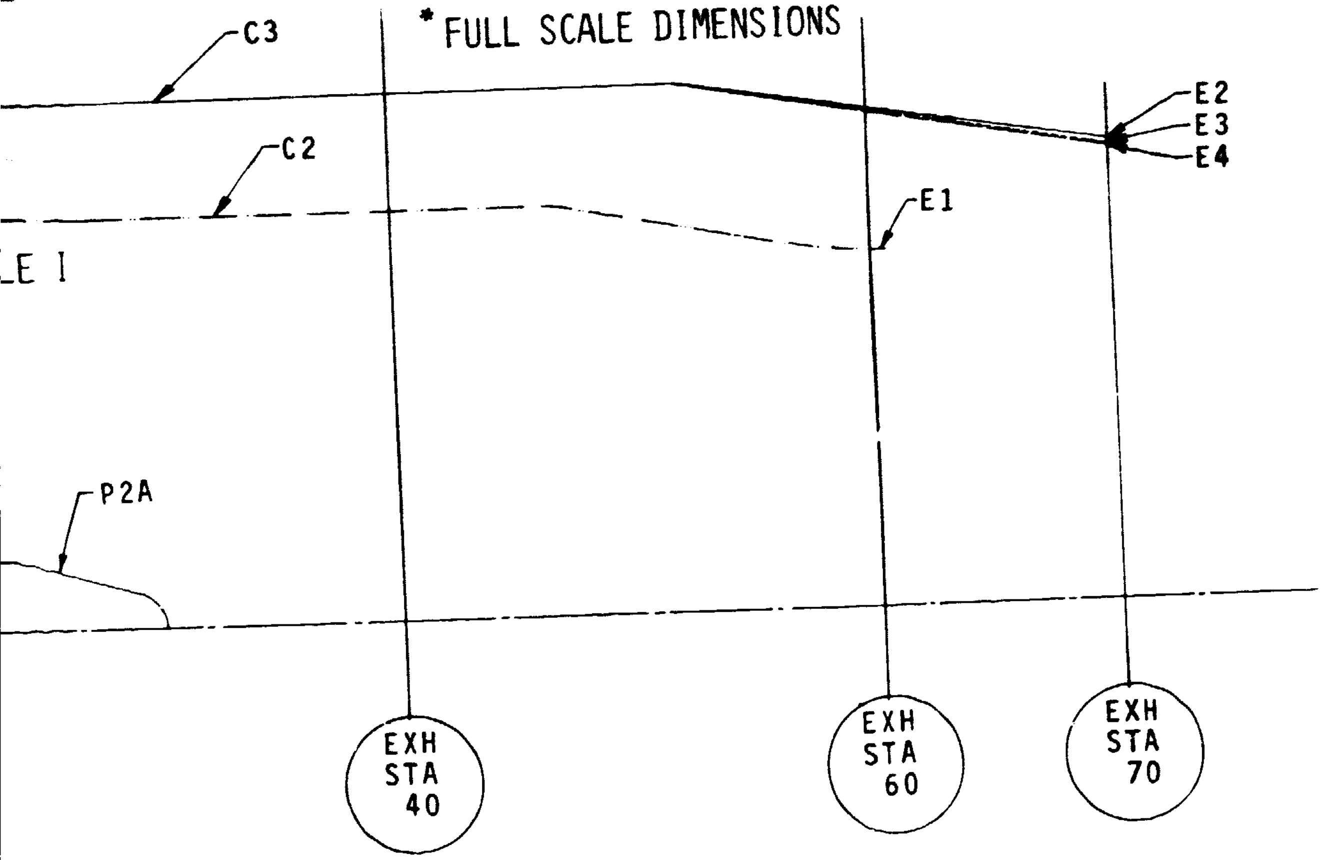

D REFERENCE NOZZLE TEST CONFIGURATIONS

EXH STA	NOZZLE OUTER WALL C4 * RADIUS~IN.
0	24.50
21.0	22.10
57.3	20.44

* FULL SCALE DIMENSIONS

EXH STA	NOZ… E… * RADIU…
	19.2
66.0	19.2
66.75	
66.99	
NOTE:	D - … A - …

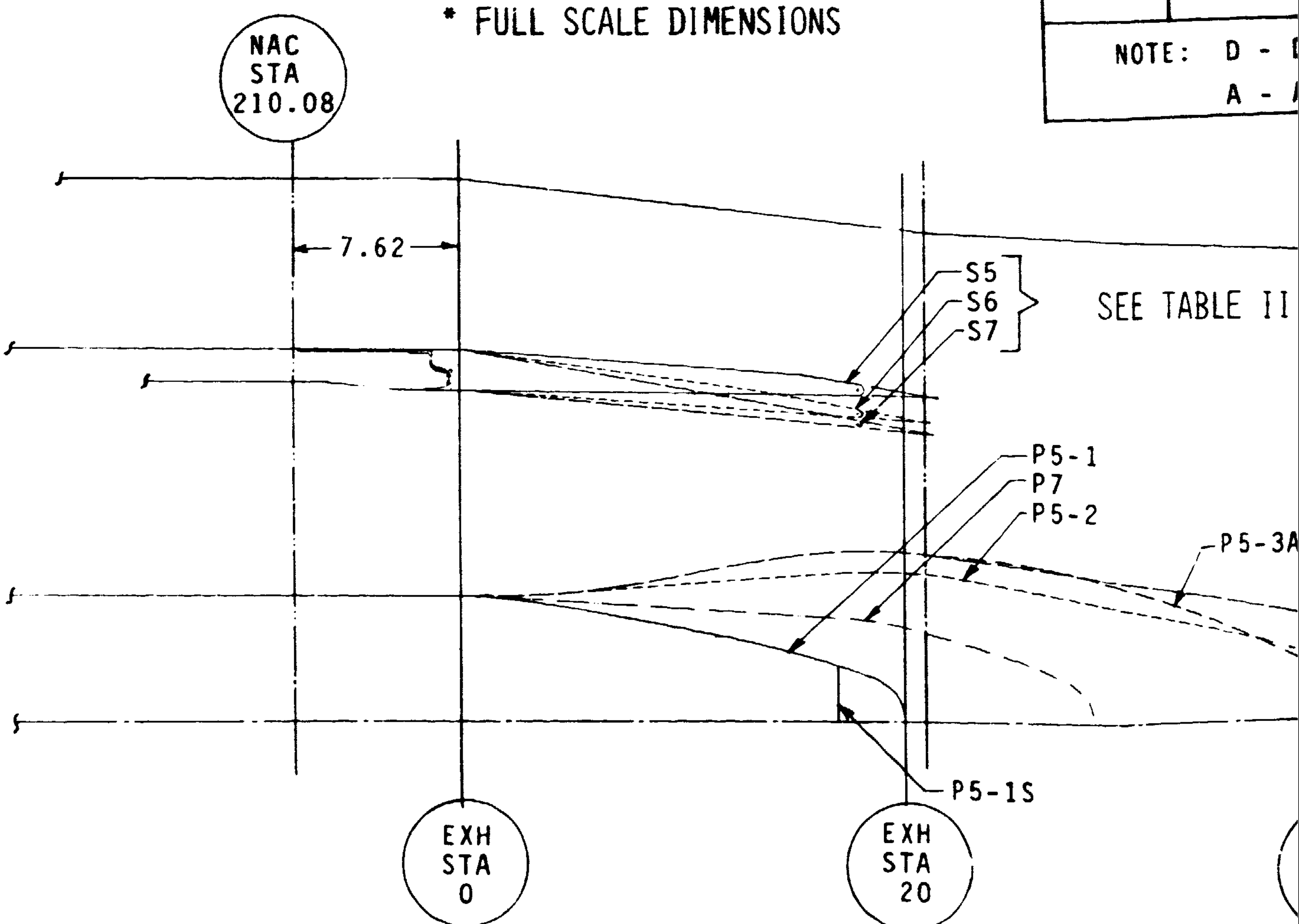

FIGURE 19 - BOEING CONFIGURATION NO. 2 EXHAUST NOZZ

FOLDOUT FRAME

FOLDOUT FRAM

EXH STA	NOZZLE EXIT CONFIGURATION NO. E5 * RADIUS ~IN.	E6 * RADIUS~IN.	E7 * RADIUS~IN.
66.0	19.24(D) 19.23(A)		
66.75		19.01(D) 19.01(A)	
66.99			18.93(D) 18.92(A)

NOTE: D - DESIGN DIMENSIONS
A - ACTUAL HARDWARE DIMENSIONS

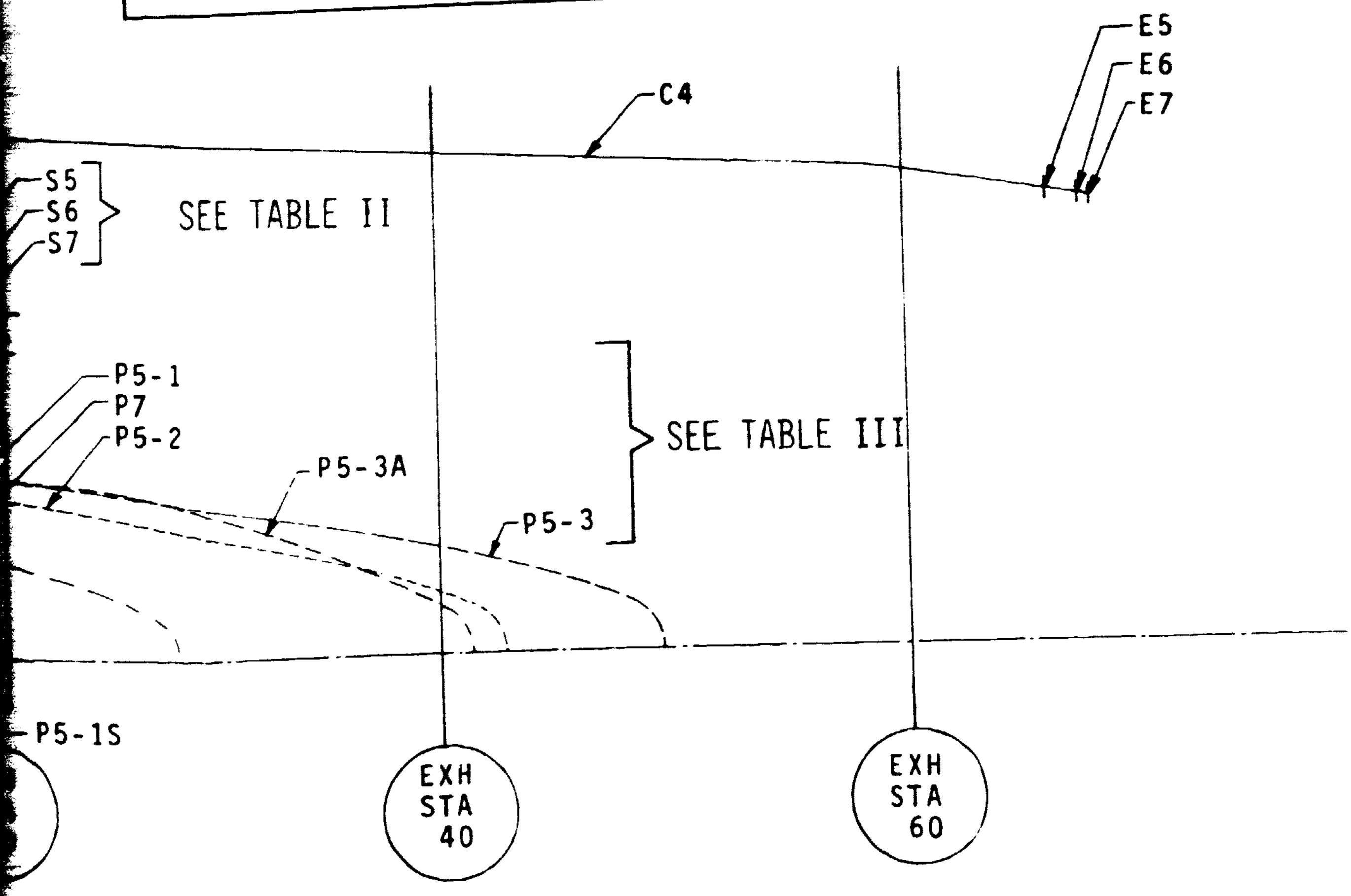

ON NO. 2 EXHAUST NOZZLE TEST CONFIGURATIONS

FOLDOUT FRAME

TABLE I - P&WA SPLITTER COORDINATES

EXH STA	SPLITTER CONFIGURATION NO.					
	S2		S3		S4	
	R_I ~ IN.	R_o ~ IN.	R_I ~ IN.	R_o ~ IN.	R_I ~ IN.	R_o ~ IN.
-1.07	------	------	------	------	14.943	16.765
-1.00	------	------	------	16.765	------	------
-0.42	14.943	16.765	14.943	16.730	14.943	------
0.0	------	------	------	------	------	16.680
0.58	14.943	16.765	14.943	16.644	14.943	------
1.00	------	------	------	------	------	16.586
1.58	15.030	16.780	14.950	16.530	14.943	------
2.00	------	------	------	------	------	16.410
2.58	15.245	16.810	15.100	16.400	14.950	------
3.00	------	------	------	------	------	16.264
3.58	15.650	16.835	15.280	16.276	14.975	------
4.00	------	------	------	------	------	16.086
4.58	16.000	16.860	15.400	16.140	15.050	------
5.00	------	------	------	------	------	15.906
5.58	16.270	16.890	15.460	15.990	15.135	------
6.00	------	------	------	------	------	15.728
6.58	16.455	16.900	15.478	15.850	15.175	------
7.00	------	------	------	------	------	15.544
7.58	16.520	16.840	15.436	15.700	15.110	------
8.00	------	------	------	------	------	15.332
8.58	16.515	16.735	15.330	15.516	14.960	------
9.00	------	------	------	------	------	15.048
9.58	16.400	16.575	------	------	14.710	------
9.85	------	------	------	------	14.630	14.790
9.86	------	------	15.140	15.300	------	------
10.00	16.330	16.500	------	------	------	------

TABLE II - BOEING SPLITTER COORDINATES

EXH STA	SPLITTER CONFIGURATION NO.					
	S5		S6		S7	
	$R_I \sim$ IN.	$R_O \sim$ IN.	$R_I \sim$ IN.	$R_O \sim$ IN.	$R_I \sim$ IN.	$R_O \sim$ IN.
0.0	14.943	16.765	14.943	16.765	14.943	16.765
2.0	14.923	16.623	14.810	16.491	14.760	16.430
4.0	14.902	16.481	14.677	16.216	14.579	16.093
6.0	14.882	16.339	14.544	15.942	14.396	15.774
8.0	14.862	16.197	14.410	15.668	14.214	15.405
10.0	14.842	16.055	14.277	15.394	14.032	15.054
12.0	14.821	15.913	14.144	15.120	13.850	14.699
14.0	14.801	15.771	14.011	14.815	13.668	14.338
16.0	14.781	15.574	13.878	14.458	13.485	13.972
18.0	14.760	15.240	13.745	14.098	13.303	13.601
20.0	14.740	14.827	13.612	13.730	13.121	13.222
21.0	14.730	14.730	13.545	13.545	13.030	13.030

TABLE III-BOEING PLUG COORDINATES

EXH STA	PLUG CONFIGURATION NO.				
	P5-1 *	P5-2	P5-3	P5-3A	P7
	R_{PL} ~ IN.	R_{PL} ~ IN.	R_{PL} ~ IN.	R_{PL} ~ IN.	R_{PL} ~ IN.
0.0	5.651	5.651	5.651	5.651	5.651
2.0	5.530	5.651	5.651	5.651	5.530
4.0	5.255	5.702	5.708	5.708	5.419
6.0	4.923	5.869	5.898	5.898	5.310
8.0	4.568	6.030	6.178	6.178	5.198
10.0	4.191	6.188	6.544	6.544	5.091
12.0	3.780	6.339	6.987	6.987	4.985
14.0	3.325	6.490	7.329	7.329	4.880
16.0	2.803	6.637	7.588	7.588	4.776
18.0	2.166	6.712	7.653	7.653	4.602
20.0	-----	6.683	7.618	7.609	4.226
21.0	-----	6.661	7.599	7.555	4.005
23.0	-----	6.351	-----	7.380	3.464
25.0	-----	6.026	7.049	7.116	2.826
27.0	-----	-----	-----	6.762	1.996
29.0	-----	5.322	6.457	6.316	-----
33.0	-----	4.517	5.841	5.134	-----
37.0	-----	3.549	5.095	3.538	-----
41.0	-----	2.192	4.263	1.477	-----
45.0	-----	-----	3.233	-----	-----

*NOTE: Plug P5-1S is the same as PS-1 but truncated at EXH STA 17.

TABLE IV - TEST CONFIGURATION GEOMETRIES

TEST CONFIG. NO.	CONFIGURATION NOTATION ①	MIXING PLANE GEOMETRY ②					NOZZLE EXIT ② PLANE GEOMETRY	
		OUTER WALL RADIUS INCHES	SPLITTER RADIUS INCHES	PLUG RADIUS INCHES	PRI. FLOW AREA @SPL PLANE SQ. IN.	FAN FLOW AREA @SPL PLANE SQ. IN.	RADIUS INCHES	AREA SQ. IN.
2	C2,S1,P1,E1(JT8D-9/727)	20.50	14.66	5.20	590.229	645.077	19.9620	703.28
3	C3,S2,P2A,E2(JT8D-109 P&WA)	23.32	16.415	6.50	713.777	861.959	19.2264	1161.28
4	C3,S2,P2A,E2,PRI. SWIRL VANES (JT8D-109 P&WA)	✓	✓	✓	✓	✓	✓	✓
5	C3,S3,P2A,E3(JT8D-115 P&WA)	23.34	15.22	6.56	592.551	983.655	18.9912	1133.06
6	C3,S4,P2A,E4(JT8D-117 P&WA)	23.36	14.71	6.58	543.771	1034.544	18.9184	1124.40
7	C4,S5,P5-1,E5(JT8D-109 TBC)	22.10	14.73	0	681.640	852.745	19.2264	1161.25
8	C4,S5,P5-2,E6(JT8D-115 TBC)	✓	✓	6.661	542.251	✓	19.0136	1135.74
9	C4,S6,P5-1S,E6(JT8D-115 TBC)	✓	13.545	0	576.379	958.007	✓	✓
10	C4,S6,P5-1,E5(JT8D-115 TBC)	✓	✓	✓	✓	✓	19.2264	1161.25
11	C4,S6,P5-1,E6(JT8D-115 TBC)	✓	✓	✓	✓	✓	19.0136	1135.74
12	C4,S6,P5-1,E7(JT8D-115 TBC)	✓	✓	✓	✓	✓	18.9240	1125.06
13	C4,S5,P5-1,E6(JT8D-115 TBC)	✓	14.73	✓	681.640	852.745	19.0136	1135.74
14	C4,S7,P5-1,E6(JT8D-115 TBC)	✓	13.03	✓	533.382	1001.003	✓	✓
15	C4,S5,P5-3,E7(JT8D-117 TBC)	✓	14.73	7.599	500.230	852.745	18.9240	1125.06
16	C4,S5,P5-3A,E7(JT8D-117TBC)	✓	✓	7.555	502.325	✓	✓	✓
17	C4,S6,P7,F7 (JT8D-117 TBC)	✓	13.545	4.005	525.987	958.007	✓	✓
18	C4,S7,P5-1,E7(JT8D-117 TBC)	✓	13.03	0	533.382	1001.003	✓	✓
19	C4,S5,P5-1,E5, PRI. SWIRL VANES (JT8D-109 TBC)	✓	14.73	✓	681.640	852.745	19.2264	1161.25

NOTES: ① TBC - THE BOEING CO.
P&WA - PRATT & WHITNEY AIRCRAFT

② FULL SCALE DIMENSIONS AND AREAS

4.3 DATA ACCURACY

The following is a list of parameters and estimated 95% confidence limits of the recorded data.

1) Measured parameters:

Parameter	Range	Accuracy*
Thrust	0-500 LB	± 0.10%
Temperature	Amb. -1000°F	± 4°F
Primary nozzle total pressure	0-50 PSIA	± 0.15%
Primary nozzle total pressure	0-50 PSIA	± 0.15%
Splitter and duct static pressure	0-50 PSIA	± 0.15%
Primary and fan venturi upstream static pressure	0-250 PSI	± 0.15%
Primary and fan throat static pressure	0-200 PSI	± 0.5%
Primary and fan venturi total temperature	Amb.-90°F	± 1°F
Traverse probe total pressure	0-50 PSI	± 0.25%
Traverse probe total temperature	Amb. -1000°F	± 5°F
Traverse probe position	0-6 IN.	± 1%

2) Calculated Parameters:

Parameter	Range	Accuracy*
Air flow	0-9.25 LB/SEC	± 0.25%

* Where accuracy is expressed as a percentage, it represents the percentage of the full range value.

For steady state data, a trap and scan scannivalve system with punched paper tape output was used with all transducers.

The accuracy of the test results is discussed in Section 5.9 of this document.

4.4 TEST PROCEDURES

The following procedures were used throughout the test program and to check both the model and data system before each day's running or configuration change.

1) All runs:

   a) Inspect the model build and check for leaks with low air pressure at model joints.

   b) Check all instrumentation lines for pressure leaks.

2) Cold runs:

   a) Zero check instrumentation. Read barometer. Set primary and fan pressure ratios in accordance with the predetermined relationship, Figure 20, for the particular configuration with cold flow in both fan and primary channels. Record data after pressures stabilize (approximately one minute) and set the next highest fan to primary pressure ratio in accordance with predetermined relationship. Repeat until data for eleven primary nozzle pressure ratios in ascending order has been obtained. Shut down air supply. Re-check zero.

   b) Repeat 2a twice.

3) Hot runs:

   a) At low primary and fan pressure ratios, ignite primary burner and warm up model for approximately 20 minutes. Shut down air supply.

b) Zero check instrumentation. Read barometer. Set primary and fan pressure ratios at low levels and ignite primary burner. Set primary and fan pressure ratio in accordance with predetermined relationship for the particular condition maintaining the primary to fan temperature ratio at 2.2. Record data after pressures stabilize (approximately one minute) and set the next highest fan to primary pressure ratio in accordance with the predetermined relationship.

Repeat until data for eleven primary nozzle pressure ratios in ascending order have been obtained. Shut down air supply and burner. Zero check instrumentation.

c) Repeat 3b twice.

4) Exit traverse:

a) Repeat 3b at only four selected pressure ratios instead of eleven. Take an exit survey using the traversing total pressure and temperature probes, recording pressure and temperature continuously as a function of a rake radial position.

b) Repeat 4a at two additional circumferential positions.

5) Mixing plane survey:

a) Repeat 2a at only four selected primary nozzle pressure ratios instead of eleven. Take a mixing plane survey using the traversing total pressure probe, recording pressure continuously as a function of probe radial position.

b) Repeat 5a at two additional circumferential positions.

Procedures 4 and 5 were used for the test configurations noted in Table V.

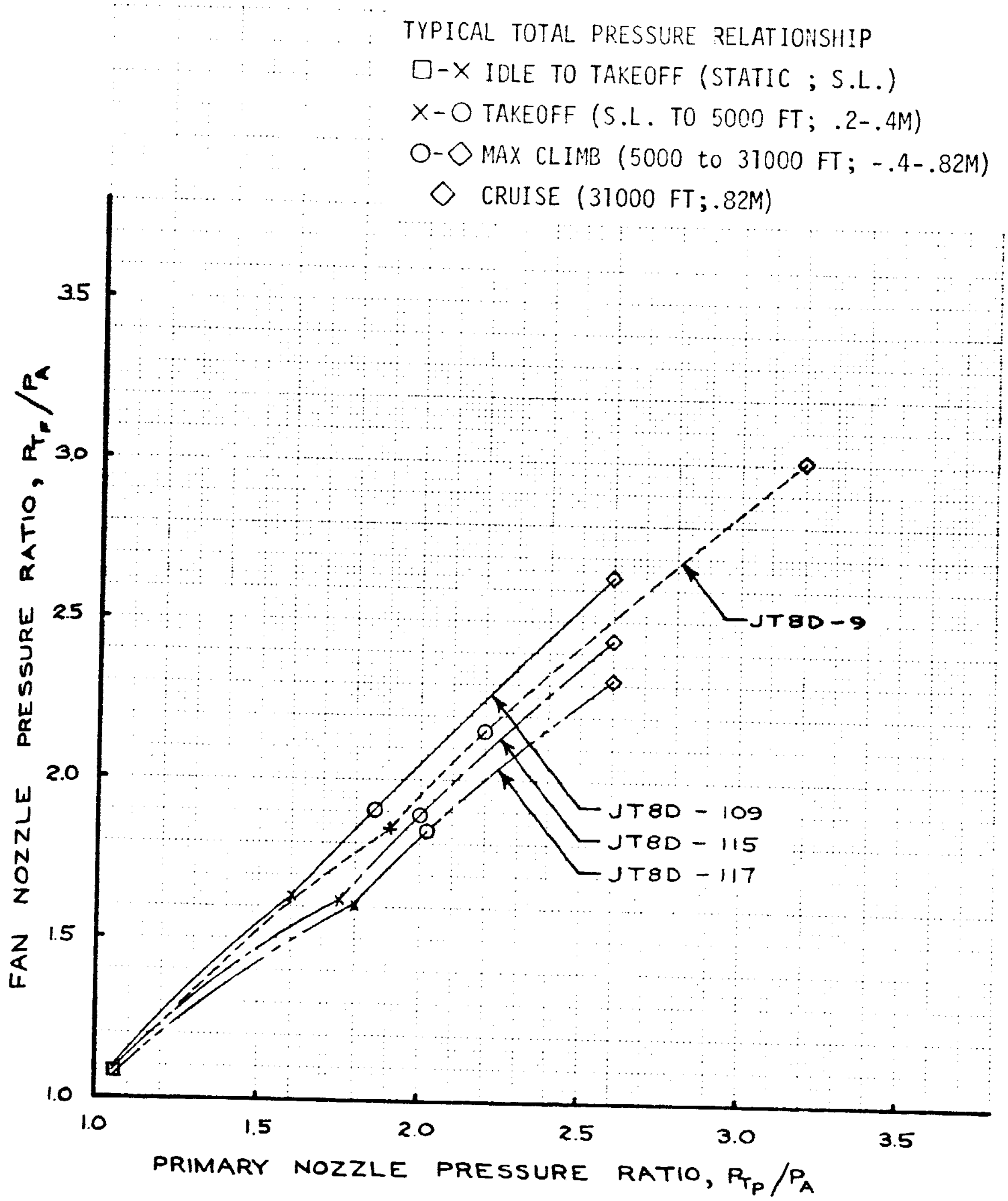

FIGURE 20 - SIMULATED ENGINE FAN AND PRIMARY NOZZLE TOTAL PRESSURE RATIOS SCHEDULES

TABLE V - TEST CONFIGURATIONS

TEST CONFIG. NO.	CONFIGURATION	HARDWARE NOTATION: OUTER NOZZLE WALL	SPLITTER	PLUG	NOZZLE EXIT	TRAVERSE DATA M=MIX PLANE E = EXIT
1.	A.S.M.E. 4-In. Nozzle	C1	--	--	--	N.A.
2.	JT8D-9/727 Production	C2	S1	P1	E1	M&E
3.	JT8D-109 P&WA Ref.	C3	S2	P2A	E2	M&E
4.	JT8D-109 P&WA Ref. (with Pri. Swirl Vanes)	C3	S2	P2A	E2	M&E
5.	JT8D-115 P&WA Ref.	C3	S3	P2A	E3	
6.	JT8D-117 P&WA Ref.	C3	S4	P2A	E4	
7.	JT8D-109 Boeing Conf. 2	C4	S5	P5-1	E5	M&E
8.	JT8D-115 Boeing Conf. 2	C4	S5	P5-2	E6	
9.	JT8D-115 Boeing Conf. 2	C4	S6	P5-1S	E6	
10.	JT8D-115 Boeing Conf. 2	C4	S6	P5-1	E5	
11.	JT8D-115 Boeing Conf. 2	C4	S6	P5-1	E6	
12.	JT8D-115 Boeing Conf. 2	C4	S6	P5-1	E7	
13.	JT8D-115 Boeing Conf. 2	C4	S5	P5-1	E6	
14.	JT8D-115 Boeing Conf. 2	C4	S7	P5-1	E6	
15.	JT8D-117 Boeing Conf. 2	C4	S5	P5-3	E7	
16.	JT8D-117 Boeing Conf. 2	C4	S5	P5-3A	E7	
17.	JT8D-117 Boeing Conf. 2	C4	S6	P7	E7	
18.	JT8D-117 Boeing Conf. 2	C4	S7	P5-1	E7	
19.	JT8D-109 Boeing Conf. 2 (with Pri. Swirl Vanes)	C4	S5	P5-1	E5	M&E

4.5 TEST DESIGN AND DATA COLLECTION

4.5.1 PRESSURE AND TEMPERATURE RATIO SELECTION

An explanation of the judgements and philosophy which determined the choice of fan/primary pressure and temperature ratio is desirable since the ratios influence the resulting data and the analysis. It was suspected that the temperature ratio has by far the biggest influence on the theoretical mixing thrust gains, but that the importance of the pressure ratio must be carefully considered. It was also suspected that on a mixed flow engine the shape and therefore the level of the velocity coefficient would be sensitive to the pressure and temperature ratio and therefore great care must be exercised in their selection to obviate confounding the experiment.

By an examination of JT8D-109 engine data, it was obvious that the fan/primary pressure ratio was by no means constant, varying typically over a range of 1.01 to 1.06. The temperature ratio varies between 2.1 and 2.3. Moreover, the range of the pressure ratios is different for each engine cycle simulated. From these data, it was apparent that some kind of representative pressure and temperature ratio schedules were required.

From studies conducted with a 100% ideal mixing analysis to examine the effects of temperature and pressure ratio variations, the following was concluded:

1. The theoretical mixing gain is a function of the absolute temperatures of the gas streams.

2. The theoretical mixing gain is dependent on the temperature ratio but relatively insensitive to the magnitude of the temperature ratio changes exemplified by the typical JT8D-100 operating envelope. Therefore, a temperature ratio of 2.2 was chosen.

3. The mixing potential is dependent and quite sensitive to, the pressure ratio variations over the typical JT8D-100 operating range. Therefore, a schedule of primary/fan pressure ratio was utilized for each engine cycle simulated, Figure 20.

The fan stream of the Thrust Vectoring Rig is not heated. The temperature ratio could therefore only be simulated by having a lower primary temperature than that in the full scale engines. It was concluded this would reduce the potential theoretical thrust gains but would not affect the ability to measure the mixing efficiency of the nozzles. That is to say, the amount of the theoretical gain recovered by mixing is a constant proportion of the theoretical gain for a particular engine cycle even though the absolute magnitude of the theoretical gain is a function of the absolute temperature.

Figure 20 shows the chosen pressure ratios for the various engine configurations. These curves are divided into roughly three segments representative of a typical engine operation of the JT8D-100 powered 727-200 airplane. The three segments represent: 1, idle to takeoff power; 2, climb to initial cruise at maximum climb power; and 3, typical cruise. The cruise curves intersect the curves shown depending on Mach number and altitude chosen. The pressure ratios chosen are therefore not rigorous but the best that can be expected for the simplification of a complex relationship.

4.5.2 SELECTION OF NUMBER OF RUNS AND DATA POINTS

Designers of experiments must take cognizance of the intended use of the data. Comparisons of configurations require enough data of the right type to perform a reliable statistical analysis. History indicates that most, if not all, nozzle performance test rigs have random errors which cause run to

run level variations of any particular configuration. For this reason a number of runs per configuration must be performed. Without excessive elaboration it will be stated here that the statistical degrees of freedom needed in the analysis are proportional to the number of runs per configuration minus one. Three runs per configuration are the minimum useful number of runs required to improve the analysis of variance (see Section 5.9) to the level of meaningfulness to conduct intelligent comparisons of configurations.

The number of data points per run is governed to a large extent by the pressure ratio range expected for the particular application of the nozzle being tested. However, certain other criteria govern the number of data points and the pressure ratio distribution:

Firstly, consideration must be taken of the order of the regression equation (polynomial curve fit) expected to fit the data. Generally, velocity coefficient curves will be second or third order, and a mathematicians rule of thumb is that n points per run are required for each of the n coefficients of the regression equation. Thus, for a least squares curve fit routine to have sufficient data to arrive at a regression curve of reasonable confidence, nine points per run are required for quadratic curve fits and sixteen points for cubic curve fits.

Secondly, any particular nozzle pressure ratios of interest and distribution of the pressure ratios around the points of interest must be considered. These points of interest in nozzle work usually pertain to the takeoff pressure ratio and cruise pressure ratio. Curve shape is also important. Whereas it might appear that taking all data points at two particular pressure ratios would suffice as far as the best estimates of the absolute values were concerned, it would violate the curve fit requirements.

For the comparison of two or more configurations, it is important that all be run with the same distribution of pressure ratios. A valid statistical comparison of two or more configurations depends on certain conditions being satisfied which depend in turn on the variance of the data between runs as well as within a run. Since the variance changes with pressure ratio it is readily apparent that the comparison of different configurations becomes more difficult if the quality of the data in one configuration is better at the particular point of comparison than in another. If sufficient number of data points could be taken this condition would not exist because it is assumed the distribution of error is normal (this is the central limit theorem) and in the limit (many runs and many data points per run) the quality at a particular point is the same. To satisfy these conditions, eleven points with the same primary pressure ratio distribution per run were considered satisfactory and within the test time available considering the number of configurations to be tested.

4.5.3 DATA COLLECTION AND REDUCTION

Data reduction was accomplished in four phases:

1) Transducer outputs and temperatures in non-engineering units, physical areas and ambient conditions were recorded on punched paper tape.

2) Calculated nozzle parameters, corrected thrust, mass flow, pressure ratios, bypass ratio and individual pressure readings were obtained on a digital computer near the test site. Output was generally available within 45-60 minutes after each run.

3) Certain parameters were selected and compiled for computer data reduction using a more elaborate computer program. Data was obtained in the same form as the above mentioned data and also with other computational methods to obtain outputs as functions of mixed flow parameters and full scale quantities. A calculation for each data point was conducted using a 100% mixed theoretical subroutine program with outputs of local velocities, Mach numbers, pressure ratios and theoretical mixed thrust gains. Least squares quadratic curve fits were put through each composite of three runs (average 33 data points) as an aid to rapid comparison.

4) Configurations were compared using a statistical analysis computer program to determine whether differences existed between configurations.

4.6 QUALITY ASSURANCE

It is necessary for any test of nozzles to have some baseline which establishes test rig performance repeatability and level. For this purpose, a long radius ASME nozzle was mounted on the rig with its own instrumentation section and was run at the same pressure ratios, mass flows and bypass ratio as the JT8D-100 nozzles. The velocity coefficient and flow coefficient of the ASME nozzle were obtained. Figures 21 and 22 show velocity coefficient and flow coefficient respectively obtained with the 4-inch ASME nozzle at the beginning of the test program. These results are compared with a recognized industry standard referred to as the G.E. level. The excellent agreement with the G.E. flow coefficient level indicates accurate mass flow measurements. The velocity coefficient level is lower than the G.E. level by approximately 1.0% over the pressure ratio range considered. Figure 23 shows a thrust correction curve generated from the difference between the G.E. level and the rig level. A curve was drawn through these data and this correction was incorporated in the data reduction program to correct all measured thrusts. The increased scatter in the data at lower pressure ratios is readily apparent in Figure 23. Figures 24 and 25 illustrate the excellent repeatability of the rig at the end of the test. Figure 26 shows the thrust errors for each individual data point after the test was completed, to be of the same family as those generated at the beginning of the test. It can be concluded that the rig repeatability was well maintained throughout the test in both thrust and mass flow measurement.

Part way through the test a failure occurred in the 1/8-scale model instrumentation section, necessitating a complete rebuild of the pressure and temperature instrumentation in the fan passage. Retesting of the same configuration which had been

tested just prior to the failure showed a level shift, not repeated by the subsequent end of test rig calibration using the ASME standard nozzle. This indicated that the instrumentation section had an influence on the absolute levels of the data.

Comparisons have been made throughout this report using only data collected for each nozzle run with the rebuilt instrumentation section. Unfortunately all nozzles to be compared were not and could not be run with the two, apparently different instrumentation sections. By combining the data for those configurations tested both before and after the instrumentation section rebuild, more valid estimates of the absolute levels of performance were obtained due to the inclusion of another experimental variable. Examination of these data reveals that the velocity coefficient estimates have 95% confidence of being within 0.10% and 0.05% of the best estimate of the true levels at takeoff and cruise conditions respectively.

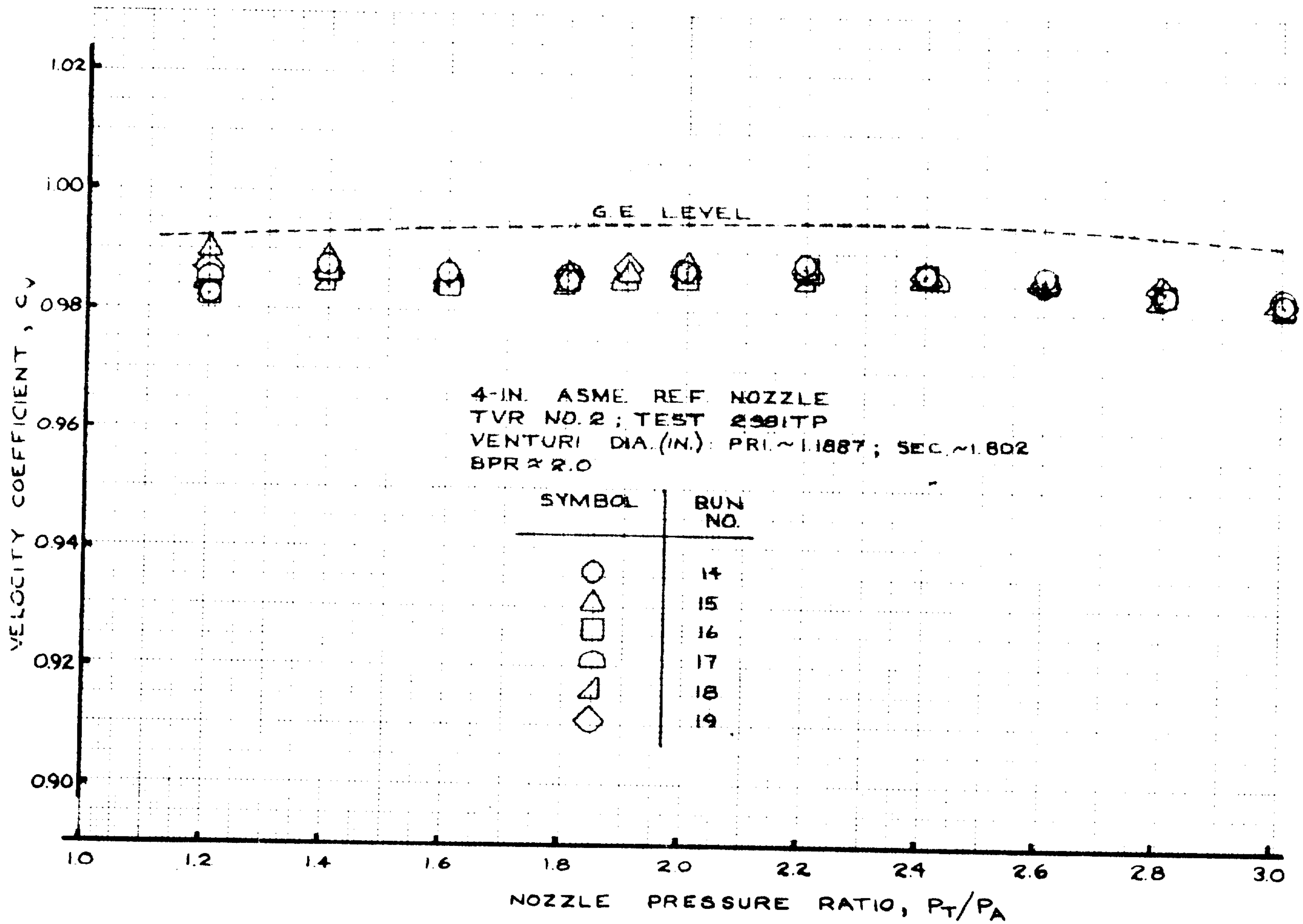

FIGURE 21 - VELOCITY COEFFICIENT; RUNS 14 - 19

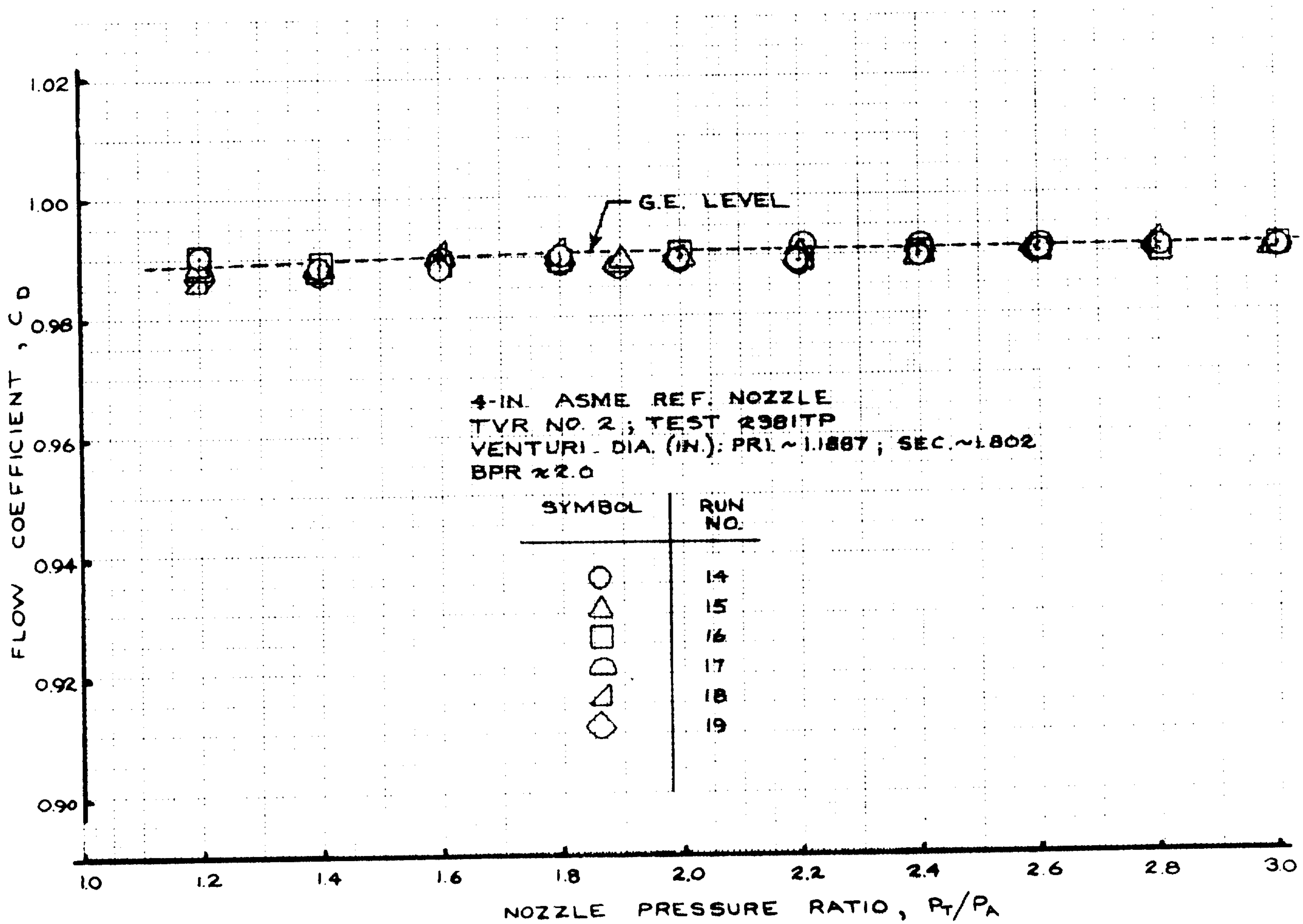

FIGURE 22 - FLOW COEFFICIENT; RUNS 14 - 19

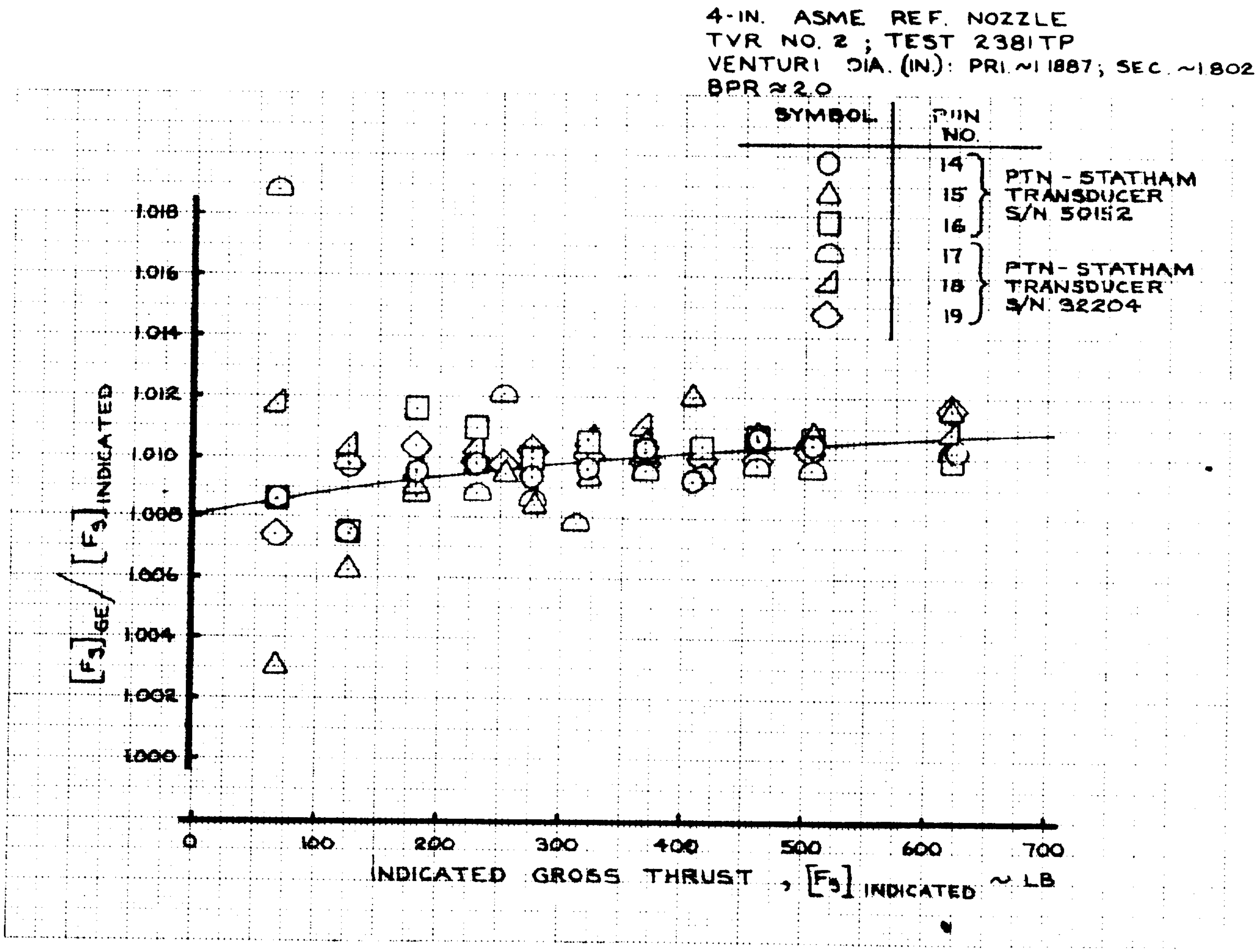

FIGURE 23 - GROSS THRUST CORRECTION; RUNS 14 - 19

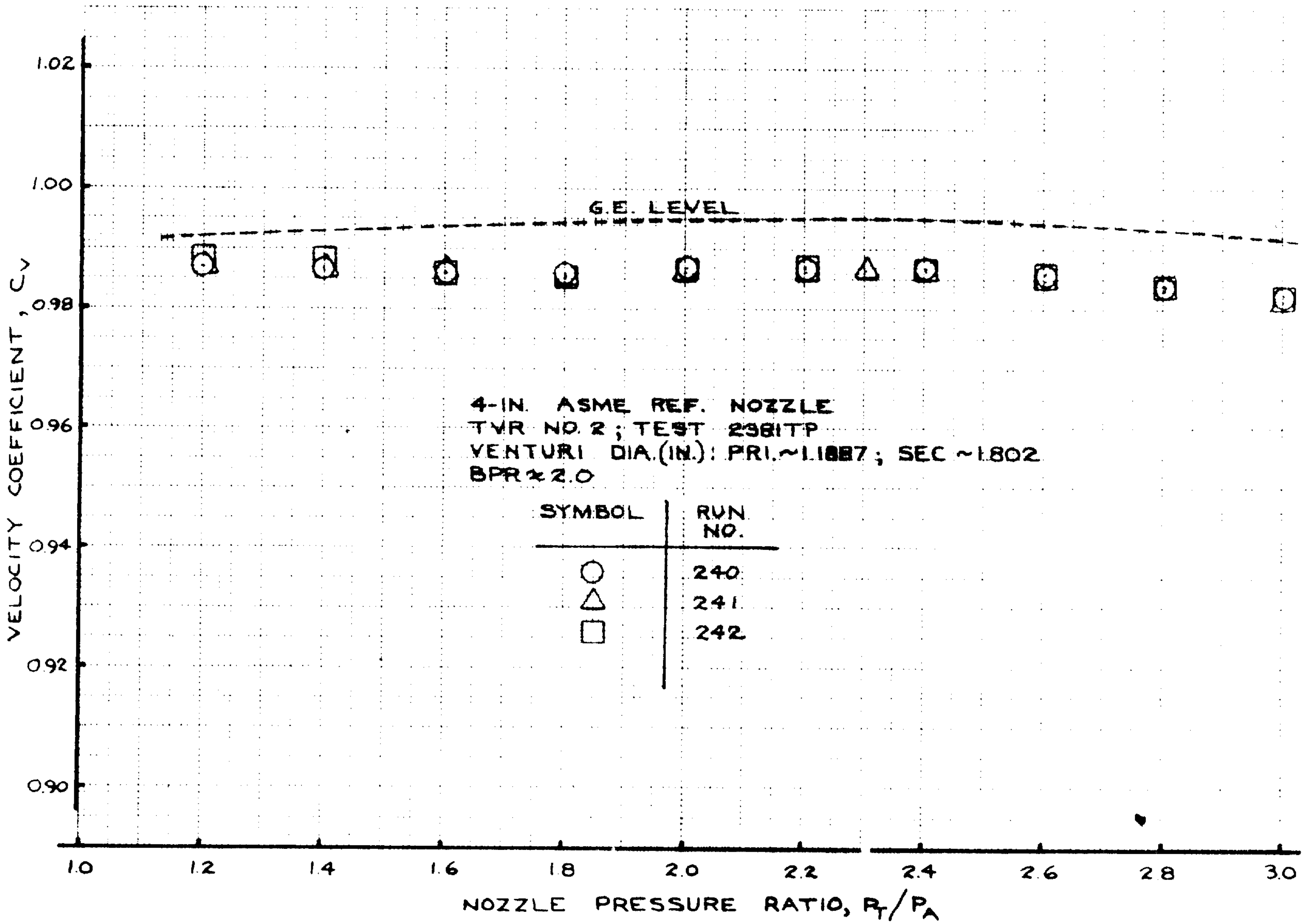

FIGURE 24 - VELOCITY COEFFICIENT; RUNS 240 - 242

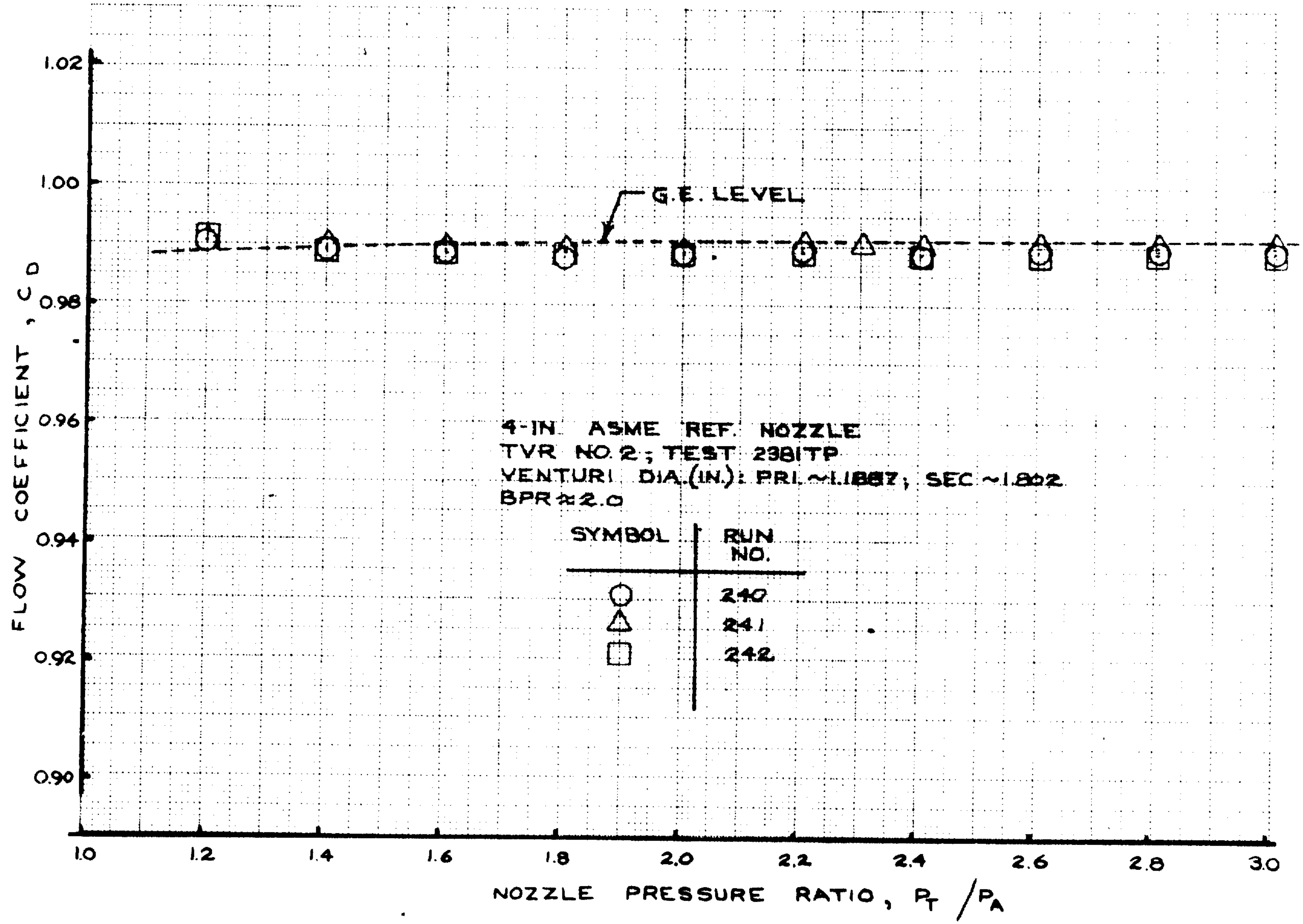

FIGURE 25 - FLOW COEFFICIENT; RUNS 240 - 242

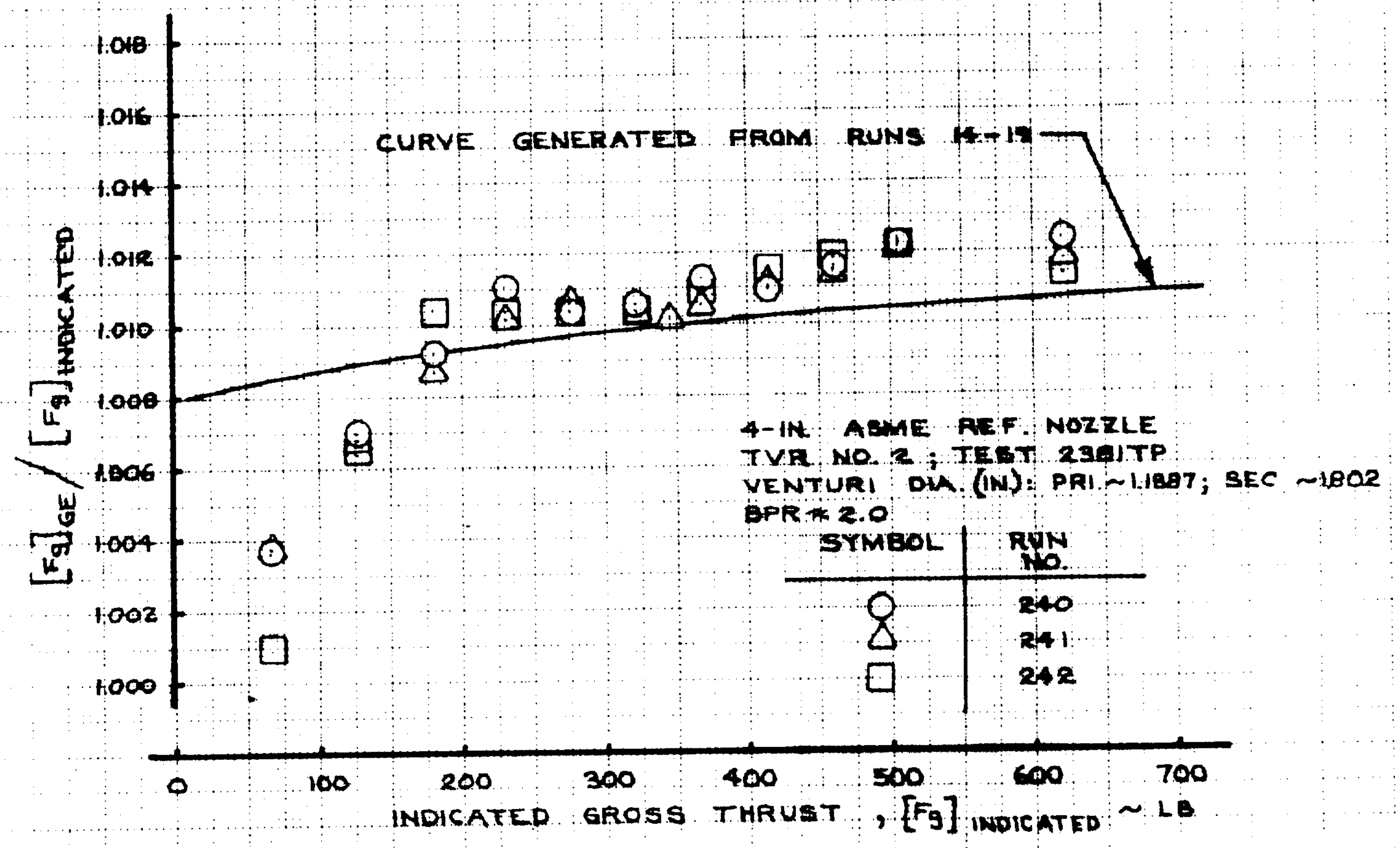

FIGURE 26 - GROSS THRUST CORRECTION; 240 - 242

5.0 TEST RESULTS AND DISCUSSION

5.1 GENERAL

Appendix A shows the equations used for the data reduction of velocity coefficient and flow coefficient. Two methods have been employed for the calculations and the following remarks concern the velocity coefficient. In one method, the ideal thrust in the denominator is the sum of the thrusts obtained by fully expanding the individual gas streams to ambient through separate ideal nozzles. The other method employs the ideal thrust resulting when the streams are fully mixed, conserving mass, momentum and energy, and then fully expanding to ambient through an ideal nozzle. Since the numerator is the same in each case and contains (when run with a hot primary and cold fan) the realized mixing gains, and the denominator in the velocity coefficient equations is different, then it follows that the velocity coefficient calculated one way is not the same as calculated the other way. The velocity coefficient calculated with cold flow in each passage is essentially the same irrespective of the method of calculation. Small differences exist, however, because the pressures in the fan and primary passage are not the same.

For the purposes of comparing absolute levels of performance of various configurations the following must be considered:

- o The hot nozzle Cv can be used to compare absolute levels of performance of the configurations irrespective of the calculation method provided the two methods are not confused.

- o To determine mixing gains the equation uses the velocity coefficients evaluated using the sum of the separately expanded flows. (See Section 5.8)

o Nozzle losses, independent of mixing gains, can be observed by comparing cold nozzle velocity coefficient at the correct fan-to-primary pressure ratio for the engine.

Pratt & Whitney Aircraft provide nozzle velocity coefficient for engine simulator work as a function of the mixed total pressure. Therefore, comparisons herein will be made on that basis. Similarly, comparisons of flow coefficient will be made on a mixed flow pressure ratio basis.

Section 5.8 presents the evaluation of mixing efficiency for selected configurations.

Section 5.9 presents a discussion of the statistical analysis used to determine the validity of differences between the various configurations.

Section 7.0 presents the velocity coefficient, flow coefficient, pressure ratio schedule, bypass ratio and splitter static pressure ratio for each configuration. In some configurations, the relationship between mixed total pressure ratio and primary nozzle pressure ratio is also included. Each configuration tested has a set of graphs in Section 7.2. The subsections are numbered as 7.2.X where the X refers to the Test Configuration (T.C.) number. In the discussion of the comparisons which follow, the sets of data for each configuration are referred to by Test Configuration number rather than the actual figure numbers, otherwise the text becomes encumbered with multi-references.

It became readily apparent from a preliminary analysis of the data that of all the Boeing Config. No. 2 options for the JT8D-109, -115 and -117 engines, those which used a common small plug terminating at the mixing plane (Exhaust station 21, see Figure 19) and altered the splitter position to accomplish the

desired mixing plane match, were the best performing Config. No. 2 nozzles. Extensive statistical analysis, Section 5.9, of these configurations, the P&WA Reference nozzles, and of configurations which varied the plug instead of the splitter were conducted.

5.2 PERFORMANCE COMPARISONS OF P&WA REFERENCE AND BOEING CONFIG. NO. 2 NOZZLES (COMMON PLUG, VARIABLE SPLITTER)

Each Boeing configuration was compared with its equivalent P&WA Reference configuration. In addition, the performance levels for each type of nozzle (Boeing or P&WA Reference) for a particular engine cycle were compared to the performance for the same type of nozzle for different engine cycles and to variants for the same cycle. Figure 27 shows comparisons of the P&WA Reference nozzles and the Boeing Config. No. 2 nozzles which have their respective common plugs and vary the splitter location to suit the individual engine cycle mixing plane area requirements. Also shown is a comparison of these JT8D-100 nozzles to the JT8D-9/727 airplane production nozzle. Levels of velocity coefficient for cold and hot conditions, at 1.6 and 2.4 mixed nozzle pressure ratios, for each configuration are based on the levels read from the data points from Section 7.0. Velocity coefficient levels determined from the statistical analysis, Section 5.9, are also shown. It is apparent from Figure 27 that in some instances there are small differences in performance indicated by reading the mean levels from the data points in Section 7.0 which the statistical analysis shows to be insubstantiable. At other points, the apparent difference is substantiated by the statistical result.

The performance comparisons of these P&WA Reference and Boeing Config. No. 2 nozzles on the various JT8D-100 engines and comparisons of the JT8D-100 configurations to the JT8D-9/727 airplane production configuration are discussed in the following subsections.

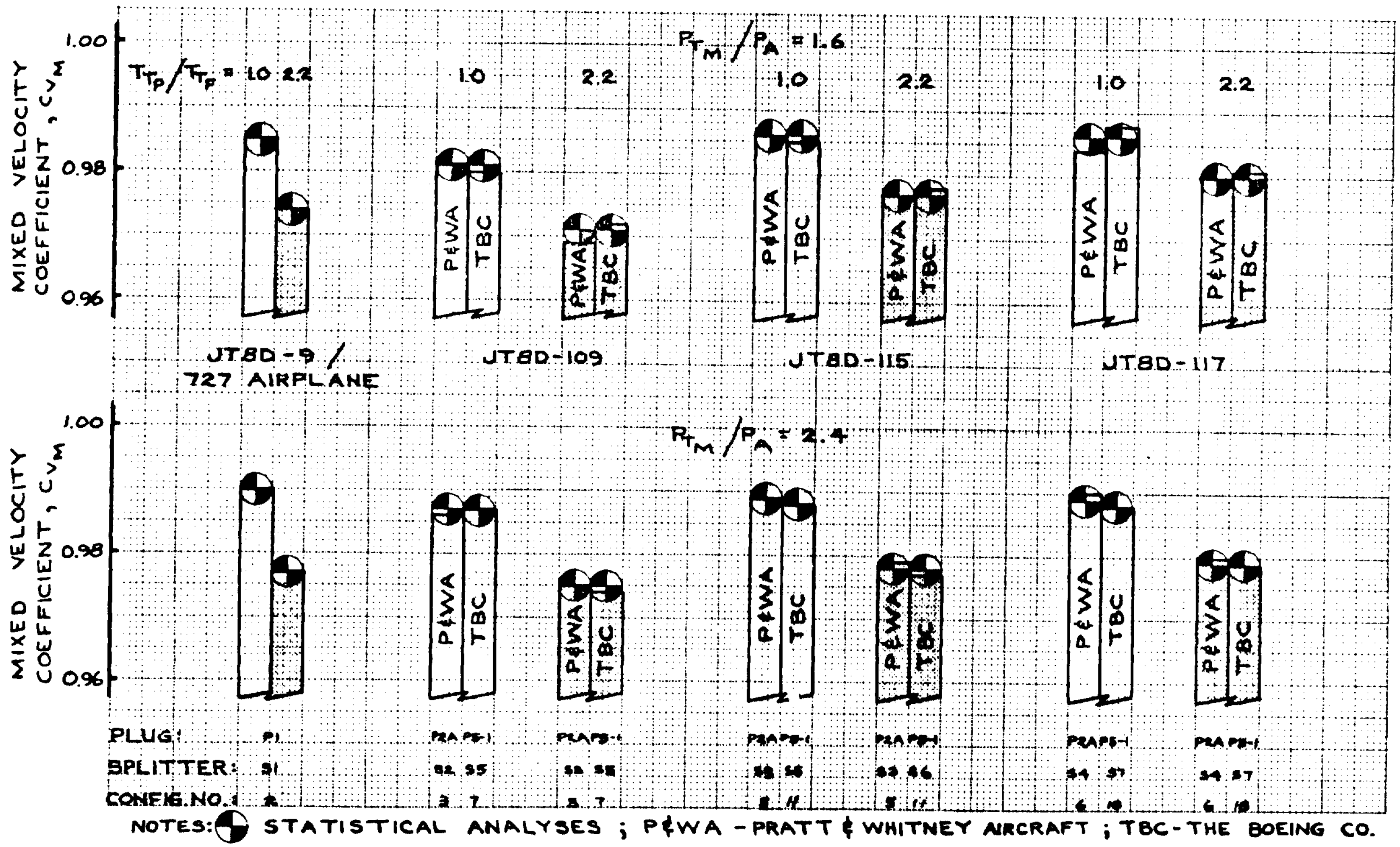

FIGURE 27 - P&WA REFERENCE NOZZLE VERSUS BOEING CONFIG. NO. 2
COMMON PLUG/VARIABLE SPLITTER COMPARISONS

5.2.1 PERFORMANCE COMPARISON OF P&WA REFERENCE (T.C.3) AND BOEING CONFIG. NO. 2 (T.C.7) NOZZLES FOR THE JT8D-109 ENGINE

The data for these two configurations were combined because the statistical analysis determined that they were the same, with 95% confidence, over the 1.6 to 2.5 mixed nozzle pressure range. Figures 28 and 29 show the combined data points and least squares curve fit through the mixed velocity coefficient data for hot (T_{T_P}/T_{T_F} = 2.2) and cold (T_{T_P}/T_{T_F} = 1.0) flow conditions, respectively. The data were obtained simulating the JT8D-109 fan-to-primary total pressure ratio. The cold level of mixed velocity coefficient is the best representation of the thermodynamic efficiency for these two nozzle configurations. Comparisons of these two nozzles with the introduction of primary flow swirl is presented in Section 5.7.2. Flow coefficient comparisons are presented in Section 5.5.

5.2.2 PERFORMANCE COMPARISON OF P&WA REFERENCE (T.C.5) AND BOEING CONFIG. NO. 2 (T.C.11) NOZZLES FOR THE JT8D-115 ENGINE

Examination of the hot nozzle performance levels using the statistical analysis (Section 5.9) shows, with 95% confidence, that the P&WA Reference nozzle is the same as the Boeing Config. No. 2 nozzle for the JT8D-115 engine between mixed pressure ratios of 1.6 and 2.5. Figure 30 shows the combined data and the least squares curve fit for the hot flow (T_{T_P}/T_{T_F} = 2.2) mixed velocity coefficient of these two nozzles.

The statistical analysis shows that the cold flow (T_{T_P}/T_{T_F} = 1.0) mixed velocity coefficients of these two nozzles are different at nozzle pressure ratios of 1.9 to 2.3 but are the same at takeoff and cruise. Furthermore, the statistical analysis shows there are differences between either the Boeing Config. No. 2 or P&WA Reference nozzle for the JT8D-115 engine

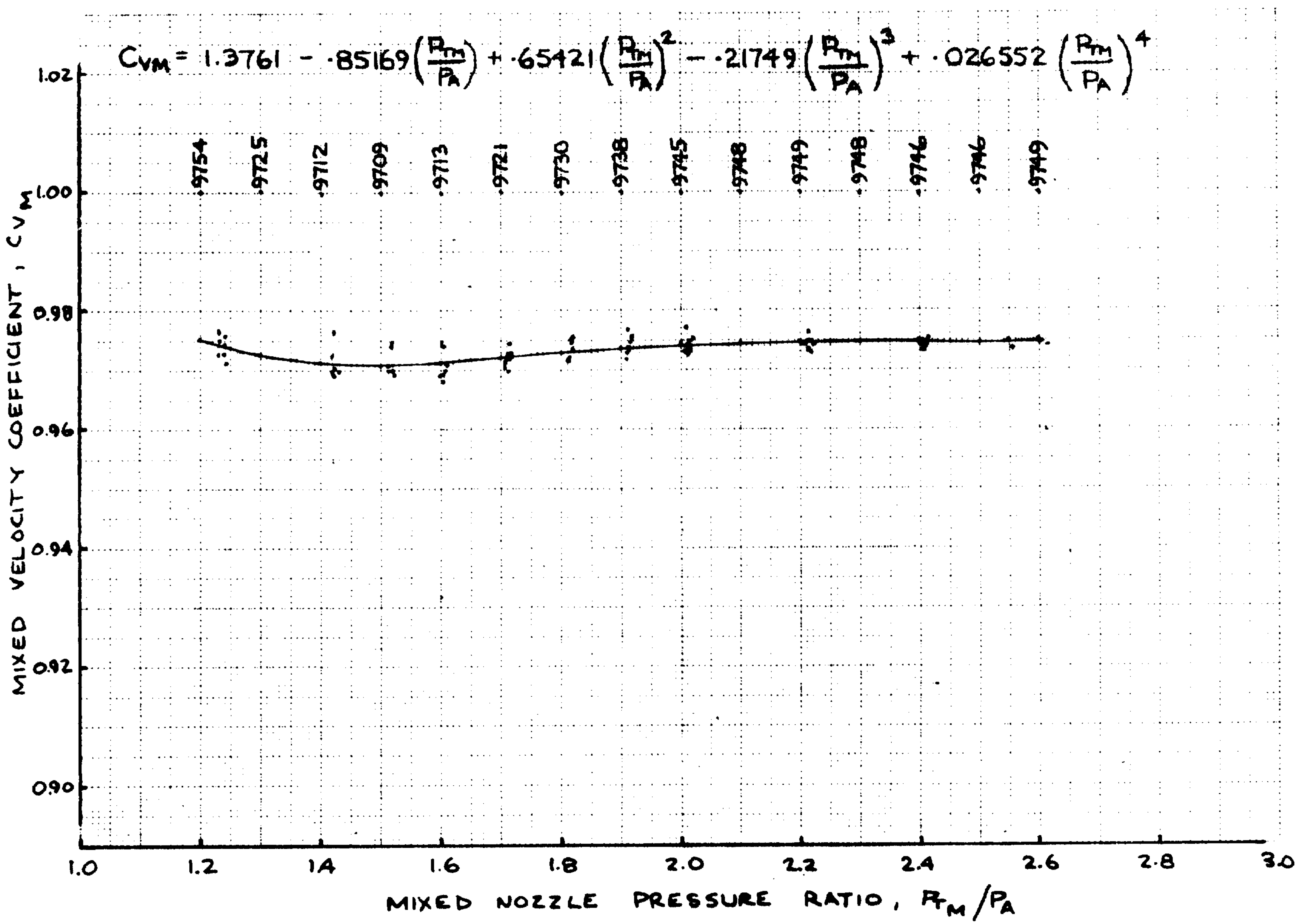

FIGURE 28 - C_{VM} FOR P&WA (T.C.3) AND BOEING CONFIG. NO. 2 (T.C.7) NOZZLES INSTALLED ON JT8D-109 (T_{Tp}/T_{TF} = 2.2)

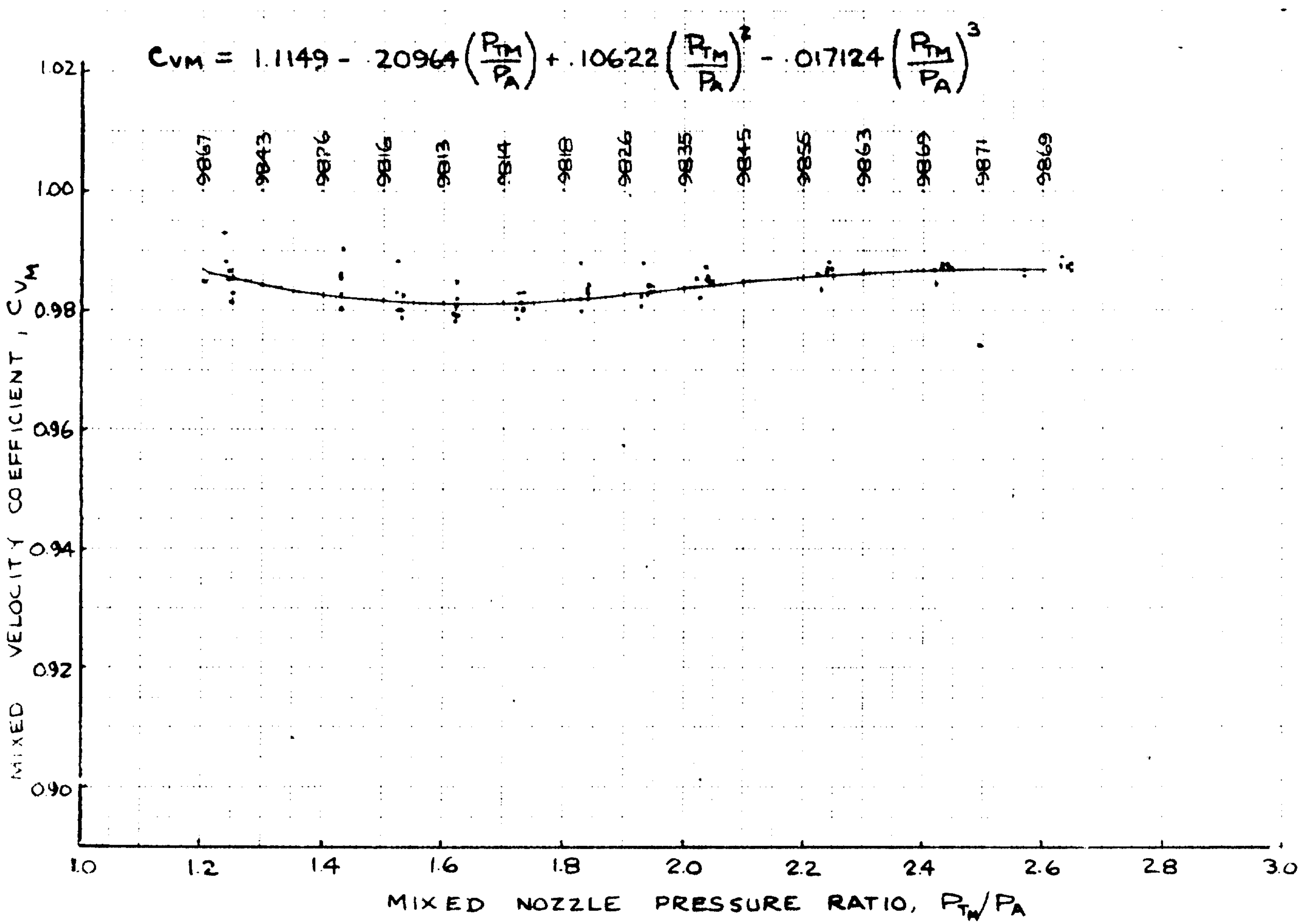

FIGURE 29 - CV_M FOR P&WA (T.C.3) AND BOEING CONFIG. NO. 2 (T.C.7) NOZZLES INSTALLED ON JT8D-109 (T_{T_P}/T_{T_F} = 1.0)

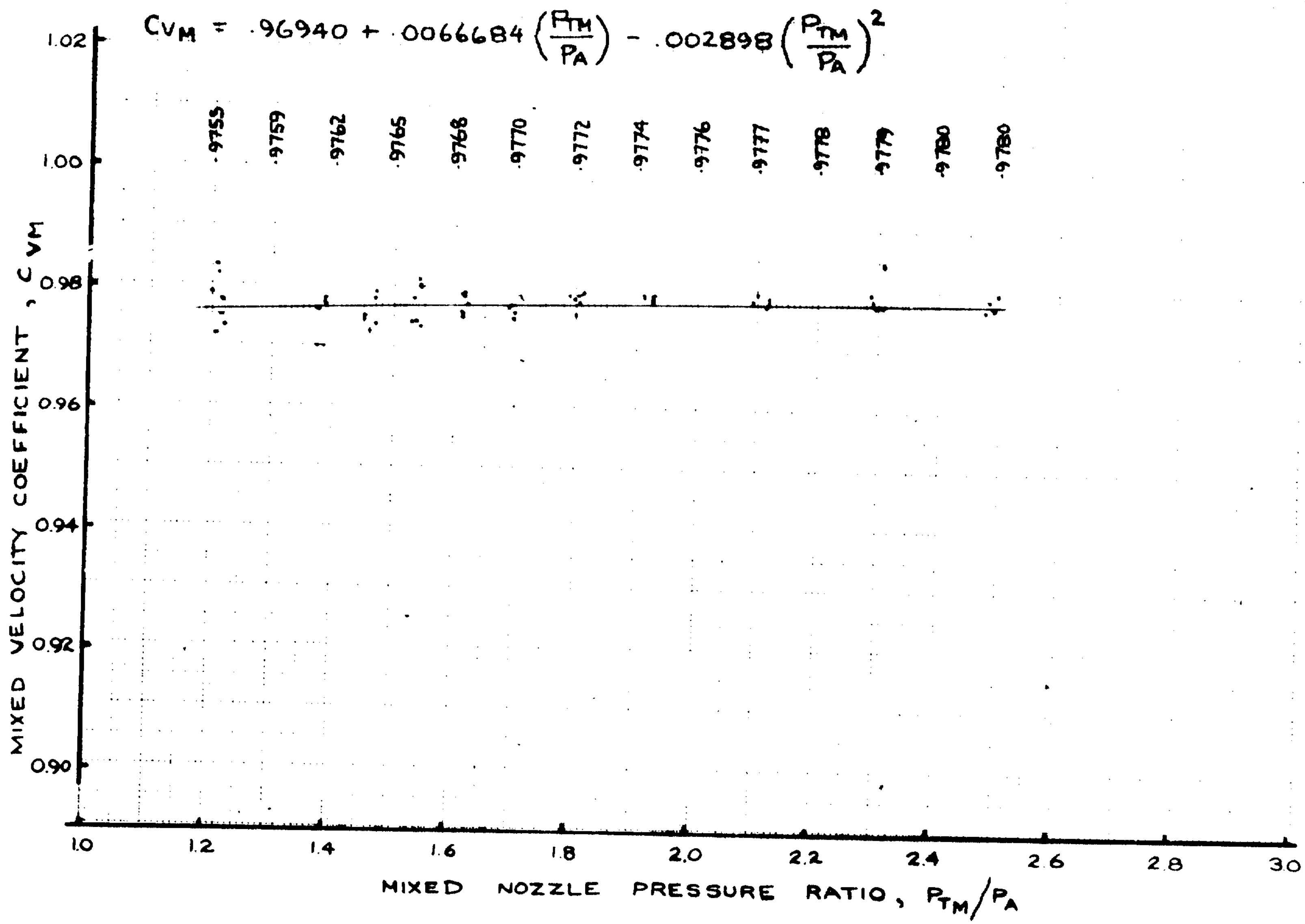

FIGURE 30 - C_{VM} FOR P&WA (T.C.5) AND BOEING CONFIG. NO. 2 (T.C.11) NOZZLES INSTALLED ON JT8D-115 (T_{T_P}/T_{T_F} = 2.2)

and the common level for the Boeing and P&WA nozzles for the JT8D-109 engine. Cold flow performance levels are presented and discussed further in the next sub-section.

5.2.3 PERFORMANCE COMPARISON OF P&WA REFERENCE (T.C.6) AND BOEING CONFIG. NO. 2 (T.C.18) NOZZLES FOR THE JT8D-117 ENGINE

Examination of the hot nozzle performance levels using the statistical analysis (Section 5.9) shows, with 95% confidence, that the P&WA Reference nozzle is the same as the Boeing Config. No. 2 nozzle for the JT8D-117 engine between mixed pressure ratios of 1.6 and 2.5. Figure 31 shows the combined data and least squares curve fit for the hot flow ($T_{T_P}/T_{T_F} = 2.2$) mixed velocity coefficient of these two nozzles.

Statistical analysis was used to determine whether the cold ($T_{T_P}/T_{T_F} = 1.0$) performance levels of the Boeing Config. No. 2 nozzle for the JT8D-115 engine was different than the Boeing design for the JT8D-117 engine. A similar analysis was conducted with the P&WA Reference nozzle data for the JT8D-115 and -117 engines. The physical differences between the JT8D-115 and -117 configurations, for the P&WA or Boeing designs, are smaller than the differences between either the JT8D-109 and the -115 configurations or between the JT8D-109 and the -117 configurations. Moreover, the engine mixing plane area match requirements are such that the primary flow passage changes from a diffusing passage in the JT8D-109, to converging passages in both the P&WA and Boeing JT8D-115 and -117 designs. These flow passage changes are beneficial for the internal aerodynamics. For these reasons it was suspected that the performance differences between the JT8D-115 and -117 configurations would be small. The statistical analysis showed that the cold flow mixed velocity coefficients for the Boeing Config. No. 2 JT8D-115 and -117 nozzles were the same for mixed

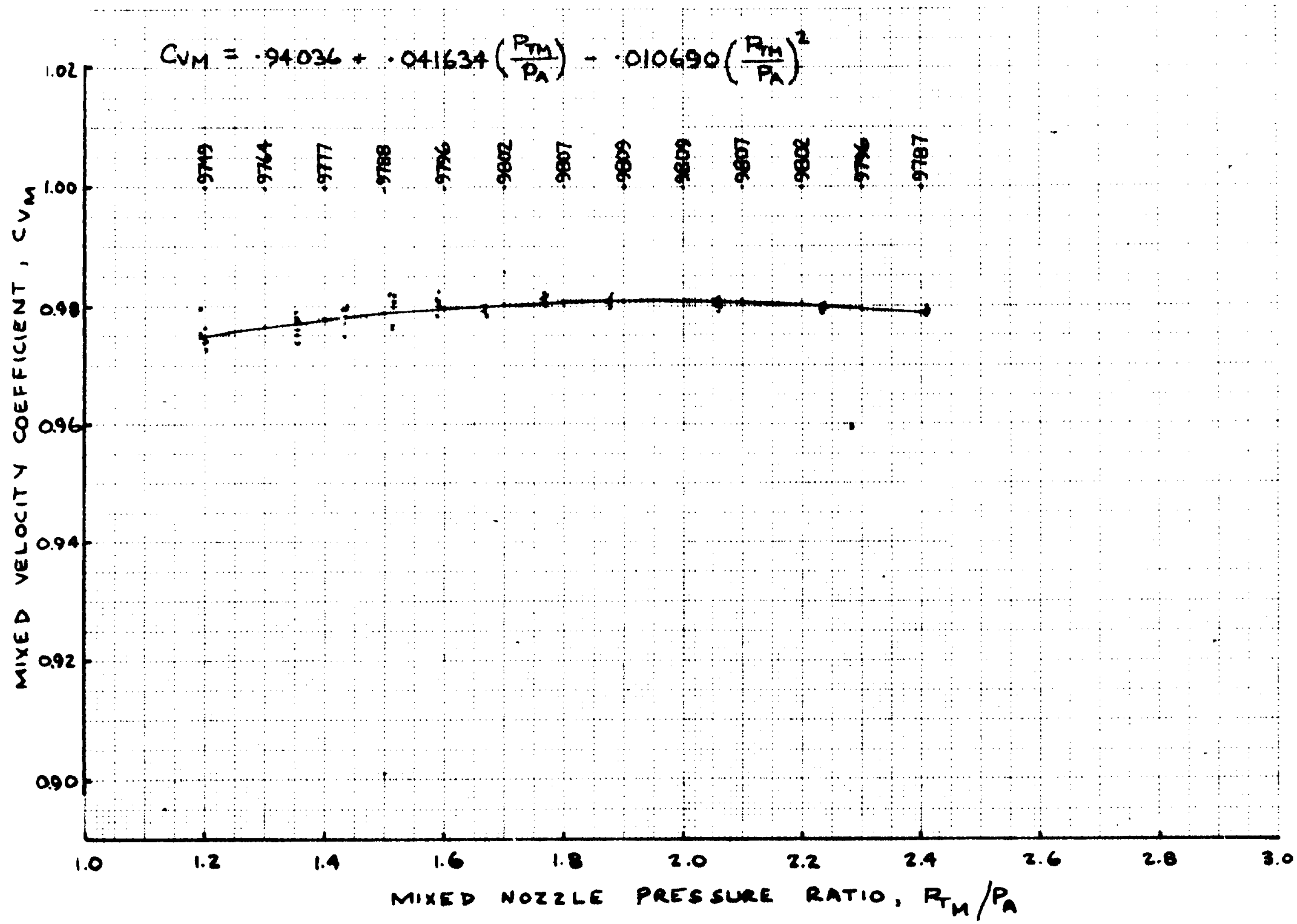

FIGURE 31 - C_{V_M} FOR P&WA (T.C.6) AND BOEING CONFIG. NO. 2 (T.C.18) NOZZLES INSTALLED ON JT8D-117 (T_{T_P}/T_{T_F} = 2.2)

pressure ratios between 1.6 and 2.5. Similarly, the P&WA Reference nozzles for the JT8D-115 and -117 engine were also the same. Figures 32 and 33 show the combined data and least squares curve fit for the cold flow ($T_{T_P}/T_{T_F} = 1.0$) mixed velocity coefficients of the Boeing Config. No. 2 and P&WA Reference nozzles, respectively, for the JT8D-115/-117 engines.

A comparison of the cold performance levels of the nozzles for the JT8D-109 engine (Figure 29) with those for the JT8D-115/-117 engines (Figures 32 and 33) reveal differences in internal losses for the three nozzle families. A similar comparison of the hot performance levels (Figure 28, 30, and 31) reflect the achieved thrust gains due to mixing as well as the internal losses. Since the theoretical mixing gains and the mixing efficiencies are different for nozzles installed on the JT8D-109, -115, and -117 engines, the differences between the cold performance levels should not necessarily be the same as the differences between the hot performance levels. The theoretical mixing gains and mixing efficiencies for these nozzles are discussed in Section 5.8.

5.2.4 PERFORMANCE COMPARISONS OF JT8D-109, -115, -117 NOZZLES (T.C. 3 & 7; 5 & 11; 6 & 18 RESPECTIVELY) WITH THE JT8D-9/727 BOEING PRODUCTION NOZZLE (T.C.2)

It is important, when making comparisons between these configurations, to appreciate that the Boeing nozzle configurations for the JT8D-100 series engines are designed (though not explicitly) for a target type thrust reverser installation. The nozzles are, therefore, representative of the smooth continuous wall construction inherent in such designs. The Boeing production JT8D-9/727 model nozzle built for this test was smooth wall and not fully representative of the configuration presently on the 727 airplane which has an internal clam-shell door type thrust reverser. To compare the JT8D-100

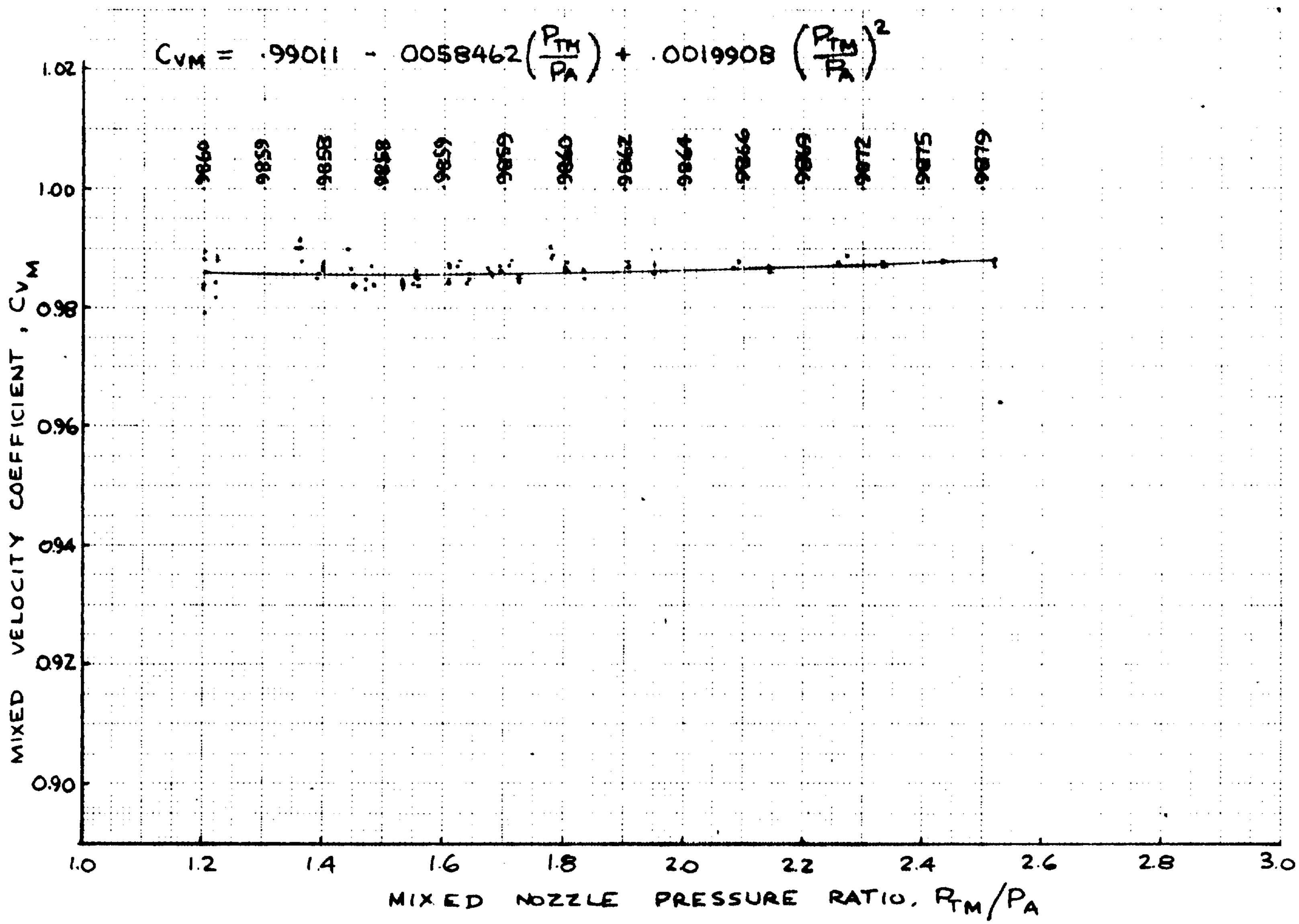

FIGURE 32 - C_{V_M} FOR BOEING CONFIG. NO. 2 (T.C.11 & 18) NOZZLES INSTALLED ON JT8D-115 & -117 (T_{T_P}/T_{T_F} = 1.0)

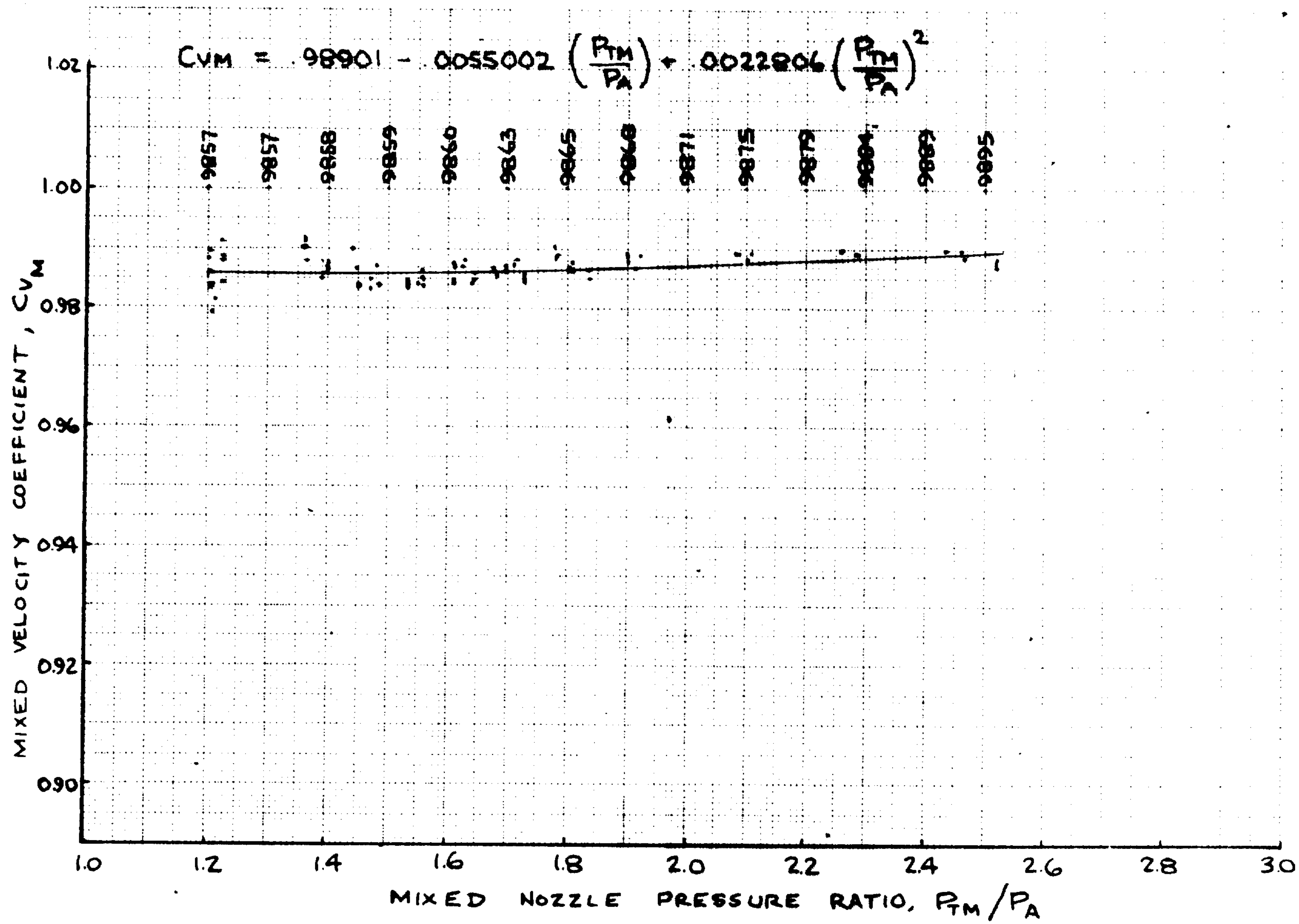

FIGURE 33 - C_{V_M} FOR P&WA (T.C.5 & 6) REFERENCE NOZZLES INSTALLED ON JT8D-115 & -117 (T_{T_P}/T_{T_F} = 1.0)

configurations with the current 727 installation, the 727 thrust reverser installation losses should be deducted from the measured JT8D-9/727 nozzle performance levels obtained during this test program. However, the performance of the JT8D-9/727 model nozzle should be representative of the P&WA JT8D-9 Reference nozzle level.

It is interesting to compare the JT8D-100 P&WA Reference and Boeing Config. No. 2 nozzle performance with this pseudo JT8D-9 standard. These comparisons have been made at 1.6 and 2.4 mixed nozzle pressure ratios which are near the takeoff and cruise pressure ratios for the JT8D-100 engines. It is proper to compare exhaust system performance at the same pressure ratios rather than at the respective takeoff and cruise pressure ratios for the respective engine cycles. The latter differences are accounted for in the total engine and airplane performance comparisons which are not the subjects for discussion in this report.

The hot flow (T_{T_P}/T_{T_F} = 2.2) JT8D-9/727 nozzle performance levels, Figure 34, are about 0.3% and 0.2% higher than the JT8D-109 P&WA Reference and Boeing Config. No. 2 nozzles at the 1.6 and 2.4 mixed pressure ratios, respectively. The JT8D-9/727 nozzle performance levels are lower than the P&WA and Boeing nozzles for the JT8D-115 and -117 engines, by 0.3% and 0.6%, respectively, at the 1.6 mixed pressure ratio and lower by 0.1% and 0.2%, respectively, at the 2.4 mixed pressure ratio.

Figure 35 shows the cold flow (T_{T_P}/T_{T_F} = 1.0) performance levels for the JT8D-9/727 nozzle to be about 0.4% and 0.3% higher than the JT8D-109 P&WA and Boeing nozzles at the 1.6 and 2.4 mixed pressure ratios, respectively. The JT8D-9/727 nozzle performance levels, at the same mixed pressure ratios, are 0.1% higher and 0.1% lower, respectively, than the nozzles for either the JT8D-115 or JT8D-117 engines.

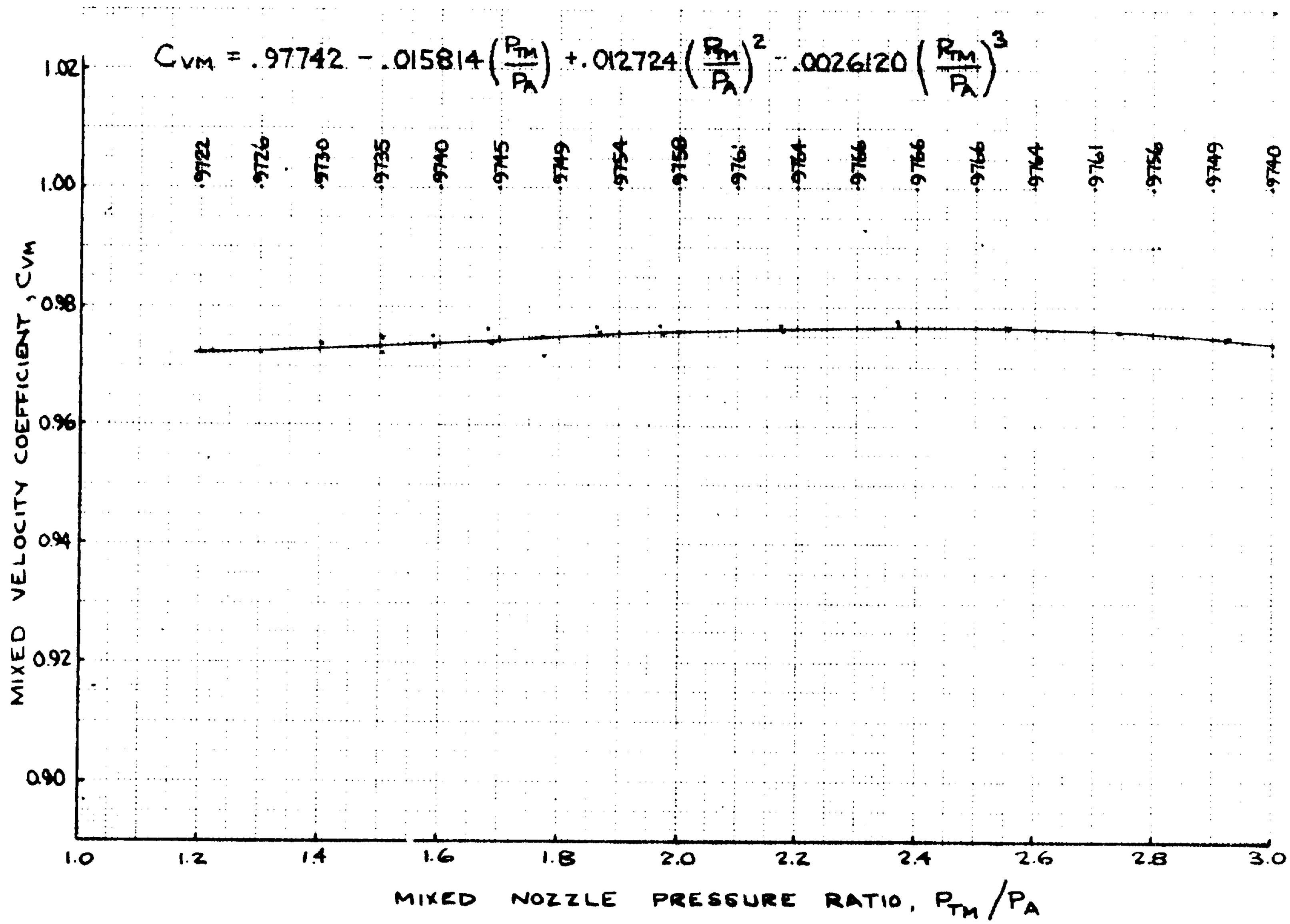

FIGURE 34 - C_{VM} FOR JT8D-9/727 AIRPLANE PRODUCTION NOZZLE (T.C.2)
AT T_{TP}/T_{TF} = 2.2

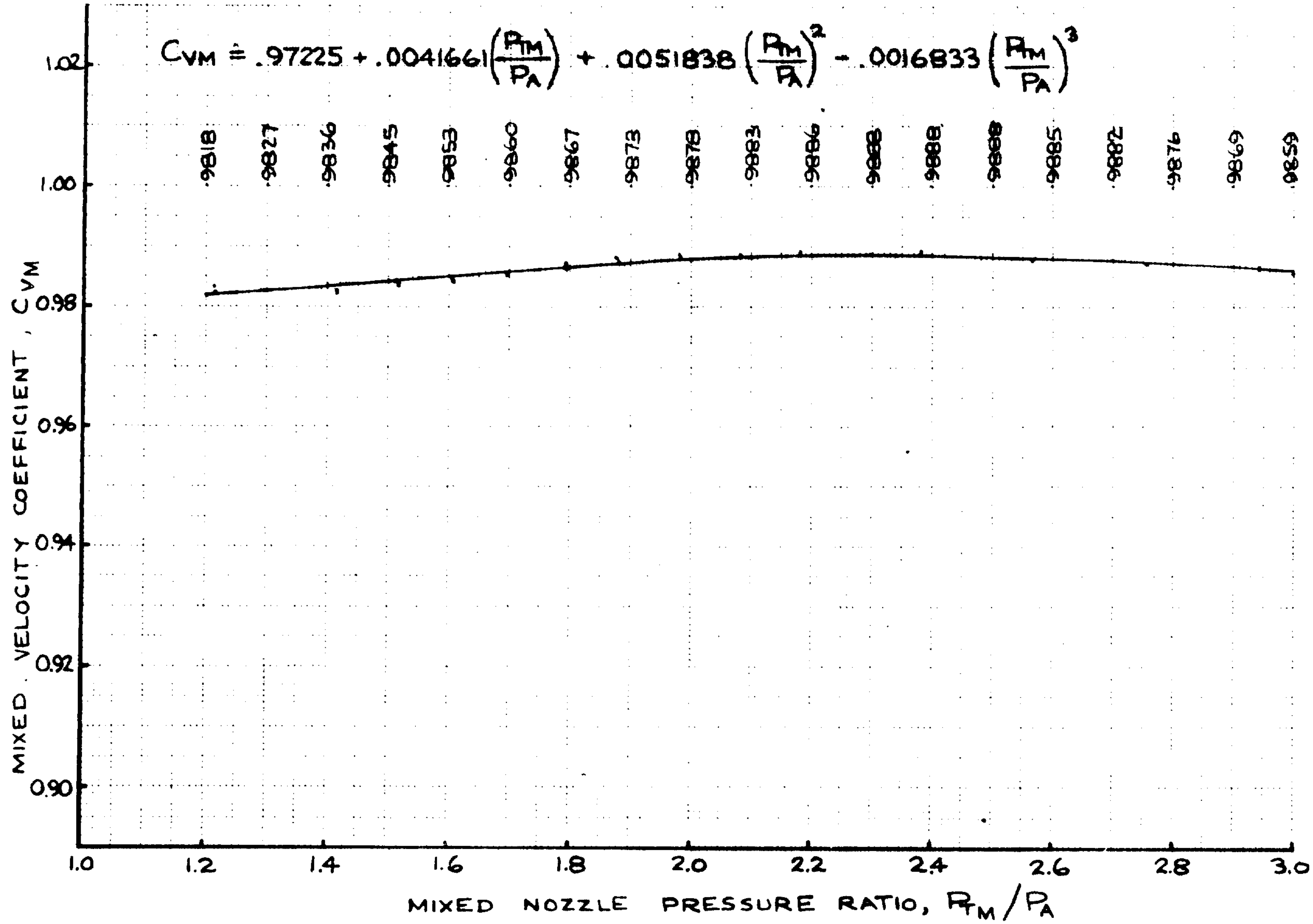

FIGURE 35 - C_{VM} FOR JT8D-9/727 AIRPLANE PRODUCTION NOZZLE (T.C.2) AT $T_{TP}/T_{TF} = 1.0$

5.3 PERFORMANCE COMPARISONS OF PLUG/SPLITTER VARIANTS FOR BOEING CONFIG. NO. 2 NOZZLE OPTIONS

The JT8D-115 and -117 engines require different fan and primary mixing plane areas than that required by the JT8D-109 engine for a given nozzle outer wall diameter. As the engine rating increases, the required mixing plane area ratio, A_F/A_P, increases. This can be accomplished by moving the splitter and using a common plug or varying the plug while maintaining a constant splitter position. Test configuration (T.C.8) is a plug variant option of T.C.11 using the JT8D-109 splitter (S5) for JT8D-115 engine application. A truncated plug variant (T.C.9) of T.C.11 was also tested for the JT8D-115 engine application. The plug variant option of T.C.18 using the JT8D-109 splitter (S5) for JT8D-117 engine application is T.C.15. A shortened plug version (T.C.16) of T.C.15 was also tested for the JT8D-117. In addition T.C.17 is a plug variant option of T.C.18 for the JT8D-117 engine application using the JT8D-115 splitter (S6).

Figure 36 shows the hot flow ($T_{T_P}/T_{T_F} = 2.2$) and cold flow ($T_{T_P}/T_{T_F} = 1.0$) performance results for the above mentioned configurations at mixed nozzle pressure ratios of 1.6 and 2.4. These comparisons show, in general, that enlarging the plus is less desirable than moving the splitter inward to obtain the required mixing plane flow areas. In addition to having a lower performance level, the larger plugs will have a weight penalty which is detrimental to the airplane performance.

The truncated plug configuration (T.C.9) was tested to determine the performance effects associated with an internally accessed attachment scheme. Any performance effects associated with the diffusion and/or separation designed into this scheme were outside the capabilities of the test rig to detect them.

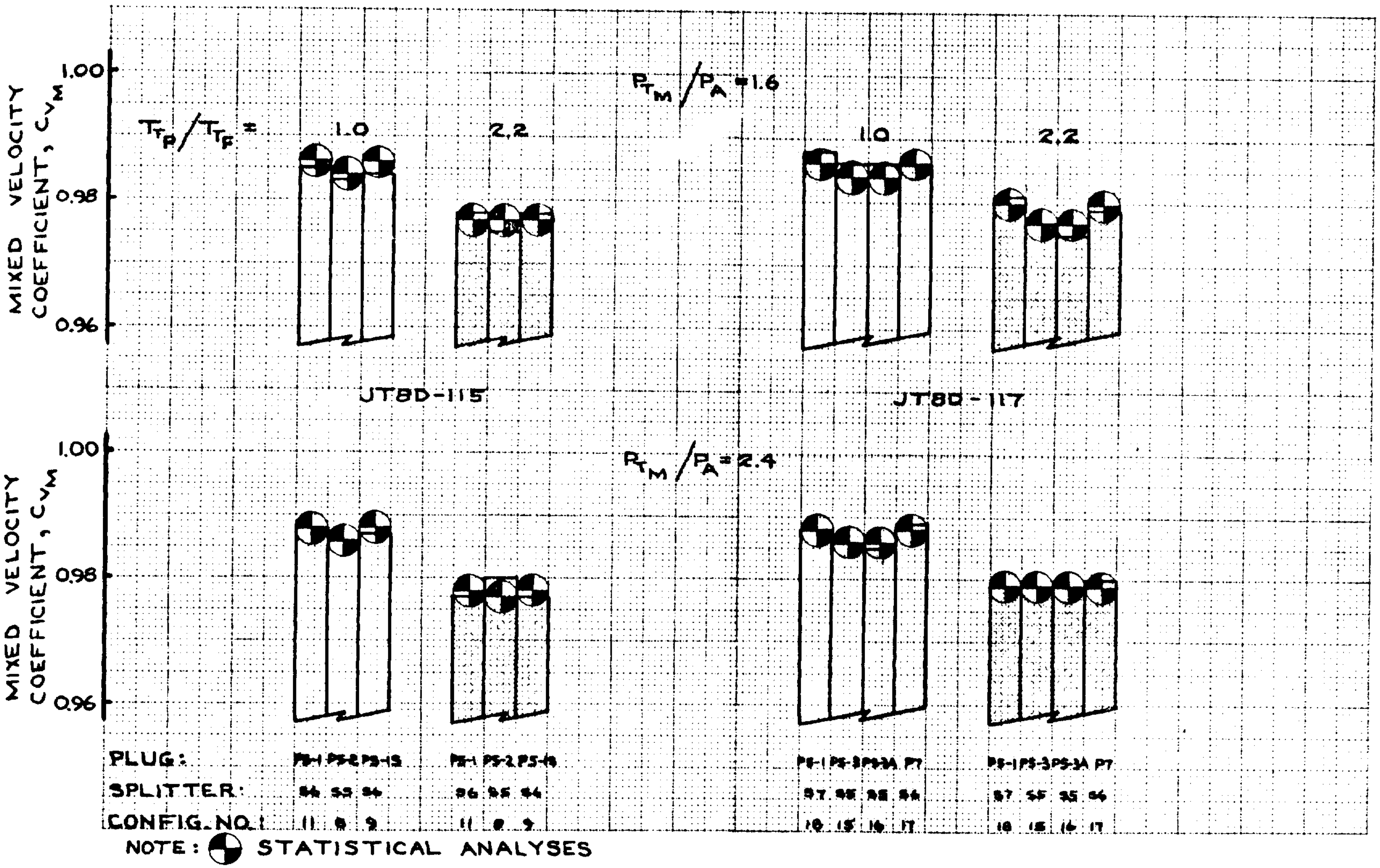

FIGURE 36 - BOEING CONFIG. NO. 2 PLUG/SPLITTER COMPARISONS

Using the JT8D-109 splitter (S5) for JT8D-117 engine application requires a very long and heavy plug configuration (T.C.15). The shortened plug version of this configuration (T.C.16) introduced a small amount of duct diffusion. There was not detectable difference in performance over the 1.6 to 2.4 mixed pressure ratio range for these two configurations.

5.3.1 INVESTIGATION OF PLUG VARIANTS TO SUIT BOEING CONFIG. NO. 2 DESIGNS FOR THE JT8D-115 AND -117 ENGINES USING THE JT8D-109 SPLITTER (T.C.8 AND T.C.15)

Statistical comparisons were made between T.C.8 and T.C.11 between T.C.15 and T.C.18, and between T.C.8 and T.C.15. The first two pairs of comparisons showed performance differences existed at some pressure ratios but no differences at others. The third pair of comparisons showed that T.C.8 and T.C.15 had the same performance at all mixed pressure ratios with either the hot flow (T_{T_P}/T_{T_F} = 2.2) or cold flow (T_{T_P}/T_{T_F} = 1.0). The combined data for T.C.8 and T.C.15, Figure 37, was then tested against the combined data of T.C.5 and T.C.11, Figure 30, and against the combined data of T.C.6 and T.C.18, Figure 31, for the hot flow conditions. The first of these combined configuration comparisons showed that the performance of these nozzles (T.C.8 and T.C.15; T.C.5 and T.C.11) were indistinguishable. The second combined comparison showed the performance of T.C.8 and T.C.15 to be equal to the combined data of configurations T.C.6 and T.C.18 at pressure ratios of 1.9 and above but a deficiency of nearly 0.5% at the 1.6 pressure ratio. Differences between the cold flow performance levels are apparent at all pressure ratios above 1.6, Figure 38 compared to Figures 32 and 33.

The statistical analysis shows for mixed pressure ratios above 1.8 that the hot flow performance levels for T.C.8 and T.C.15, T.C.5 and T.C.11, as well as T.C.6 and T.C.18 are the same. However, the cold flow performance levels for T.C.8 and T.C.15 are different and lower than those for T.C.5 and T.C.11 or

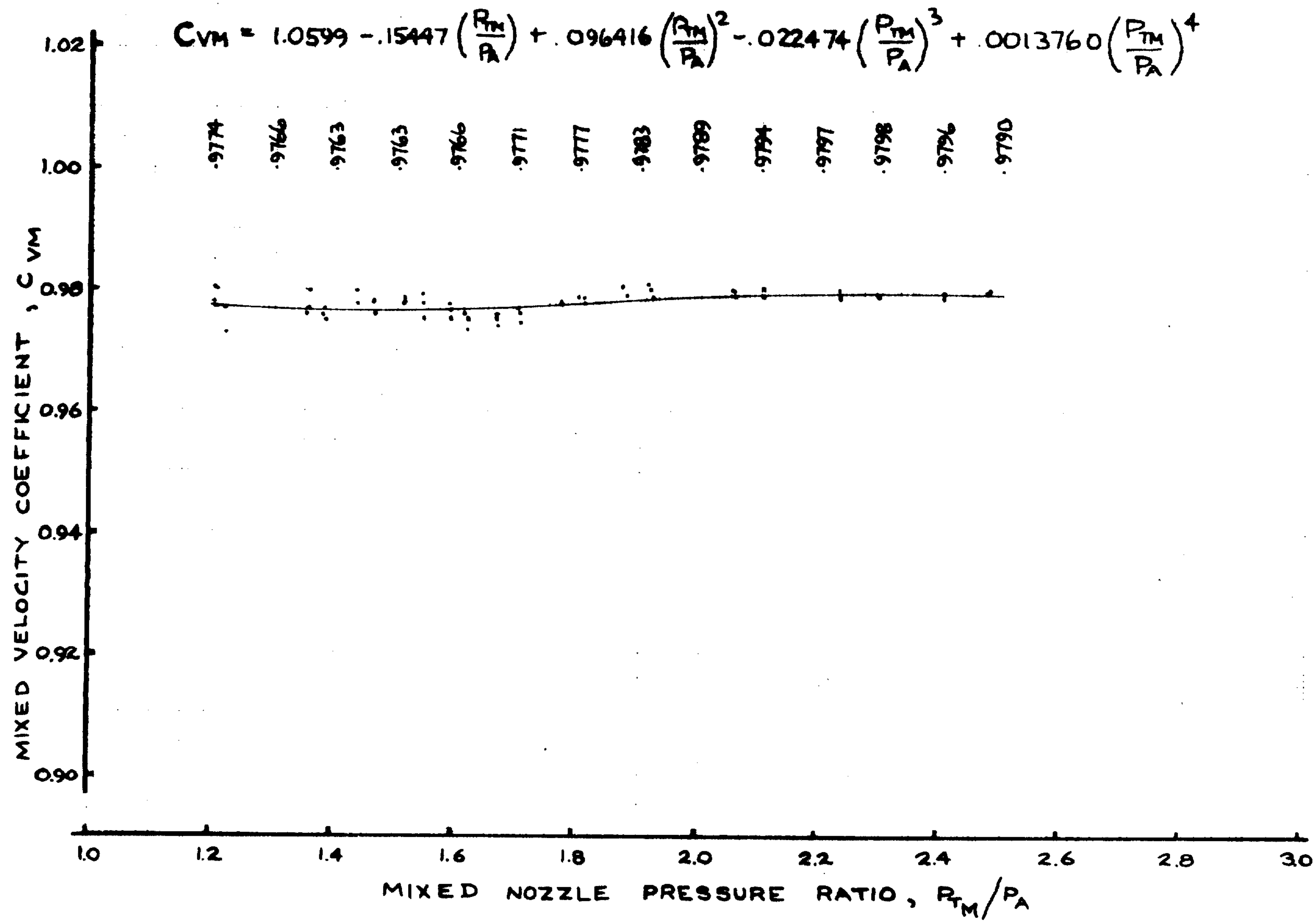

FIGURE 37 - C_{VM} FOR PLUG VARIANT BOEING CONFIG. NO. 2 NOZZLES WITH JT8D-109 SPLITTER ON JT8D-115 (T.C.8) AND JT8D-117 (T.C.15) AT T_{TP}/T_{TF} = 2.2

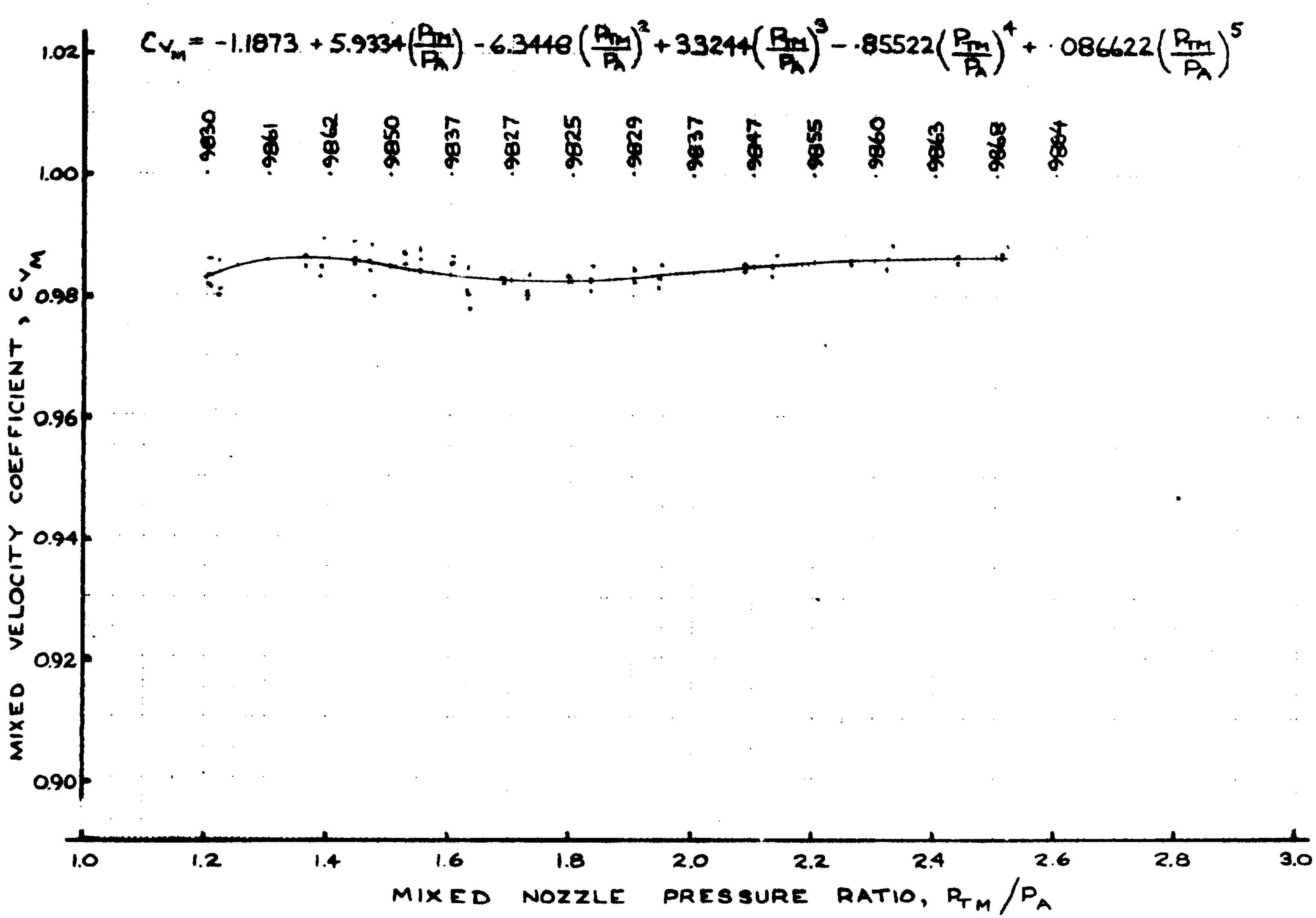

FIGURE 38 - C_{V_M} FOR PLUG VARIANT BOEING CONFIG. NO. 2 NOZZLES WITH JT8D-109 SPLITTER ON JT8D-115 (T.C.8) AND JT8D-117 (T.C.15) AT T_{T_P}/T_{T_F} = 1.0

T.C.6 and T.C.18, which are the same. This means the mixing efficiency for T.C.8 and T.C.15 must be greater in order to result in the same hot flow performance levels; i.e. the higher internal losses are somehow neutralized by better mixing efficiency.

5.3.2 INVESTIGATION OF PLUG VARIANTS TO SUIT BOEING CONFIG. NO. 2 DESIGNS FOR JT8D-117 ENGINES USING THE JT8D-115 SPLITTER (T.C.17)

There are no performance differences detectable by statistical analysis of the data for either the hot or cold flow conditions between the larger plug tailored for JT8D-117 application using the JT8D-115 splitter (T.C.17) and the short plug JT8D-117 configuration (T.C.18), as shown by Figure 36, over the engine operation range of pressure ratios from 1.6 to 2.4.

It is interesting to compare the performance of configuration T.C.17 which uses the JT8D-115 splitter and configuration T.C.15 which uses the JT8D-109 splitter for JT8D-117 engine application (see Sections 7.2.15 and 7.2.17 for mixed velocity coefficient data). The hot flow (T_{T_P}/T_{T_F} = 2.2) performance data shows the nozzles to be equal except between 1.6 and 1.8 mixed nozzle pressure ratios. But in this instance, it is again apparent from the cold flow (T_{T_P}/T_{T_F} = 1.0) data that the internal nozzle losses for the plug tailored to the JT8D-109 splitter (T.C.15) is greater (i.e., lower C_{V_m} levels) than for the plug tailored for the JT8D-115 splitter (T.C.17). The only way the hot flow performance can be equal outside the noted pressure ratio range, while the internal losses are different is that the mixing efficiency must have been better for T.C.15 configuration than for T.C.17.

From these results, one must tentatively conclude for the configurations tested. the smaller the annulus height at the

mixing plane for a given cross-sectional area, the better the mixing of the two flow streams for a given tailpipe length. Opposing this effect is the increase of the internal nozzle losses due to the larger plug. Care must be taken not to assume that this is a generalized theorem, concerning annulus height and mixing, as it certainly depends on the geometry and flow characteristics of the engine to which the mixer nozzle is being applied.

5.4 EFFECTS OF FAN/PRIMARY PRESSURE RATIO ON MEASURED NOZZLE PERFORMANCE

It became increasingly obvious as the test was being conducted that the fan/primary pressure ratio schedules chosen as described in Section 4.5.1 and shown on Figure 20 had an appreciable influence on the shape of the velocity and the flow coefficient curves. Furthermore, the influence appeared to increase with the size of the plug or the decrease in the mixing plane area.

It was decided that the influence of the pressure ratio schedule on curve shape should be investigated. For this reason, a linear approximation of the pressure ratio schedule and a pressure ratio of one (equal fan and primary total pressures) were run for Boeing Config. No. 2 nozzles T.C.11 and T.C.18 for JT8D-115 and -117 engine applications, respectively.

The above changes in the fan/primary pressure ratio schedule reduced the inflection in the velocity coefficient data but the change was less dramatic for the hot flow than the cold flow data (see Section 7.2.11 and 7.2.18 for the mixed velocity coefficient data). It can be stated for these test results, being careful not to generalize, that the effect of fan/primary pressure ratio on the hot flow performance is negligible and that the levels are identical within statistical probability. However, the cold flow velocity coefficient (i.e., the internal nozzle loss) is dramatically influenced by the fan/primary pressure ratio. With these splitter/nozzle geometries, the internal nozzle losses become less as the pressure ratio schedules (Figure 20) for the JT8D-115 and JT8D-117 engines are first linearized and then set to a slope of one. This is probably explained by the changes which occur in the local duct Mach numbers for the fan and primary as the pressure ratio schedule changes. The increase in fan duct Mach number and

decrease in primary duct Mach number as the pressure split was made equal seems contrary to what would be expected for reduced nozzle losses. Even though the fan/primary pressure ratio does have an influence on the nozzle losses, this influence must somehow be compensated for by changes in mixing gains, otherwise the hot flow performance data could not show equality.

The observations are interesting, but there is no justification to use the cold Cv at a pressure ratio of one as a measure of the nozzle losses because the nozzles do not operate under these conditions.

5.5 NOZZLE FLOW COEFFICIENTS

Comparisons of the nozzle flow coefficients are made in this document based on the hot flow runs and the 100% mixed flow pressure and temperature conditions. Appendix A.2 shows the equation used to calculate these flow coefficients which are compatible with the presented hot flow mixed velocity coefficients based on 100% mixed flow conditions. This method is used herein because P&WA provide nozzle coefficients for the engine simulator work based on the 100% mixed conditions, using the same Cv_M and C_{D_M} curves for the JT8D-9, -109, -115 and -117 engines.

Two aspects of the flow coefficient are worthy of discussion:

- o Comparison of the JT8D-100 nozzles with the Boeing JT8D-9/727 production nozzle.
- o Comparison of the Boeing Config. No. 2 nozzles with the P&WA Reference nozzles for the JT8D-100 engines.

It is pertinent, at this point, to mention that the Boeing configurations maintain a constant nozzle exit half-angle between the JT8D-109, -115, and -117 engines (see Figure 3). For the P&WA configurations, the nozzle half-angle changes slightly from configuration to configuration (see Figure 2). These nozzles were designed with approximately 10^{o} half-angle convergence in an effort to reduce the flow coefficient at the engine idle nozzle pressure ratio, with as little detriment as possible at takeoff and cruise.

A comparison of the P&WA and Boeing JT8D-109 configurations (T.C.3 and T.C.7) shows that the flow coefficients are identical, Figure 39. Compared to the JT8D-9/727 production nozzle, the JT8D-109 configuration flow coefficients are about 2% lower at 1.6 pressure ratio and 1% lower at 2.4 pressure ratio. A

reduction of nearly 4% was accomplished by the 10^0 half-angle in the region of idle pressure ratio.

Comparison of the flow coefficient data of the Boeing Config. No. 2 nozzle with the P&WA Reference nozzle for JT8D-115 engine application shows that these nozzles are not choked until the mixed nozzle pressure ratio is above 2.1 (Figure 40). The flow coefficients for both nozzles are identical above choke and about 1% higher than those for the JT8D-109 engine shown on Figure 39. At a 1.6 pressure ratio, the Boeing Config. No. 2 nozzle flow coefficient is approximately 0.8% higher than the P&WA Reference nozzle, Figure 40, and 1.4% higher than the JT8D-109 nozzle levels, Figure 39. These data indicate that the geometric nozzle areas specified for the various engines by P&WA may have to be changed in relation to one another by about 1% one way or the other for the JT8D-109 and JT8D-115 Reference nozzles.

A very similar situation exists with the P&WA Reference and Boeing Config. No. 2 nozzles (T.C.6 and T.C.18, respectively) for JT8D-117 engine application. In this instance, the flow coefficients above choke are the same and 0.5% higher than the JT8D-115 configurations and 1.5% higher than the JT8D-109 configurations (comparing Figure 41 with Figures 40 and 39, respectively). The Boeing configuration is again 0.8% higher than the P&WA Reference nozzle at 1.6 pressure ratio (Figure 41). Flow coefficients for the P&WA Reference and Boeing Config. No. 2 nozzles for the JT8D-117 engine are about 0.5% higher than the corresponding P&WA and Boeing configurations for JT8D-115 engine application.

It is interesting to compare the flow coefficients of various Boeing Config. No. 2 splitter/plug options for JT8D-115 and -117 engine applications using either the JT8D-109 or -115 splitter for the short plug design. The data indicates that the

configuration using the JT8D-109 splitter (T.C.8) for JT8D-115 engine application matches the flow coefficient of the P&WA JT8D-115 Reference nozzle (T.C.5) at low mixed pressure ratios and is 0.4% lower at choked pressure ratios. When the JT8D-109 splitter is used for the JT8D-117 engine application (T.C.15), its flow coefficient matches that for the P&WA JT8D-117 Reference nozzle (T.C.6) at all mixed pressure ratios. The flow coefficient for the configuration using the JT8D-115 splitter for JT8D-117 application (T.C.17) matches that of the Boeing Config. No. 2 JT8D-117 short plug/splitter design (T.C.18) which is about 0.8% higher than and matched to the P&WA JT8D-117 Reference nozzle flow coefficient at the 1.6 and 2.4 pressure ratios, respectively.

The important result from these comparisons is that the discharge coefficient curve shape for the Boeing Config. 2 nozzles and the P&WA Reference nozzles for the respective engines are very similar. It follows that no major problem is envisaged in satisfying the engine match requirements with either Boeing Config. No. 2 or P&WA Reference nozzles on the full scale engines.

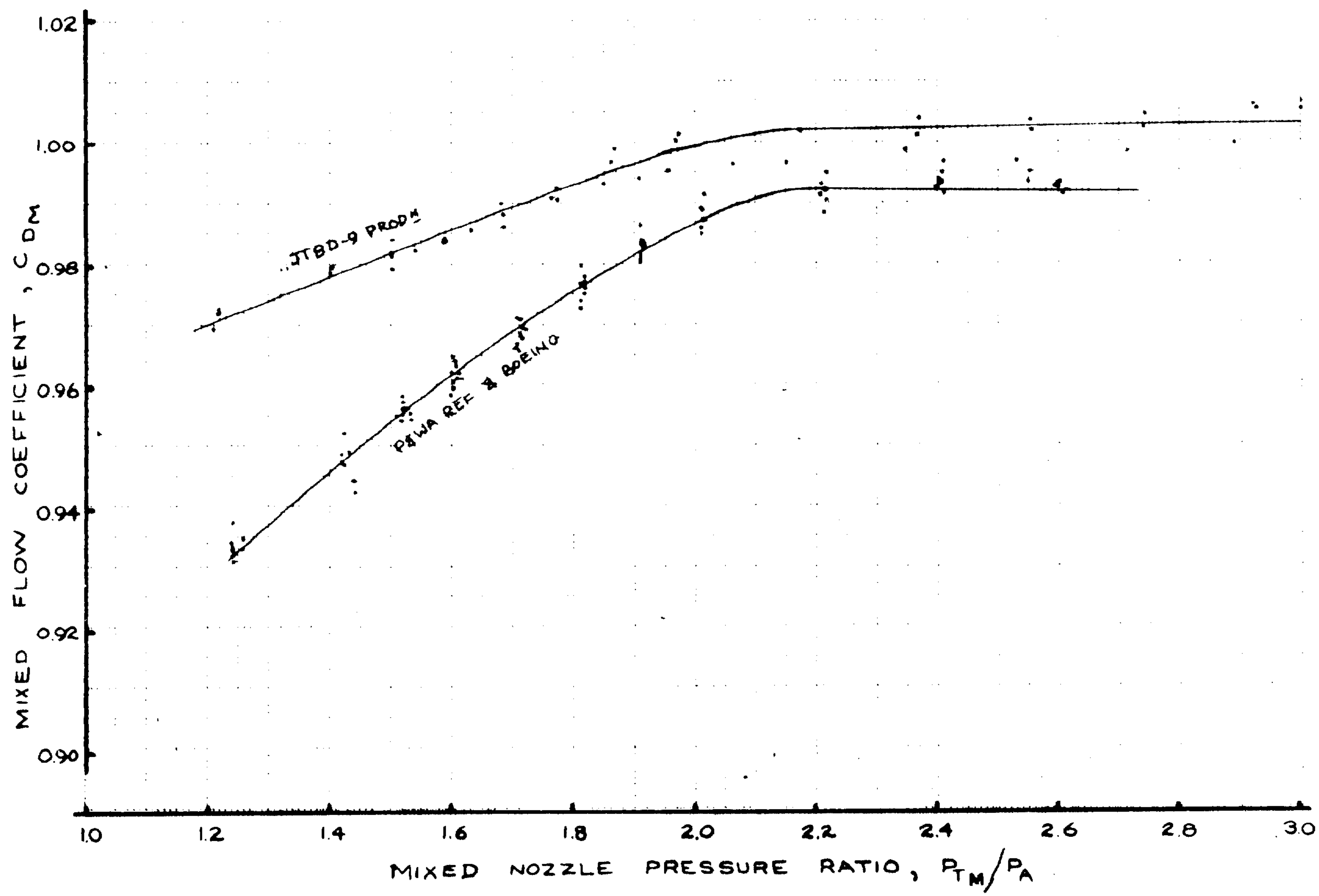

FIGURE 39 - C_{DM} FOR JT8D-9/727 PROD. (T.C.2); P&WA (T.C.3) AND BOEING CONFIG. NO. 2 (T.C.7) ON JT8D-109 AT T_{TP}/T_{TF} = 2.2

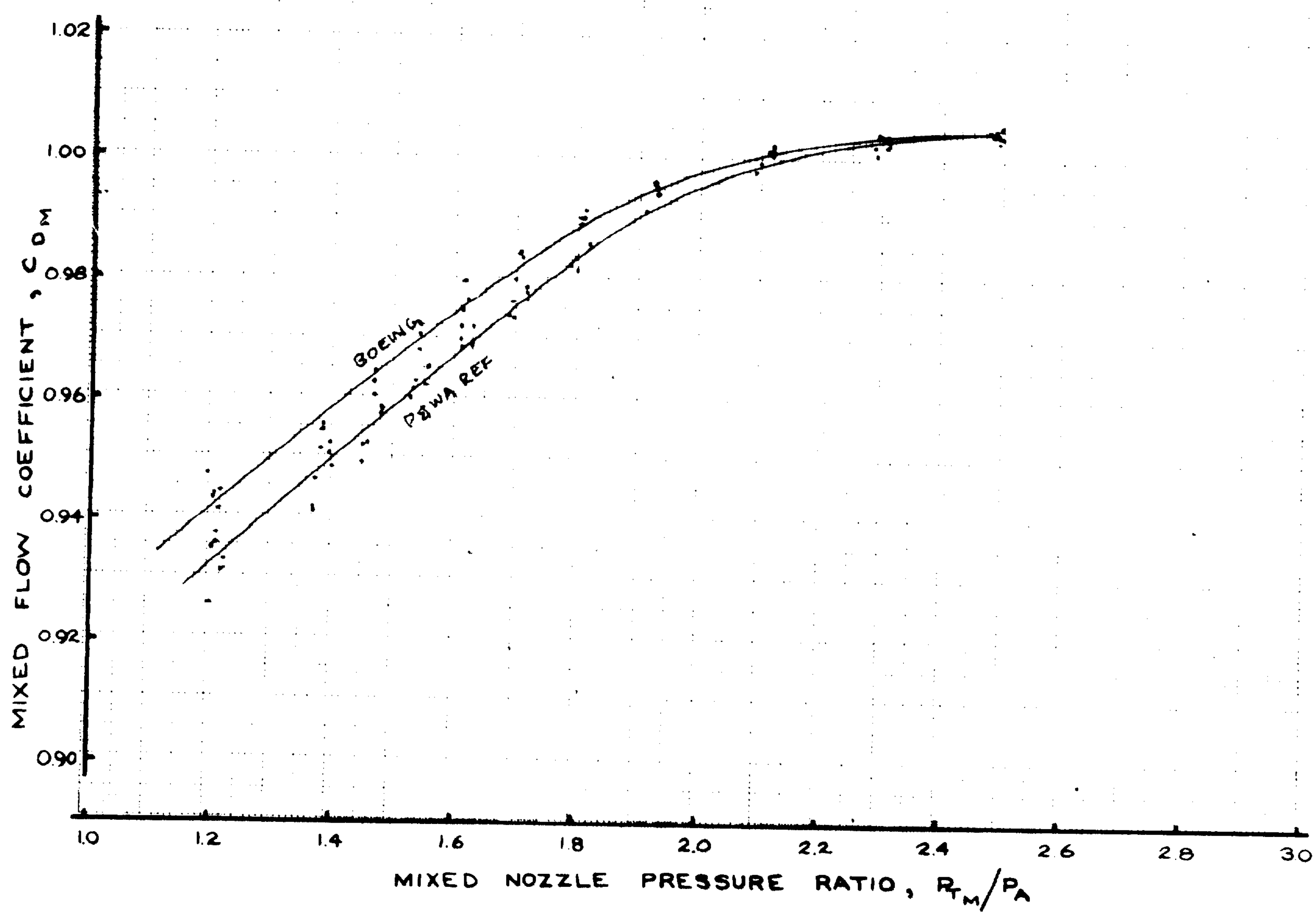

FIGURE 40 - C_{D_M} FOR P&WA (T.C.5) AND BOEING CONFIG. NO. 2 (T.C.11) ON JT8D-115 AT T_{T_P}/T_{T_F} = 2.2

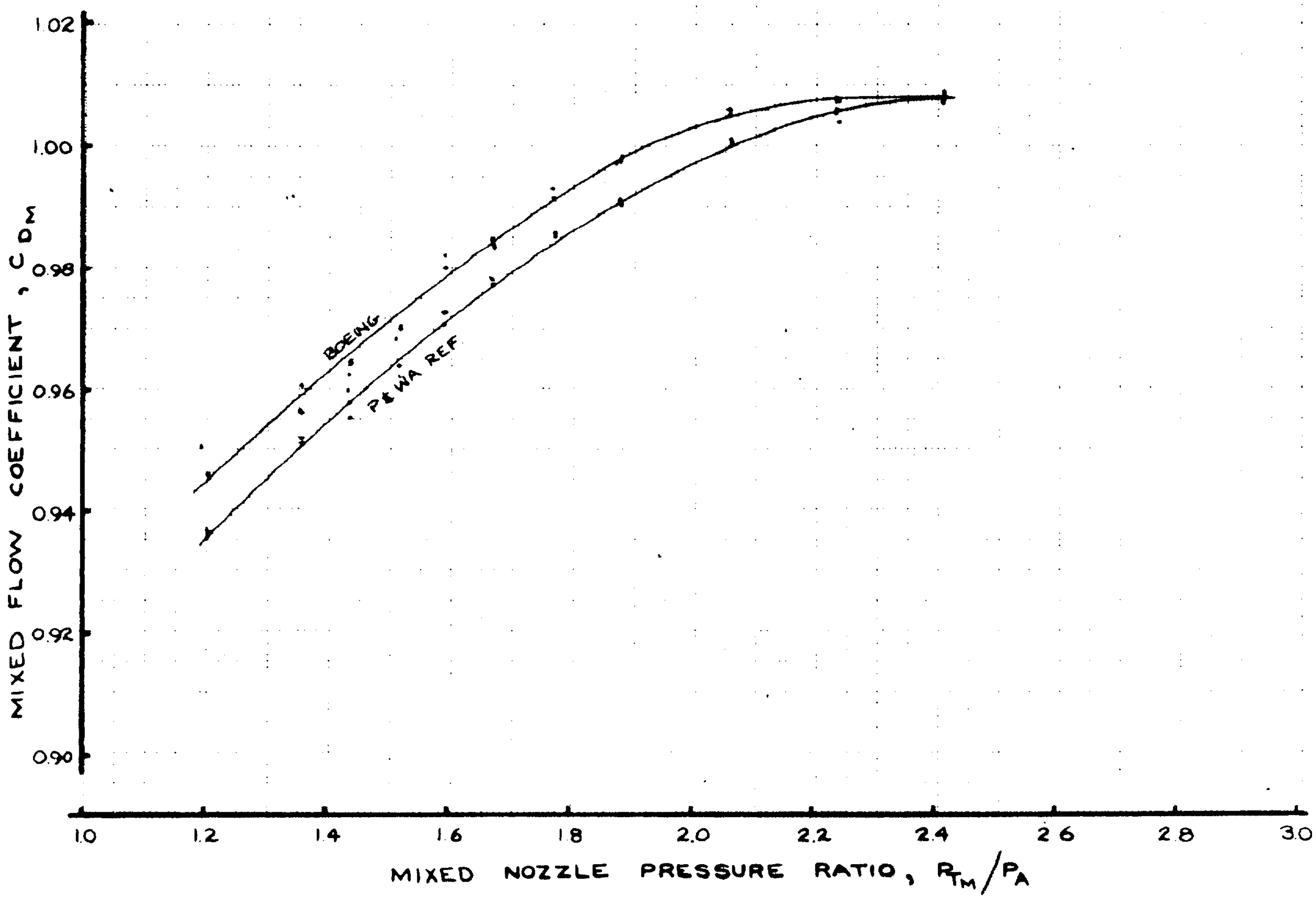

FIGURE 41 - C_{DM} FOR P&WA (T.C.6) AND BOEING CONFIG. NO. 2 (T.C.18) ON JT8D-117 AT T_{TP}/T_{TF} = 2.2

5.6 MIXING PLANE MATCH INVESTIGATIONS

As well as being able to produce thrust with minimum internal losses, the exhaust systems for the mixed flow JT8D-100 engines must be able to provide the correct bypass ratio for the engine to be operating at its optimum design point as specified by the engine manufacturer, P&WA. The exit area of the exhaust system influences both total engine mass flow and bypass ratio while the fan-to-primary area ratio at the mixing plane primarily effects the bypass ratio.

P&WA has established the required bypass ratios for the JT8D-100 engines needed to match their computer simulations of these engines. Figure 42 shows the required engine bypass ratio, including the fuel flow, as a function of the primary nozzle pressure ratio (P_{T_P}/P_A) for static, sea level conditions. This primary nozzle pressure ratio is the total pressure existing at the mixing plane due to the flow from the engine turbine section.

Also to ensure that the dividing splitter between the fan and primary flow streams has low aerodynamic losses, the leaving stagnation streamline must satisfy the Kutta condition at the trailing edge so that the flow will not separate. The Kutta condition will be satisfied if the wall static pressures on each side of the splitter, near the trailing edge, are equal (or balanced). As mentioned in Section 4.2.2, the splitter static pressures were measured on the P&WA and Boeing designs equivalent to 4.16 and 3.32 inches full scale upstream of the respective splitter trailing edges. Static pressure data for each test configuration are shown in Section 7.2.

Figure 43 shows the splitter static pressure unbalance versus the deviation from the required engine bypass ratio at the take-off primary pressure ratio. Due to the inability to set the fan-to-primary total pressure ratio exactly on the model test rig,

the bypass ratio was divided by P_{T_F}/P_{T_P} which can be considered an adjusted bypass ratio. This figure shows that the P&WA exhaust system designs for the JT8D-100 engines are within ±4.2% of matching the required engine bypass ratio with a splitter static pressure unbalance of -2.0% to +10.3%. Boeing exhaust system designs (exclusive of the A_E, A_F/A_P, and P_{T_F}/P_{T_P} variation studies) are within -1.6% to +6.5% of matching the required engine bypass ratio with a splitter static pressure unbalance of +2.0% to +0.3%, respectively. The P&WA designs show a larger static pressure unbalance than the Boeing designs because their splitters and plugs have more curvature than the Boeing designs. Also, since the static pressures were so far upstream of the splitter trailing edge, the static pressure data for both the P&WA and Boeing designs are not a good indicator of what is really happening at the trailing edge. Section 7.3.1 shows the physical position of the splitter trailing edge relative to the measured wake from the splitter. These data tend to show that the splitter position is not optimum in the Boeing or P&WA configurations for the JT8D-109 engine, with the P&WA Reference nozzle being slightly worse than the Boeing Config. No. 2 nozzle. This indicates that the required effective areas at the mixing plane are different than those provided by the model physical geometry which were presumed to satisfy the nozzle upstream flow conditions. The apparent mismatch of the Boeing JT8D-115 Config. No. 2 nozzle is less than on the Boeing JT8D-109 Config. No. 2 nozzle indicating that the JT8D-115 model geometry is closer to the correct mixing plane matched area. It should be emphasized here that the required engine bypass ratio has been that obtained from computer simulations of the engines and it is not known at the time of this writing what the actual engine bypass ratios will be. In practice, when the full scale engine is run on a ground rig test stand with the Boeing designed exhaust system both the mixing plane A_F/A_P ratio and the nozzle exit area may require small changes until the bypass ratio and

the bypass ratio and the total engine mass flow match that required by the engine manufacturer, P&WA.

The effect of splitter location on bypass ratio was investigated for the JT8D-115 engine and Boeing Config. No. 2 designs. Changes in the geometric A_F/A_P ratio of -25.7% to +12.9% resulted in bypass ratio changes of -22.6% to +13.7%, respectively, relative to the base A_F/A_P ratio for the JT8D-115 which has a 1% bypass ratio deviation (Figure 43). As was expected, a 1% change in A_F/A_P ratio is a 1% change in bypass ratio for fixed stagnation conditions in the fan and primary streams. Performance data, in terms of C_{V_M} and C_{D_M}, were also recorded and are summarized on Figure 44 at 1.6 and 2.4 mixed total pressure ratios for both hot and cold flow conditions.

The effect of changing the nozzle exit area on bypass ratio was also investigated on the Boeing Config. No. 2 design for the JT8D-115 engine. A change in the geometric exit area of -0.9% and +2.2% resulted in a -0.6% and +2.4% change, respectively, in the bypass ratio (Figure 43), again relative to the 1% JT8D-115 bypass ratio deviation. Hence, a 1% change in bypass ratio was found for a 1% change in nozzle exit area for given stagnation conditions in the fan and primary streams. This was an unexpected result as it showed that for the model the bypass ratio is as sensitive to nozzle exit area as it is to the splitter position (A_F/A_P). The performance data showing the effect of nozzle exit area is presented on Figure 45 at 1.6 and 2.4 mixed nozzle pressure ratio for both hot and cold flow conditions.

The fan-to-primary total pressure ratio, P_{T_F}/P_{T_P}, was varied on the Boeing Config. No. 2 design for the JT8D-115 engine to determine the effects on bypass ratio. A +3.7% and +7.5% change in the P_{T_F}/P_{T_P} ratio resulted in a +9.6% and +23.6% change, respectively, in bypass ratio (Figure 43), again relative to the 1% JT8D-115 bypass ratio deviation. This is nominally a 2.8%

change in bypass ratio for each 1% change in the P_{T_F}/P_{T_P} ratio.

The sensitivities of bypass ratio to A_E, A_F/A_P, and P_{T_F}/P_{T_P} found during this model test program may not be the same as those for the actual JT8D-100 engines. This is because the engine rematches by interaction through the engine rotating machinery in a way that the model with its independent flow supplies cannot do.

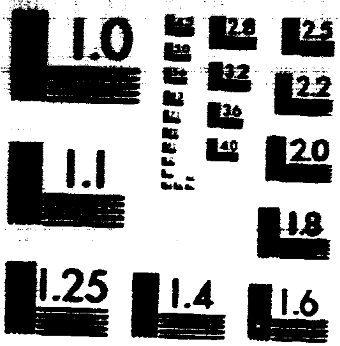

MICROCOPY RESOLUTION TEST CHART
NATIONAL BUREAU OF STANDARDS-1963-A

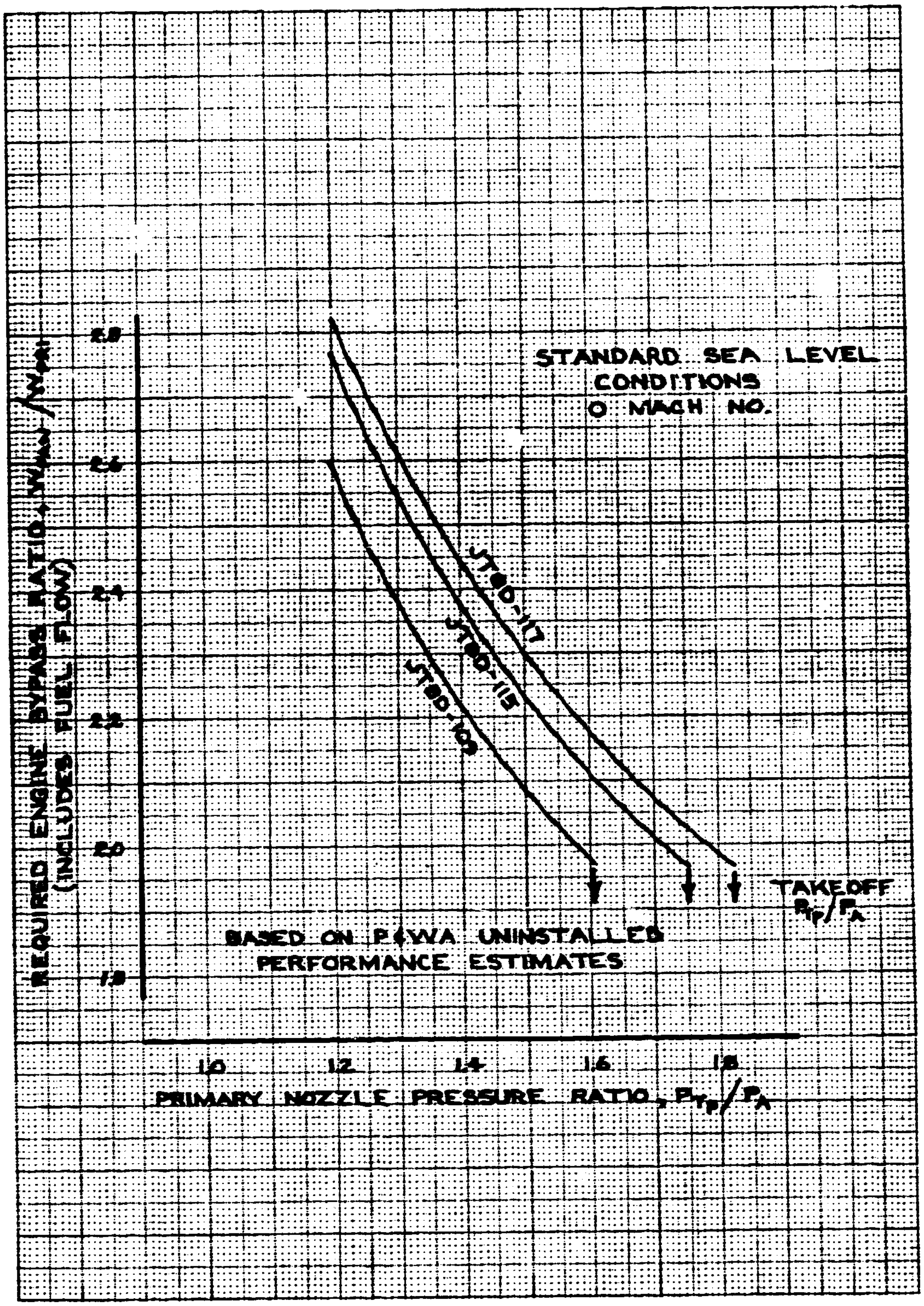

FIGURE 42 - REQUIRED JT8D-100 ENGINE BYPASS RATIO

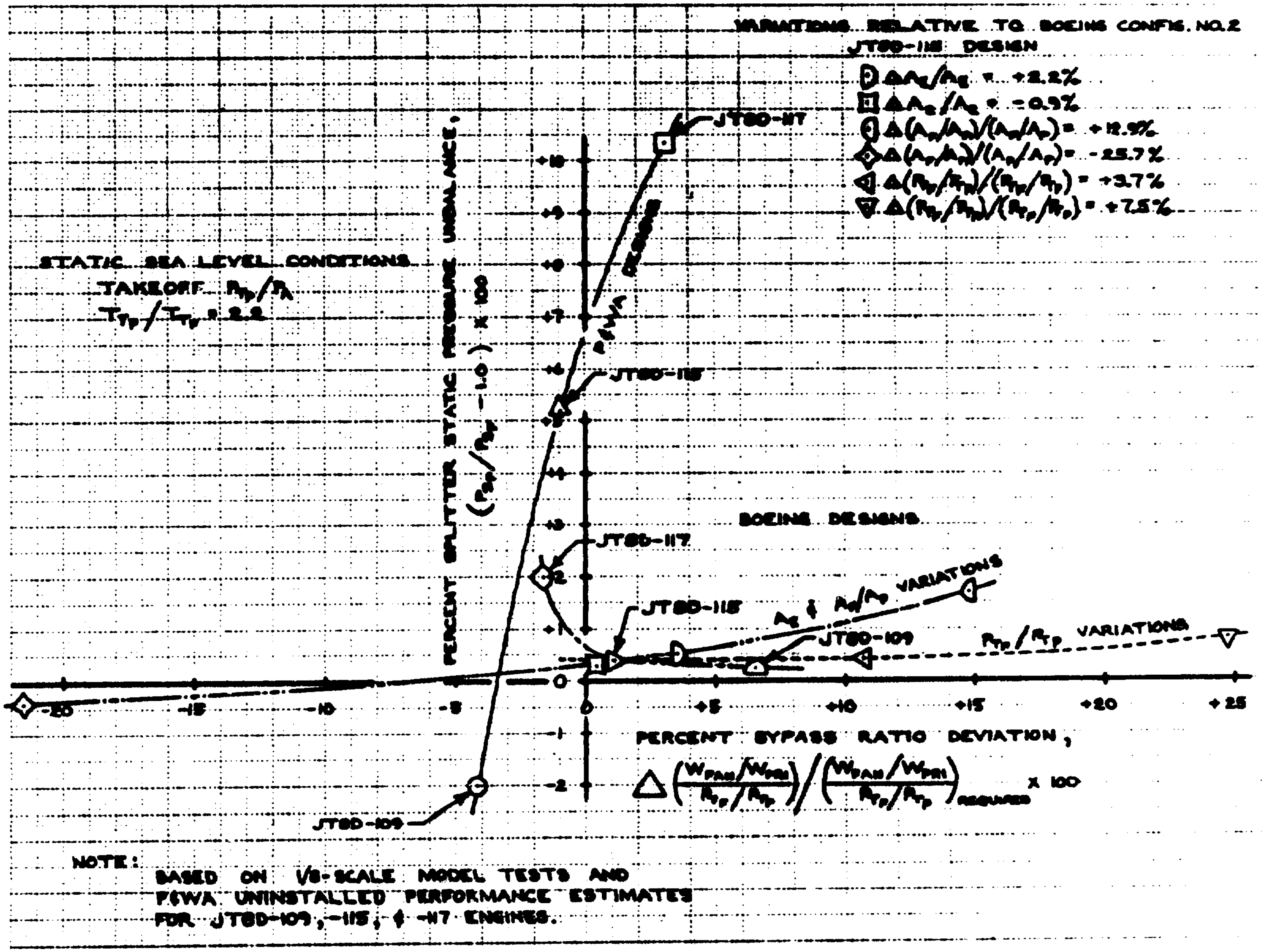

FIGURE 43 - P&WA AND BOEING JT8D-100 ENGINE SPLITTER BYPASS RATIO DEVIATIONS

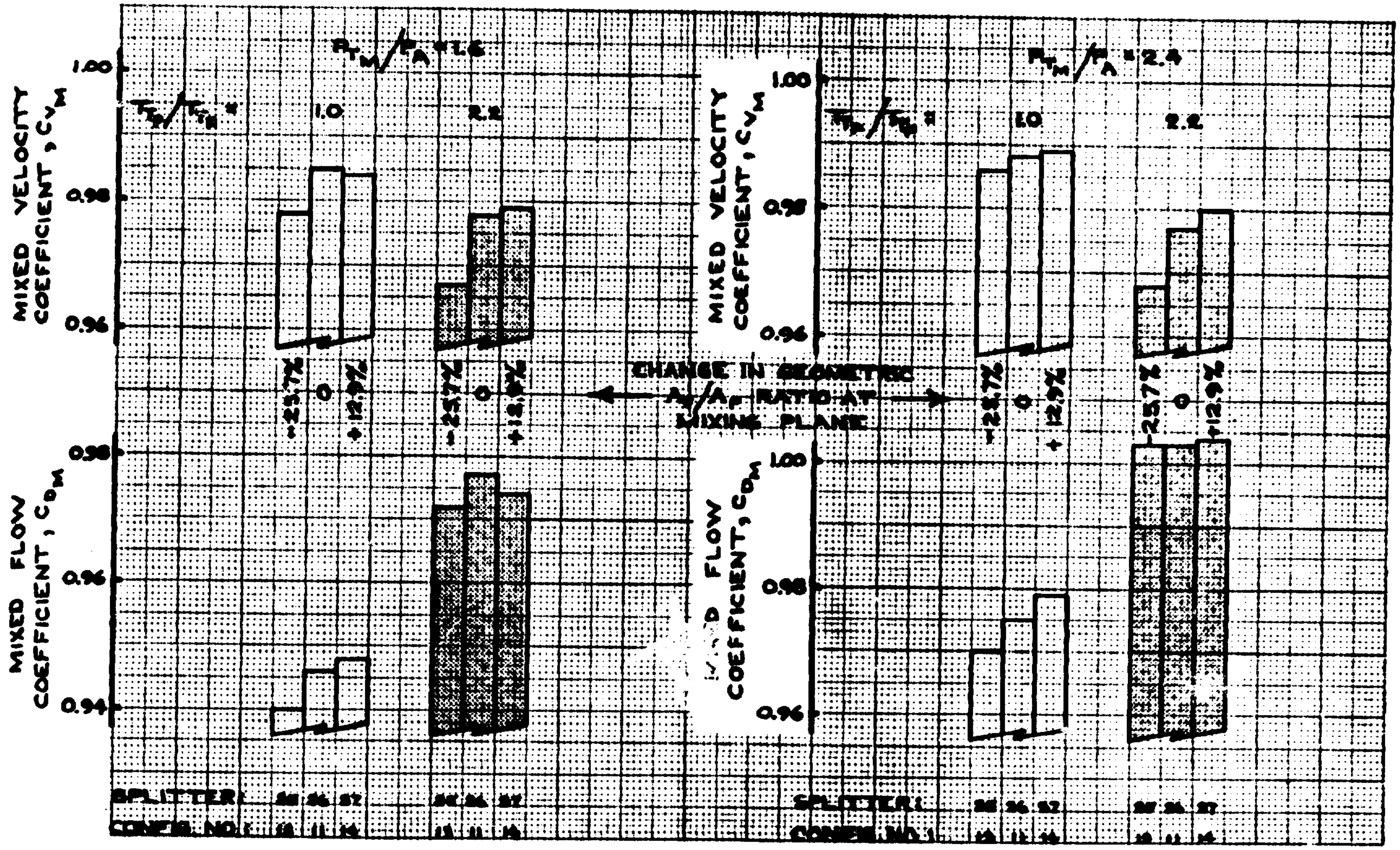

FIGURE 44 - JT8D-115 BOEING CONFIG. NO. 2 SPLITTER LOCATION VARIATIONS

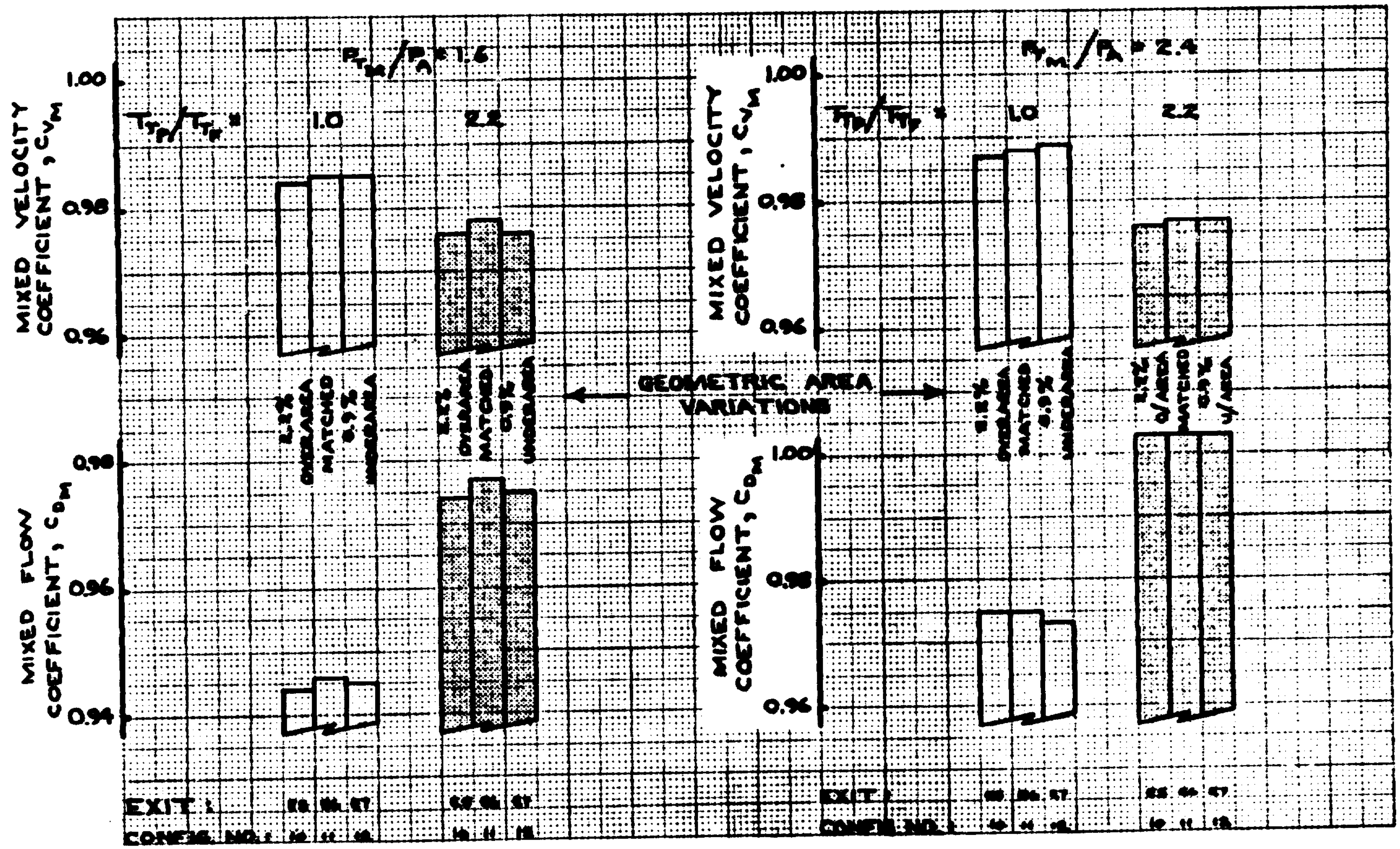

FIGURE 45 - JT8D-115 BOEING CONFIG. NO. 2 EXIT AREA VARIATIONS

5.7 INVESTIGATION OF THE EFFECT OF PRIMARY FLOW SWIRL

5.7.1 MEASUREMENT OF SWIRL ANGLES AND PROFILES

The JT8D-109 series engine, according to P&WA best estimates at the time of planning this test, would experience swirl in the primary stream at takeoff which varies linearly from 0° at the outer wall, to 18° on the inner wall downstream of the turbine exit guide vanes.

In order to determine the effects of such swirl on the performance (velocity coefficient, flow coefficient, mixing plane match, nozzle exit profile, etc.) a set of turning vanes were manufactured for incorporation downstream of the instrumentation section to reproduce the predicted JT8D-109 swirl. Swirl cannot be introduced ahead of the measurement station without rather elaborate measurements to ensure correct orientation of the total pressure probes for proper measurement of the nozzle charging station pressures. Therefore, swirl is introduced downstream of the measurement station and consequently the losses of the swirl vanes increased the nozzle losses and were recorded as a reduction in the nozzle Cv, together with any effects of the swirl itself.

Figure 46 shows the measurement of swirl angle on the P&WA JT8D-109 Reference configuration (T.C.3) at a 315° circumferential location without swirl vanes installed (angles are measured in a rear view clockwise from the top centerline). The yaw probe zero was obtained by aligning the probe perpendicular to the model fixture flanges. The yaw probe was located about 6 inches (full scale) downstream of the mixing plane pressure traverse (data presented in Section 7.3) for both the P&WA Reference configurations and the Boeing configurations. The mixing plane in the Boeing configuration is further downstream than in the P&WA configuration. In the

Boeing configuration, there is no plug at that location whereas in the P&WA configuration, the plug is quite large at the mixing plane. Due to the presence of the plug at the mixing plane and the design of the yaw probe, the probe was unable to reach the plug surface in the P&WA configuration; therefore, approximately 30% of the inner primary annulus height could not be surveyed. Figure 46 shows less than 2° swirl in the primary passage at the center of the flow, and approximately 4.5° swirl in the fan passage. Figure 47 shows the total pressure profile at various nozzle pressure ratios taken during the yaw traverse.

Figures 48, 50, and 52 show the swirl angle at the 300°, 315°, and 330° circumferential location respectively, after installation of the swirl vanes in the P&WA JT8D-109 Reference (T.C.4). Figures 49, 51, and 53 show the corresponding total pressure profiles at the same locations. These positions correspond to the wake and the pressure and suction sides of the swirl inducing airfoils in an attempt to ascertain that no separation was occurring. It will be noted that the linear variation of swirl angle with percentage of primary annulus height was not achieved. However, extrapolation of the mean curves through the various sets of data shows approximately 18° of counter-clockwise swirl (looking up-stream) at the plug surface. It is obvious that no increase in swirl was induced into the fan passage by the device.

Before proceeding to a discussion of the nozzle performance aspects, perusal of Figures 54 and 55 show the effect of the swirl device on the Boeing JT8D-109 Config. No. 2 (T.C.19). The fan swirl was the same as on the P&WA Reference Nozzle. The primary swirl induced in the Boeing configuration is no different than on the P&WA configuration at the swirl vane trailing edge, but because the splitter is longer on the Boeing Config. No. 2 than on the P&WA Reference nozzle, the swirl angle measurements were not made in the same axial location. Therefore,

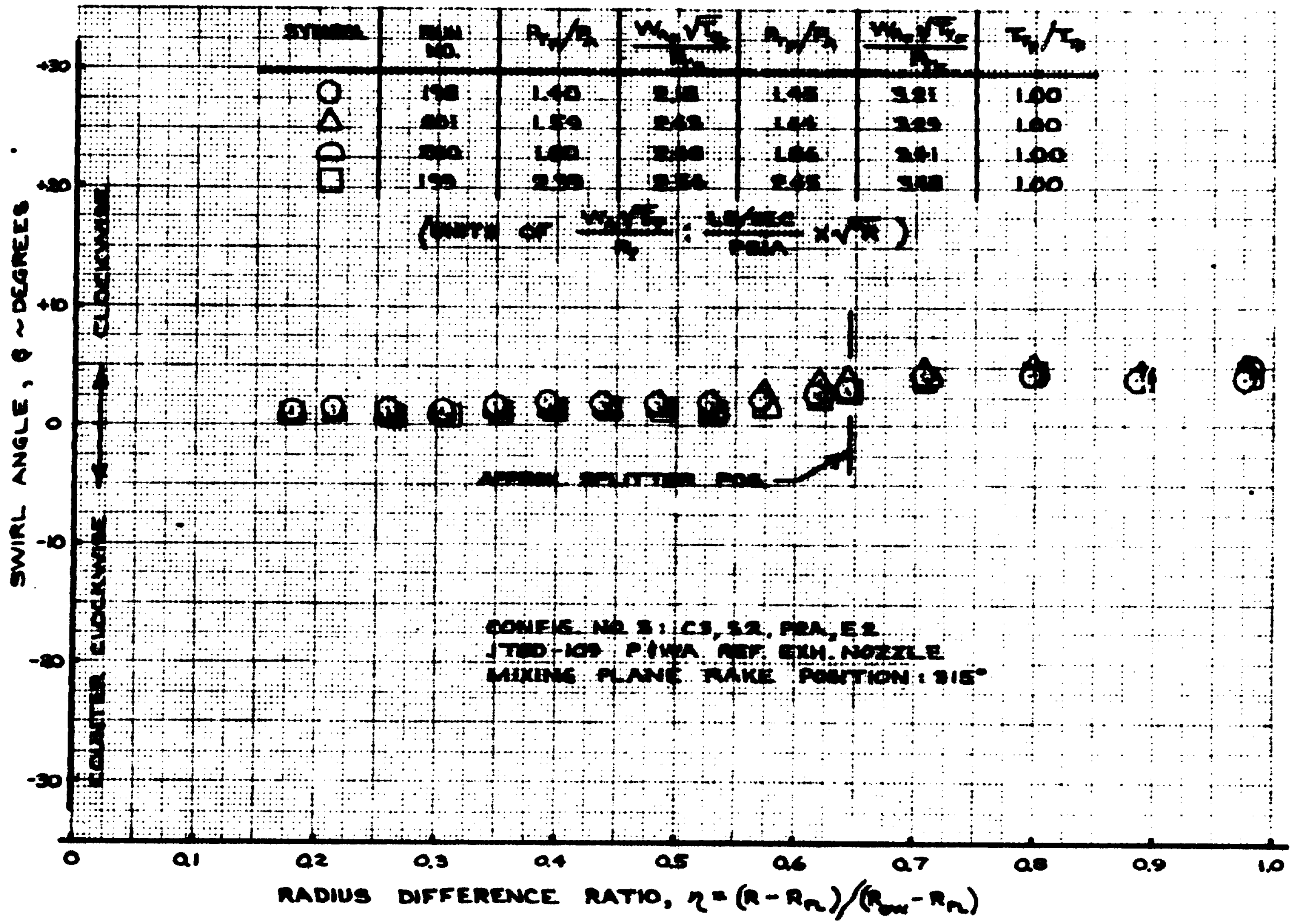

FIGURE 46 - MIXING PLANE SWIRL ANGLE PROFILES
TEST CONFIG. NO. 3; RAKE POSITION - 315 DEG.

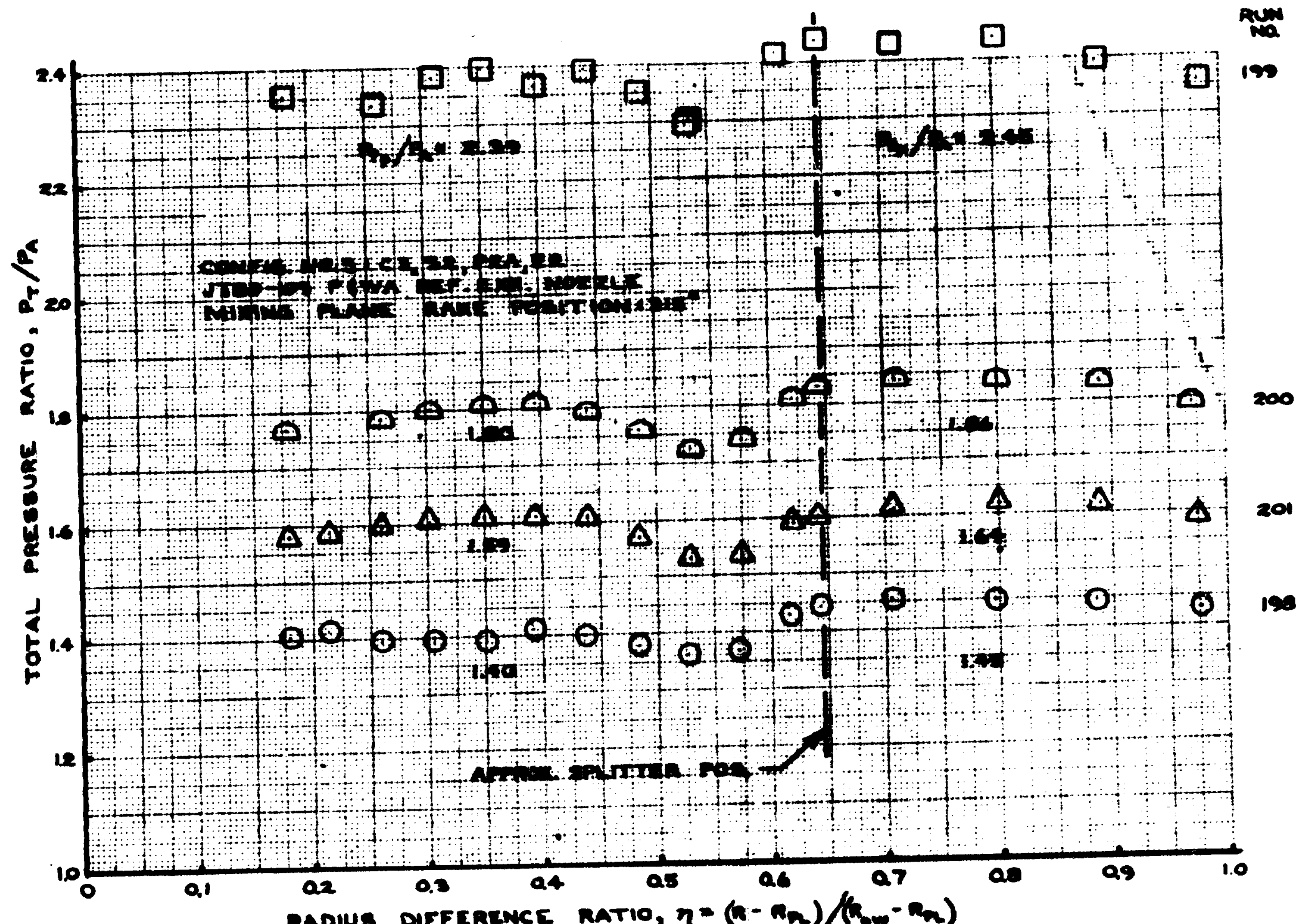

FIGURE 47 - MIXING PLANE TOTAL PRESSURE PROFILE (SWIRL PROBE)
TEST CONFIG. NO. 3; RAKE POSITION - 315 DEG.

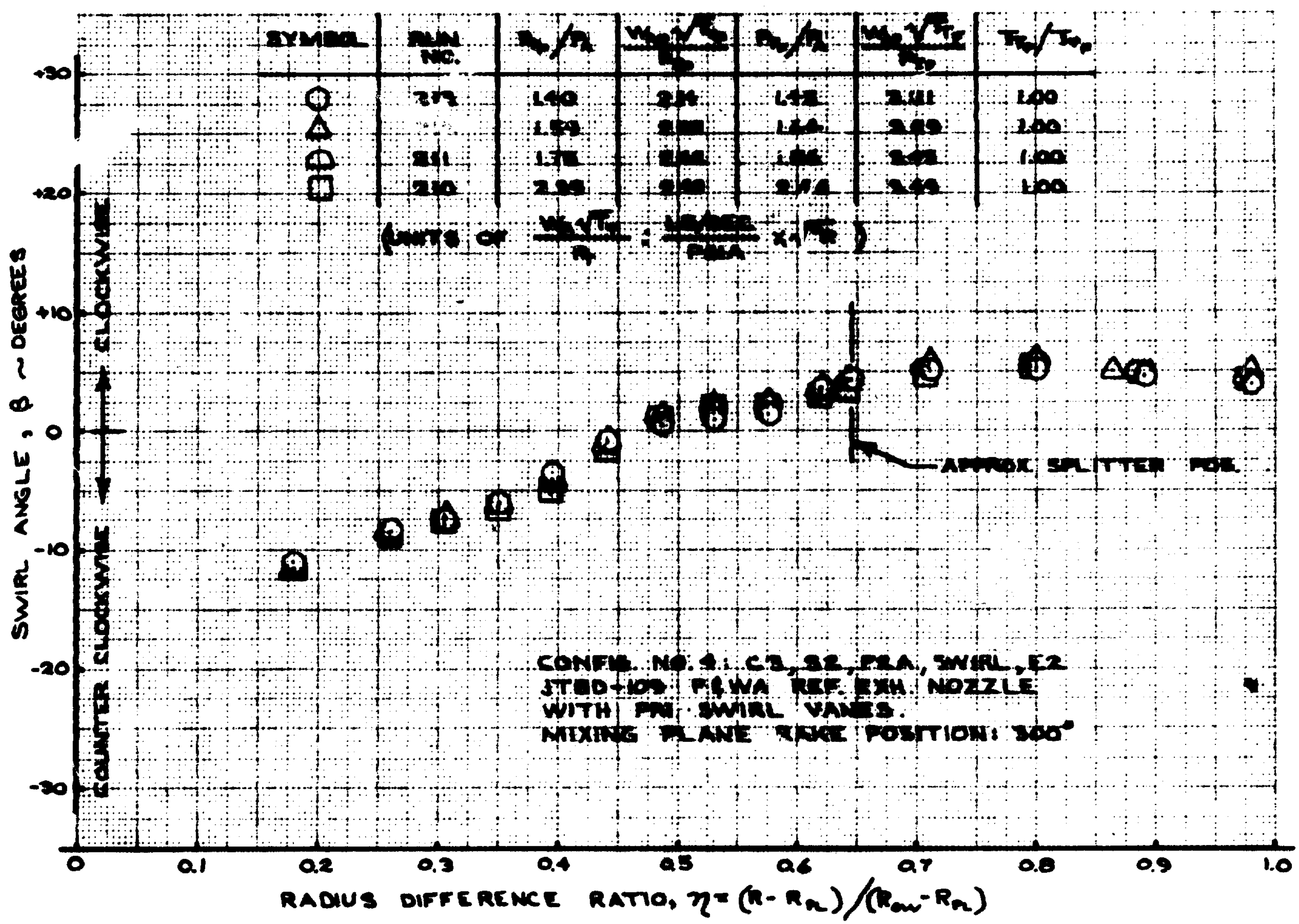

FIGURE 48 - MIXING PLANE SWIRL ANGLE PROFILES
TEST CONFIG. NO. 4; RAKE POSITION - 300 DEG.

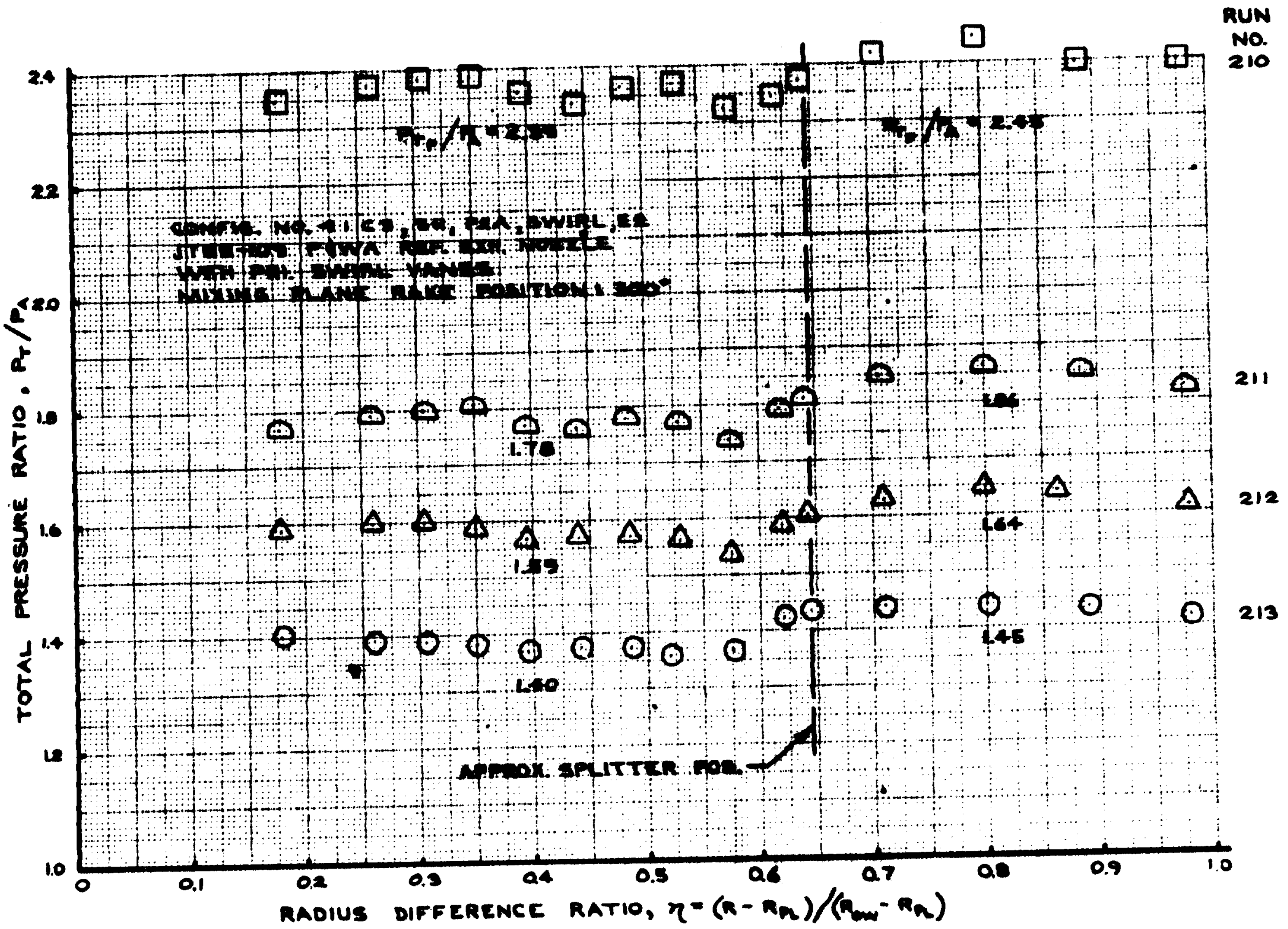

FIGURE 49 - MIXING PLANE TOTAL PRESSURE PROFILE (SWIRL PROBE)
TEST CONFIG. NO. 4; RAKE POSITION - 300 DEG.

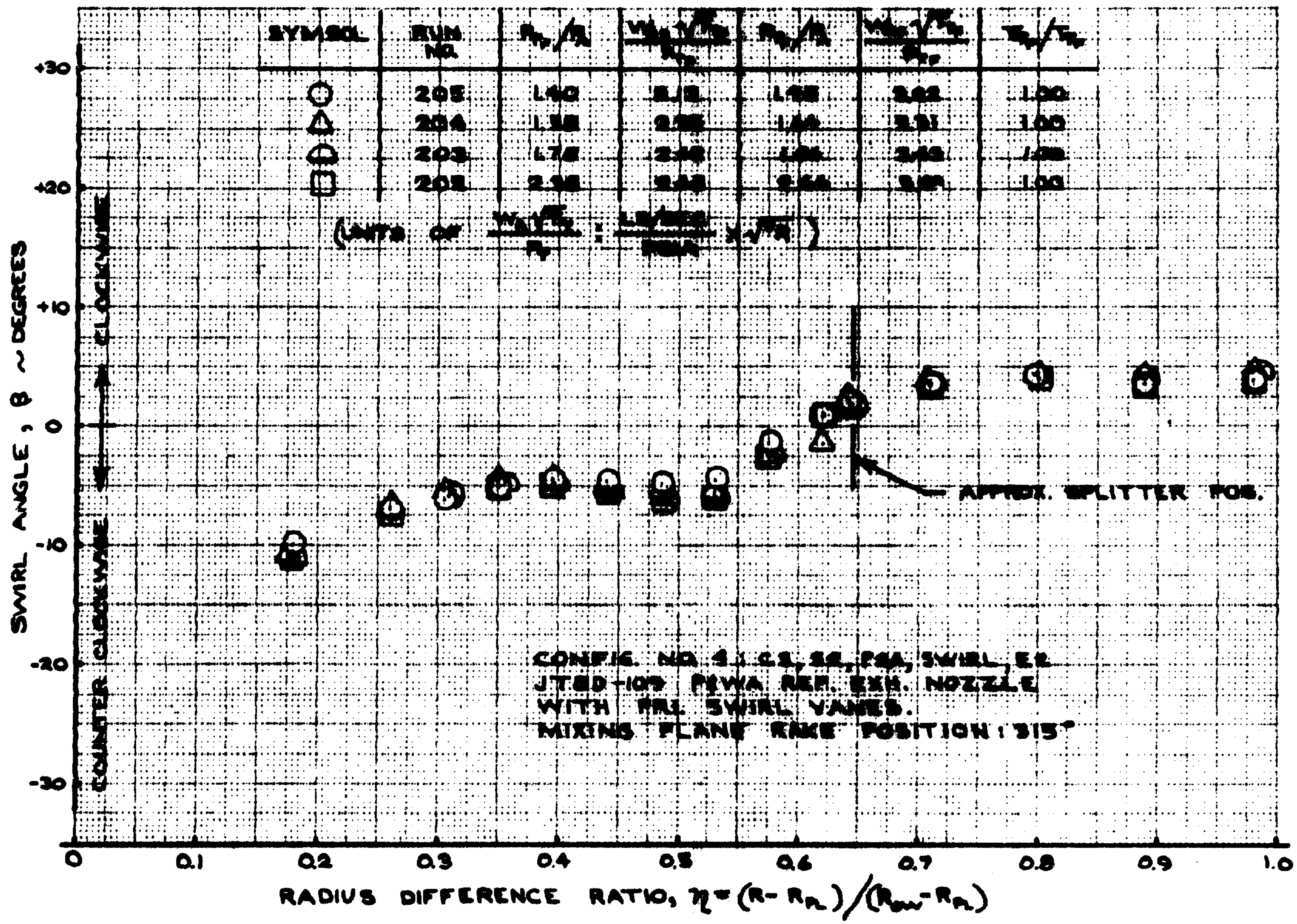

FIGURE 50 - MIXING PLANE SWIRL ANGLE PROFILES
TEST CONFIG. NO. 4; RAKE POSITION - 315 DEG.

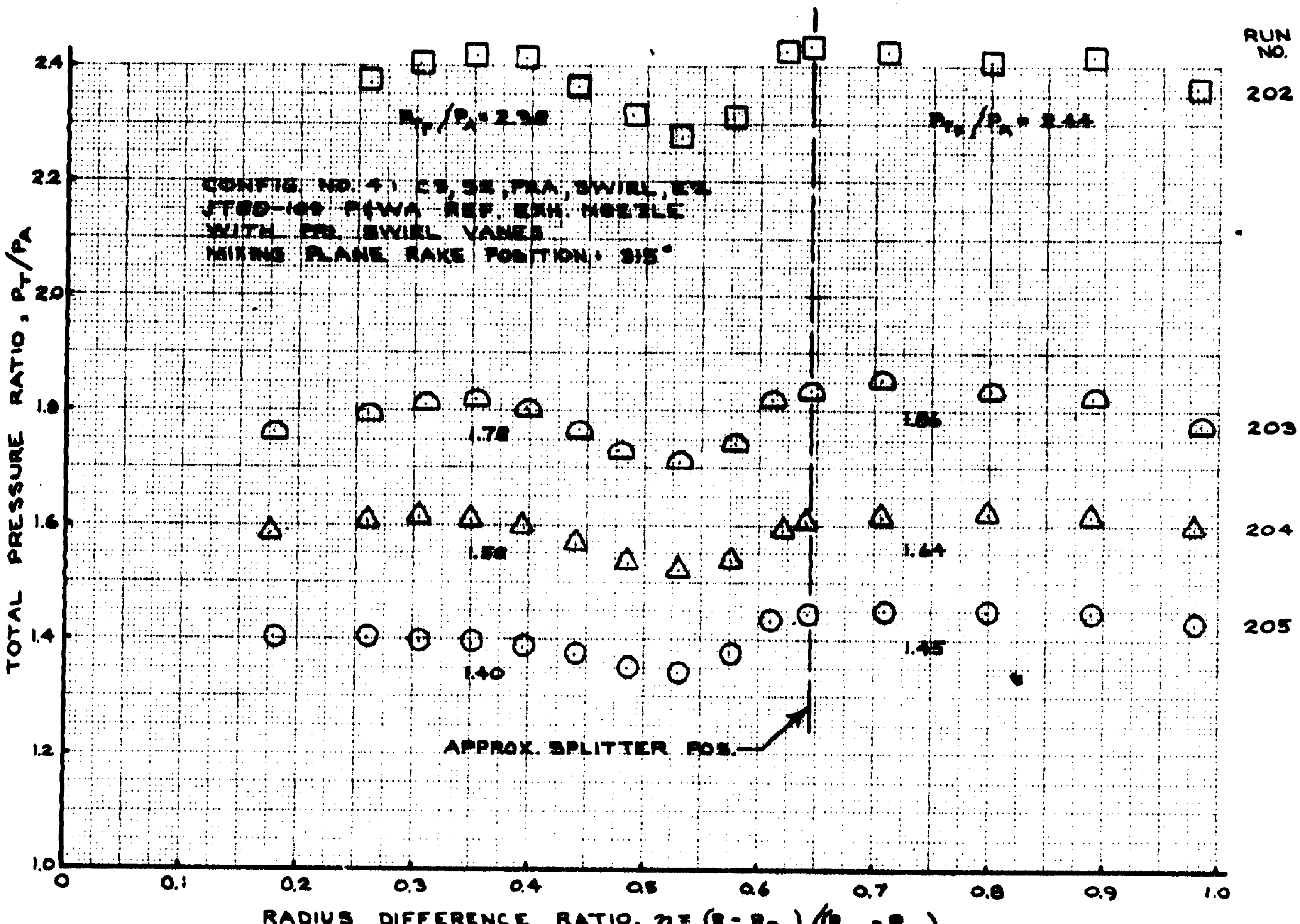

FIGURE 51 - MIXING PLANE TOTAL PRESSURE PROFILE (SWIRL PROBE) TEST CONFIG. NO. 4; RAKE POSITION -315 DEG.

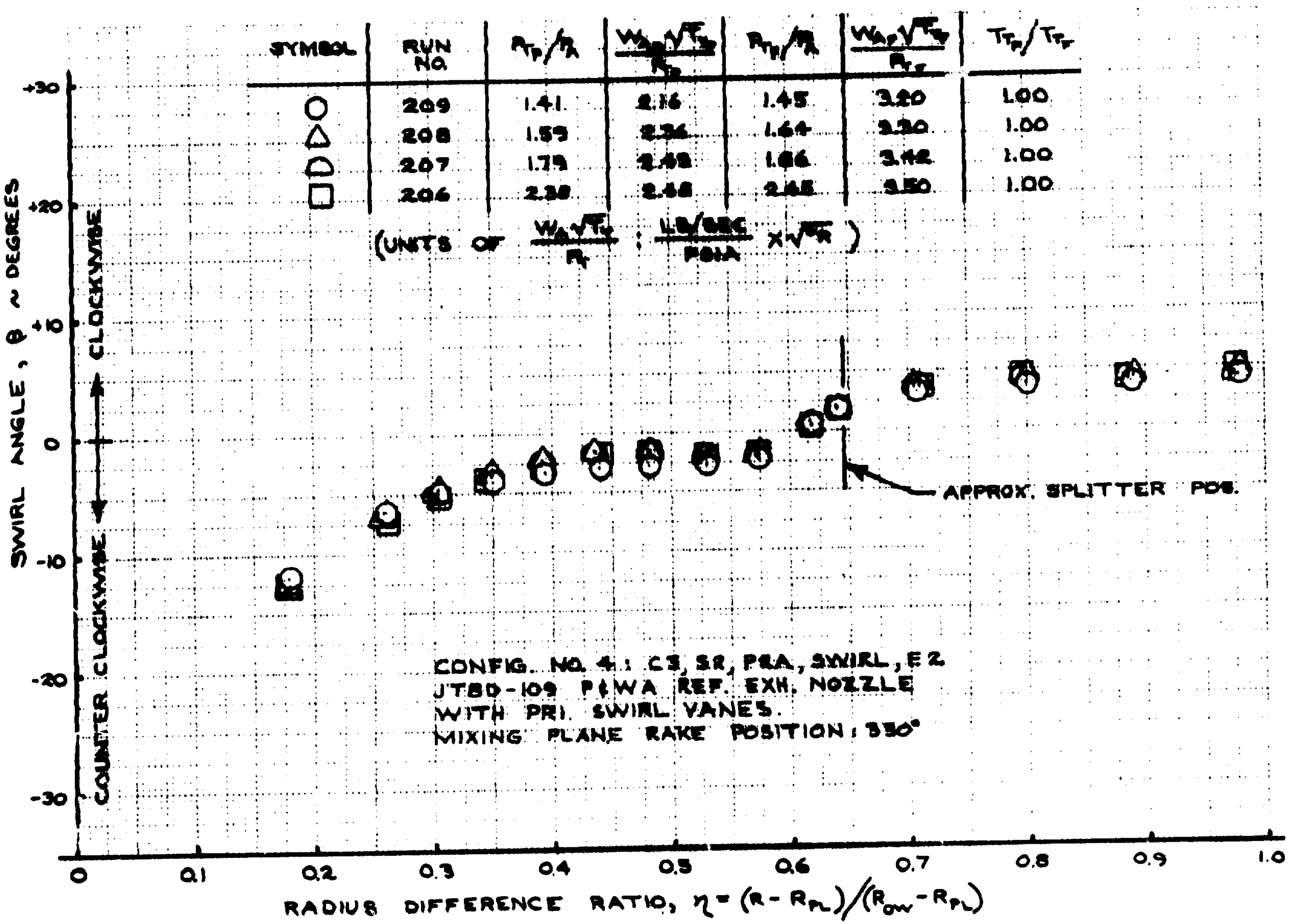

FIGURE 52 - MIXING PLANE SWIRL ANGLE PROFILES
TEST CONFIG. NO. 4; RAKE POSITION - 330 DEG

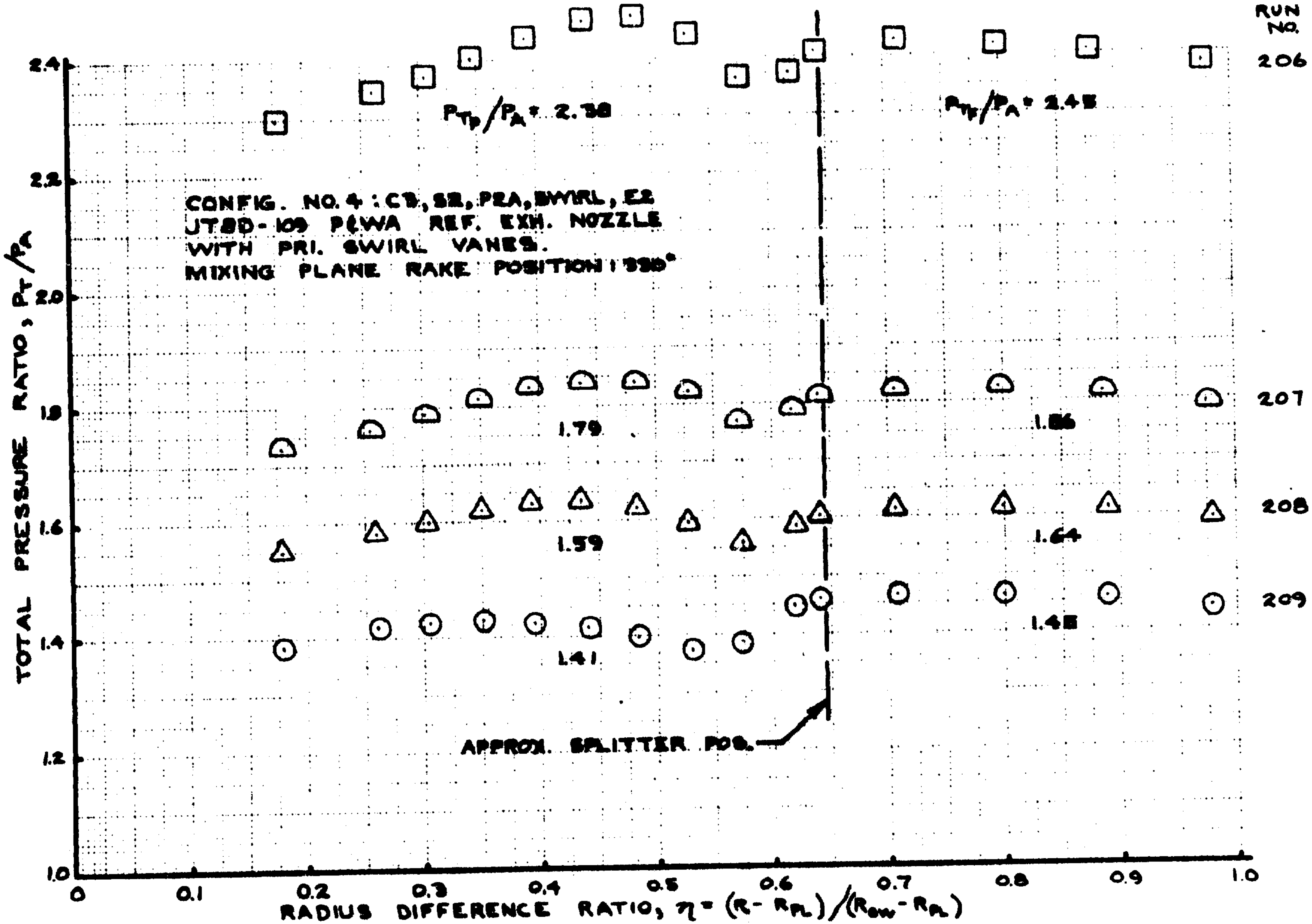

FIGURE 53 - MIXING PLANE TOTAL PRESSURE PROFILE (SWIRL PROBE)
TEST CONFIG. NO. 4; RAKE POSITION - 330 DEG.

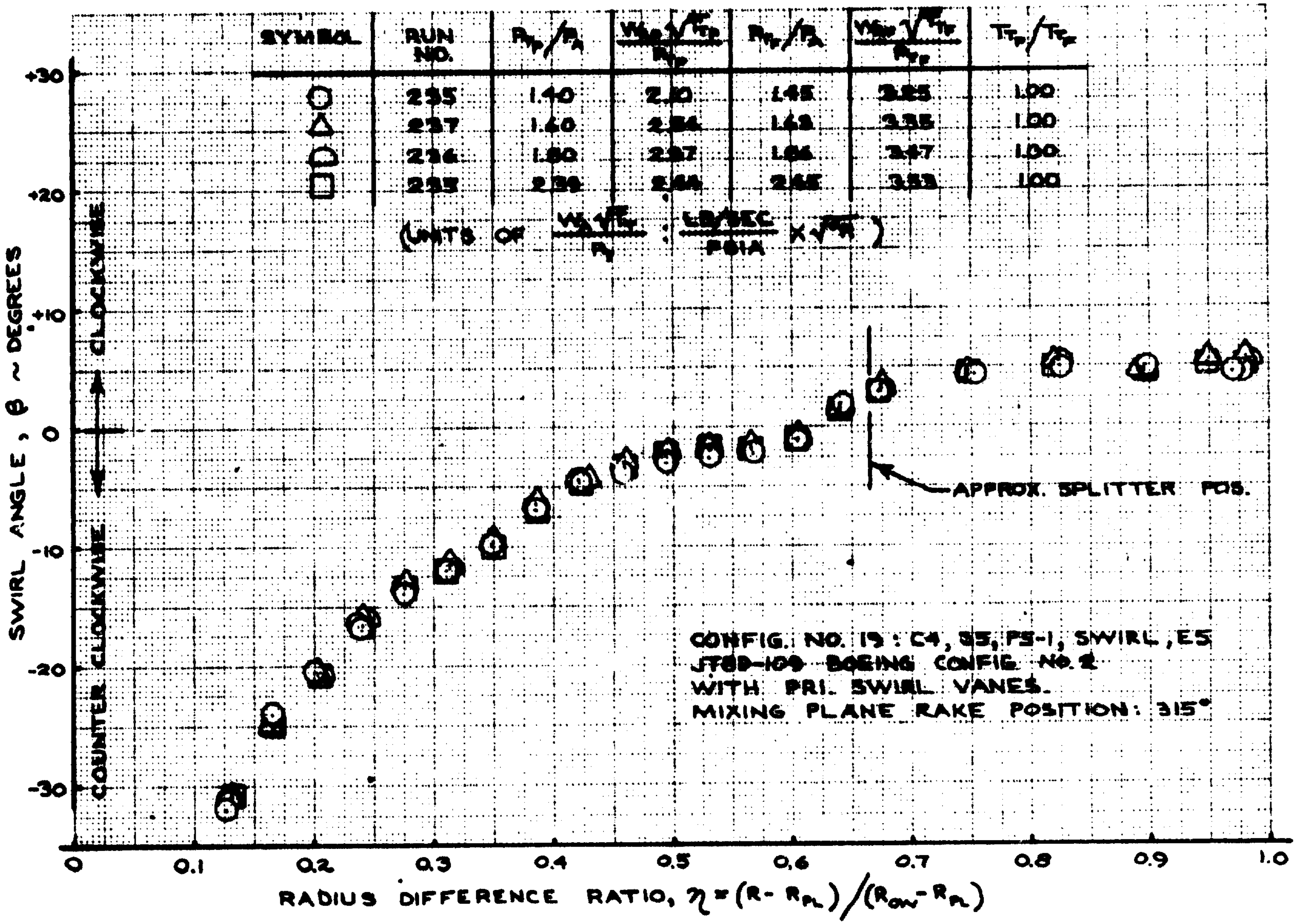

FIGURE 54 - MIXING PLANE SWIRL ANGLE PROFILES
TEST CONFIG. NO. 19; RAKE POSITION - 315 DEG.

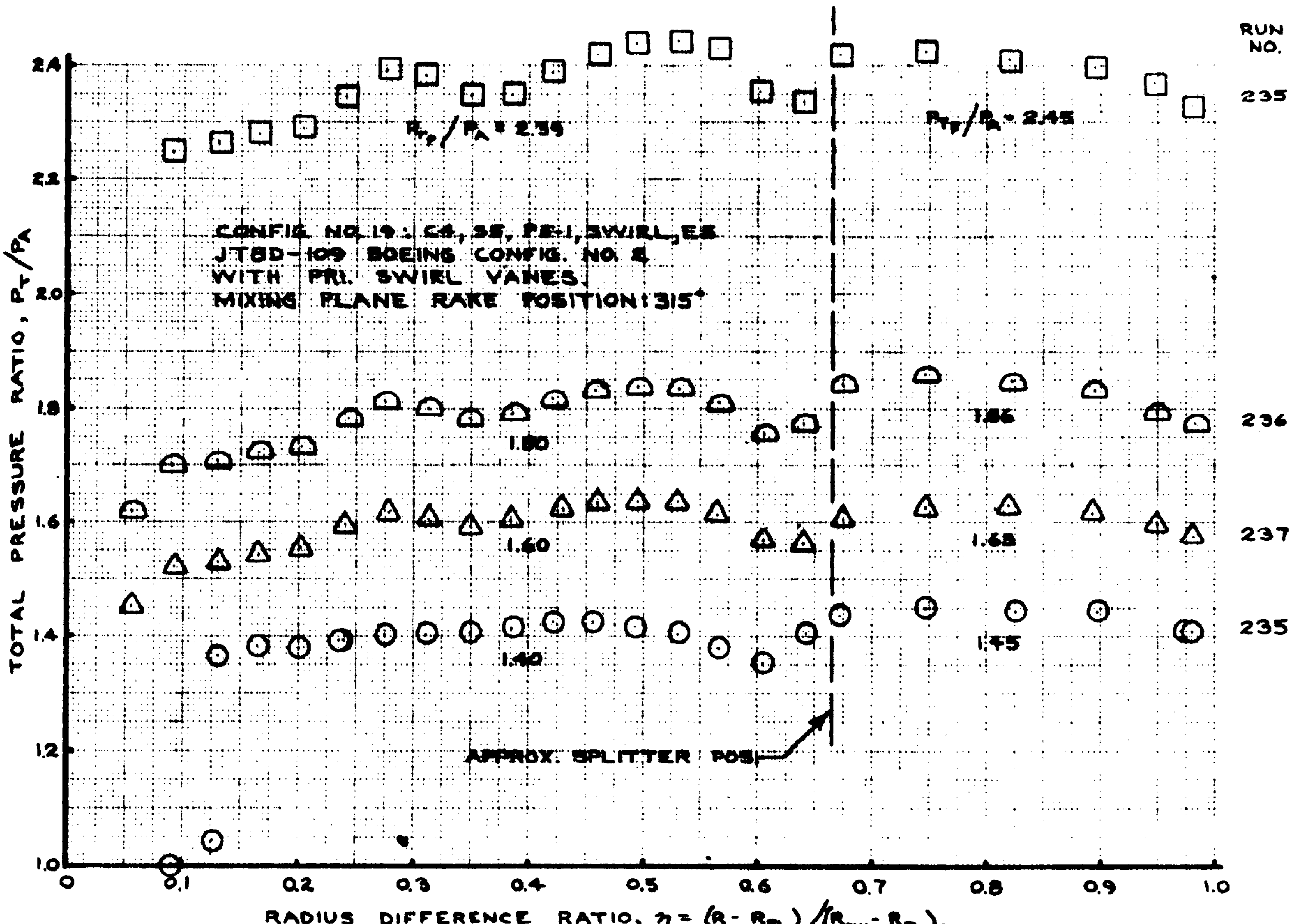

FIGURE 55 - MIXING PLANE TOTAL PRESSURE PROFILE (SWIRL PROBE)
TEST CONFIG. NO. 19; RAKE POSITION - 315 DEG.

the swirl angle measurements in the primary flow for the two nozzle configurations are different as shown in Figures 48, 50, 52, and 54. Theoretically, to maintain no loss of angular momentum, the swirl angle must approach 90° as the radius (percentage of annulus or duct height) of the induced vortex approaches zero. In practical systems, the static pressure gradient needed to support such a system is incompatible with the static pressure gradients of the main flow and a vortex is formed in the center of the flow. It is apparent from Figure 54 that at 13% of the duct height, the yaw angle has reached 31° (the limit of the probe angle calibration) and is rapidly increasing with reduced radius. As discussed in Section 7.3.2, the exit survey data shows that a vortex exists in this region, with reverse flow.

5.7.2 EFFECT OF PRIMARY SWIRL ON NOZZLE VELOCITY AND FLOW COEFFICIENTS

The swirl introduced for this testing was only representative of the engine swirl above takeoff pressure ratio. Therefore, data at lower pressure ratios should be viewed with caution.

A statistical comparison of the P&WA Reference and the Boeing Config. No. 2 (T.C.4 and T.C.19) nozzles for JT8D-109 application showed that the hypothesis of equality was accepted (see Section 5.9). For this reason, the data from the two configurations was combined and is presented in Figure 56 where the hot flow performance level (C_{V_M}) is shown as a function of the mixed total pressure ratio.

Compared to Figure 28 without swirl, there is a marked reduction in mixed velocity coefficient of 0.8% at a pressure ratio of 1.6 (takeoff) and 0.4% at a pressure ratio of 2.4 (cruise). Similarly, the nozzle flow coefficient shows a reduction relative to the common level of the P&WA Reference and Boeing

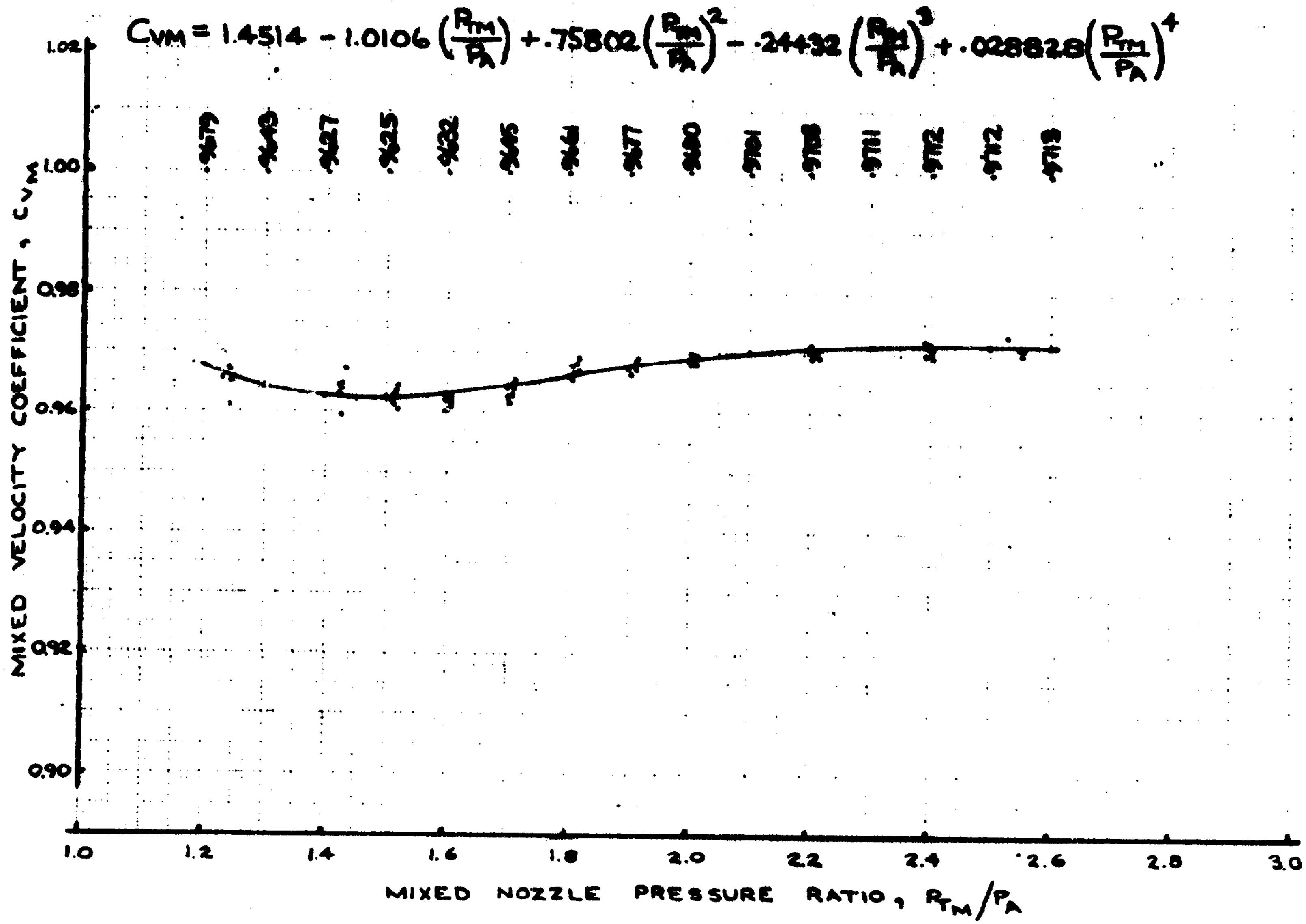

FIGURE 56 - C_{VM} FOR P&WA (T.C.4) AND BOEING CONFIG. NO. 2 (T.C.19) NOZZLES ON JT8D-109 WITH PRIMARY FLOW SWIRL

Config. No. 2, as exemplified by Figure 39 (T.C.3 and T.C.7), by about 0.6% for the Boeing Config. No. 2 with swirl (T.C.19) and 1.0% for the P&WA JT8D-109 Reference nozzle with swirl (T.C.4).

The nozzle performance loss can probably be explained as a combination of three components; the loss of the device producing the swirl, the cosine loss introduced into the primary thrust component, and an increase in the existing pressure losses in the primary passage due to both skin friction and increased pressure loss due to flow turning. In this instance, the velocity coefficient loss at cruise pressure ratio is half that at takeoff (2.4 compared to 1.6) and is characteristic of a constant pressure loss.

Estimates of the swirl device pressure loss ($\Delta P_T/P_T$) are about 0.25%. This results in a reduction in velocity coefficient of 0.25% at takeoff pressure ratio (1.6) and 0.13% at cruise (2.4) relative to the no swirl case. These losses should be accounted for to obtain the best estimate of the true level of velocity coefficient. Therefore, the introduction of primary swirl produced a net reduction in the velocity coefficient of the JT8D-109 configuration of approximately 0.55% at takeoff and 0.27% at cruise. These reductions in velocity coefficient are essentially applicable to the JT8D-115 and -117 engines at the quoted pressure ratios.

The effects of swirl on bypass ratio are difficult to assess and no positive tendency to increase or decrease bypass ratio when swirl is introduced can be detected. Bypass ratio is a very sensitive parameter to fan-to-primary duct total pressure ratio with a 2.3 to one magnifying factor. Therefore, small errors in setting pressure ratio while satisfying the other requirements of the test can cause large perturbations on bypass ratio.

In an engine, more complex reactions may occur. It is therefore, impossible to relate the model effects of swirl on bypass ratio to those in a full scale engine. It is, however, reasonable to expect a similar behavior on the nozzle flow coefficient. An engine with residual swirl is likely to require a bigger exhaust nozzle for correct match than one without.

5.8 MIXING EFFICIENCY

5.8.1 EQUATIONS FOR MIXING EFFICIENCY

The equation used to calculate mixing efficiency is based on the following fundamental equation:

$$\%\ \text{Mixing} = \frac{(Fg_{\text{partial mixed}} - \Sigma Fg_{\text{separate}})_{\text{ideal}}}{(Fg_{\text{100\% mixed}} - \Sigma Fg_{\text{separate}})_{\text{ideal}}} \qquad 1)$$

where $Fg_{\text{partial mixed}}$ is the mixed thrust without hardware losses.

All testing determines $Fg_{\text{partial mixed}}$ in combination with losses, therefore, to obtain the ideal $Fg_{\text{partial mixed}}$, the nozzle losses must be accounted for as follows:

$$\%\ \text{Mixing} = \frac{(Fg_{\text{partial mixed measured}} + Fg_{\text{losses}} - \Sigma Fg_{\text{separate ideal}})}{(Fg_{\text{100\% mixed}} - \Sigma Fg_{\text{separate}})_{\text{ideal}}}$$

The distinction must now be made that $(\Sigma Fg_{\text{separate ideal}})$ is the sum of the thrust from the primary and fan flows separately expanded, through ideal nozzles. For hot primary flows the above equation can be written as:

$$\%\ \text{Mixing} = \frac{\left(\dfrac{Fg_{\text{partial mixed measured}}}{\Sigma Fg_{\text{separate ideal hot}}} + \dfrac{Fg_{\text{losses}}}{\Sigma Fg_{\text{separate ideal hot}}} - 1\right)}{\left(\dfrac{Fg_{\text{100\% mixed}}}{\Sigma Fg_{\text{separate hot}}}\right)_{\text{ideal}} - 1}$$

$$\frac{Fg_{\text{partial mixed measured}}}{\Sigma Fg_{\text{separate ideal hot}}} = C_{V\ \text{hot}}$$

where $\Sigma Fg_{\text{separate ideal hot}}$ is the sum of the thrusts from the hot primary and the cold fan flows separately expanded through ideal nozzles.

Internal losses are as follows:

$$\frac{Fg_{losses}}{\sum Fg_{separate\ ideal\ hot}} = \frac{Fg_{losses}}{\sum Fg_{separate\ ideal\ cold}} \times \frac{\sum Fg_{separate\ ideal\ cold}}{\sum Fg_{separate\ ideal\ hot}}$$

$$= (1 - Cv_{cold}) \frac{\sum Fg_{separate\ ideal\ cold}}{\sum Fg_{separate\ ideal\ hot}}$$

where $\sum Fg_{separate\ ideal\ cold}$ is the sum of the thrusts from the cold primary and cold fan flows separately expanded through ideal nozzles.

The mixing efficiency equation becomes:

$$\%\ Mixing = \frac{Cv_{hot} + (1 - Cv_{cold})\left(\frac{\sum Fg_{separate\ ideal\ cold}}{\sum Fg_{separate\ ideal\ hot}}\right) - 1}{\left(\frac{Fg_{100\%\ mixed}}{\sum Fg_{separate\ hot}} - 1\right)_{ideal}} \qquad 2)$$

It is generally assumed in the industry that this equation can be reduced to:

$$\%\ Mixing = \frac{Cv_{hot} - Cv_{cold}}{\left(\frac{Fg_{100\%\ mixed}}{\sum Fg_{separate\ hot}}\right)_{ideal} - 1} \qquad 3)$$

This is only true if the nozzle area is reduced for the cold Cv determination and $\frac{W\sqrt{T_T}}{P_T}$ primary is kept constant for the hot and cold case, in which case $\sum Fg_{\text{separate ideal hot}} = \sum Fg_{\text{separate ideal cold}}$.

In this report the analysis has been conducted using Equation 3 rather than the more complex Equation 2. Use of Equation 3 reduced the mixing efficiency by approximately 3% relative to the values obtained by Equation 2.

It will be readily apparent that the use of the above equation requires the simultaneous determination of a cold Cv and a hot Cv at the same primary/secondary pressure ratios. It will be obvious that to accomplish this experimentally would require needless complication of the test procedure. Therefore, a polynomial curve fit through the Cv determined from the cold testing for each particular configuration is used to obtain a value of cold Cv at the same pressure ratio as obtained in the hot runs, allowing bypass ratio to vary. The mixing efficiency is then calculated for the individual points of the hot data runs using the individually calculated 100% mixing potential and the hot and cold Cv for each point, and plotted versus the mixed nozzle pressure ratio.

5.8.2 THEORETICAL MIXING POTENTIAL

It is important to recognize that the denominator in the equation is the 100% mixed potential. The geometry of the duct in which the mixing is accomplished and the local Mach numbers, even for the same inlet conditions of total pressure and temperature, influence the potential mixing gains. Thus, for any two configurations which produce the same pratical measurements of hot and cold Cv, the mixing efficiency can be different, merely because the duct geometry of one is different from the

other. The practical consideration of mixer design within certain physical constraints is therefore considered.

Figure 57 shows the 100% mixing potential for the JT8D-9, -109, -115 and -117 engine cycles based on the typical 727-200 takeoff roll and climb schedule of fan/primary pressure ratio as shown in Figure 20. This shows quite clearly that because of the slightly larger mixing plane area of the P&WA Reference configurations, the potential mixing benefit is greater, but not at all conditions. For the JT8D-117 engine, for instance, the potential of the Boeing configuration is greater at cruise than that for the P&WA configuration, indicating for that engine cycle, that the Boeing mixing area is closer to the optimum than the P&WA. Figure 57 also shows how sensitive the mixing potential is to the pressure ratio. The reduction in mixing potential is marked at the takeoff pressure ratio for the JT8D-117 engine in particular and the JT3D-115 less so, but these are purely dependent on the engine cycle fan/primary pressure ratio and reflect the real life situation in the engine.

It is noteable that the magnitude of the potential is not a large quantity. The differences between the Boeing and P&WA potentials are close to the bounds of the ability of any rig to differentiate real differences with any significance, even for a well designed test. In some instances where Cv-hot minus Cv-cold is the same for two configurations, it is impossible to legitimately show mixing efficiency differences even though it is known that there should be a mixing efficiency difference because of the denominator of the relationship.

5.8.3 PRACTICAL MIXING EFFICIENCY

Since mixing efficiency is a function of the difference between two velocity coefficients (each of which is subject to both the within run and between run errors, as discussed in Section 5.9),

and this difference is compared to a small maximum potential, it is to be expected that the data scatter of mixing efficiency would be large. Figures 58 and 59 showing the mixing efficiencies for the JT8D-9, -109, -115, and -117 engines, respectively, comparing the P&WA and Boeing Configurations, illustrate clearly that this is so. Non-mathematical mean lines have been ascribed to the respective configurations. Statistically, there is no justification whatsoever to support any difference between the respective configurations in any one engine group. The maximum mixing potential is only 1.80% for the JT8D-109 thus an error in either hot or cold velocity coefficient of 0.0016 (for one standard deviation) will result in approximately a 10% change in mixing efficiency. The typical standard deviation about any run is of this magnitude, which means the 95% confidence limit for velocity coefficient is 0.0032 which is reflected as 20% on the mixing efficiency curves. Thus the scatter of the data in mixing efficiency does not appear unreasonable. The detection of 6% and 5% changes due to mixing potential, therefore, becomes impossible and is buried in the total data scatter.

The magnitude of the mixing efficiency is higher than was expected for these configurations particularly at takeoff where about 25-30% was customarily expected. The cruise levels are close to expectations.

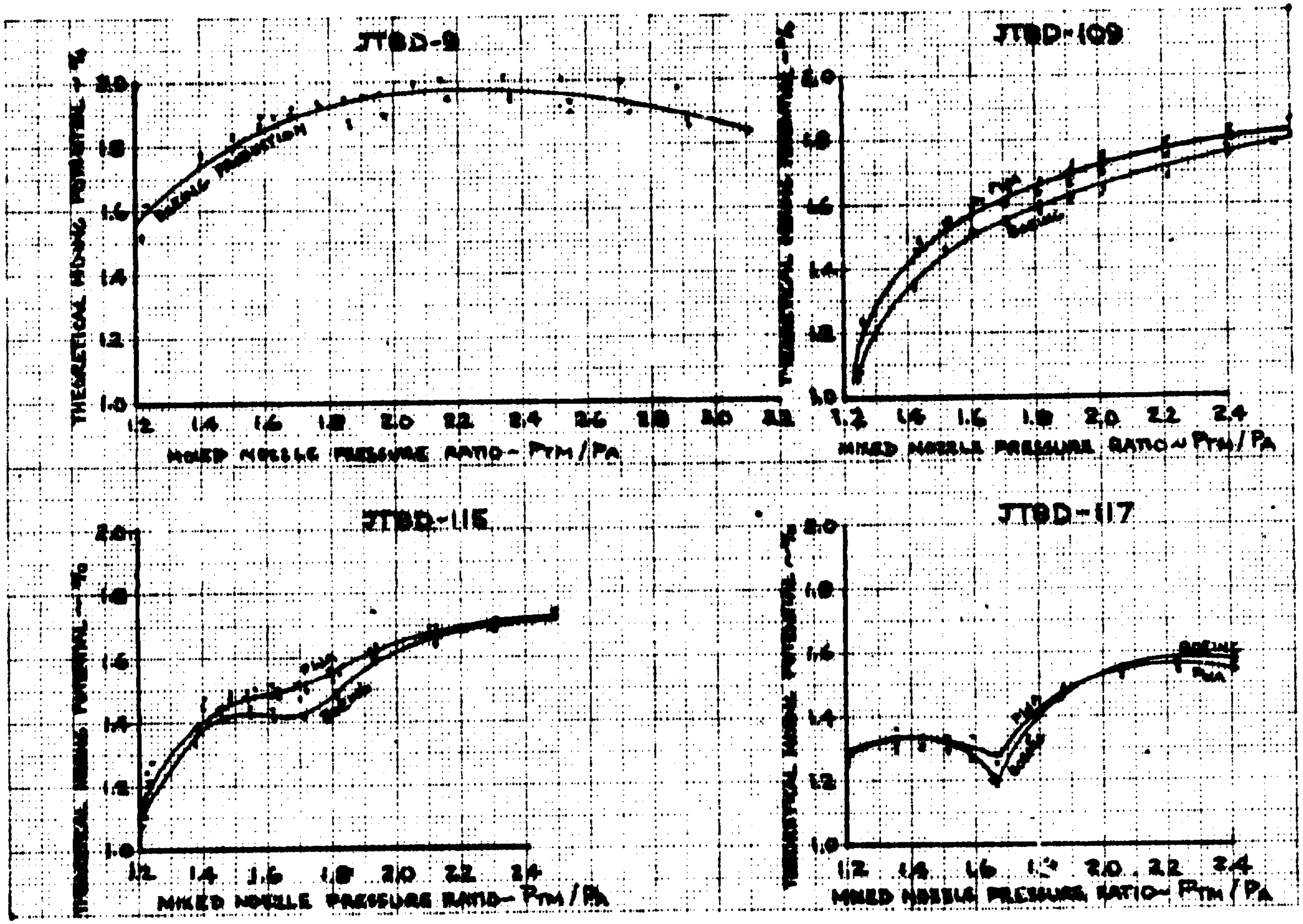

FIGURE 57 - 100% THEORETICAL MIXING POTENTIAL

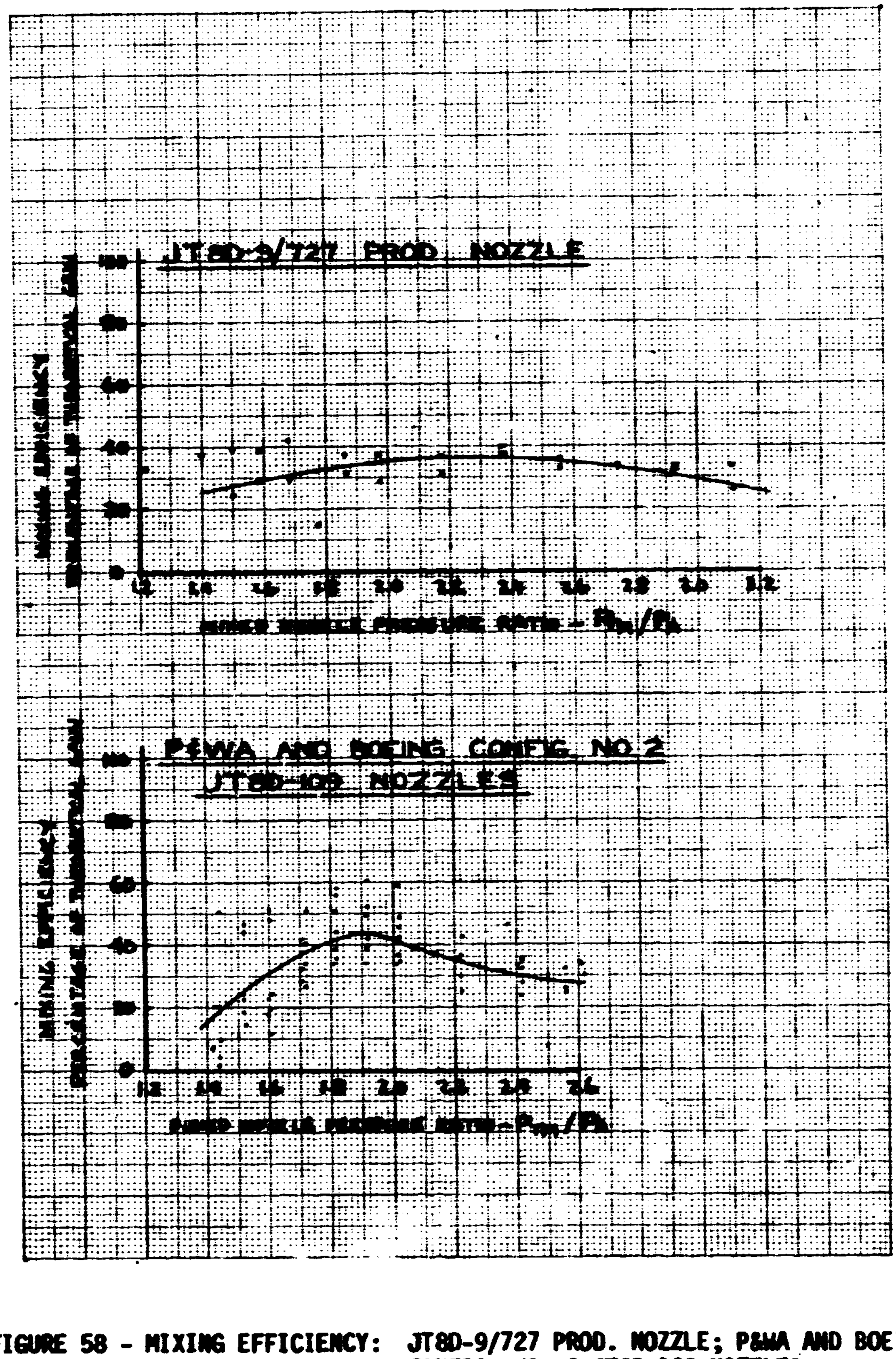

FIGURE 58 - MIXING EFFICIENCY: JT8D-9/727 PROD. NOZZLE; P&WA AND BOEING CONFIG. NO. 2 JT8D-109 NOZZLES

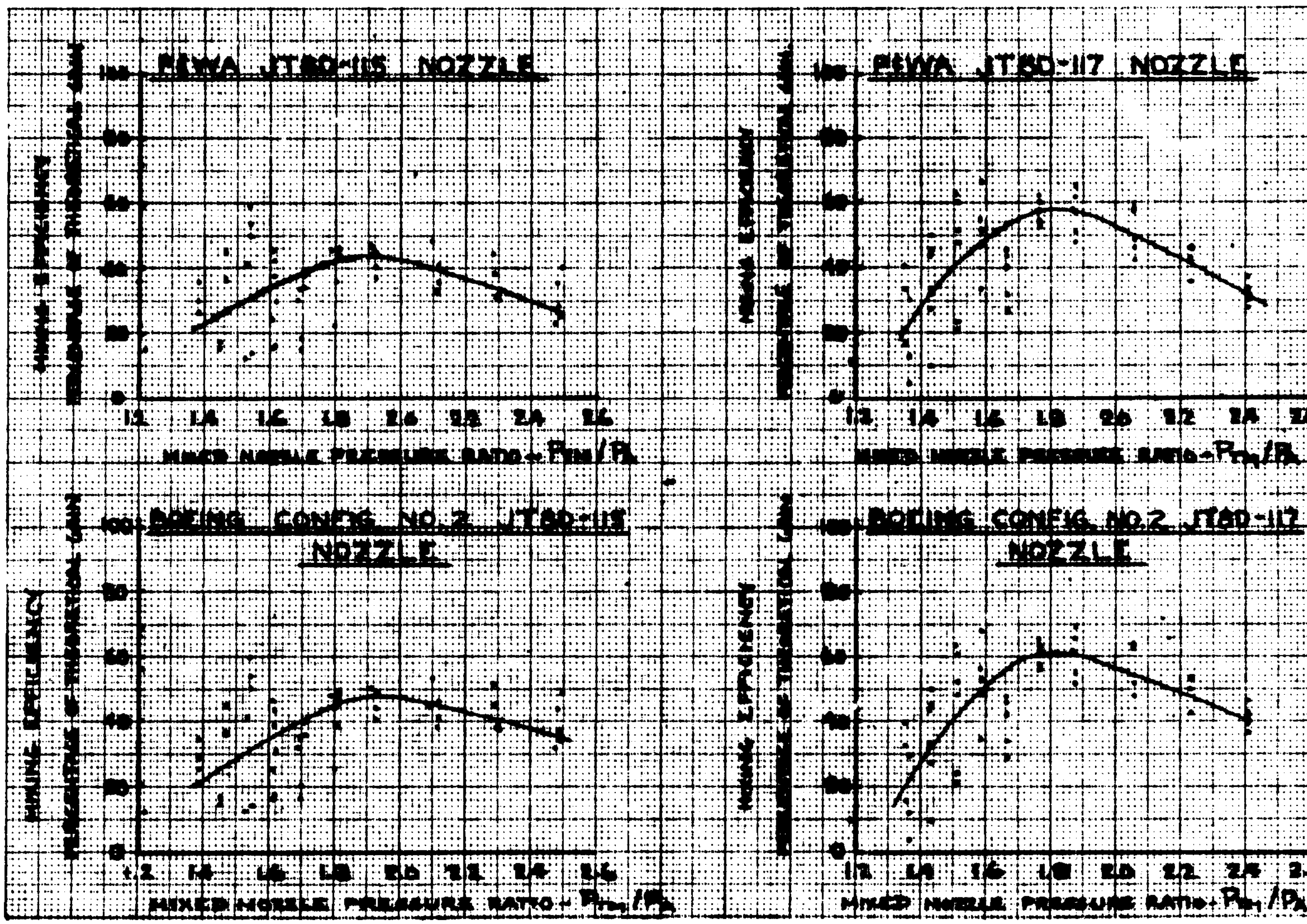

FIGURE 59 - MIXING EFFICIENCY: P&WA AND BOEING CONFIG. NO. 2 JT8D-115 AND -117 NOZZLES

5.9 DATA ACCURACY

5.9.1 GENERAL DISCUSSION OF ERRORS AND TEST TECHNIQUE

Section 4.5.2 discussed the design of the test in terms of selecting the number of data points per run and the number of runs.

The aim of all testing is usually to determine either the absolute performance level for a configuration or the difference between two or more configurations or both. The absolute levels or the comparative levels of performance can never be determined precisely. All test data is, therefore, aimed at getting the best estimate or an adequate estimate (for the purposes of the test) of the true absolute or comparative levels of the parameters by which the test articles will be compared. These estimates will have a degree of confidence, or measurement of the reliability, with which the estimated level is known. The greater the surety required in the comparison, the greater the confidence which must be established for each configuration. This, in essence, means more data.

The question now is, what kind of data? It can be shown that errors in many independent and dependent variables contribute to the error in any particular parameter which is used as the final comparison in the data sequence, for instance, nozzle velocity coefficient. These factors include instrumentation accuracy, random force balance errors due to the rig shifts, environmental effects on hardware, model instrumentation installation and running stresses, and test hardware assembly differences from build to build. It is well known that if, for a particular test run, the number of data points is increased, the confidence with which the resulting level for that particular configuration, of that particular build, on that particular day, on that particular rig, under that particular set of rig zero

shifts etc., can be improved. This is true whether the number of points is increased at a particular point (as at a particular pressure ratio setting) or over the range of pressure ratios of interest. However, the two methods have different impact on the knowledge and deductions one can make concerning the data, and care must be taken as to how the data is used, being cognizant of how it was recorded. This is again a part of the "design of the experiment." Knowledge of the intended use of the data must be considered in order to determine how the data is to be taken.

Returning to the above example, it will be clear that unless more than one run is made, certain errors will not influence the total knowledge of a configuration. Again, if the rig is not shut down between runs and the rig instrumentation re-zeroed, if only one build of the test hardware is made, or if all the testing is done on one day very close together in time; then the knowledge of certain errors which influence the measured performance of a configuration will be unknown. Obviously, certain requirements for the best estimate of the true level of performance of a configuration are costly to obtain mainly due to increased rig occupancy time to permit the incorporation of the above requirements. Therefore, only certain elements of all the variables can be incorporated with the inevitable consequence of reduced confidence in the true level of a particular configuration. Note that it is the inclusion of factors which are known to contribute to errors, not their rejection, that improves the final confidence.

The first and obvious requirement is the need to increase the number of runs. If by fortuitous circumstances these runs are distributed in time (as in the case of this test) then certain of the other errors will be partially incorporated. To a certain extent, the same basis that controls the improvement in the knowledge of any particular level of one run by increasing

the number of data points taken applies to the number of runs; two runs are vastly better than one, and three are better than two. Increasing the number of runs for the statistical analysis is the only way that improvement in the ability to determine differences in configurations can be accomplished if the number of data points per run has already reached the point of diminishing returns to improve the within run variance. In this case, it is the between run variance which is dominant.

All tests aimed at determining best estimates of true level with any degres of reasonable confidence should aim to have two builds of the configuration. Here again, this prolongs the test time. For this test, the desire to measure mixing plane and exit plane pressure and temperature surveys made it convenient to run all performance work first and then rebuild the configurations for the surveys. This gave the opportunity to retake data for some configurations and thereby introduce the build-to-build errors.

5.9.2 BASIC PRINCIPLES OF THE STATISTICAL ANALYSIS

An existing Boeing analysis of variance computer program was used to examine the data points of each individual run, (eleven per run in the majority of the test described herein) and a least squares curve fitted through each run. The computer program then calculates the variance of the data about the curve at any desired pressure ratio, weighting the contribution that the data at pressure ratios further from the point of interest has on the determination of the variance at the point of interest and the best estimate of that point. It does this for each configuration. Currently, the computer program requires a choice of curve fit order by the operator. As stated in Section 4.5.2 the velocity coefficient curve is usually a third or second order curve, moreover the quantity of data per run taken in this test does not justify higher order curve fits even were this desirable.

In general, the selected curve fit is that which has the lowest order such that the next higher order does not significantly alter the variance about the curve. Naturally, the higher the order of curve fit, the lower the within run variance, but the increasing amount of waviness introduced with increasing order eventually defeats the purpose of the curve fit which is to obtain the best estimate at any particular point based on the weighted contribution of all the data recorded. This introduction of waviness can be overcome by a significance check on the polynomial terms and eliminating insignificant terms, but this computer program addition is not yet available.

For any one configuration, the curve fits through all the runs together with the within run variance are needed to calculate a variance between runs. The variance between runs and about each run and the data distribution versus pressure ratio for each of the configurations tested, together with the best estimate of the value of the coefficient being compared at the point of interest, are submitted to a statistical "F Test." This type of test examines whether differences exist between two or more collections of data or whether they belong to an indistinguishable family. An "F statistic" is computed at the 95% confidence level for (I-1), (J-1)(I) degrees of freedom, where I is the number of configurations being compared and J is the number of runs per configuration. The analysis of variance program computes the data necessary to perform an "F-Test." This is then used to compare the "F statistic" value computed with a standard statistics text book "F" value at 95% confidence for (I-1), (J-1)(I) degrees of freedom.

The "F statistic" is computed to test the hypothesis that there are no differences between the configurations being examined. If the "F statistic" computed from the data is greater than the "F statistic" calculated for the same number of degrees of

freedom in a standard statistics text book, the hypothesis is rejected. The implications of the acceptance or rejection of the hypothesis will be discussed later.

Basically two things are of importance here. First, the value of the "F statistic" computed for the data of the configurations being compared is dependent on the variance about each run and the variance between runs. It is important that both configurations have the same number of runs to ensure that, if possible, the distribution of the errors in the data, both within and between runs, be normally distributed. This is why it is important that the data be recorded in a similar manner for each configuration. This ensures that, provided the errors introduced are normally distributed, there is an even chance for cases with insufficient data that the random introduction of error is at least of even probability. In simpler words, the configurations have at least been run with the best chance of getting data of equal quality, so that the experiment is not compounded at the outset and the statistical examination can operate within the normal error distribution constraints imposed upon it. The "F statistic" computed will become larger for better quality data and smaller for smaller differences between the configurations being examined. Second, the value of the "F statistic" from the standard statistics text book gets smaller for a higher number of degrees of freedom. It is obvious that, for (I-1), (J-1)(I) degrees of freedom, the larger I or J, the greater the degrees of freedom. This shows that the fewer the configurations being compared (I), the greater the number of runs per configuration (J) must be to avoid making the acceptance of the hypothesis too coarse. Note that the probability of making the error of accepting the hypothesis when it should be rejected and vice versa is always reduced by increasing both I and J. It is also important to note that any statistical test is invalid for only one run per configuration.

5.9.3 HYPOTHESIS ACCEPTANCE AND REJECTION AND POSSIBILITY OF TYPE 2 ERRORS

To understand the concept of "sameness" it is important to appreciate the meaning of certainty and that nothing is known with absolute precision. If the performance of two nozzles for instance were known precisely, then they would only be the "same" if they were identical. But the performance is not known precisely; some tolerance on the absolute true level exists. Statistics, therefore, compares two performances which are known indistinctly and estimates whether there is enough evidence to conclude they are different, when they are different, or they are the same, when they are the same.

Testing of the hypothesis in this test report was conducted on each configuration at all pressure ratios, between 1.6 and 2.5 at 0.1 intervals. Acceptance of the hypothesis at the 95% confidence level states: there is 95% confidence that the nozzle performance levels are the same, when the data says they are the same. Similarly, rejection of the hypothesis states: there is 5% chance the nozzles are the same when the data says they are different. The "F Test" of the hypothesis is thus a go/no-go test. These statements leave something to be desired and lead to the discussion of what is terms in statistical parlance, Type II errors. Type II errors are always associated with a tolerance band. Stated simply, Type II errors are a measure of the risk of making an incorrect decision.

This is where the important concept of "sameness" links up with the design of the experiment. A decision has to be made as to what qualifies as "the same". Assume for a moment that two nozzles will be counted the same if the velocity coefficients are within 0.0010 of each other. If the data is of sufficient accuracy to resolve differences to this order of magnitude, then two things happen. First, if the nozzles are the "same"

then the hypothesis will be accepted. Second, there is a small probability, say 5%, of accepting the hypothesis they are the same when they are really different by 0.005. There is a larger probability, say 40% of accepting the hypothesis they are the same when they are really different by 0.003, and a larger probability, say 70%, of accepting them as the same when they are really 0.0015 different. Now assume for this same set of data that the definition of "sameness" is changed to 0.0020. It will be apparent that nothing changes regarding the acceptance or rejection of the hypothesis by the "F statistic" as the data hasn't changed. However, the percentage probability of the Type II error at the level of the new acceptance tolerance is lower than it was for the more critical acceptance.

In practice, the percentage probability of Type II error for any particular chosen tolerance of "sameness" can be regarded as a measure of the quality of the test. If, for instance, the probability of accepting the hypothesis that two nozzles are the same when they are really different by 0.0020 is 80%, and the experimenter really wanted to be sure the nozzles were no different than 0.0010, then the data is telling him that it is inadequate for the task. This can be due to insufficient data, usually runs per configuration, or points per run if these have been small and insufficient to support the order of regression curve through the data. It may also indicate, that for all practical purposes, the rig is of insufficient quality to obtain data in a cost effective manner to satisfy the experiment.

In this case, the experimenter must either change his rig or his "criteria of acceptance of sameness."

Currently, the statistical analysis of variance program does not calculate the Type II errors. An estimate of the Type II error for this test indicates a 50% probability of there being a 0.0020 difference in two configurations when the hypothesis is accepted.

5.9.4 RESULTS OF COMPARISONS AND DATA MERGING

When the hypothesis is accepted, the best estimate of the weighted mean at the point of comparison is provided. In this case, all the points and runs of the configurations being compared are combined. Because of the increased number of points a least squares curve fit of much higher order is permissible. The technique used was to use the least order curve fit which showed the curve fitted velocity coefficient at any pressure ratio to vary by no more than 0.0002 from the velocity coefficient at any pressure ratio for the next highest order regression curve.

When the hypothesis is rejected, a similar technique is used through the respective data points for each configuration and the statistics program output is the best esitmate of the weighted coefficients at the point of comparison.

Table VI shows the configurations compared, the run numbers, the degrees of freedom of the F statistic, the value of the F statistic from a standard statistics text book for the same number of degrees of freedom, the pressure ratio at which the hypothesis was accepted or rejected, and the standard deviation about the runs and between runs.

Based upon the statistical results of Table VI, two curves for the JT8D-109 nozzles, one hot CV, the other cold CV, were generated for the P&WA and Boeing nozzle data combined (see Figures 28 and 29).

Hot Cv for the Boeing Config. No. 2 and P&WA Reference JT8D-115 nozzles were combined to produce Figure 30. Similarly the hot Cv for the JT8D-117 combined the data for Boeing Config. No. 2 and P&WA reference to produce Figure 31.

The cold Cv for the P&WA Reference JT8D-115 and JT8D-117 nozzles is the same and was obtained by combining the two sets of data to produce one curve, Figure 33. Similarly the cold Cv for the Boeing Config. No. 2 JT8D-115 and JT8D-117 nozzles uses the combined data to produce Figure 32.

The statistical analysis showed that there was a definite difference between the first set of runs for the P&WA Reference JT8D-109 and JT8D-115 nozzles and the second set following a failure and subsequent rebuild of the fan duct instrumentation section. The decision was made to reject the first set of data so that the comparisons between the configurations were made with a common instrumentation section build. This did not detract from the build-to-build differences between the same nozzle because in many cases this was still accomplished. However, it did eliminate a source of difference, the inclusion of which must add to the validity of the absolute level. Since all nozzles were not run with two instrumentation section builds, the elimination of the earlier run was unfortunate, but necessary.

In every comparison, the number of runs for each configuration must be the same. Therefore, a doubling of a run or runs to make up a run deficit on a configuration devoid of a second build run was used.

The method of analysis used in this report will become gradually more sophisticated as the computer program is further developed. Suffice it to say, the current analysis is considered a superior technique to the blind acceptance of the data represented by one run of a few data points as adequate representation of a configuration for comparative analysis. It also avoids the pitfalls of considering two configurations different when the quality of the data does not permit that conclusion.

TABLE VI - STATISTICAL ANALYSIS COMPARISONS

TEST CONFIGURATION (T.C.)	RUNS USED	ENGINE CYCLE JT8D	NO. OF RUNS COMPARED	DEGREES OF FREEDOM (I-1)(J-1)(I)	95% CONF. 'F' TEST FOR (I-1)(J-1)(I) DEGREES OF FREEDOM	HYPOTHESIS OF SAMENESS ACCEPTANCE OR REJECTION: PRESSURE RATIOS AT WHICH HYPOTHESIS REJECTED	HYPOTHESIS OF SAMENESS ACCEPTANCE OR REJECTION: PRESSURE RATIOS AT WHICH HYPOTHESIS ACCEPTED	TYPICAL STANDARD DEVIATION ABOUT RUNS ΔC_{V_N}	AVERAGE STD. DEV. BETWEEN RUNS WHEN HYPOTHESIS ACCEPTED ΔC_{V_N}
3 P&WA 7 TBC	187,194,195 64,65,182	-109	3 3	1,4	7.7086	—	ALL	.00145 .00157	.00065
4 P&WA 19 TBC	216,221,222 226-228	-109 (with swirl)	3 3	1,4	7.7086	—	ALL	.00207 .00241	.00036
3 P&WA 5 P&WA	187,194,195 48-50	-115	3 3	1,4	7.7086	ALL	—	.00145 .00173	—
3 P&WA 6 P&WA	187,194,195 54-56	-109 -117	3 3	1,4	7.7086	ALL	—	.00145 .00114	—
7 TBC 11 TBC	64,65,182 109-111	-109 -115	3 3	1,4	7.7086	1.6-2.3	2.4,2.5	.00157 .00119	—
7 TBC 18 TBC	64,65,182 136-138	-109 -117	3 3	1,4	7.7086	ALL	—	.00157 .00119	—
5 P&WA 6 P&WA	48,48,49 54-56	-115 -117	3 3	1,4	7.7086	1.7-2.0	1.6,2.1,*2.2* 2.3,2.4	.00147 .00114	—
11 TBC 18 TBC	109-111,170 136,137,2X138	-115 -117	4 4	1,6	5.9874	1.8-2.4	1.6,1.7*	.00120 .00112	—
5 P&WA 11 TBC	2X48,49,50 109-111,170	-115 -115	4 4	1,6	5.9874	—	ALL	.00156 .00120	.00067
6 P&WA 18 TBC	54-56 136-138	-117 -117	3 3	1,4	7.7086	—	ALL	.00114 .00119	.00044
11 TBC 9 TBC	109-111 101-103	-115 W/W.O. SHORT PLUG	3 3	1,4	7.7086	—	ALL	.00108 .00108	.00025
5 P&WA 9 TBC	48-50 101-103	-115 REF TO SHORT PLUG	3 3	1,4	7.7086	—	ALL	.00173 .00108	.00050

* THE PROBABILITY OF TYPE II ERROR IS LARGE FOR THESE CASES, WHERE, ALTHOUGH THE HYPOTHESIS IS ACCEPTED OR REJECTED AS A GO/NO-GO TEST, THE DIFFERENCES IN THE "F" TEST VALUES ARE SMALL.

TABLE VI - (CON'T) STATISTICAL ANALYSIS COMPARISON

TEST CONFIGURATION (T.C.)	RUNS USED	ENGINE CYCLE JT8D	NO. OF RUNS COMPARED	DEGREES OF FREEDOM (I-1), (J-1)(I)	95% CONF. 'F' TEST FOR (I-1),(J-1)(I) DEGREES OF FREEDOM	HYPOTHESIS OF SAMENESS ACCEPTANCE OR REJECTION: PRESSURE RATIOS AT WHICH HYPOTHESIS REJECTED	PRESSURE RATIOS AT WHICH HYPOTHESIS ACCEPTED	TYPICAL STANDARD DEVIATION ABOUT RUNS ΔC_{V_M}	AVERAGE STD DEV. BETWEEN RUNS WHEN HYPOTHESIS ACCEPTED ΔC_{V_M}
8 TBC 15 TBC	75-77 88-90	-115 -117	3 3	1,4	7.7086	—	ALL	.00154 .00151	.00021
8 TBC 11 TBC	75-77,77 109-116,170	-115 -115	4 4	1,6	5.9874	2.2-2.5	1.6-2.1	.00154 .00120	—
5,11 PAMA/TBC 8,15 TBC/TBC	48,48-50,109-111,170 75-77,77;88,88-90	-115 -115/117	6 6	1,14	4.6001	2.1-2.2	1.6-2.0,2.3*	.00138 .00154	—
15 TBC 18 TBC	88-90 136-138	-117 -117	3 3	1,4	7.7086	1.6-2.2	2.3-2.4	.00151 .00119	—
6,18 PAMA/TBC 8,15 TBC/TBC	54-56,136-138 75-77,88-90	-117 -115/-117	6 6	1,14	4.9646	1.7-2.1	2.2-2.4	.00117 .00153	—
15 TBC 16 TBC	88-90 94-96	-117 -117	3 3	1,4	7.7086	—	ALL	.00151 .00164	.00037
17 TBC 18 TBC	82-84 136-138	-117 -117	3 3	1,4	7.7086	1.8-2.1	1.6,1.7 2.2-2.4	.00125 .00119	—
3 PAMA 7 TBC	186,2X196,197 57-60	-109 COLD -109 COLD	4 4	1,6	5.9874	—	ALL	.00166 .00222	.00100
5 PAMA 11 TBC	2X46,47 104-106	-115 COLD -115 COLD	3 3	1,4	7.7086	1.9-2.3	1.6-1.8*,2.4	.00093 .00113	—
6 PAMA 18 TBC	51-53 143-145	-117 COLD -117 COLD	3 3	1,4	7.7086	2.0-2.4	1.6-1.9*,2.5	.00236 .00196	—
5 PAMA 6 PAMA	2X46,47 51-53	-115 COLD -117 COLD	3 3	1,4	7.7086	—	ALL	.00093 .00236	.00024
11 TBC 18 TBC	104-106 143-145	-115 COLD -117 COLD	3 3	1,4	7.7086	—	ALL	.00113 .00196	.00026

* THE PROBABILITY OF TYPE II ERROR IS LARGE FOR THESE CASES, WHERE, ALTHOUGH THE HYPOTHESIS IS ACCEPTED OR REJECTED AS A GO/NO-GO TEST, THE DIFFERENCES IN THE "F" TEST VALUES ARE SMALL.

6.0 CONCLUSIONS

The following is a summary of the conclusions drawn during this model test program:

- The objectives of the test were accomplished with adequate accuracy and all nozzles tested showed good performance.
- The Boeing Config. No. 2 and P&WA Reference nozzles for the JT8D-109 have the same performance which is slightly lower than the current uninstalled performance for the JT8D-9/727 Boeing production nozzle (i.e. without thrust reverser).
- The Boeing Config. No. 2 and P&WA Reference nozzles for the JT8D-115 have the same performance which is slightly better than the current uninstalled performance for the JT8D-9/727 Boeing production nozzle (i.e. without thrust reverser).
- The Boeing Config. No. 2 and P&WA Reference nozzles for the JT8D-117 have the same performance which is better than the current uninstalled performance for the JT8D-9/727 Boeing production nozzle (i.e. without thrust reverser).
- Larger plug options for the Boeing Config. No. 2 nozzles result in reduced takeoff performance but, in general, suffer no losses at cruise.
- The Boeing Config. No. 2 and P&WA Reference nozzles for the JT8D-109 have the same flow coefficient at all pressure ratios and accomplished the desired flow coefficient reduction at low pressure ratios to reduce the engine idle thrust.
- The Boeing Config. No. 2 and P&WA Reference nozzles for the JT8D-115 have small differences in flow coefficient except at the cruise pressure ratios where they are the same.

PRECEDING PAGE BLANK NOT FILMED

- The Boeing Config. No. 2 and P&WA Reference nozzles for the JT8D-117 have small differences in flow coefficient except at the cruise pressure ratios where they are the same.

- The splitter surface static pressures on the models were not sufficiently close to the splitter trailing edge to provide any useful data regarding mixing plane match.

- The Boeing Config. No. 2 and P&WA Reference nozzles show that the bypass ratio required was reasonably well achieved, indicating the configurations were close to the required mixing plane match.

- The effect of nozzle area variation on the model mixing plane match (bypass ratio) was found to be as great as the effect of splitter position.

- Swirl in the primary flow passage of the magnitude simulated in this test reduced the nozzle performance of the Boeing Config. No. 2 and P&WA Reference nozzles by an equal amount. The reduction amounted to approximately 0.55% at takeoff and 0.27% at cruise.

- Mixing efficiency of the JT8D-100 series nozzles was better than had been expected with 30% to 60% of the theoretical thrust gains available at takeoff pressure ratio and 30% to 40% at cruise.

- Mixing plane and exit plane survey data were obtained which indicated all nozzles were behaving as expected.

7.0 DATA PRESENTATION

7.1 DATA DESCRIPTION

Each configuration tested has a set of graphs plotted for it which consist mostly of the following and are in groups for each configuration in Section 7.2:

1) Velocity coefficient (C_V), as a function of primary nozzle pressure ratio showing both hot and cold runs at the engine designated fan-to-primary total pressure ratio.

2) Mixed velocity coefficient (C_{V_M}) as a function of the mixed nozzle pressure ratio showing both hot and cold runs at the engine designated fan-to-primary total pressure ratio.

3) Flow coefficient (C_D) for hot and cold runs as a function of primary nozzle pressure ratio.

4) Mixed flow coefficient (C_{D_M}) for hot and cold runs as a function of mixed nozzle pressure ratio.

5) Fan-to-primary total pressure ratio (P_{T_F}/P_{T_P}) compared to the engine pressure ratio schedule versus primary nozzle pressure ratio.

6) Mixed nozzle pressure ratio (P_{T_M}/P_A) versus primary nozzle pressure ratio.

7) Bypass ratio (W_{FAN}/W_{PRI}) versus primary pressure ratio.

8) Splitter static pressure ratio (P_{S_P}/P_{S_F}) versus primary nozzle pressure ratio.

7.2 PLOTTED DATA FOR EACH TEST CONFIGURATION

7.2.1 TEST CONFIGURATION (T.C.) NO. 1

Configuration Description: Long radius 4-inch ASME nozzle.
Plotted Data: (See Section 4.6 for figures)

Figure 21 - Velocity Coefficient; Runs 14-19.
Figure 22 - Flow Coefficient; Runs 14-19.
Figure 23 - Gross Thrust Correction; Runs 14-19.
Figure 24 - Velocity Coefficient; Runs 240-242.
Figure 25 - Flow Coefficient; Runs 240-242.
Figure 26 - Gross Thrust Correction; 240-242.

7.2.2 TEST CONFIGURATION (T.C.) NO. 2

Configuration Description: JT8D-9/727 production nozzle.

Hardware Designations:

Outer Nozzle Wall	Splitter	Plug	Exit
C2	S1	P1	E2

Plotted Data:

Figure 60 - Velocity Coefficient; Runs 20-23, 155-158.
Figure 61 - Mixed Velocity Coefficient; Runs 20-23, 155-158.
Figure 62 - Flow Coefficient; Runs 20-23, 155-158.
Figure 63 - Mixed Flow Coefficient; Runs 20-23, 155-158.
Figure 64 - Fan/Primary Total Pressure Ratio; Runs 20-23, 155-158.
Figure 65 - Mixed Nozzle Pressure Ratio; Runs 20-23, 155-158.
Figure 66 - Bypass Ratio; Runs 20-23, 155-158.

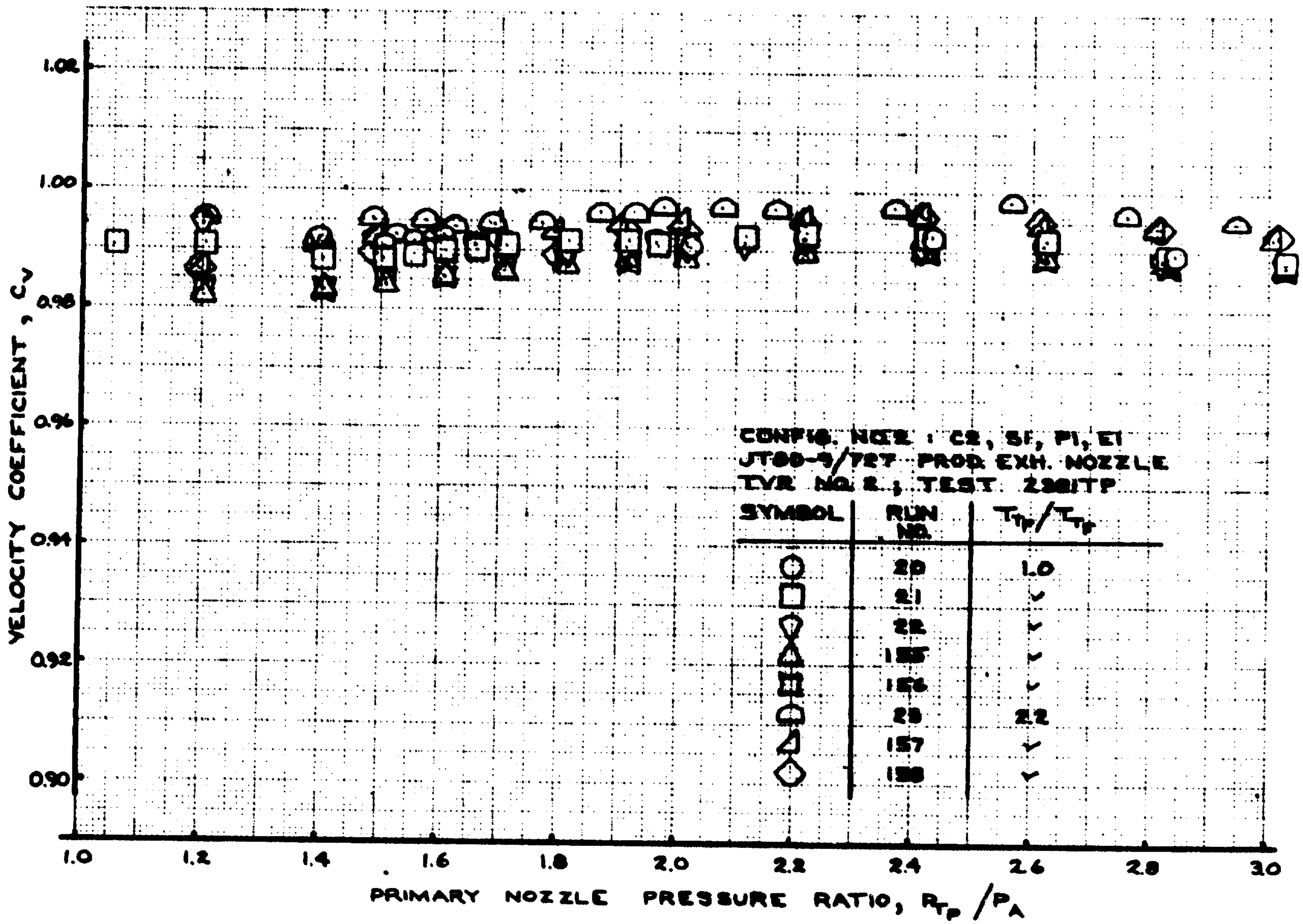

FIGURE 60 - VELOCITY COEFFICIENT
TEST CONFIG. NO. 2; RUNS 20-23, 155-158

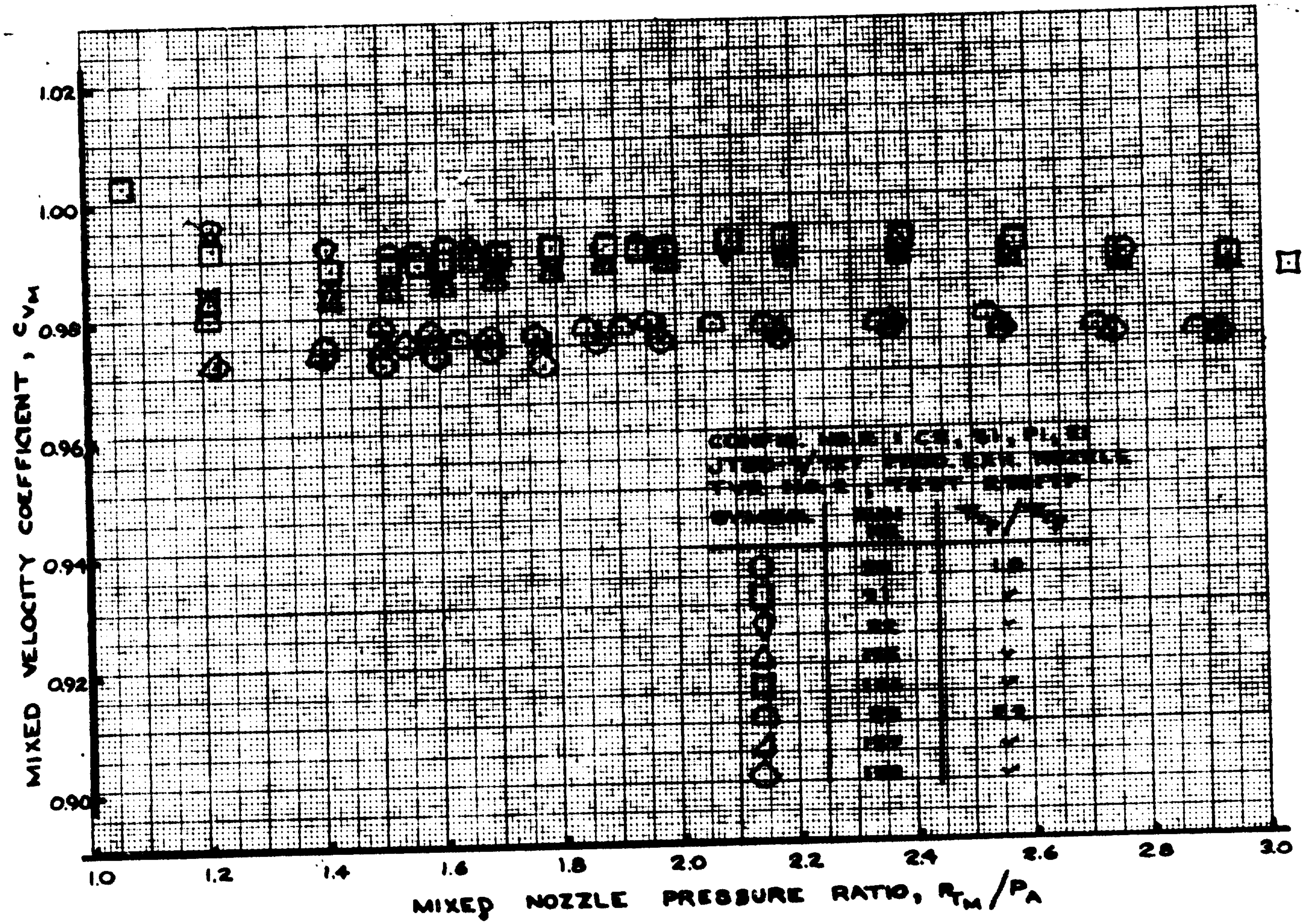

FIGURE 61 - MIXED VELOCITY COEFFICIENT
TEST CONFIG. NO. 2; RUNS 20-23, 155-158

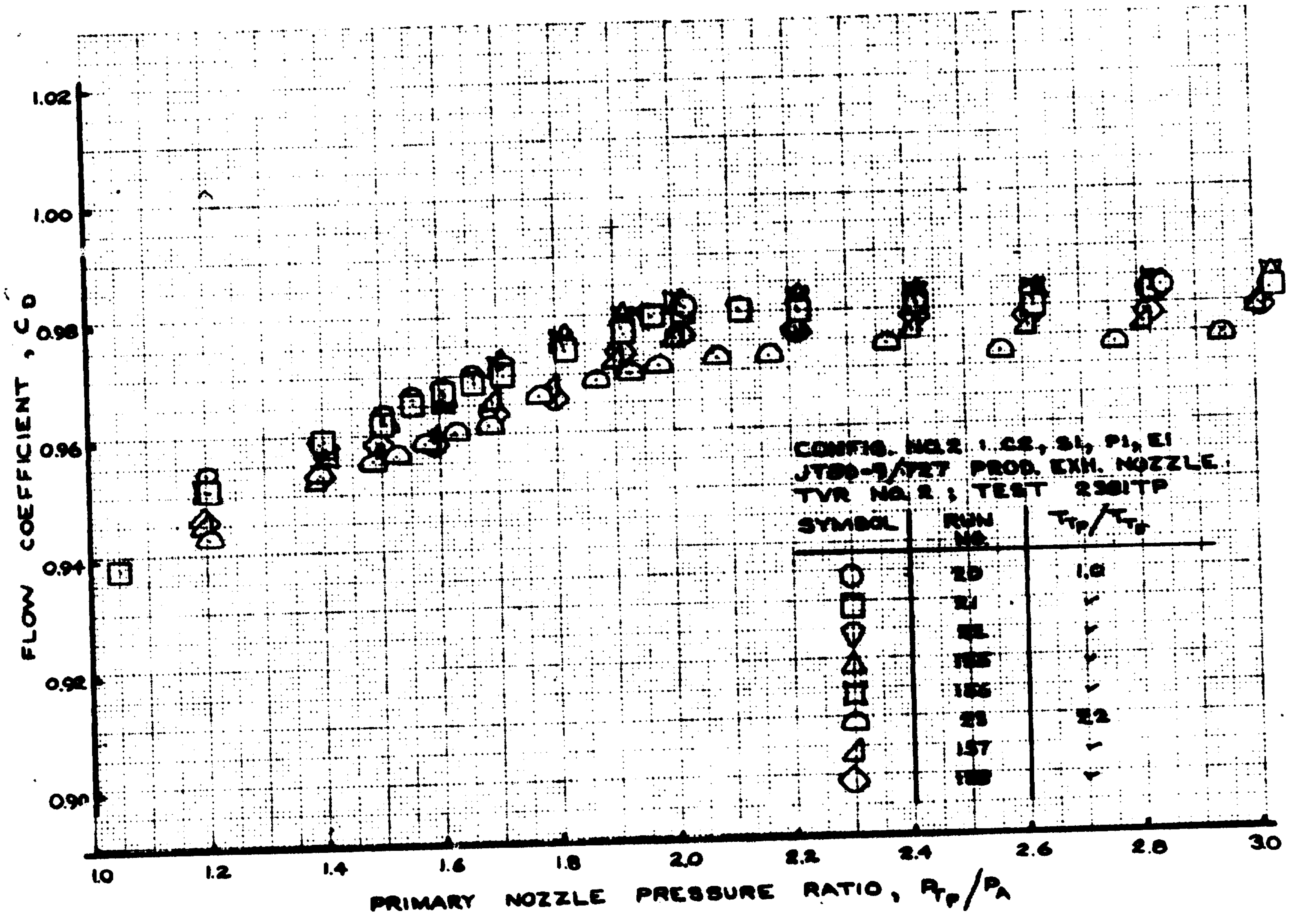

FIGURE 62 - FLOW COEFFICIENT
TEST CONFIG. NO. 2; RUNS 20-23, 155-158

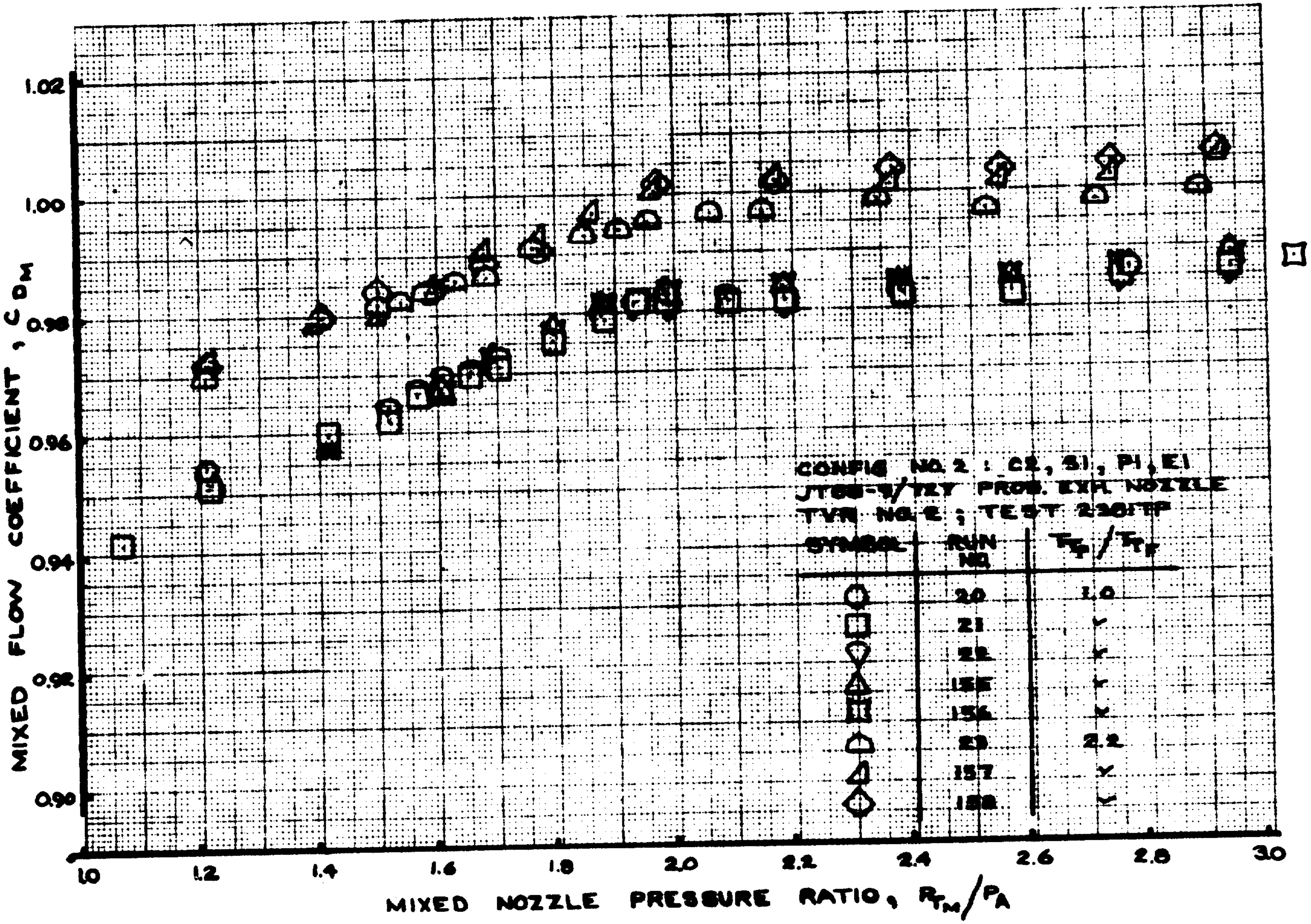

FIGURE 63 - MIXED FLOW COEFFICIENT
TEST CONFIG. NO. 2; RUNS 20-23, 155-158

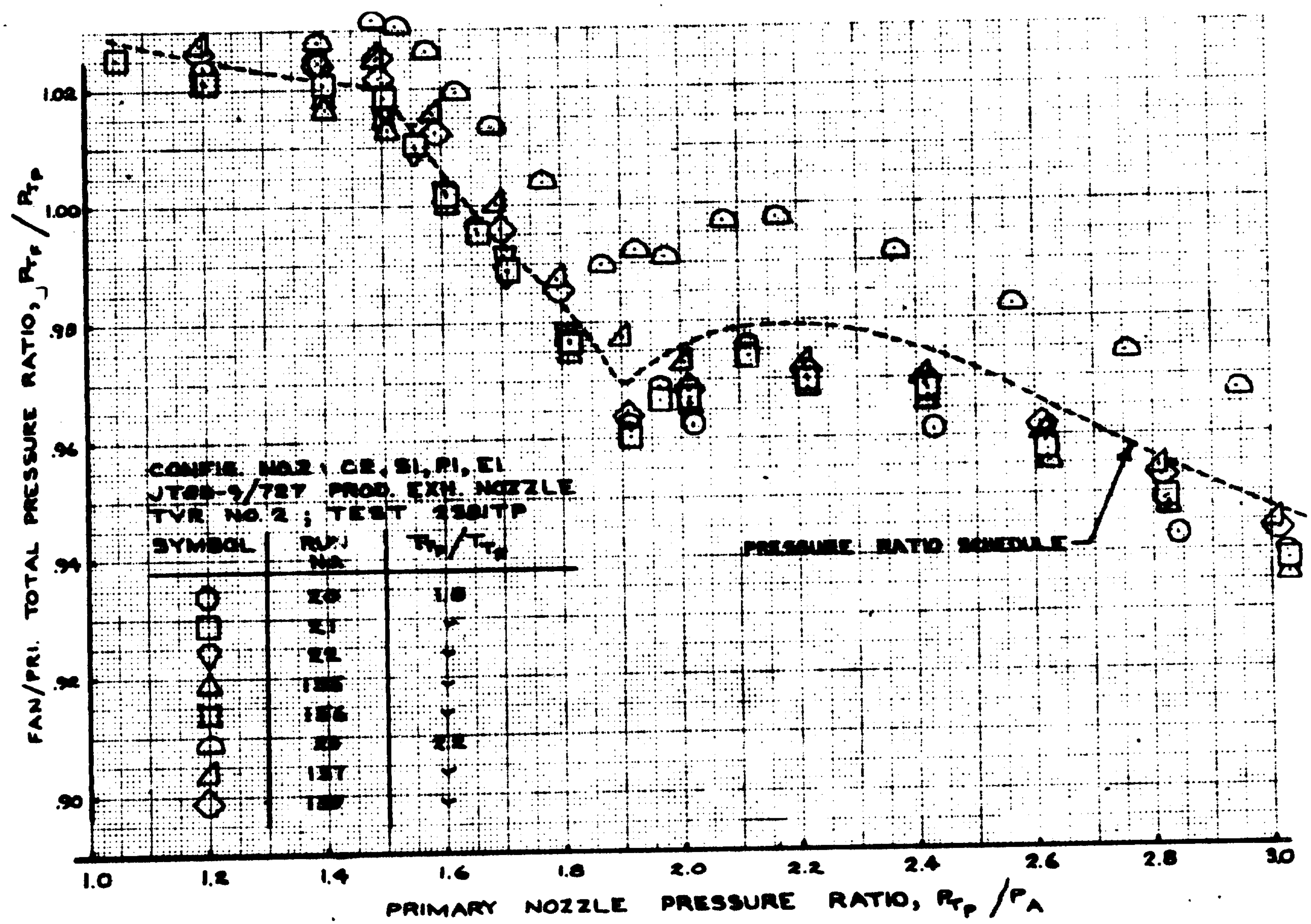

FIGURE 64 - FAN/PRIMARY TOTAL PRESSURE RATIO
TEST CONFIG. NO. 2; RUNS 20-23, 155-158

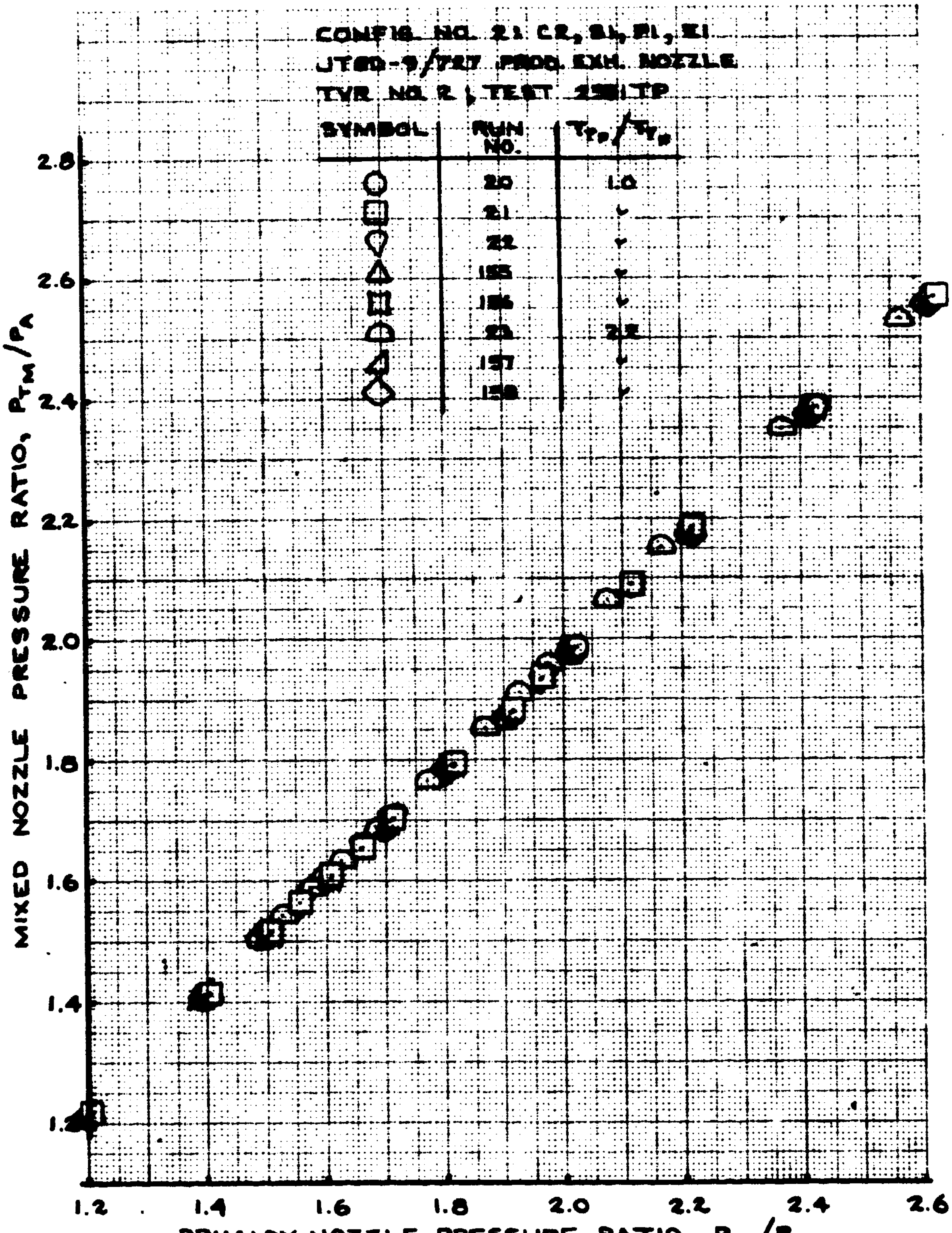

FIGURE 65 - MIXED NOZZLE PRESSURE RATIO
TEST CONFIG. NO. 2; RUNS 20-23, 155-158

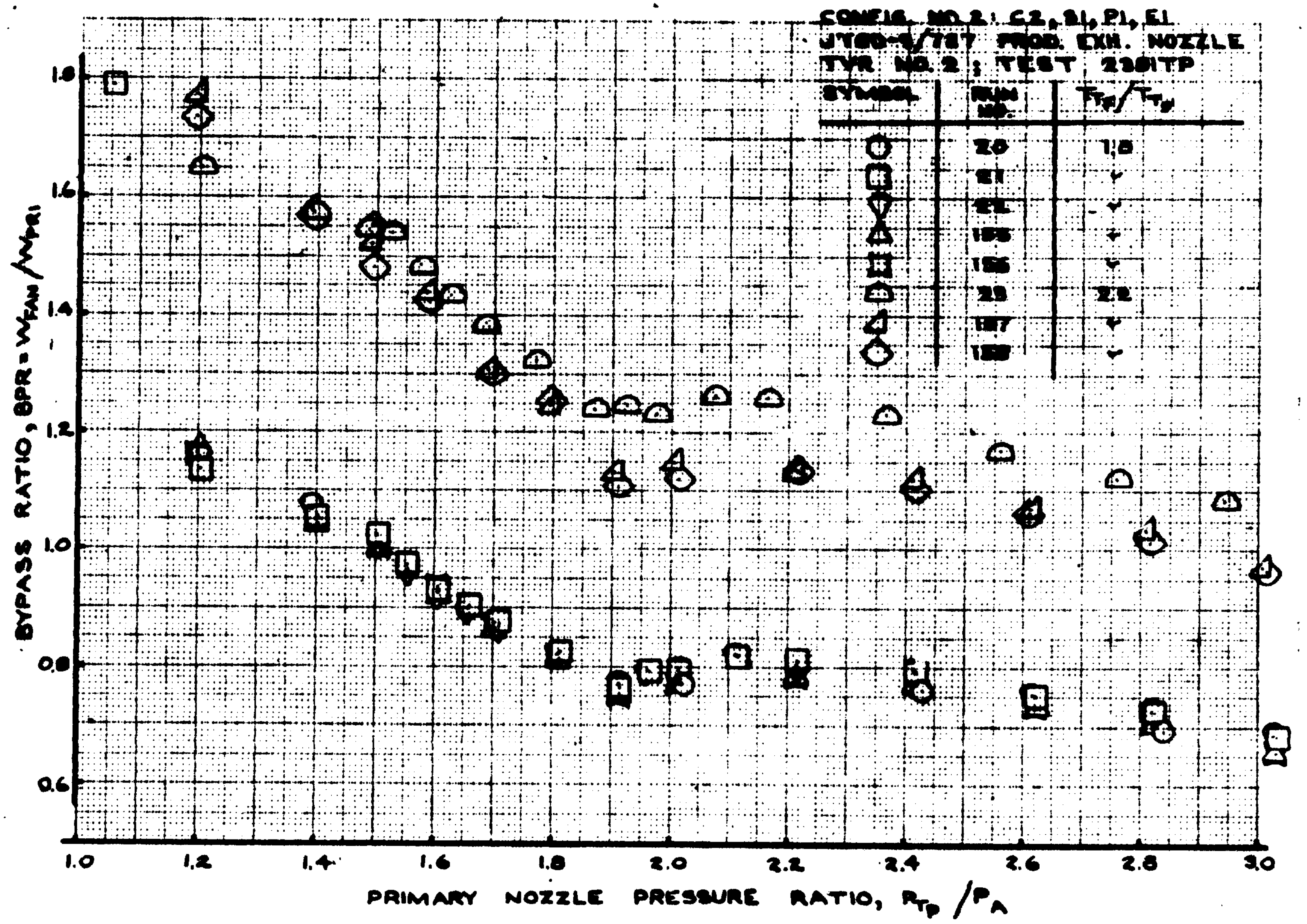

FIGURE 66 - BYPASS RATIO
TEST CONFIG. NO. 2; RUNS 20-23, 155-158

7.2.3 TEST CONFIGURATION (T.C.) NO. 3

Configuration Description: P&WA Reference nozzle for JT8D-109

Hardware Designations:

Outer Nozzle Wall	Splitter	Plug	Exit
C3	S2	P2A	E2

Plotted Data:

Figure 67 - Velocity Coefficient; Runs 27-32.
Figure 68 - Mixed Velocity Coefficient; Runs 27-32.
Figure 69 - Flow Coefficient; Runs 27-32.
Figure 70 - Mixed Flow Coefficient; Runs 27-32.
Figure 71 - Fan/Primary Total Pressure Ratio; Runs 27-32.
Figure 72 - Mixed Nozzle Pressure Ratio; Runs 27-32.
Figure 73 - Bypass Ratio; Runs 27-32.
Figure 74 - Splitter Static Pressure Ratio; Run 31.
Figure 75 - Velocity Coefficient; Runs 186, 187, 194-197.
Figure 76 - Mixed Velocity Coefficient; Runs 186, 187, 194-197.
Figure 77 - Flow Coefficient; Runs 186, 187, 194-197.
Figure 78 - Mixed Flow Coefficient; Runs 186, 187, 194-197.
Figure 79 - Fan/Primary Total Pressure Ratio; Runs 186, 187, 194-197.
Figure 80 - Bypass Ratio; Runs 186, 187, 194-197.

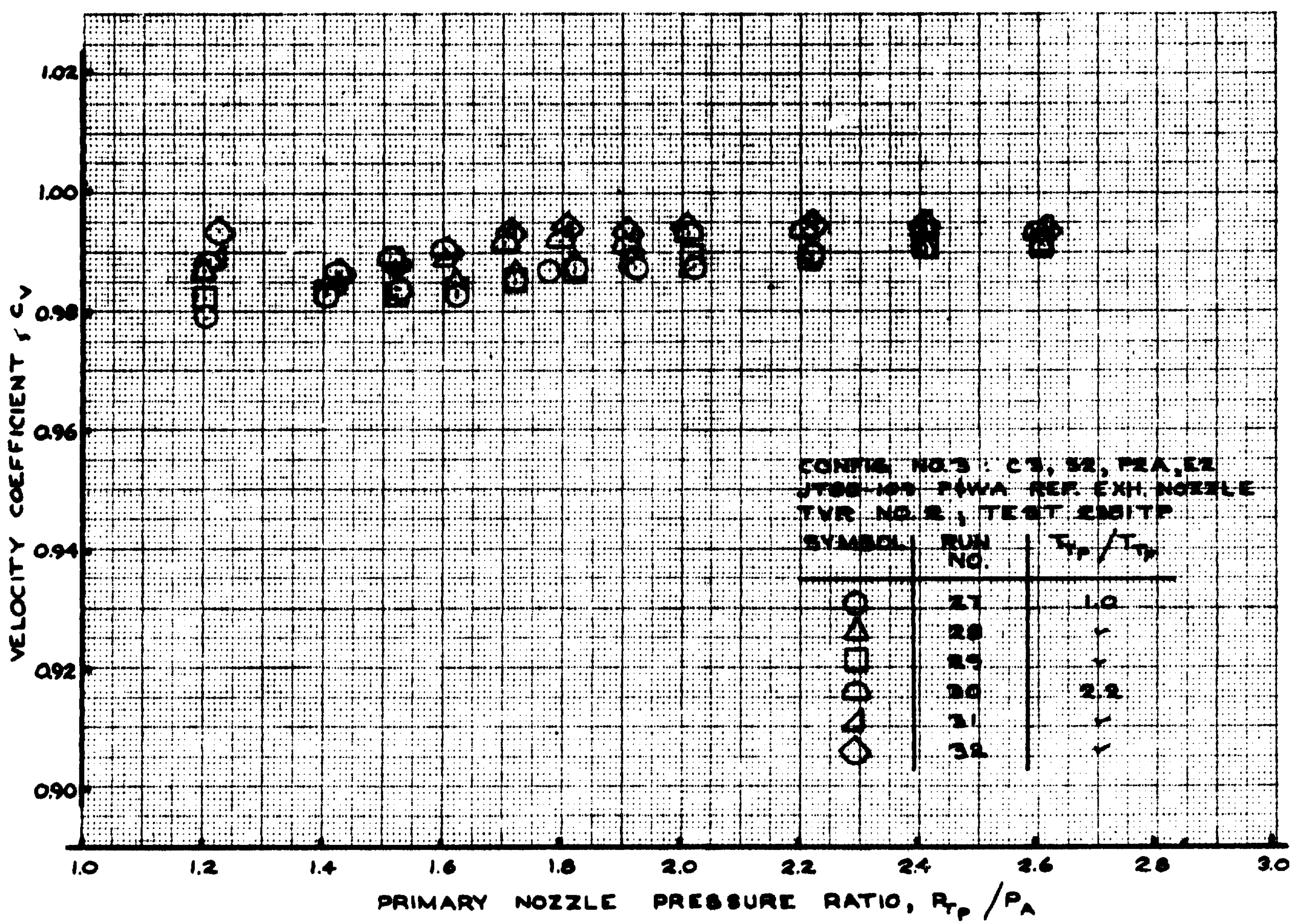

FIGURE 67 - VELOCITY COEFFICIENT
TEST CONFIG. NO. 3; RUNS 27-32

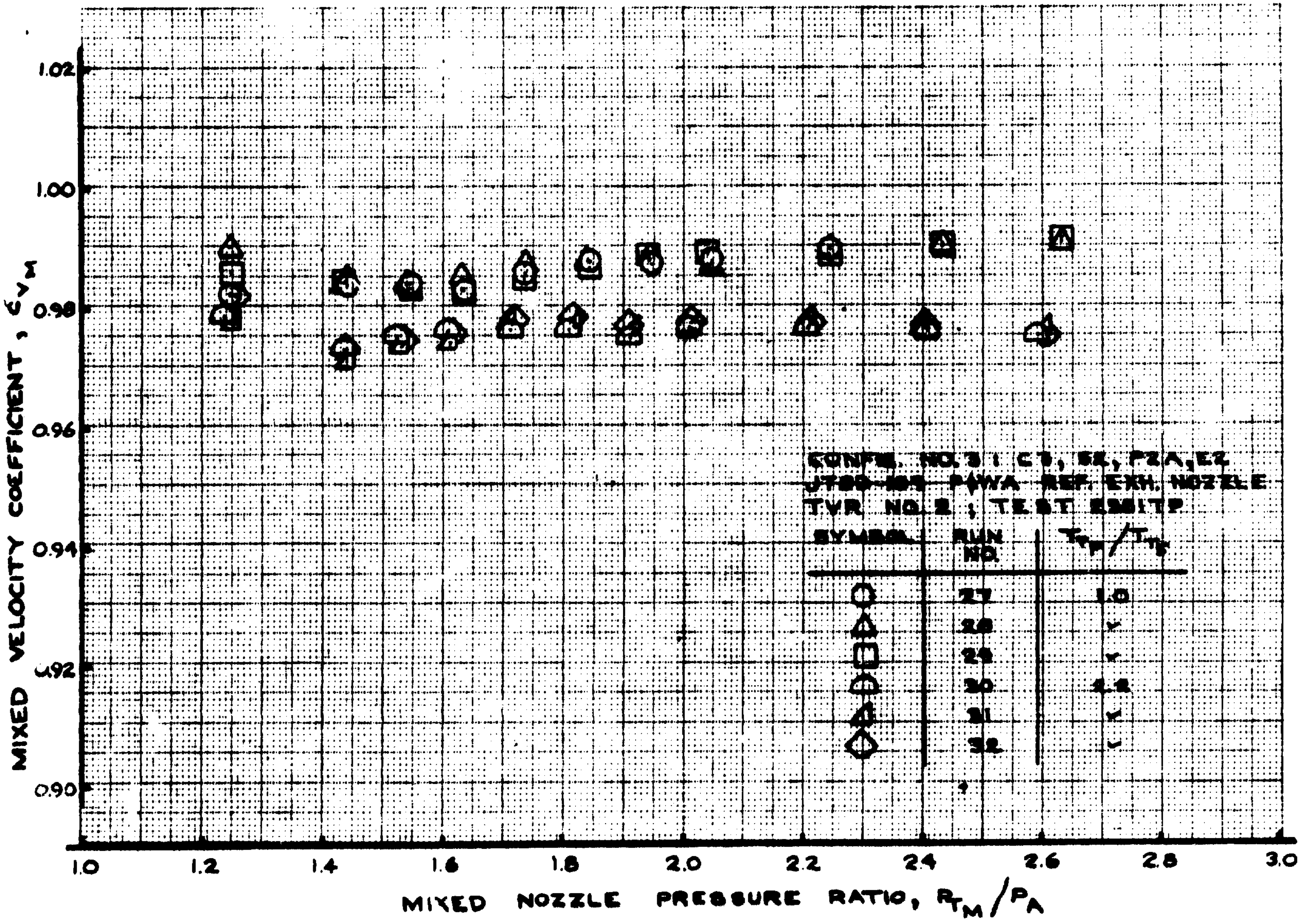

FIGURE 68 - MIXED VELOCITY COEFFICIENT
TEST CONFIG. NO. 3; RUNS 27-32

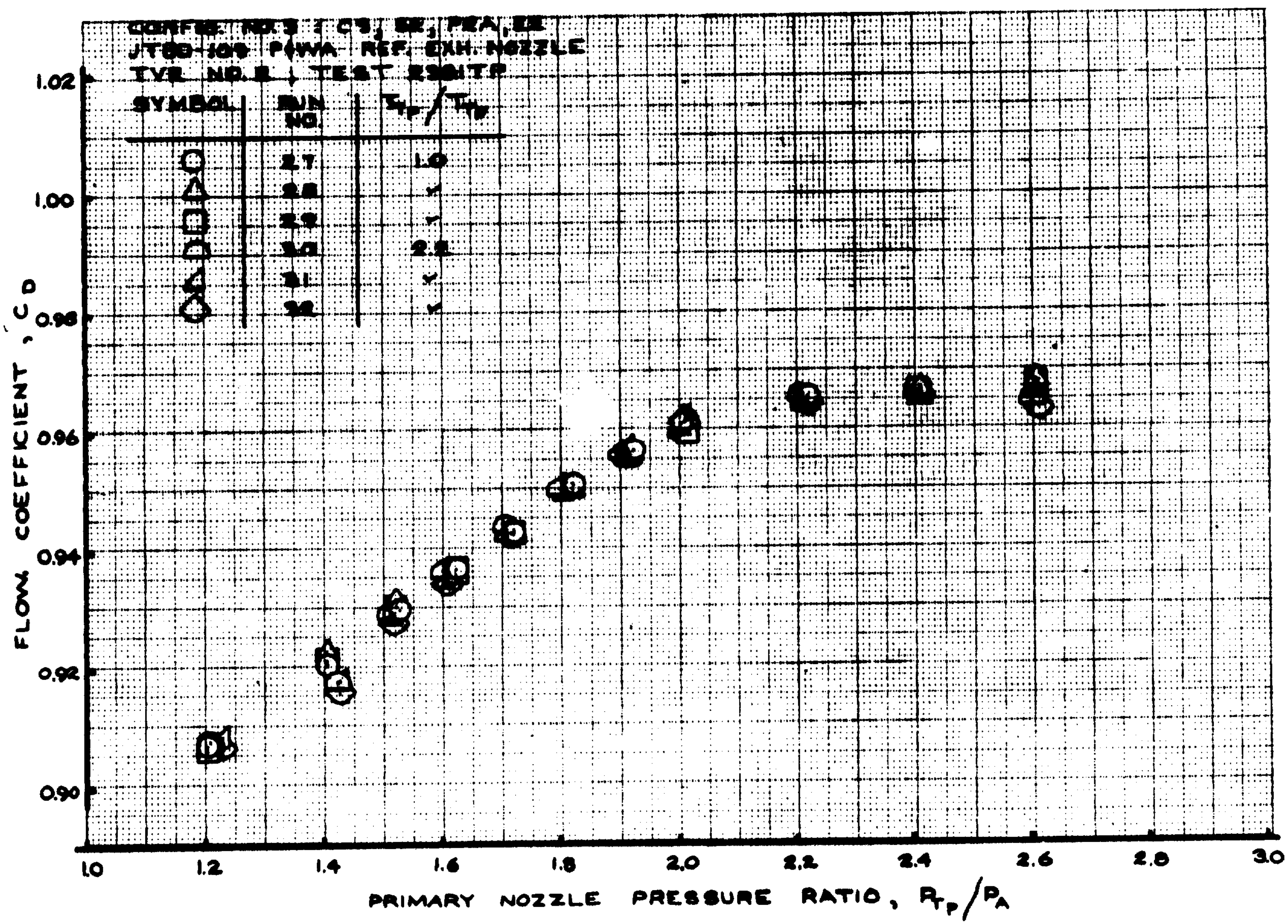

FIGURE 69 - FLOW COEFFICIENT
TEST CONFIG. NO. 3; RUNS 27-32

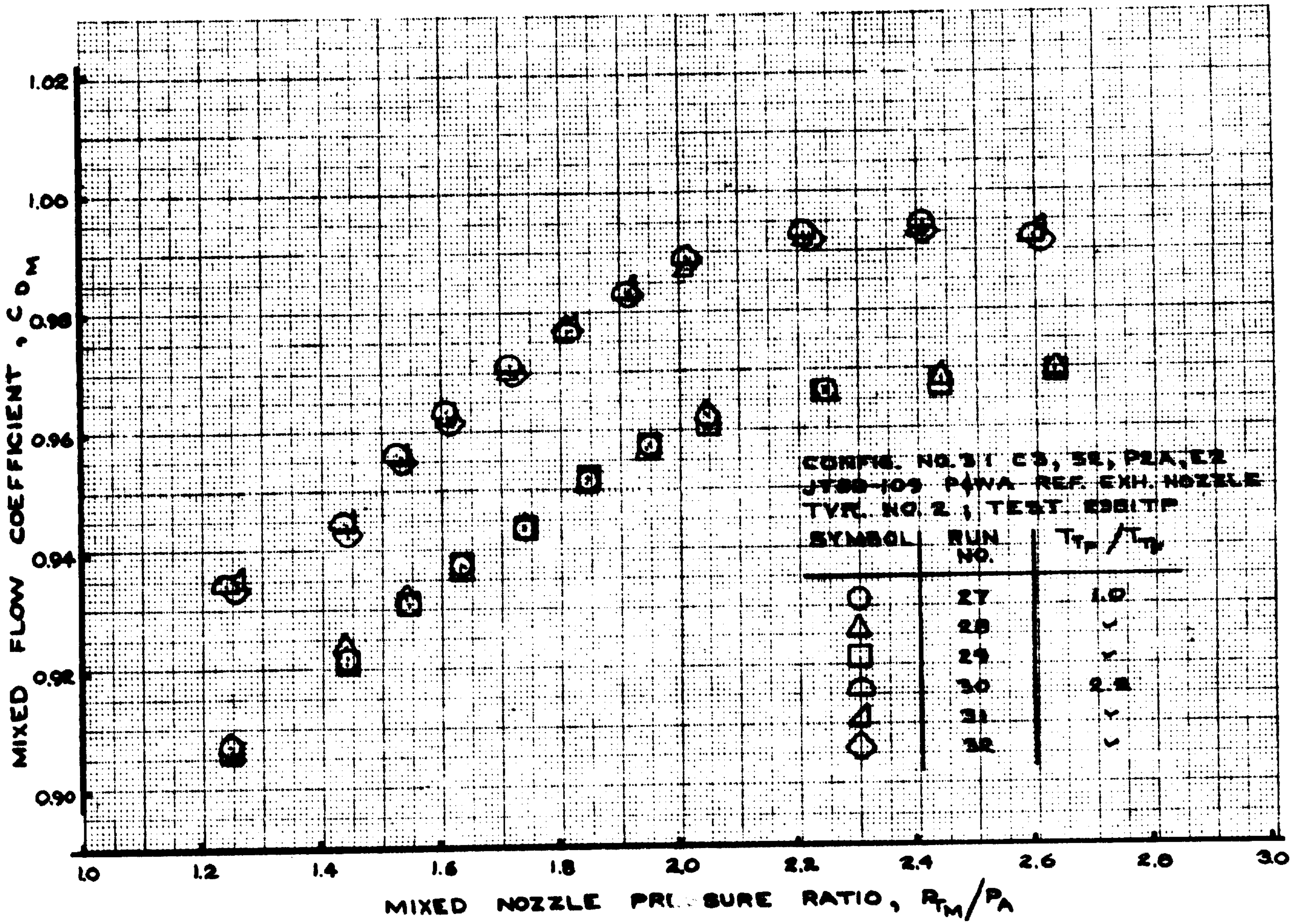

FIGURE 70 - MIXED FLOW COEFFICIENT
TEST CONFIG. NO. 3; RUNS 27-32

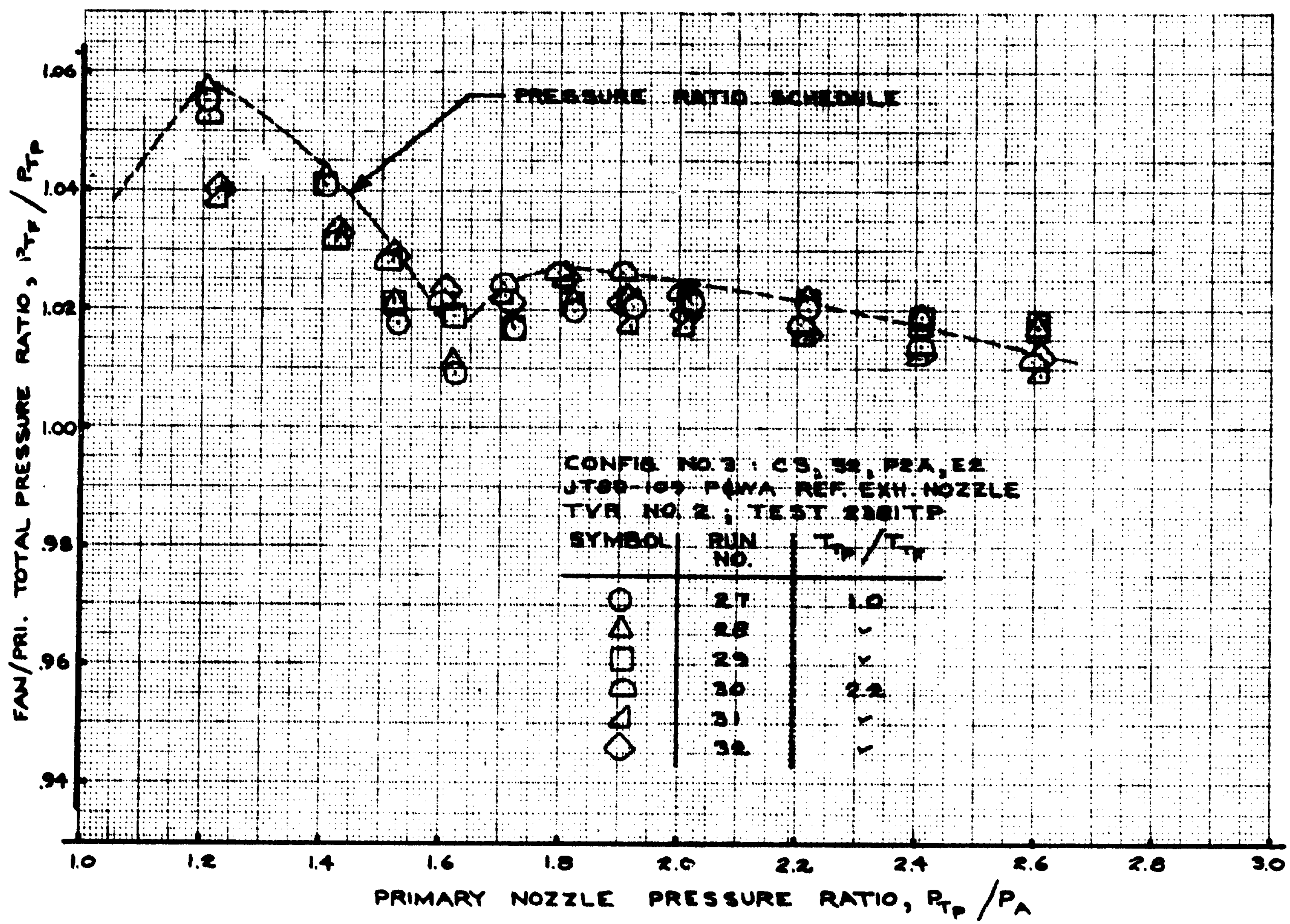

FIGURE 71 - FAN/PRIMARY TOTAL PRESSURE RATIO
TEST CONFIG. NO. 3; RUNS 27-32

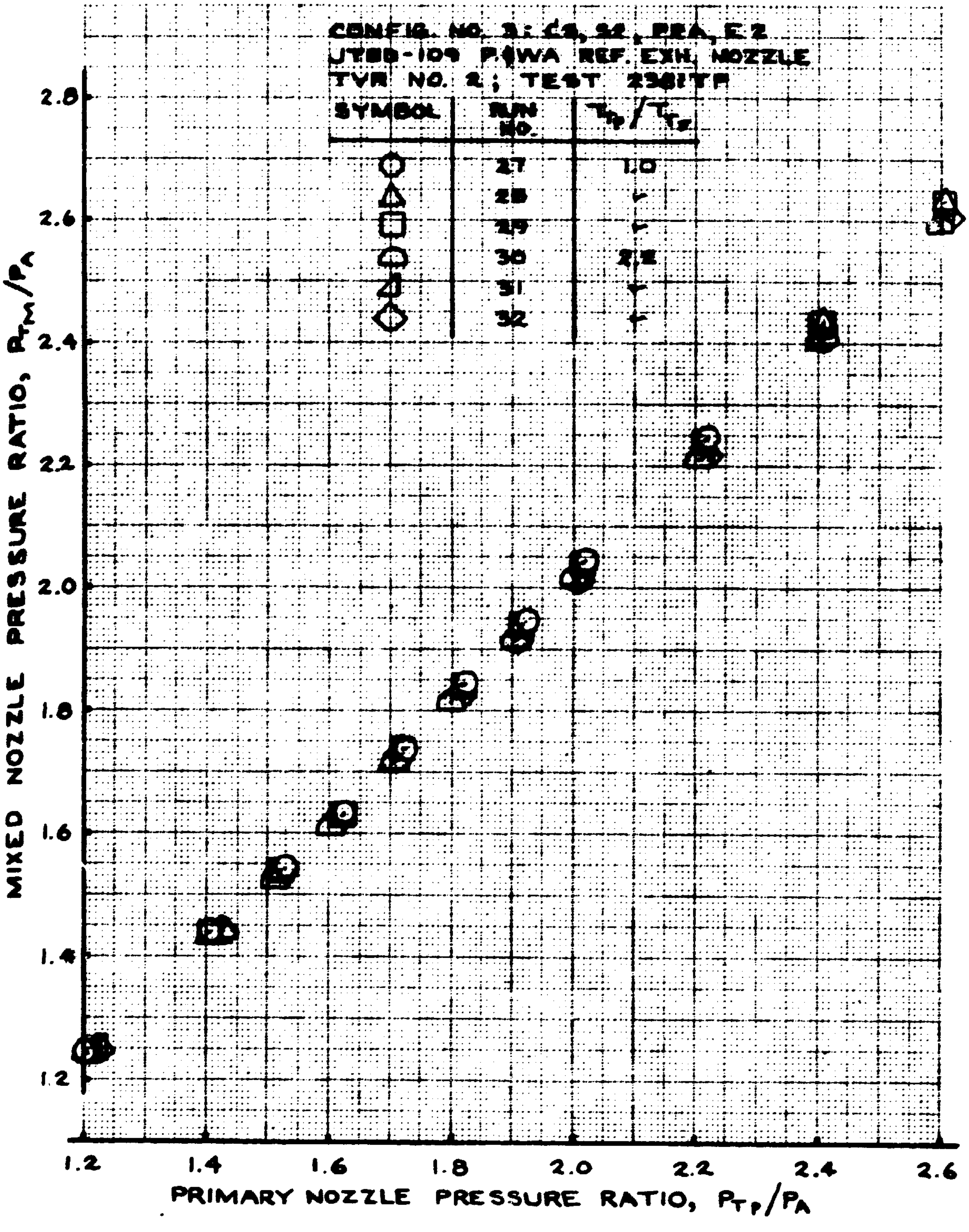

FIGURE 72 - MIXED NOZZLE PRESSURE RATIO
TEST CONFIG. NO. 3; RUNS 27-32

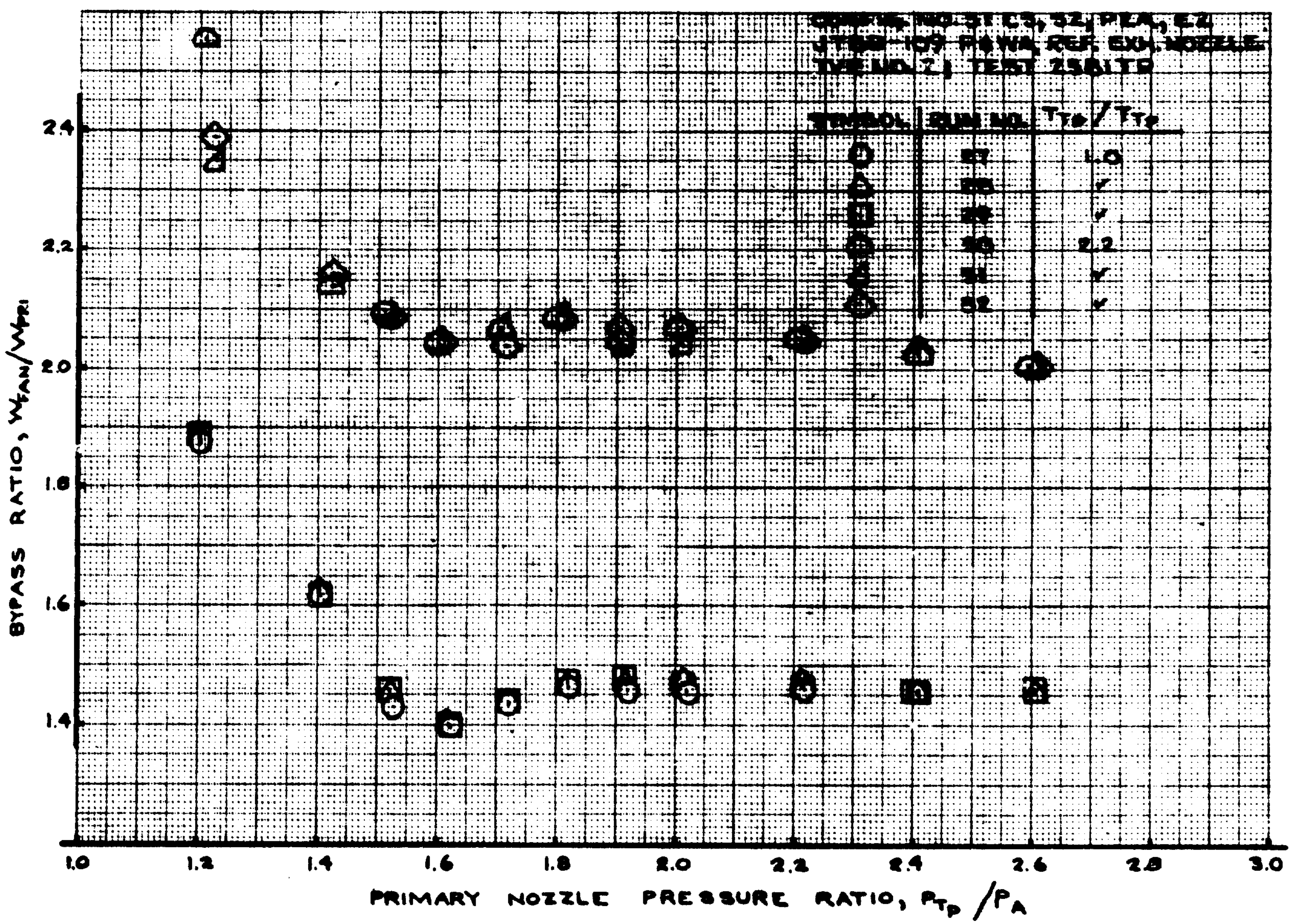

FIGURE 73 - BYPASS RATIO
TEST CONFIG. NO. 3; RUNS 27-32

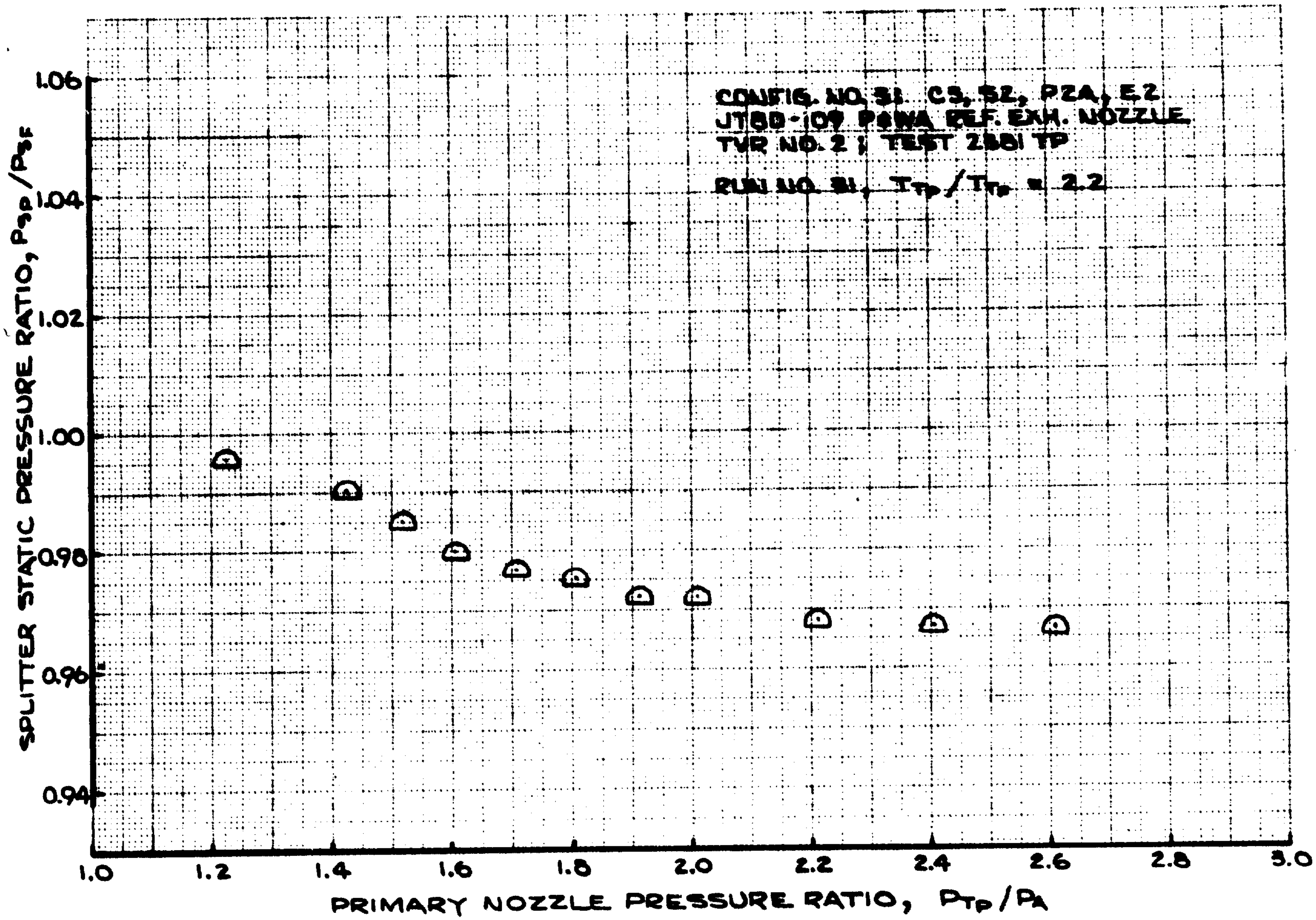

FIGURE 74 - SPLITTER STATIC PRESSURE RATIO
TEST CONFIG. NO. 3; RUN 31

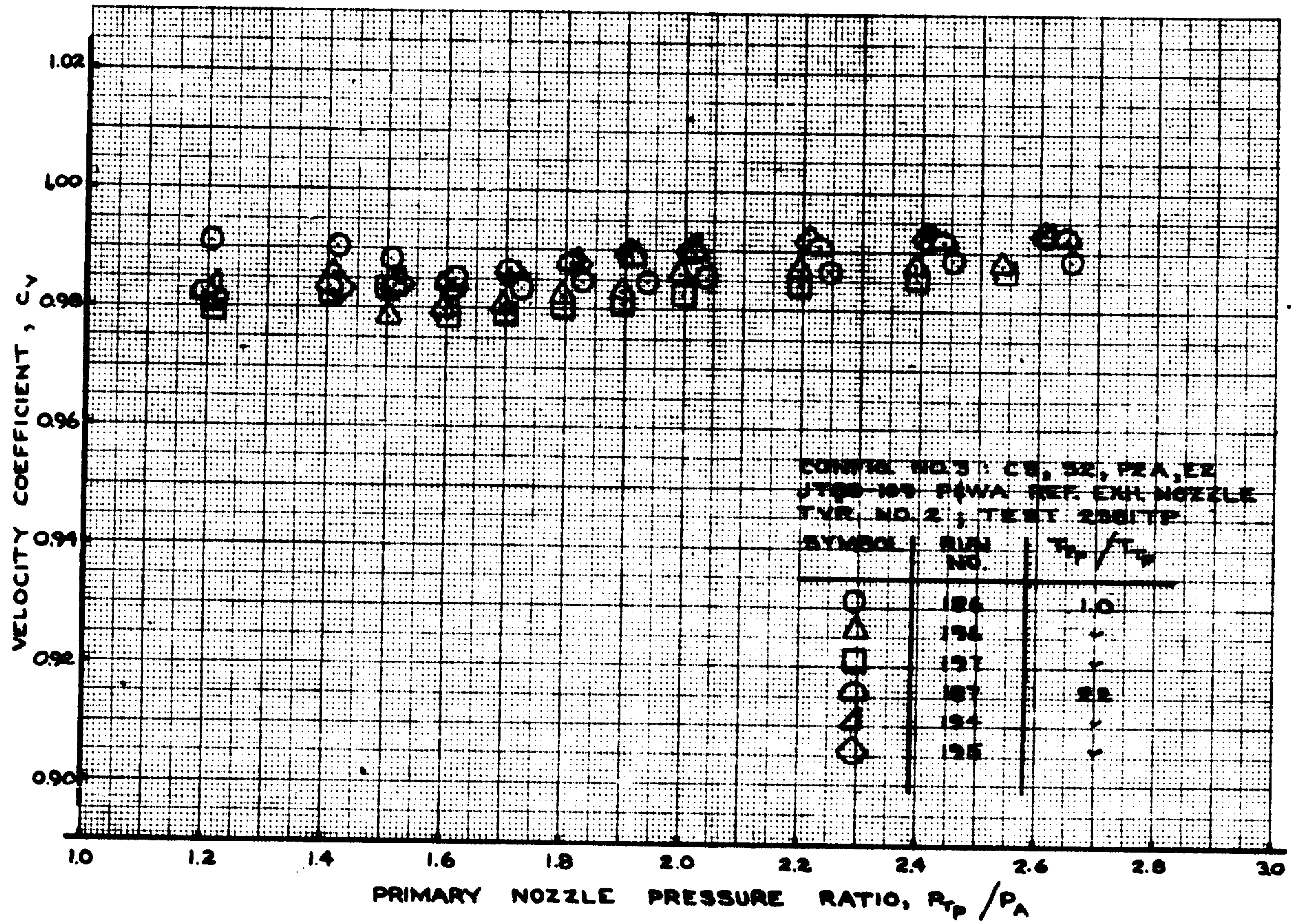

FIGURE 75 - VELOCITY COEFFICIENT
TEST CONFIG. NO. 3; RUNS 186, 187, 194-197

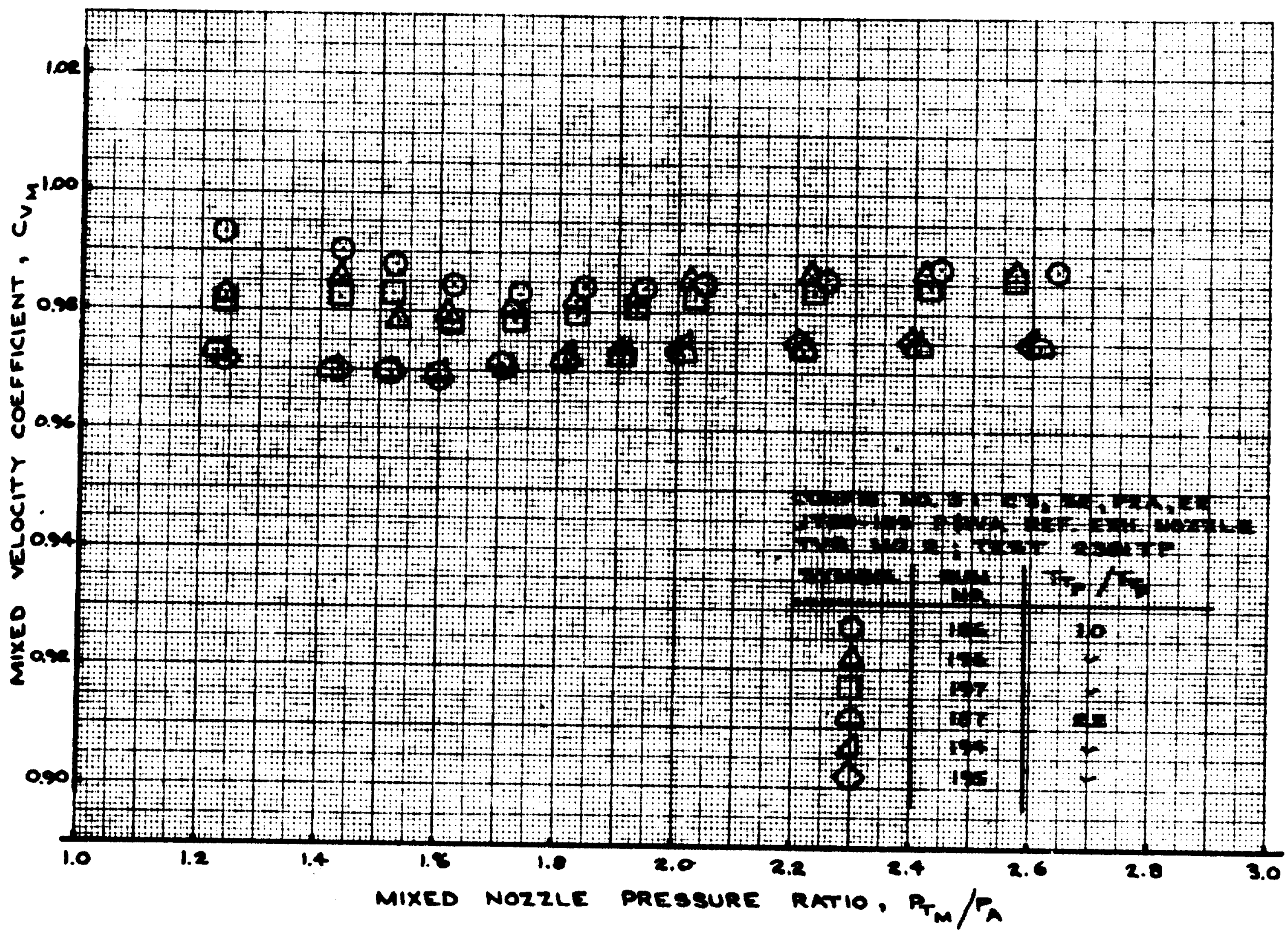

FIGURE 76 - MIXED VELOCITY COEFFICIENT
TEST CONFIG. NO. 3; RUNS 186, 187, 194-197

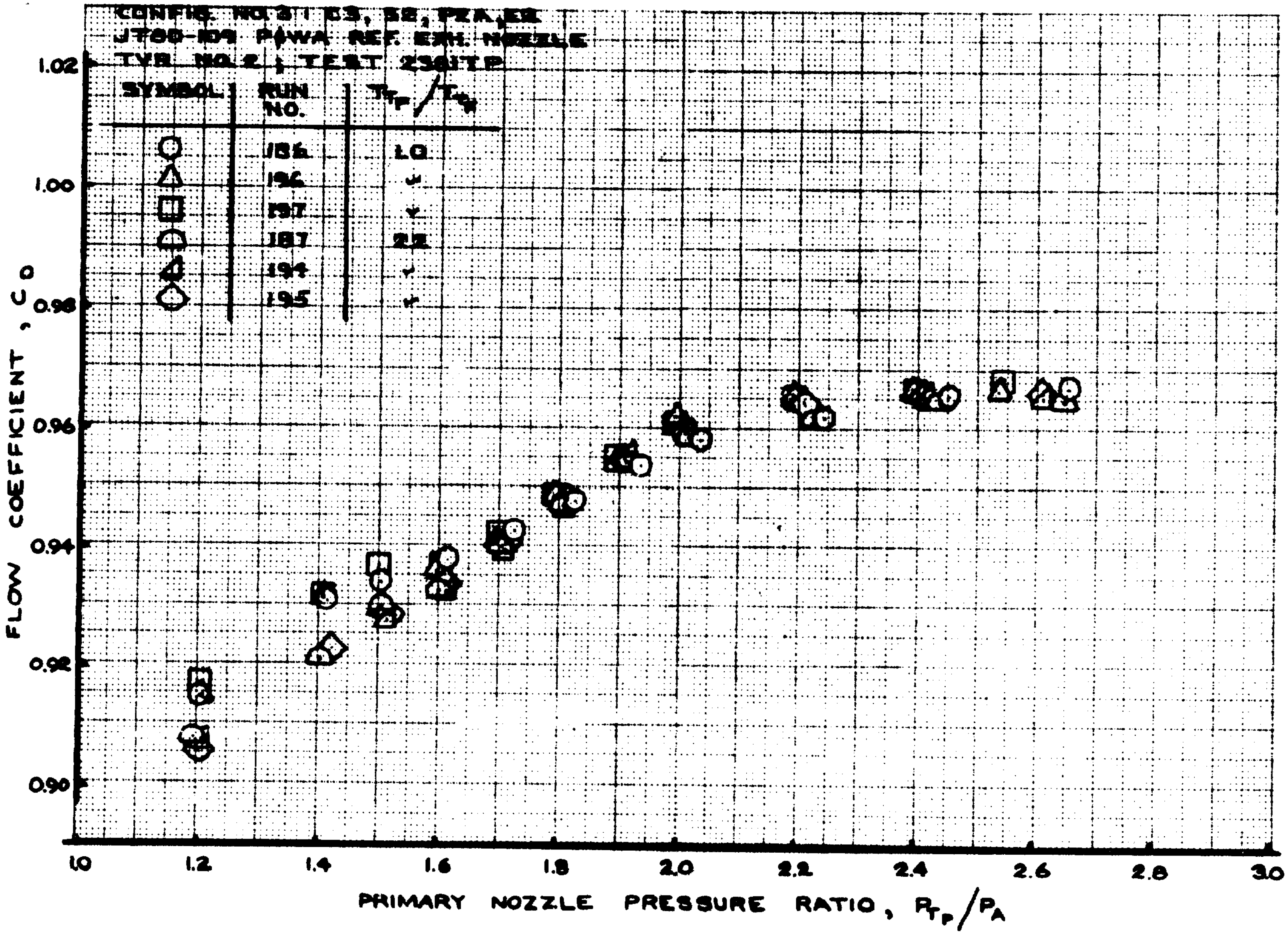

FIGURE 77 - FLOW COEFFICIENT
TEST CONFIG. NO. 3; RUNS 186, 187, 194-197

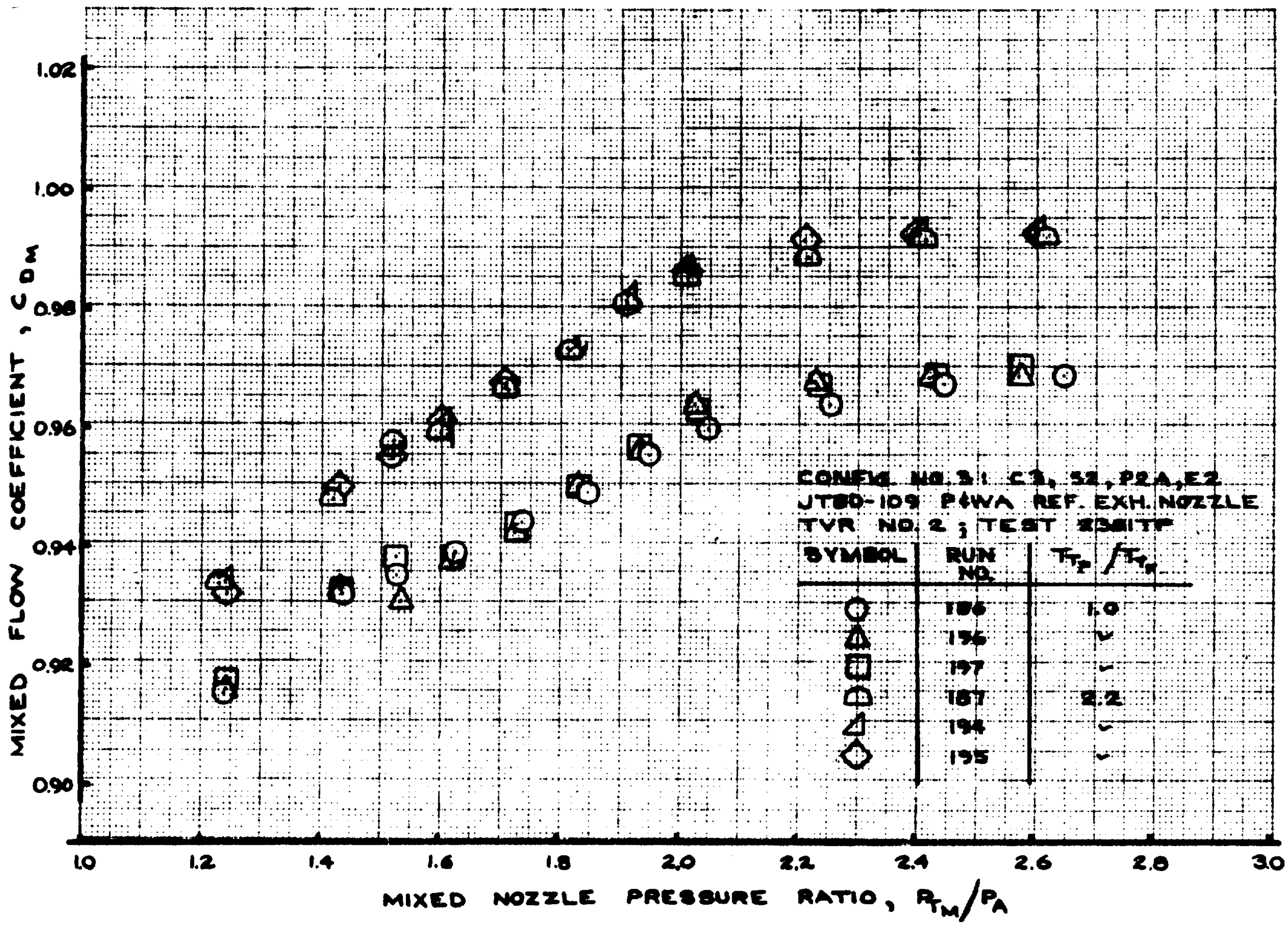

FIGURE 78 - MIXED FLOW COEFFICIENT
TEST CONFIG. NO. 3; RUNS 186, 187, 194-197

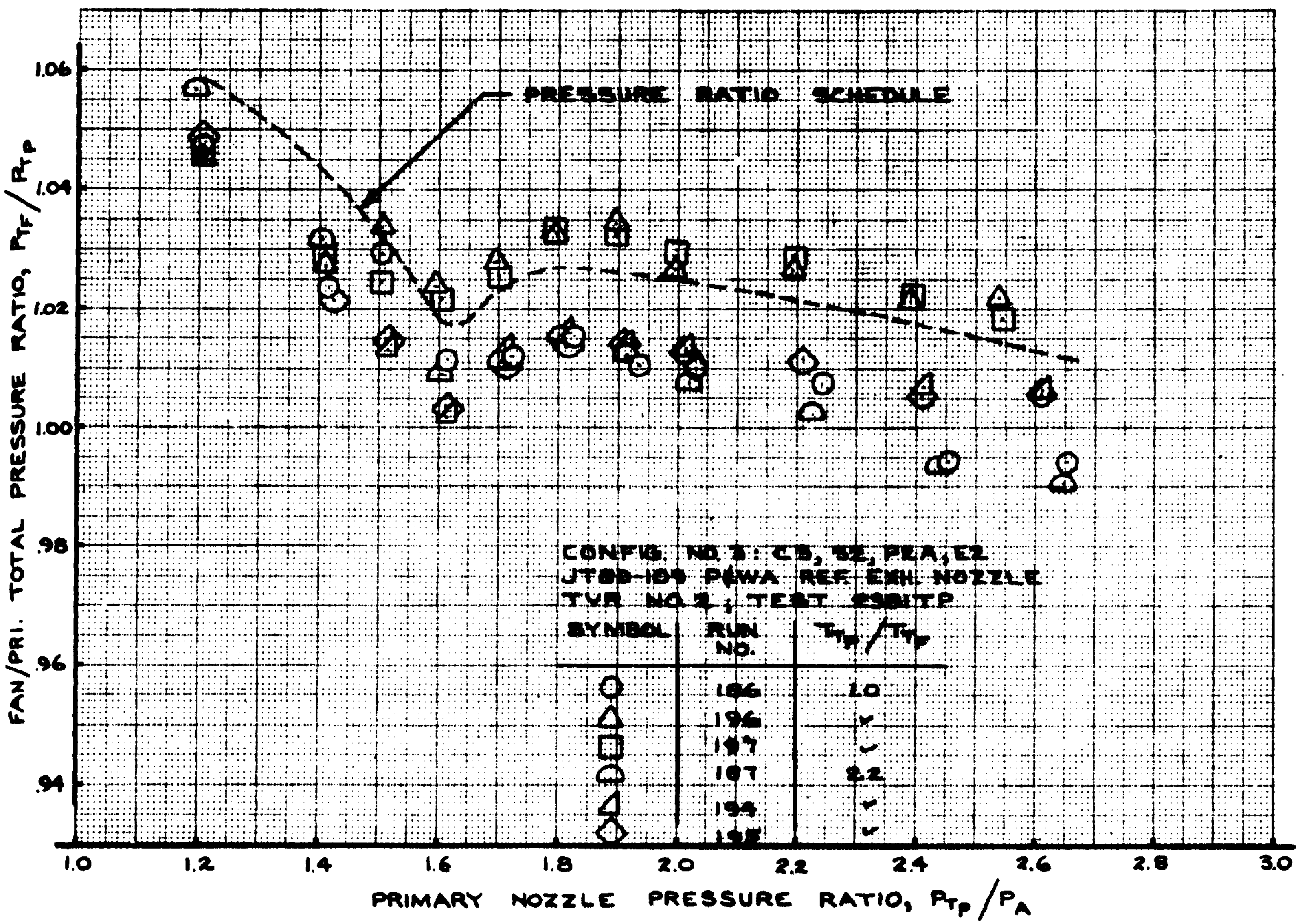

FIGURE 79 - FAN/PRIMARY TOTAL PRESSURE RATIO
TEST CONFIG. NO. 3; RUNS 186, 187, 194-197

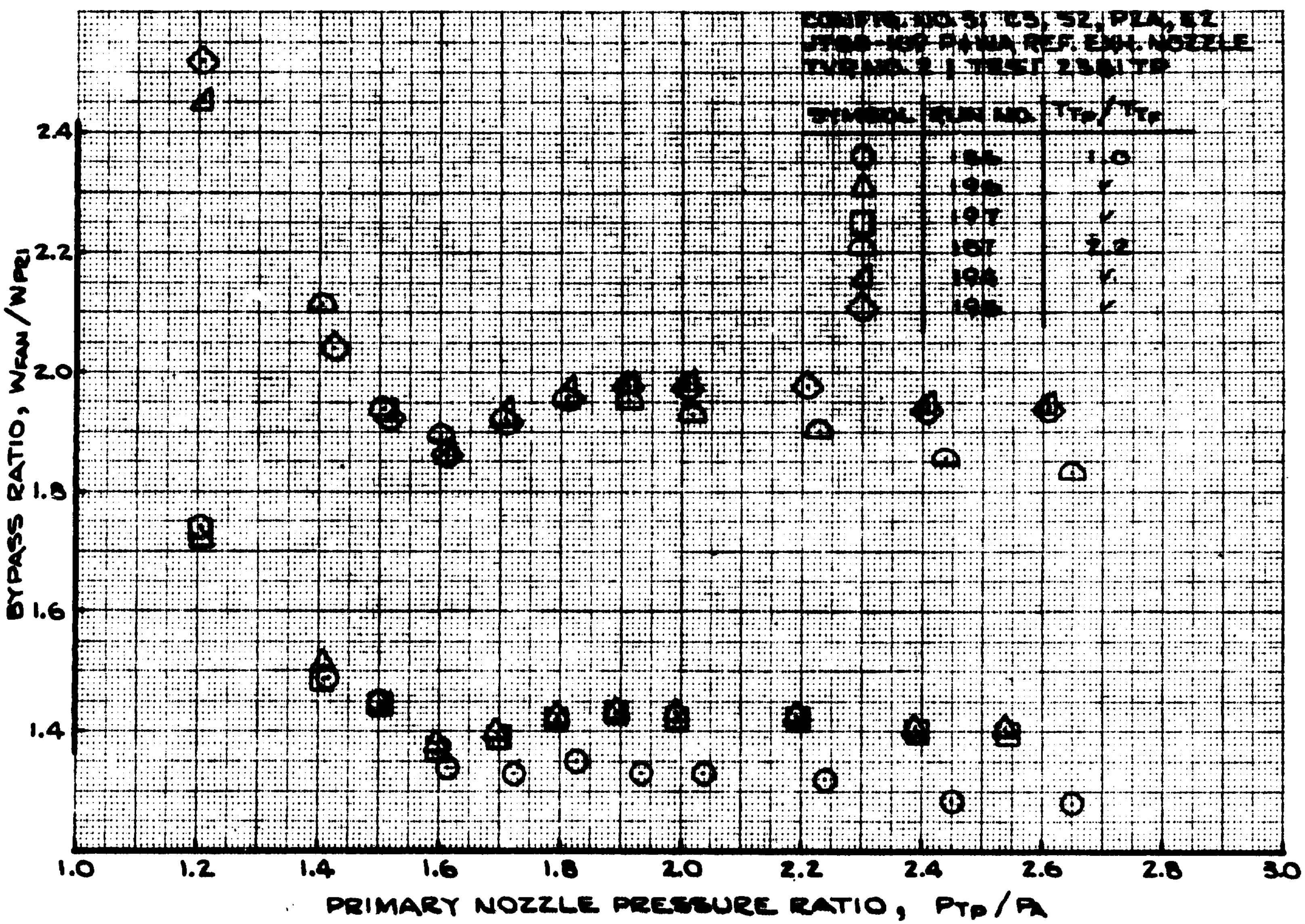

FIGURE 80 - BYPASS RATIO
TEST CONFIG. NO. 3; RUNS 186, 187, 194-197

7.2.4 TEST CONFIGURATION (T.C.) NO. 4

Configuration Description: P&WA Reference nozzle for JT8D-109 with primary swirl.

Hardware Designations:

Outer Nozzle Wall	Splitter	Plug	Exit
C3	S2	P2A	E2

Plotted Data:

Figure 81 - Velocity Coefficient; Runs 33-39.
Figure 82 - Mixed Velocity Coefficient; Runs 33-39.
Figure 83 - Flow Coefficient; Runs 33-39.
Figure 84 - Mixed Flow Coefficient; Runs 33-39.
Figure 85 - Fan/Primary Total Pressure Ratio; Runs 33-39.
Figure 86 - Bypass Ratio; Runs 33-39.
Figure 87 - Splitter Static Pressure Ratio; Run 36.
Figure 88 - Velocity Coefficient; Runs 216, 217, 221-224.
Figure 89 - Mixed Velocity Coefficient; Runs 216, 217, 221-224.
Figure 90 - Flow Coefficient; Runs 216, 217, 221-224.
Figure 91 - Mixed Flow Coefficient; Runs 216, 217, 221-224.
Figure 92 - Fan/Primary Total Pressure Ratio; Runs 216, 217, 221-224.
Figure 93 - Bypass Ratio; Runs 216, 217, 221-224.

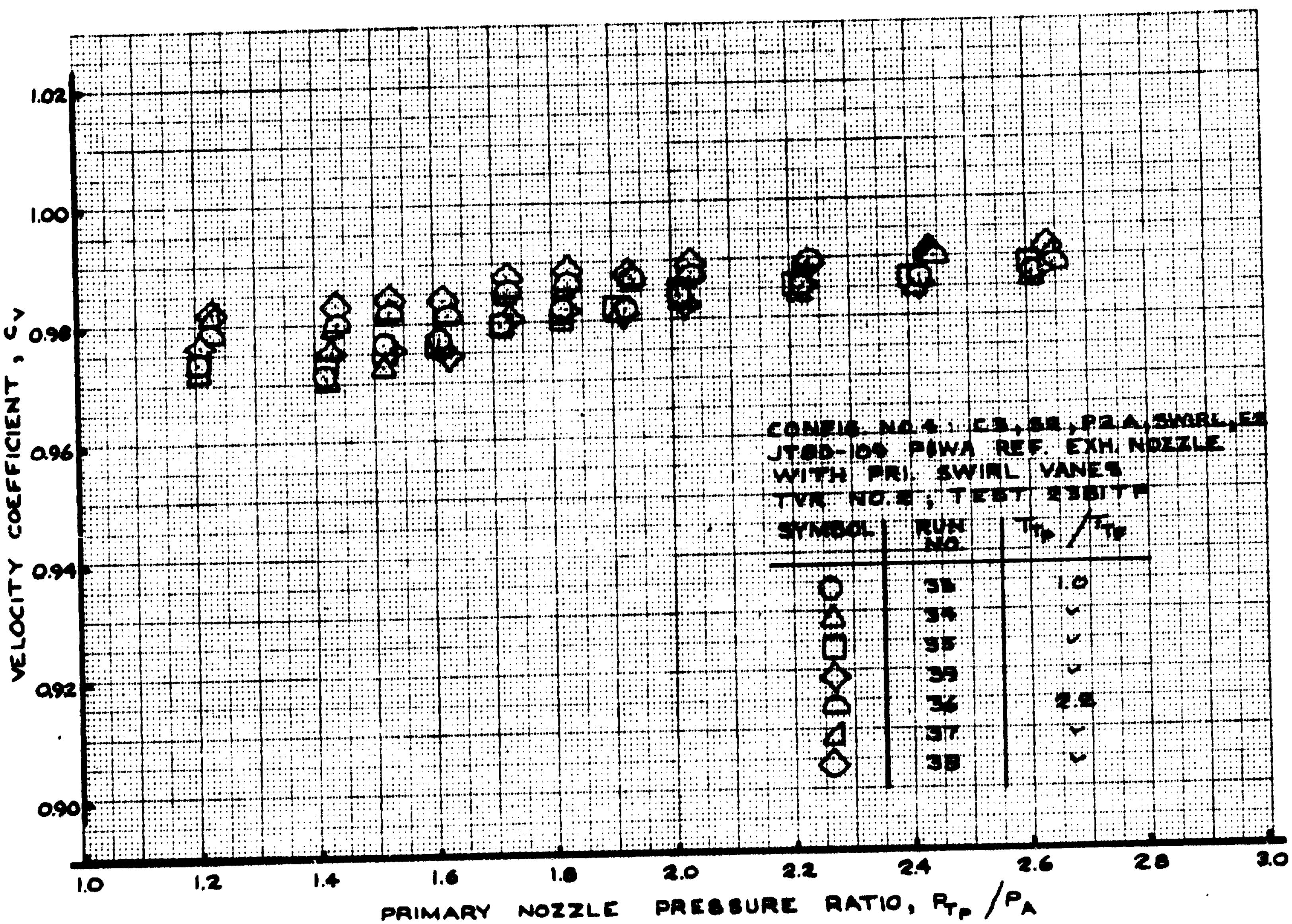

FIGURE 81 - VELOCITY COEFFICIENT
TEST CONFIG. NO. 4; RUNS 33-39

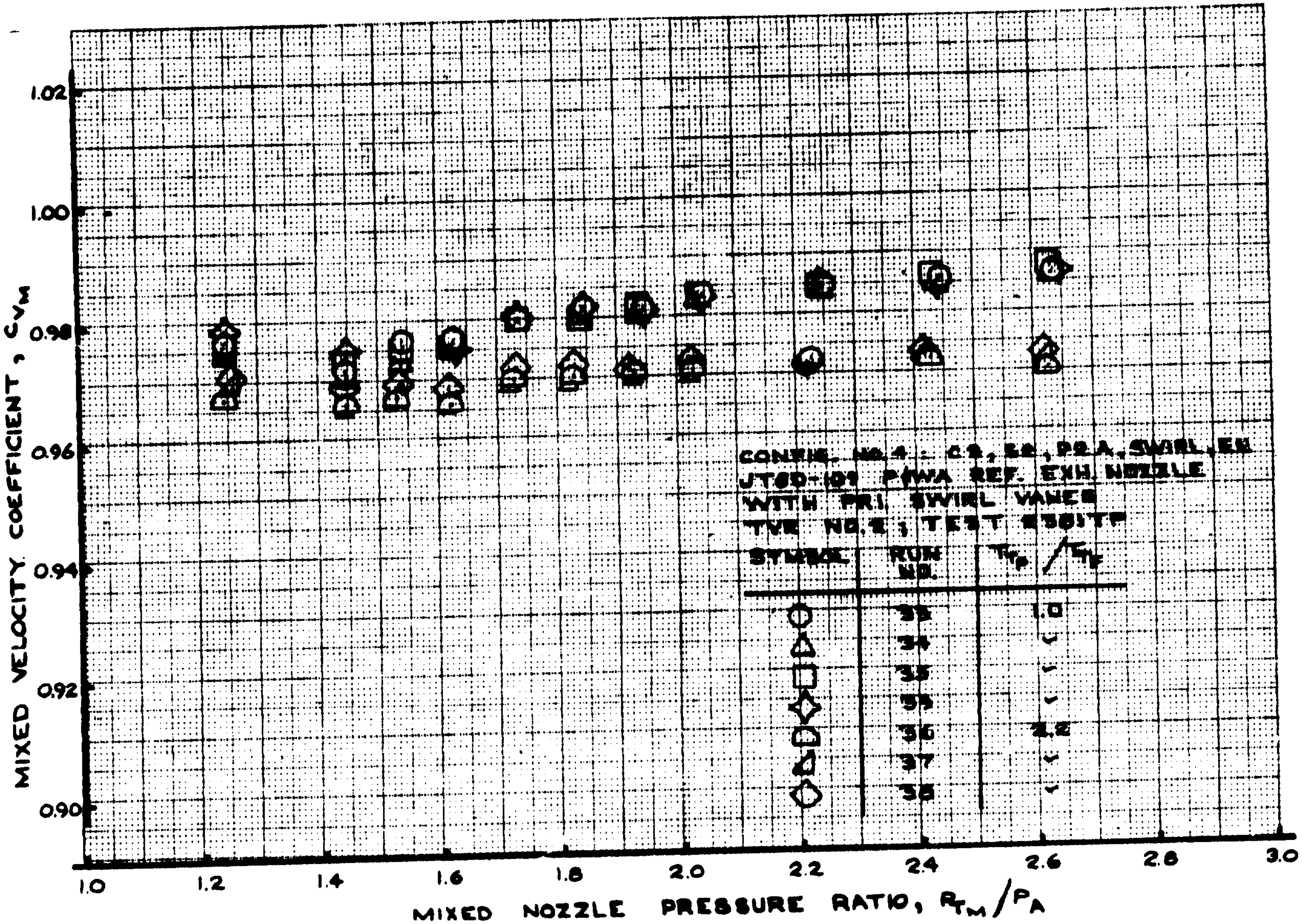

FIGURE 82 - MIXED VELOCITY COEFFICIENT
TEST CONFIG. NO. 4; RUNS 33-39

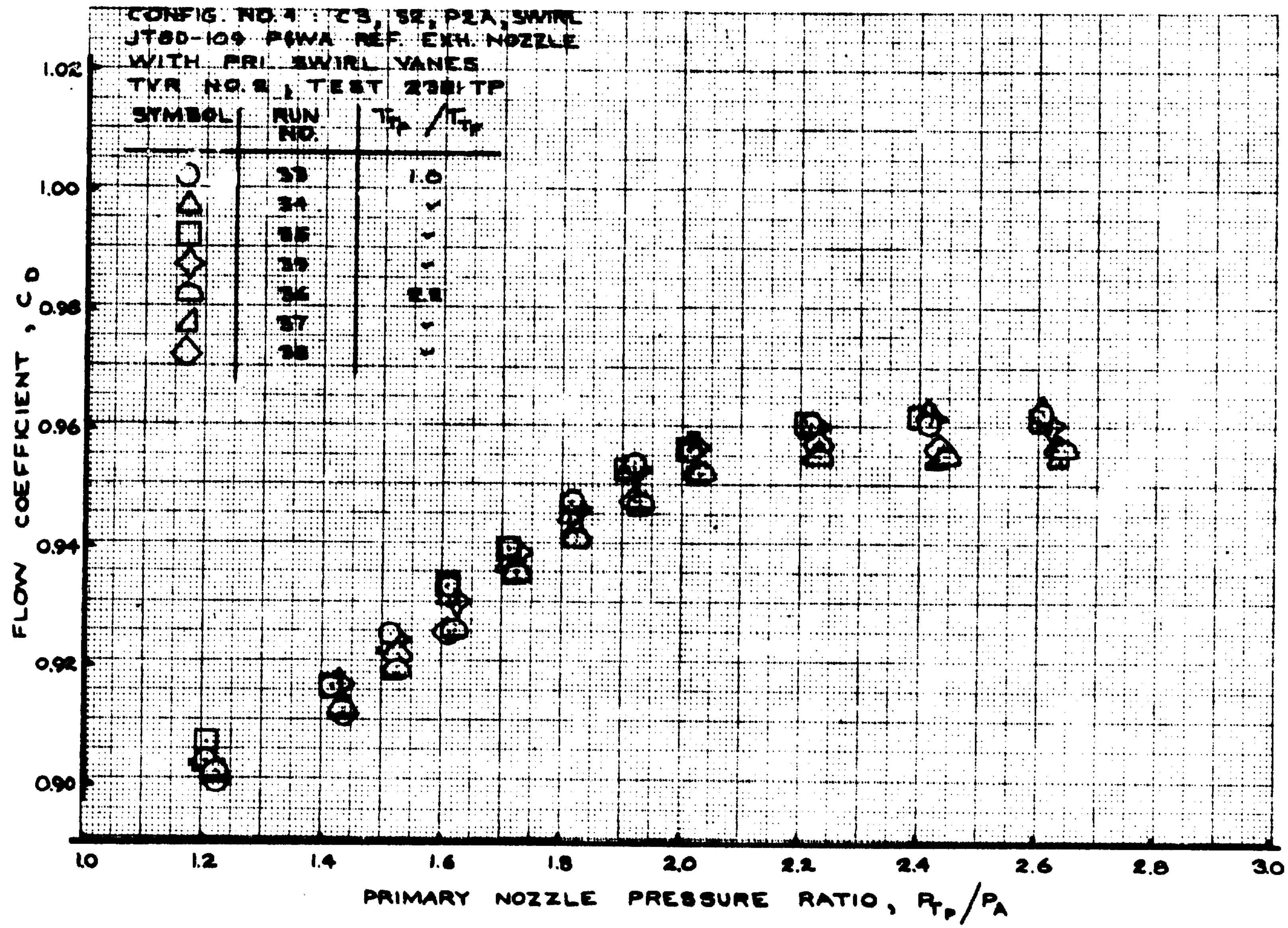

FIGURE 83 - FLOW COEFFICIENT
TEST CONFIG. NO. 4; RUNS 33-39

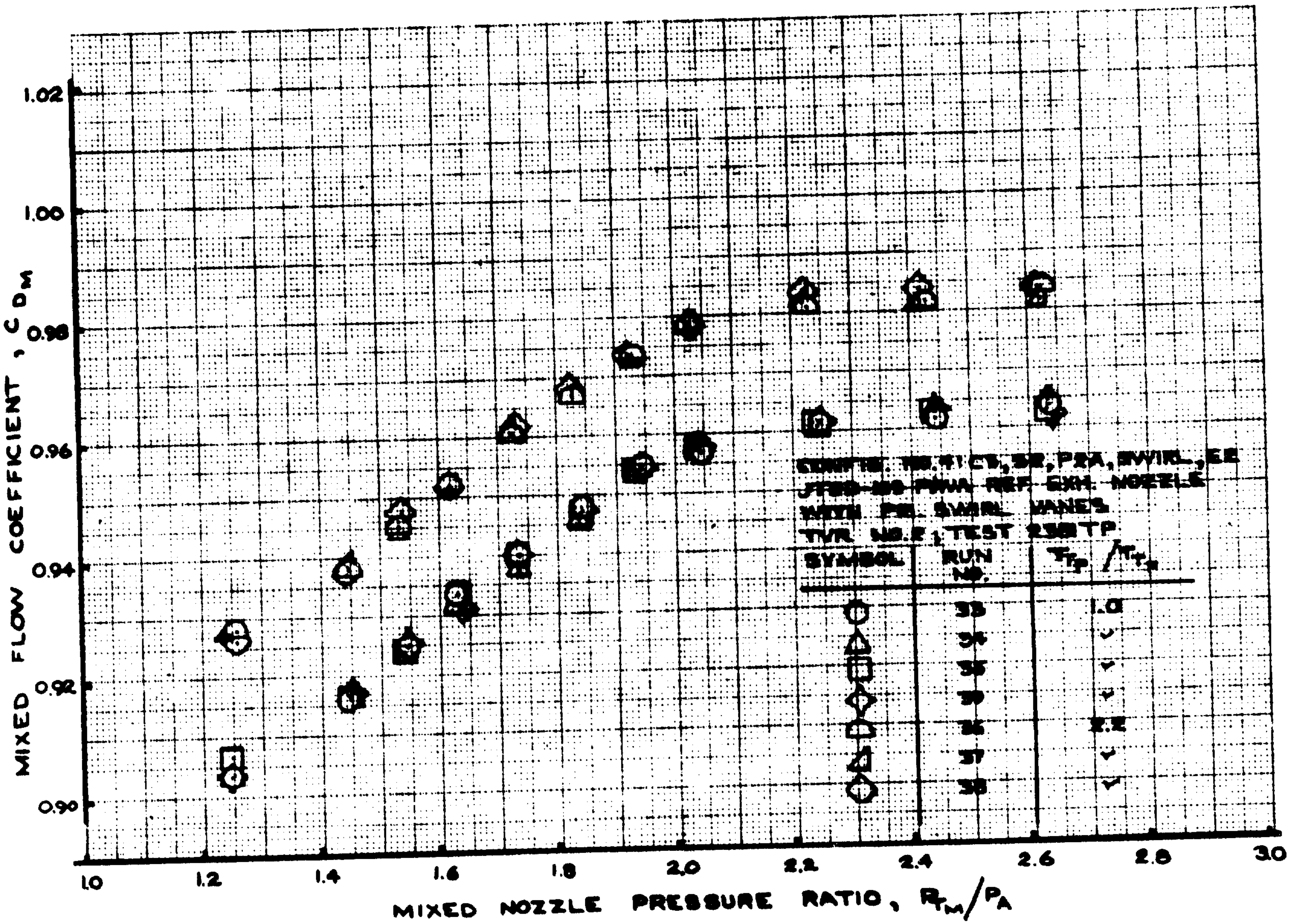

FIGURE 84 - MIXED FLOW COEFFICIENT
. TEST CONFIG. NO. 4; RUNS 33-39

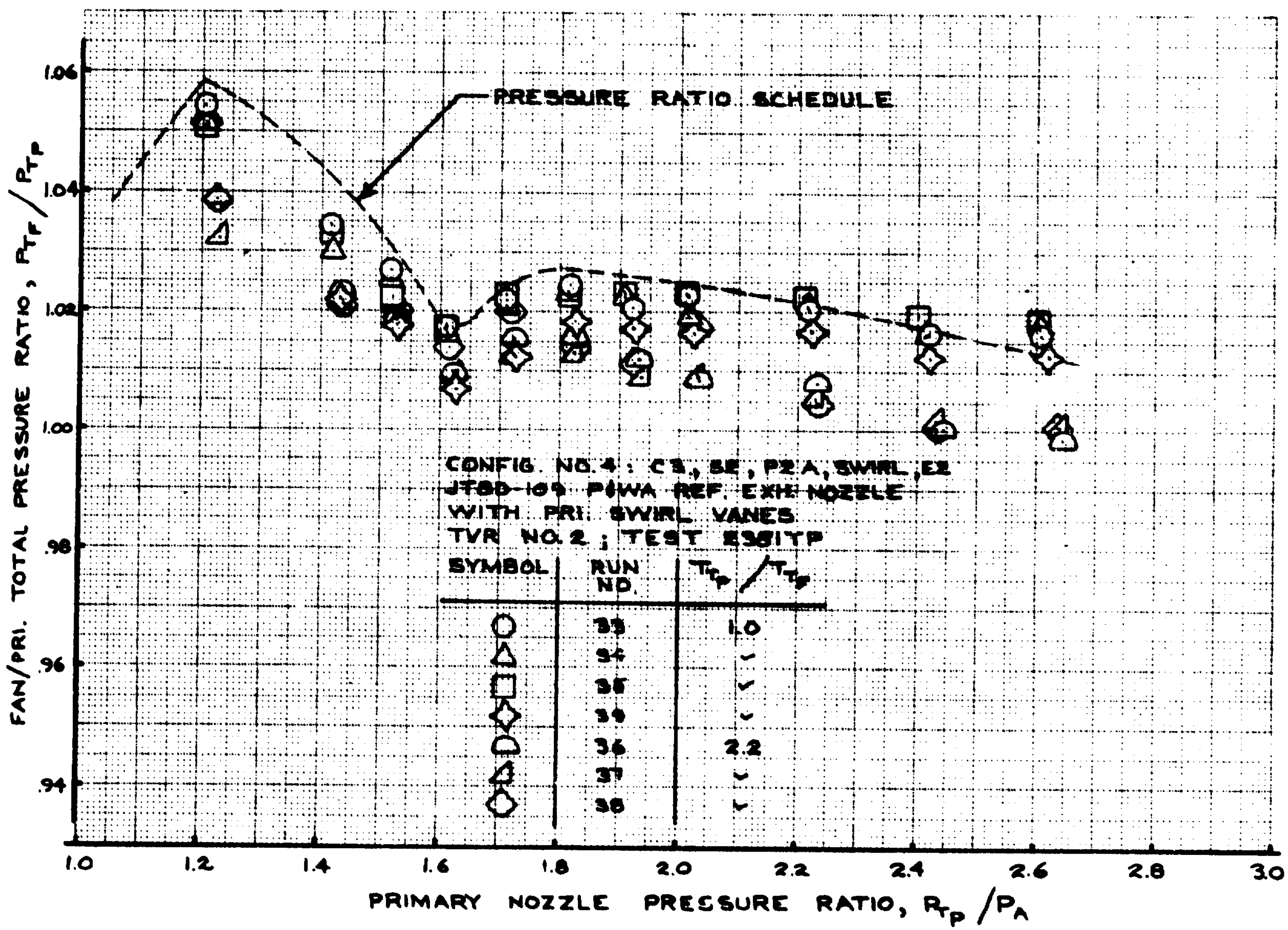

FIGURE 85 - FAN/PRIMARY TOTAL PRESSURE RATIO
TEST CONFIG. NO. 4; RUNS 33-39

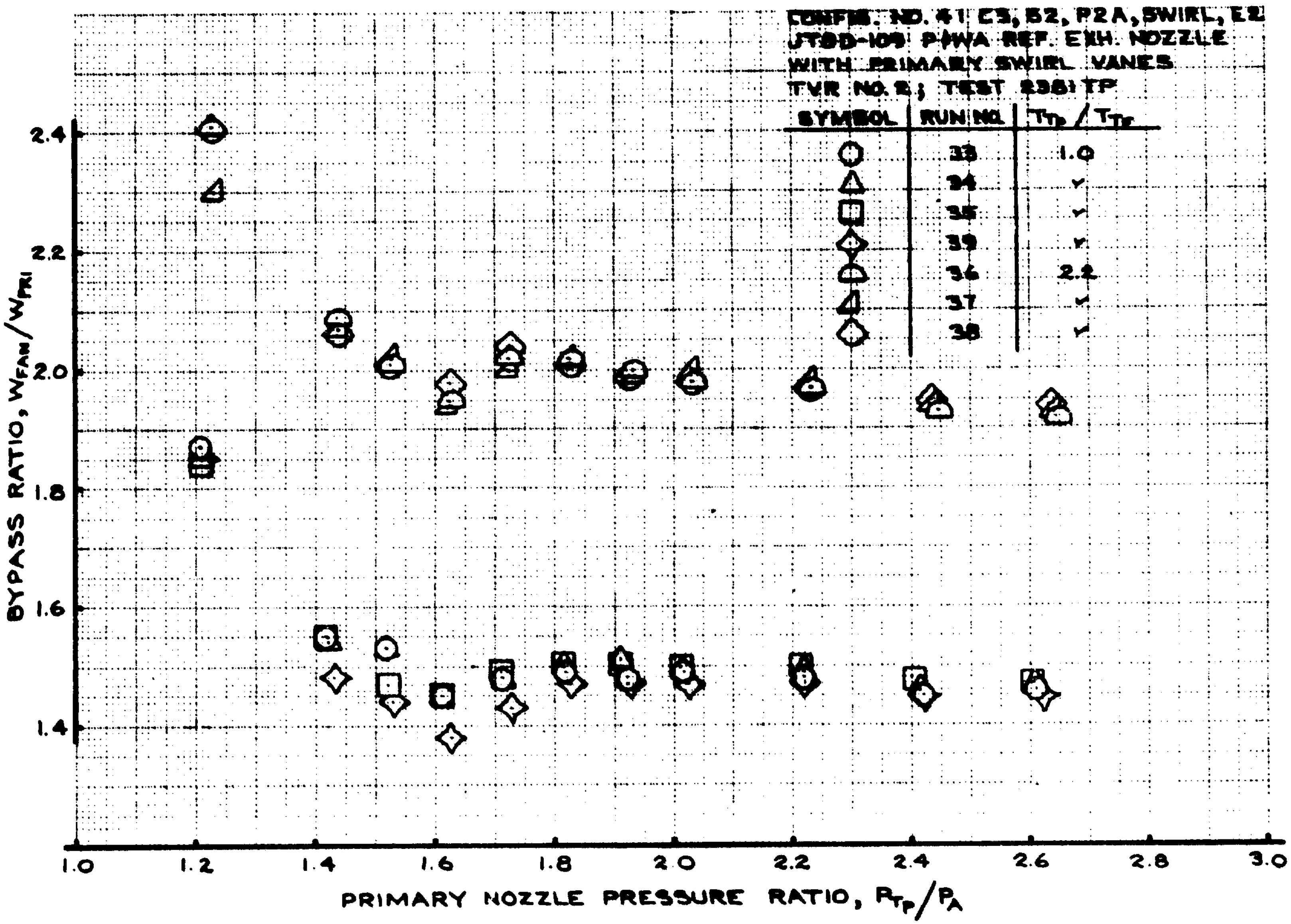

FIGURE 86 - BYPASS RATIO
TEST CONFIG. NO. 4; RUNS 33-39

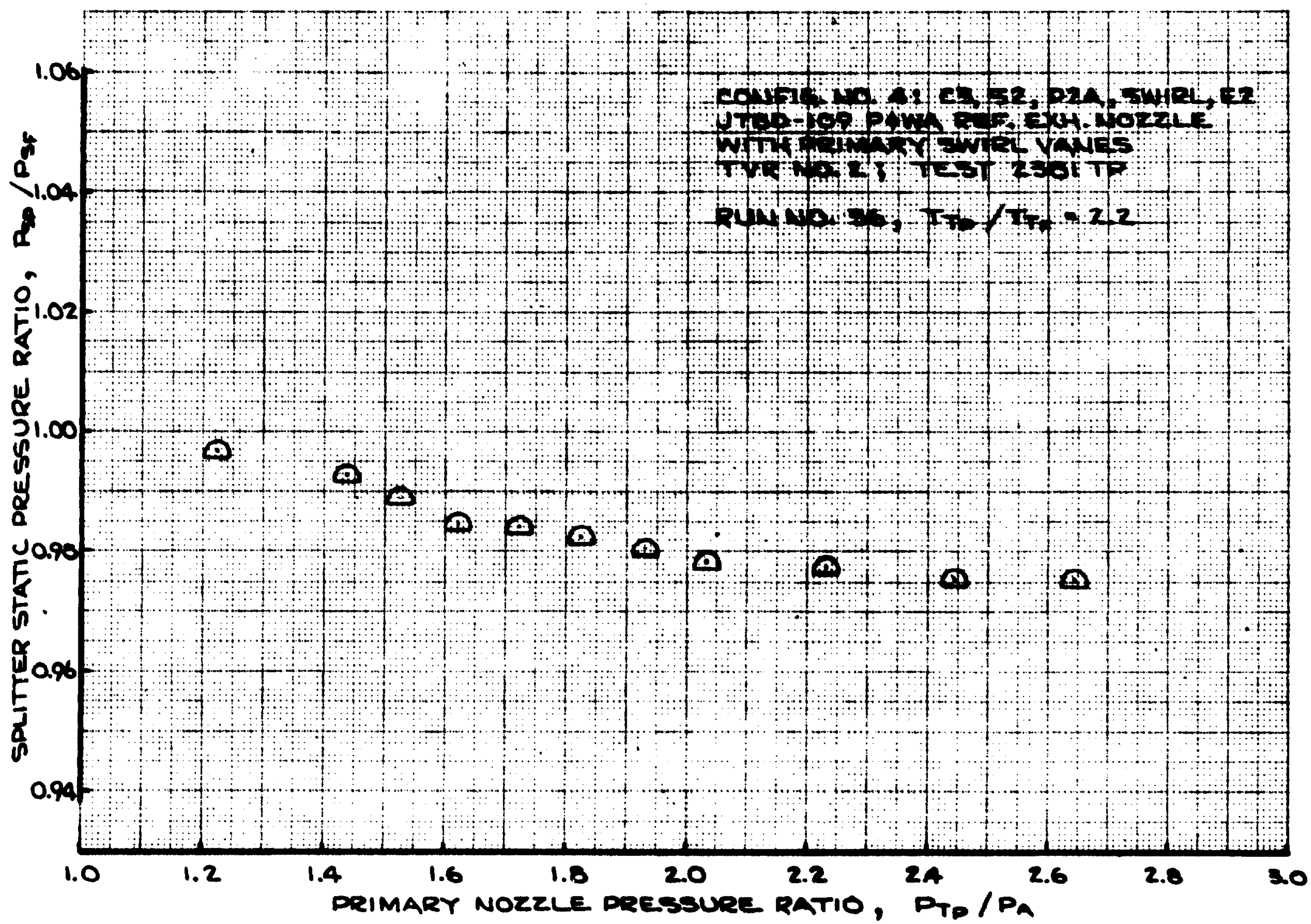

FIGURE 87 - SPLITTER STATIC PRESSURE RATIO
TEST CONFIG. NO. 4; RUN 36

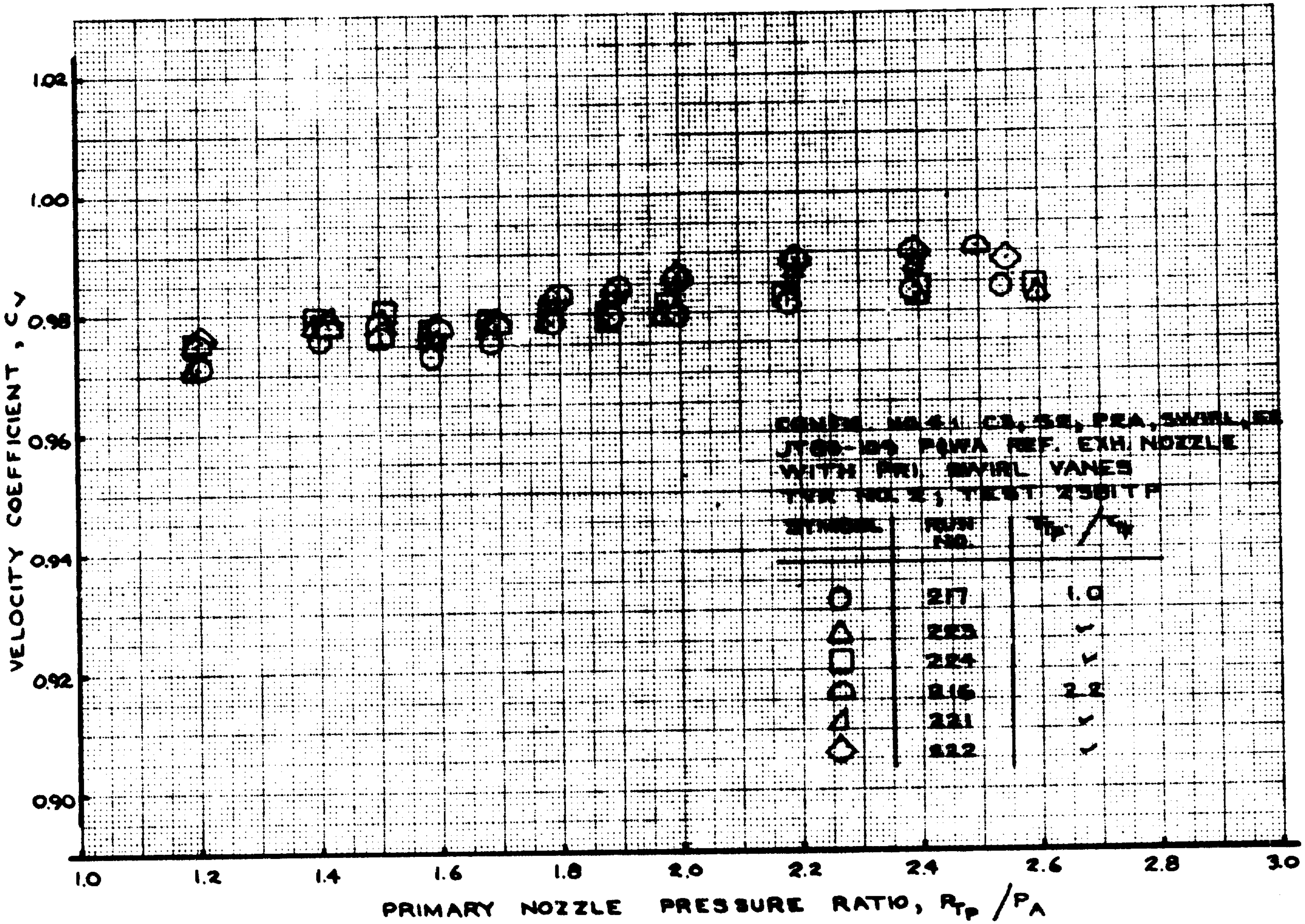

FIGURE 88 - VELOCITY COEFFICIENT
TEST CONFIG. NO. 4; RUNS 216, 217, 221-224

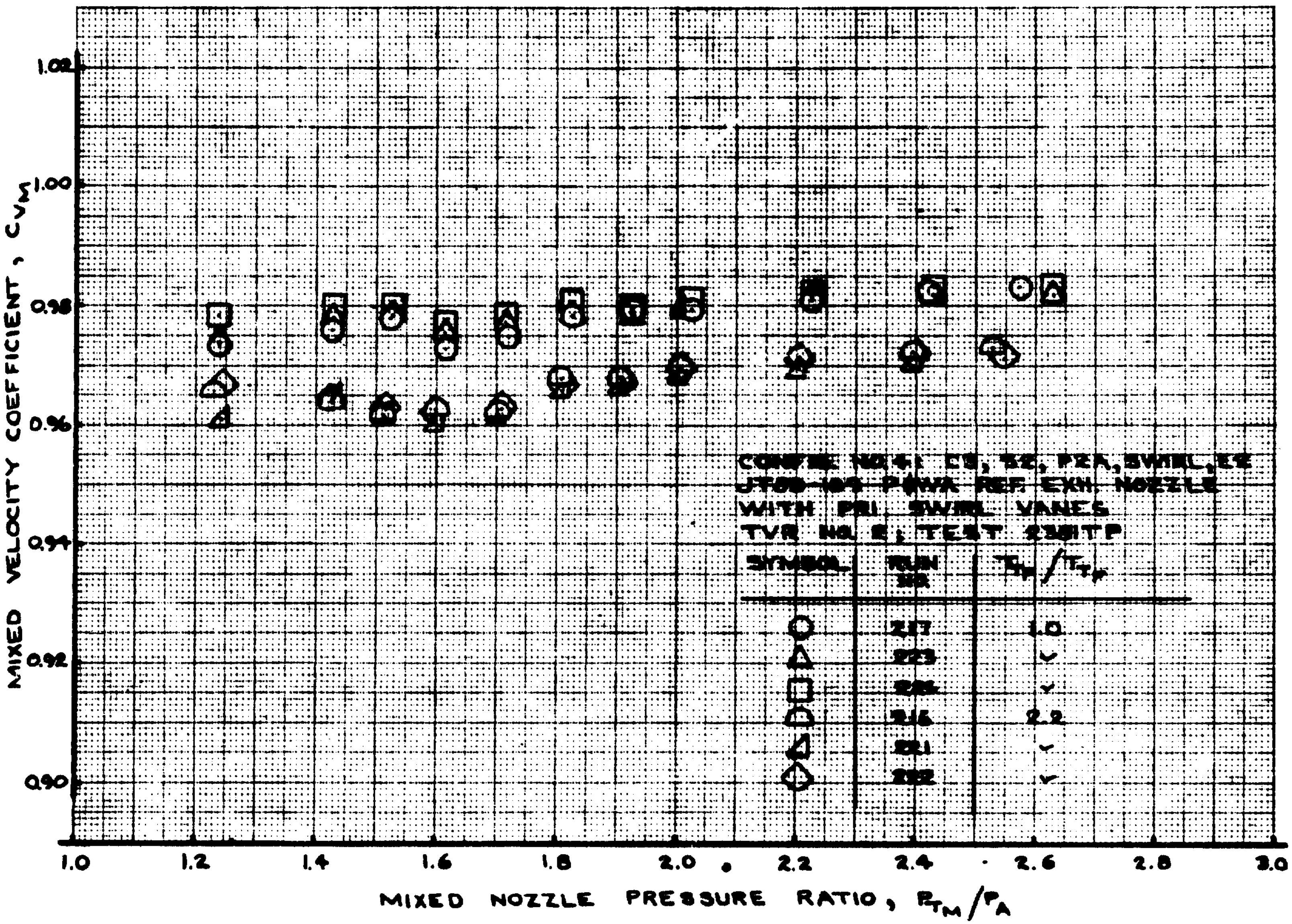

FIGURE 89 - MIXED VELOCITY COEFFICIENT
TEST CONFIG. NO. 4; RUNS 216, 217, 221-224

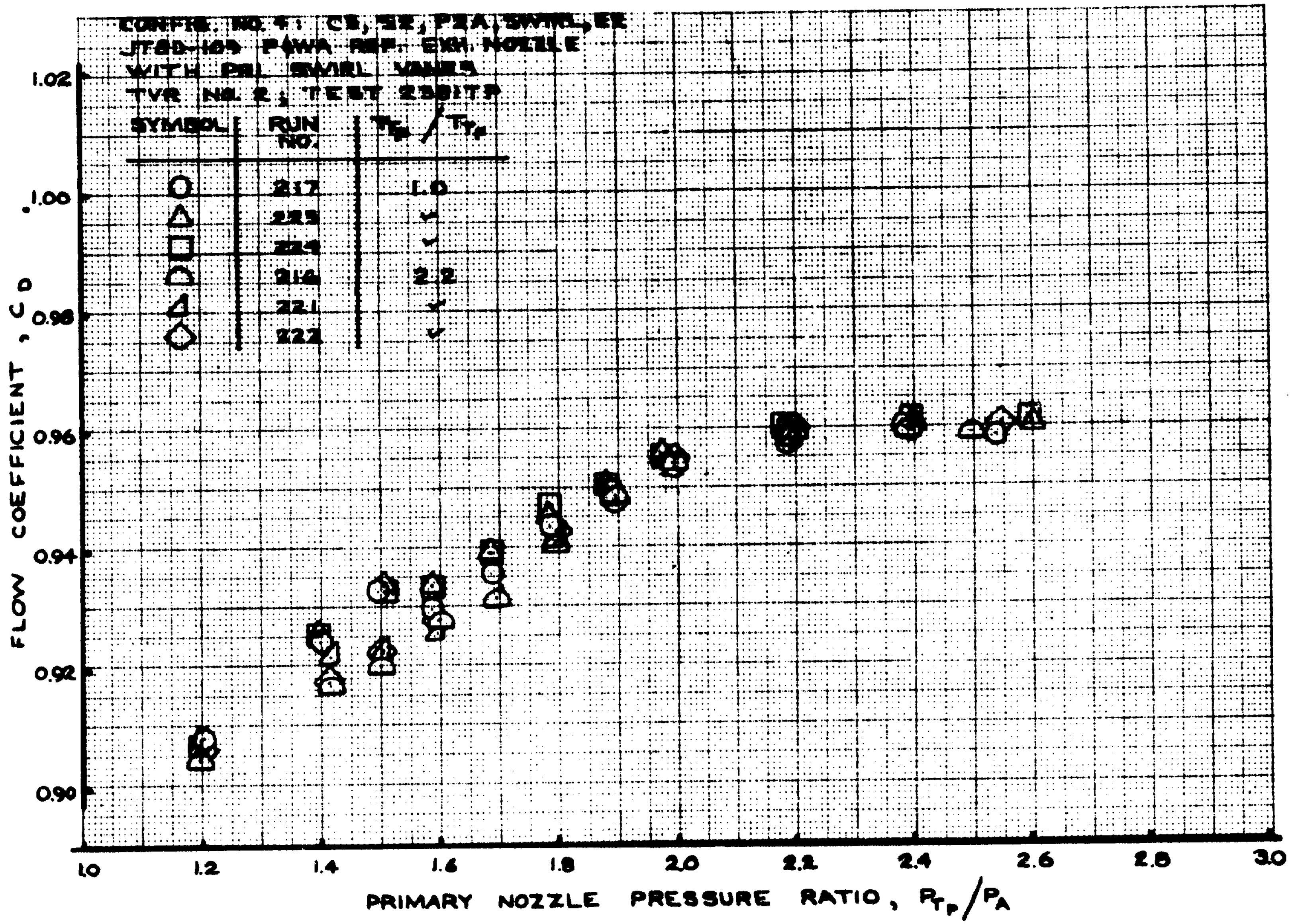

FIGURE 90 - FLOW COEFFICIENT
TEST CONFIG. NO. 4; RUNS 216, 217, 221-224

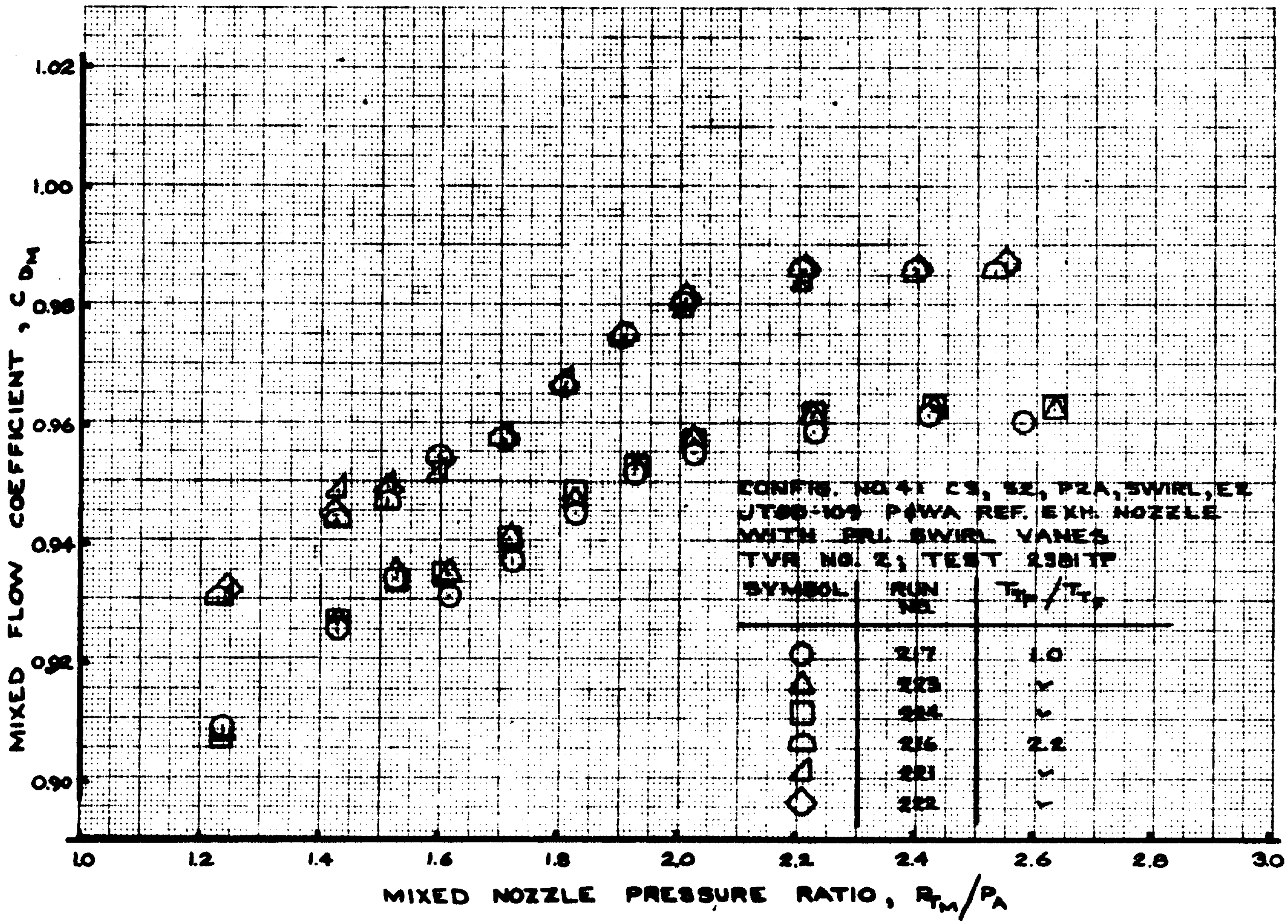

FIGURE 91 - MIXED FLOW COEFFICIENT
TEST CONFIG. NO. 4; RUNS 216, 217, 221-224

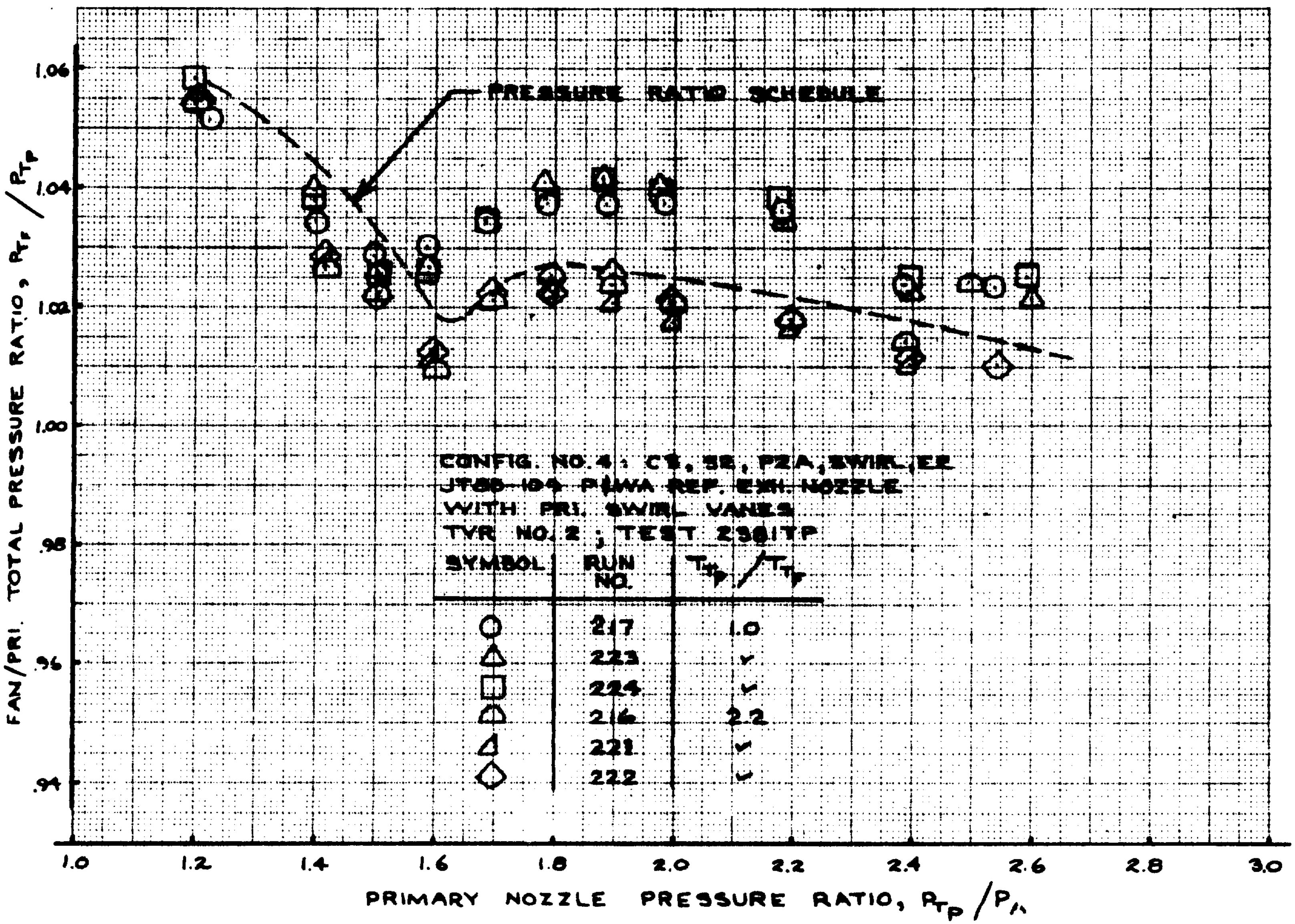

FIGURE 92 - FAN/PRIMARY TOTAL PRESSURE RATIO
TEST CONFIG. NO. 4; RUNS 216, 217, 221-224

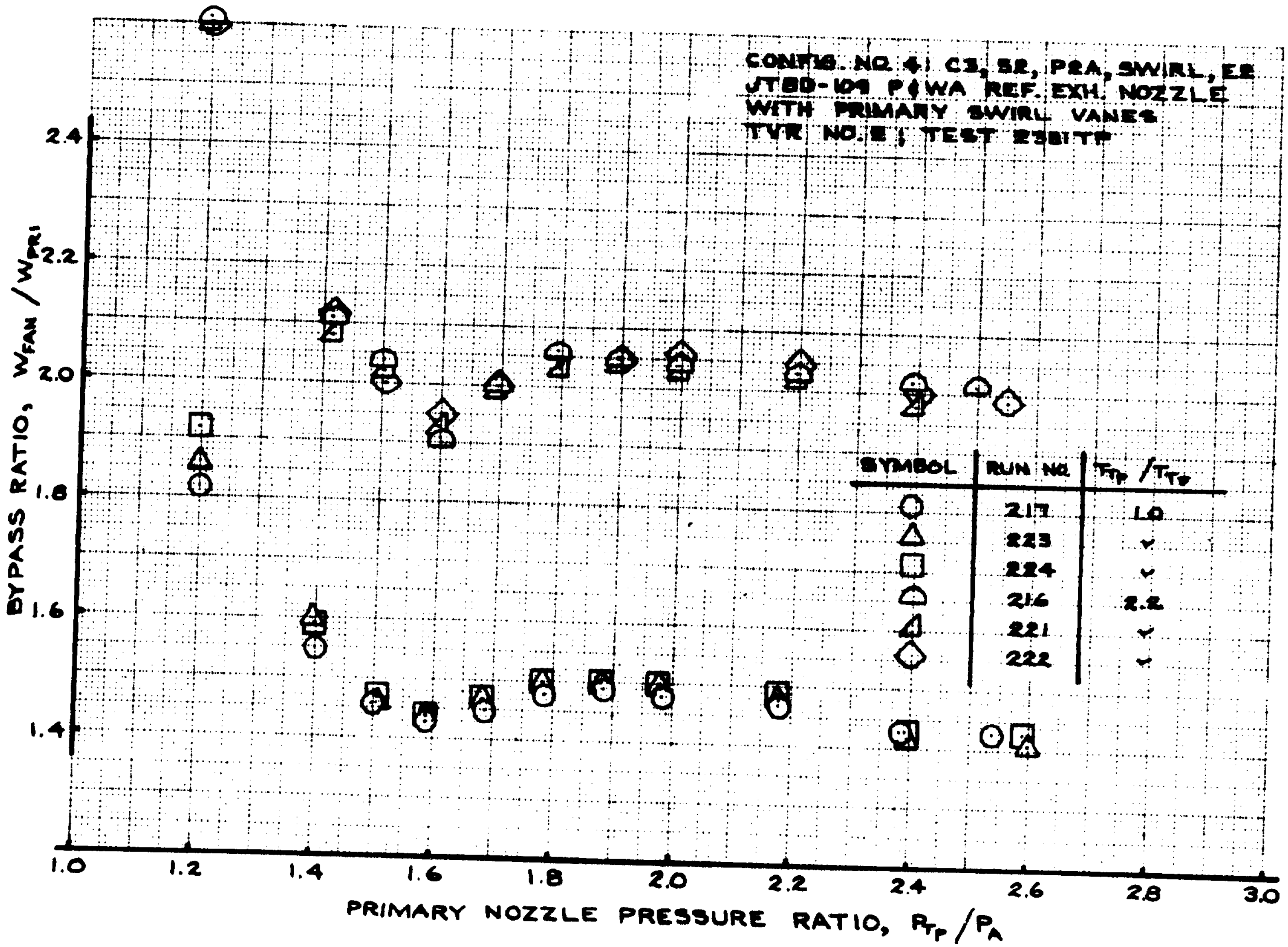

FIGURE 93 - BYPASS RATIO
TEST CONFIG. NO. 4; RUNS 216, 217, 221-224

7.2.5 TEST CONFIGURATION (T.C.) NO. 5

Configuration Description: P&WA Reference nozzle for JT8D-115.

Hardware Designations:

Outer Nozzle Wall	Splitter	Plug	Exit
C3	S3	P2A	E3

Plotted Data:

Figure 94 - Velocity Coefficient; Runs 40-45.
Figure 95 - Mixed Velocity Coefficient; Runs 40-45.
Figure 96 - Flow Coefficient; Runs 40-45.
Figure 97 - Mixed Flow Coefficient; Runs 40-45.
Figure 98 - Fan/Primary Total Pressure Ratio; Runs 40-45.
Figure 99 - Bypass Ratio; Runs 40-45.
Figure 100- Splitter Static Pressure Ratio; Run 43.
Figure 101- Velocity Coefficient; Runs 46-50.
Figure 102- Mixed Velocity Coefficient; Runs 46-50.
Figure 103- Flow Coefficient; Runs 46-50.
Figure 104- Mixed Flow Coefficient; Run 46-50.
Figure 105- Fan/Primary Total Pressure Ratio; Run 46-50.
Figure 106- Bypass Ratio; Runs 46-50.

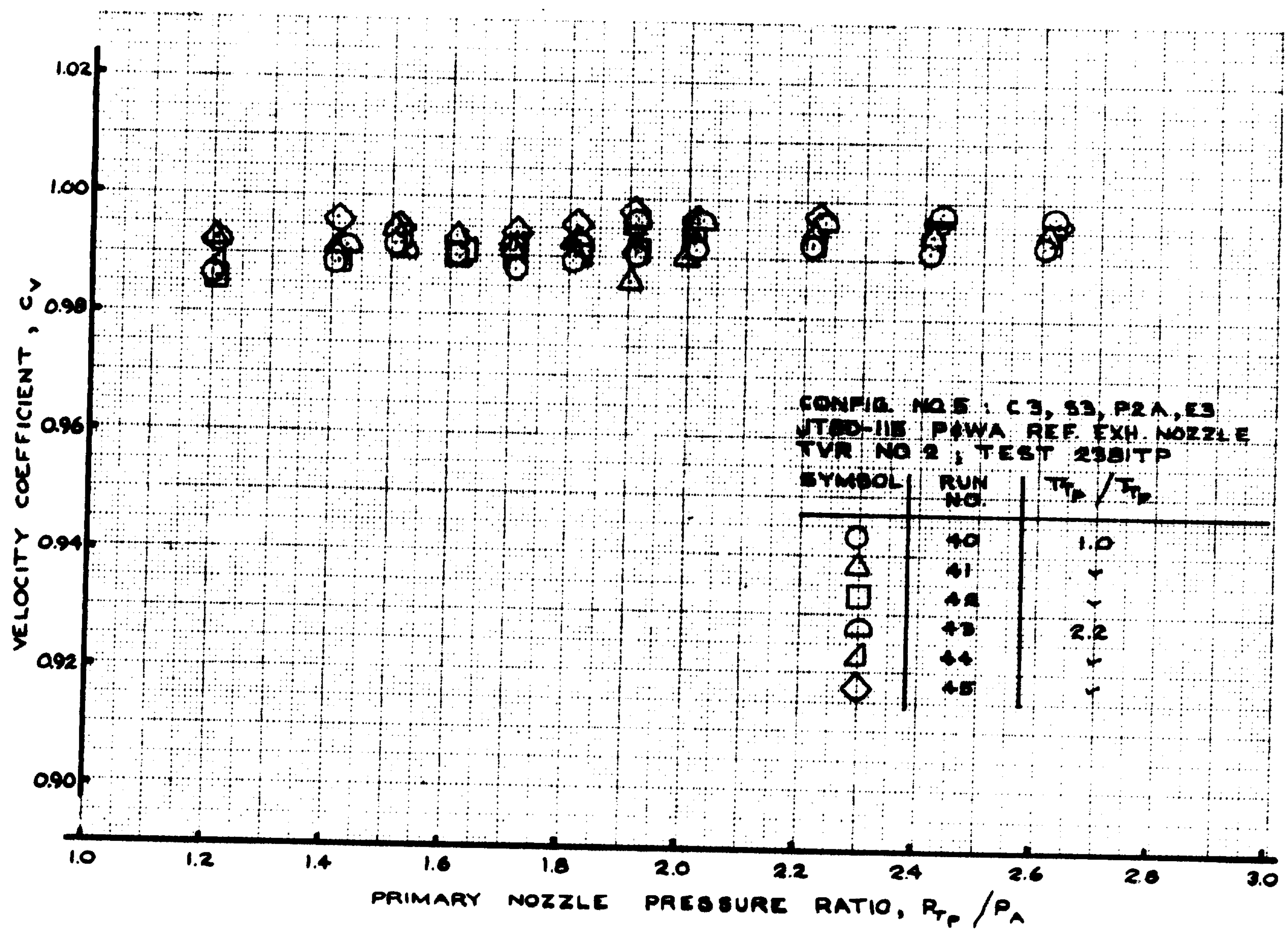

FIGURE 94 - VELOCITY COEFFICIENT
TEST CONFIG. NO. 5; RUNS 40-45

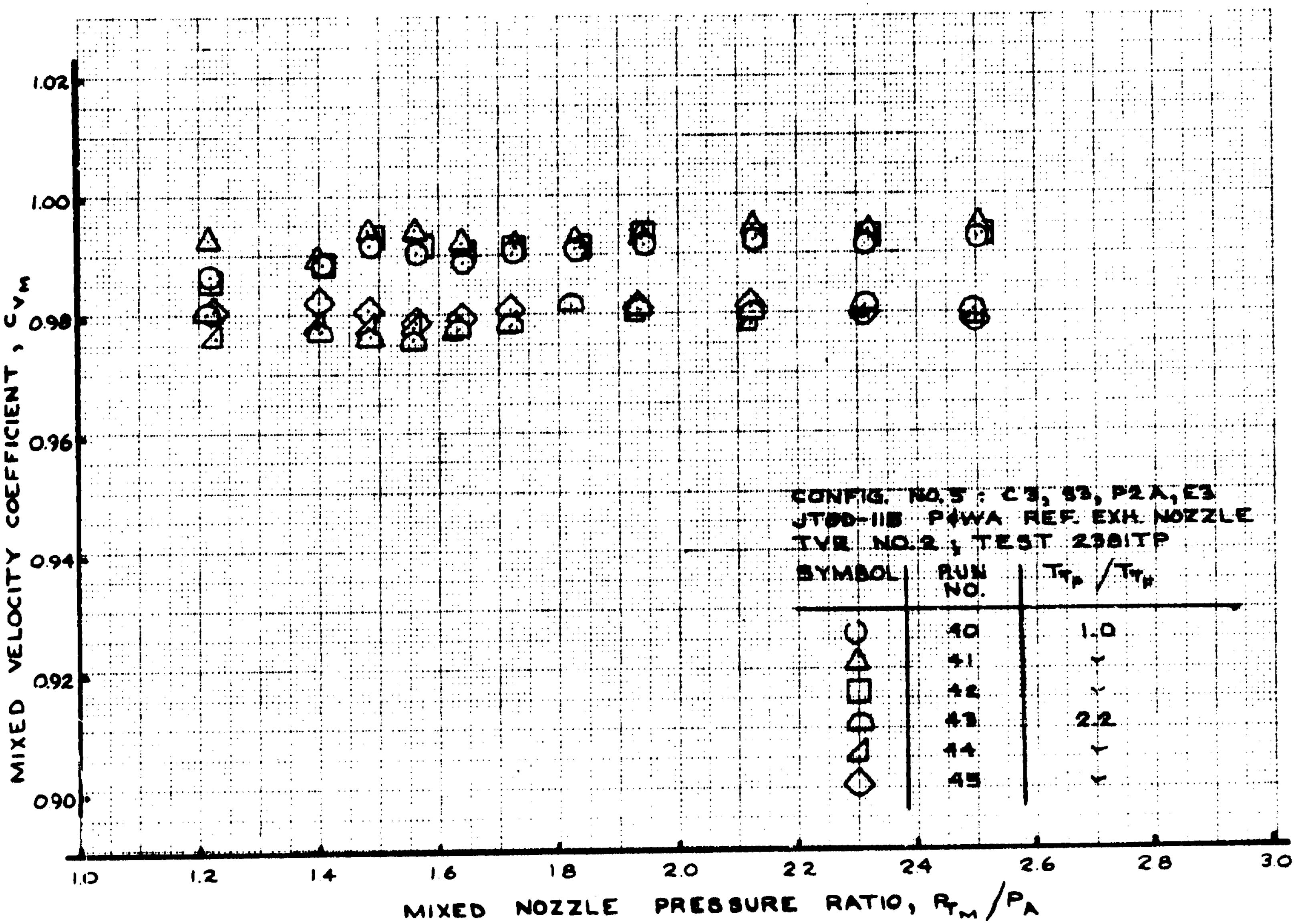

FIGURE 95 - MIXED VELOCITY COEFFICIENT
TEST CONFIG. NO. 5; RUNS 40-45

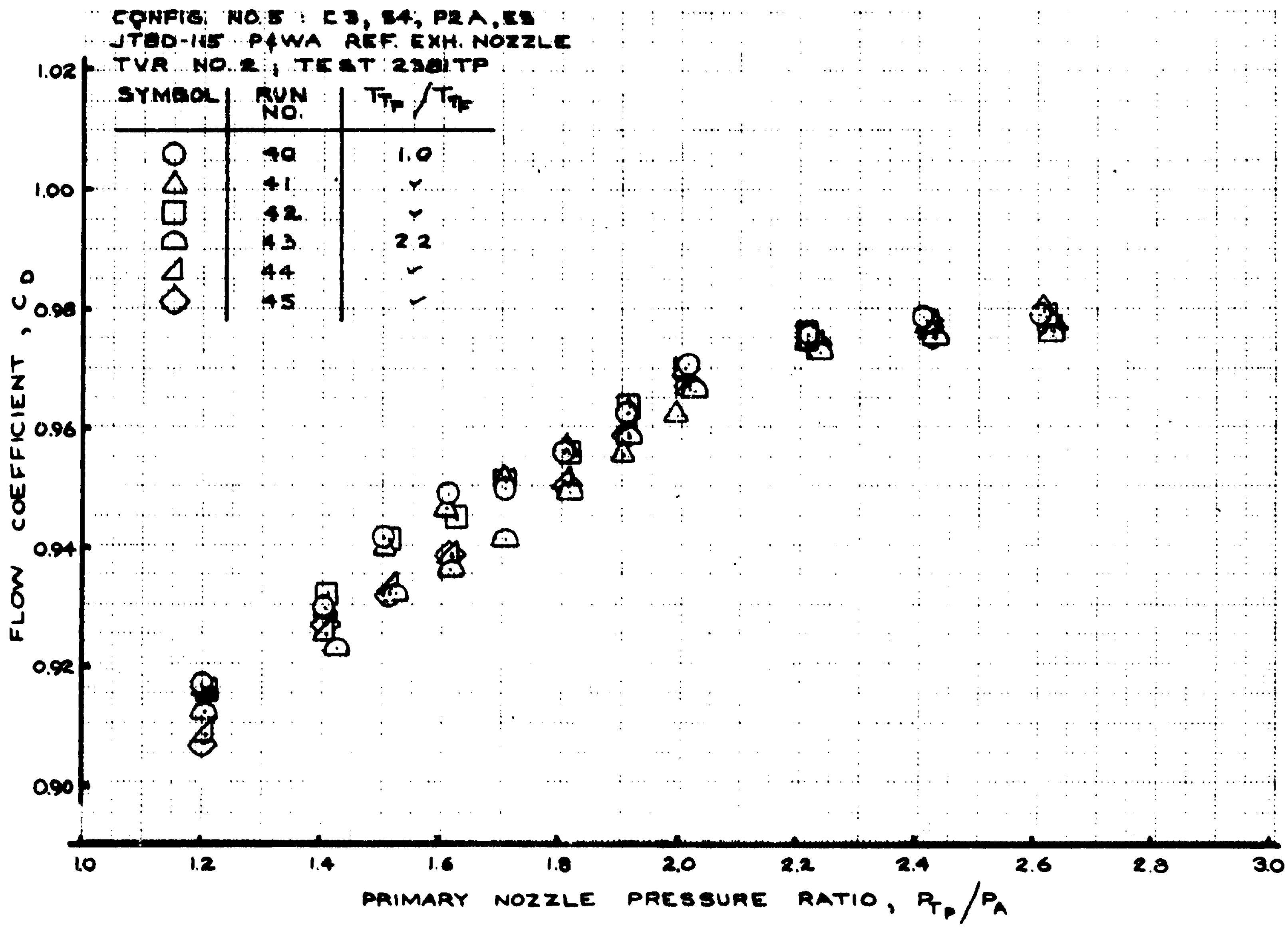

FIGURE 96 - FLOW COEFFICIENT
TEST CONFIG. NO. 5; RUNS 40-45

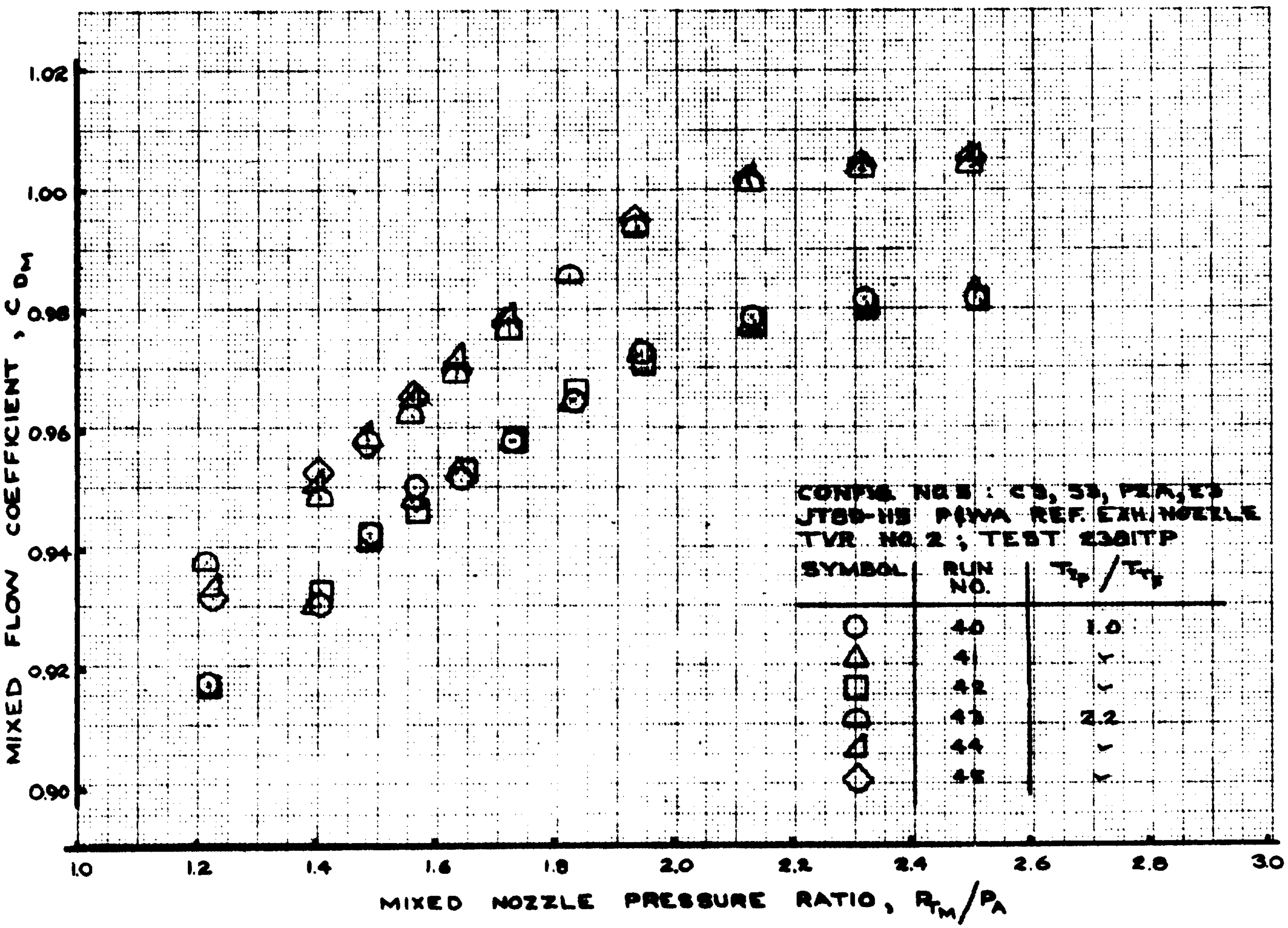

FIGURE 97 - MIXED FLOW COEFFICIEN.
TEST CONFIG. NO. 5; RUNS 40-45

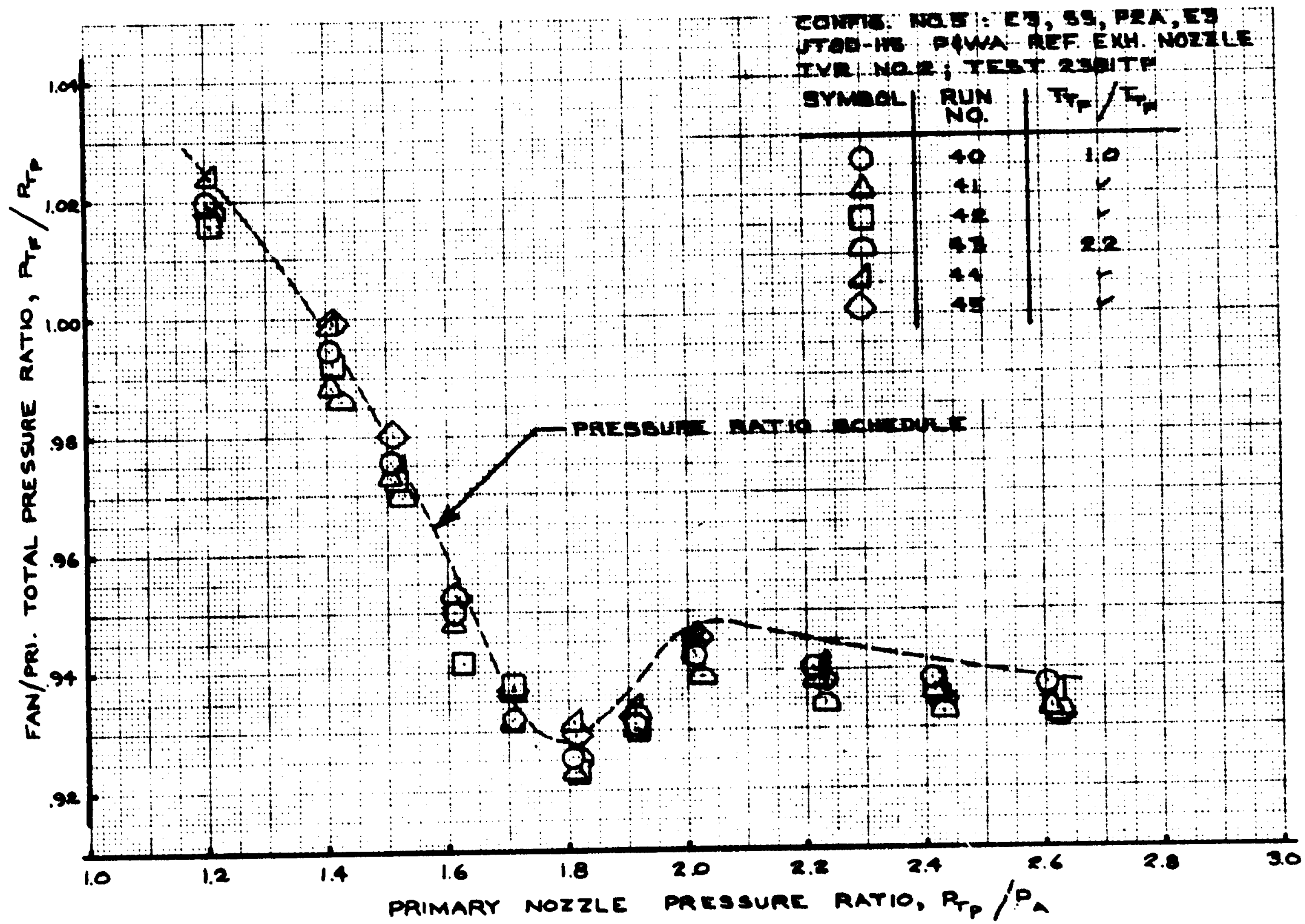

FIGURE 98 - FAN/PRIMARY TOTAL PRESSURE RATIO
TEST CONFIG. NO. 5; RUNS 40-45

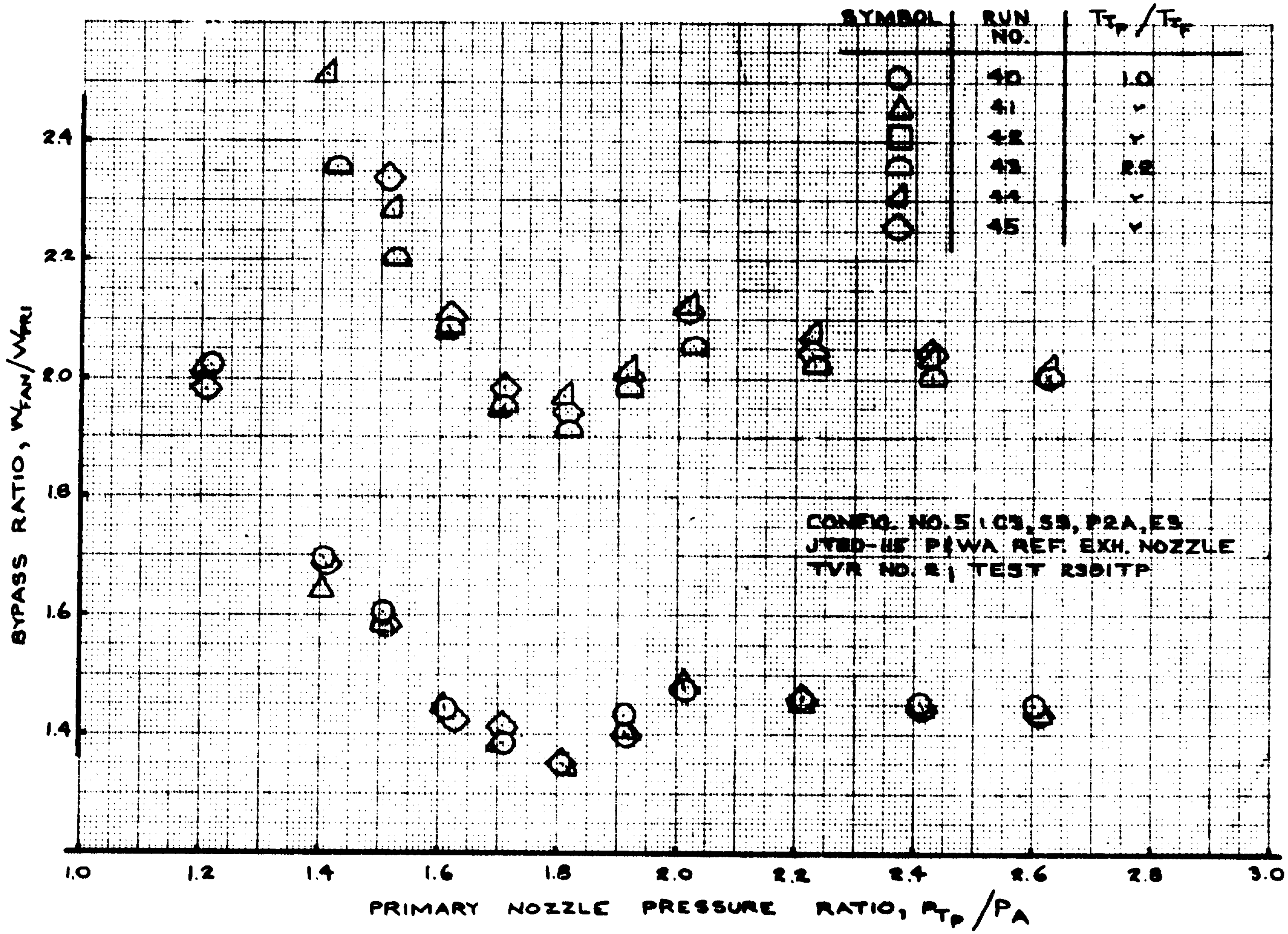

FIGURE 99 - BYPASS RATIO
TEST CONFIG. NO. 5; RUNS 40-45

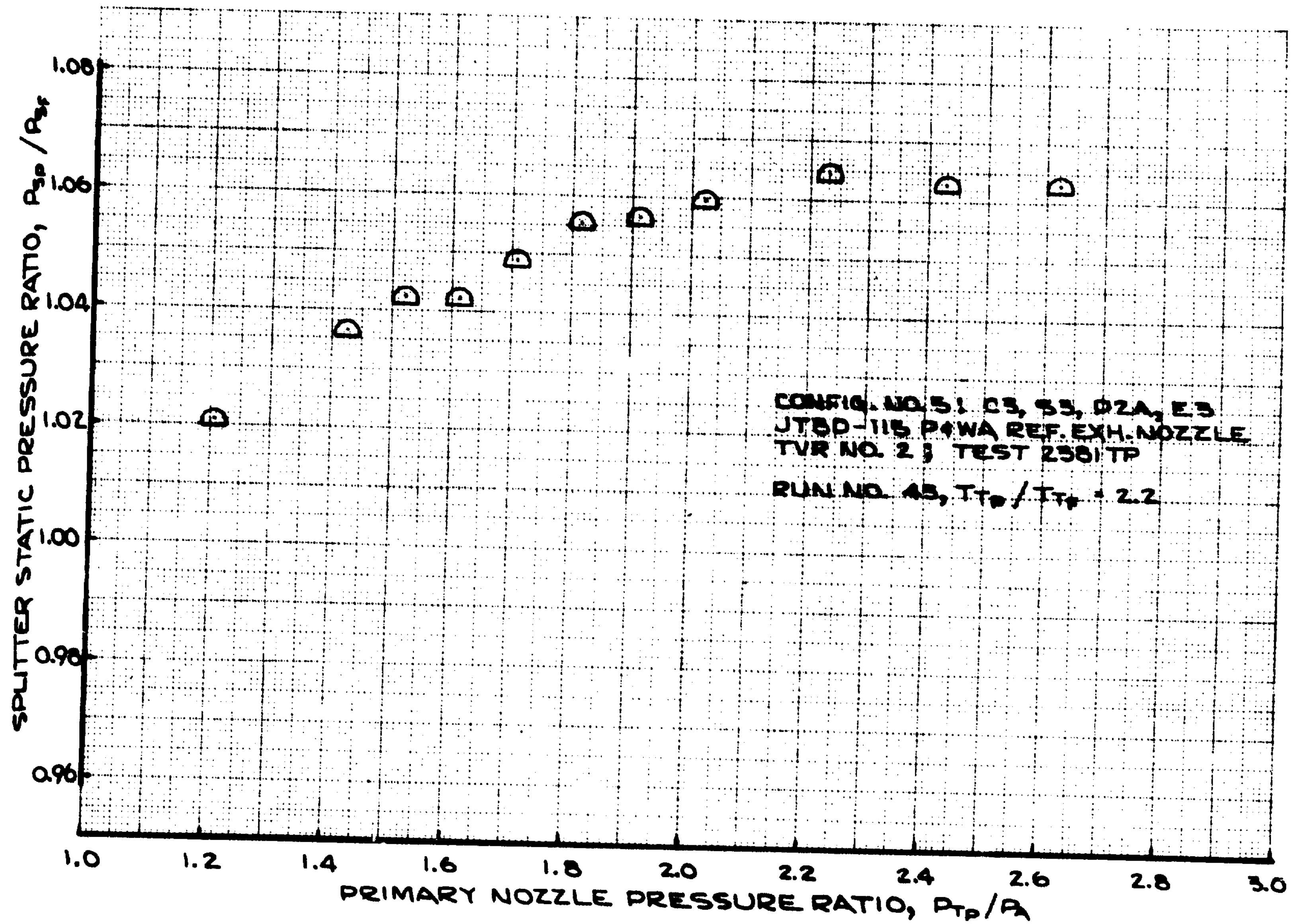

FIGURE 100 - SPLITTER STATIC PRESSURE RATIO
TEST CONFIG. NO. 5; RUN 43

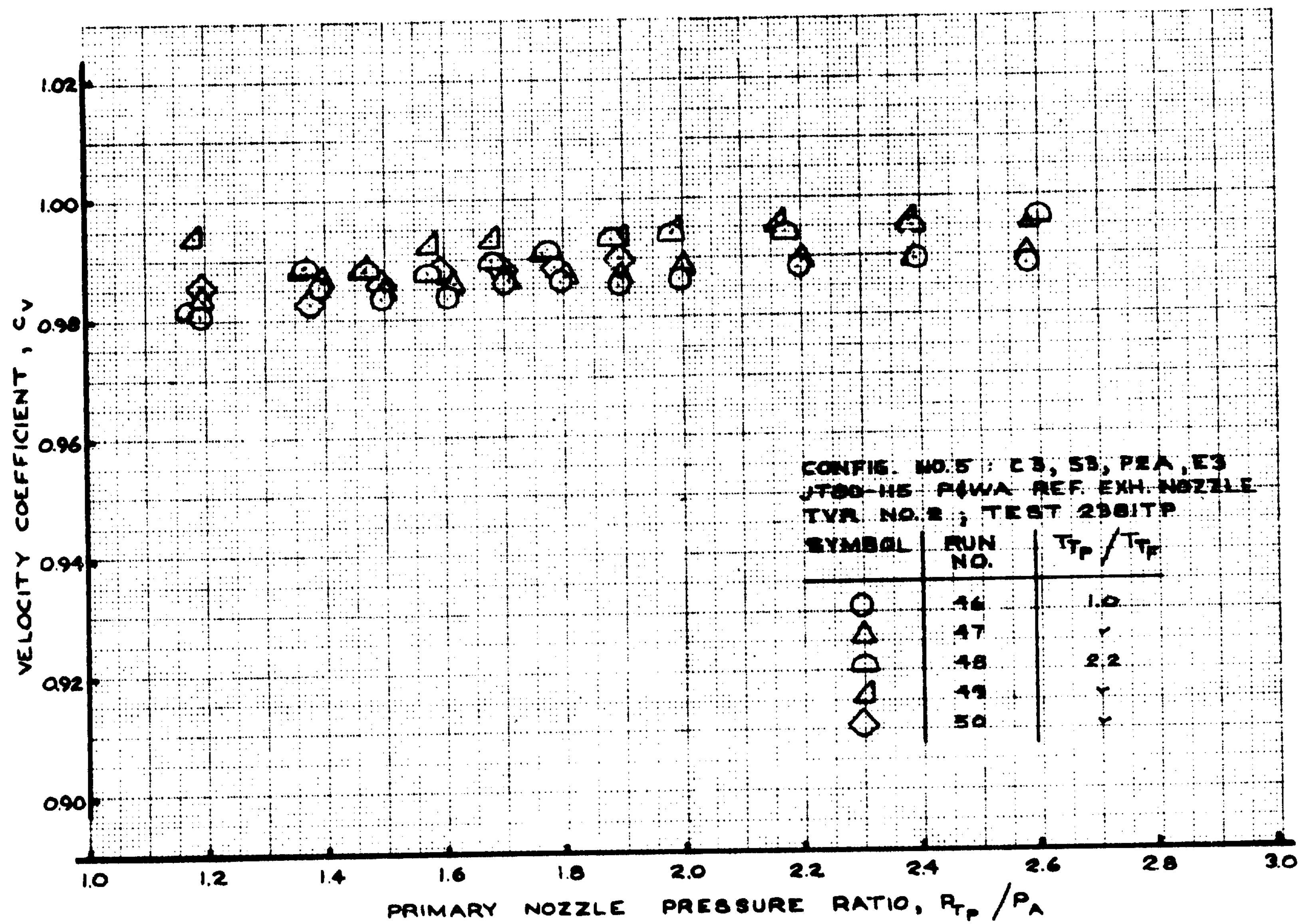

FIGURE 101- VELOCITY COEFFICIENT
TEST CONFIG. NO. 5; RUNS 46-50

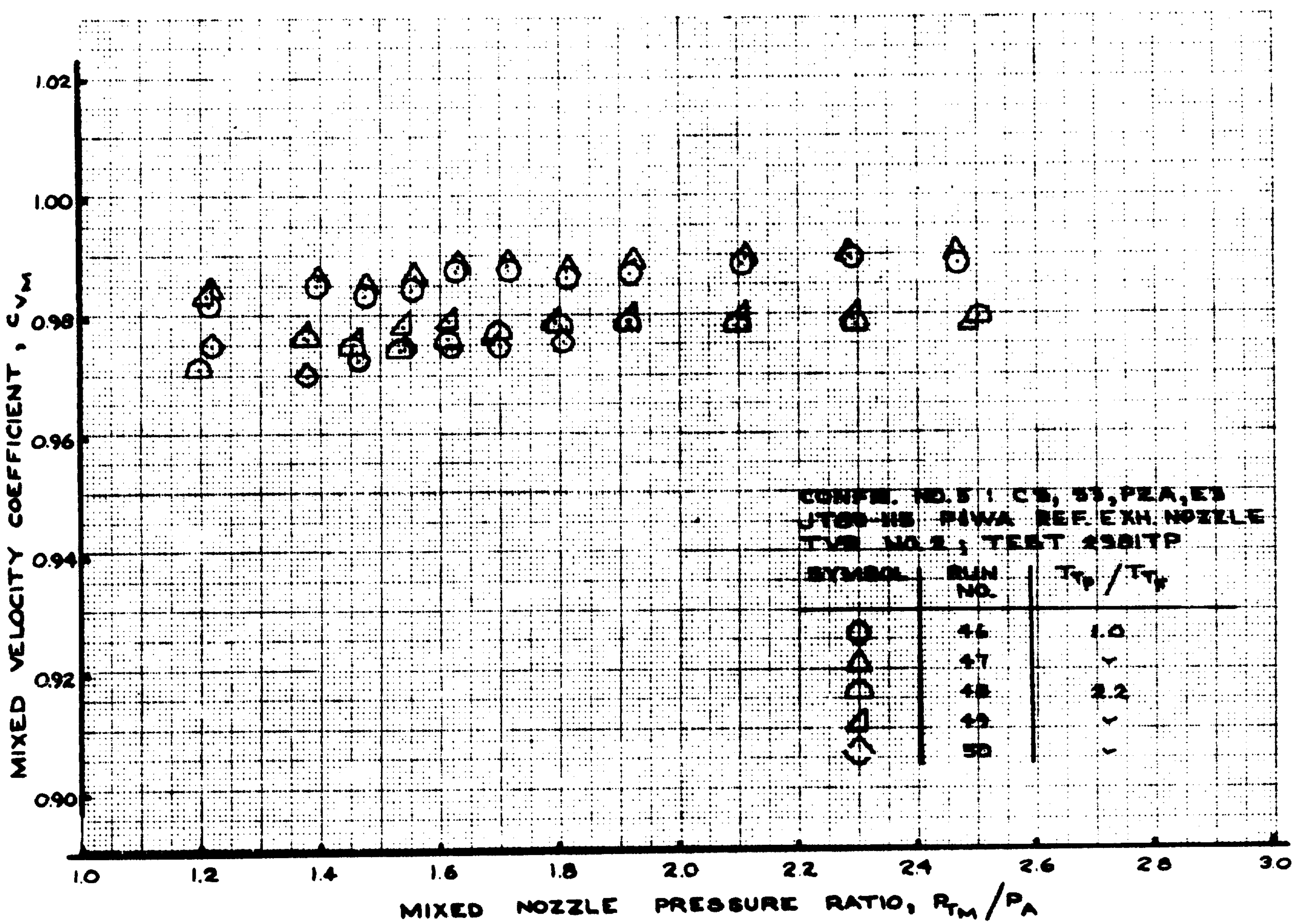

FIGURE 102- MIXED VELOCITY COEFFICIENT
TEST CONFIG. NO. 5; RUNS 46-50

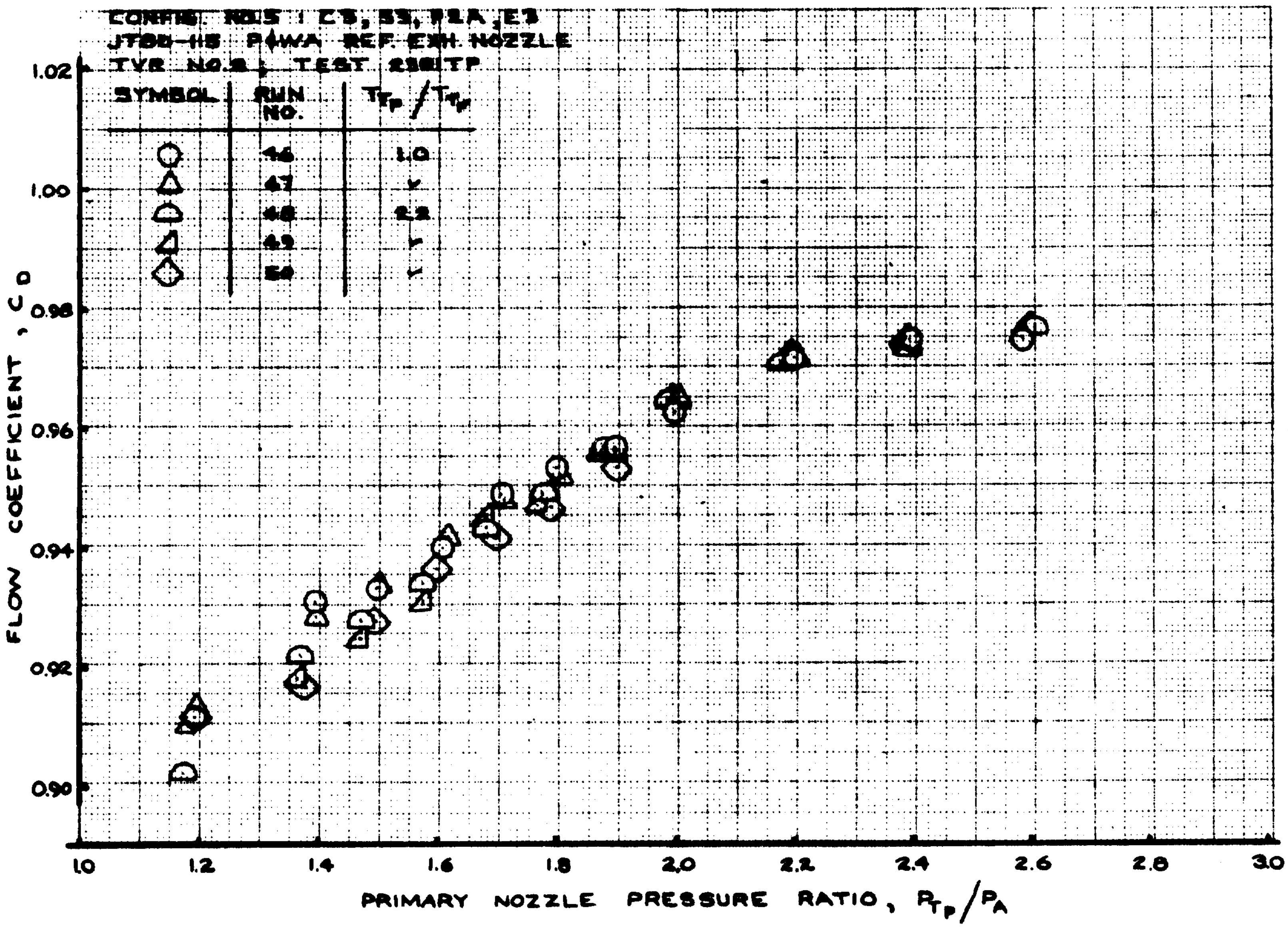

FIGURE 103- FLOW COEFFICIENT
TEST CONFIG. NO. 5; RUNS 46-50

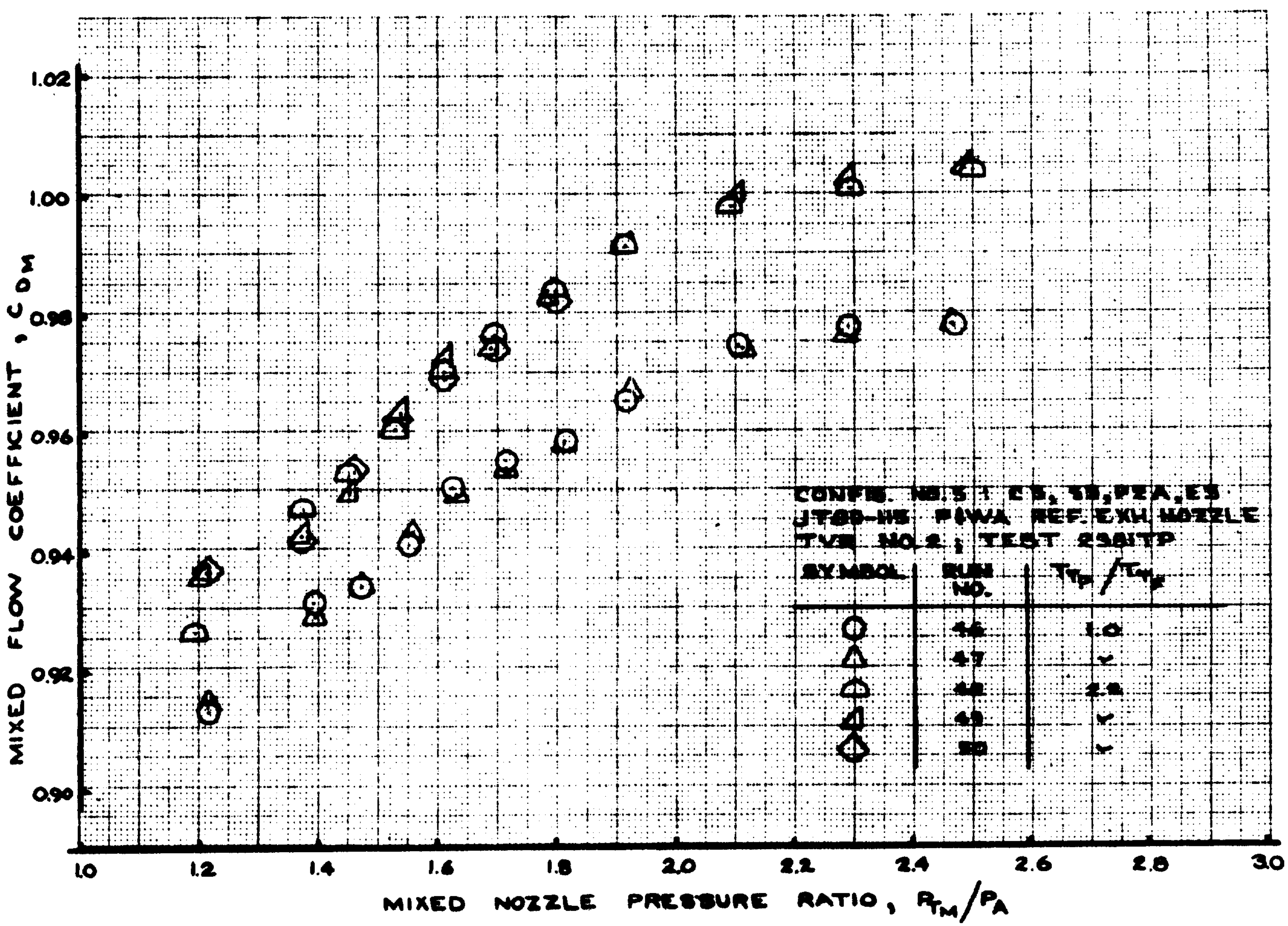

FIGURE 104- MIXED FLOW COEFFICIENT
TEST CONFIG. NO. 5; RUNS 46-50

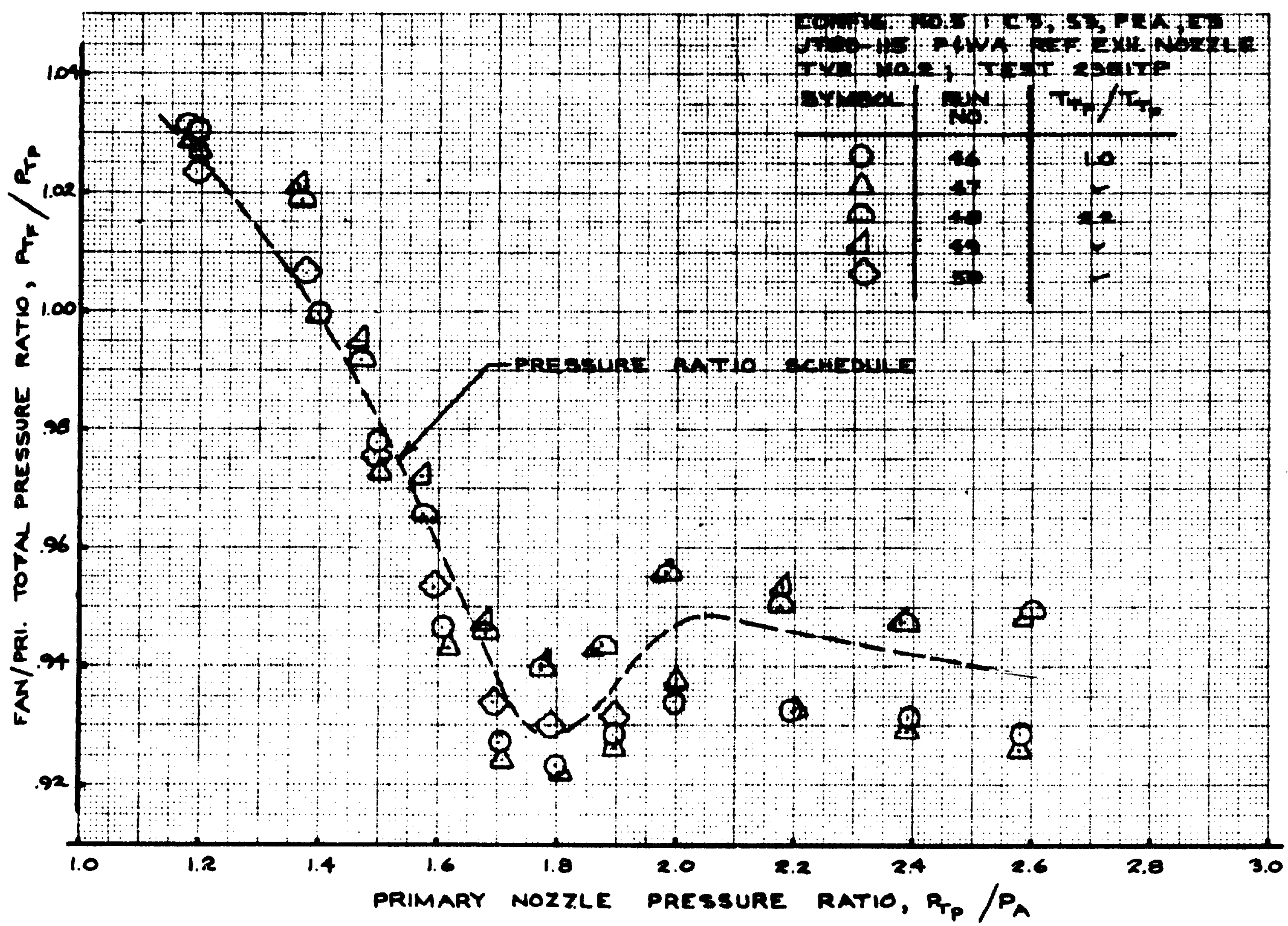

FIGURE 105- FAN/PRIMARY TOTAL PRESSURE RATIO
TEST CONFIG. NO. 5; RUNS 46-50

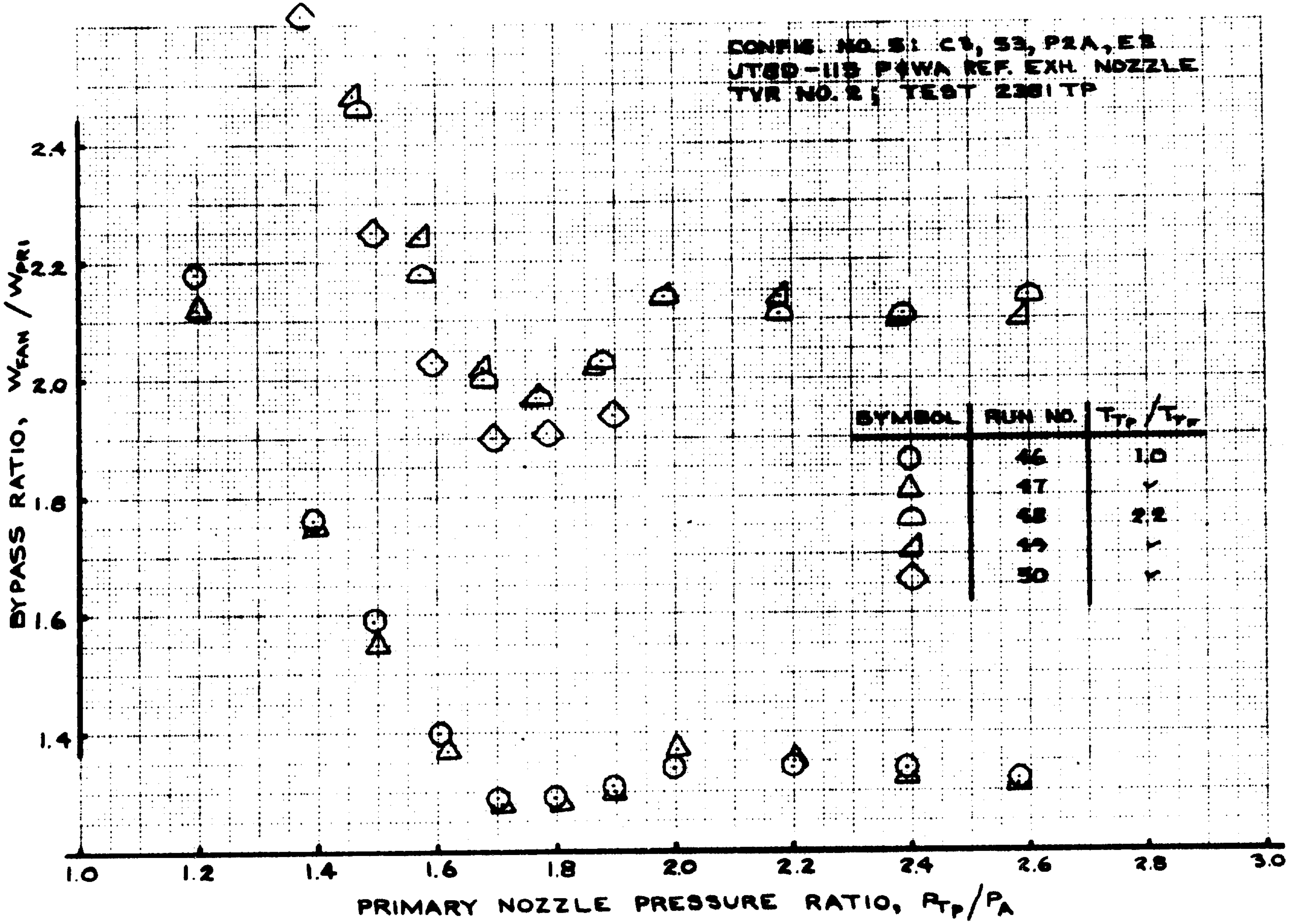

FIGURE 106- BYPASS RATIO
TEST CONFIG. NO. 5; RUNS 46-50

7.2.6 TEST CONFIGURATION (T.C.) NO. 6

Configuration Description: P&WA Reference nozzle for JT8D-117.

Hardware Designations:

Outer Nozzle Wall	Splitter	Plug	Exit
C3	S4	P2A	E3

Plotted Data:

Figure 107 - Velocity Coefficient; Runs 51-56.

Figure 108 - Mixed Velocity Coefficient; Runs 51-56.

Figure 109 - Flow Coefficient; Runs 51-56.

Figure 110 - Mixed Flow Coefficient; Runs 51-56.

Figure 111 - Fan/Primary Total Pressure Ratio; Runs 51-56.

Figure 112 - Bypass Ratio; Runs 51-56.

Figure 113 - Splitter Static Pressure Ratio; Run 55.

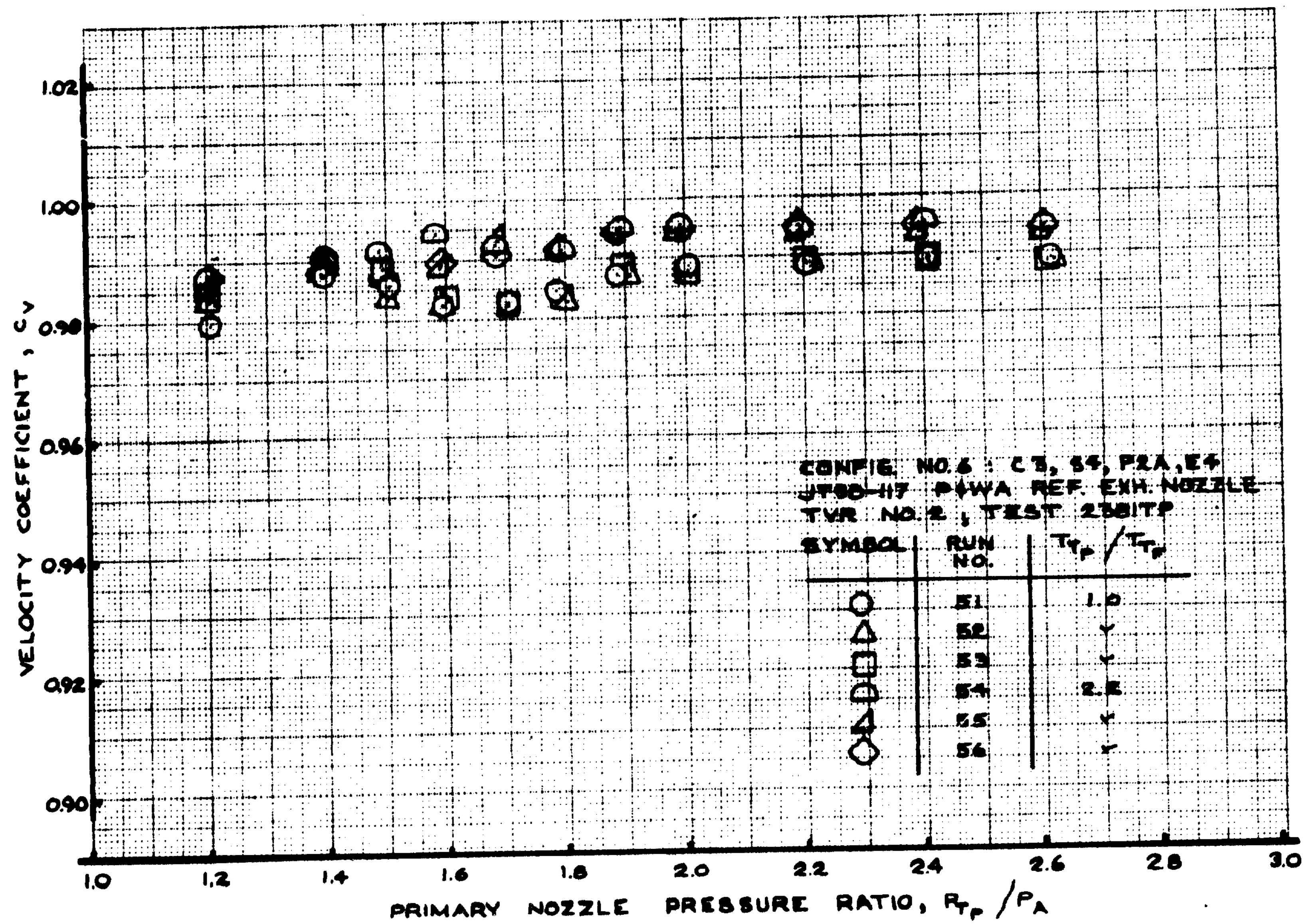

FIGURE 107- VELOCITY COEFFICIENT
TEST CONFIG. NO. 6; RUNS 51-56

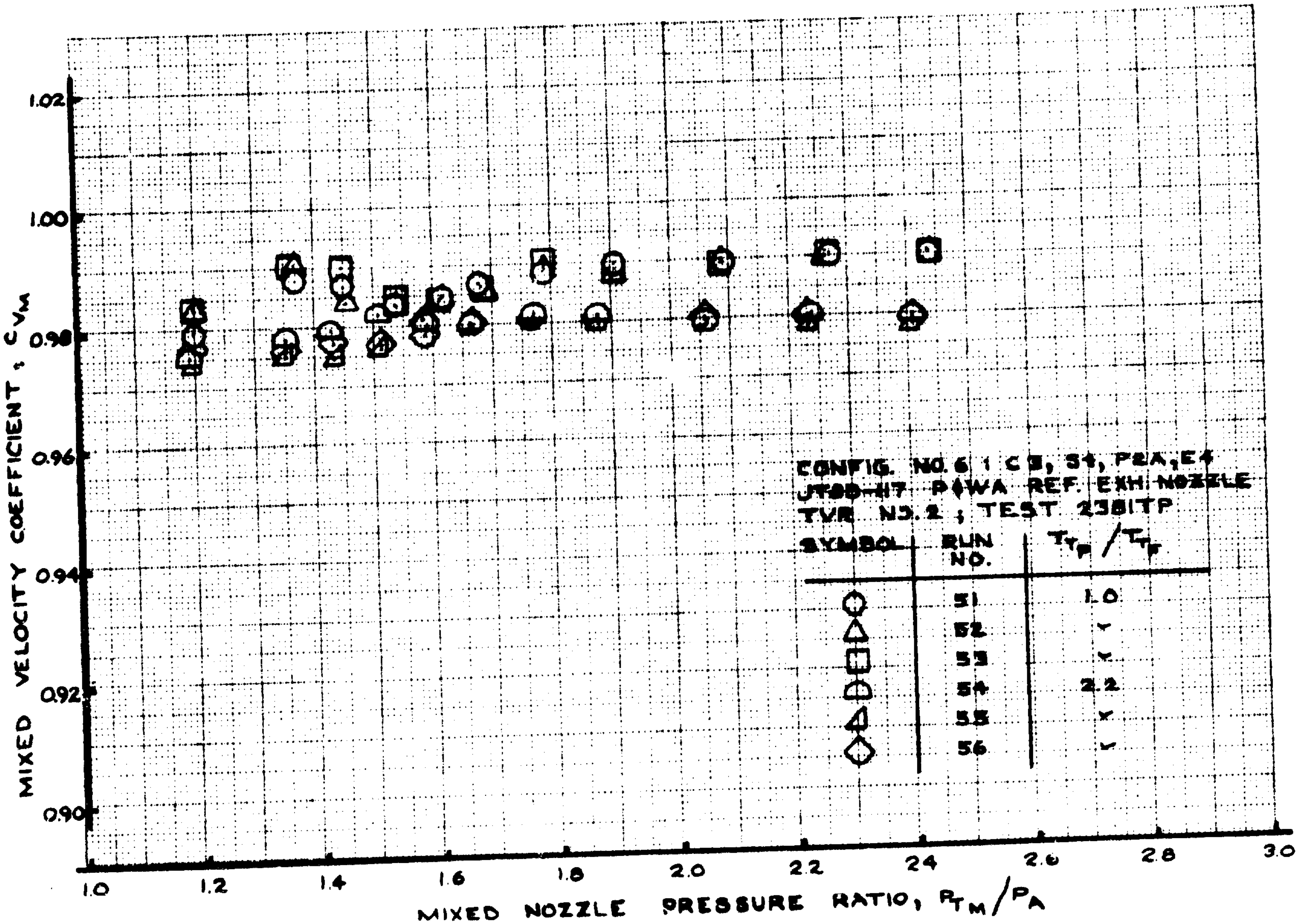

FIGURE 108- MIXED VELOCITY COEFFICIENT
TEST CONFIG. NO. 6; RUNS 51-56

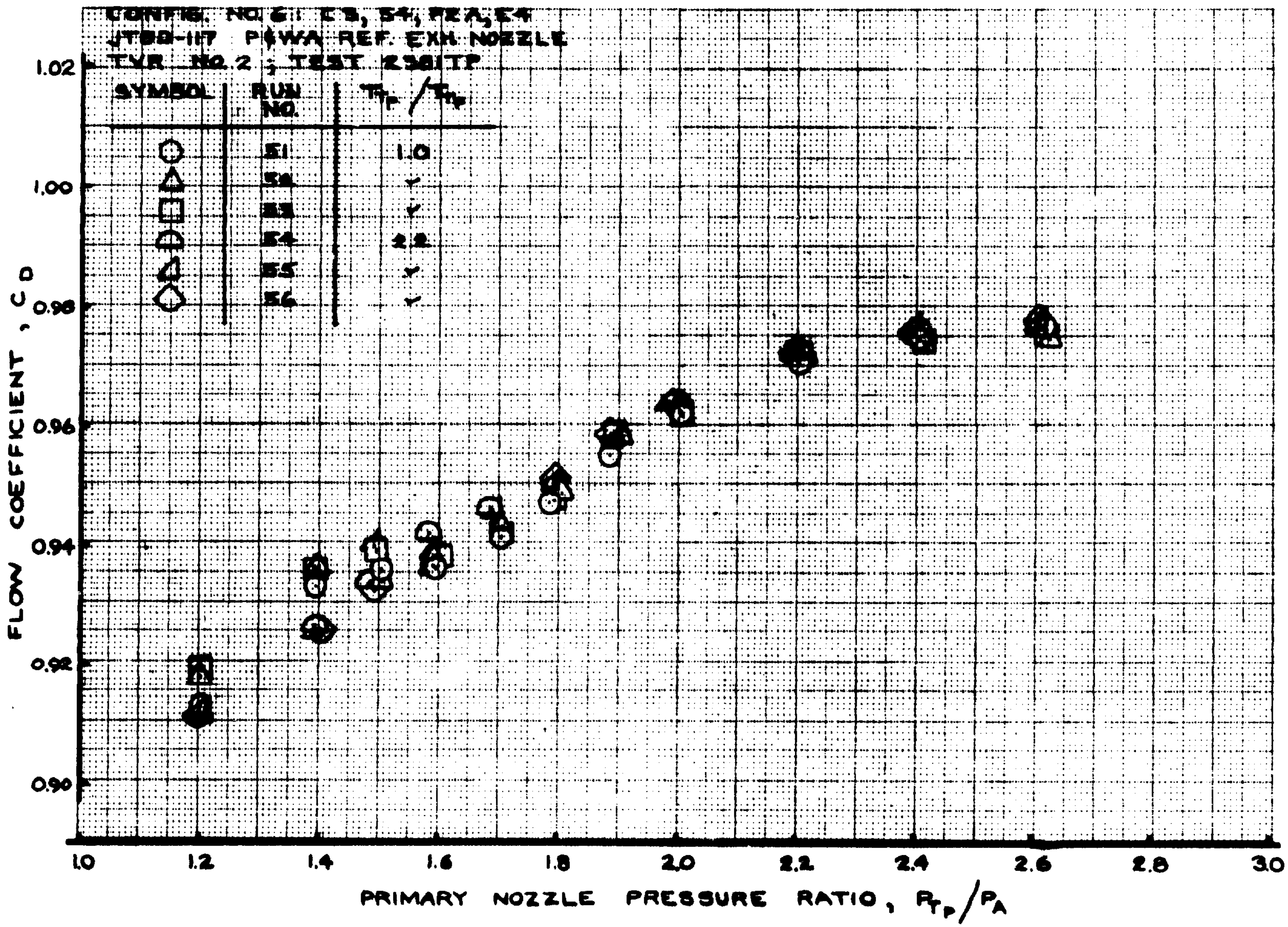

FIGURE 109- FLOW COEFFICIENT
TEST CONFIG. NO. 6; RUNS 51-56

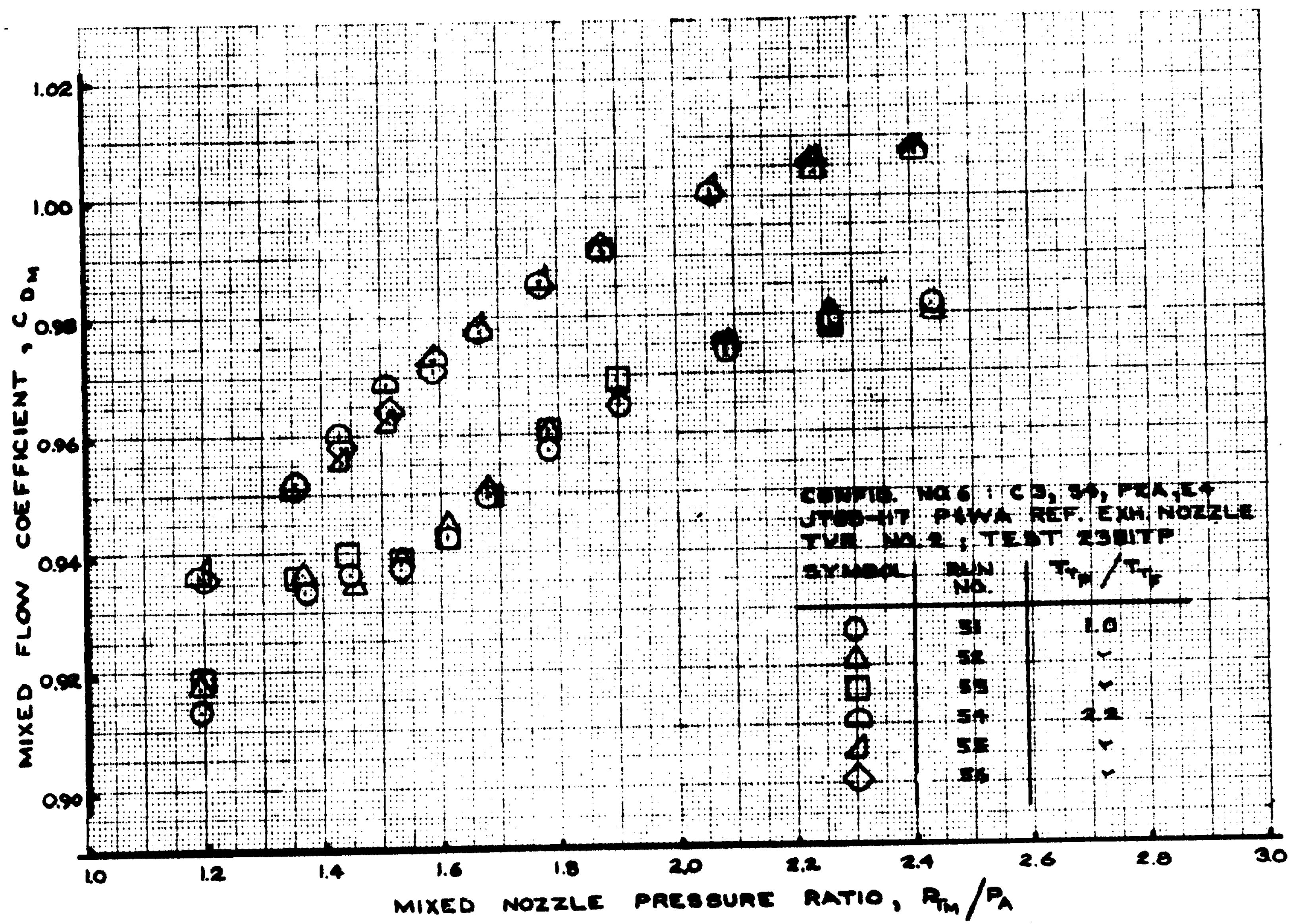

FIGURE 110- MIXED FLOW COEFFICIENT
TEST CONFIG. NO. 6; RUNS 51-56

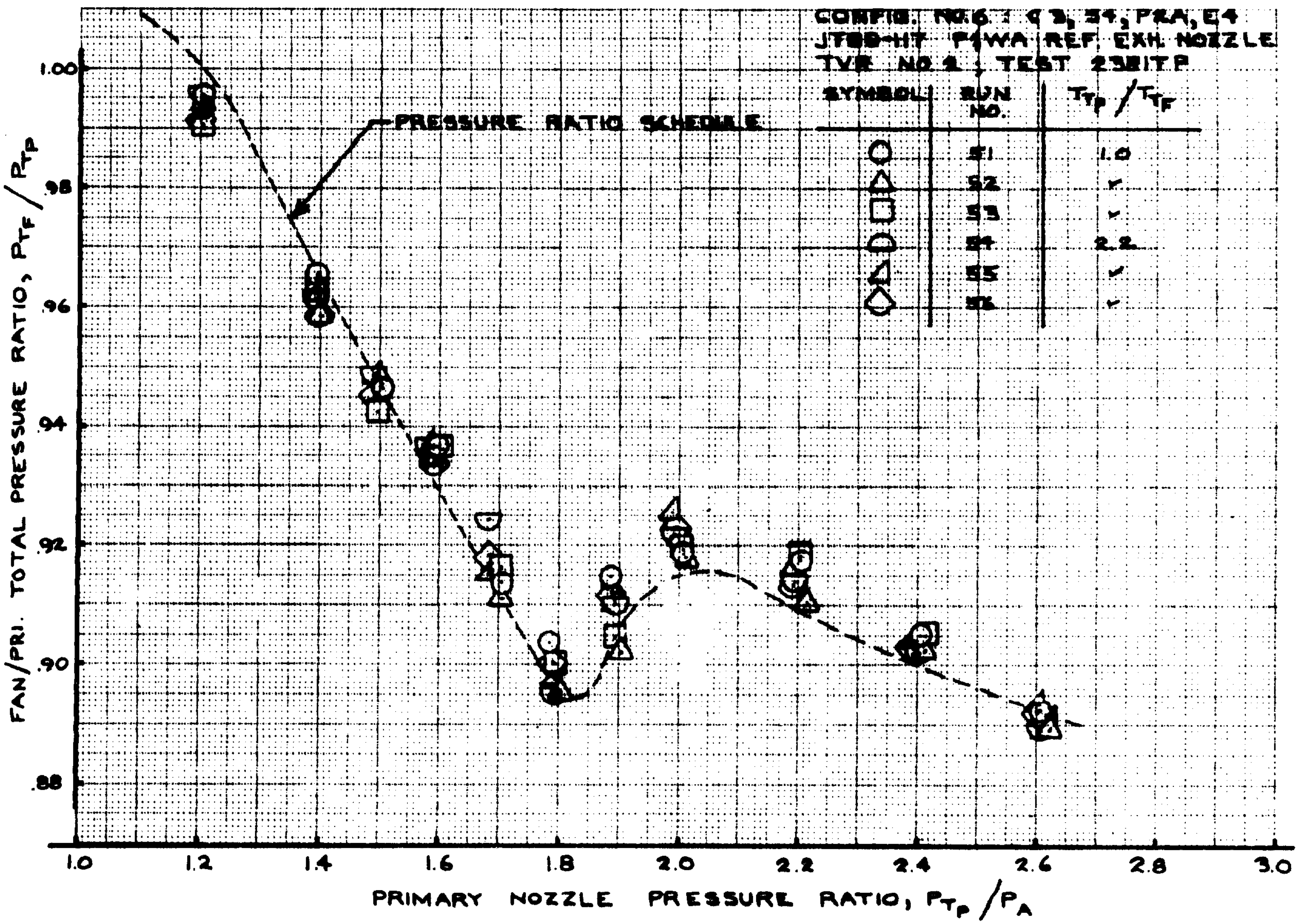

FIGURE 111- FAN/PRIMARY TOTAL PRESSURE RATIO
TEST CONFIG. NO. 6; RUNS 51-56

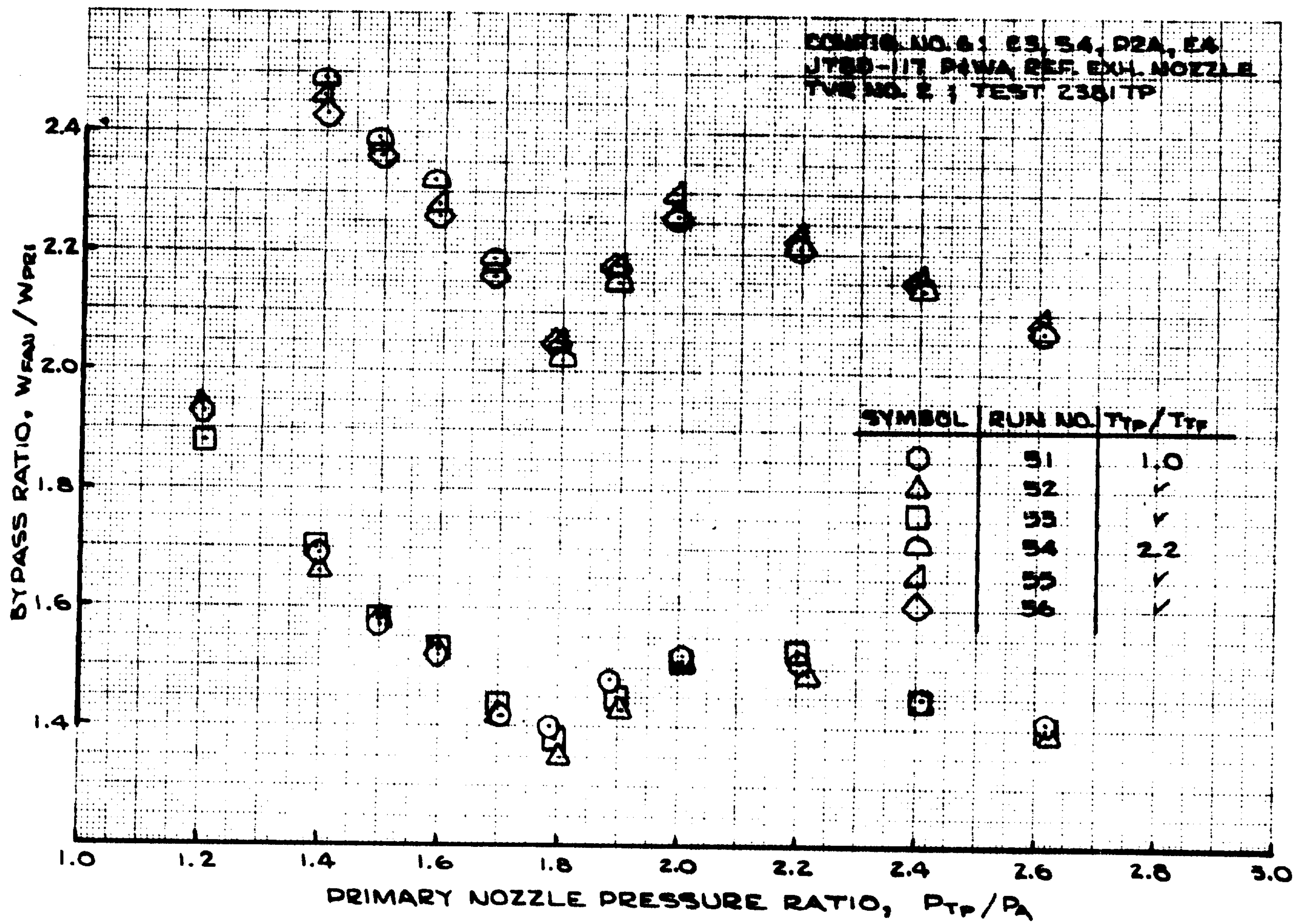

FIGURE 112 - BYPASS RATIO
TEST CONFIG. NO. 6; RUNS 51-56

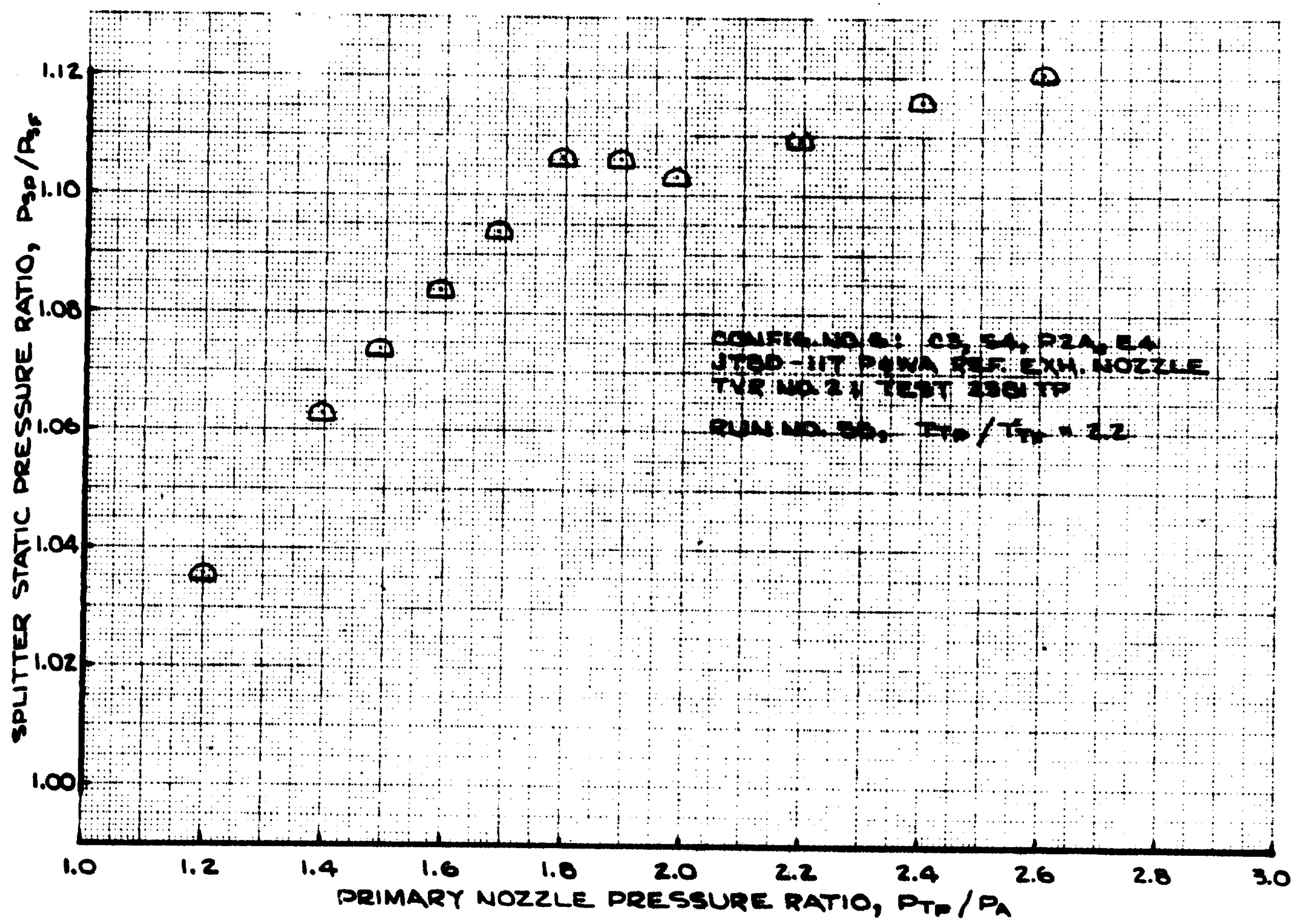

FIGURE 113 - SPLITTER STATIC PRESSURE RATIO
TEST CONFIG. NO. 6; RUN 55

7.2.7 TEST CONFIGURATION (T.C.) NO. 7

Configuration Description: Boeing Config. No. 2 design for JT8D-109.

Hardware Designations:

Outer Nozzle Wall	Splitter	Plug	Exit
C4	S5	P5-1	E5

Plotted Data:

Figure 114 - Velocity Coefficient; Runs 57-65.
Figure 115 - Mixed Velocity Coefficient; Runs 57-65.
Figure 116 - Flow Coefficient; Runs 57-65.
Figure 117 - Mixed Flow Coefficient; Runs 57-65.
Figure 118 - Fan/Primary Total Pressure Ratio; Runs 57-65.
Figure 119 - Mixed Nozzle Pressure Ratio; Runs 57-65.
Figure 120 - Bypass Ratio; Runs 57-65.
Figure 121 - Splitter Static Pressure Ratio; Run 64.
Figure 122 - Velocity Coefficient; Runs 181-182.
Figure 123 - Mixed Velocity Coefficient; Runs 181-182.
Figure 124 - Flow Coefficient; Runs 181-182.
Figure 125 - Mixed Flow Coefficient; Runs 181-182.
Figure 126 - Fan/Primary Total Pressure Ratio; Runs 181-182.
Figure 127 - Bypass Ratio; Runs 181-182.

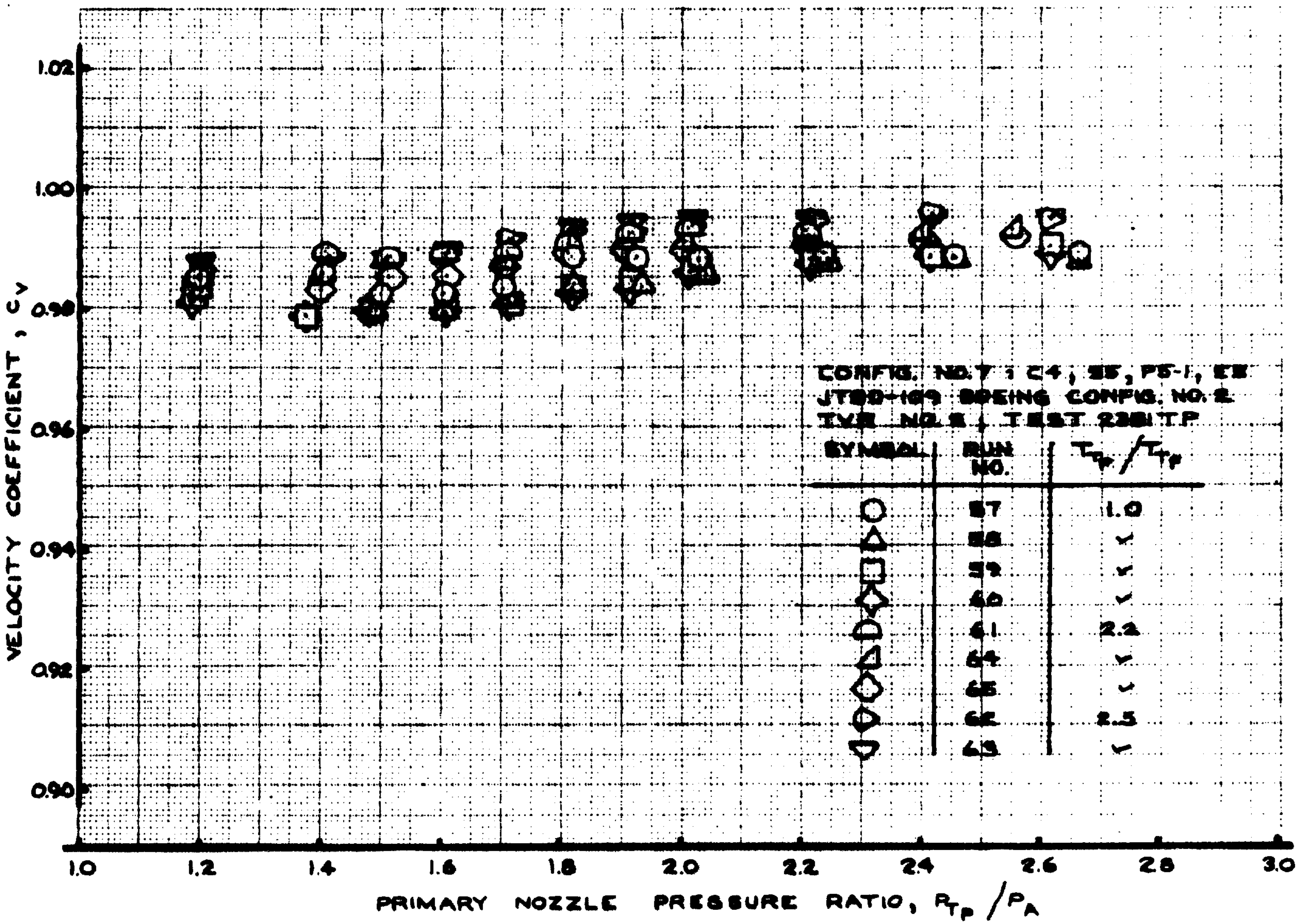

FIGURE 114- VELOCITY COEFFICIENT
TEST CONFIG. NO. 7; RUNS 57-65

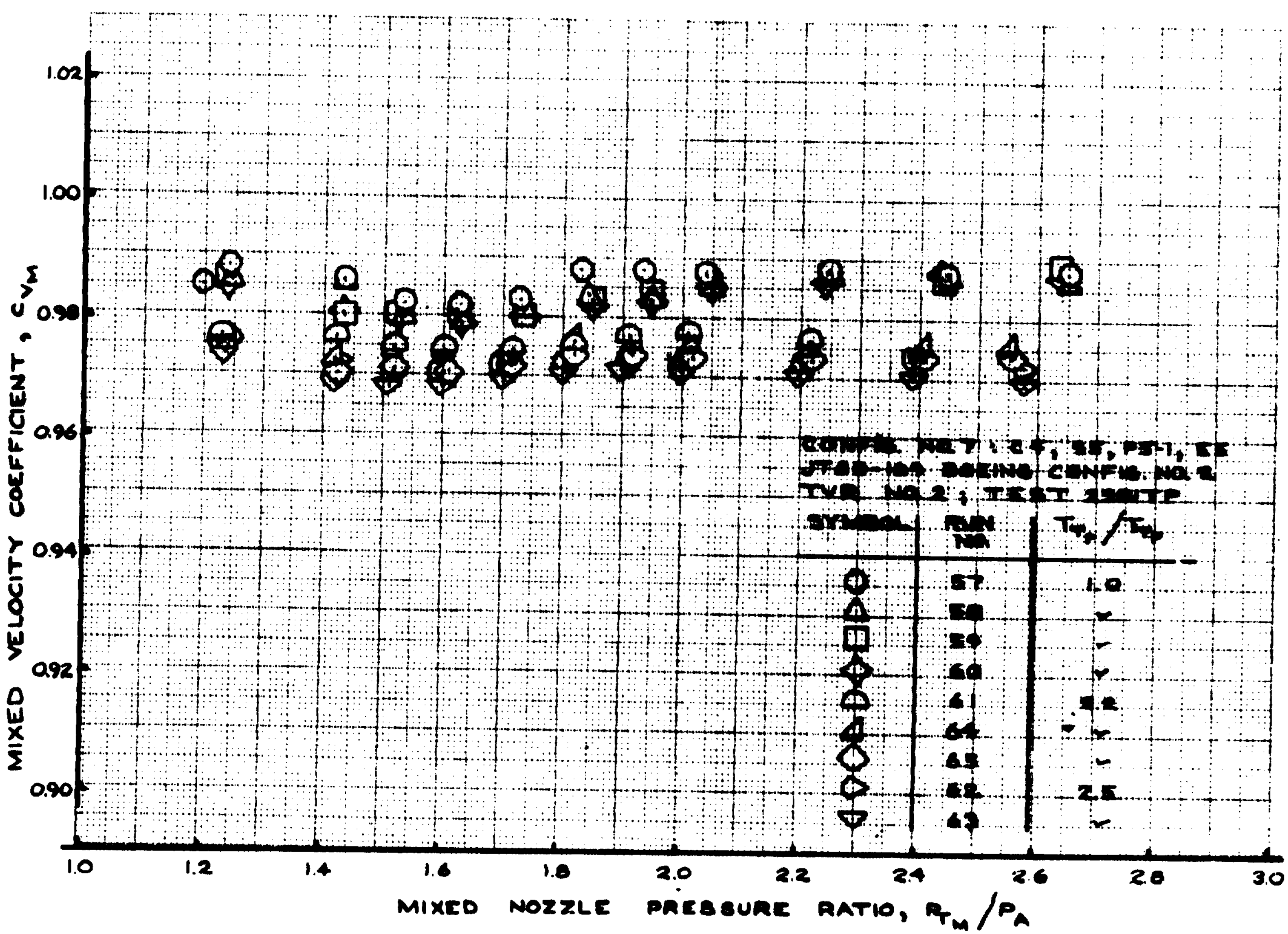

FIGURE 115- MIXED VELOCITY COEFFICIENT
TEST CONFIG. NO. 7; RUNS 57-65

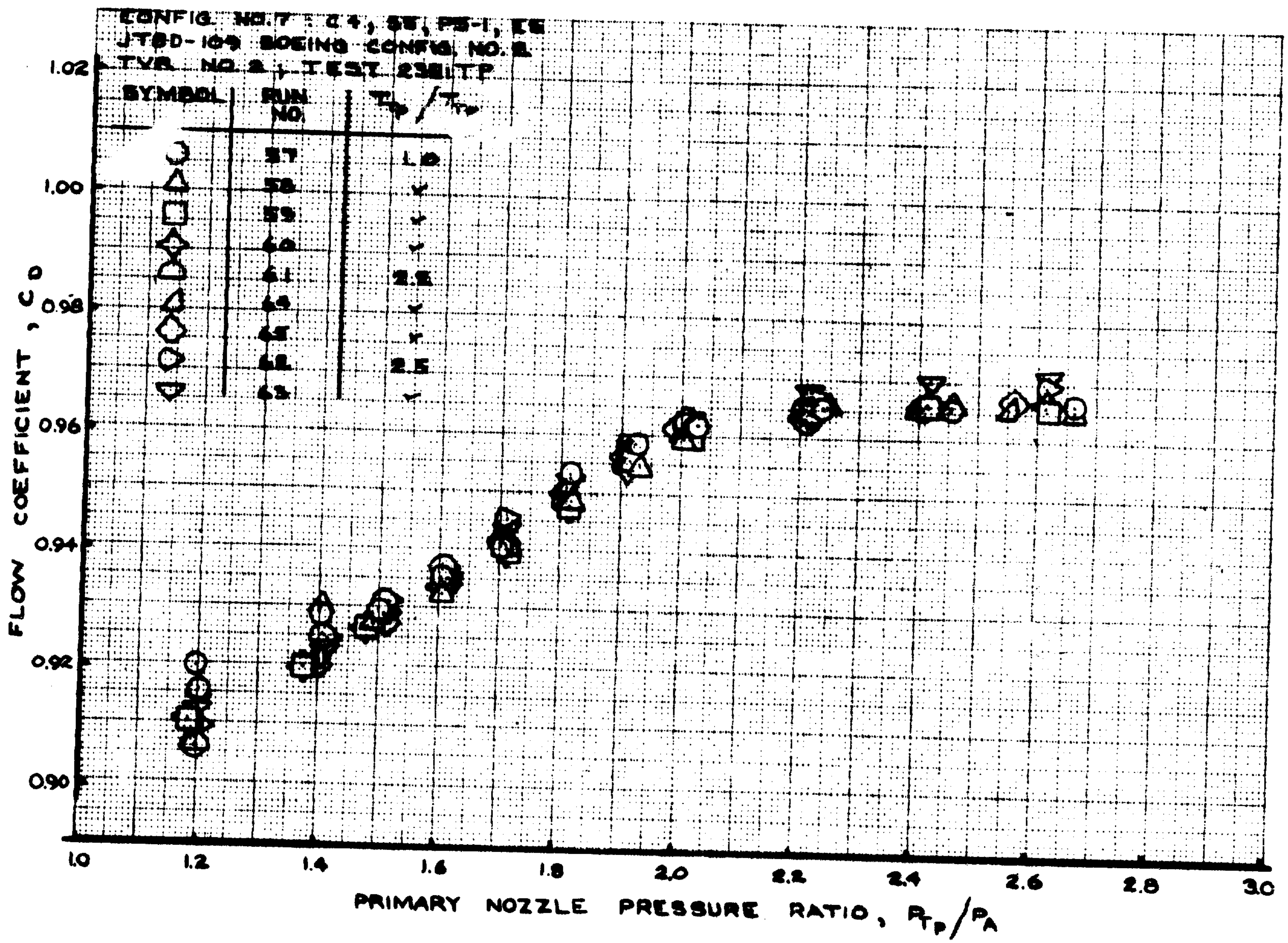

FIGURE 116- FLOW COEFFICIENT
TEST CONFIG. NO. 7; RUNS 57-65

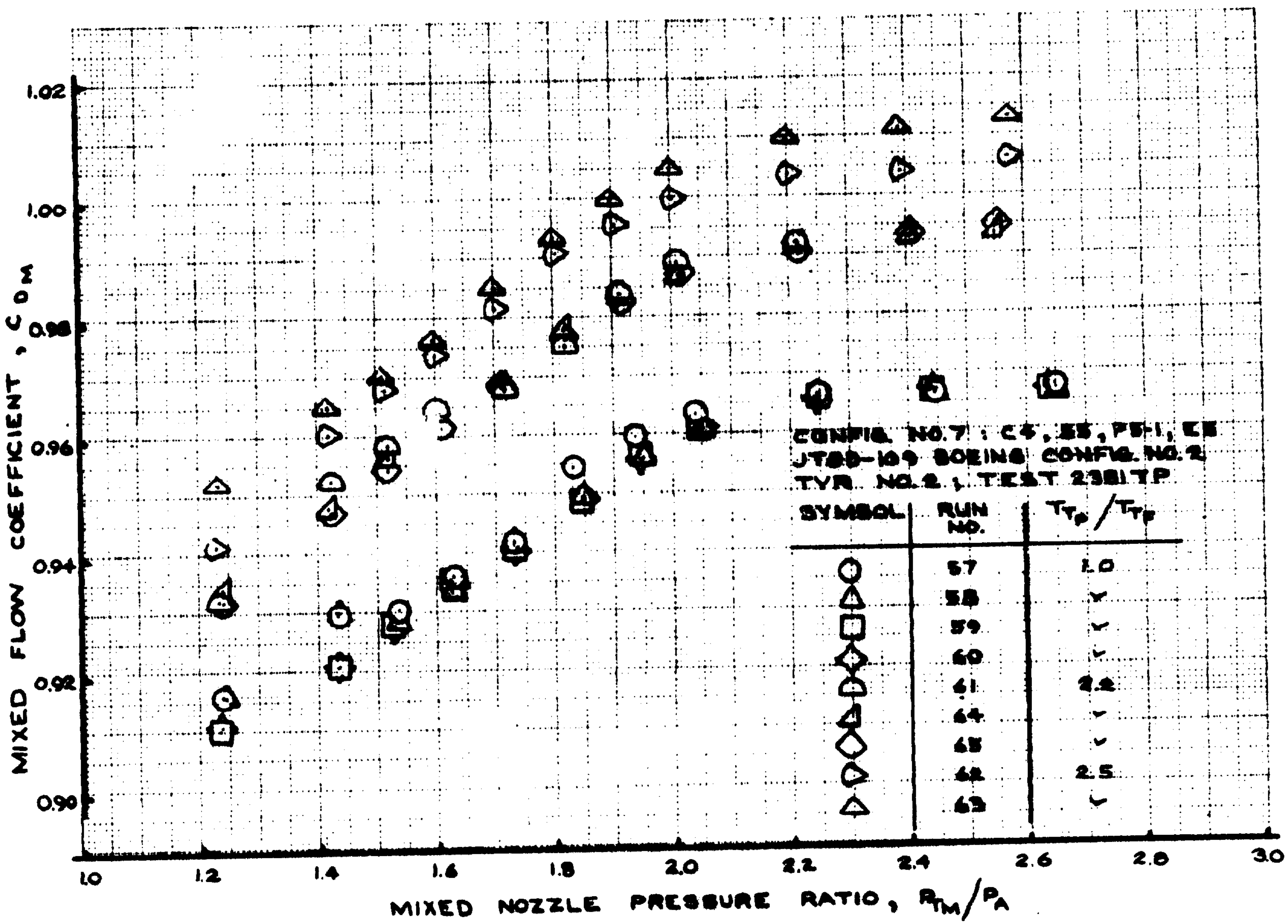

FIGURE 117- MIXED FLOW COEFFICIENT
TEST CONFIG. NO. 7; RUNS 57-65

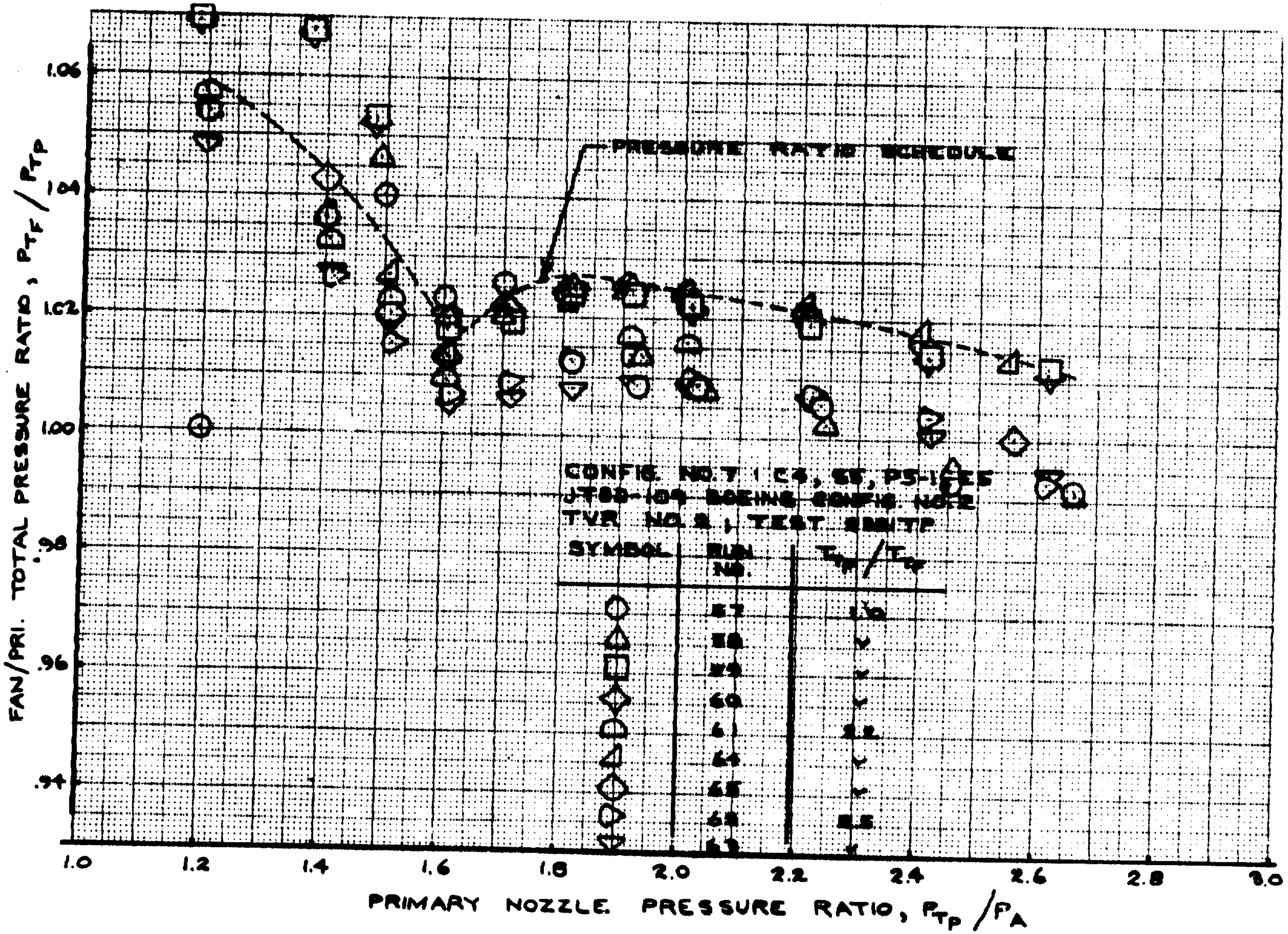

FIGURE 118- FAN/PRIMARY TOTAL PRESSURE RATIO
TEST CONFIG. NO. 7; RUNS 57-65

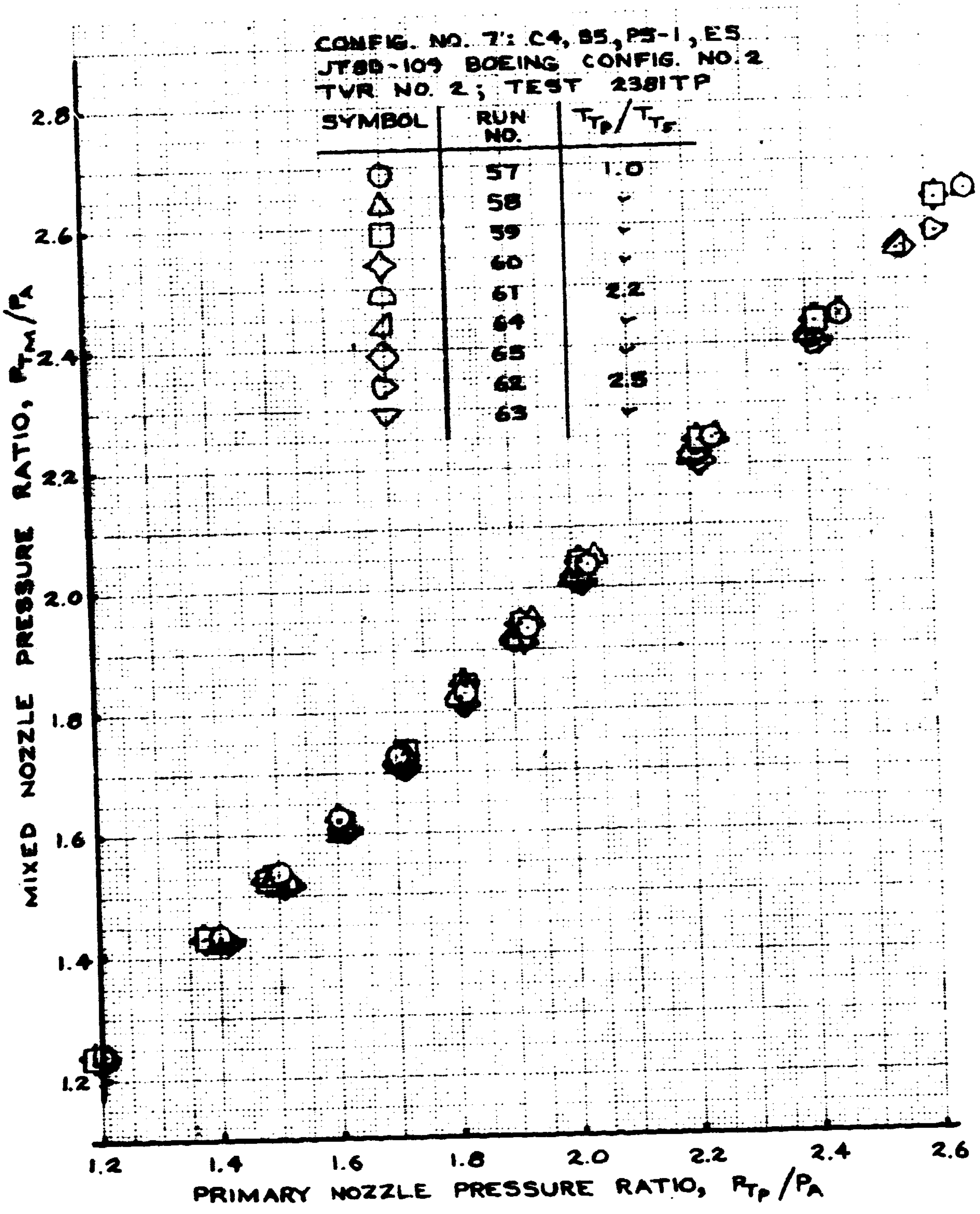

FIGURE 119- MIXED NOZZLE PRESSURE RATIO
TEST CONFIG. NO. 7; RUNS 57-65

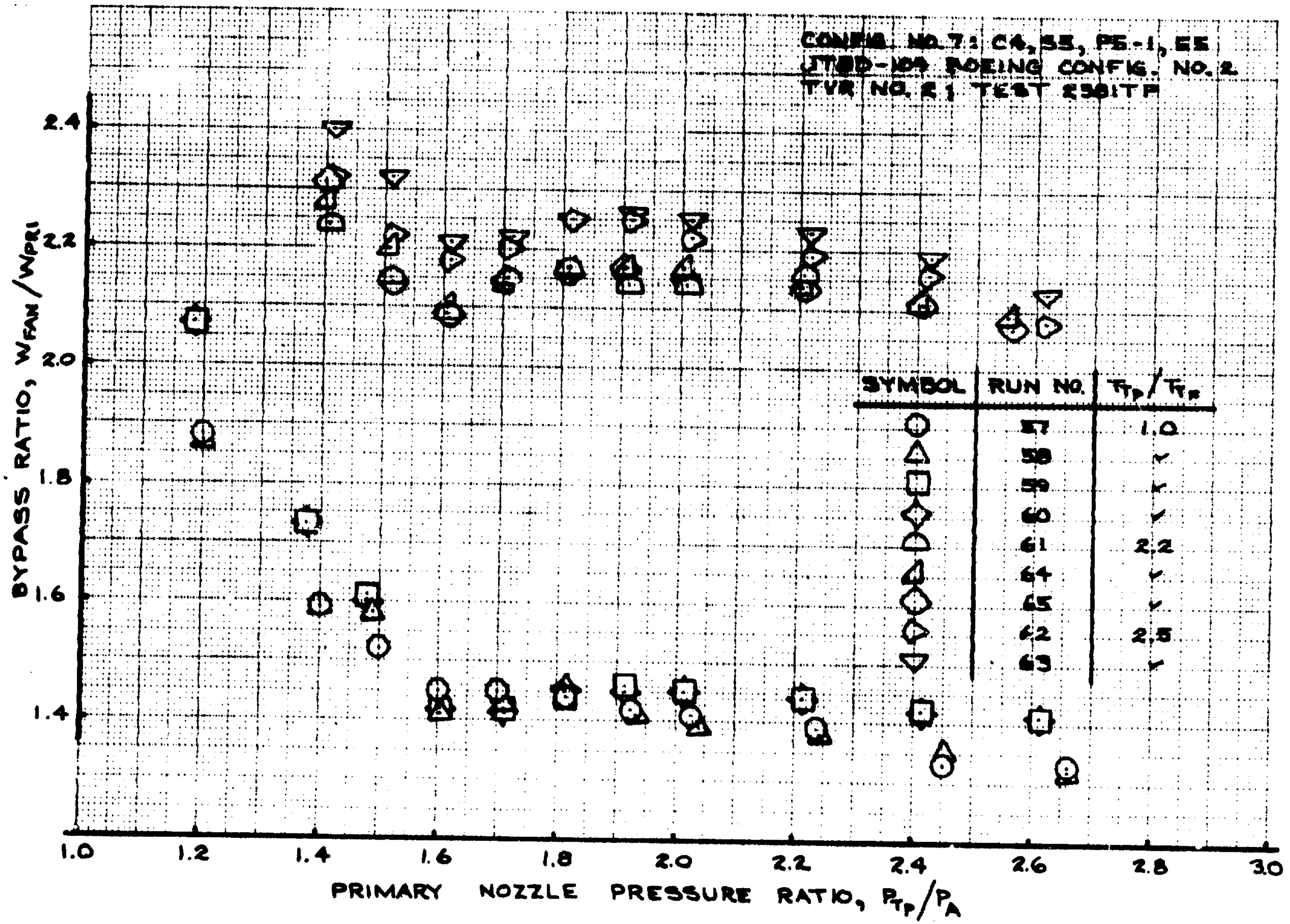

FIGURE 120- BYPASS RATIO
TEST CONFIG. NO. 7; RUNS 57-65

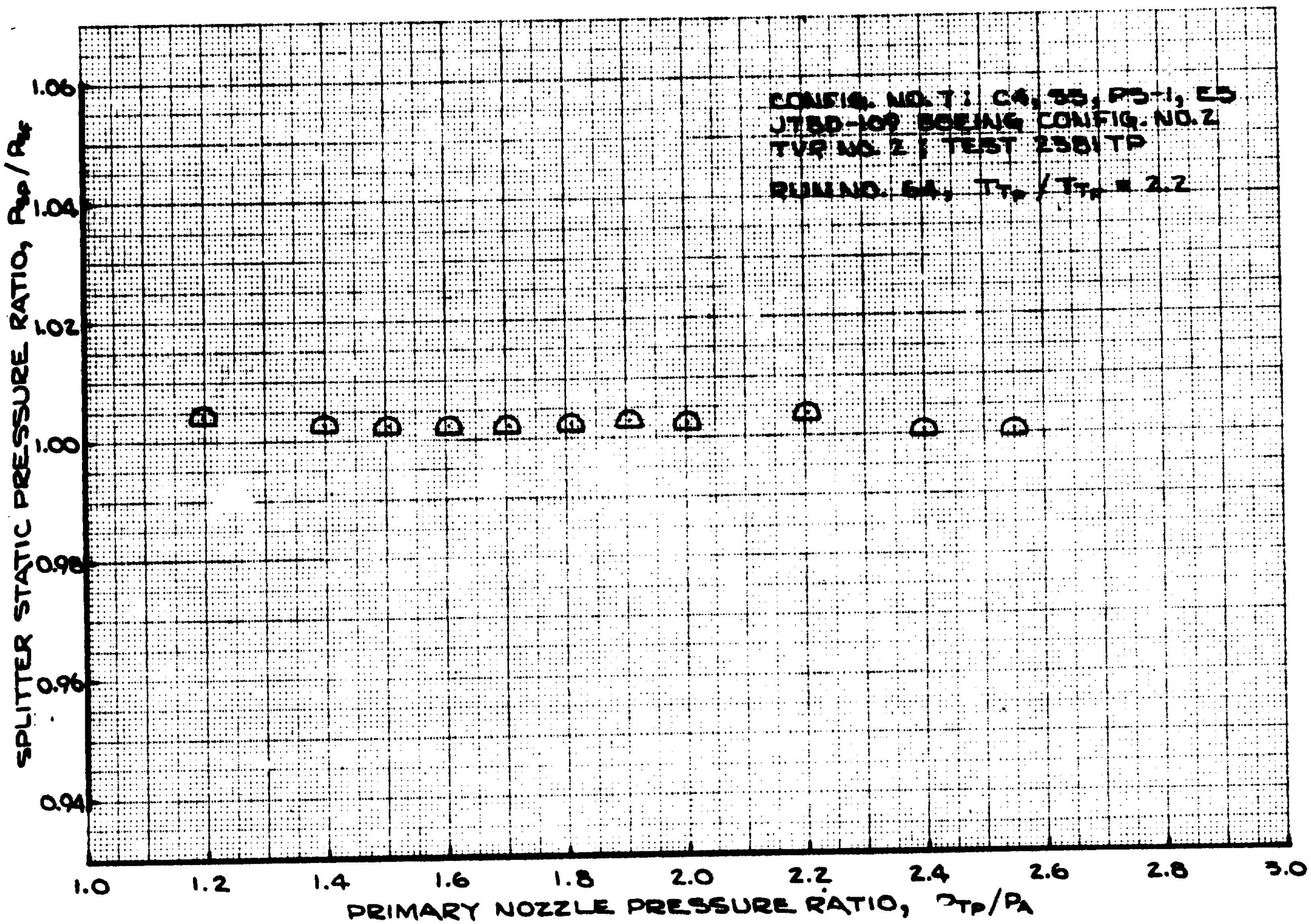

FIGURE 121 - SPLITTER STATIC PRESSURE RATIO
TEST CONFIG. NO. 7; RUN 64

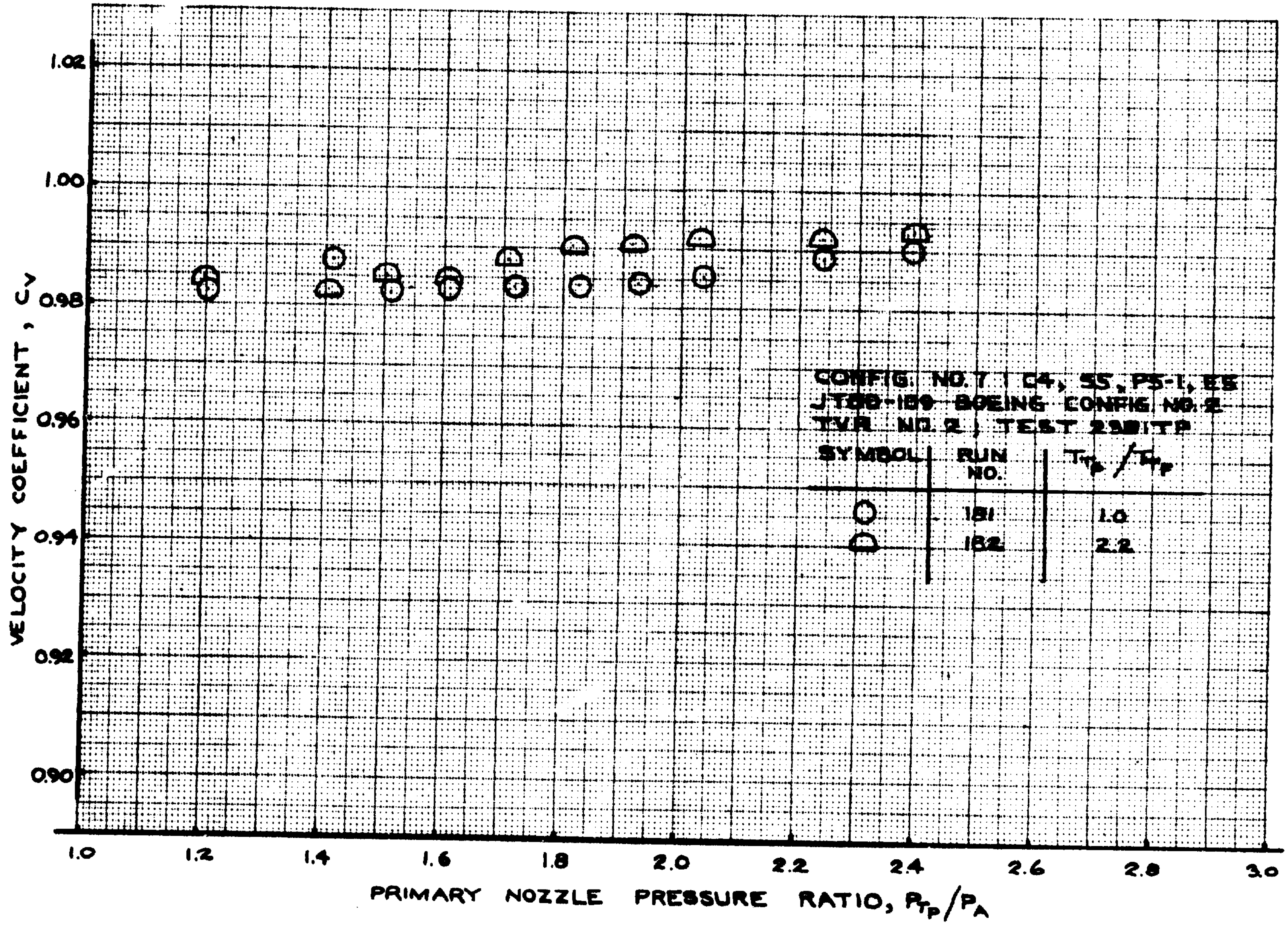

FIGURE 122 - VELOCITY COEFFICIENT
TEST CONFIG. NO. 7; RUNS 181-182

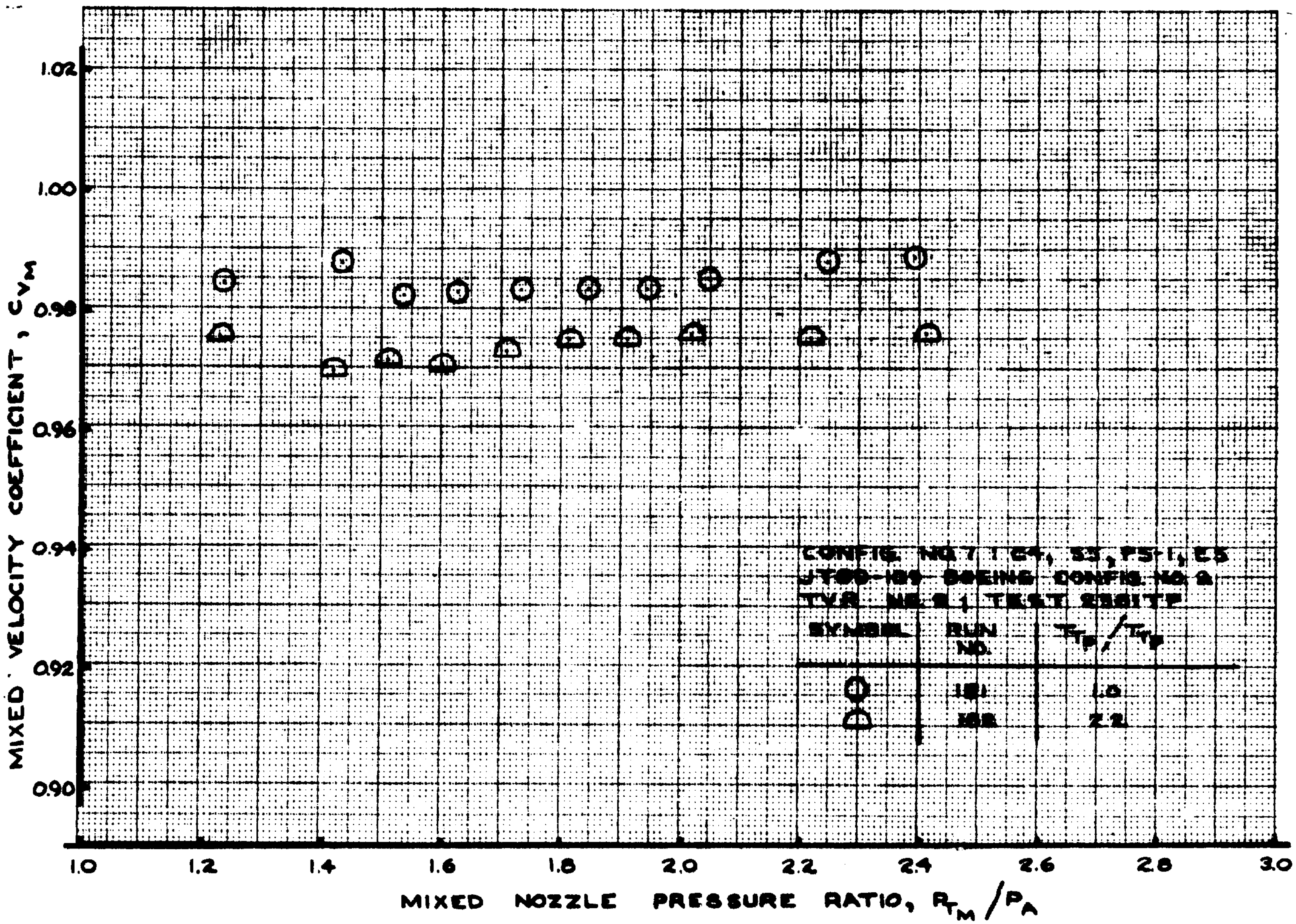

FIGURE 123 - MIXED VELOCITY COEFFICIENT
TEST CONFIG. NO. 7; RUNS 181-182

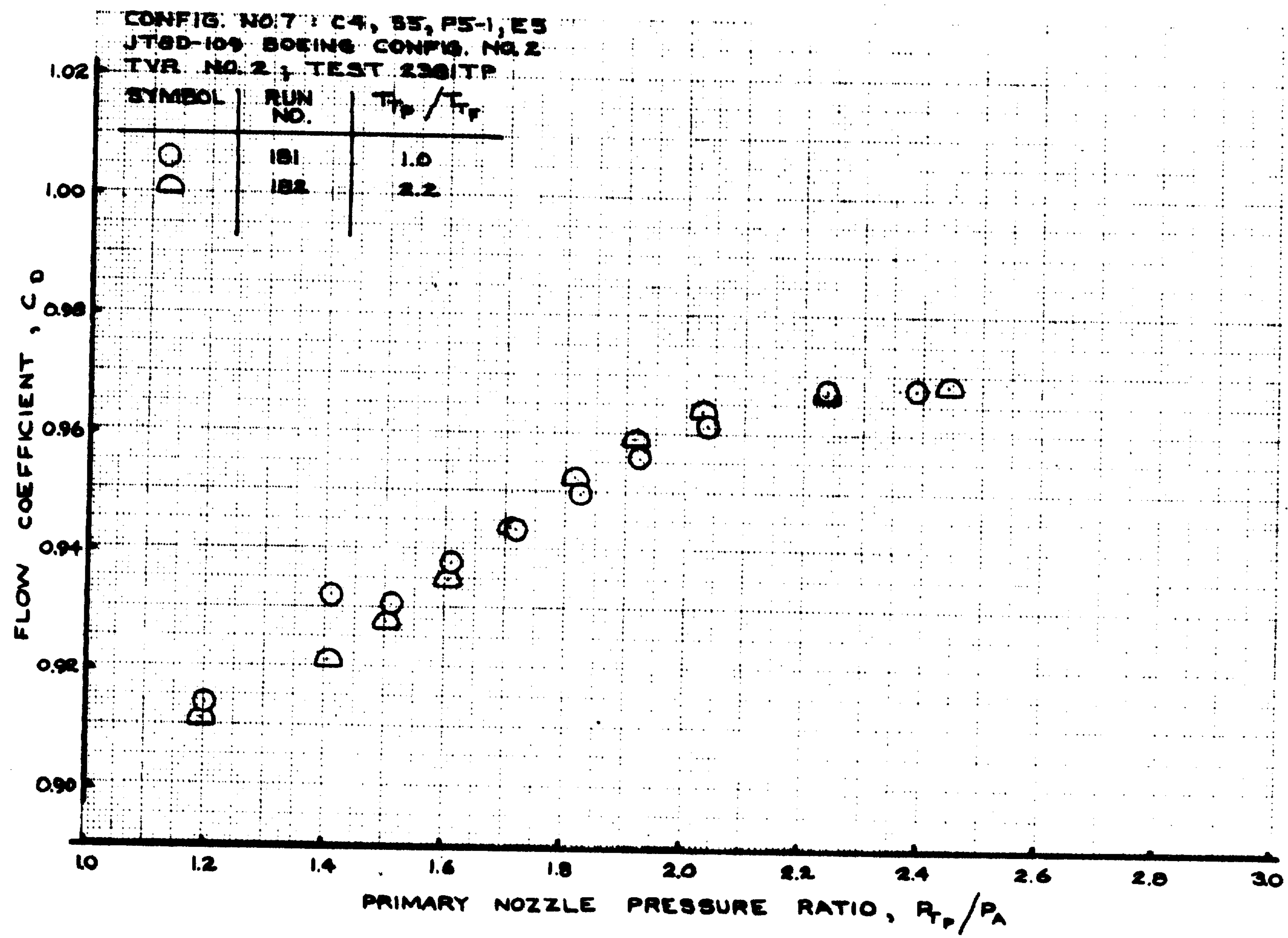

FIGURE 124 - FLOW COEFFICIENT
TEST CONFIG. NO. 7; RUNS 181-182

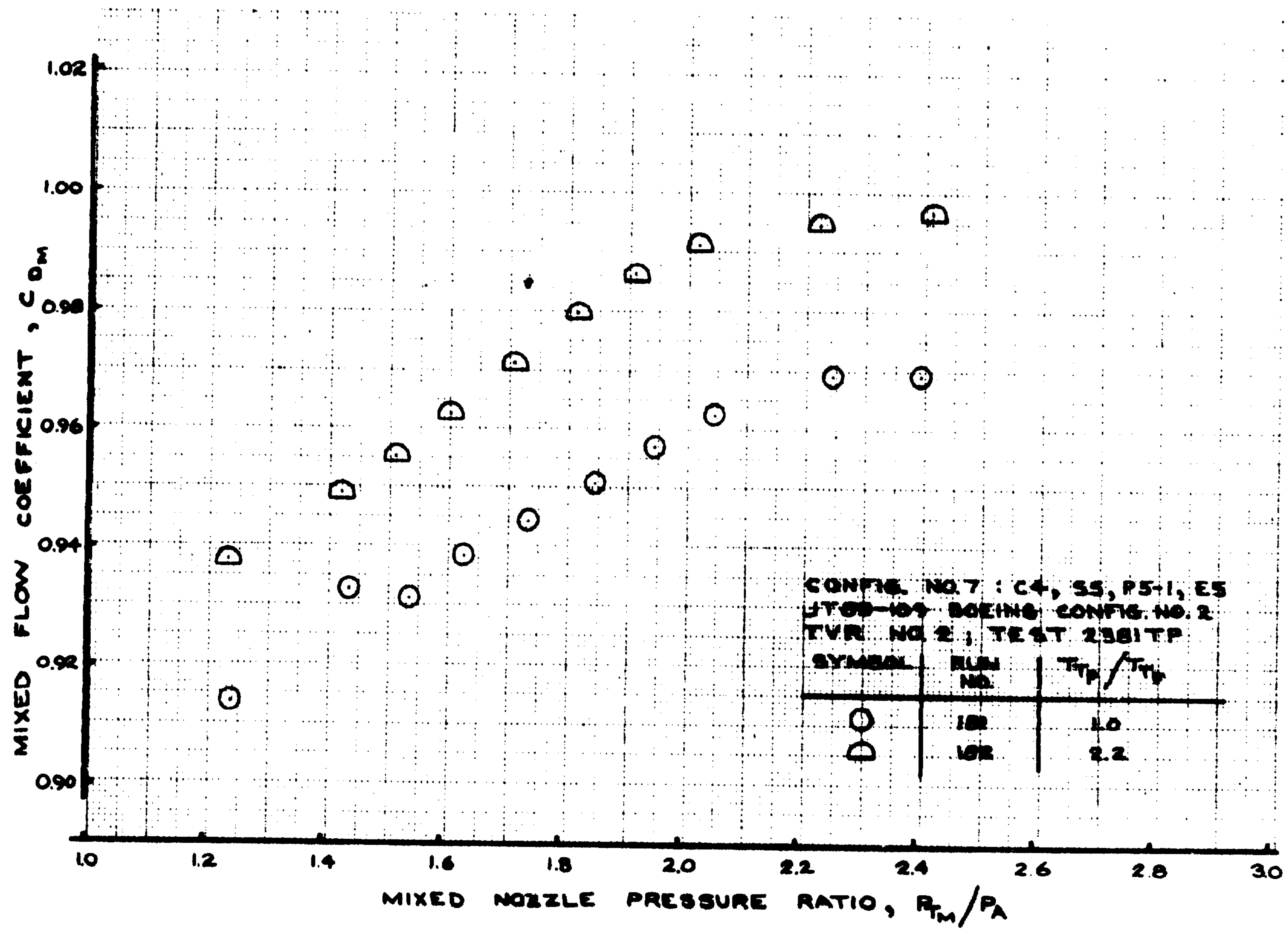

FIGURE 125 - MIXED FLOW COEFFICIENT
TEST CONFIG. NO. 7; RUNS 181-182

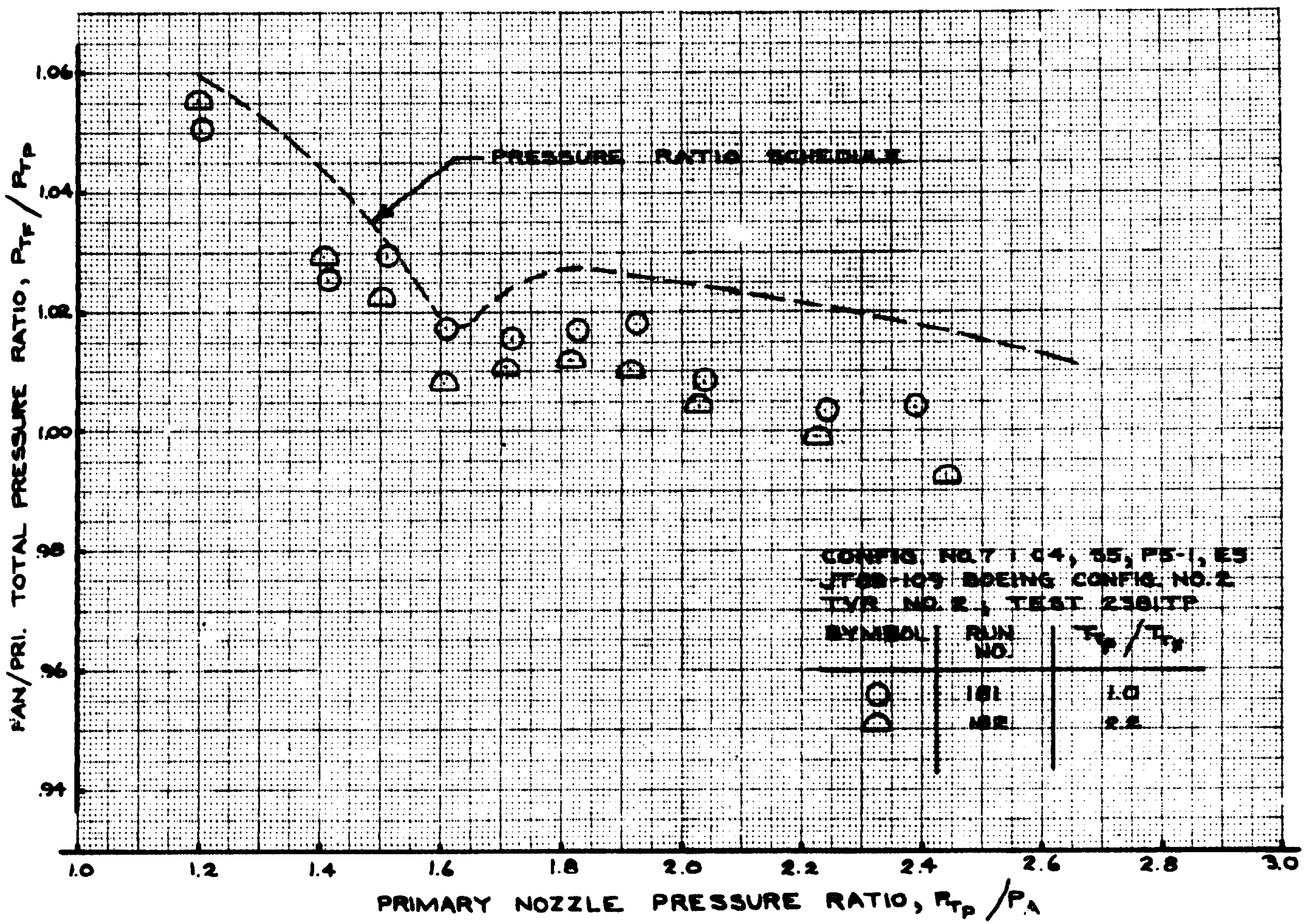

FIGURE 126 - FAN/PRIMARY TOTAL PRESSURE RATIO
TEST CONFIG. NO. 7; RUNS 181-182

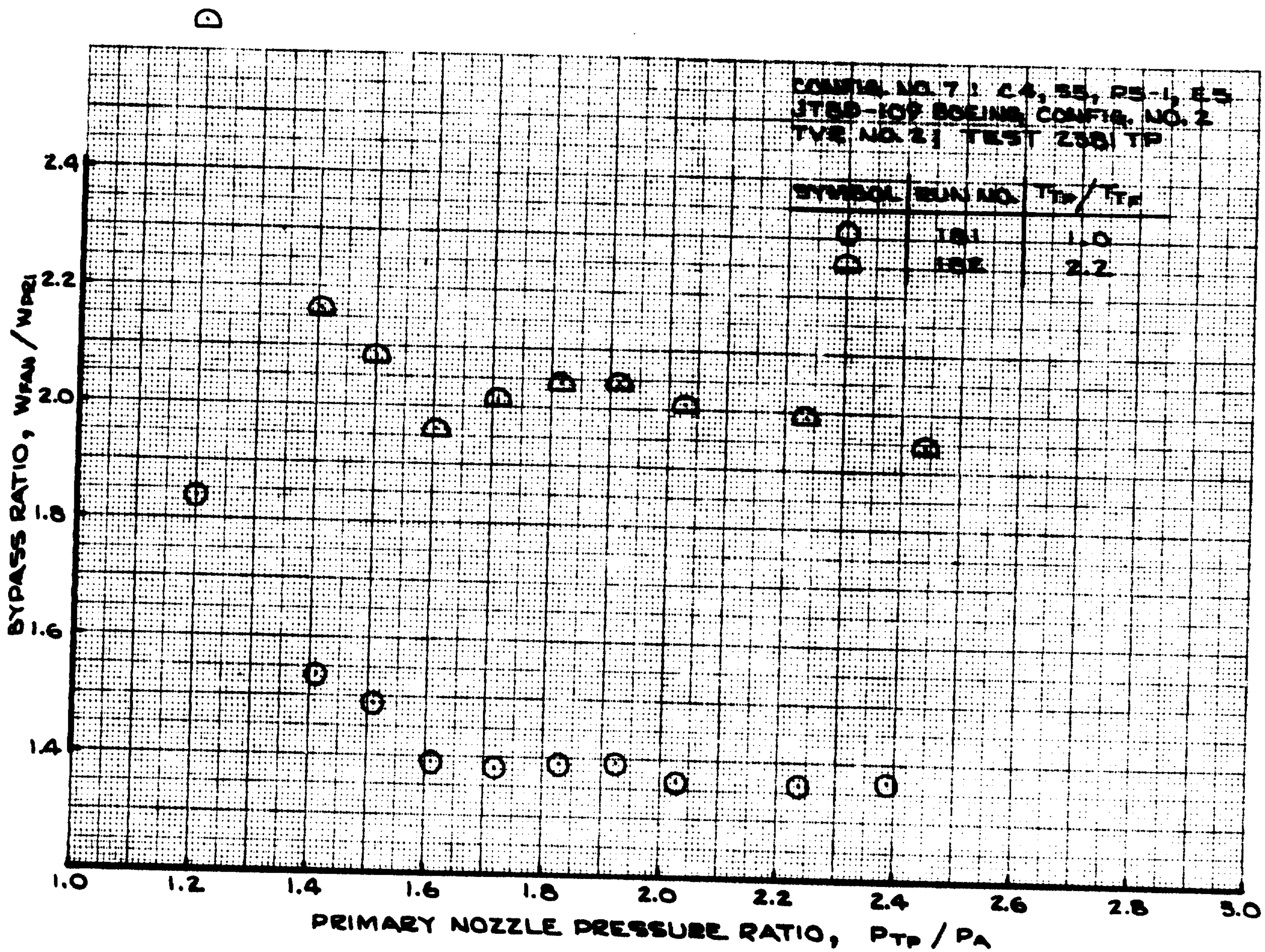

FIGURE 127 - BYPASS RATIO
TEST CONFIG. NO. 7; RUNS 181-182

7.2.8 TEST CONFIGURATION (T.C.) NO. 8

Configuration Description: Boeing Config. No. 2 variant using the JT8D-109 splitter and redesigned plug for JT8D-' 5.

Hardware Designations:

Outer Nozzle Wall	Splitter	Plug	Exit
C4	S5	P5-2	E6

Plotted Data:

- Figure 128 - Velocity Coefficient; Runs 72-78.
- Figure 129 - Mixed Velocity Coefficient; Runs 72-78.
- Figure 130 - Flow Coefficient; Runs 72-78.
- Figure 131 - Mixed Flow Coefficient; Runs 72-78.
- Figure 132 - Fan/Primary Total Pressure Ratio; Runs 72-78.
- Figure 133 - Bypass Ratio; Runs 72-78.
- Figure 134 - Splitter Static Pressure Ratio; Run 76.

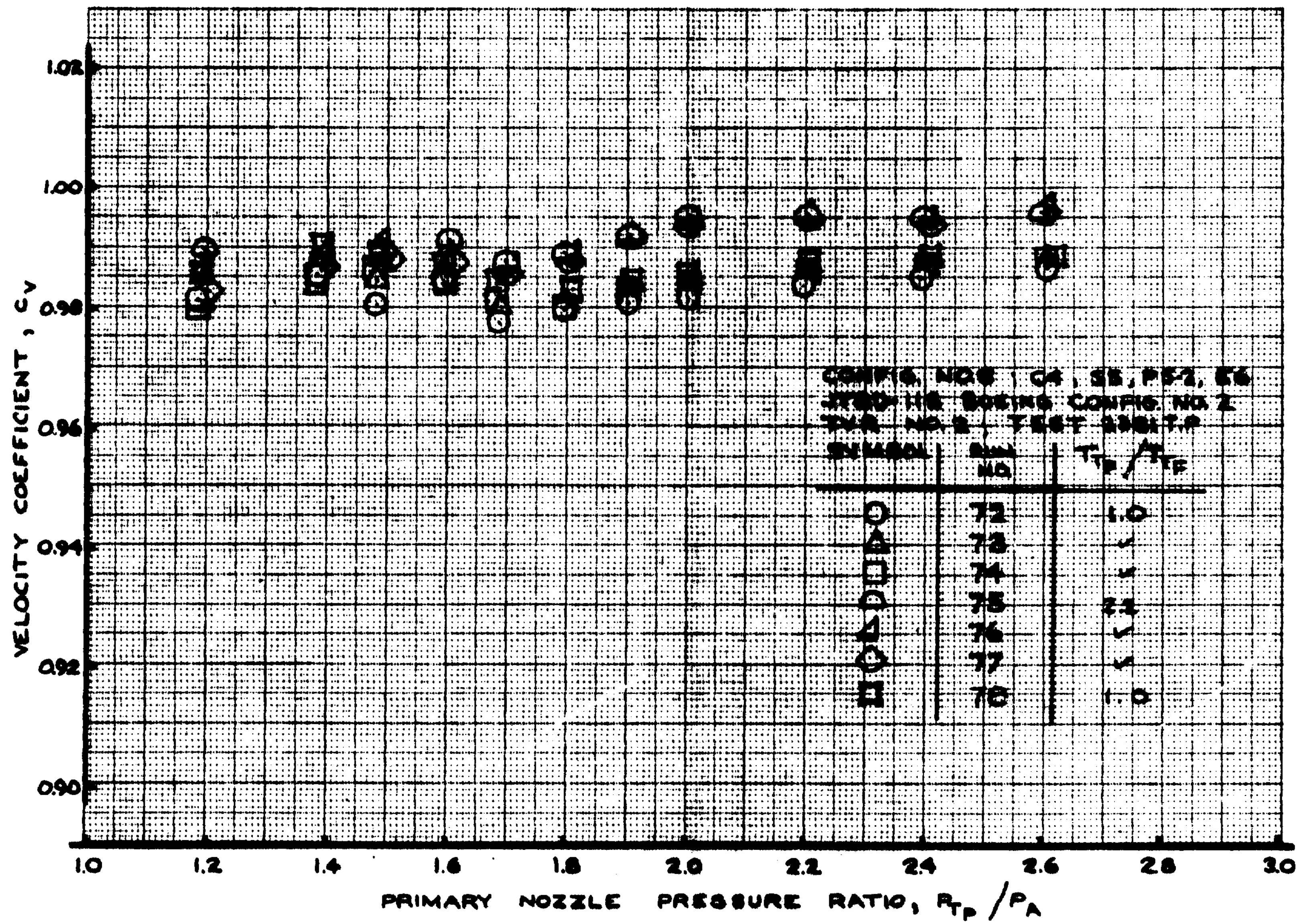

FIGURE 128- VELOCITY COEFFICIENT
TEST CONFIG. NO. 8; RUNS 72-78

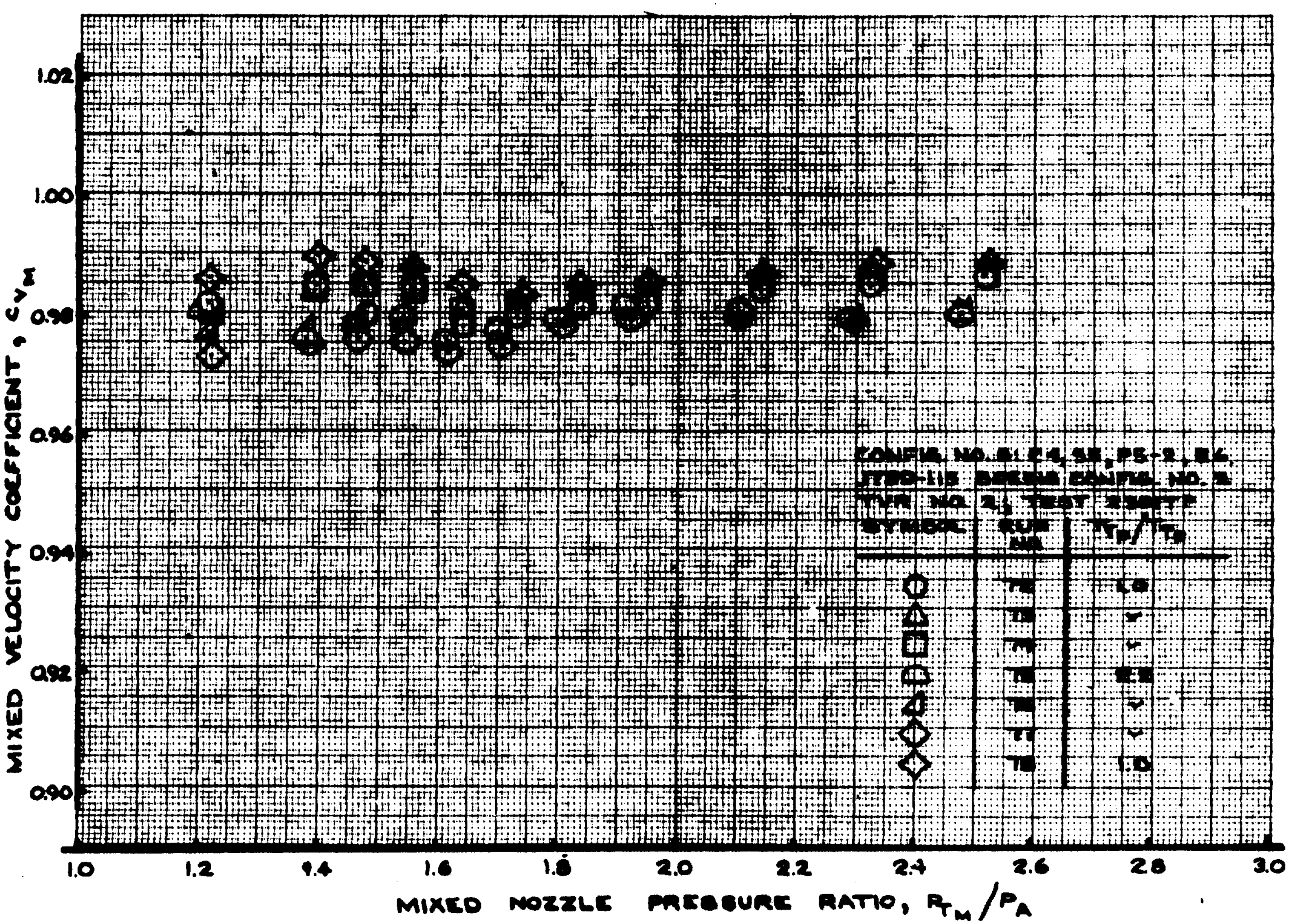

FIGURE 129- MIXED VELOCITY COEFFICIENT
TEST CONFIG. NO. 8; RUNS 72-78

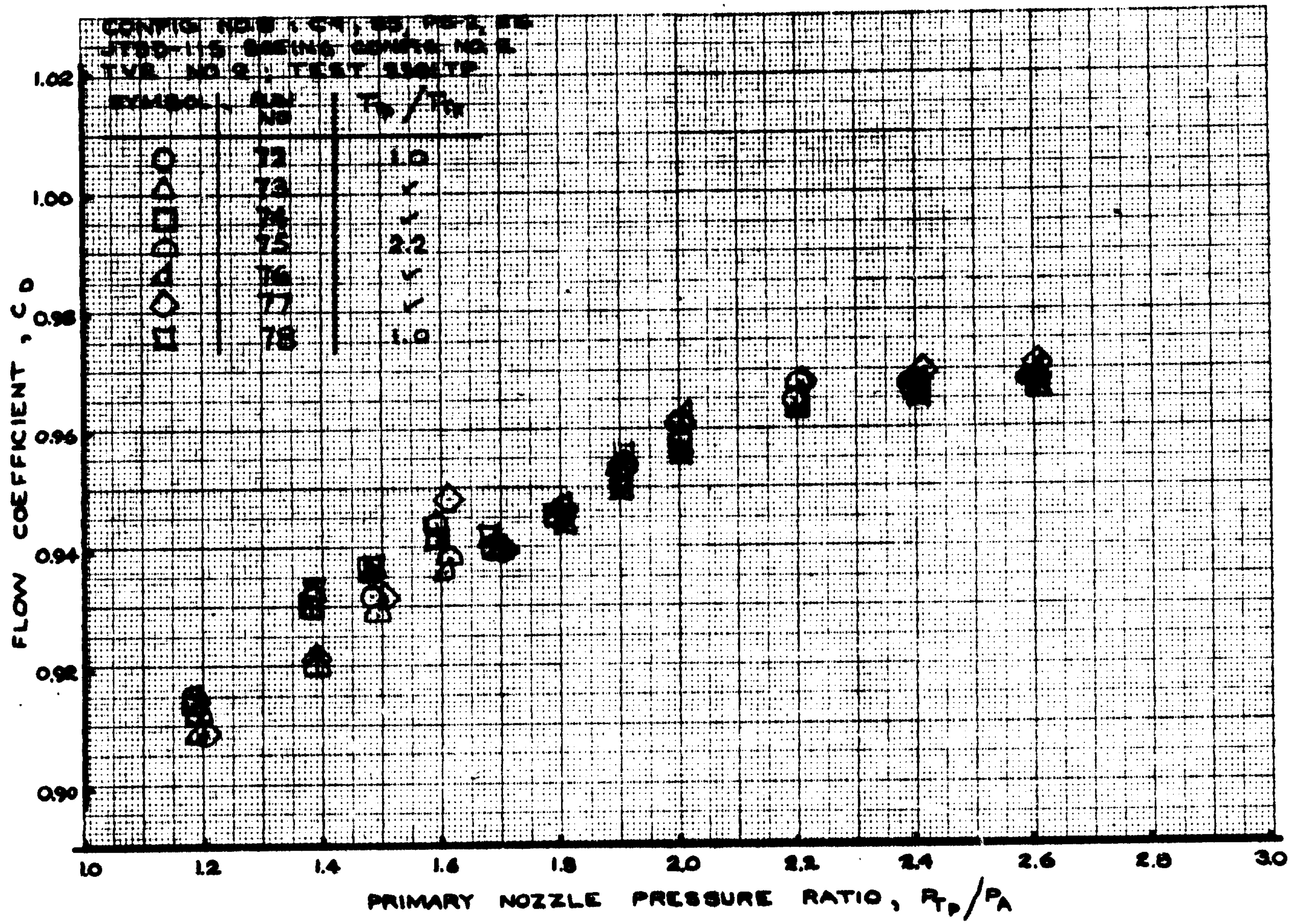

FIGURE 130 - FLOW COEFFICIENT
TEST CONFIG. NO. 8; RUNS 72-78

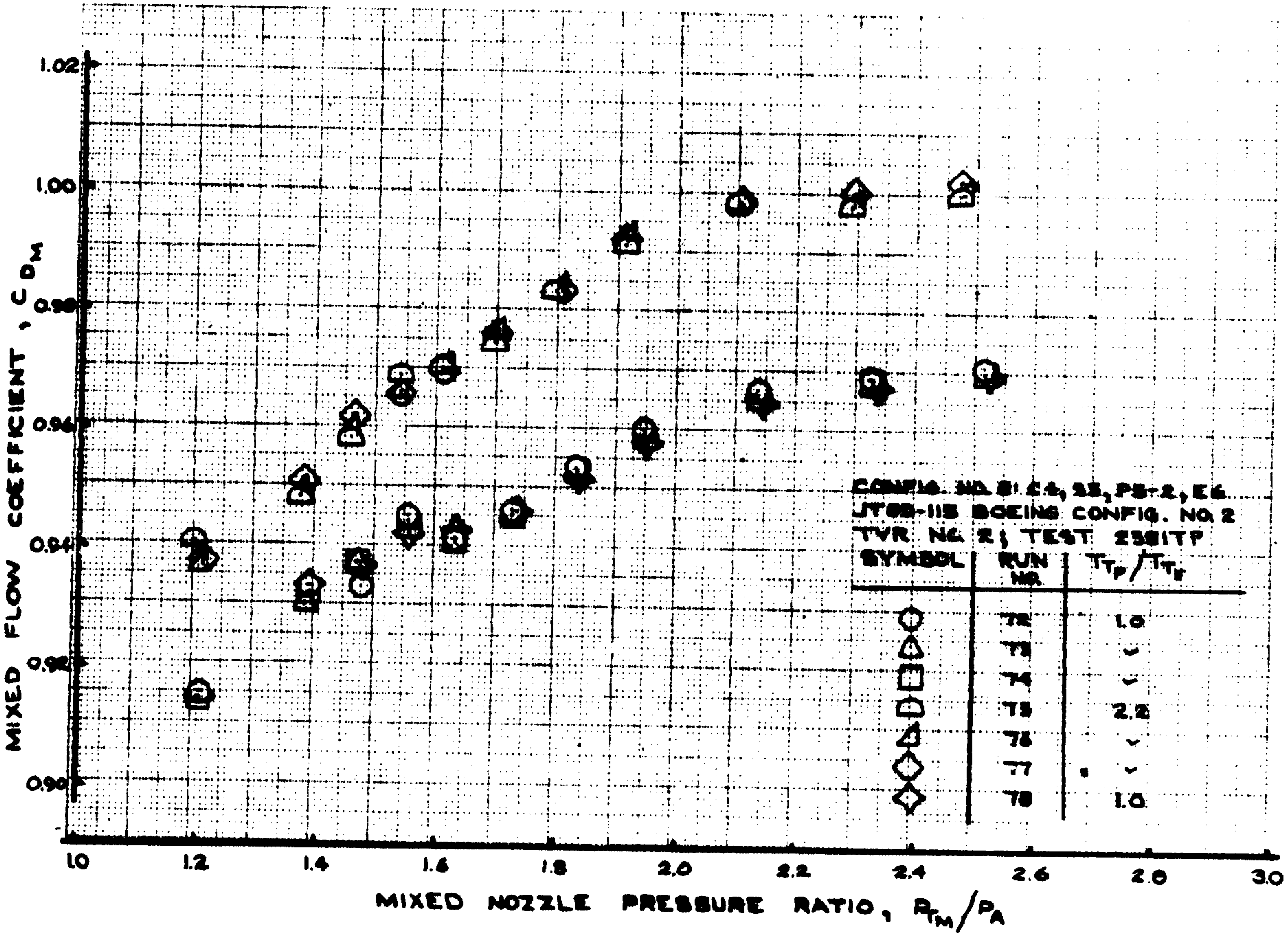

FIGURE 131- MIXED FLOW COEFFICIENT
TEST CONFIG. NO. 8; RUNS 72-78

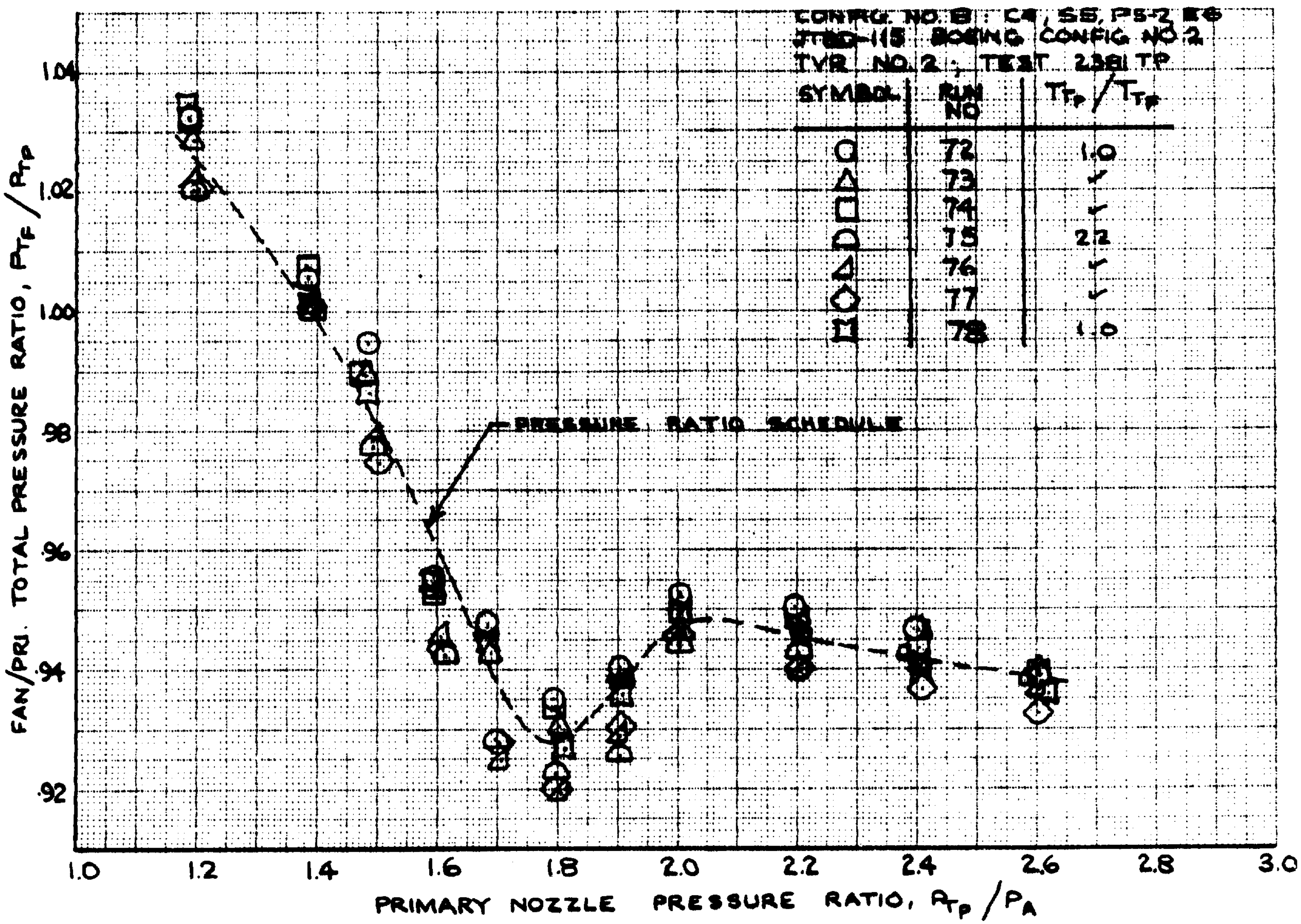

FIGURE 132- FAN/PRIMARY TOTAL PRESSURE RATIO
TEST CONFIG. NO. 8; RUNS 72-78

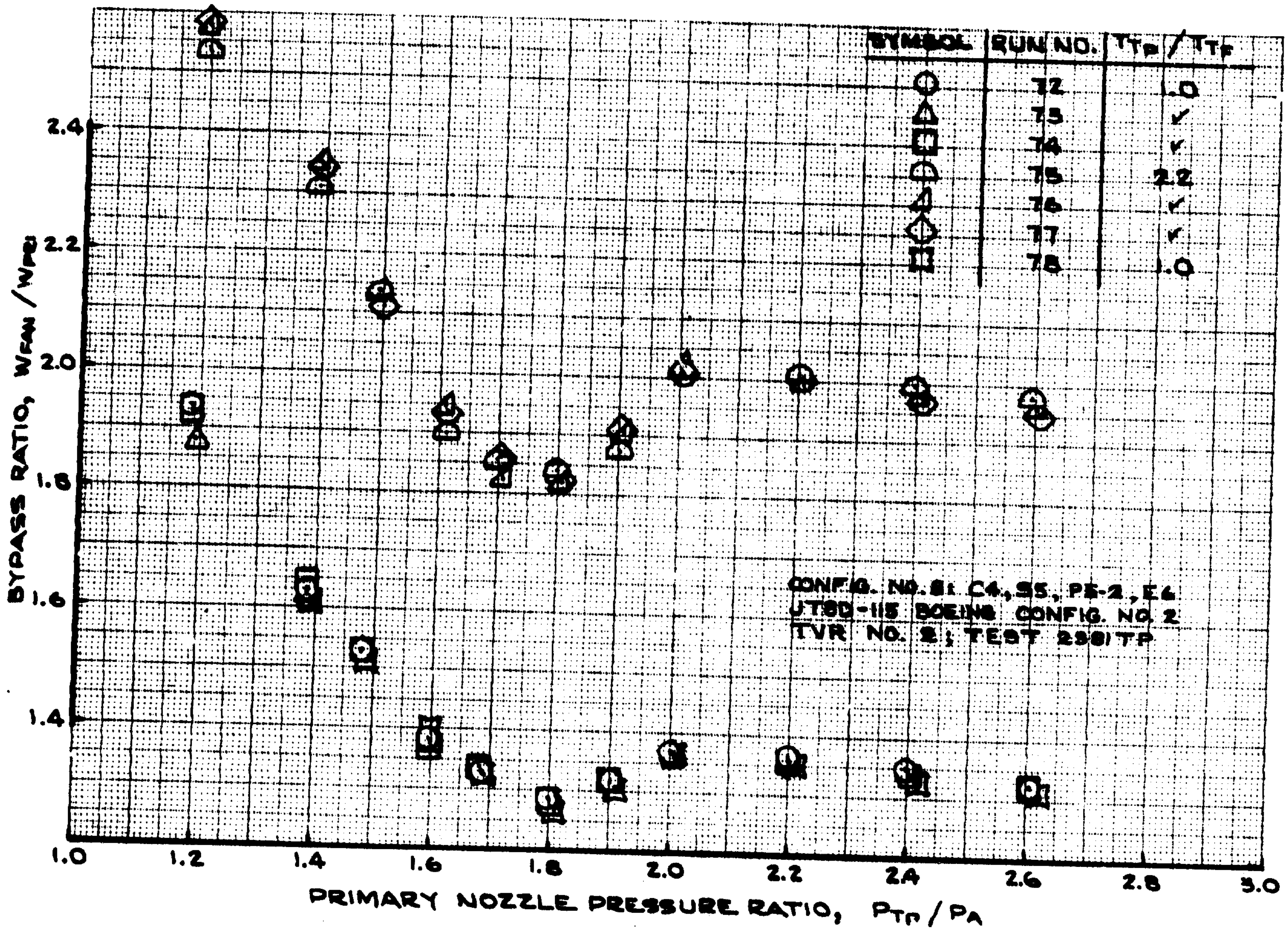

FIGURE 133- BYPASS RATIO
TEST CONFIG. NO. 8; RUNS 72-78

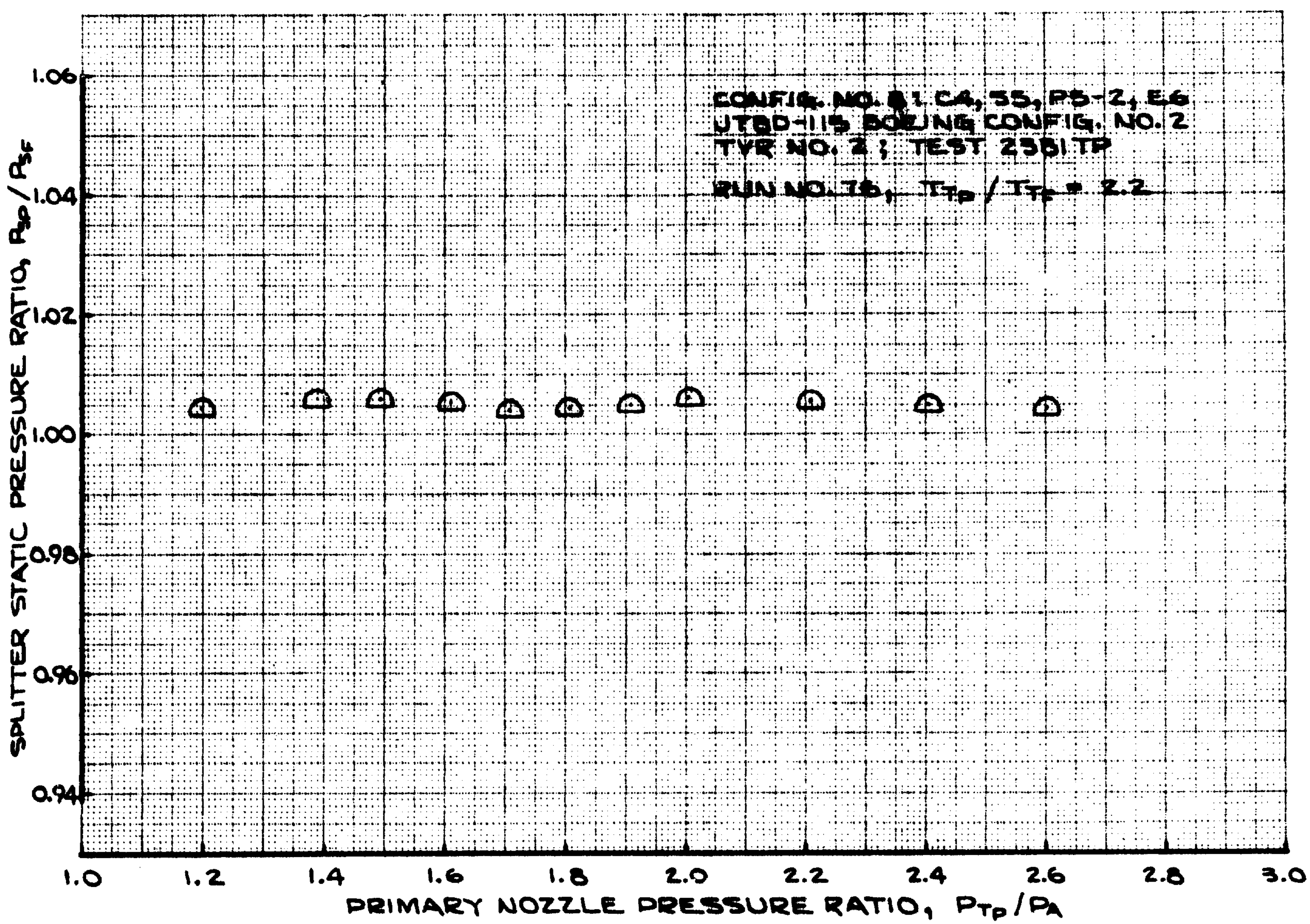

FIGURE 134 - SPLITTER STATIC PRESSURE RATIO
TEST CONFIG. NO. 8; RUN 76

7.2.9 TEST CONFIGURATION (T.C.) NO. 9

Configuration Description: Boeing Config. No. 2 design for JT8D-115 with truncated plug.

Hardware Designations:

Outer Nozzle Wall	Splitter	Plug	Exit
C4	S6	P5-1S	E6

Plotted Data:

- Figure 135 - Velocity Coefficient; Runs 98-103.
- Figure 136 - Mixed Flow Coefficient; Runs 98-103.
- Figure 137 - Flow Coefficient; Runs 98-103.
- Figure 138 - Mixed Flow Coefficient; Runs 98-103.
- Figure 139 - Fan/Primary Total Pressure Ratio; Runs 98-103.
- Figure 140 - Bypass Ratio; Runs 98-103.
- Figure 141 - Splitter Static Pressure Ratio; Run 101.

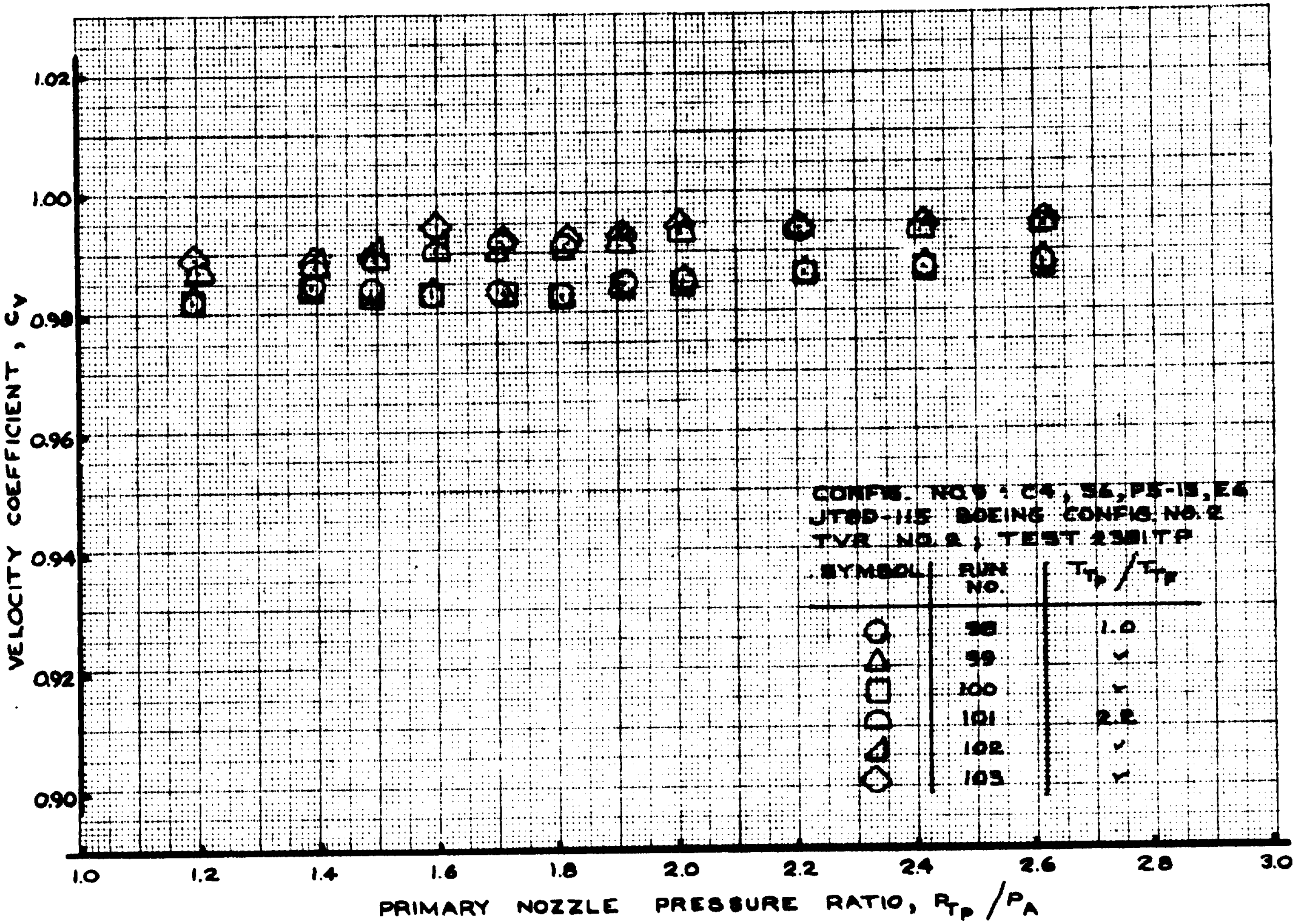

FIGURE 135- VELOCITY COEFFICIENT
TEST CONFIG. NO. 9; RUNS 98-103

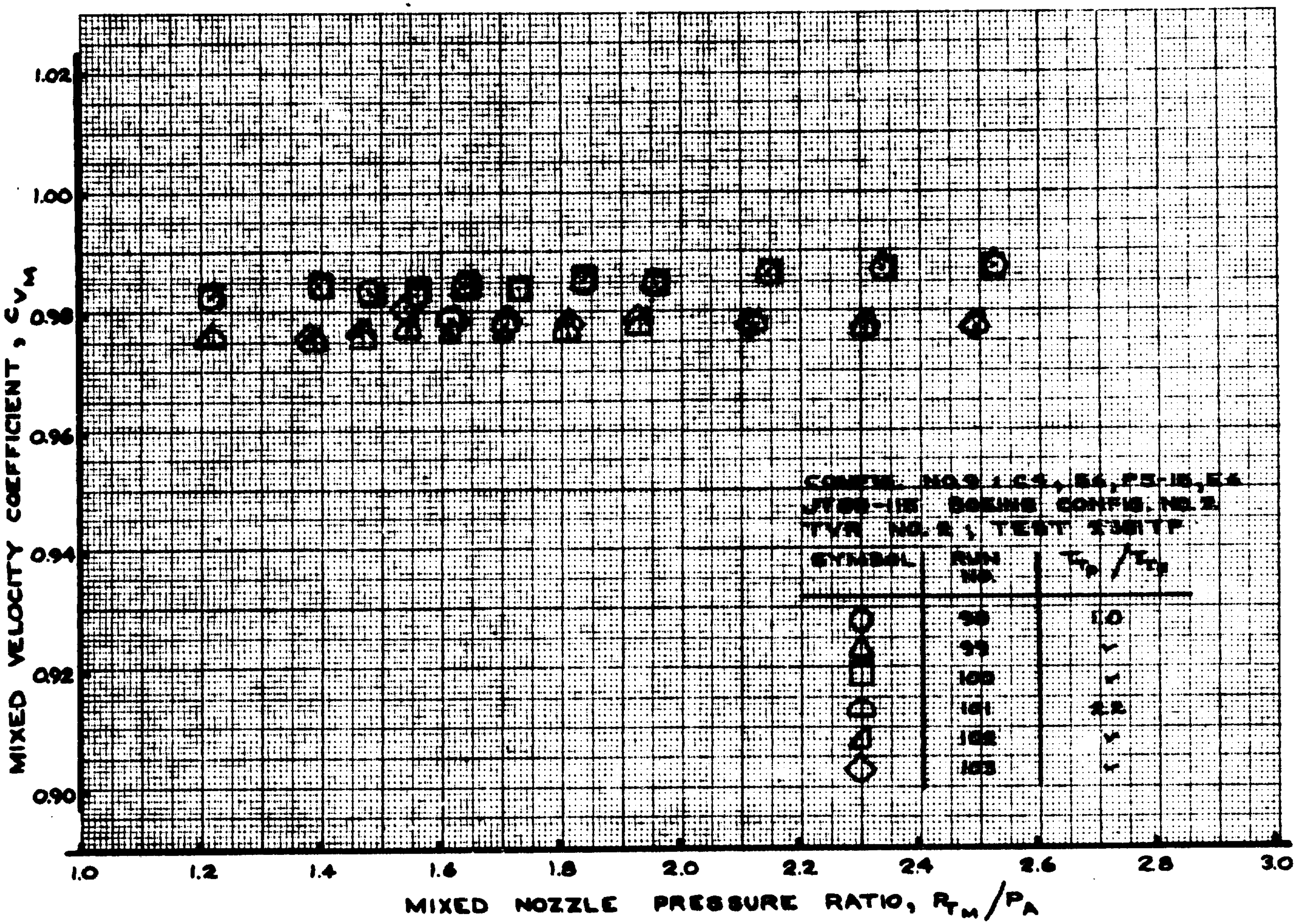

FIGURE 136. MIXED VELOCITY COEFFICIENT
TEST CONFIG. NO. 9; RUNS 98-103

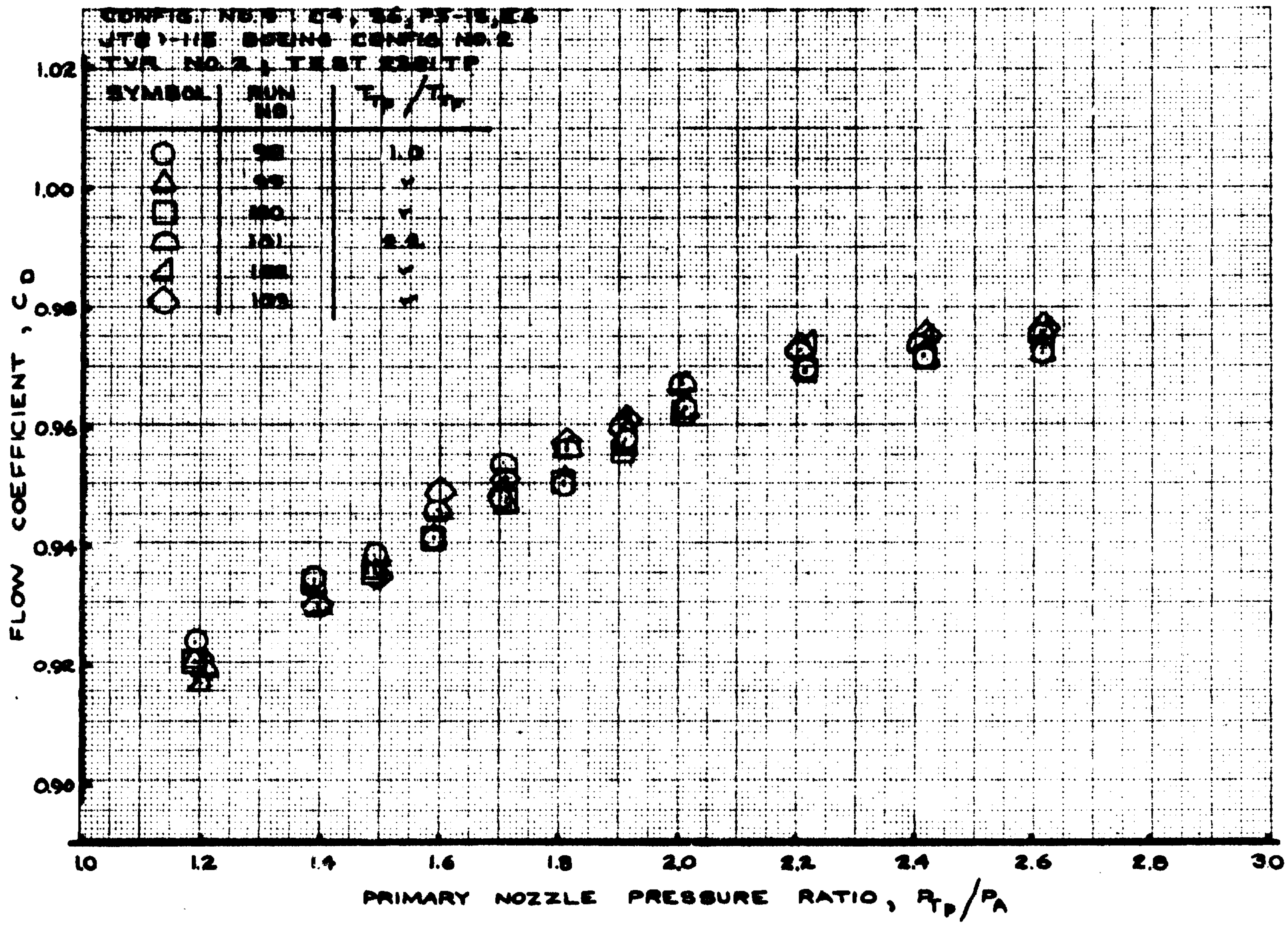

FIGURE 137- FLOW COEFFICIENT
TEST CONFIG. NO. 9; RUNS 98-103

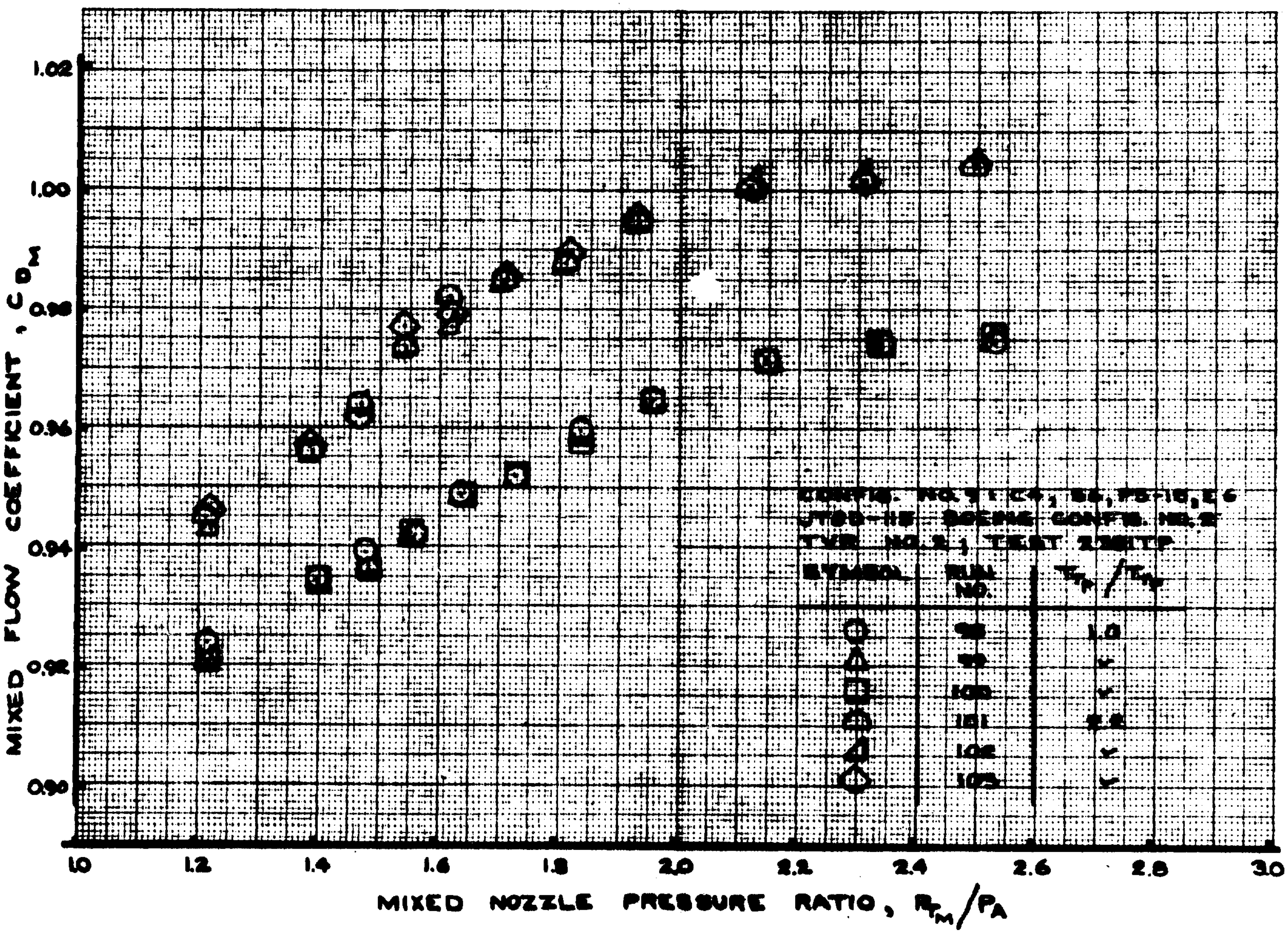

FIGURE 138- MIXED FLOW COEFFICIENT
TEST CONFIG. NO. 9; RUNS 98-103

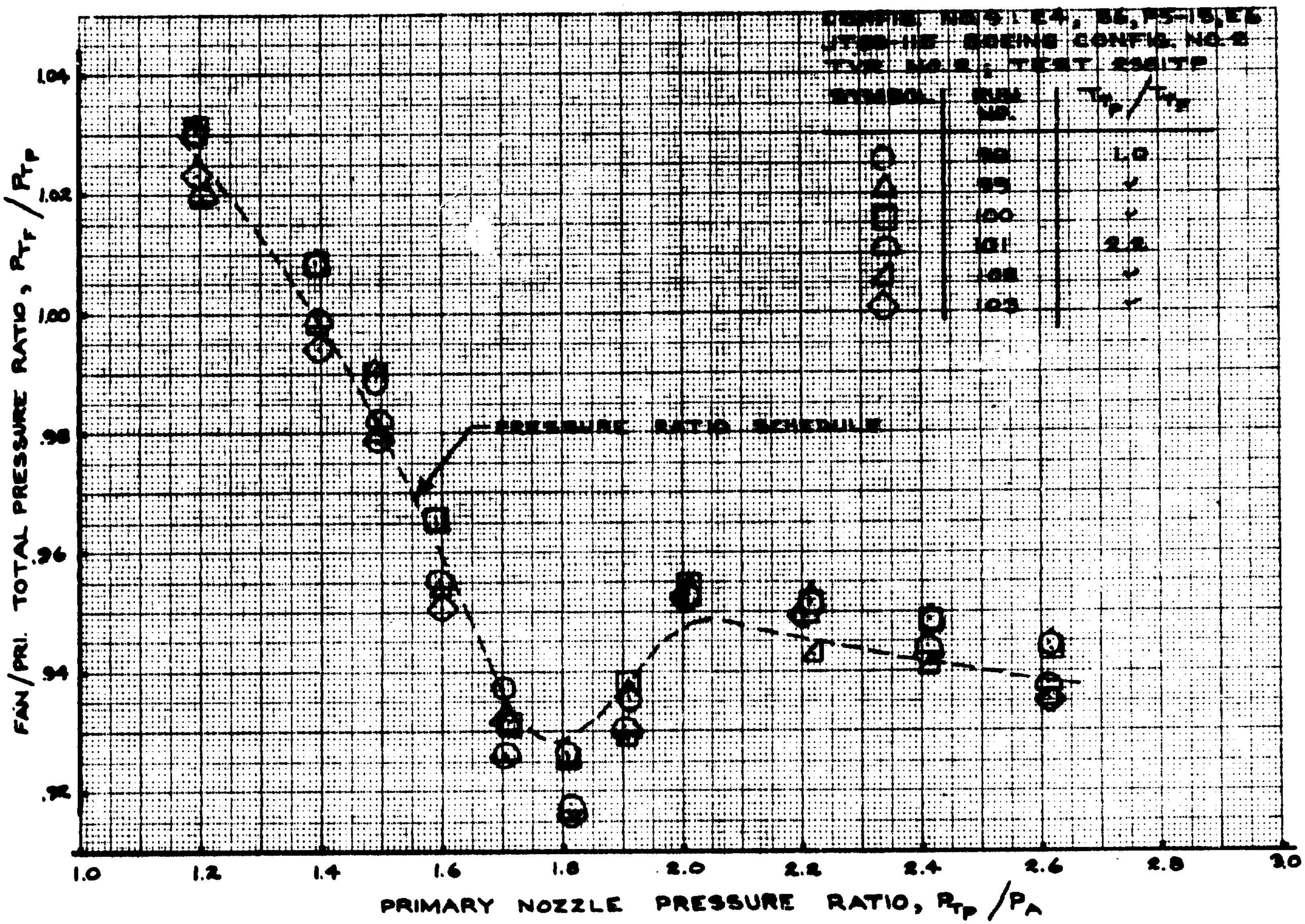

FIGURE 139- FAN/PRIMARY TOTAL PRESSURE RATIO
TEST CONFIG. NO. 9; RUNS 98-103

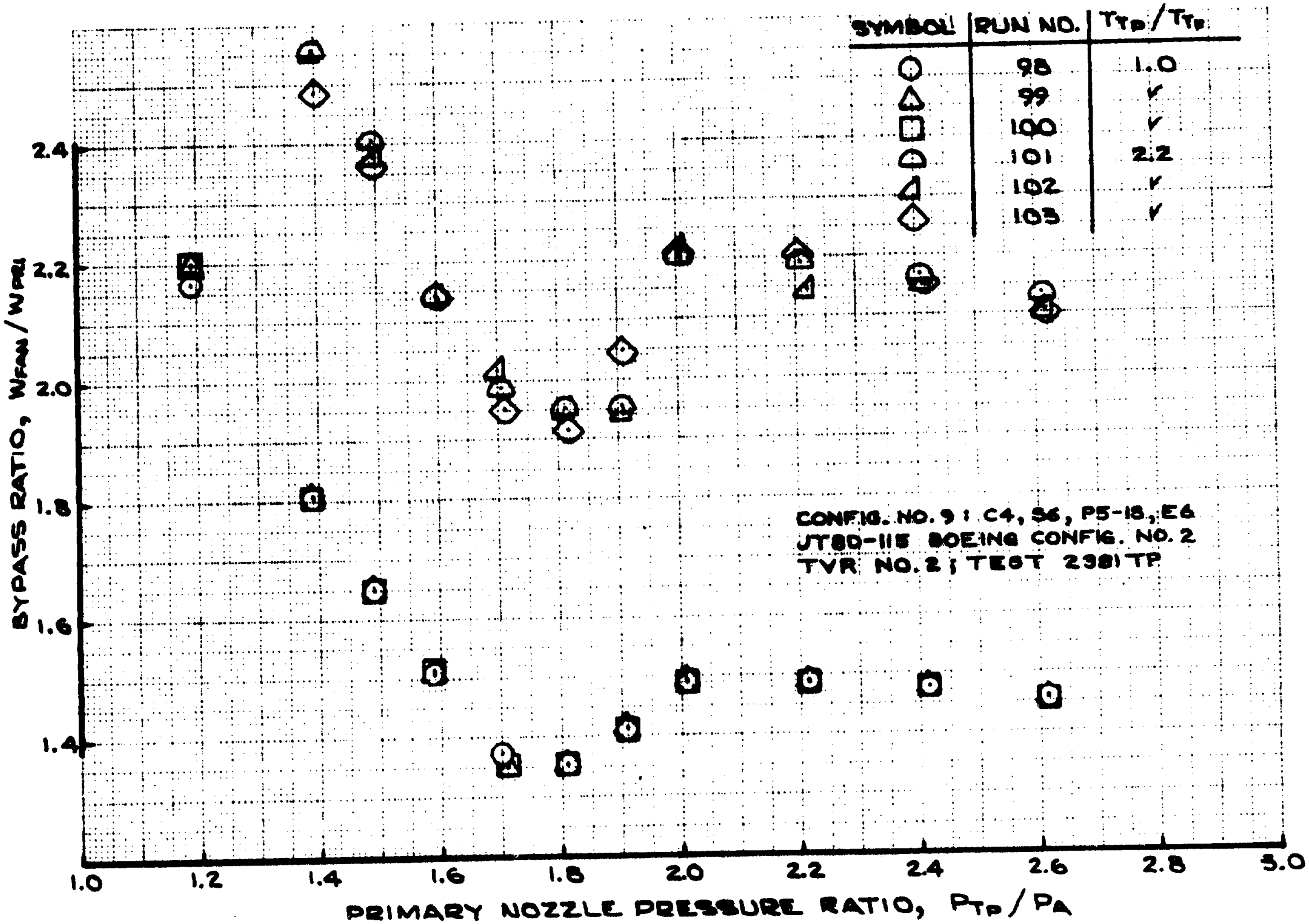

FIGURE 140- BYPASS RATIO
TEST CONFIG. NO. 9; RUNS 98-103

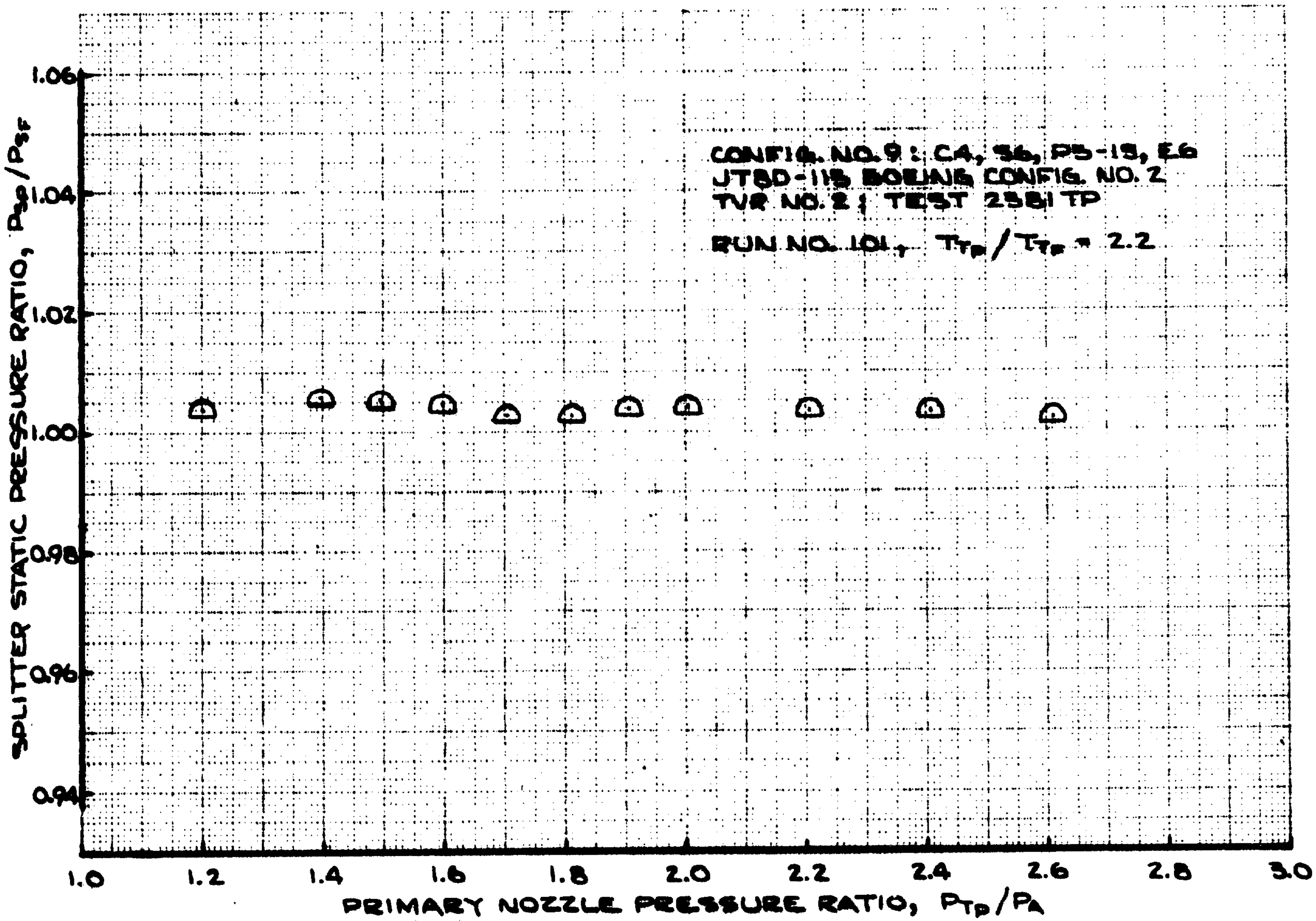

FIGURE 141 - SPLITTER STATIC PRESSURE RATIO
TEST CONFIG. NO. 9; RUN 101

7.2.10 TEST CONFIGURATION (T.C.) NO. 10

Configuration Description: Boeing Config. No. 2 design for JT8D-115 with the JT8D-109 exit area.

Hardware Designations:

Outer Nozzle Wall	Splitter	Plug	Exit
C4	S6	P5-1	E5

Plotted Data:

Figure 142 - Velocity Coefficient; Runs 118-123.
Figure 143 - Mixed Velocity Coefficient; Runs 118-123.
Figure 144 - Flow Coefficient; Runs 118-123.
Figure 145 - Mixed Flow Coefficient; Runs 118-123.
Figure 146 - Fan/Primary Total Pressure Ratio; Runs 118-123.
Figure 147 - Bypass Ratio; Runs 118-123.
Figure 148 - Splitter Static Pressure Ratio; Run 122.

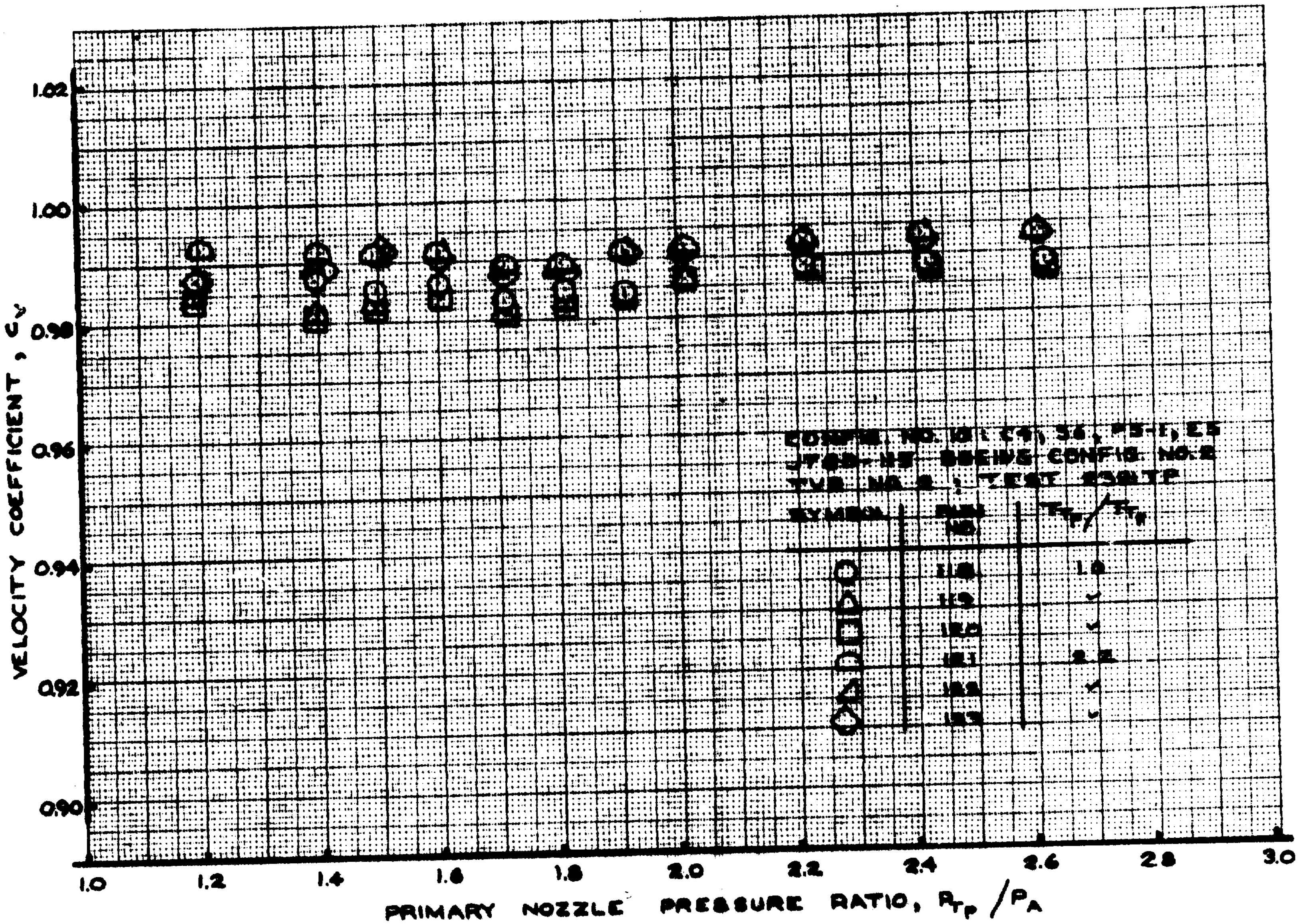

FIGURE 142- VELOCITY COEFFICIENT
TEST CONFIG. NO. 10; RUNS 118-123

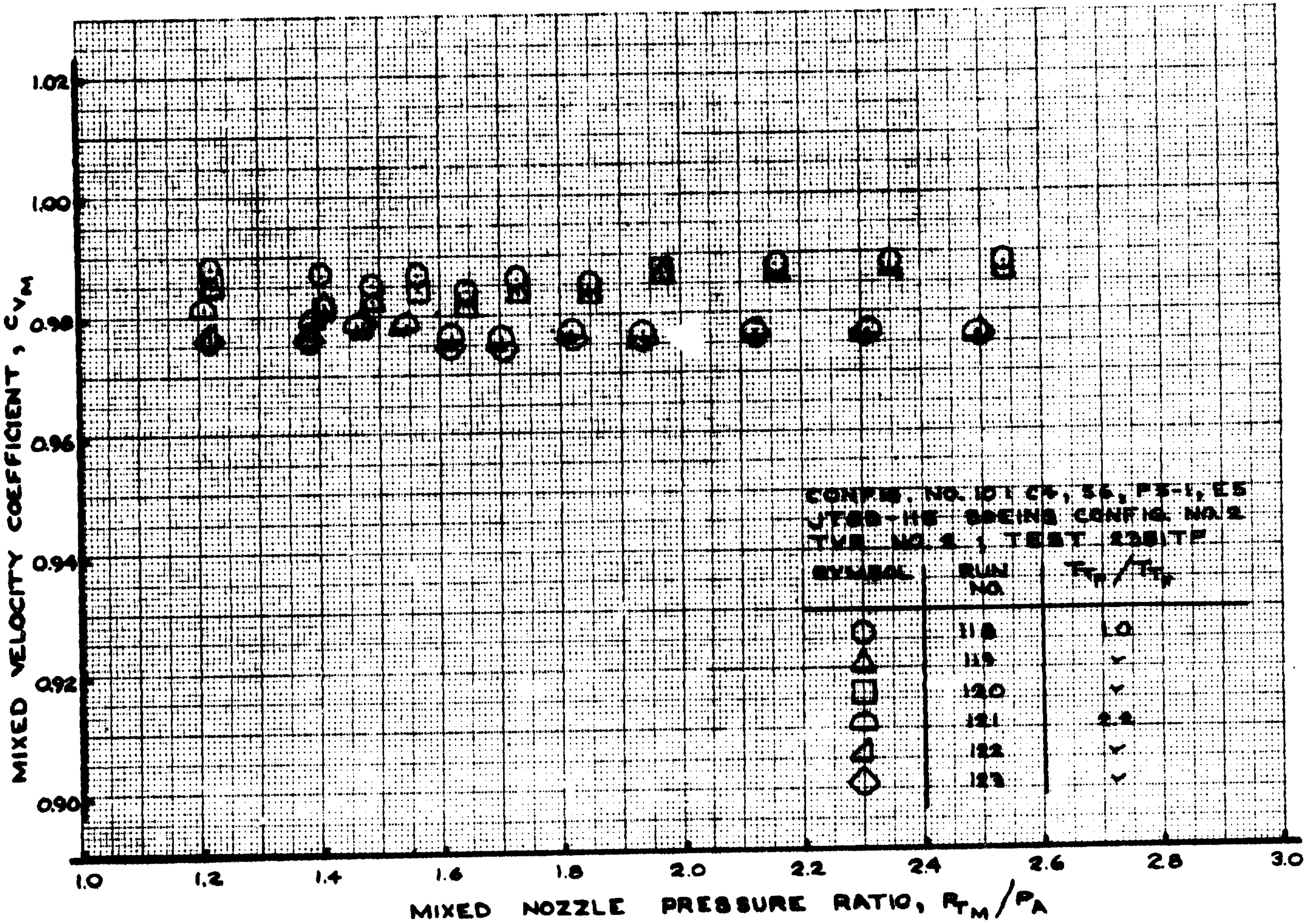

FIGURE 143- MIXED VELOCITY COEFFICIENT
TEST CONFIG. NO. 10; RUNS 118-123

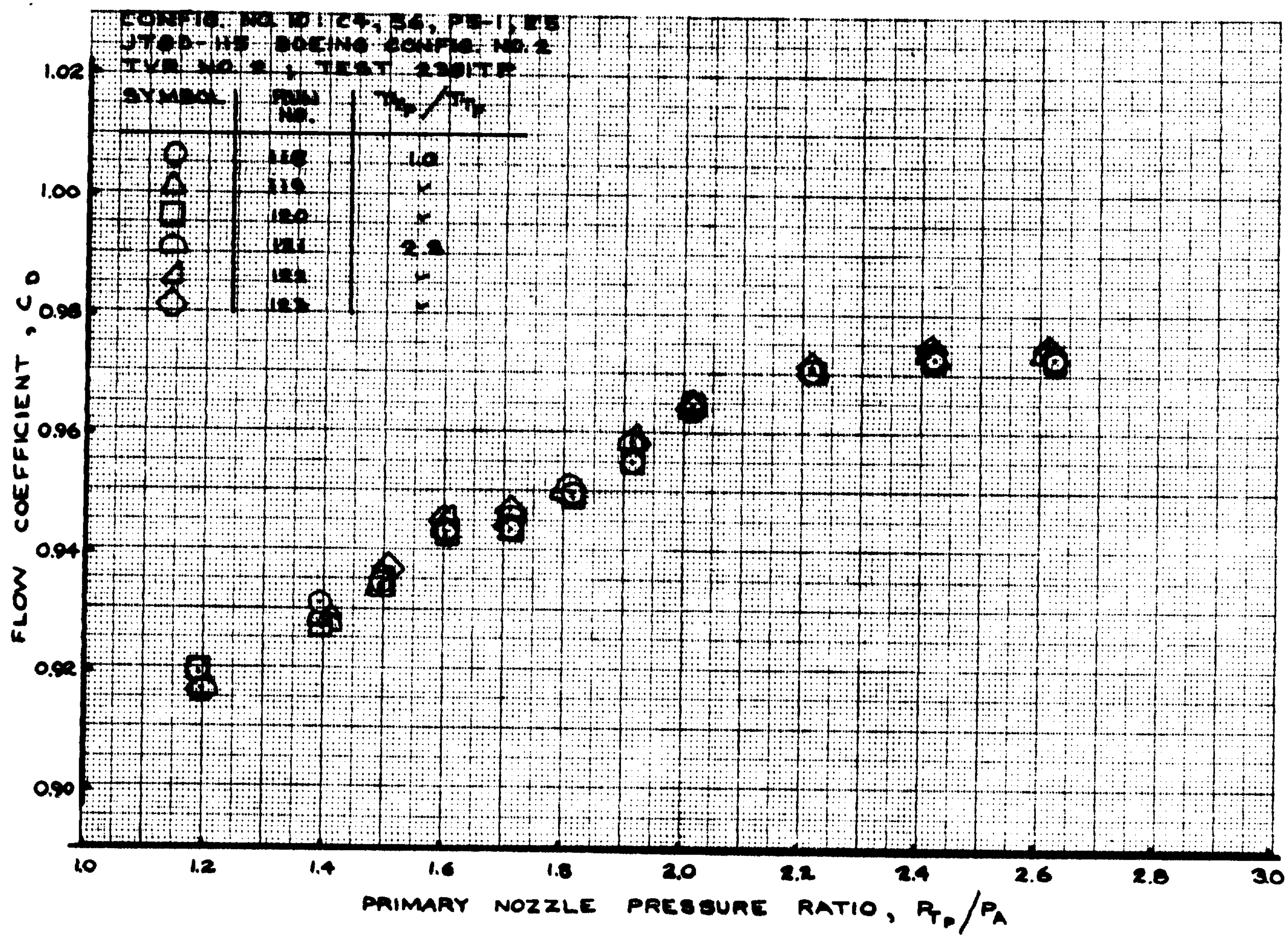

FIGURE 144- FLOW COEFFICIENT
TEST CONFIG. NO. 10; RUNS 118-123

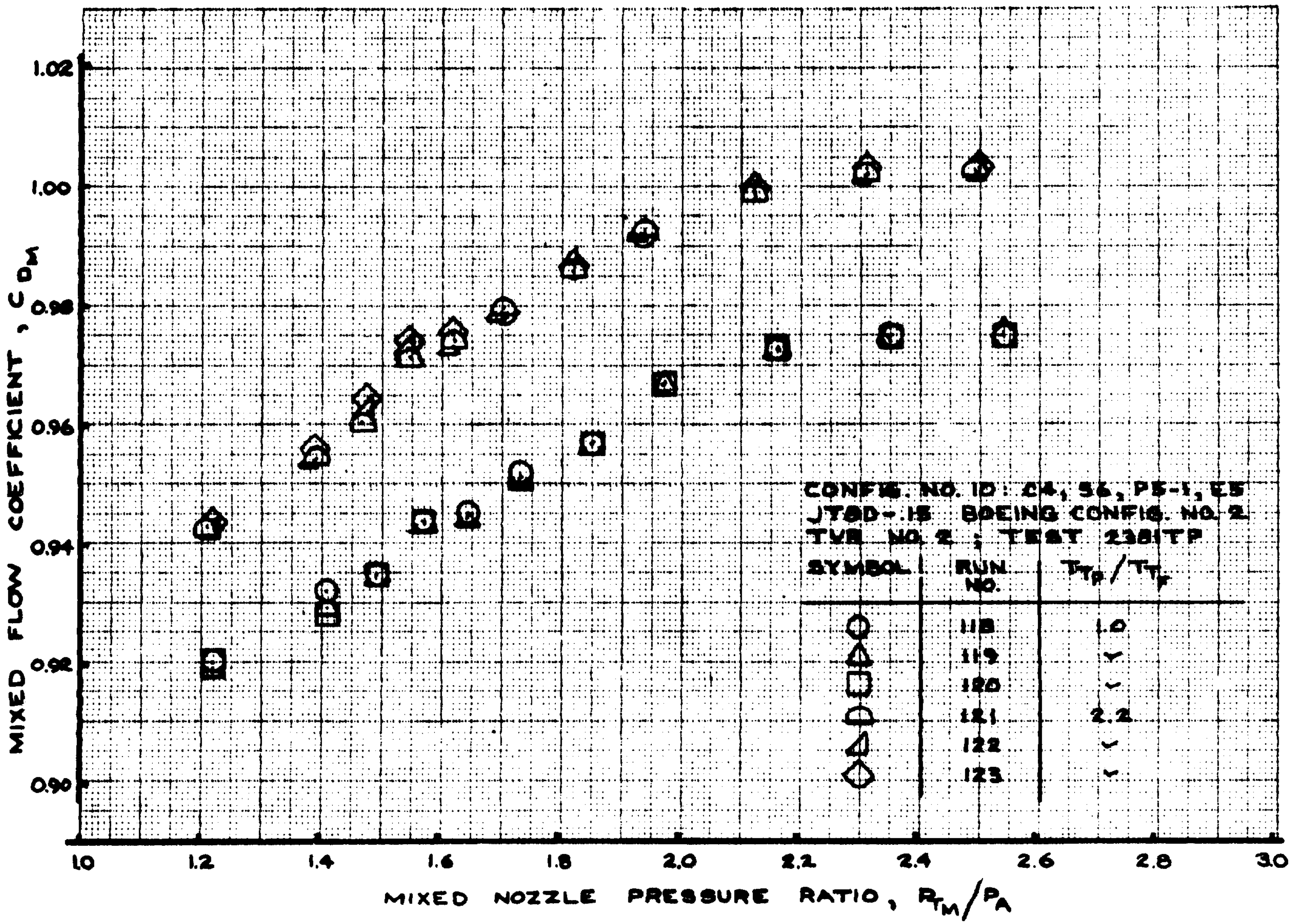

FIGURE 145- MIXED FLOW COEFFICIENT
TEST CONFIG. NO. 10; RUNS 118-123

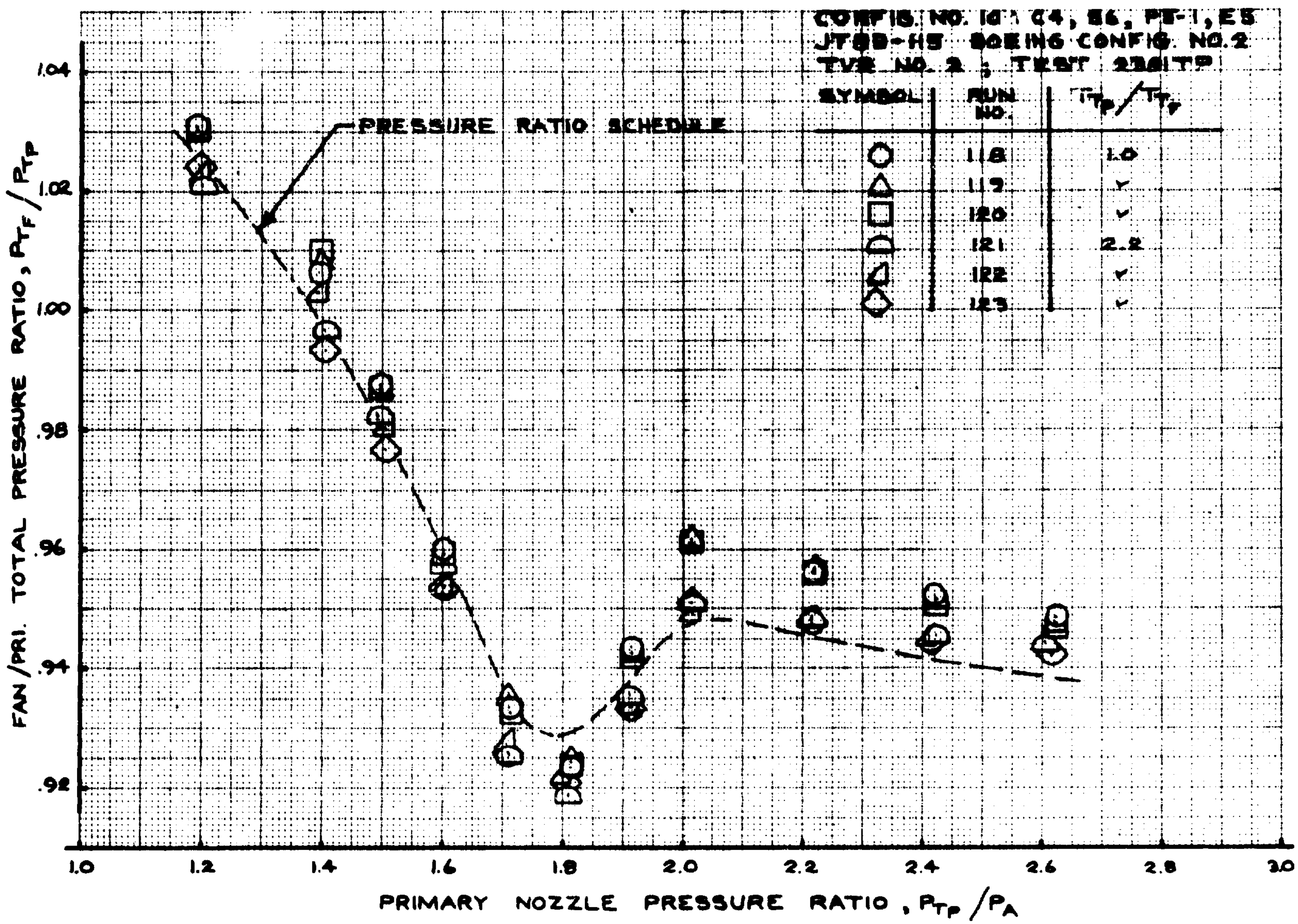

FIGURE 146- FAN/PRIMARY TOTAL PRESSURE RATIO
TEST CONFIG. NO. 10; RUNS 118-123

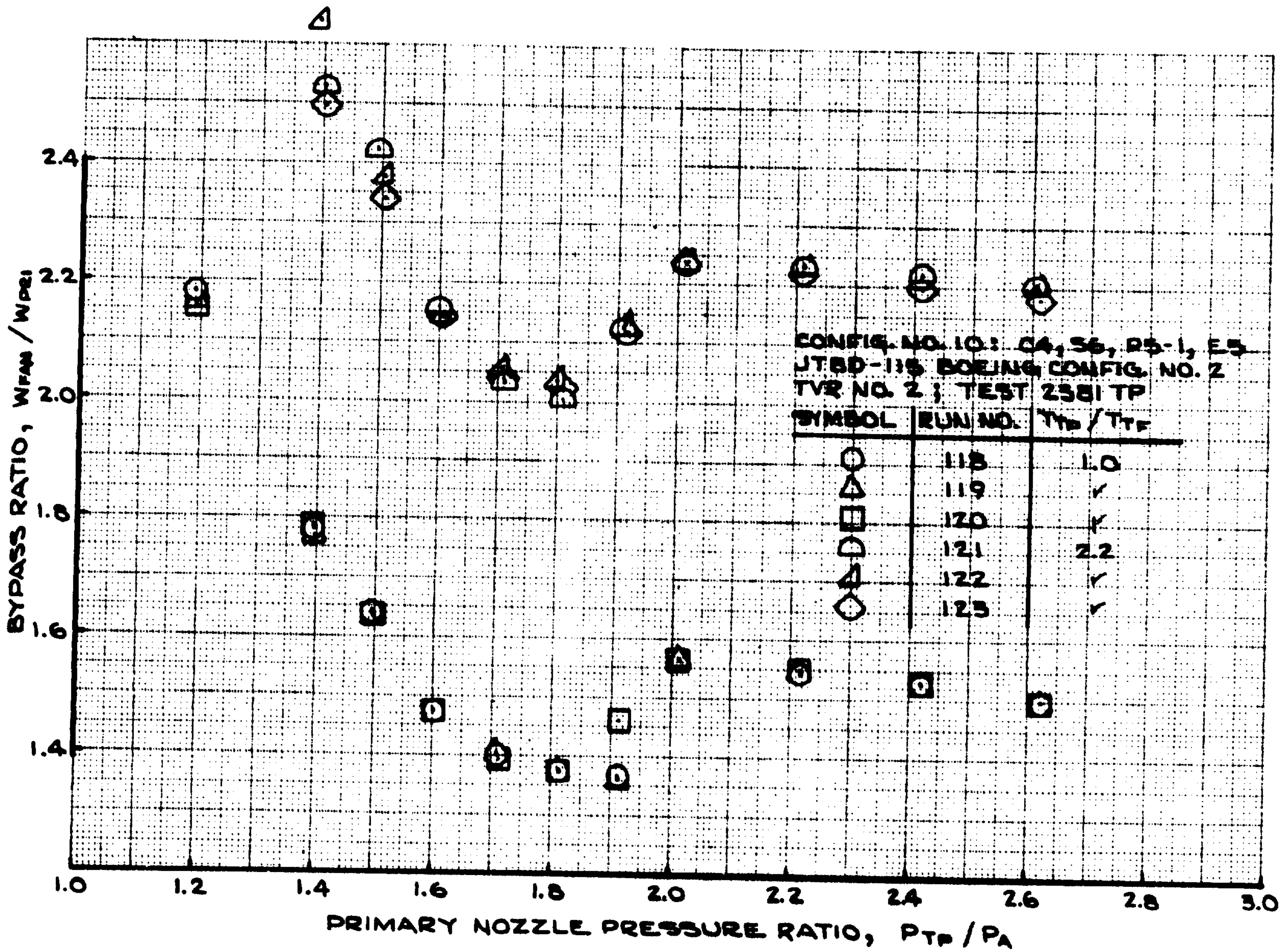

FIGURE 147- BYPASS RATIO
TEST CONFIG. NO. 10; RUNS 118-123

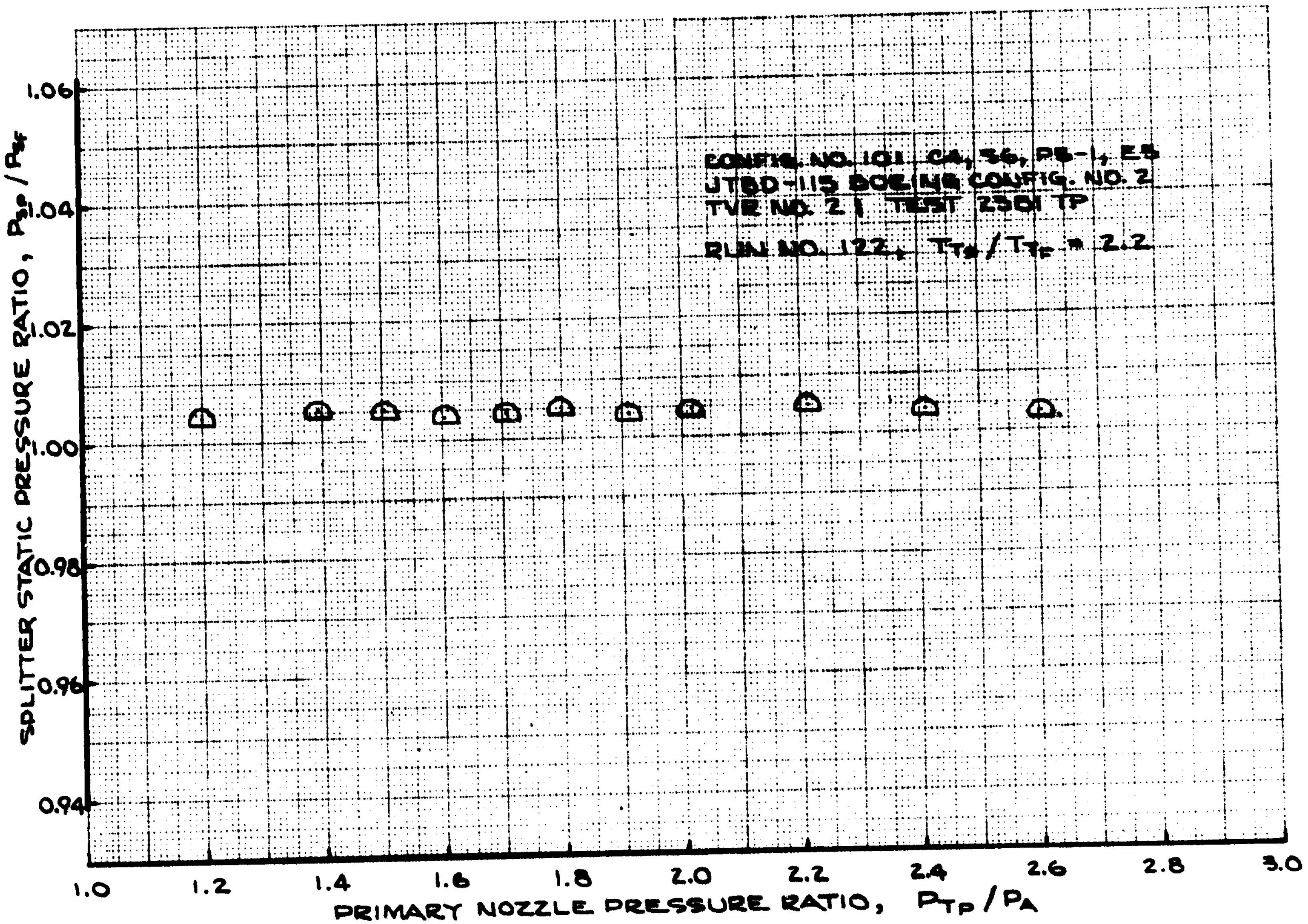

FIGURE 148 - SPLITTER STATIC PRESSURE RATIO
TEST CONFIG. NO. 10; RUN 122

7.2.11 TEST CONFIGURATION (T.C.) NO. 11

Configuration Description: Boeing Config. No. 2 design for JT8D-115.

Hardware Designations:

Outer Nozzle Wall	Splitter	Plug	Exit
C4	S6	P5-1	E6

Plotted Data:

Figure 149 - Velocity Coefficient; Runs 104-106, 109-111, 169-170.

Figure 150 - Mixed Velocity Coefficient; Runs 104-106, 109-111, 169-170.

Figure 151 - Flow Coefficient; Runs 104-106, 109-111, 169-170.

Figure 152 - Mixed Flow Coefficient; Runs 104-106, 109-111, 169-170.

Figure 153 - Fan/Primary Total Pressure Ratio; Runs 104-106, 109-111, 169-170.

Figure 154 - Bypass Ratio; Runs 104-106, 109-111, 169-170.

Figure 155 - Velocity Coefficient; Runs 114-117.

Figure 156 - Mixed Velocity Coefficient; Runs 114-117.

Figure 157 - Flow Coefficient; Runs 114-117.

Figure 158 - Mixed Flow Coefficient; Runs 114-117.

Figure 159 - Fan/Primary Total Pressure Ratio; Runs 114-117.

Figure 160 - Bypass Ratio; Runs 114-117.

Figure 161 - Velocity Coefficient; Runs 107-108, 112-113.

Figure 162 - Mixed Velocity Coefficient; Runs 107-108, 112-113.

Figure 163 - Flow Coefficient; Runs 107-108, 112-113.

Figure 164 - Mixed Flow Coefficient; Runs 107-108, 112-113.

Figure 165 - Fan/Primary Total Pressure Ratio; Runs 107-108, 112-113.

Figure 166 - Bypass Ratio; Runs 107-108, 112-113.

Figure 167 - Splitter Static Pressure Ratio; Runs 109, 112, 114.

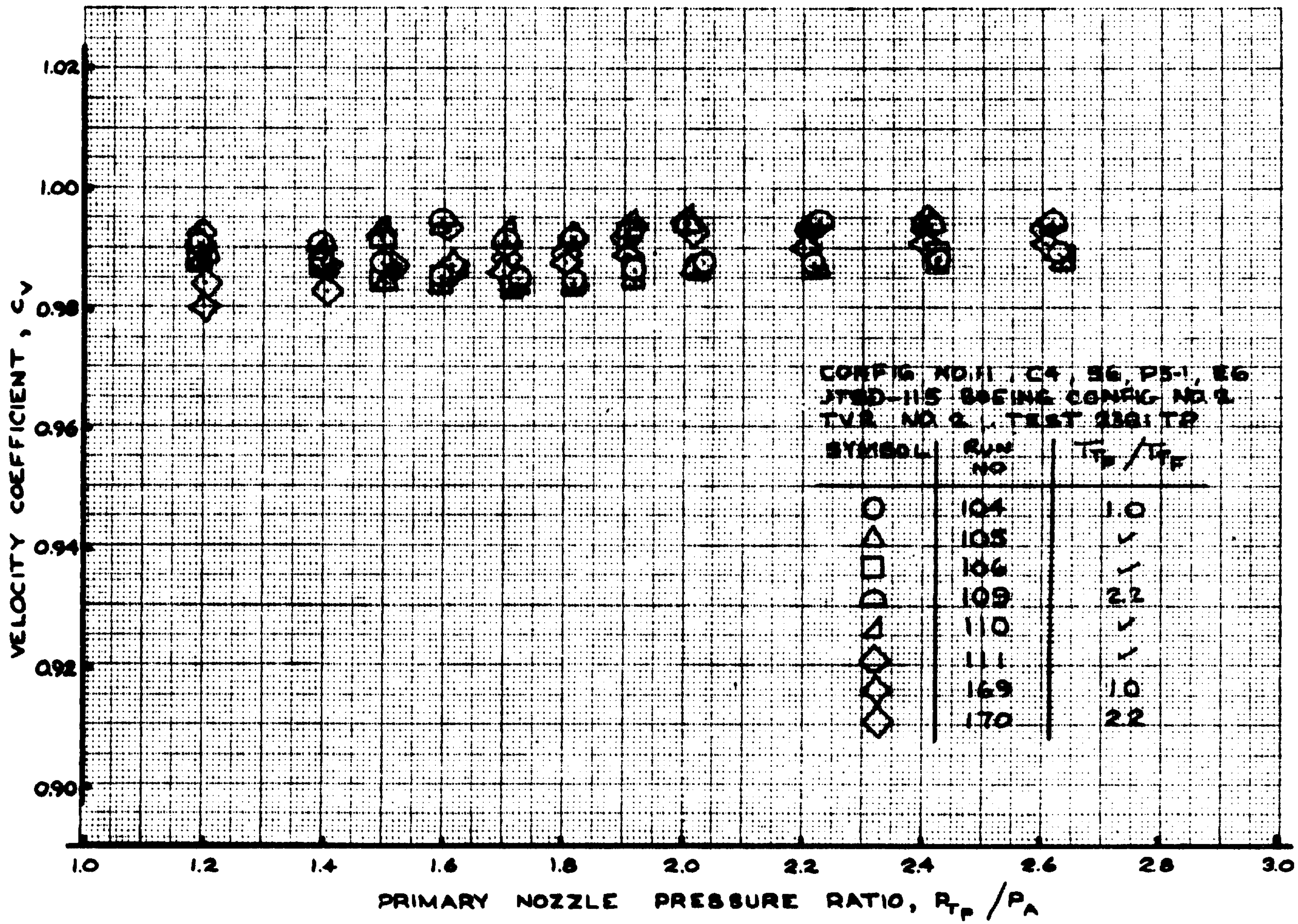

FIGURE 149- VELOCITY COEFFICIENT
TEST CONFIG. NO. 11; RUNS 104-106, 109-111, 169-170

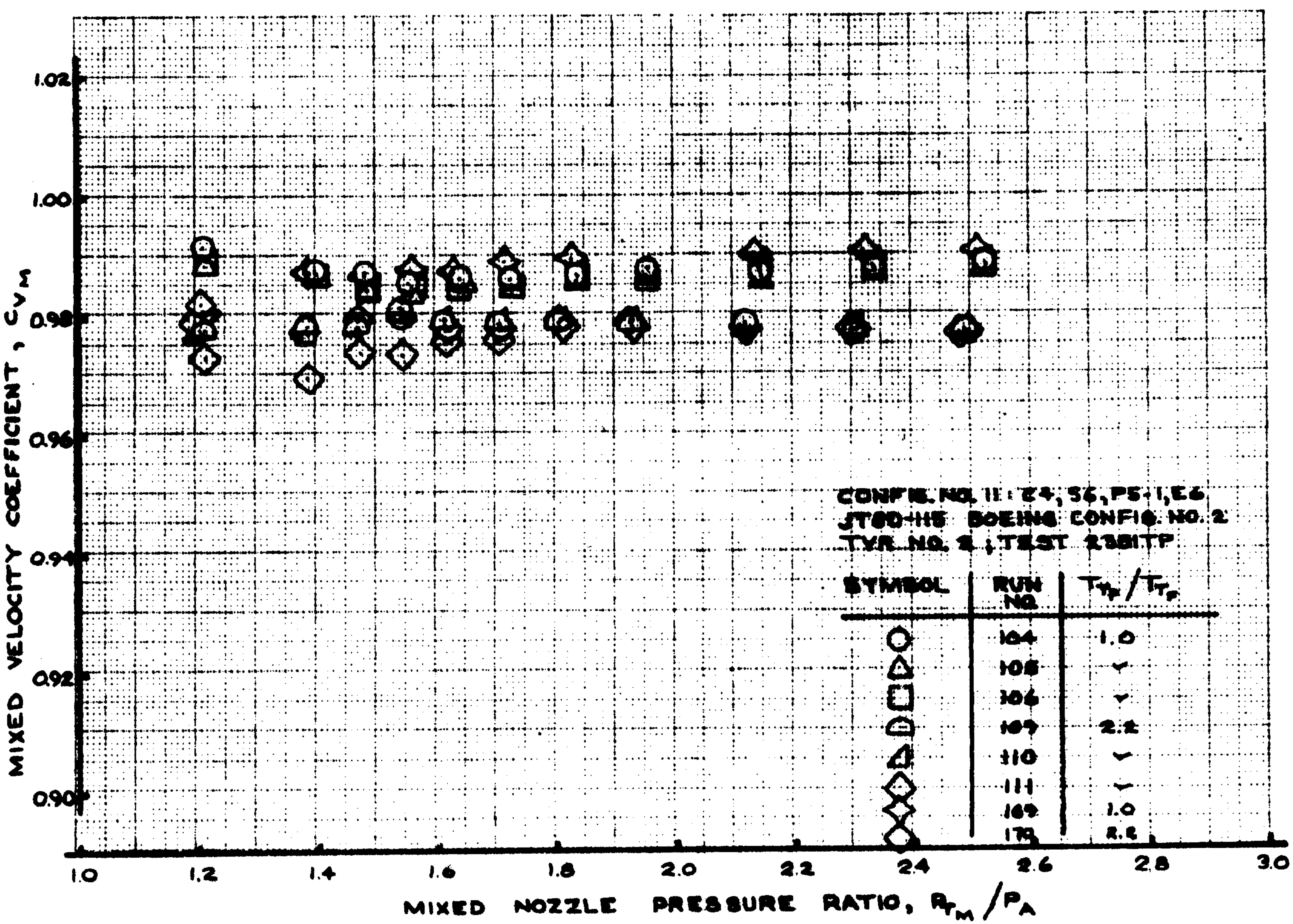

FIGURE 150- MIXED VELOCITY COEFFICIENT
TEST CONFIG. NO. 11; RUNS 104-106, 109-111, 169-170

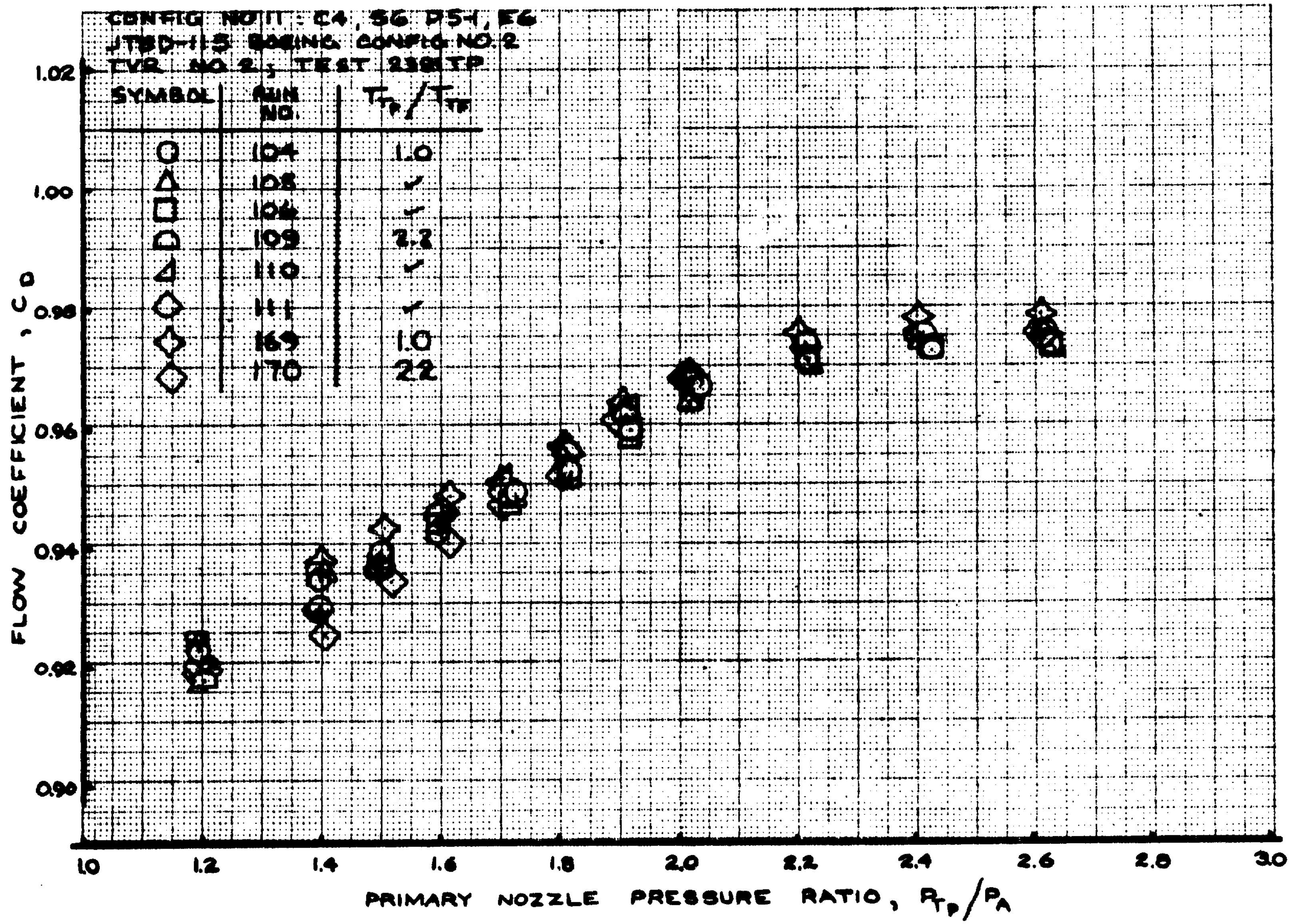

FIGURE 151 - FLOW COEFFICIENT
TEST CONFIG. NO. 11; RUNS 104-106, 109-111, 169-170

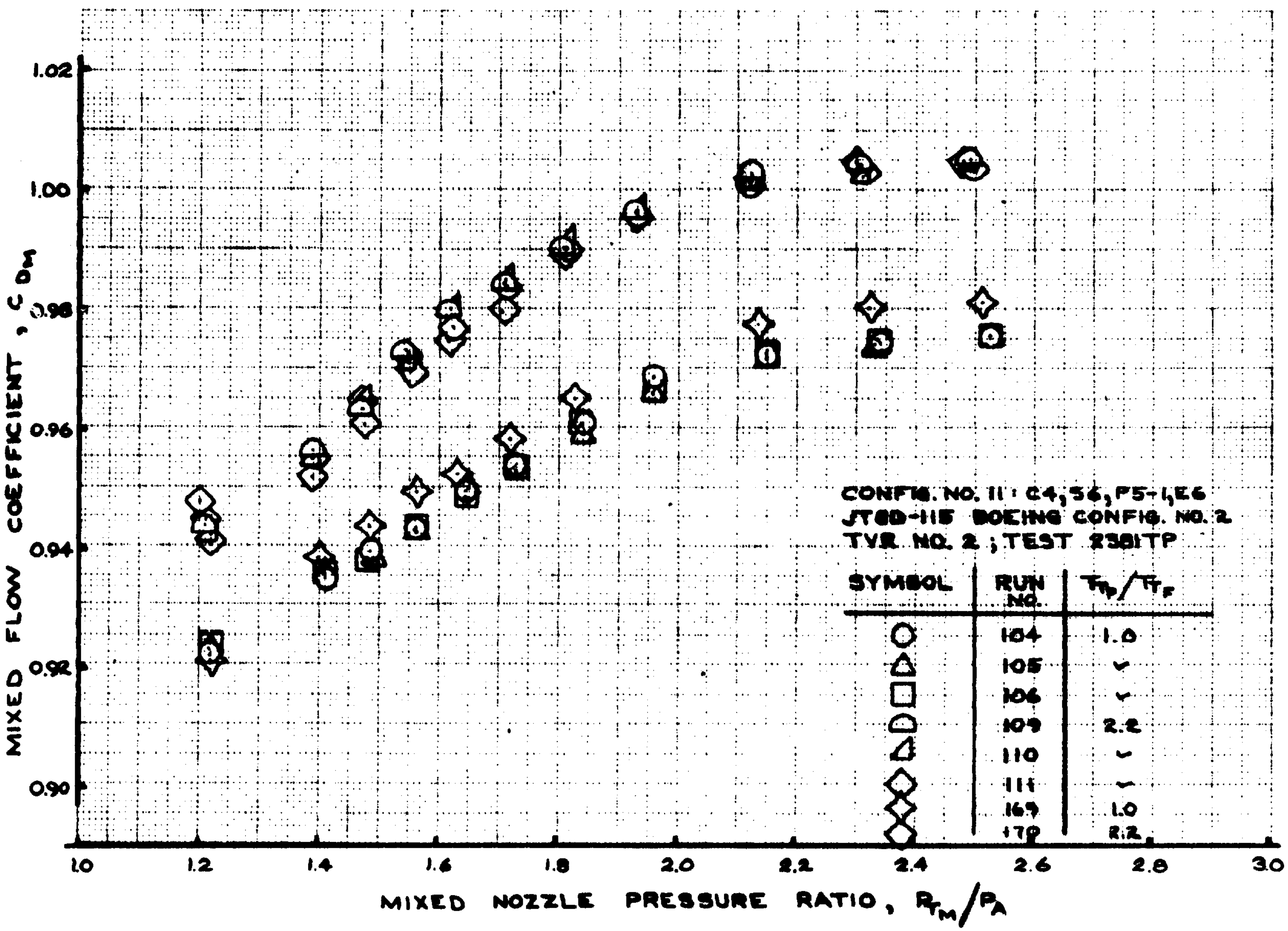

FIGURE 152- MIXED FLOW COEFFICIENT
TEST CONFIG. NO. 11; RUNS 104-106, 109-111, 169-170

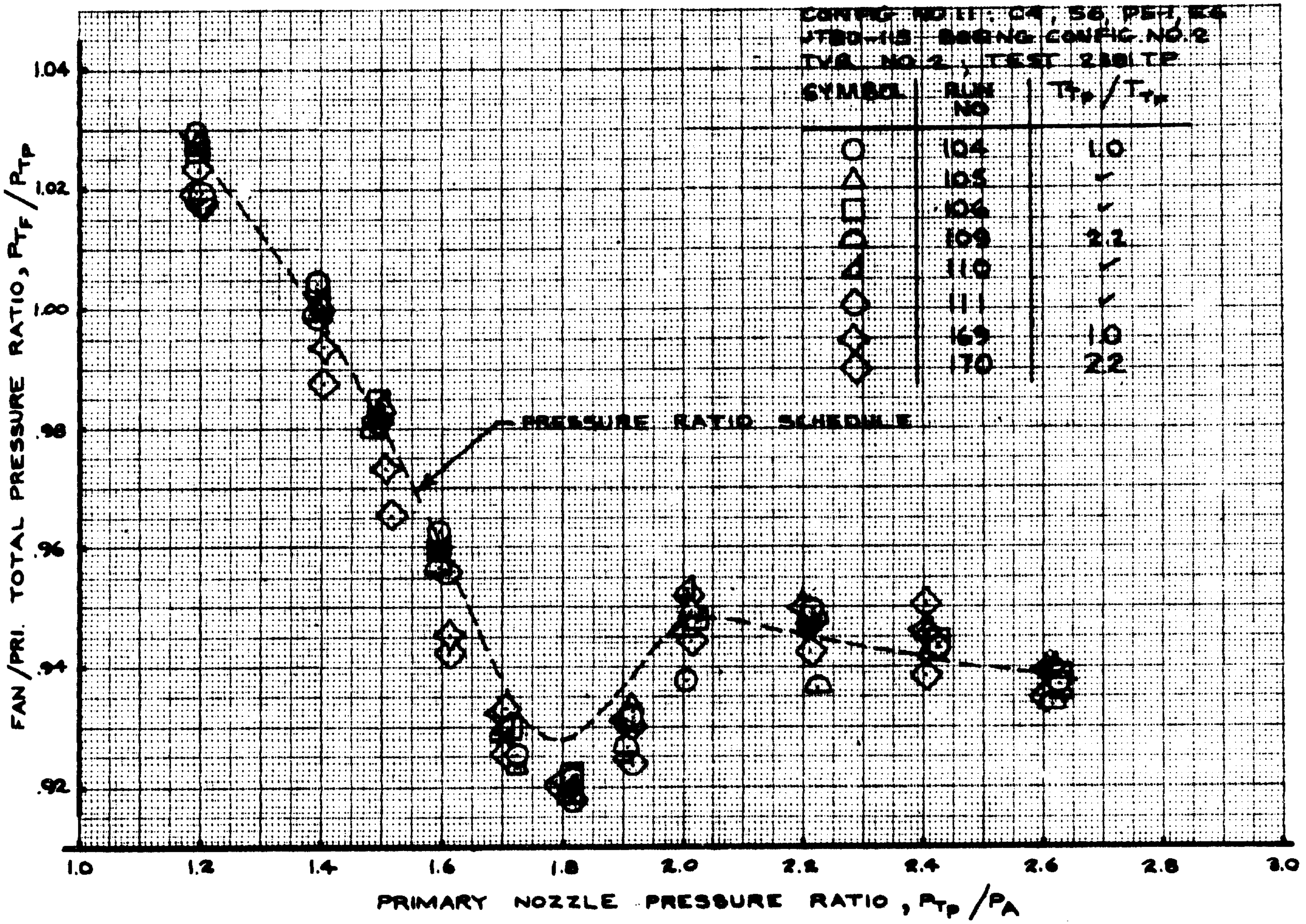

FIGURE 153 - FAN/PRIMARY TOTAL PRESSURE RATIO
TEST CONFIG. NO. 11; RUNS 104-106, 109-111, 169-170

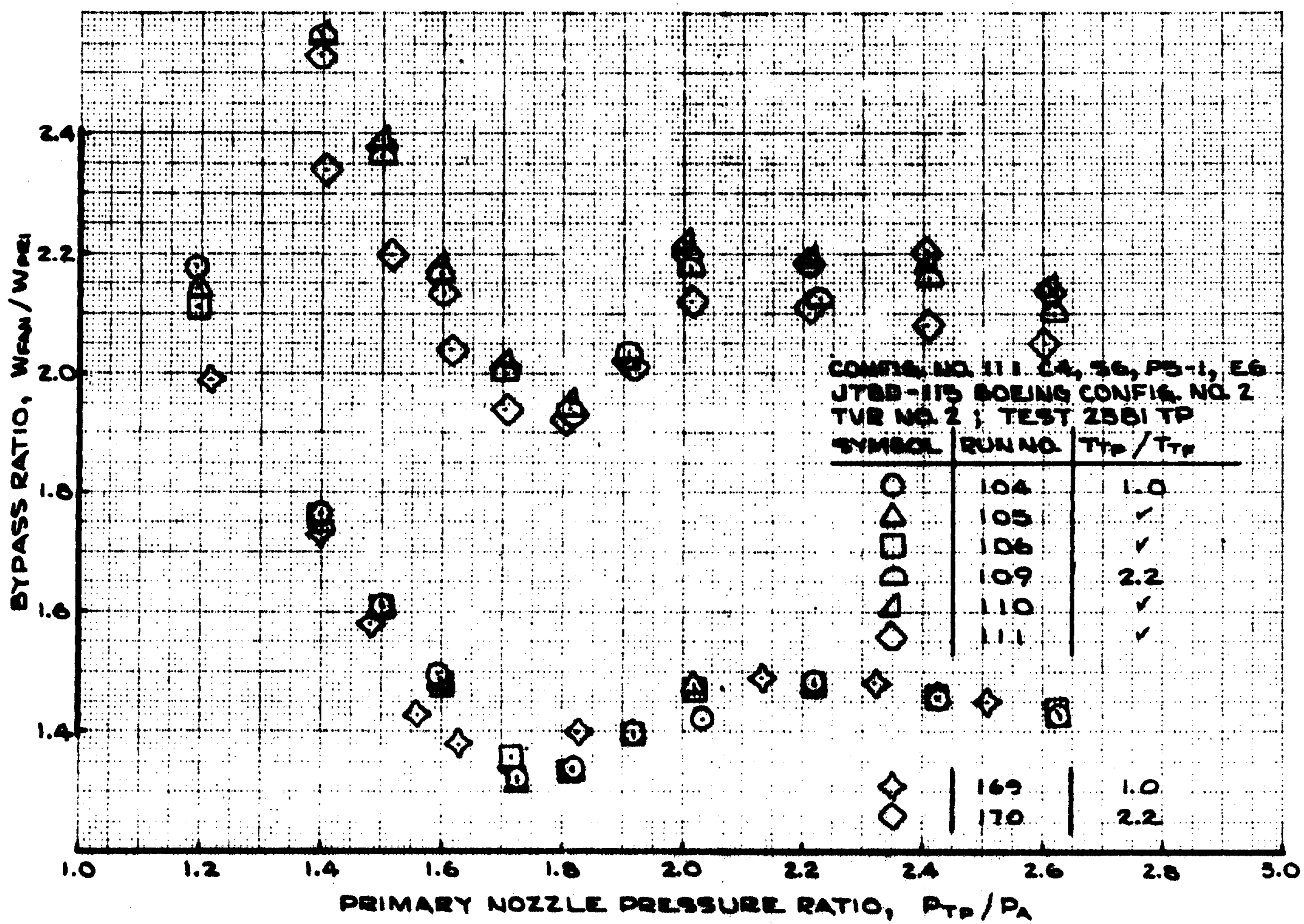

FIGURE 154- BYPASS RATIO
TEST CONFIG. NO. 11; RUNS 104-106, 109-11, 169-170

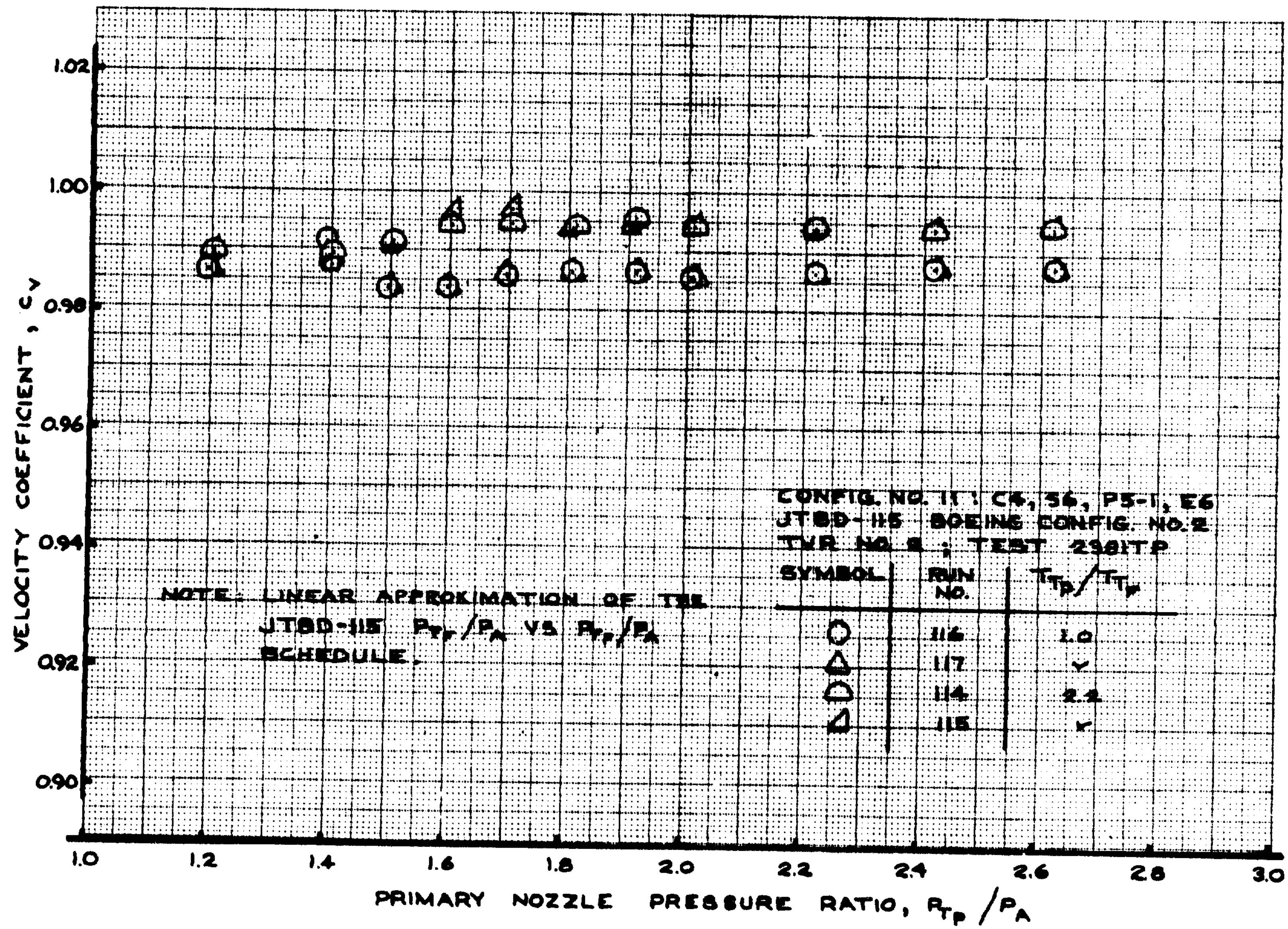

FIGURE 155- VELOCITY COEFFICIENT
TEST CONFIG. NO. 11; RUNS 114-117

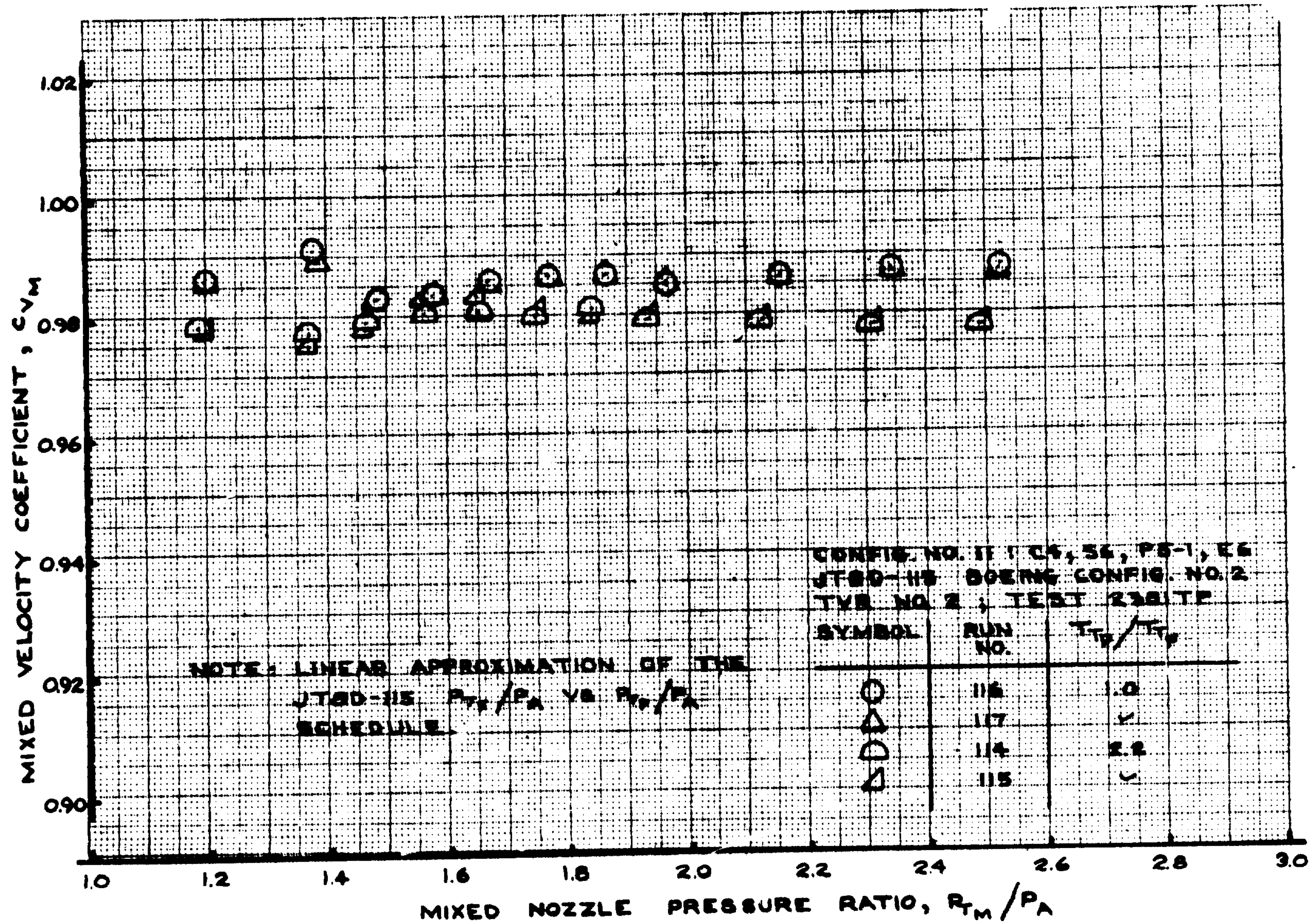

FIGURE 156- MIXED VELOCITY COEFFICIENT
TEST CONFIG. NO. 11; RUNS 114-117

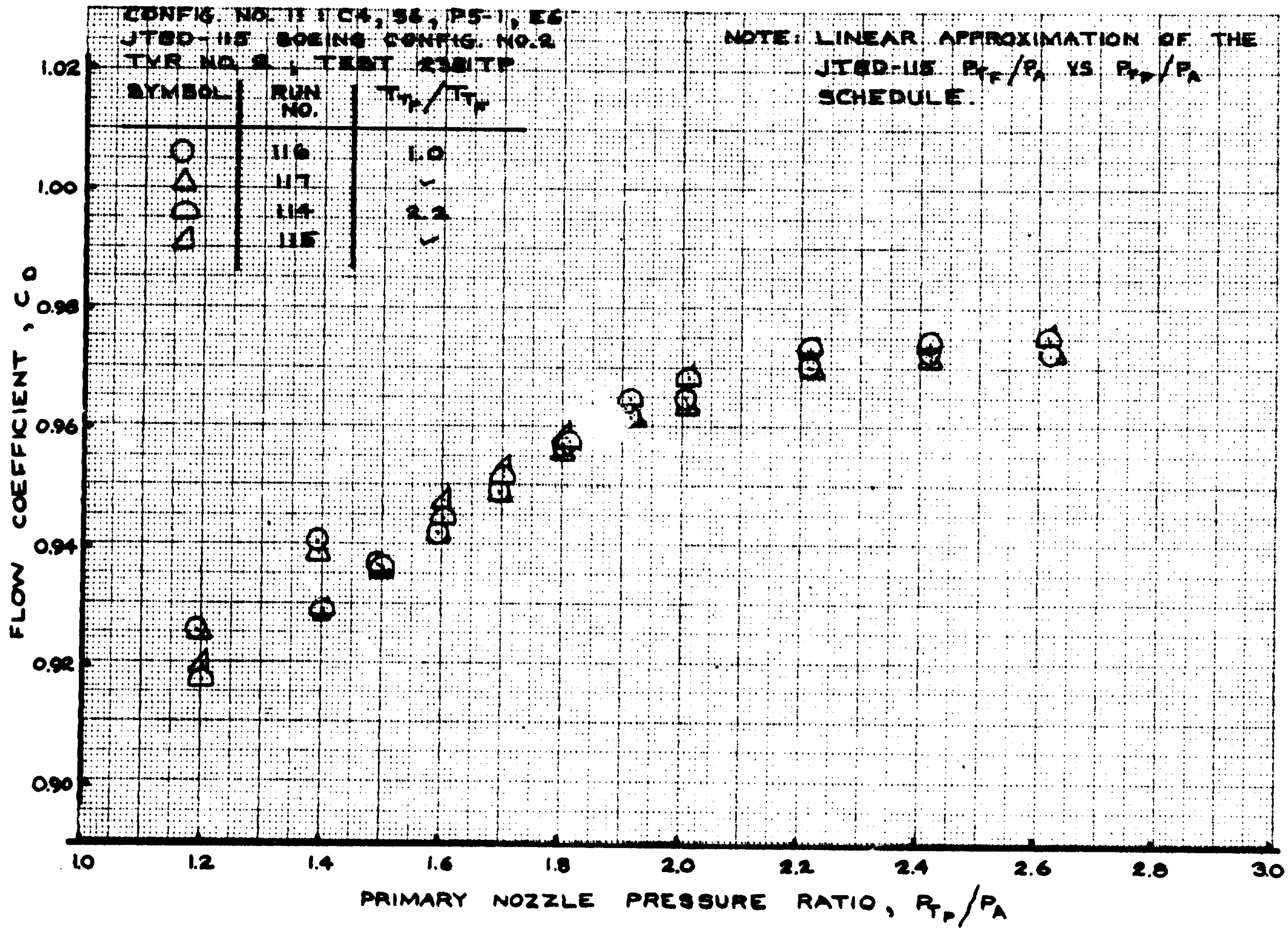

FIGURE 157 - FLOW COEFFICIENT
TEST CONFIG. NO. 11; RUNS 114-117

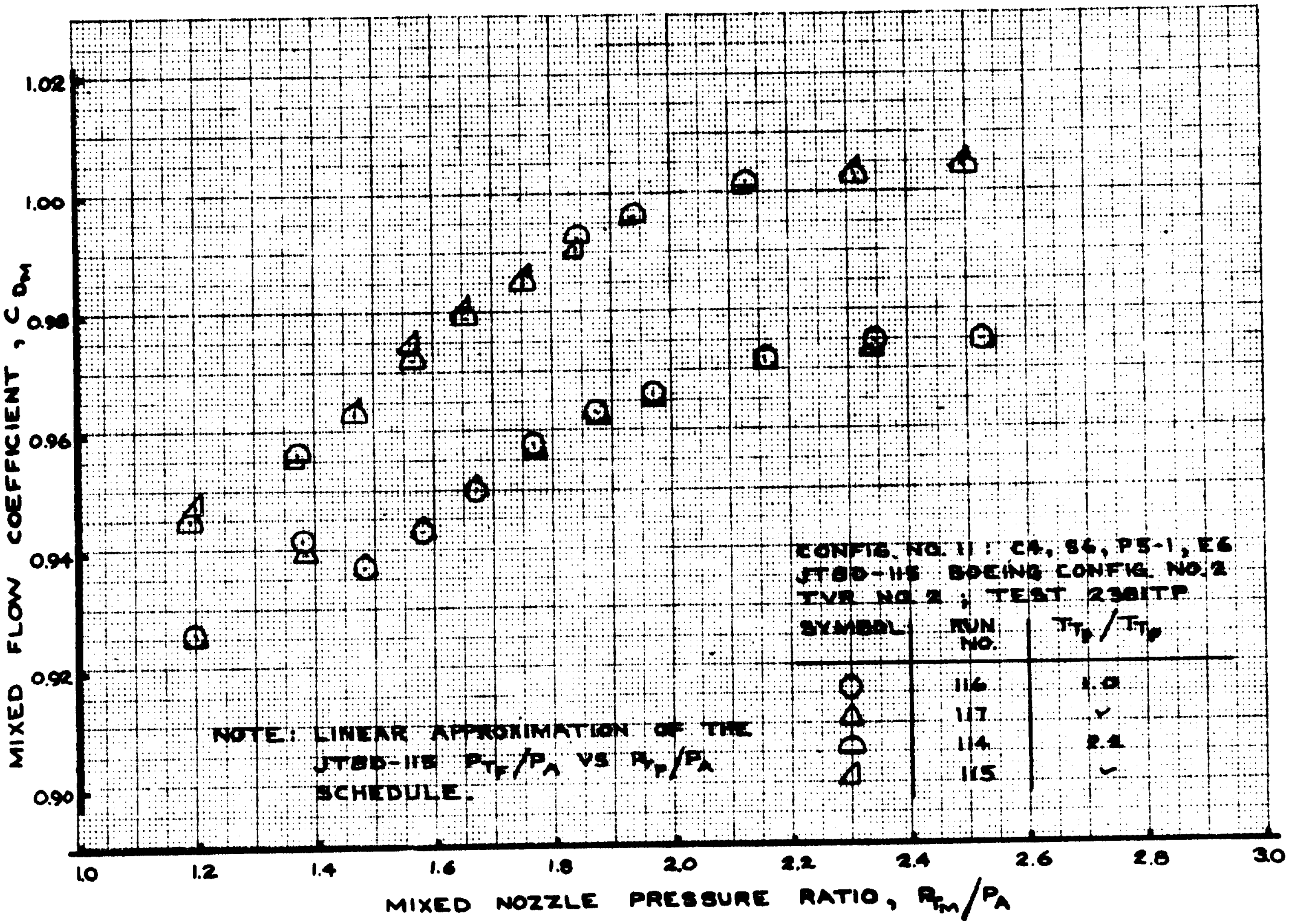

FIGURE 158- MIXED FLOW COEFFICIENT
TEST CONFIG. NO. 11; RUNS 114-117

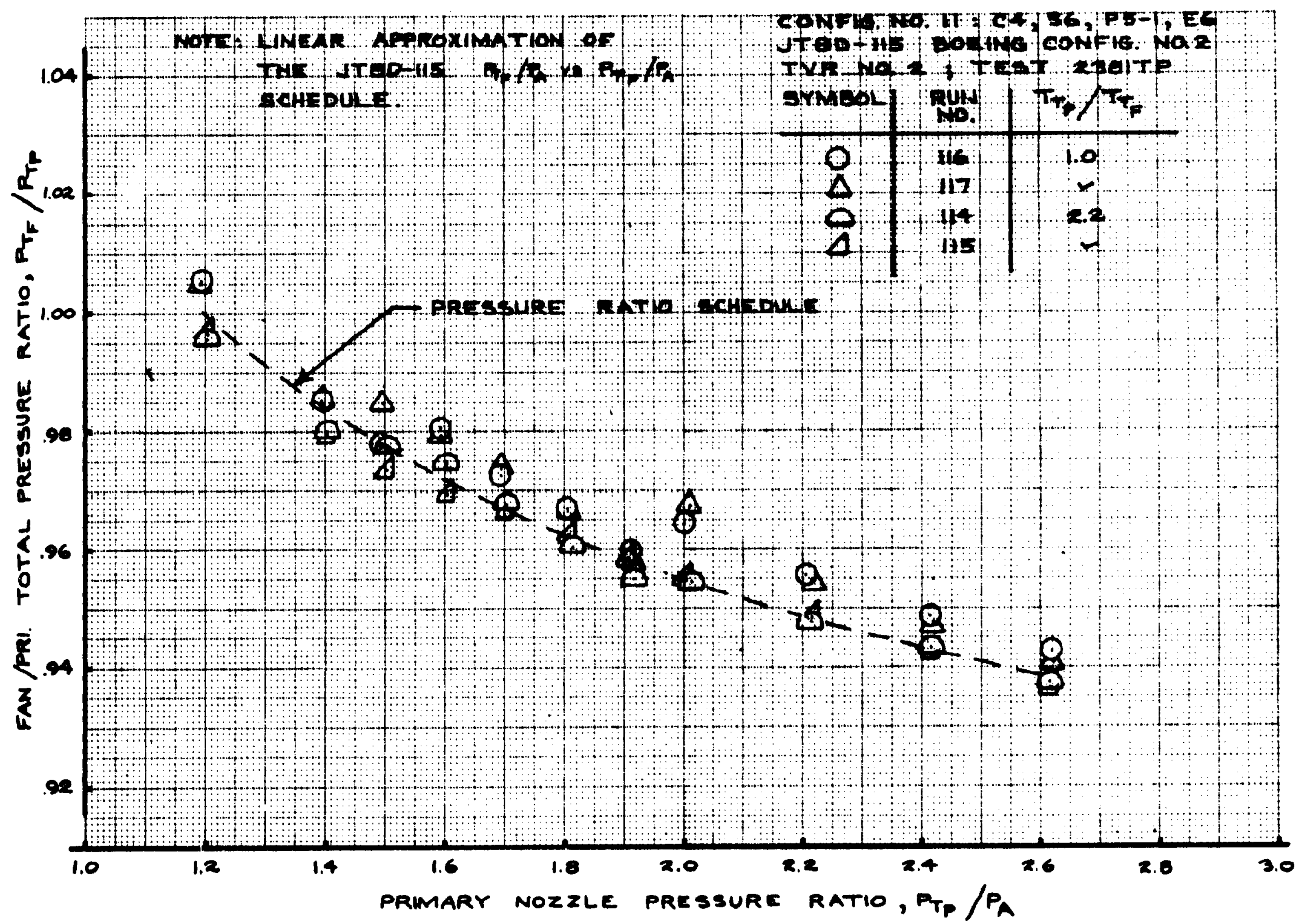

FIGURE 159- FAN/PRIMARY TOTAL PRESSURE RATIO
TEST CONFIG. NO. 11; RUNS 114-117

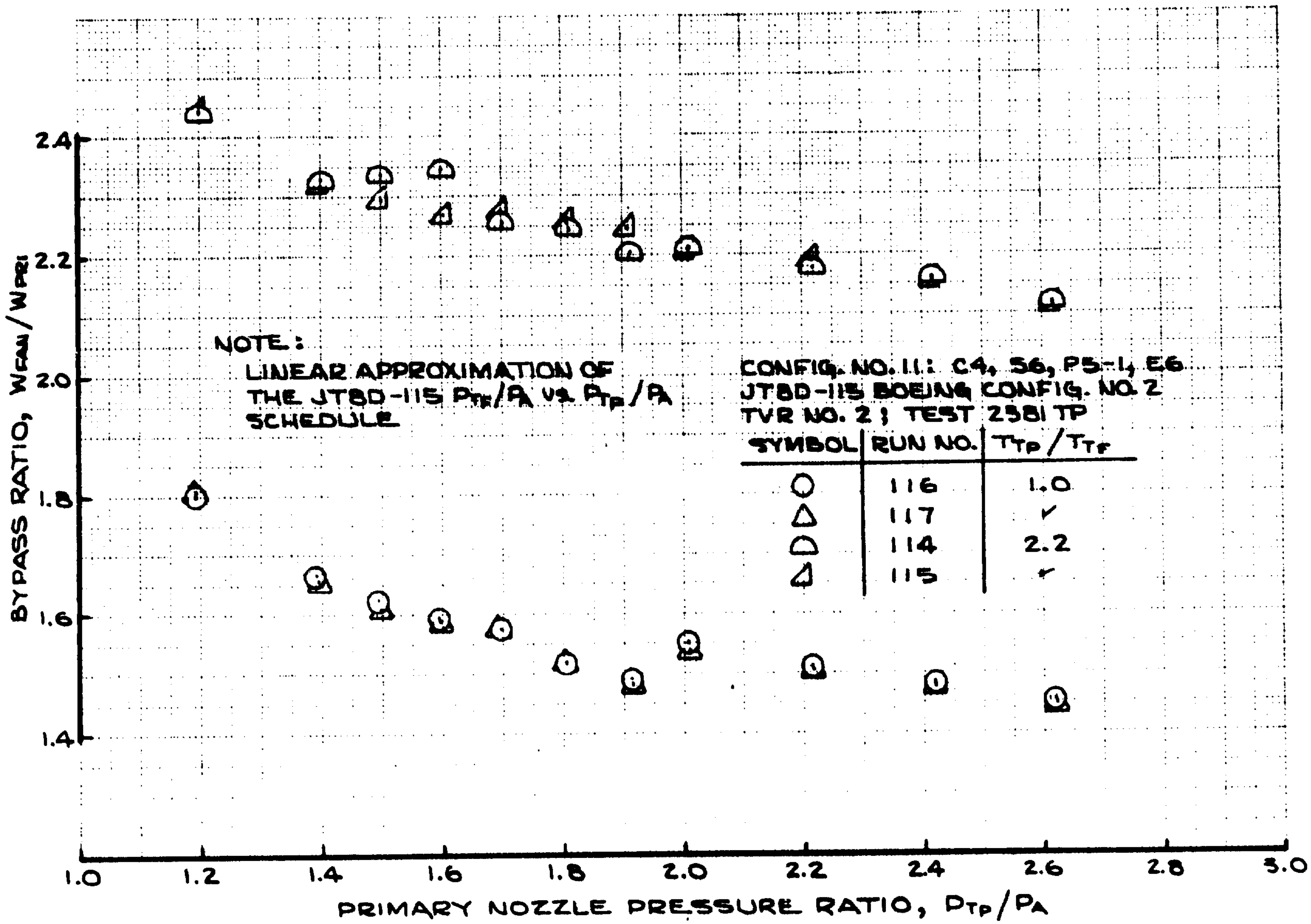

FIGURE 160.- BYPASS RATIO
TEST CONFIG. NO. 11; RUNS 114-117

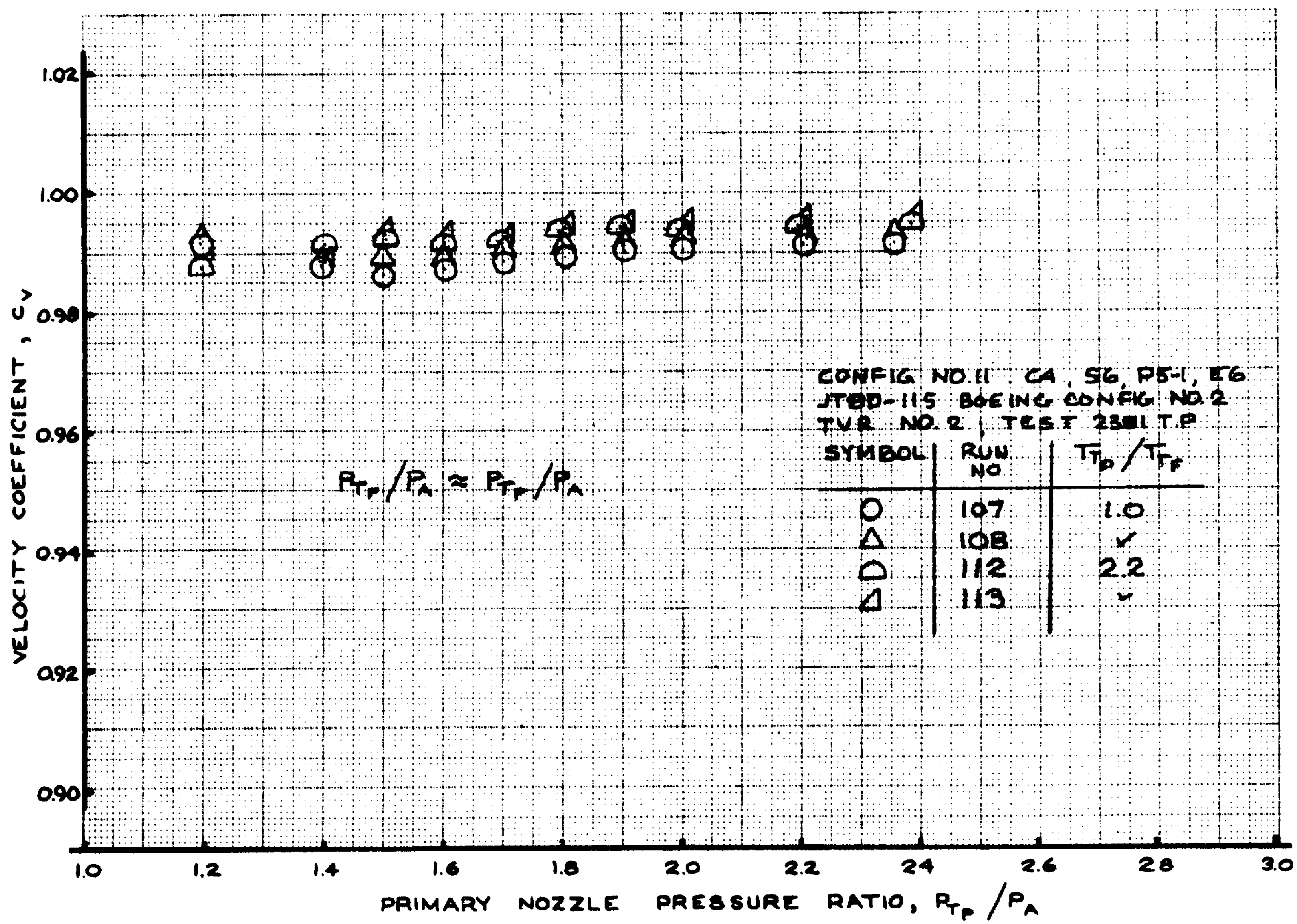

FIGURE 161- VELOCITY COEFFICIENT
TEST CONFIG. NO. 11; RUNS 107-108, 112-113

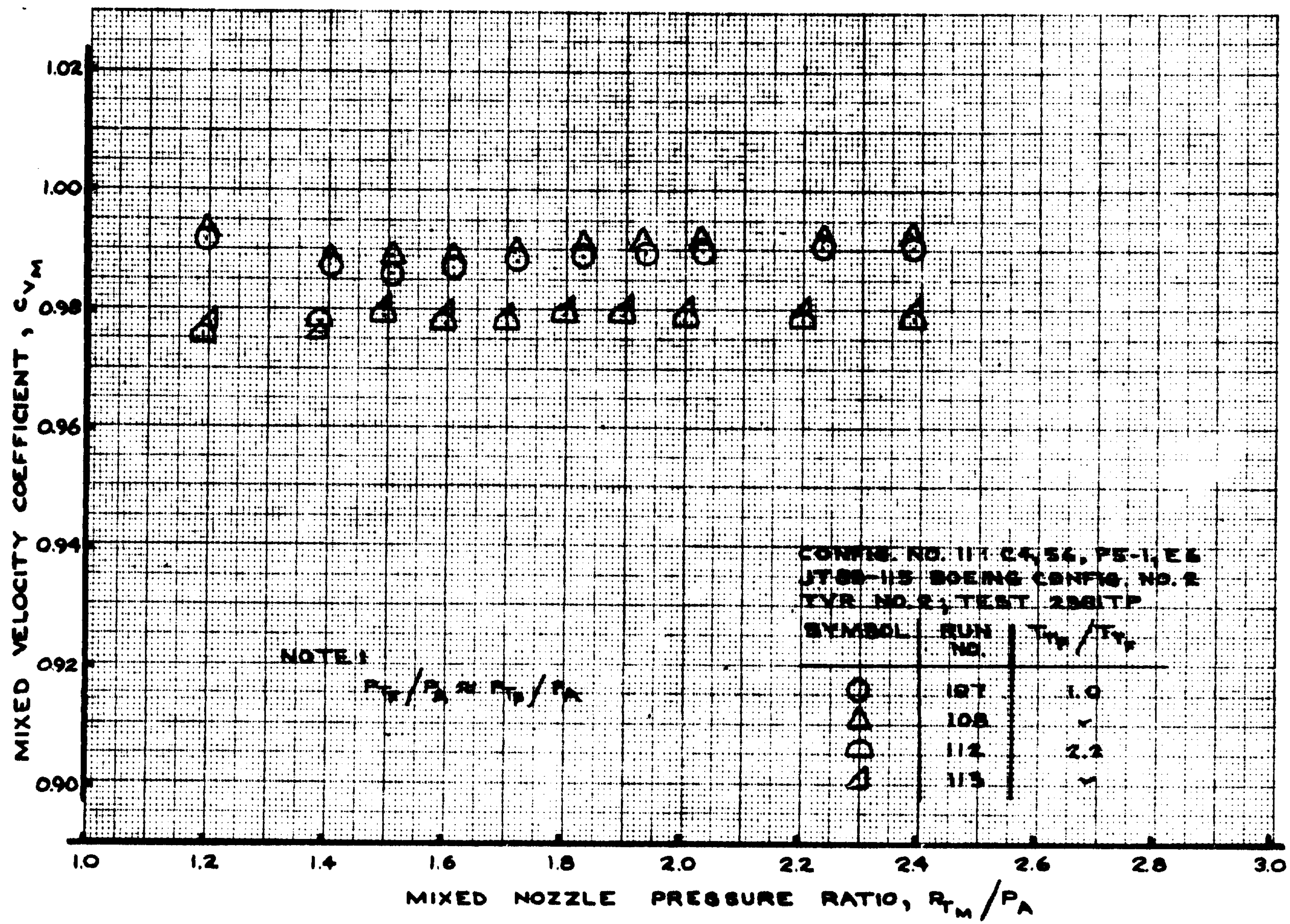

FIGURE 162- MIXED VELOCITY COEFFICIENT
TEST CONFIG. NO. 11; RUNS 107-108, 112-113

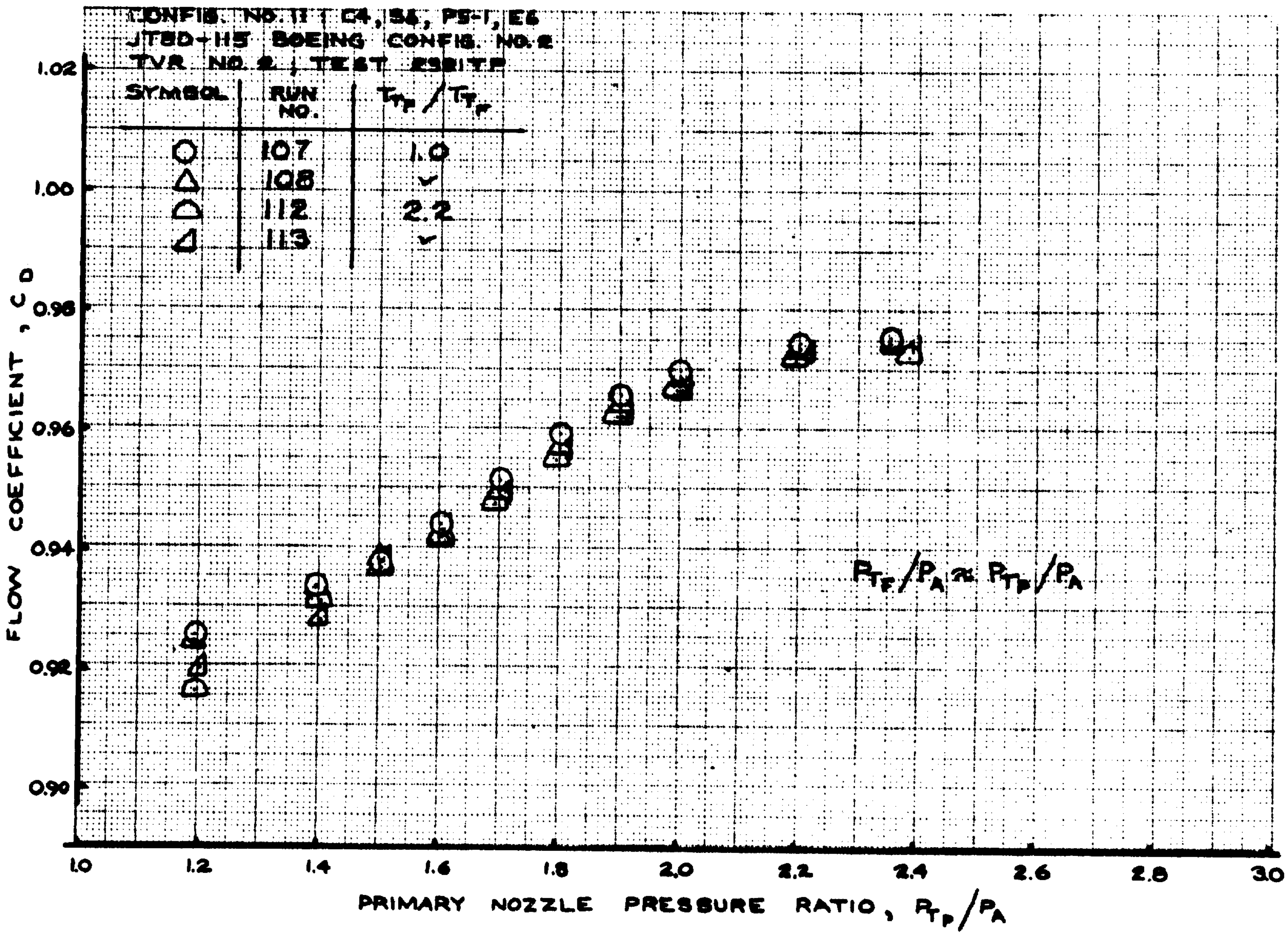

FIGURE 163- FLOW COEFFICIENT
TEST CONFIG. NO. 11; RUNS 107-108, 112-113

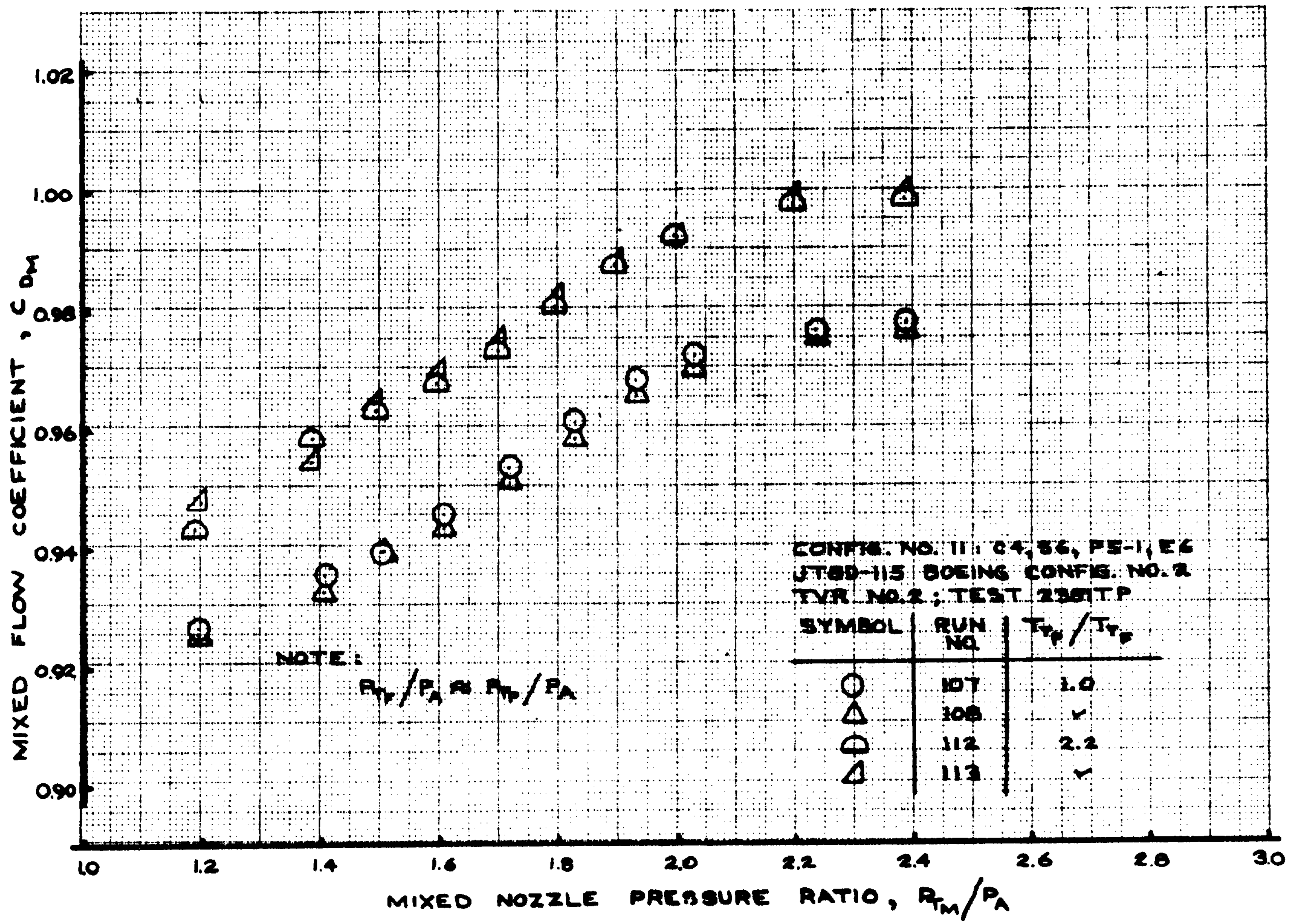

FIGURE 164- MIXED FLOW COEFFICIENT
TEST CONFIG. NO. 11; RUNS 107-108, 112-113

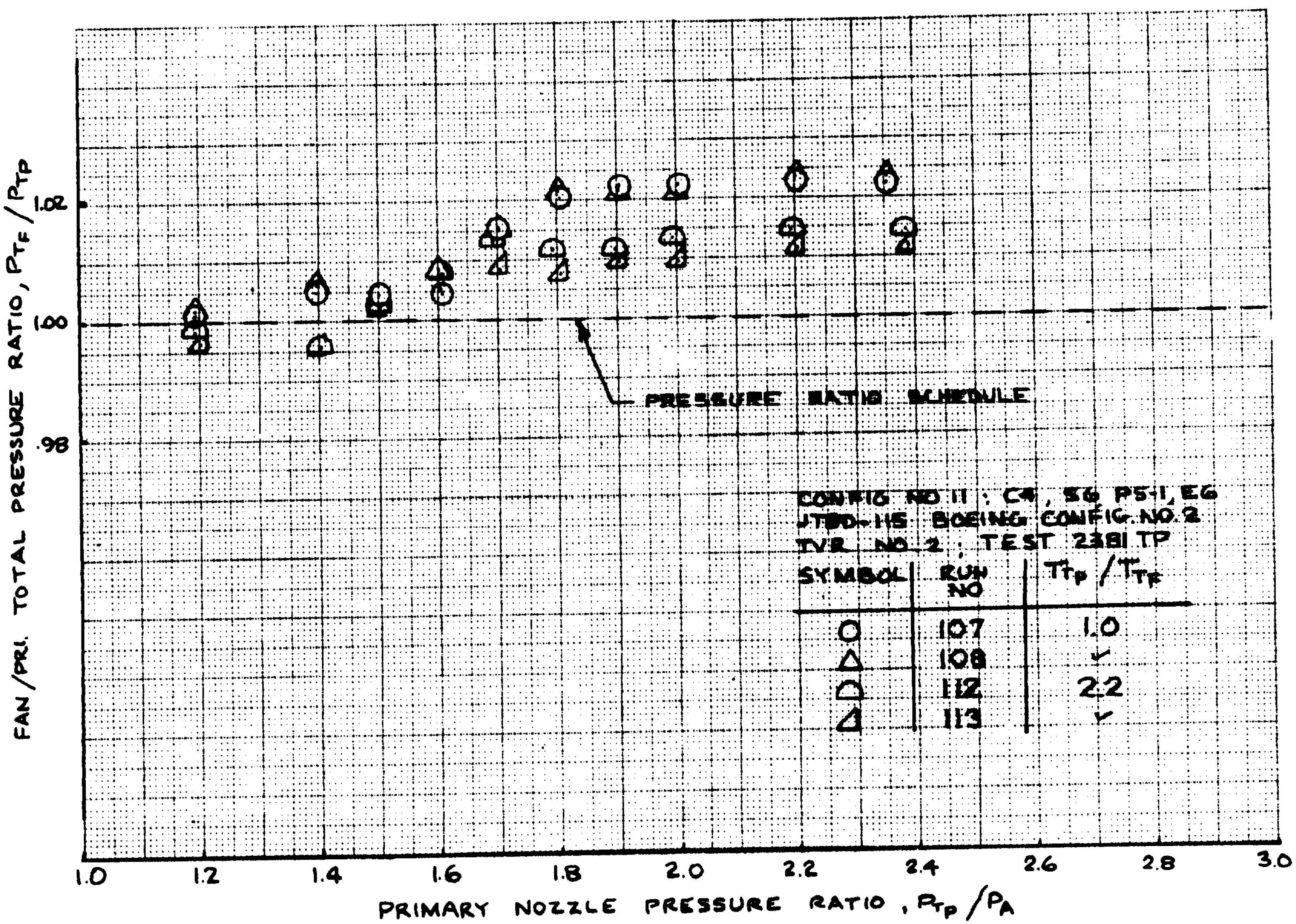

FIGURE 165- FAN/PRIMARY TOTAL PRESSURE RATIO
TEST CONFIG. NO. 11; RUNS 107-108, 112-113

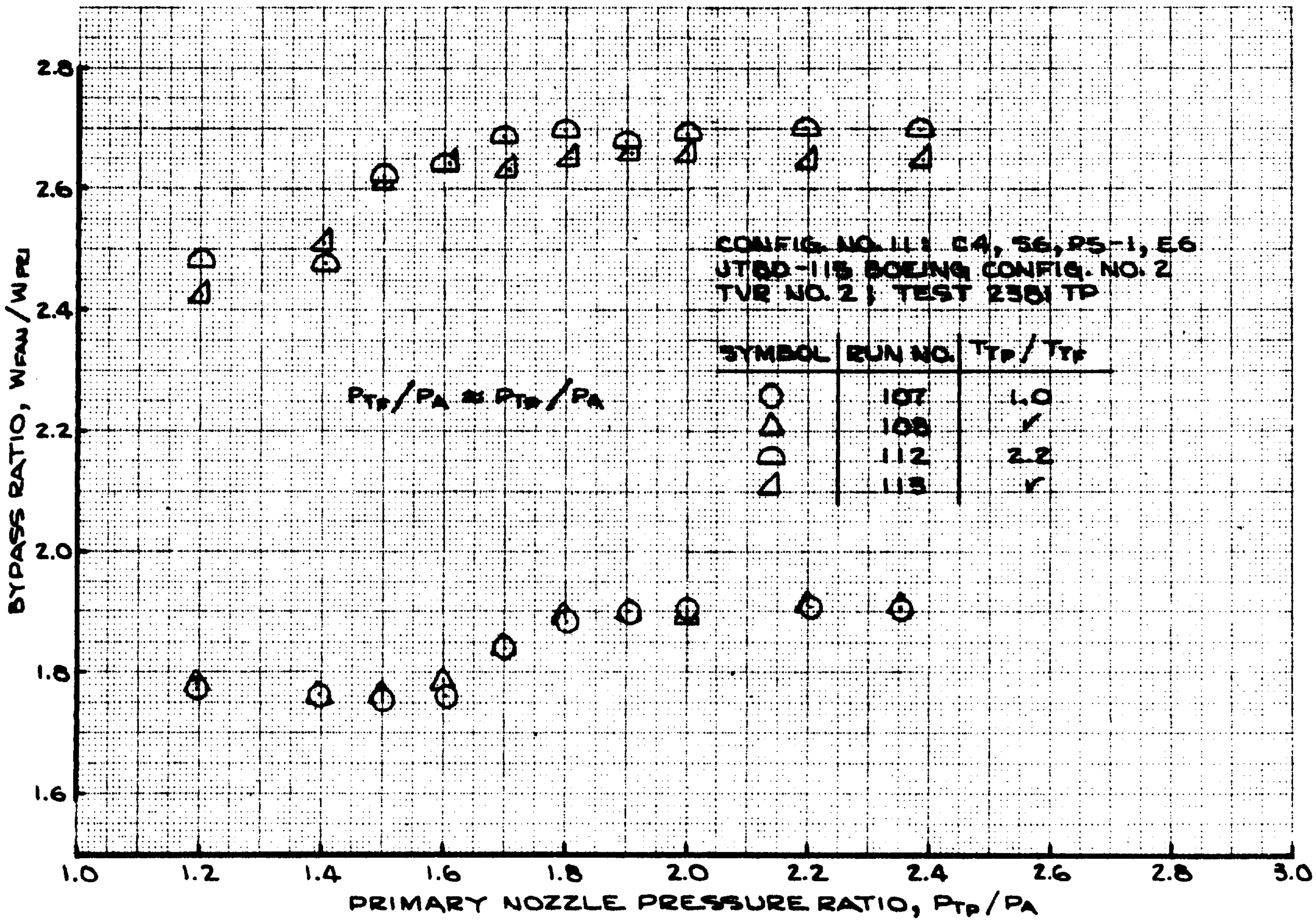

FIGURE 166- BYPASS RATIO
TEST CONFIG. NO. 11; RUNS 107-108, 112-113

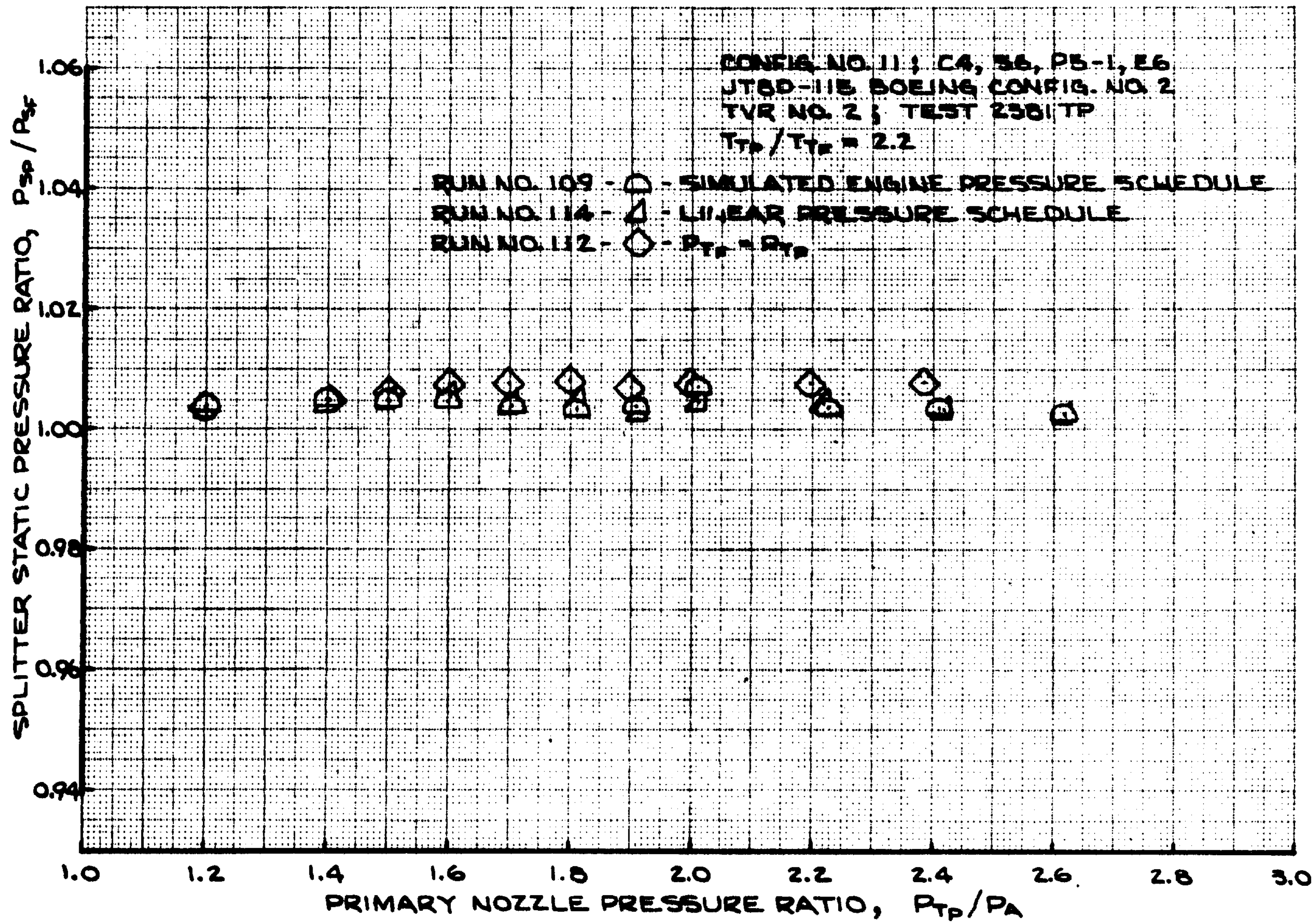

FIGURE 167 - SPLITTER STATIC PRESSURE RATIO
TEST CONFIG. NO. 11; RUNS 109, 112, 114

7.2.12 TEST CONFIGURATION (T.C.) NO. 12

Configuration Description: Boeing Config. No. 2 design for JT8D-115 with the JT8D-117 exit area.

Hardware Designations:

Outer Nozzle Wall	Splitter	Plug	Exit
C4	S6	P5-1	E7

Plotted Data:

- **Figure 168 - Velocity Coefficient; Runs 124-129.**
- Figure 169 - Mixed Velocity Coefficient; Runs 124-129.
- Figure 170 - Flow Coefficient; Runs 124-129.
- Figure 171 - Mixed Flow Coefficient; Runs 124-129.
- Figure 172 - Fan/Primary Total Pressure Ratio; Runs 124-129.
- Figure 173 - Bypass Ratio; Runs 124-129.
- Figure 174 - Splitter Static Pressure Ratio; Run 128.

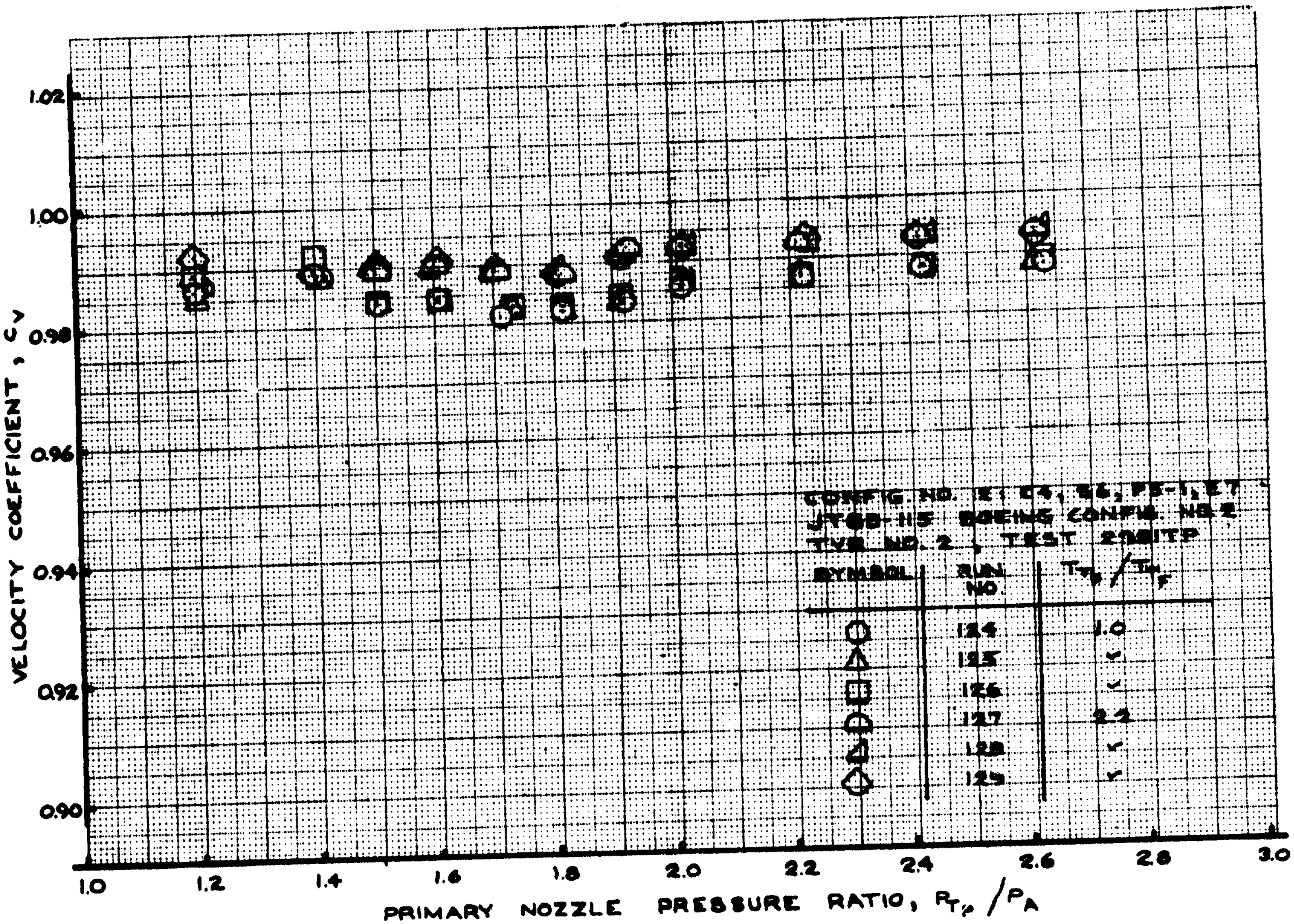

FIGURE 168- VELOCITY COEFFICIENT
TEST CONFIG. NO. 12; RUNS 124-129

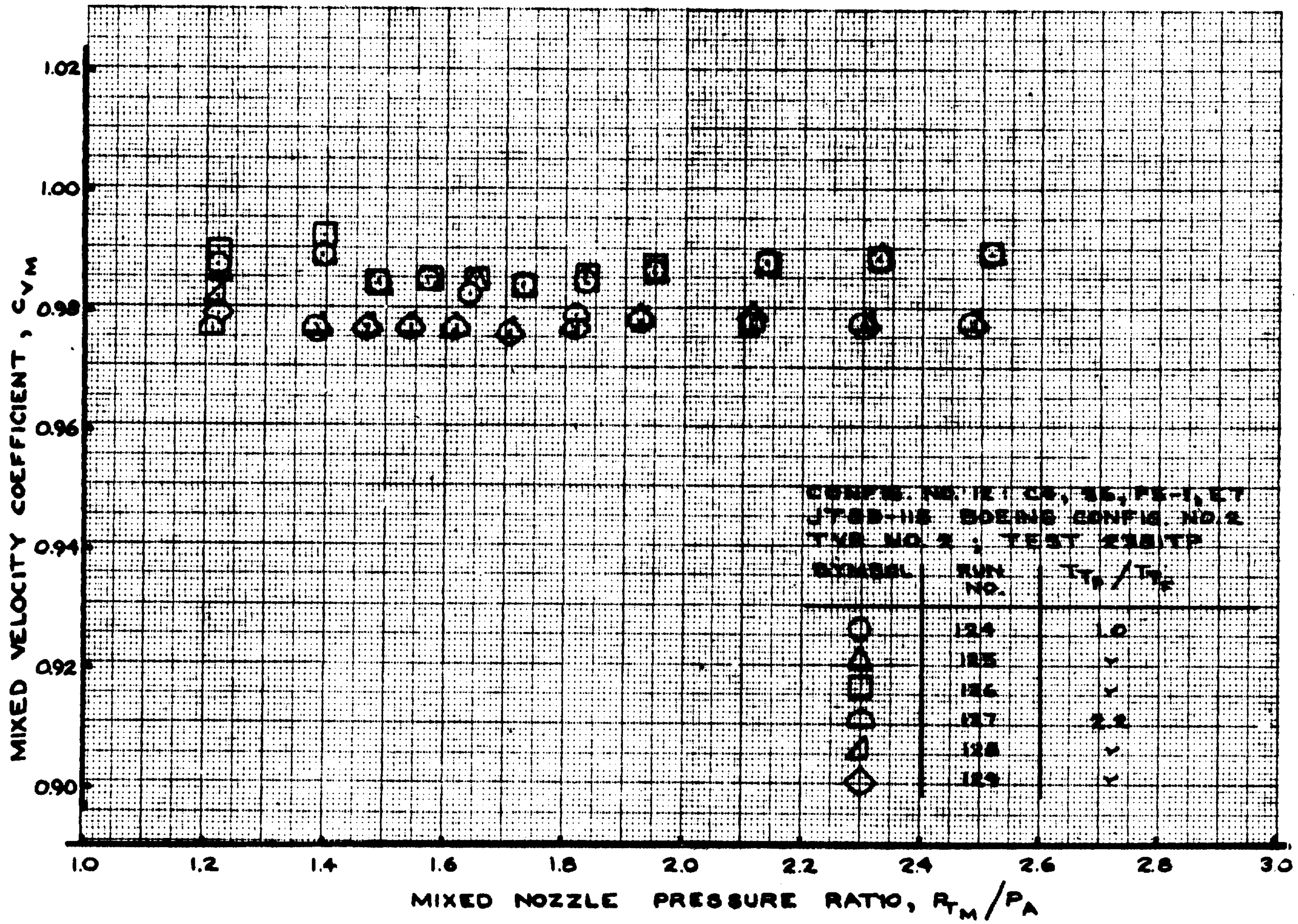

FIGURE 169- MIXED VELOCITY COEFFICIENT
TEST CONFIG. NO. 12; RUNS 124-129

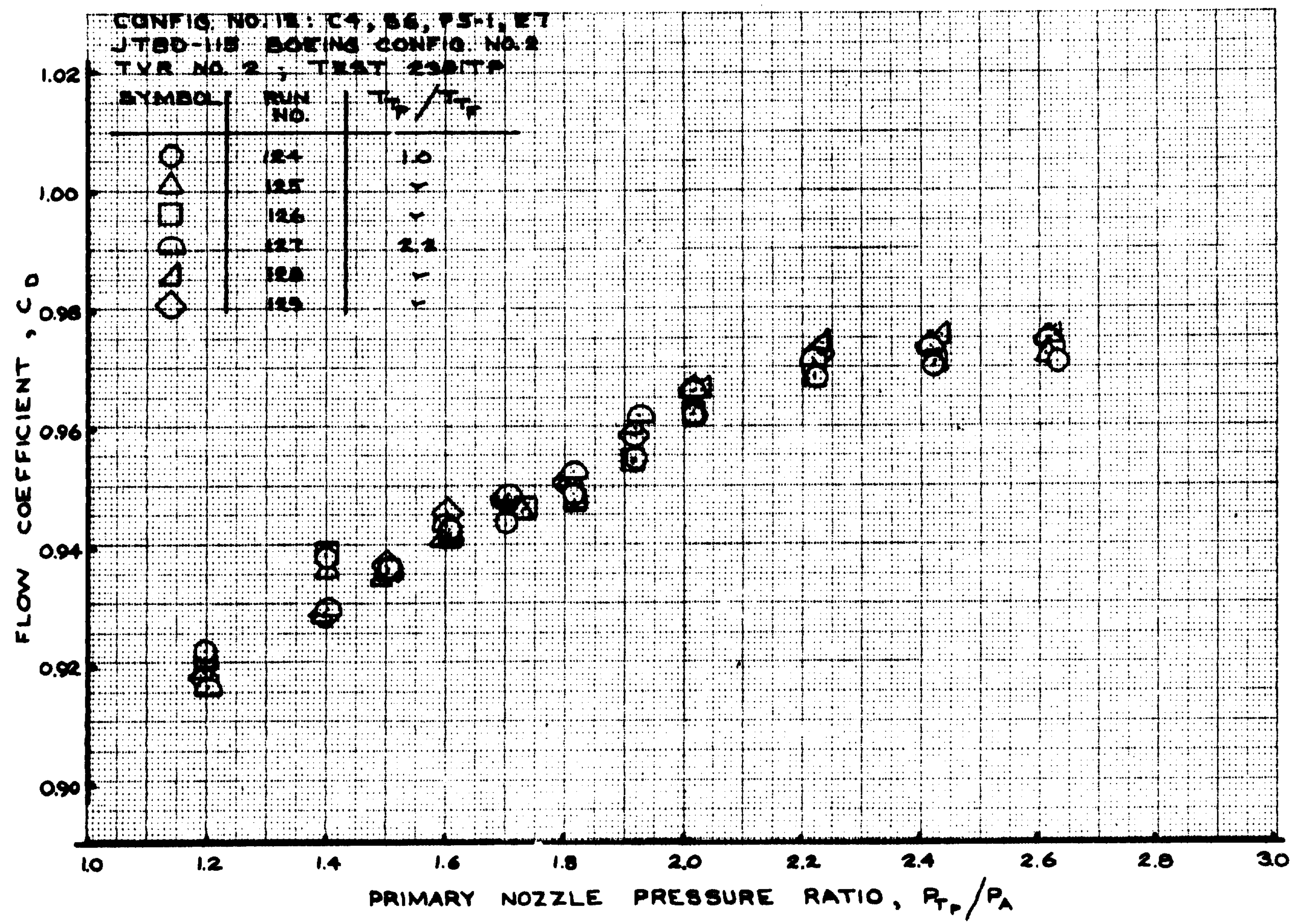

FIGURE 170- FLOW COEFFICIENT
TEST CONFIG. NO. 12; RUNS 124-129

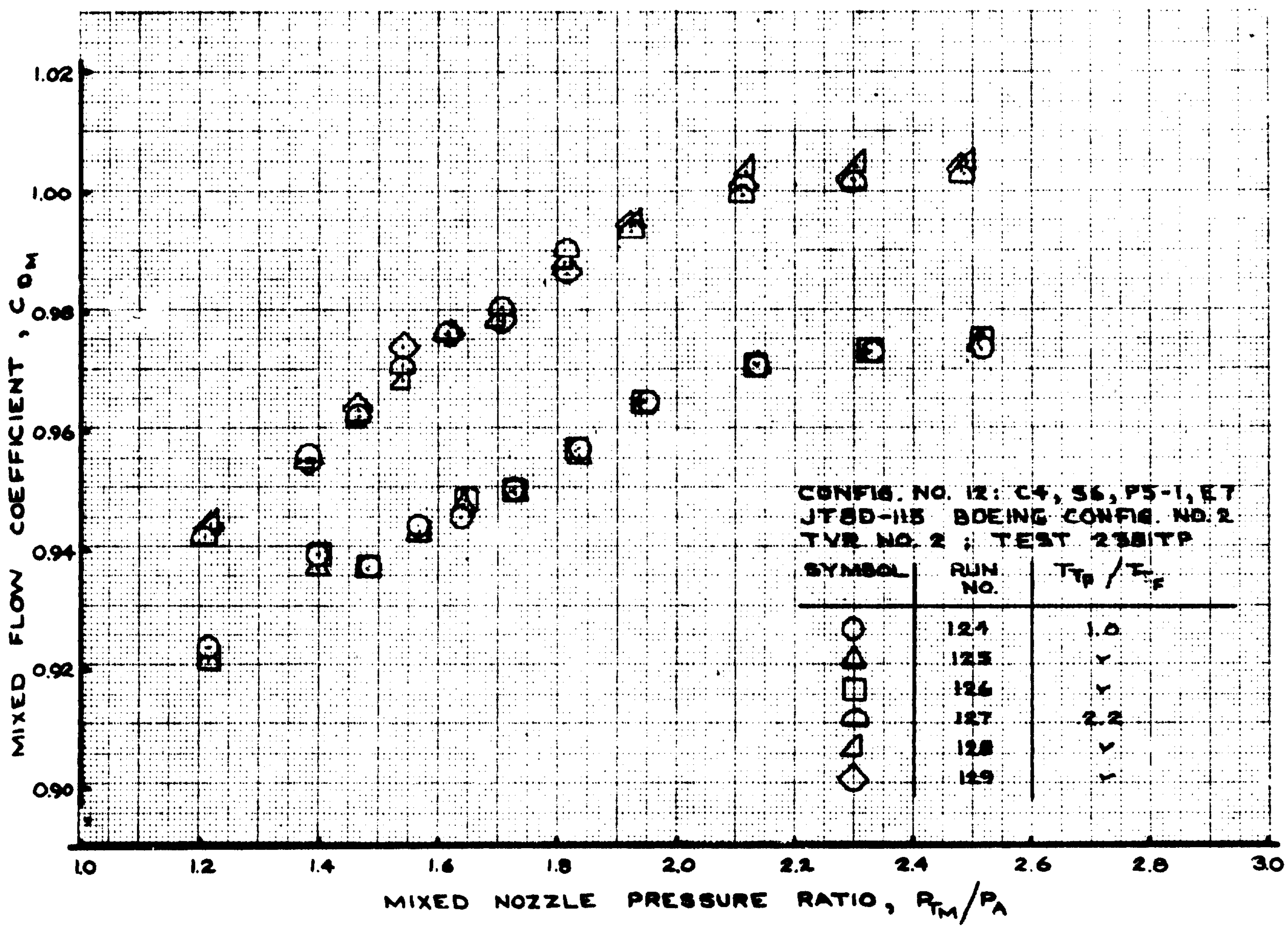

FIGURE 171 - MIXED FLOW COEFFICIENT
TEST CONFIG. NO. 12; RUNS 124-129

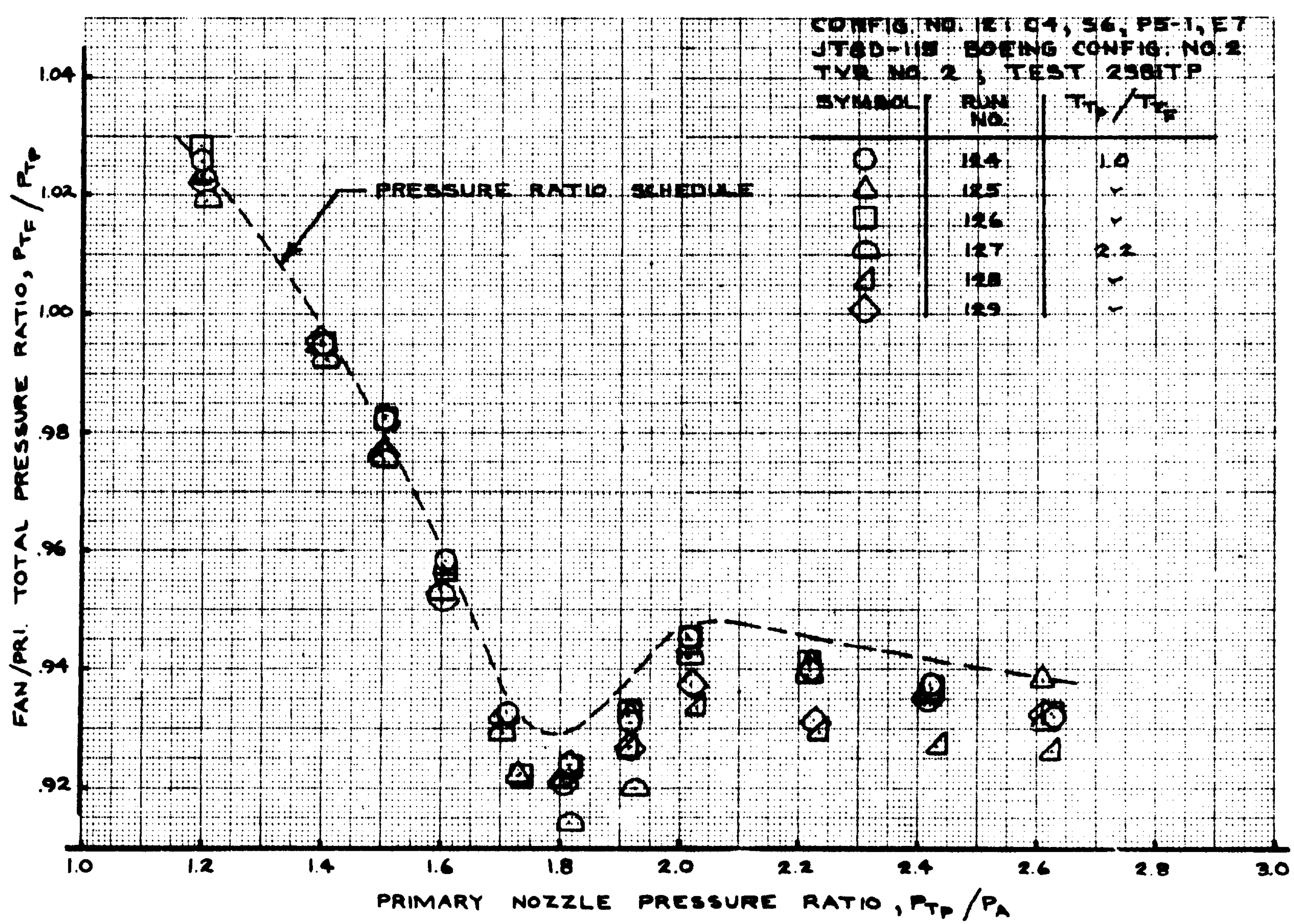

FIGURE 172- FAN/PRIMARY TOTAL PRESSURE RATIO
TEST CONFIG. NO. 12; RUNS 124-129

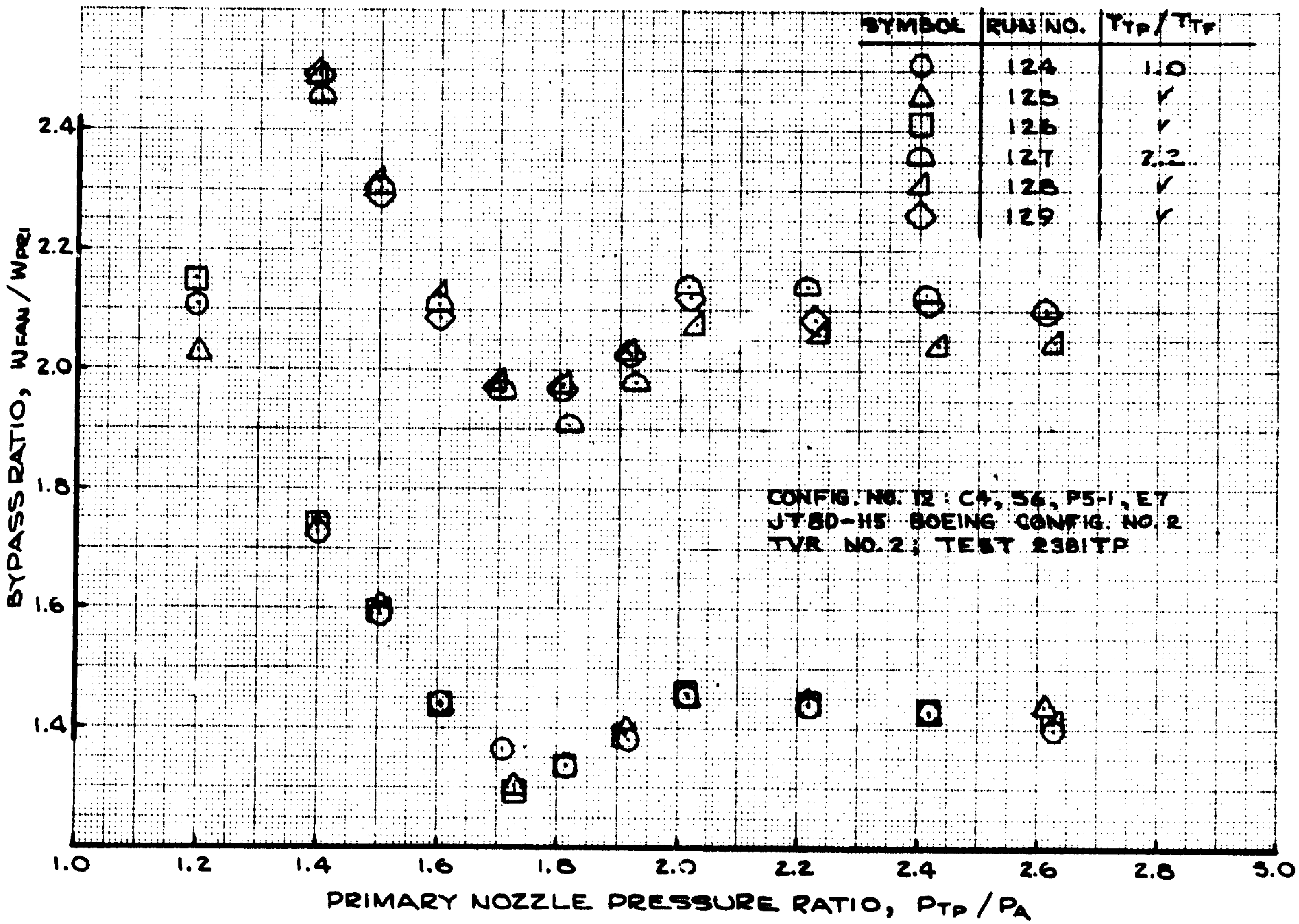

FIGURE 173- BYPASS RATIO
TEST CONFIG. NO. 12; RUNS 124-129

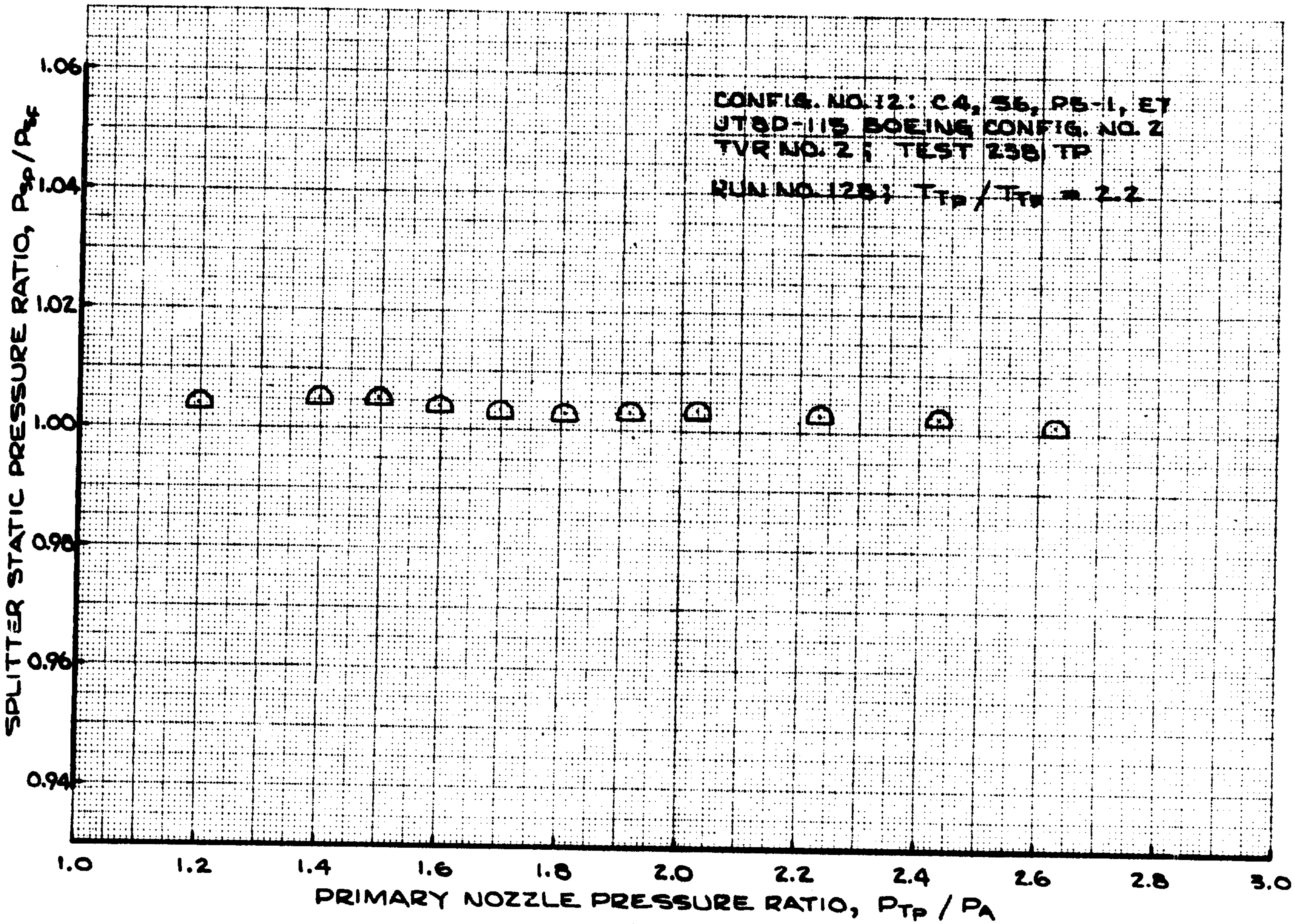

FIGURE 174 - SPLITTER STATIC PRESSURE RATIO
TEST CONFIG. NO. 12; RUN 128

7.2.13 TEST CONFIGURATION (T.C.) NO. 13

Configuration Description: Boeing Config. No. 2 variant using JT8D-109 splitter for A_F/A_P investigations on JT8D-115.

Hardware Designations:

Outer Nozzle Wall	Splitter	Plug	Exit
C4	S5	P5-1	E6

Plotted Data:

Figure 175 - Velocity Coefficient; Runs 66-71.
Figure 176 - Mixed Velocity Coefficient; Runs 66-71.
Figure 177 - Flow Coefficient; Runs 66-71.
Figure 178 - Mixed Flow Coefficient; Runs 66-71.
Figure 179 - Fan/Primary Total Pressure Ratio; Runs 66-71.
Figure 180 - Bypass Ratio; Runs 66-71.
Figure 181 - Splitter Static Pressure Ratio; Run 69.

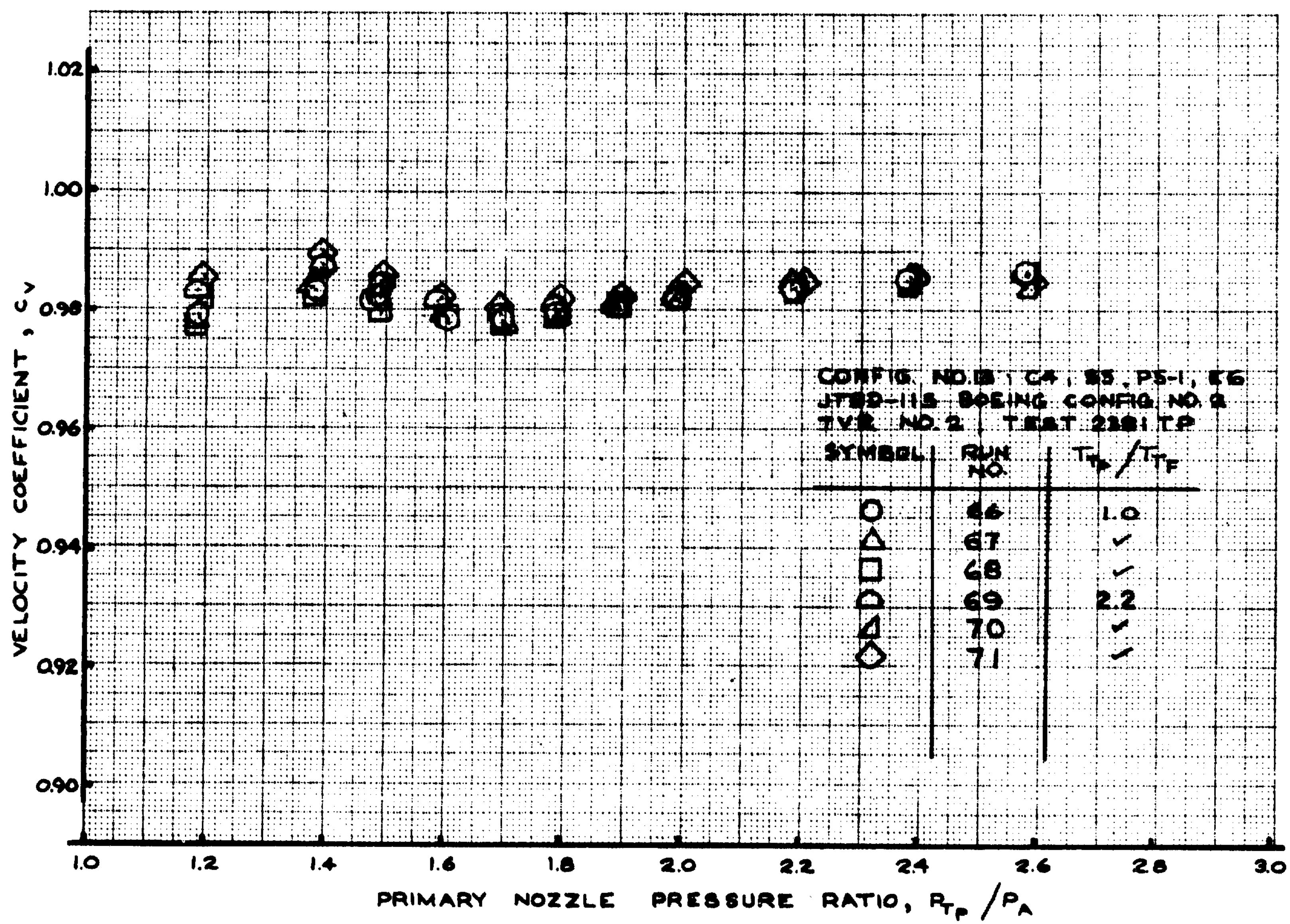

FIGURE 175- VELOCITY COEFFICIENT
TEST CONFIG. NO. 13; RUNS 66-71

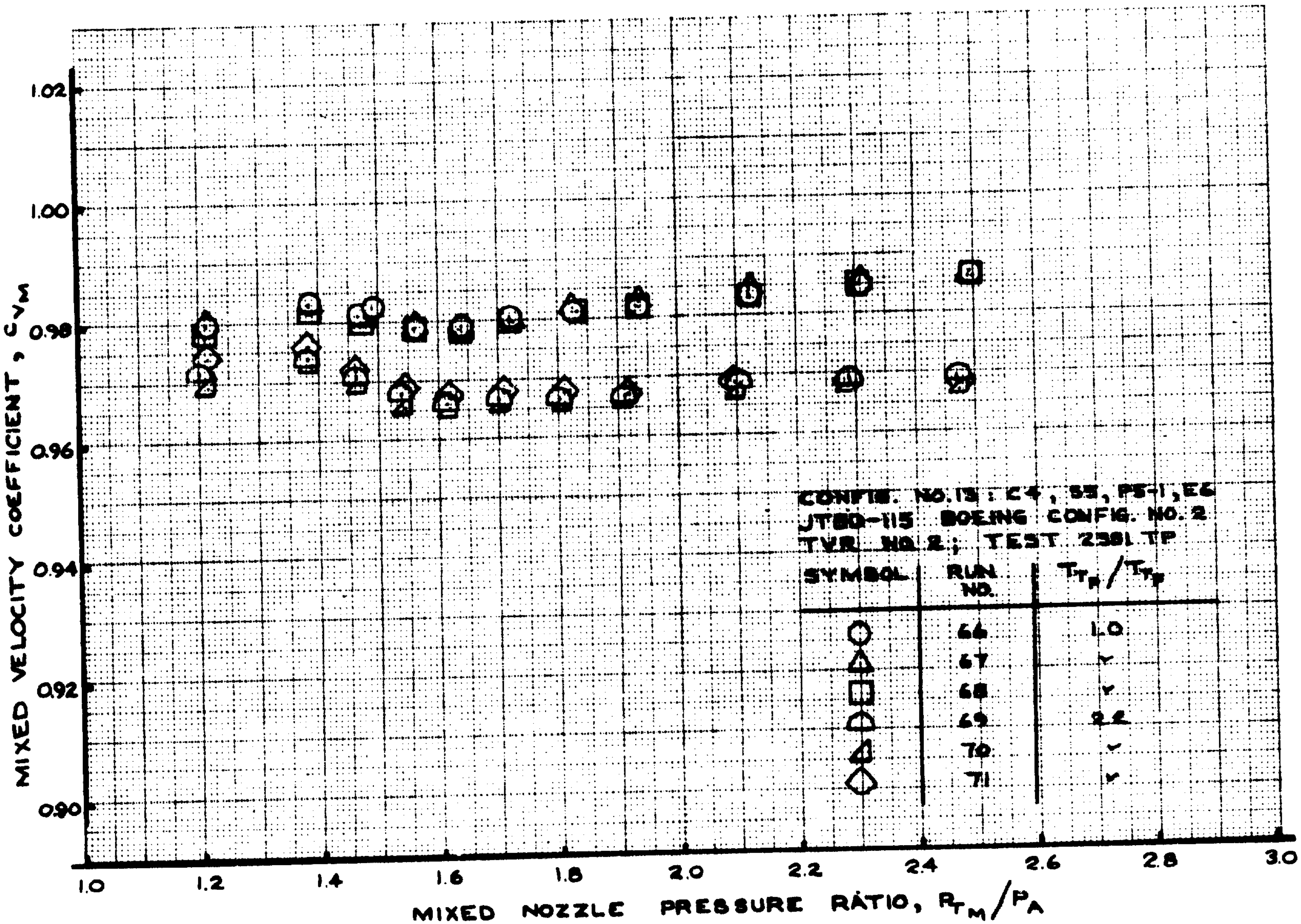

FIGURE 176- MIXED VELOCITY COEFFICIENT
TEST CONFIG. NO. 13; RUNS 66-71

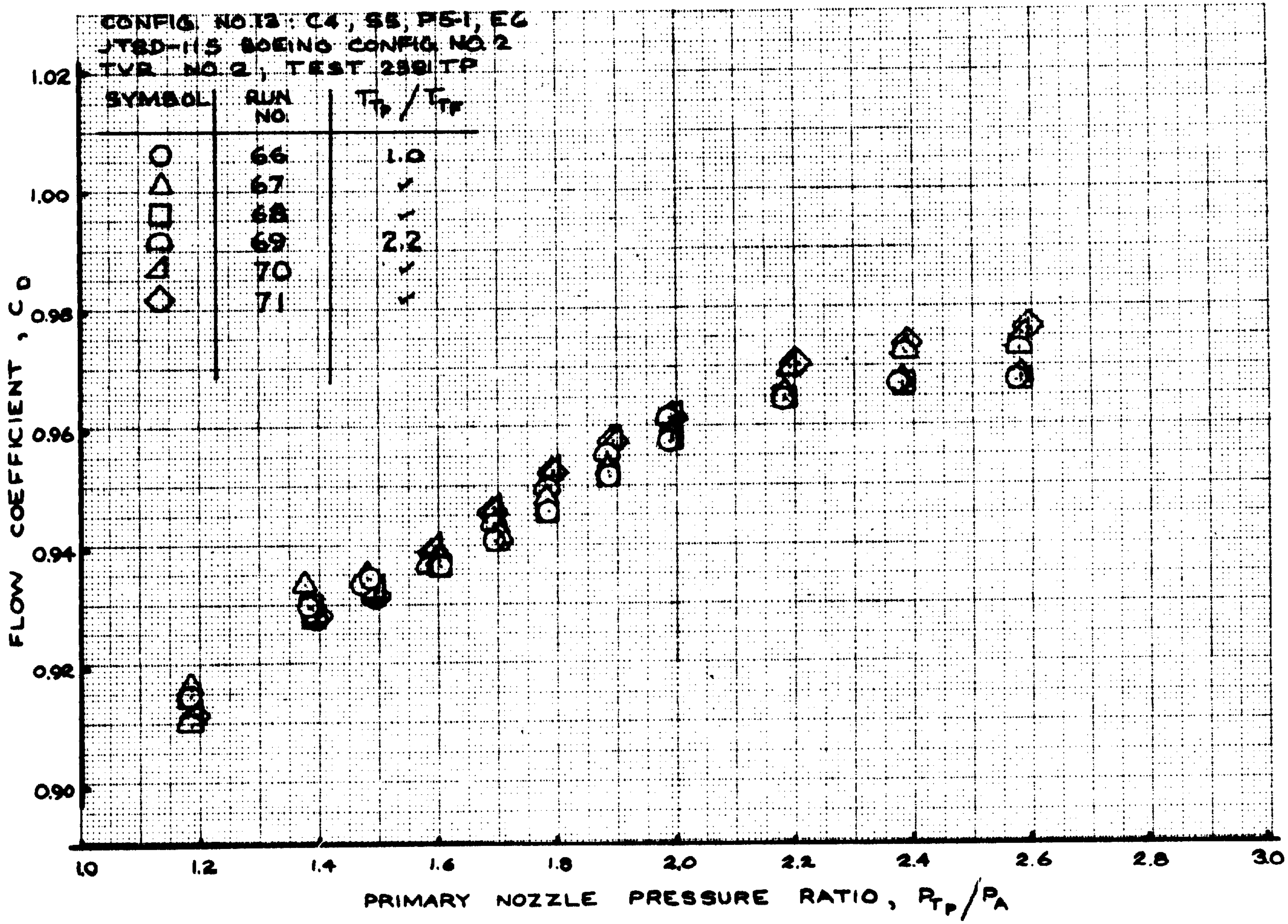

FIGURE 177- FLOW COEFFICIENT
TEST CONFIG. NO. 13; RUNS 66-71

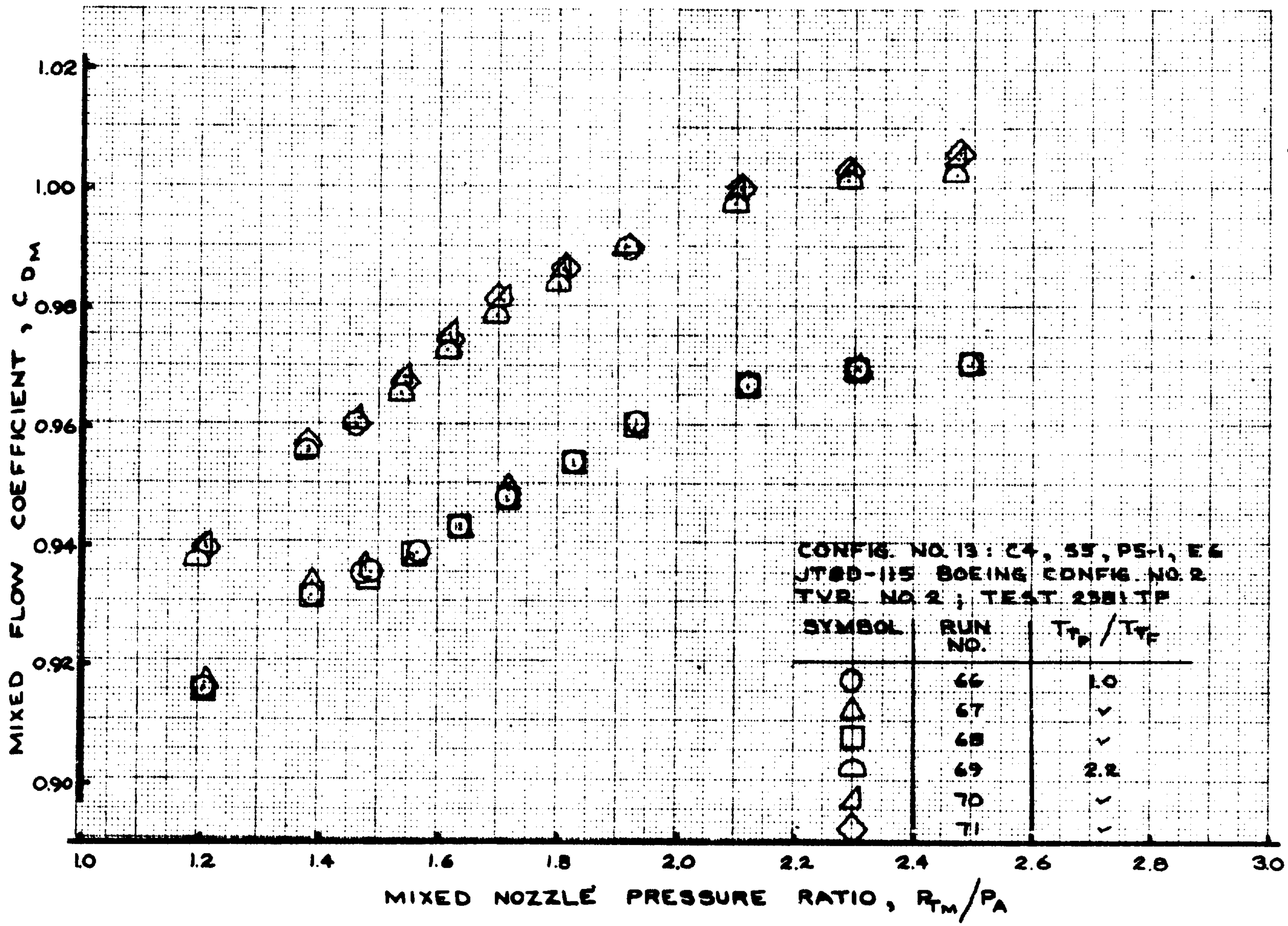

FIGURE 178- MIXED FLOW COEFFICIENT
TEST CONFIG. NO. 13; RUNS 66-71

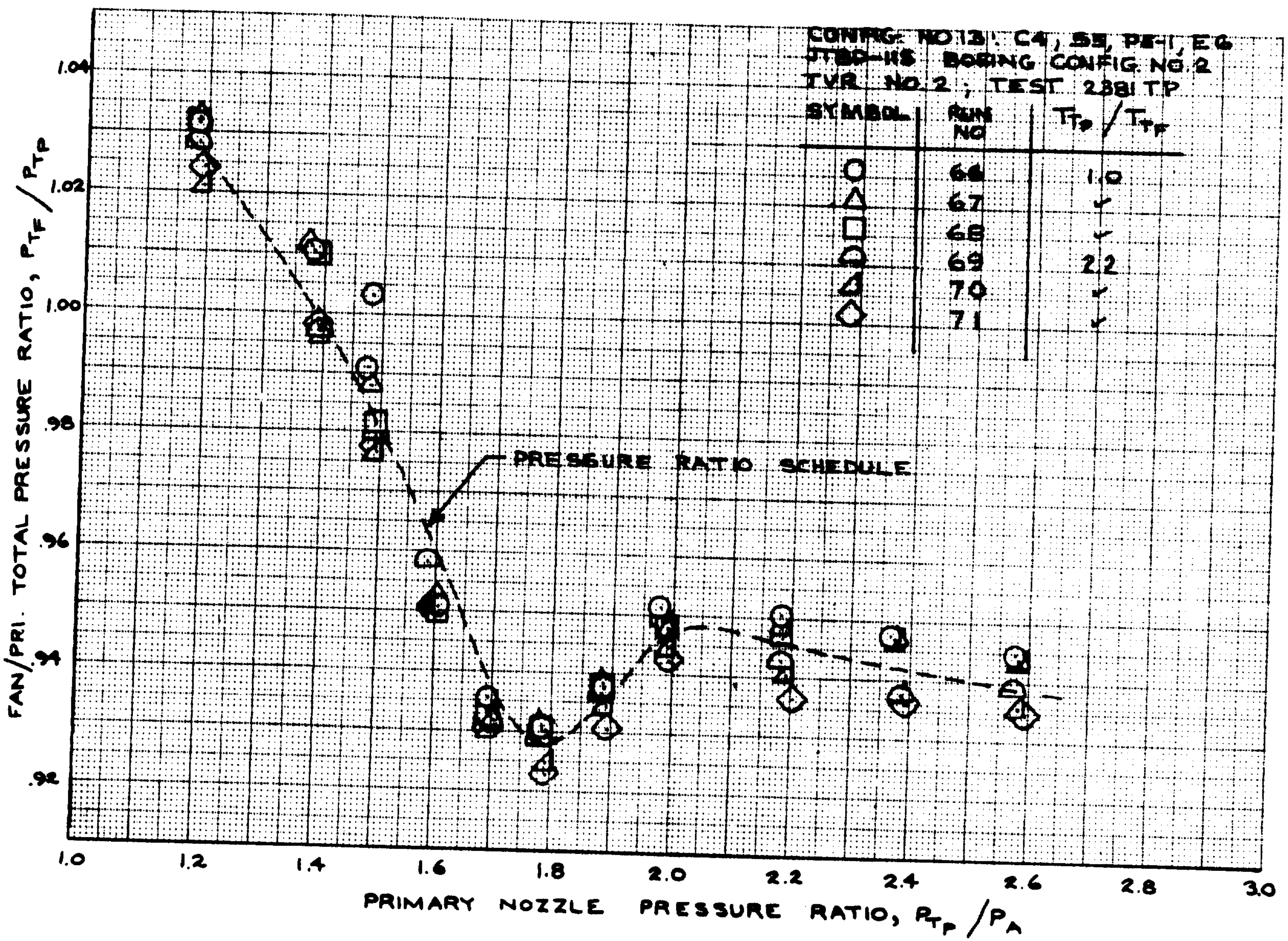

FIGURE 179. FAN/PRIMARY TOTAL PRESSURE RATIO
TEST CONFIG. NO. 13; RUNS 66-71

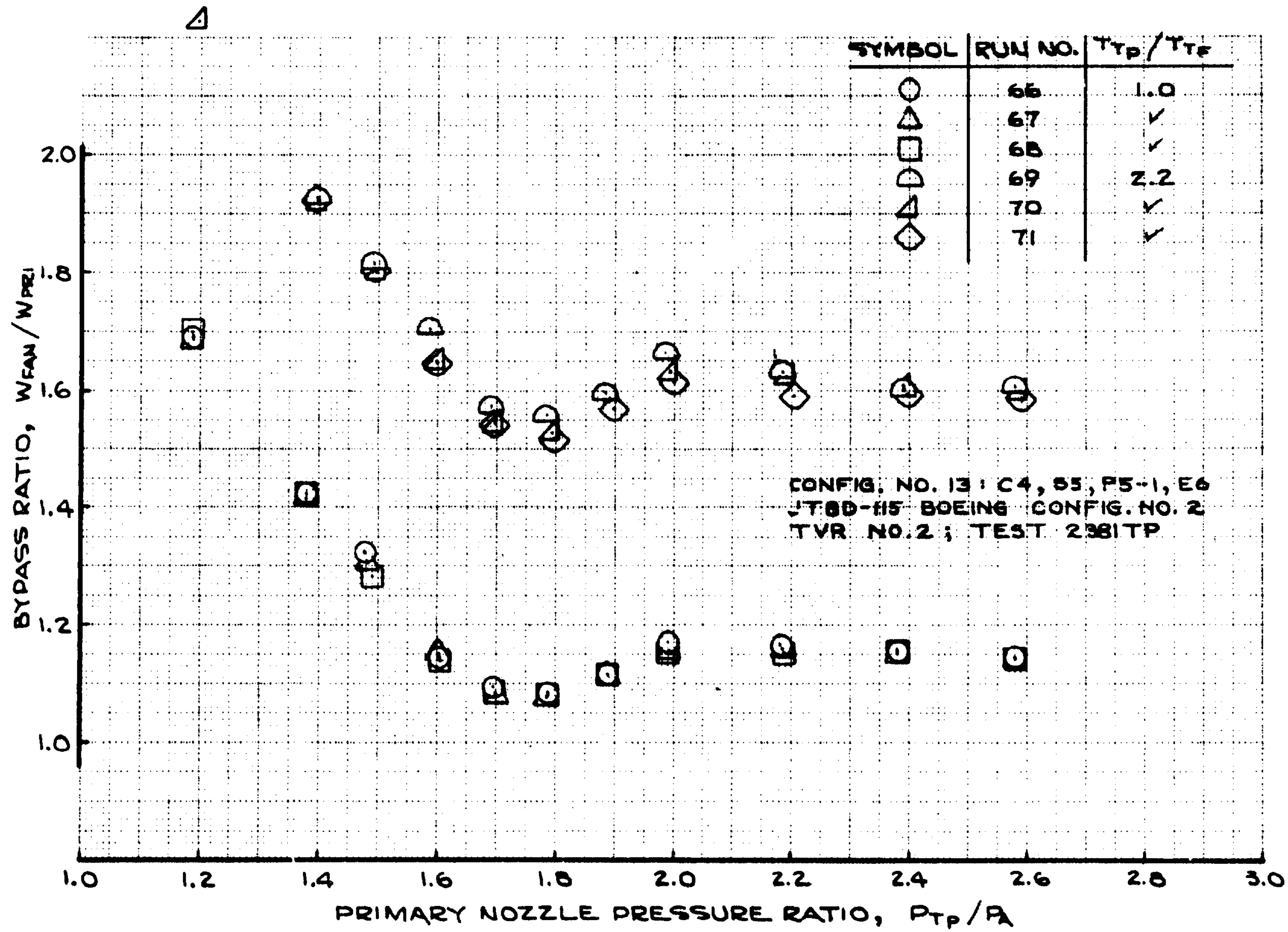

FIGURE 180- BYPASS RATIO
TEST CONFIG. NO. 13; RUNS 66-71

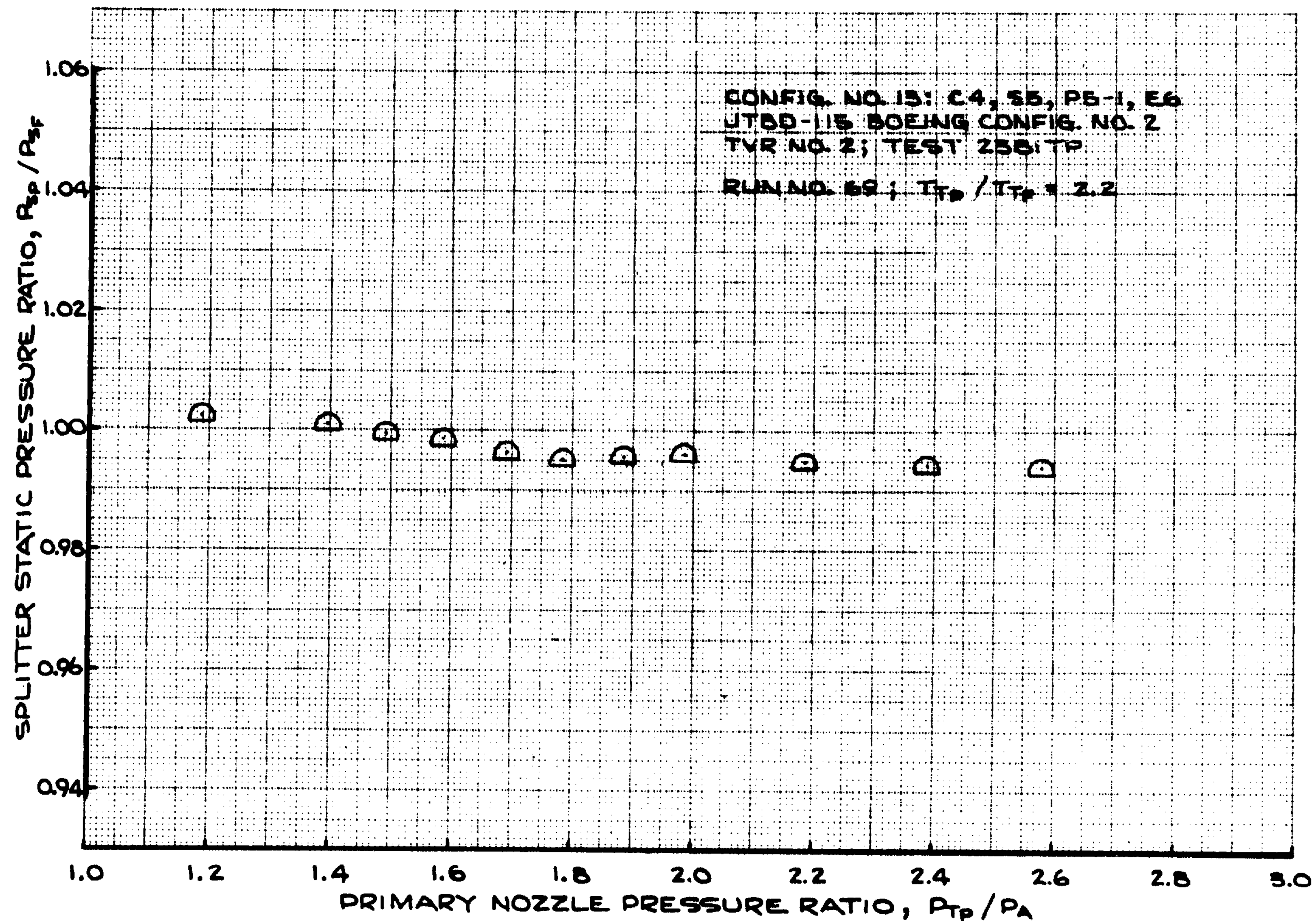

FIGURE 181 - SPLITTER STATIC PRESSURE RATIO
TEST CONFIG. NO. 13; RUN 69

7.2.14 TEST CONFIGURATION (T.C.) NO. 14

Configuration Description: Boeing Config. No. 2 variant using JT8D-117 splitter for A_F/A_P investigation on JT8D-115.

Hardware Designations:

Outer Nozzle Wall	Splitter	Plug	Exit
C4	S7	P5-1	E6

Plotted Data:

- Figure 182 - Velocity Coefficient; Runs 130-135.
- Figure 183 - Mixed Velocity Coefficient; Runs 130-135.
- Figure 184 - Flow Coefficient; Runs 130-135.
- Figure 185 - Mixed Flow Coefficient; Runs 130-135.
- Figure 186 - Fan/Primary Total Pressure Ratio; Runs 130-135.
- Figure 187 - Bypass Ratio; Runs 130-135.
- Figure 188 - Splitter Static Pressure Ratio; Run 133.

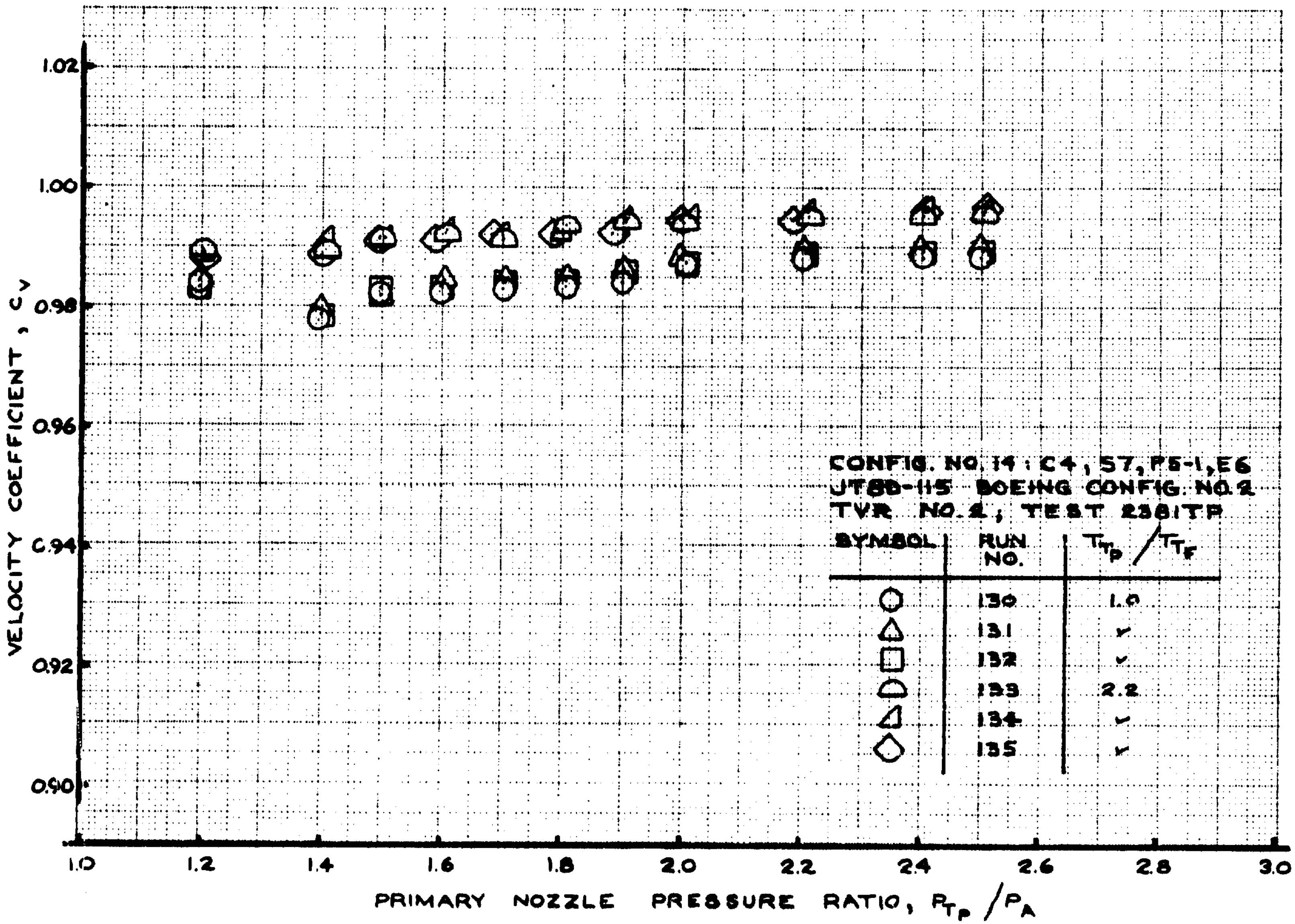

FIGURE 182- VELOCITY COEFFICIENT
TEST CONFIG. NO. 14; RUNS 130-135

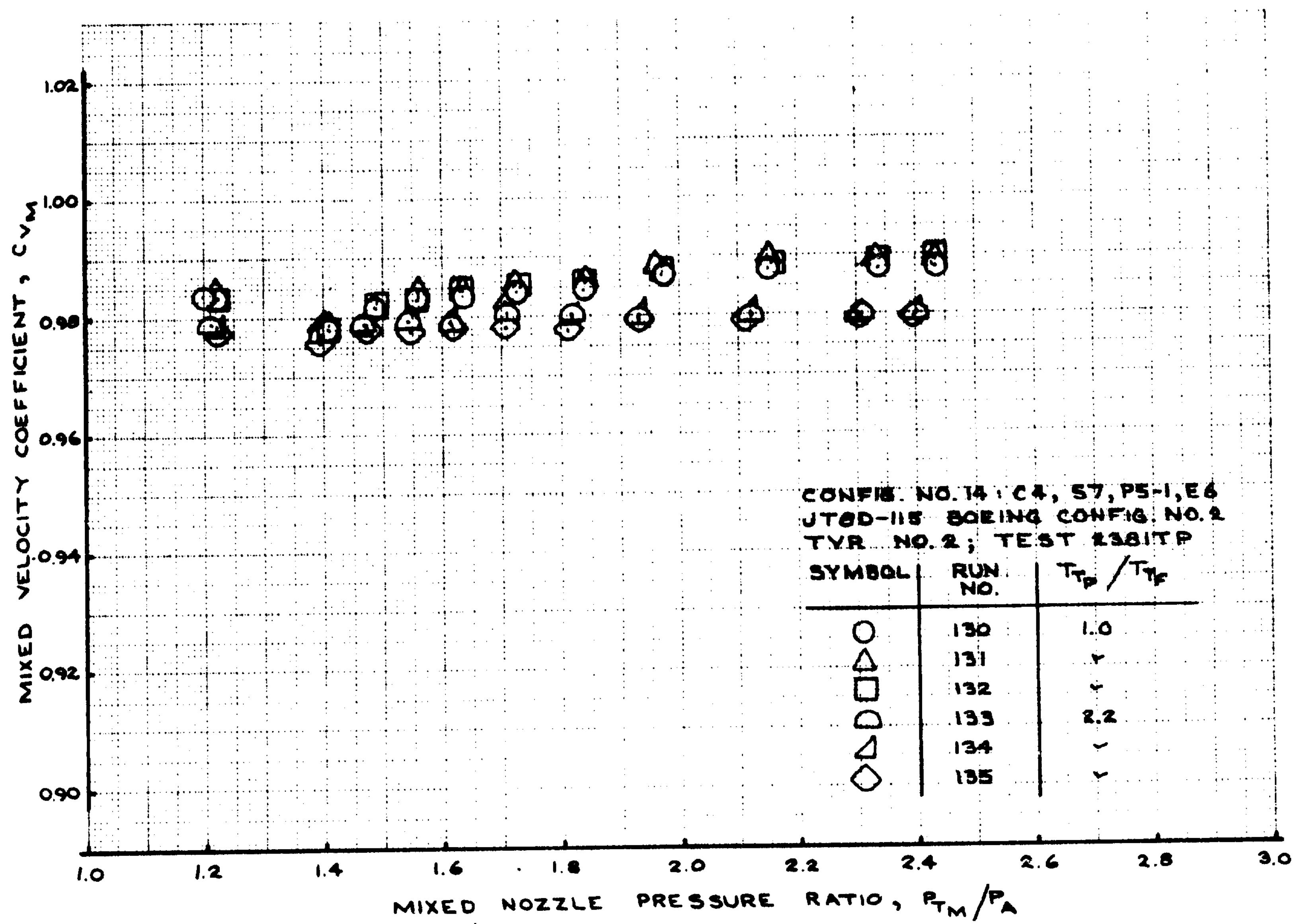

FIGURE 183 - MIXED VELOCITY COEFFICIENT
TEST CONFIG. NO. 14; RUNS 130-135

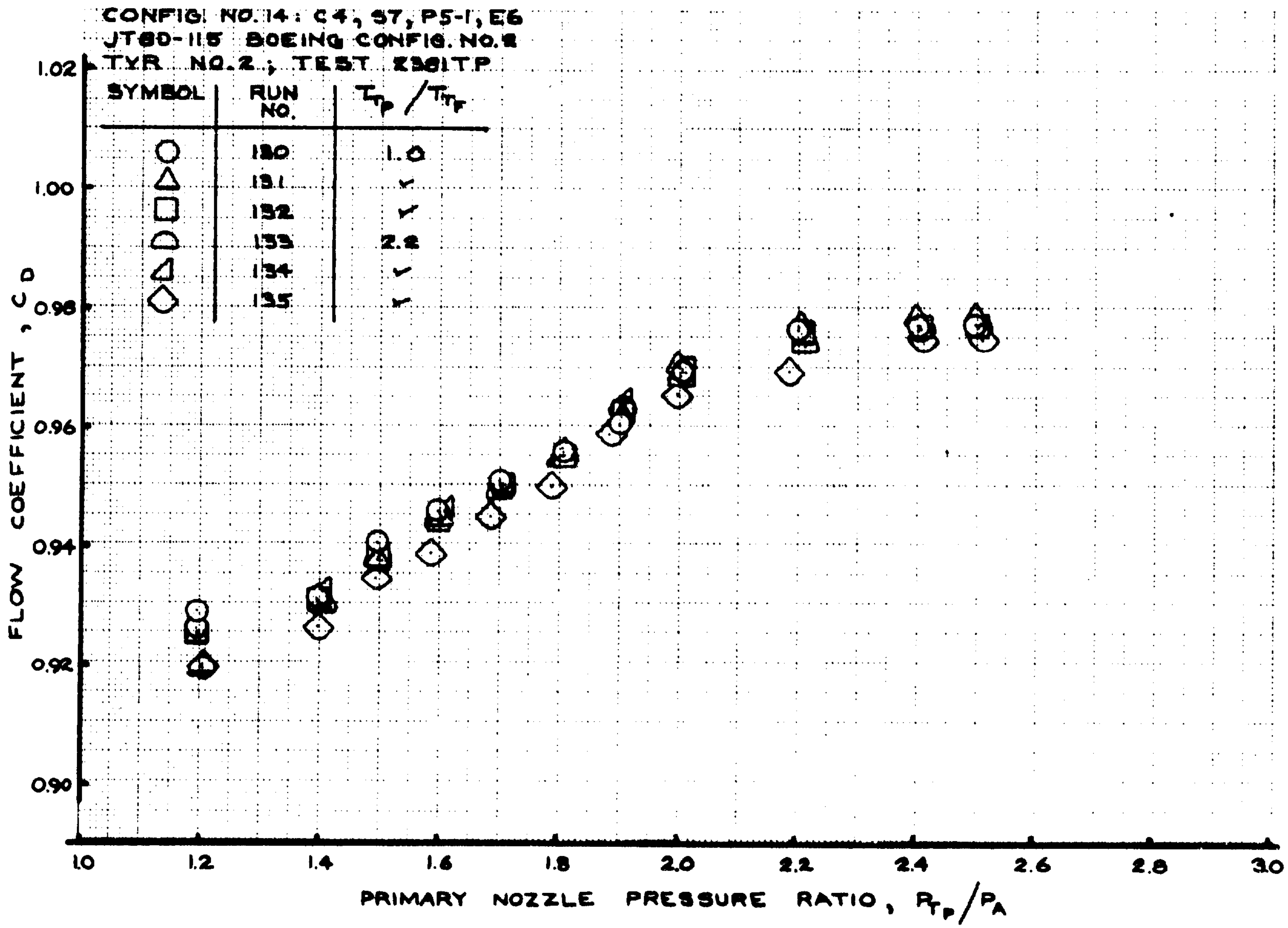

FIGURE 184- FLOW COEFFICIENT
TEST CONFIG. NO. 14; RUNS 130-135

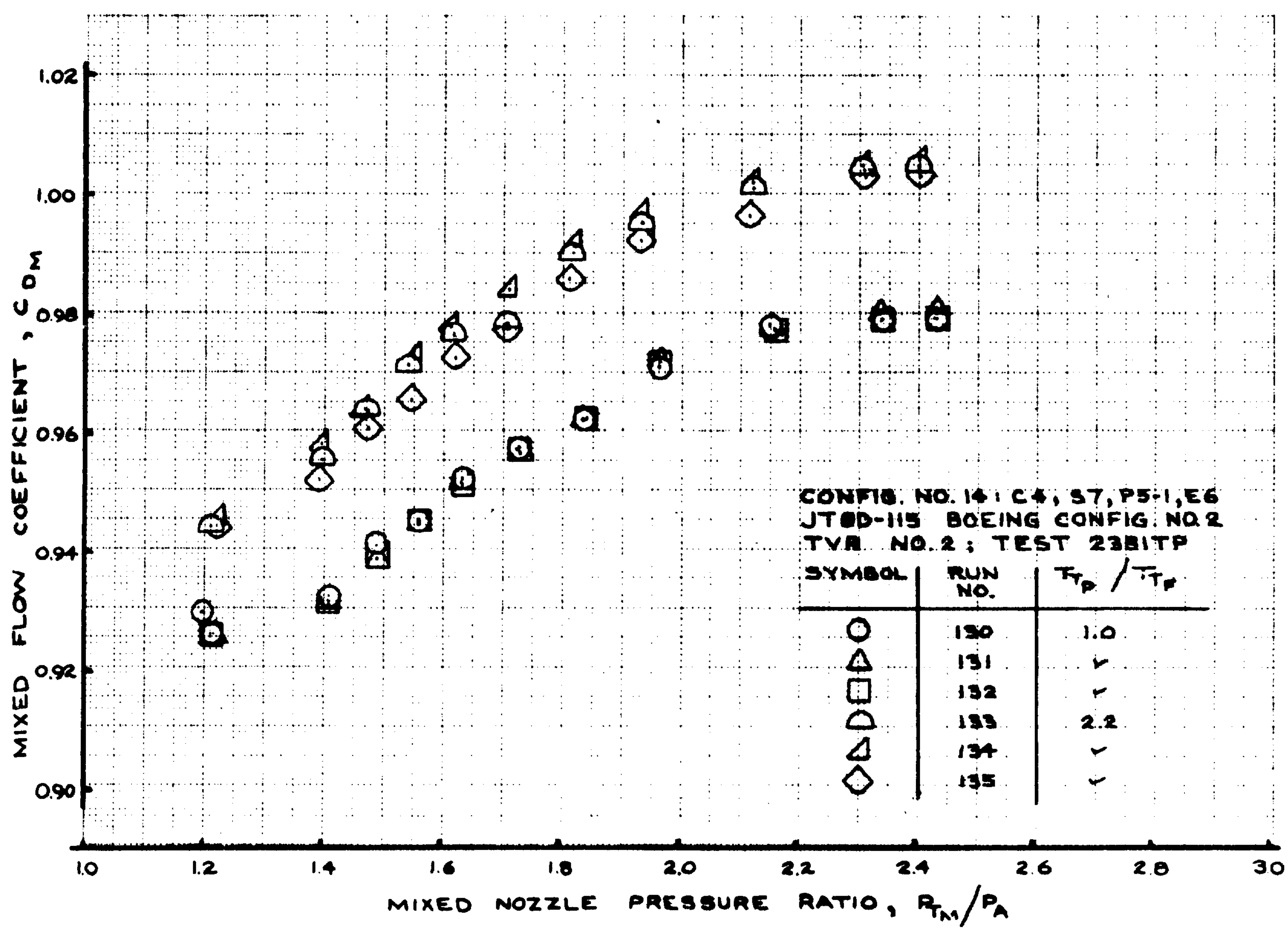

FIGURE 185- MIXED FLOW COEFFICIENT
TEST CONFIG. NO. 14; RUNS 130-135

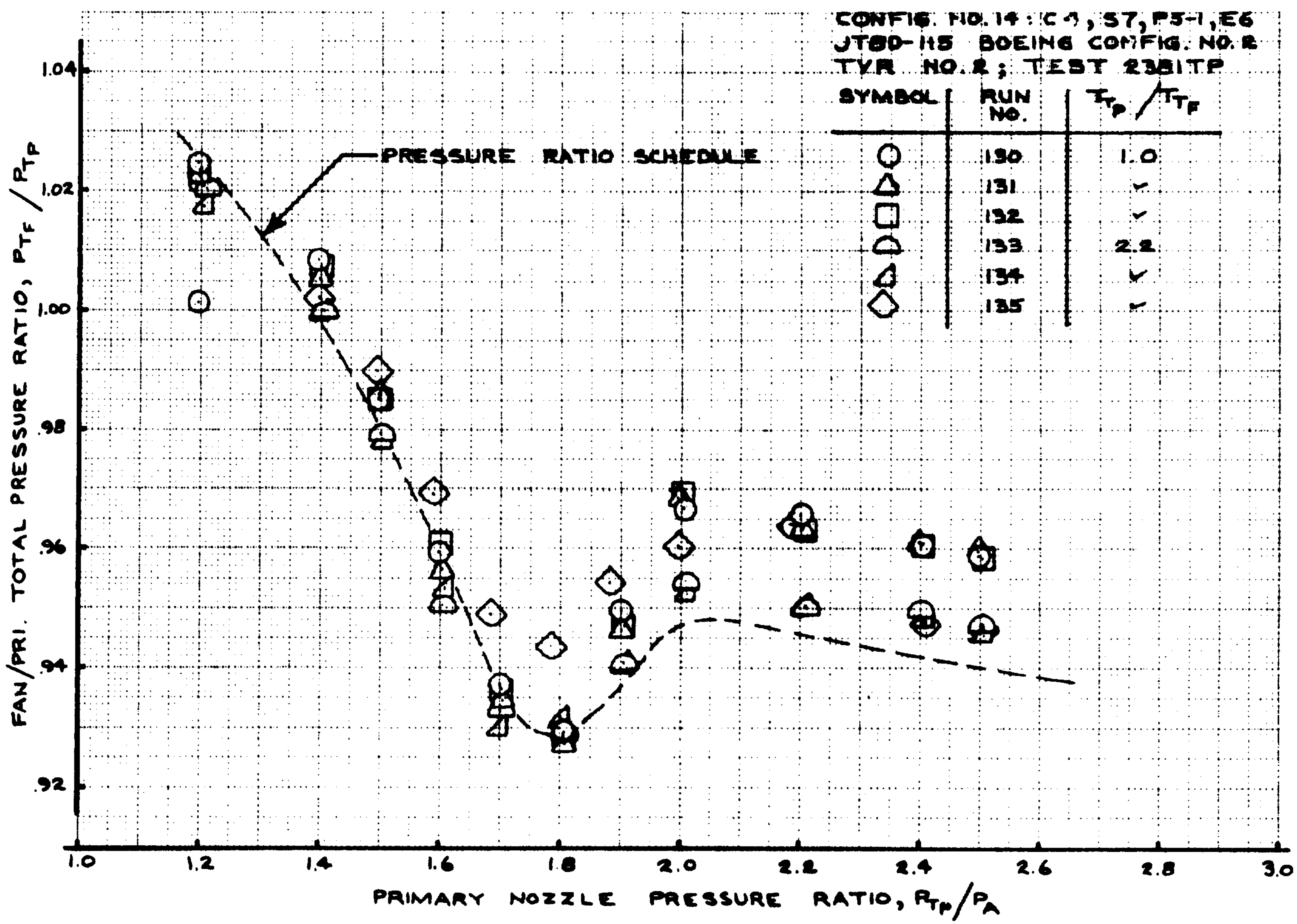

FIGURE 186- FAN/PRIMARY TOTAL PRESSURE RATIO
TEST CONFIG. NO. 14; RUNS 130-135

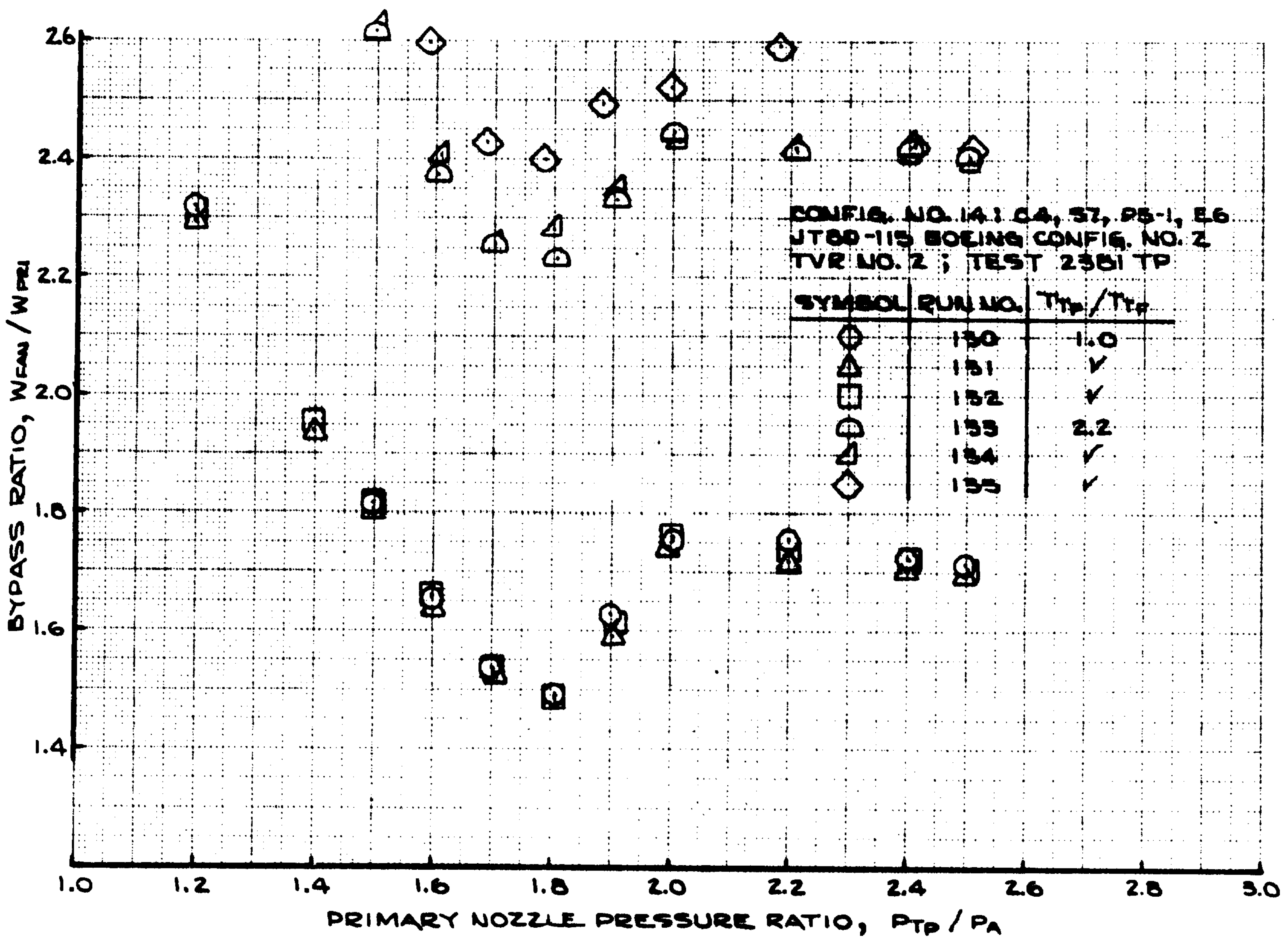

FIGURE 187- BYPASS RATIO
TEST CONFIG. NO. 14; RUNS 130-135

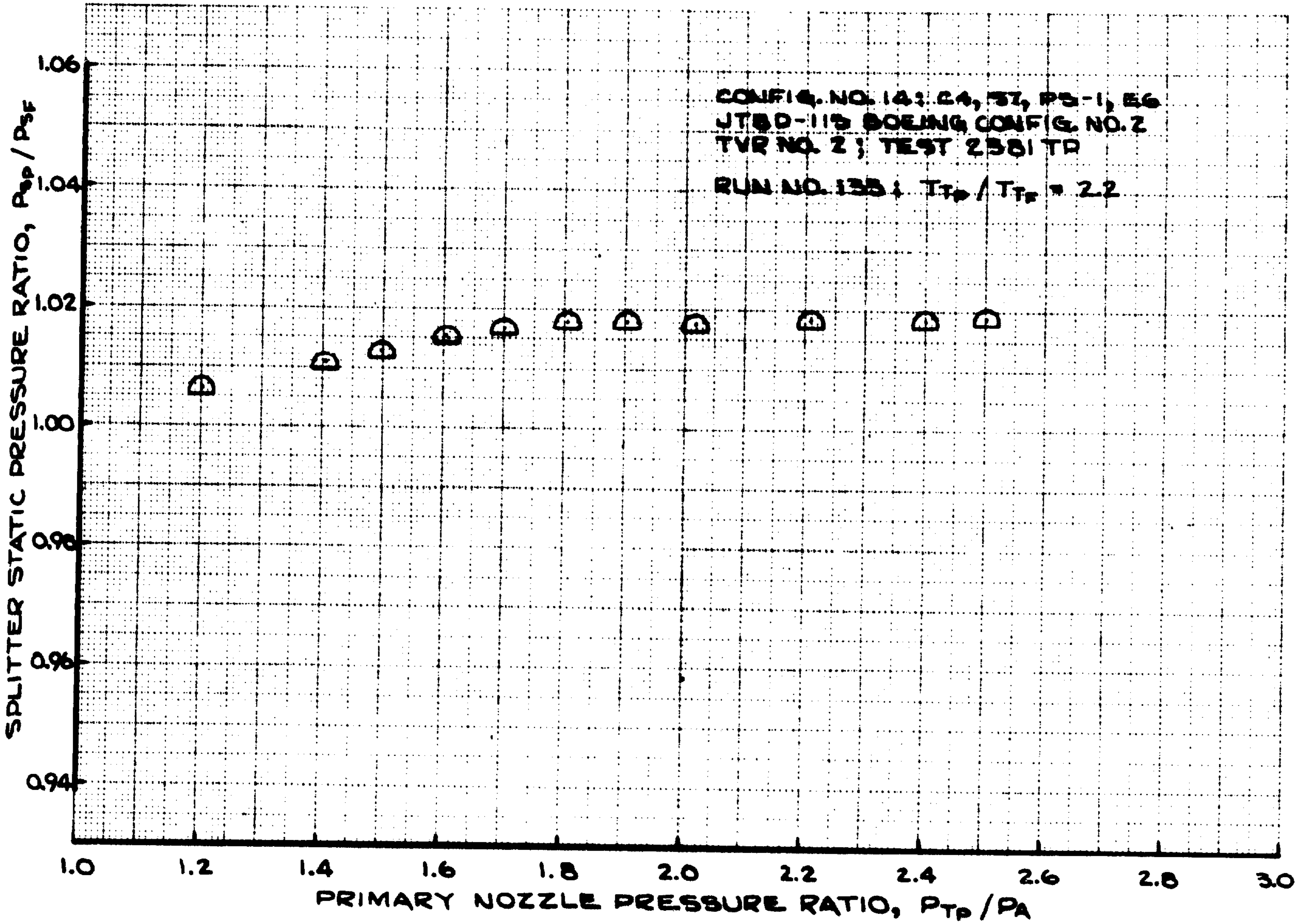

FIGURE 188 - SPLITTER STATIC PRESSURE RATIO
TEST CONFIG. NO. 14; RUN 133

7.2.15 TEST CONFIGURATION (T.C.) NO. 15

Configuration Description: Boeing Config. No. 2 variant using the JT8D-109 splitter and redesigned plug for JT8D-117.

Hardware Designations:

Outer Nozzle Wall	Splitter	Plug	Exit
C4	S5	P5-3	E7

Plotted Data:

- **Figure 189 - Velocity Coefficient; Runs 85-90.**
- **Figure 190 - Mixed Velocity Coefficient; Runs 85-90.**
- **Figure 191 - Flow Coefficient; Runs 85-90.**
- **Figure 192 - Mixed Flow Coefficient; Runs 85-90.**
- **Figure 193 - Fan/Primary Total Pressure Ratio; Runs 85-90.**
- **Figure 194 - Bypass Ratio; Runs 85-90.**
- **Figure 195 - Splitter Static Pressure Ratio; Run 88.**

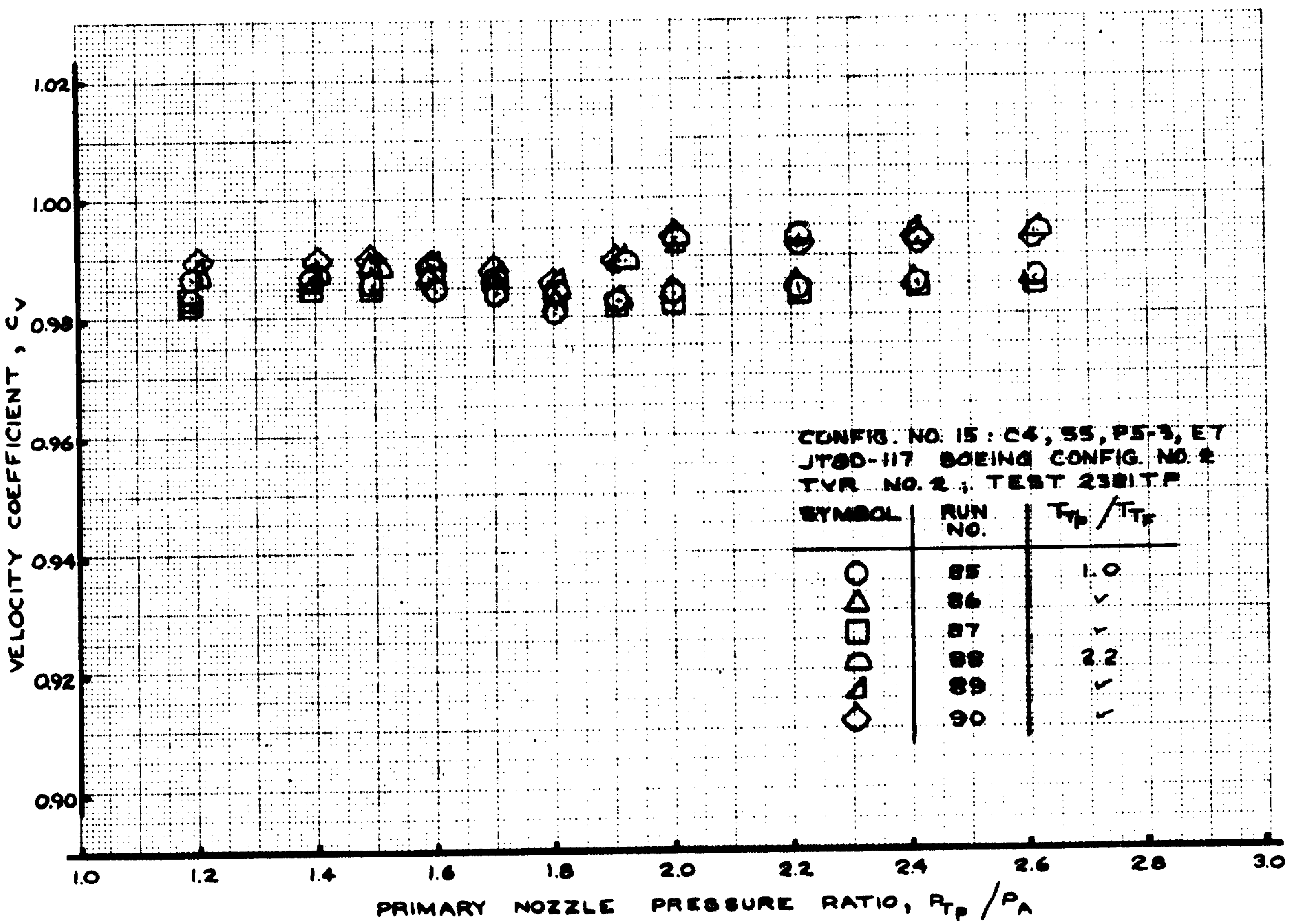

FIGURE 189- VELOCITY COEFFICIENT
TEST CONFIG. NO. 15; RUNS 85-90

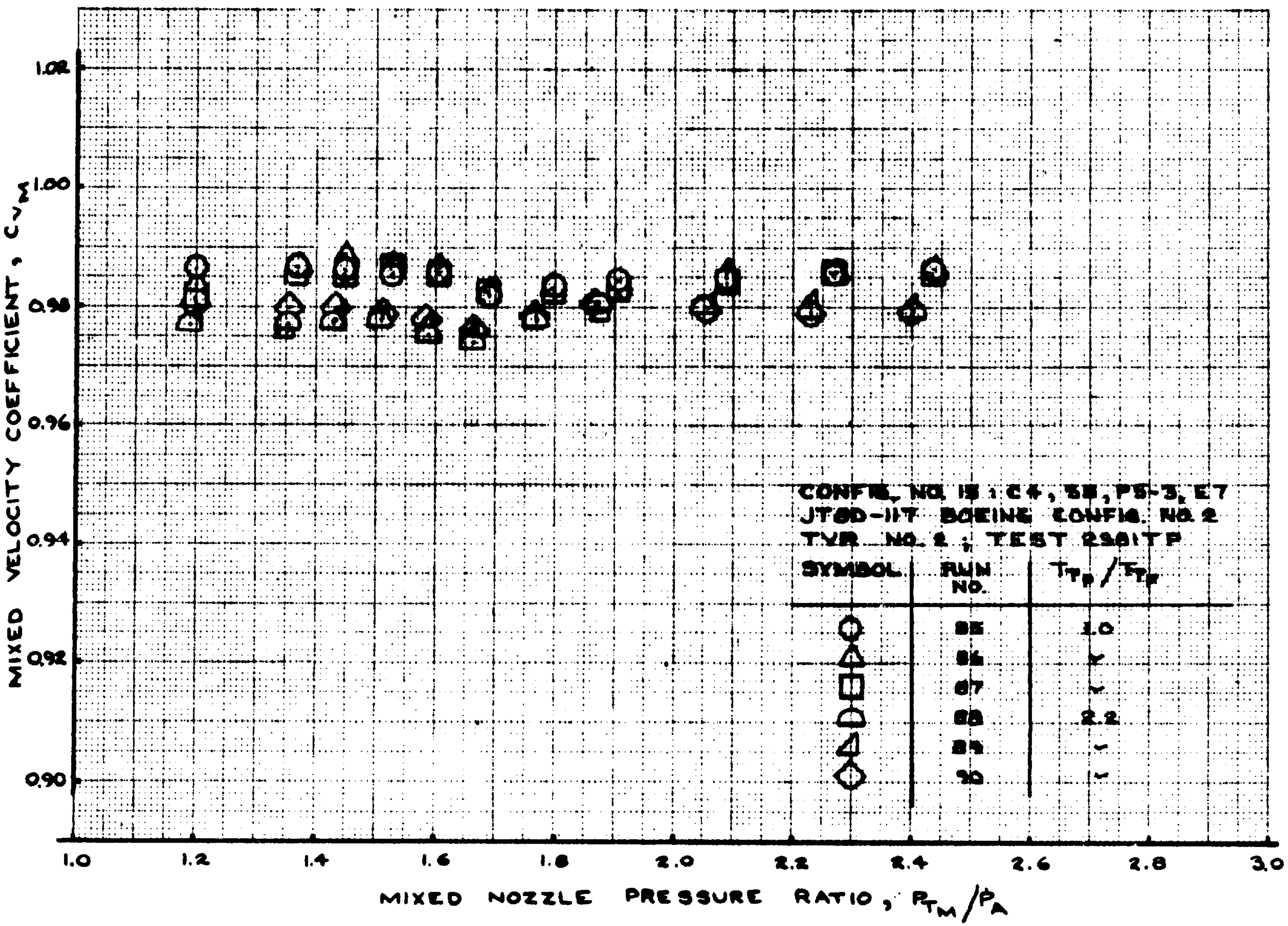

FIGURE 190- MIXED VELOCITY COEFFICIENT
TEST CONFIG. NO. 15; RUNS 85-90

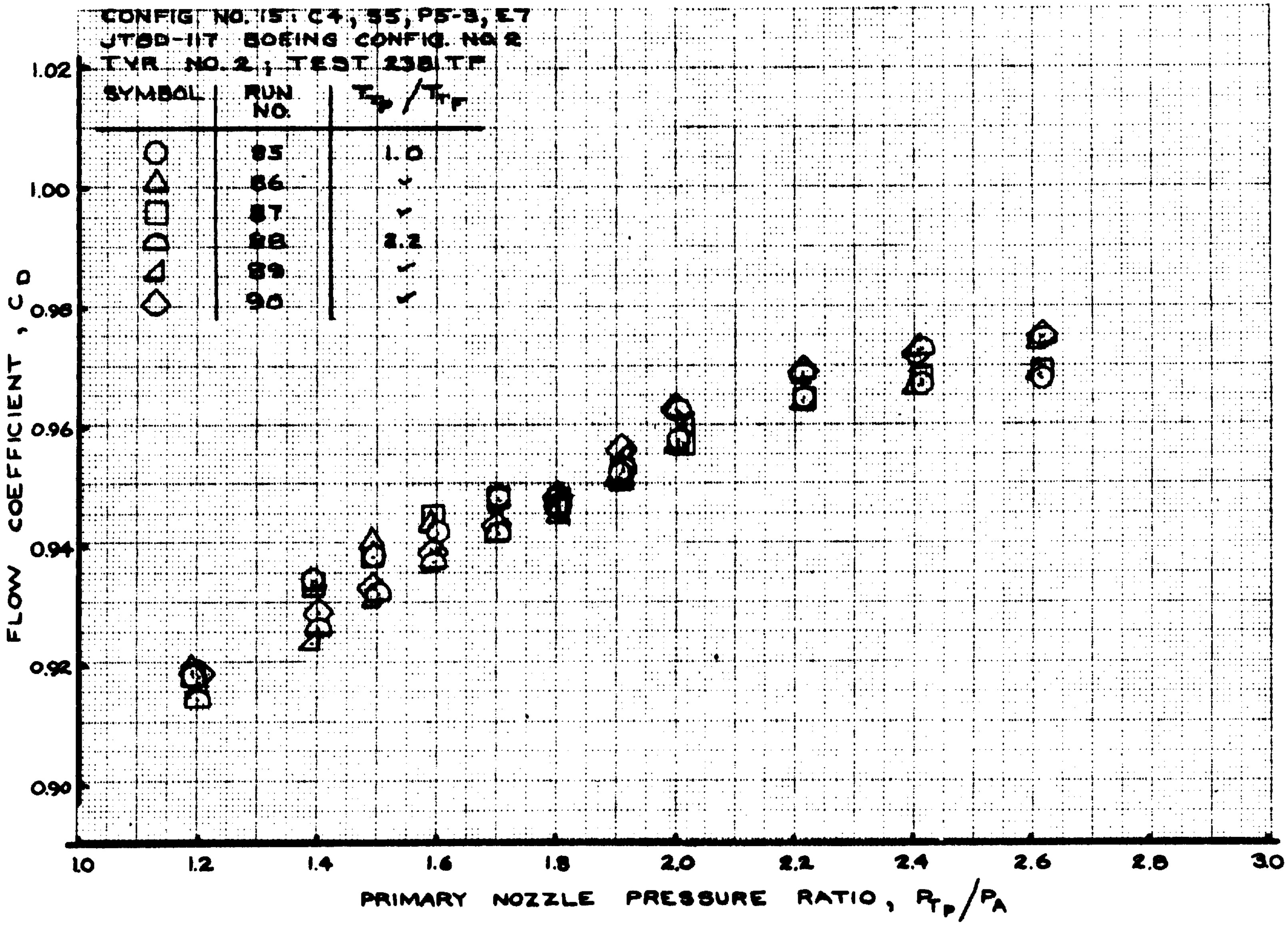

FIGURE 191- FLOW COEFFICIENT
TEST CONFIG. NO. 15; RUNS 85-90

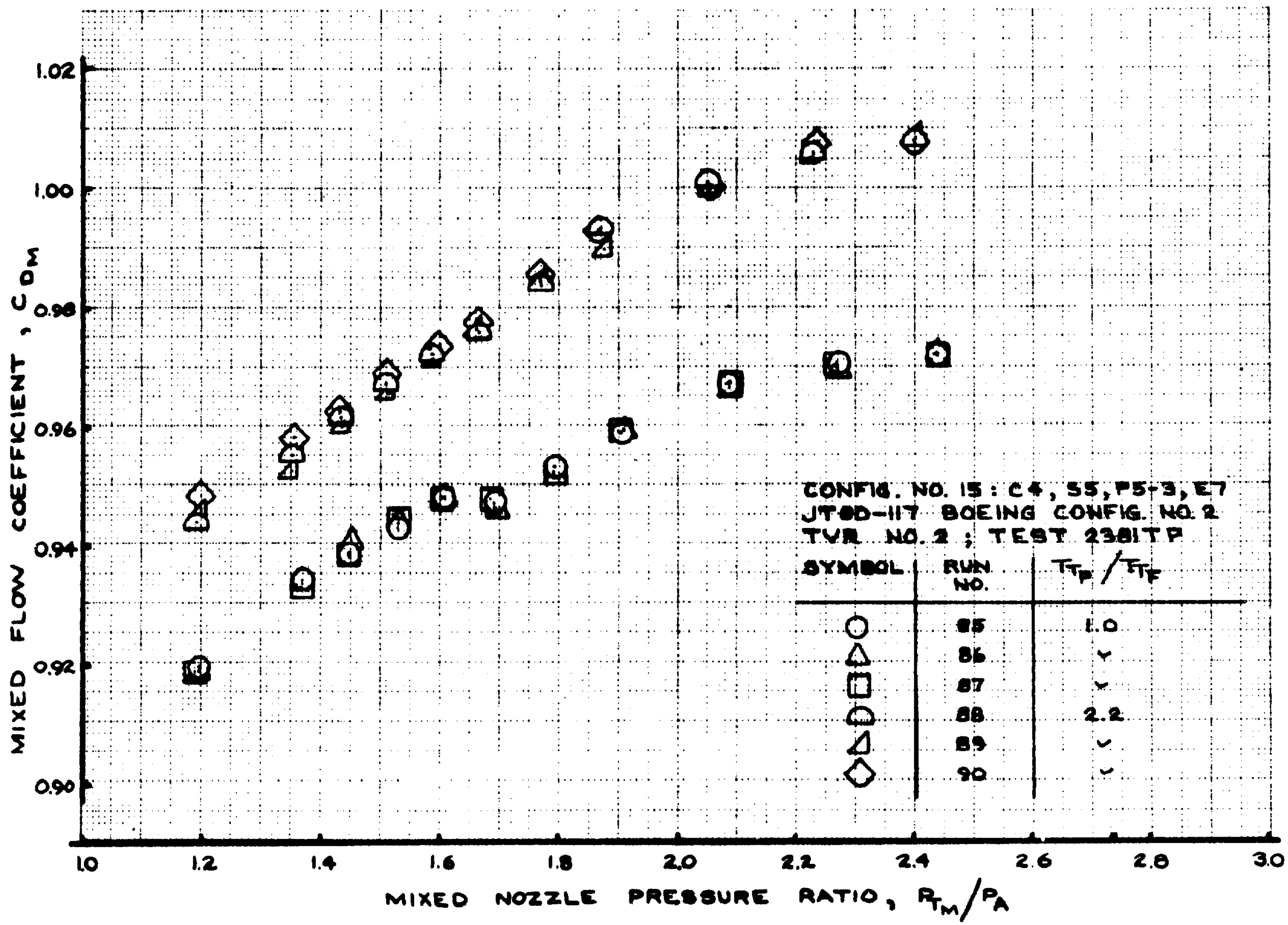

FIGURE 192- MIXED FLOW COEFFICIENT
TEST CONFIG. NO. 15; RUNS 85-90

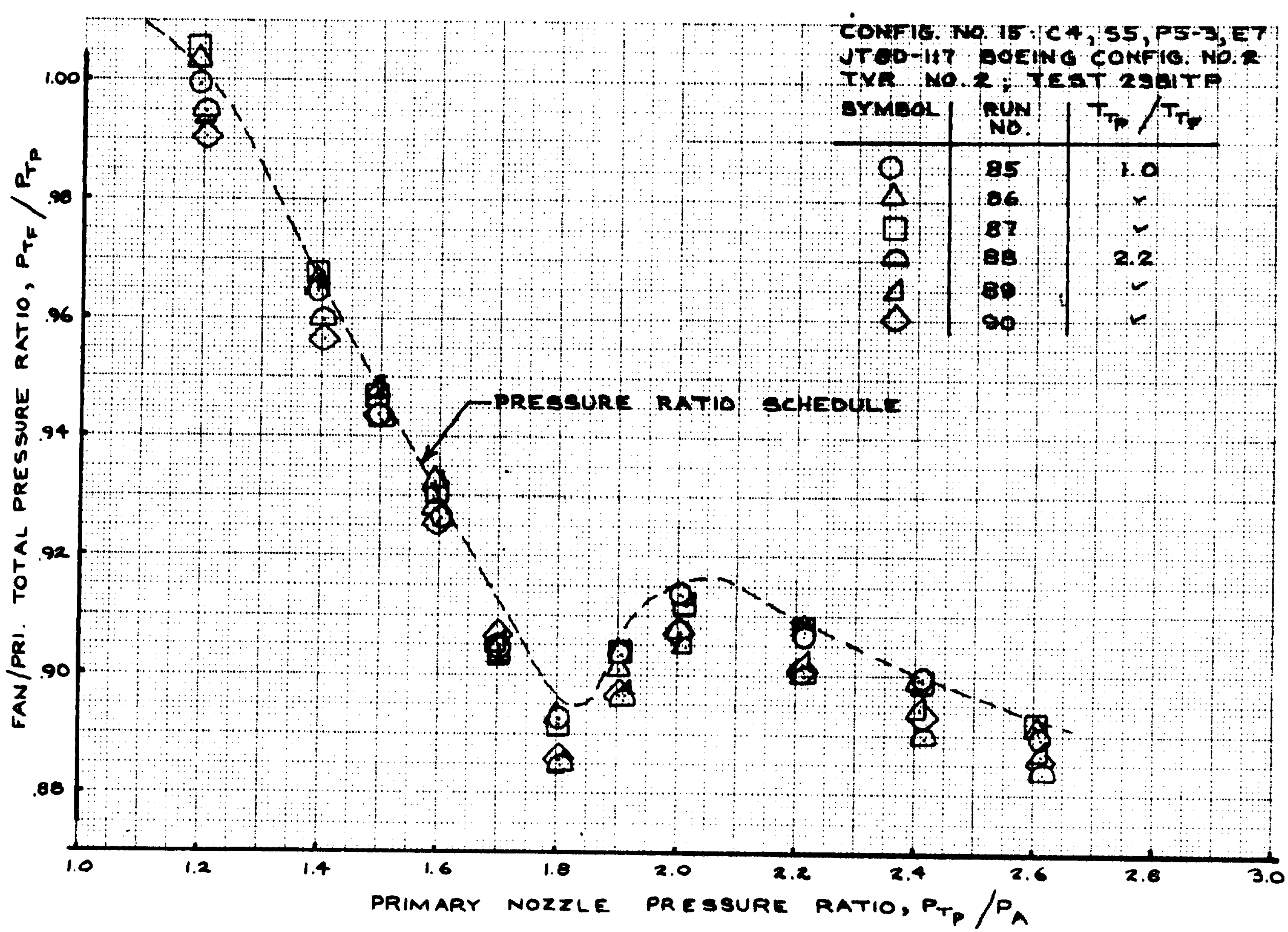

FIGURE 193- FAN/PRIMARY TOTAL PRESSURE RATIO
TEST CONFIG. NO. 15; RUNS 85-90

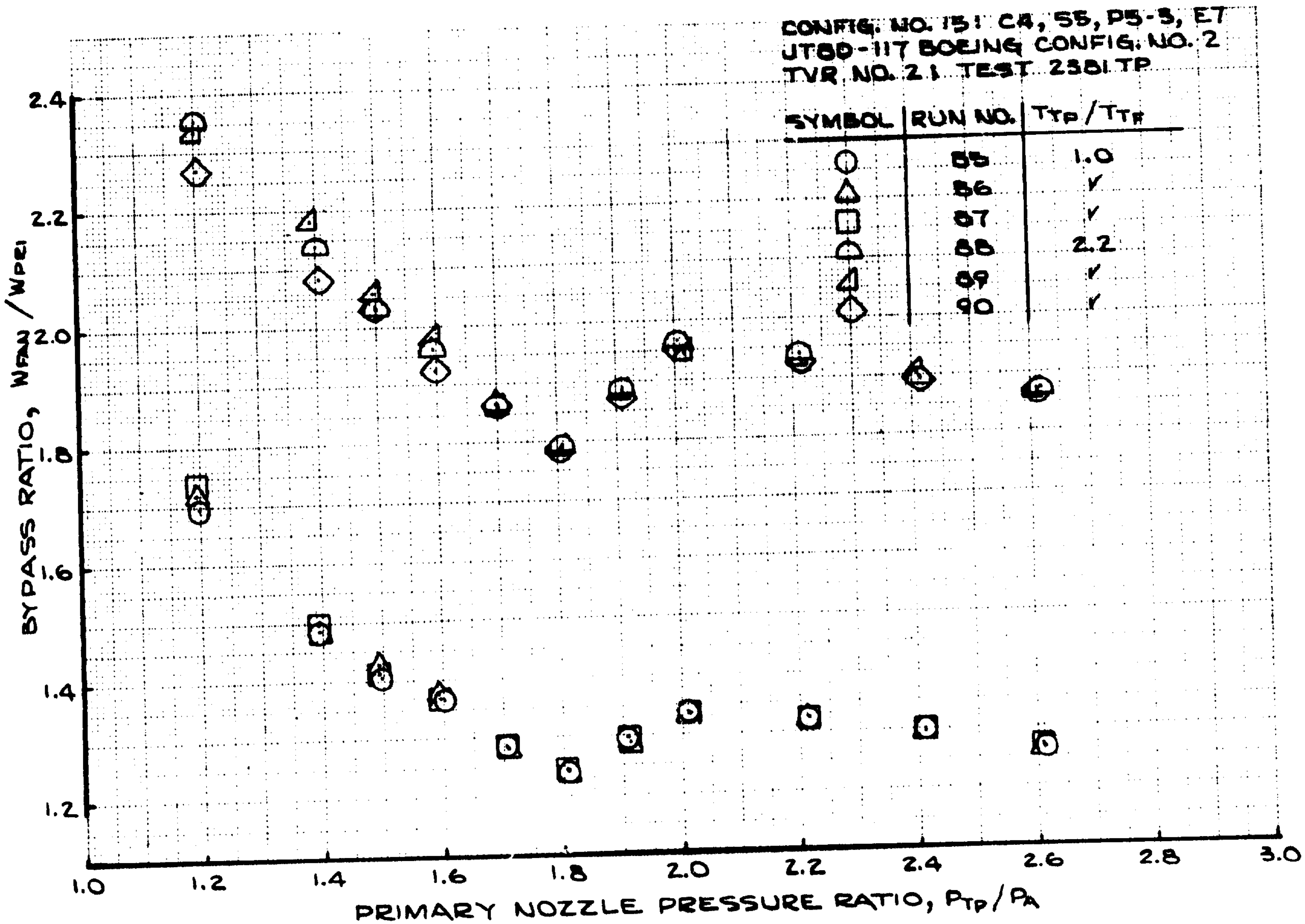

FIGURE 194- BYPASS RATIO
TEST CONFIG. NO. 15; RUNS 85-90

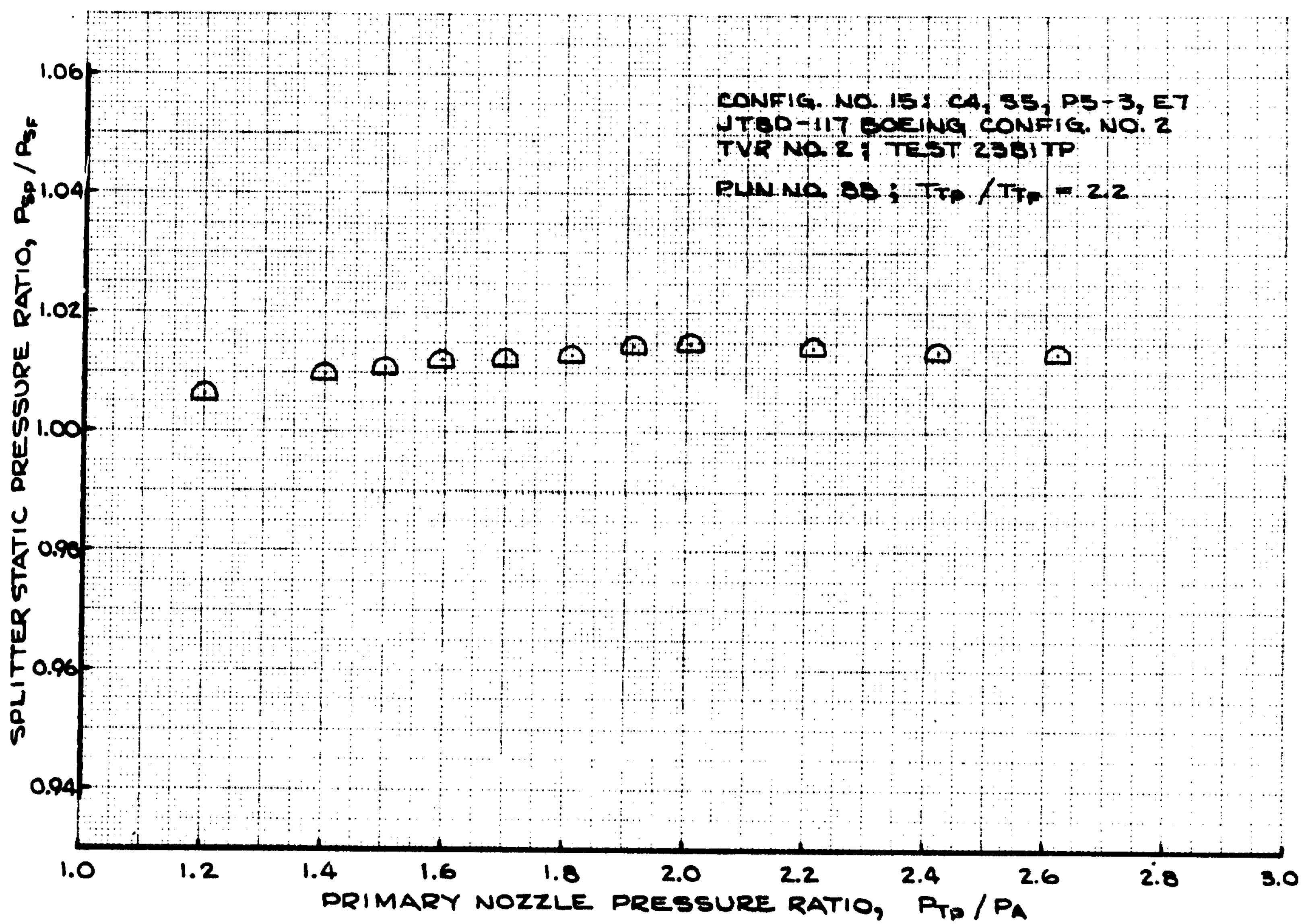

FIGURE 195 - SPLITTER STATIC PRESSURE RATIO
TEST CONFIG. NO. 15; RUN 88

7.2.16 TEST CONFIGURATION (T.C.) NO. 16

Configuration Description: Boeing Config. No. 2 variant using tne JT8D-109 splitter and redesigned plug for JT8D-117.

Hardware Designations:

Outer Nozzle Wall	Splitter	Plug	Exit
C4	S5	P5-3A	E7

Plotted Data:

Figure 196 - Velocity Coefficient; Runs 91-96

Figure 197 - Mixed Velocity Coefficient; Runs 91-96.

Figure 198 - Flow Coefficient; Runs 91-96.

Figure 199 - Mixed Flow Coefficient; Runs 91-96.

Figure 200 - Fan/Primary Total Pressure Ratio; Runs 91-96.

Figure 201 - Bypass Ratio; Runs 91-96.

Figure 202 - Splitter Static Pressure Ratio; Run 94.

C4

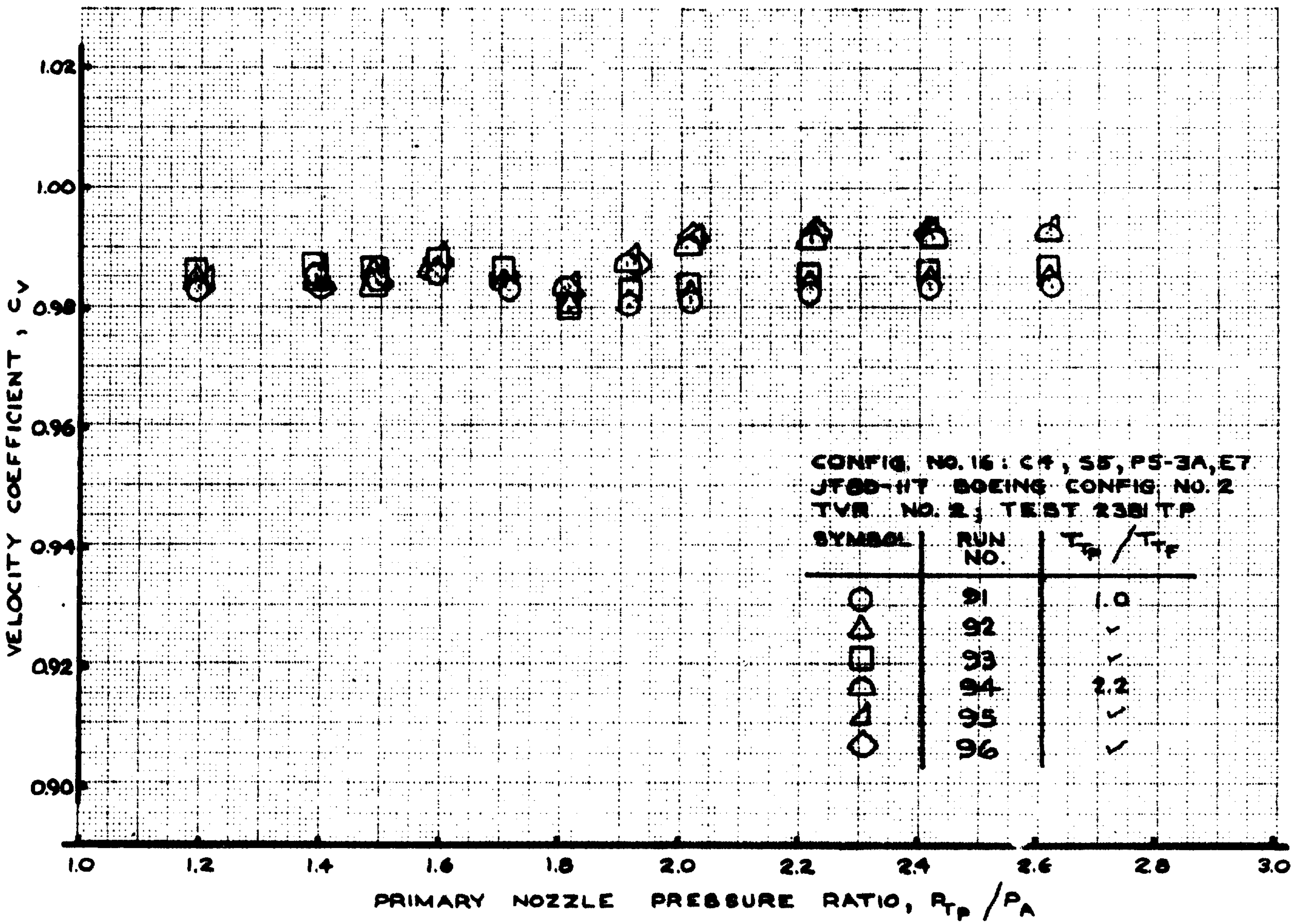

FIGURE 196- VELOCITY COEFFICIENT
TEST CONFIG. NO. 16; RUNS 91-96

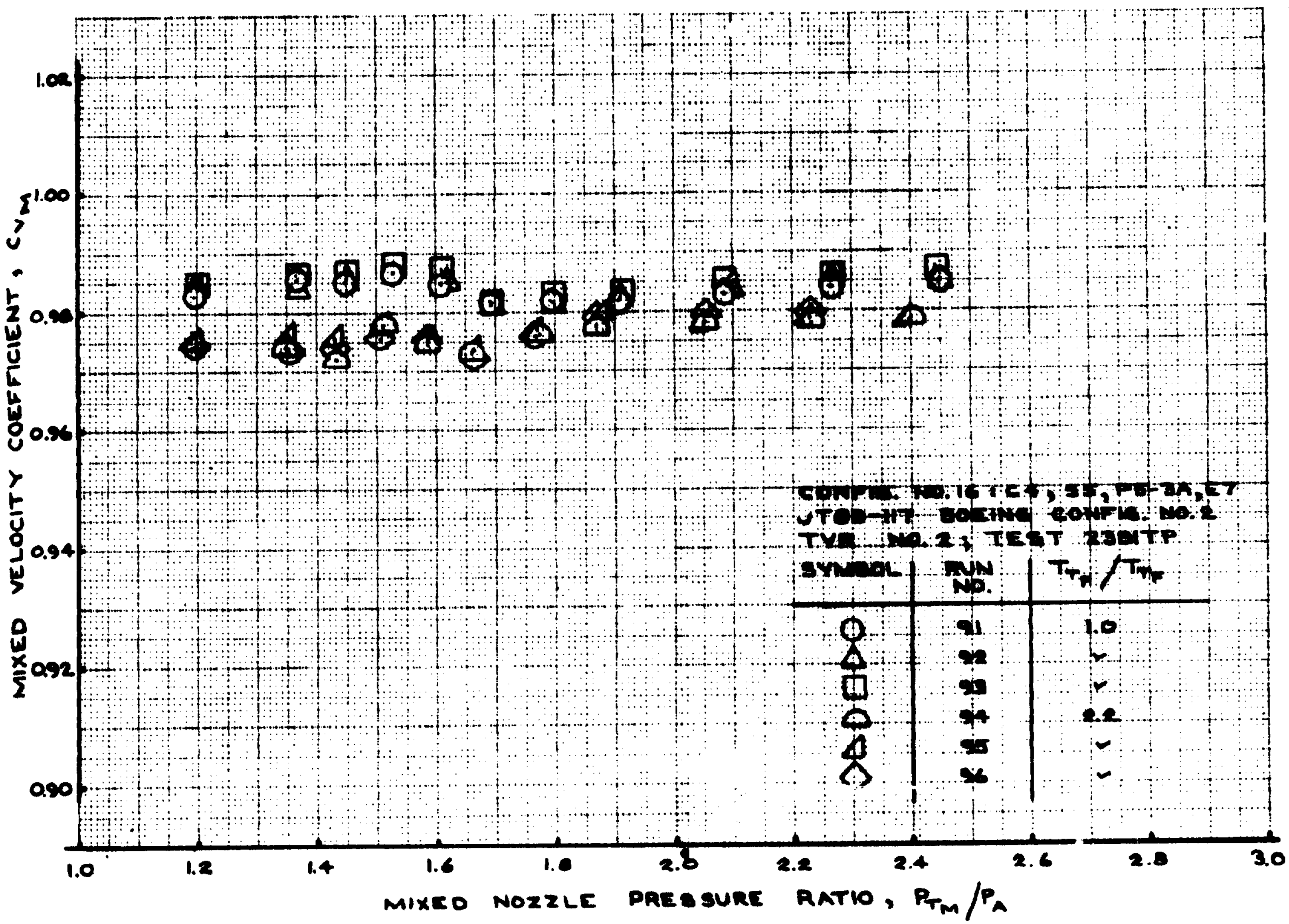

FIGURE 197- MIXED VELOCITY COEFFICIENT
TEST CONFIG. NO. 16; RUNS 91-96

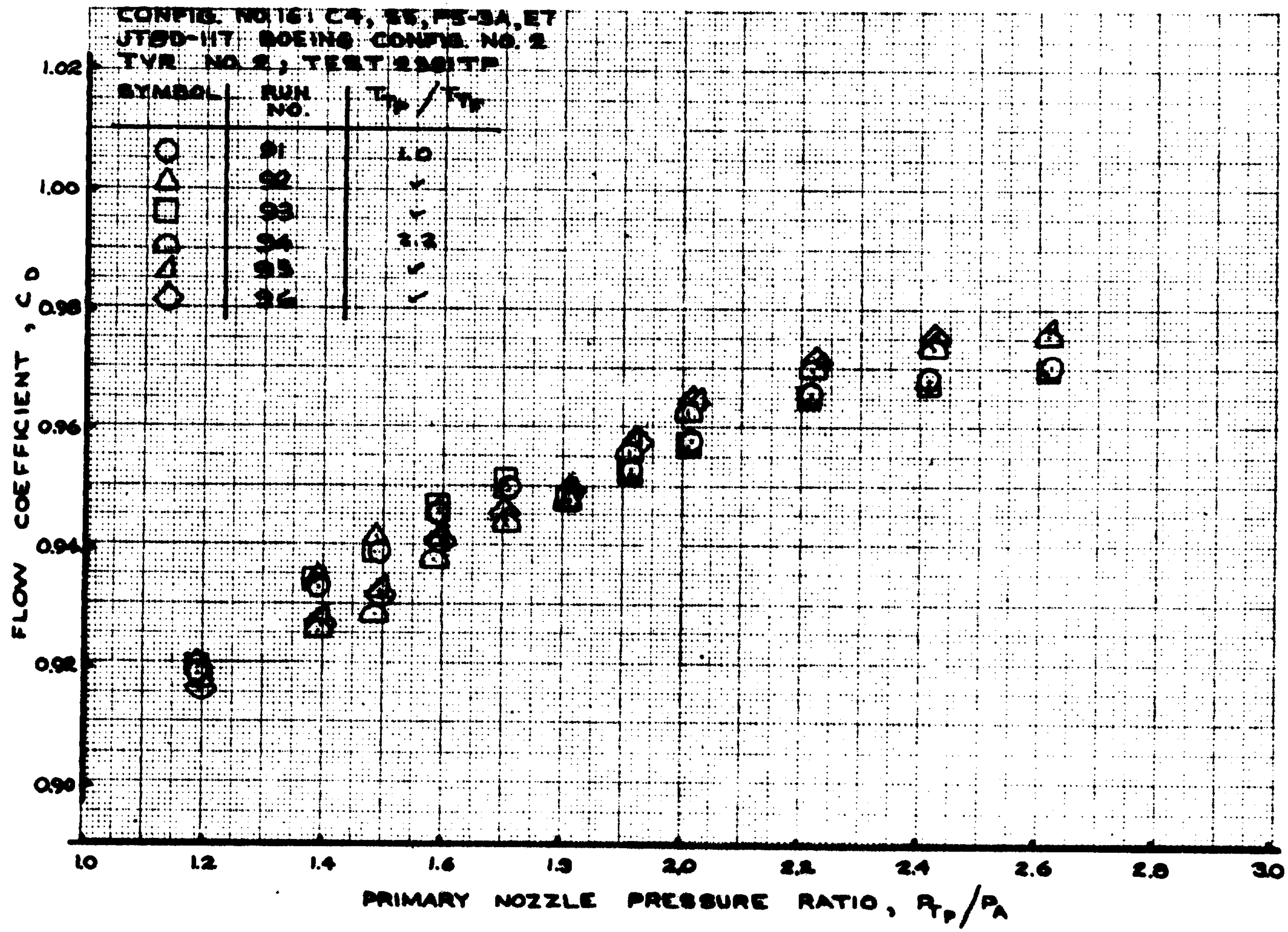

FIGURE 198- FLOW COEFFICIENT
TEST CONFIG. NO. 16; RUNS 91-96

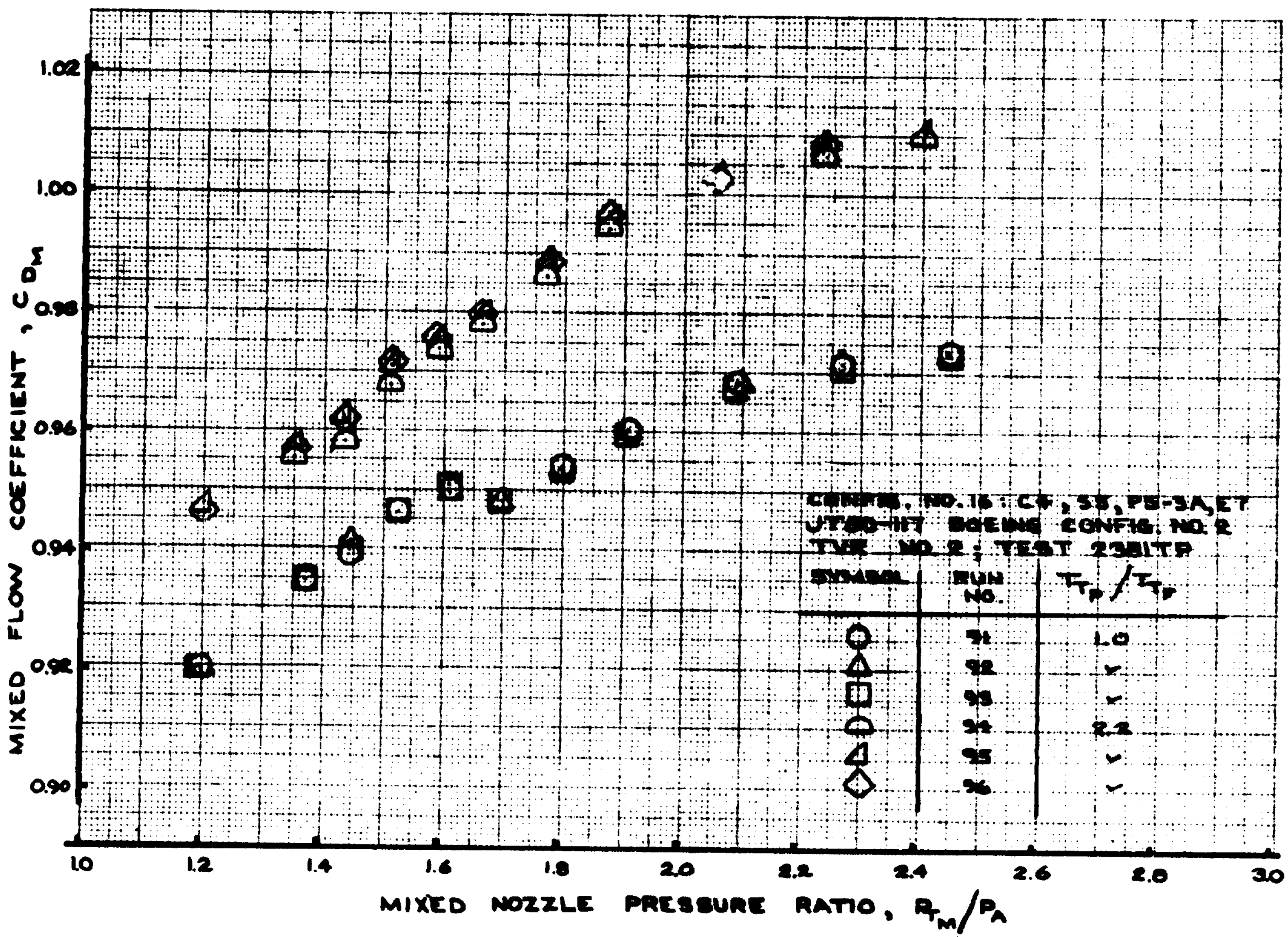

FIGURE 199- MIXED FLOW COEFFICIENT
TEST CONFIG. NO. 16; RUNS 91-96

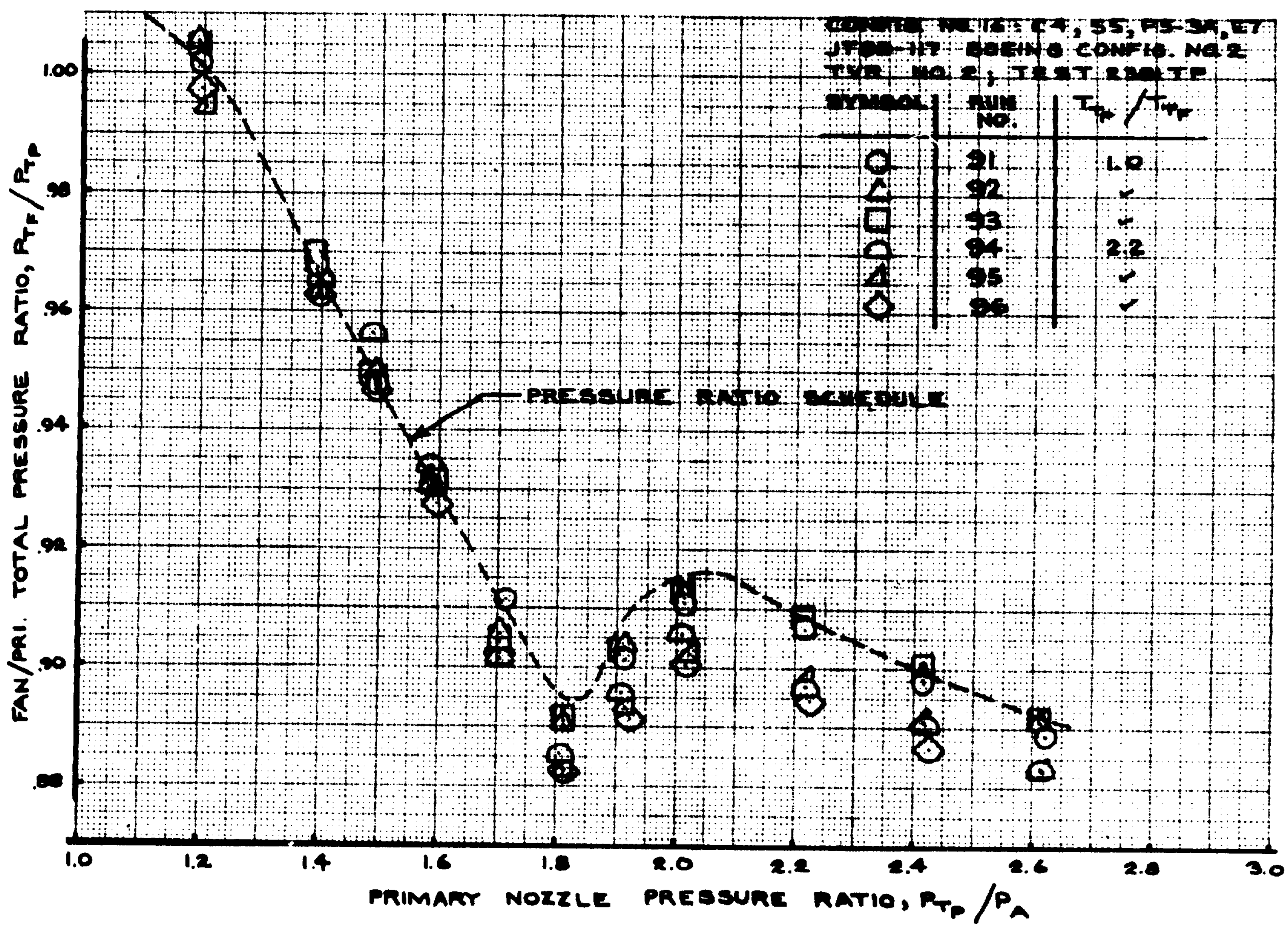

FIGURE 200- FAN/PRIMARY TOTAL PRESSURE RATIO
TEST CONFIG. NO. 16; RUNS 91-96

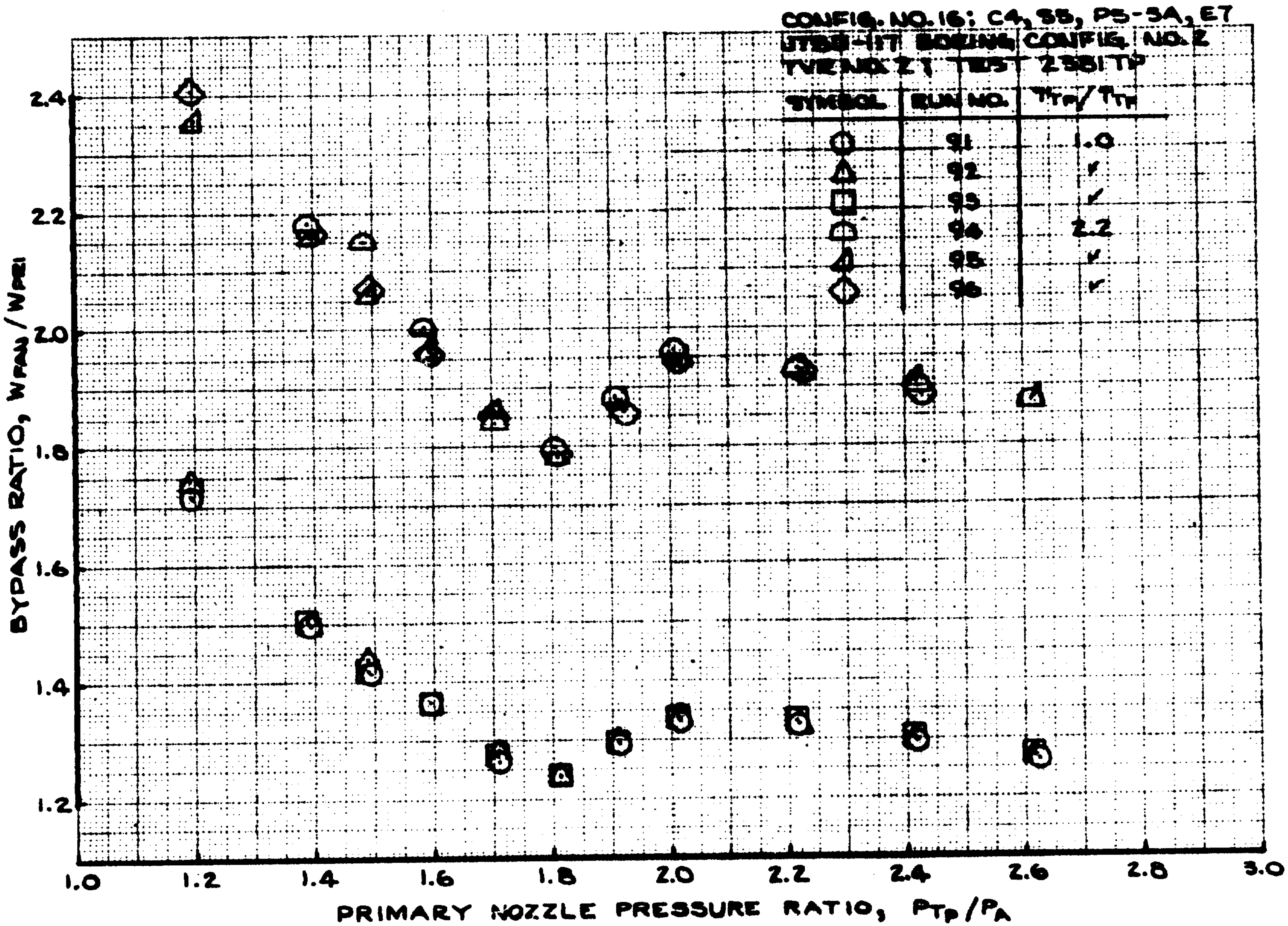

FIGURE 201- BYPASS RATIO
TEST CONFIG. NO. 16; RUNS 91-96

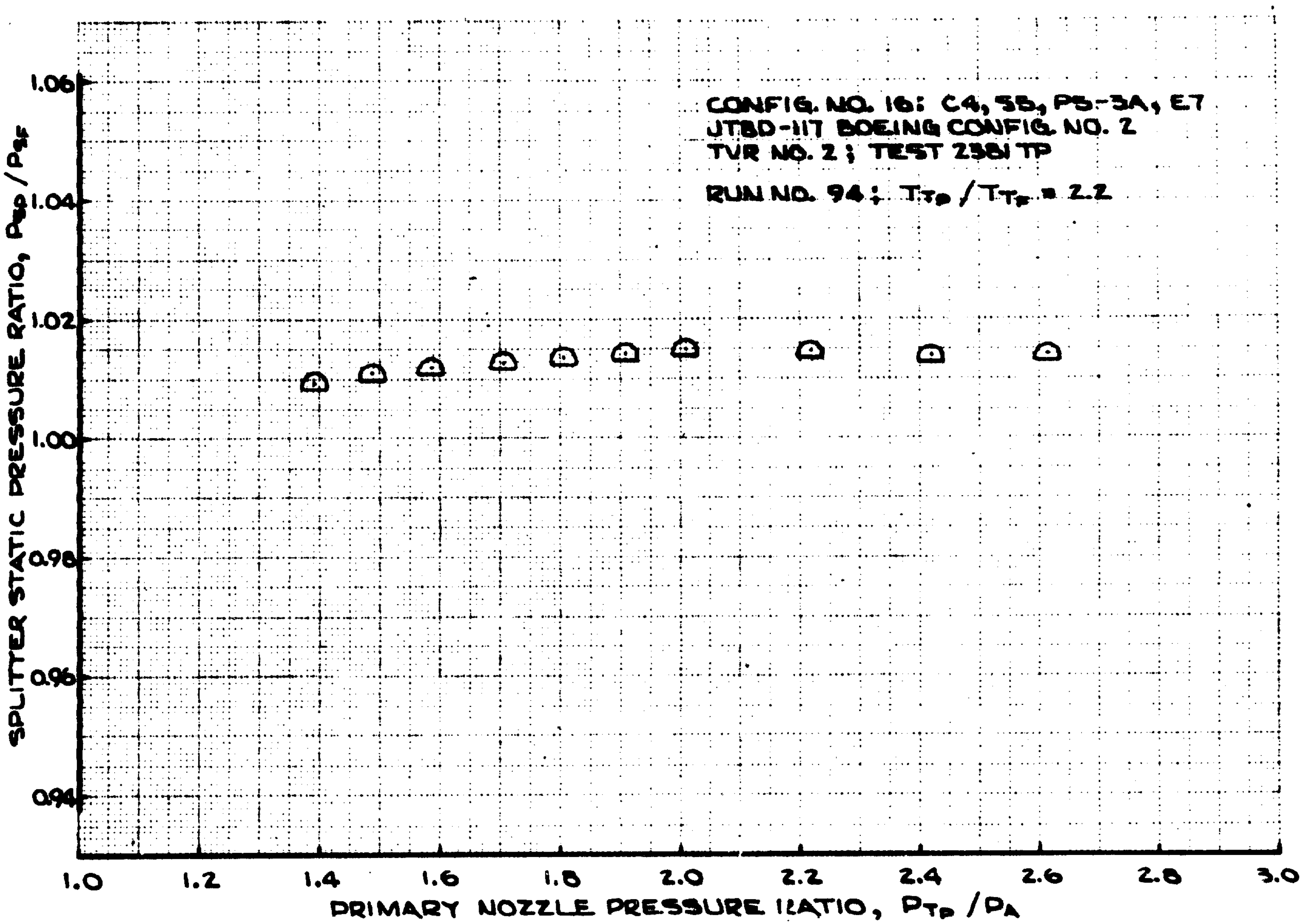

FIGURE 202 - SPLITTER STATIC PRESSURE RATIO
TEST CONFIG. NO. 16; RUN 94

7.2.17 TEST CONFIGURATION (T.C.) NO. 17

Configuration Description: Boeing Config. No. 2 variant using JT8D-115 splitter and redesigned plug for JT8D-117.

Hardware Designations:

Outer Nozzle Wall	Splitter	Plug	Exit
C4	S6	P7	E7

Plotted Data:

Figure 203 - Velocity Coefficient; Runs 79-84.
Figure 204 - Mixed Velocity Coefficient; Runs 79-84.
Figure 205 - Flow Coefficient; Runs 79-84.
Figure 206 - Mixed Flow Coefficient; Runs 79-84.
Figure 207 - Fan/Primary Total Pressure Ratio; Runs 79-84.
Figure 208 - Bypass Ratio; Runs 79-84.
Figure 209 - Splitter Static Pressure Ratio; Run 82.

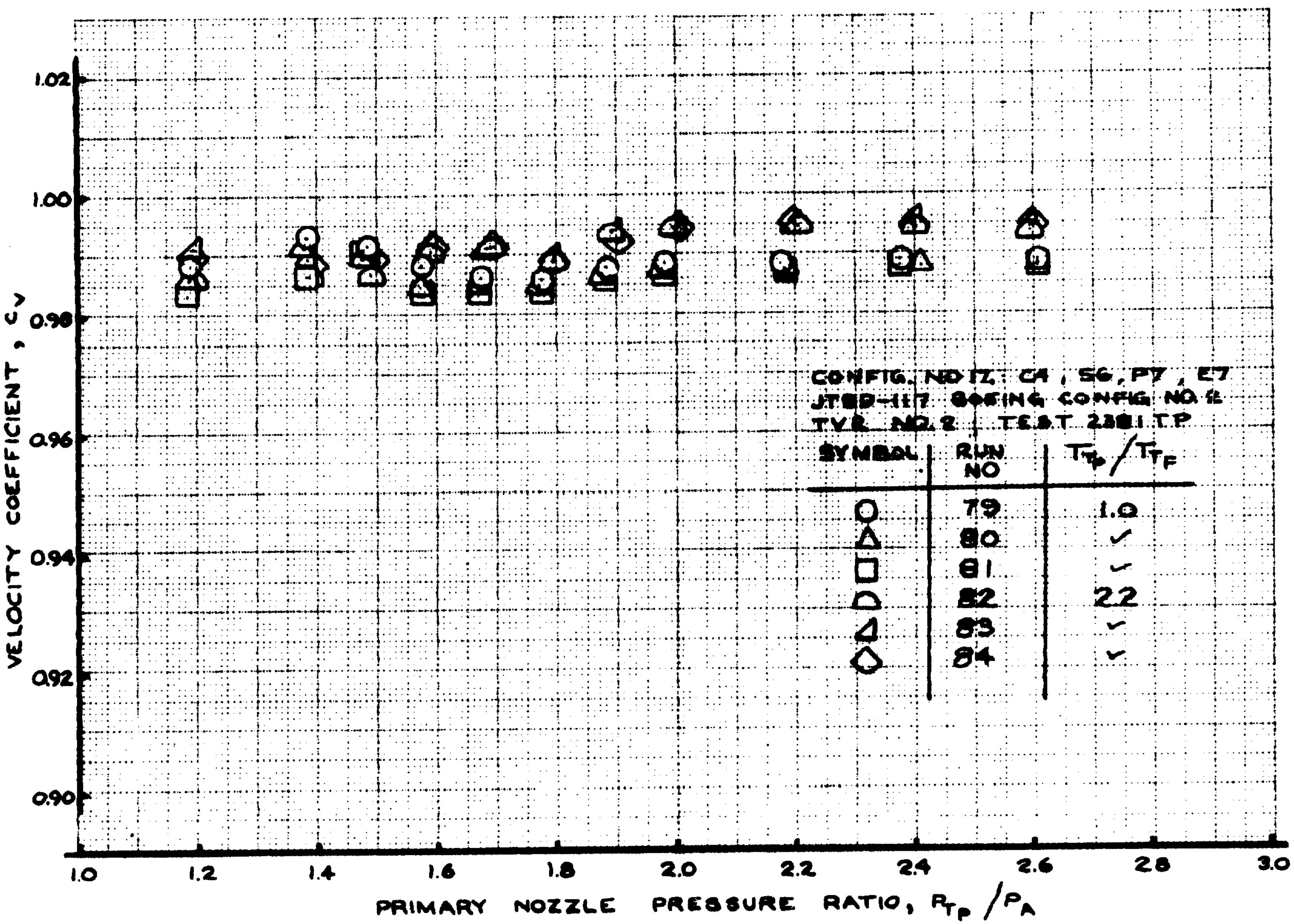

FIGURE 203- VELOCITY COEFFICIENT
TEST CONFIG. NO. 17; RUNS 79-84

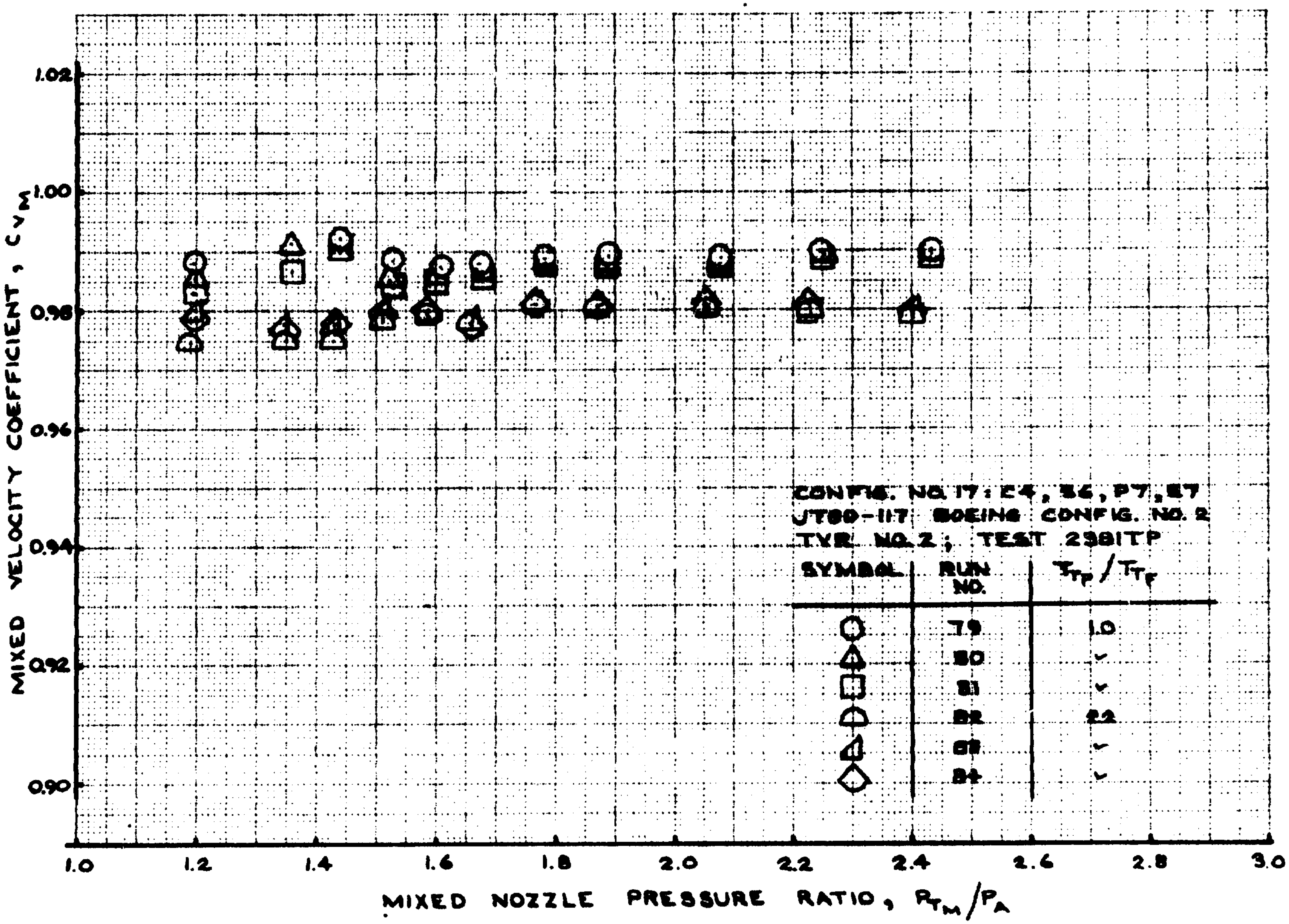

FIGURE 204- MIXED VELOCITY COEFFICIENT
TEST CONFIG. NO. 17; RUNS 79-84

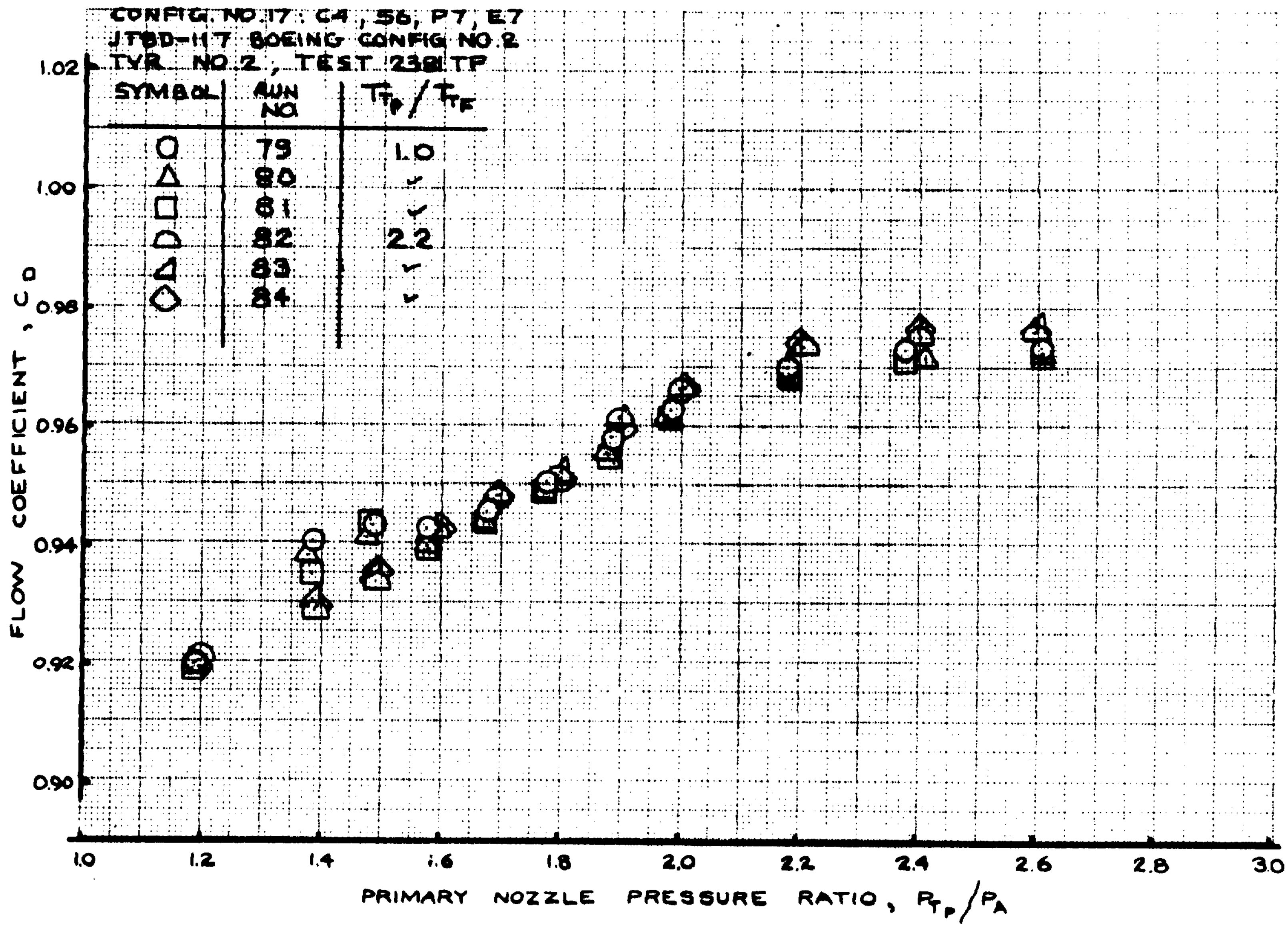

FIGURE 205- FLOW COEFFICIENT
TEST CONFIG. NO. 17; RUNS 79-84

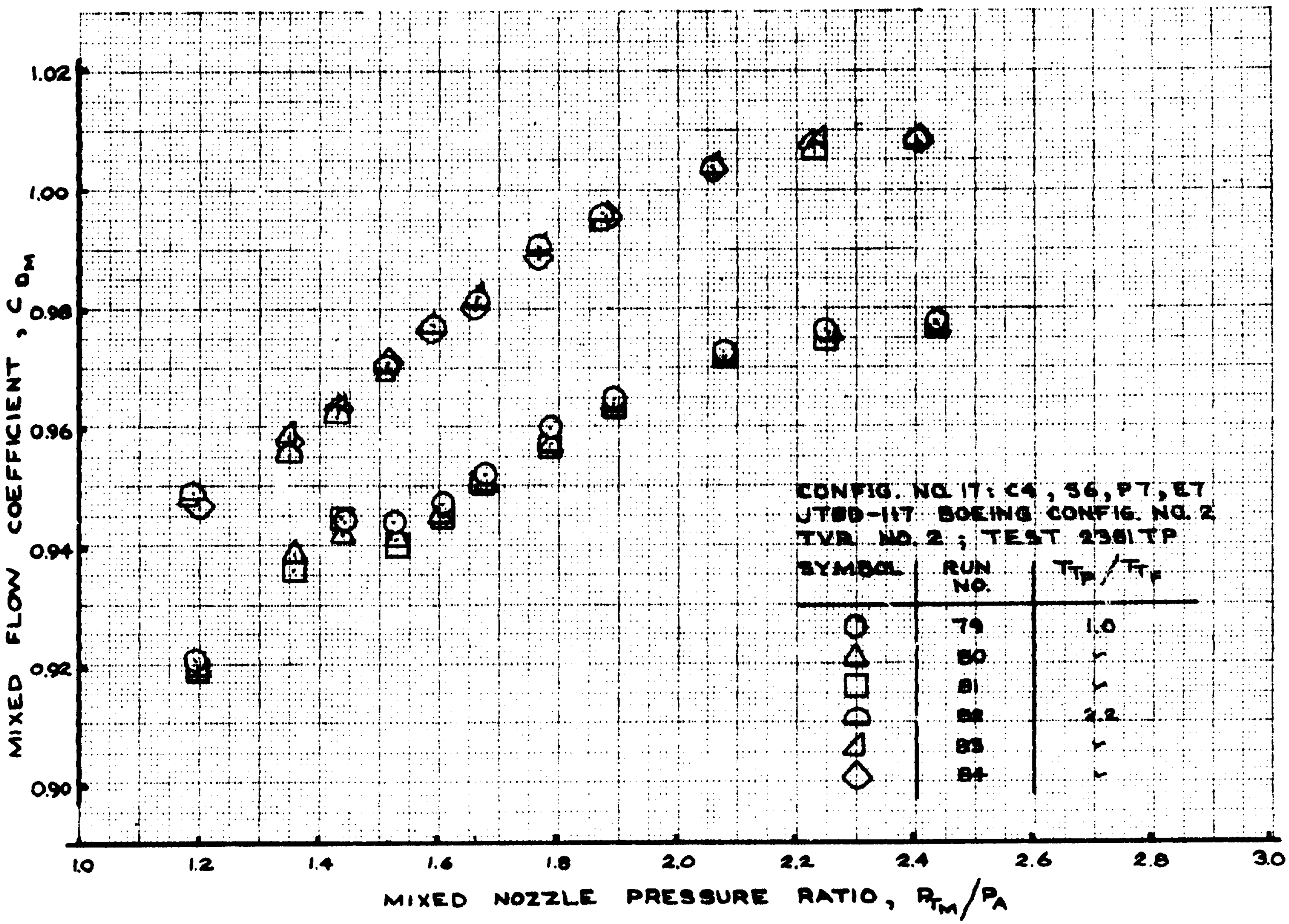

FIGURE 206- MIXED FLOW COEFFICIENT
TEST CONFIG. NO. 17; RUNS 79-84

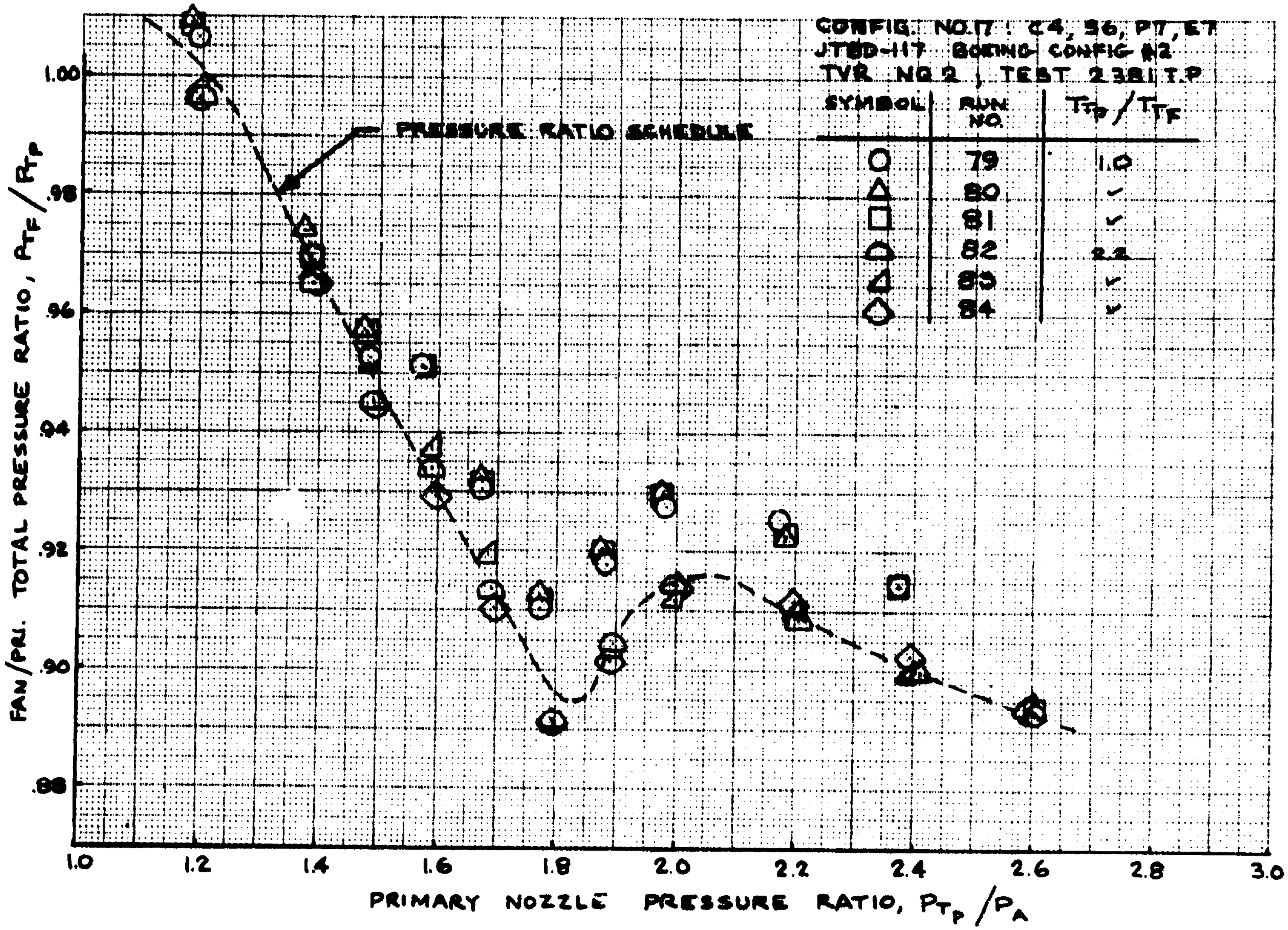

FIGURE 207 - FAN/PRIMARY TOTAL PRESSURE RATIO
TEST CONFIG. NO. 17; RUNS 79-84

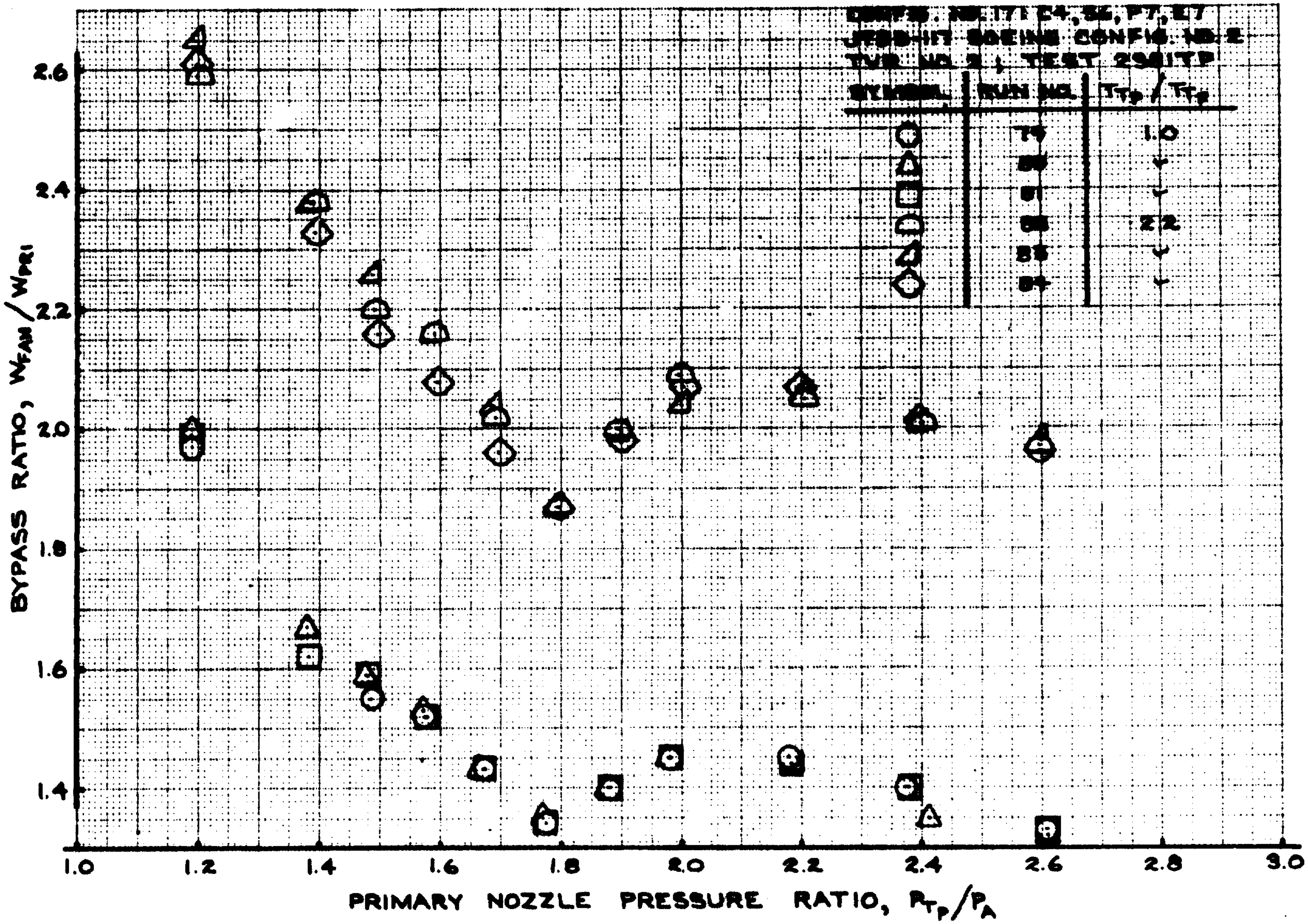

FIGURE 208- BYPASS RATIO
TEST CONFIG. NO. 17; RUNS 79-84

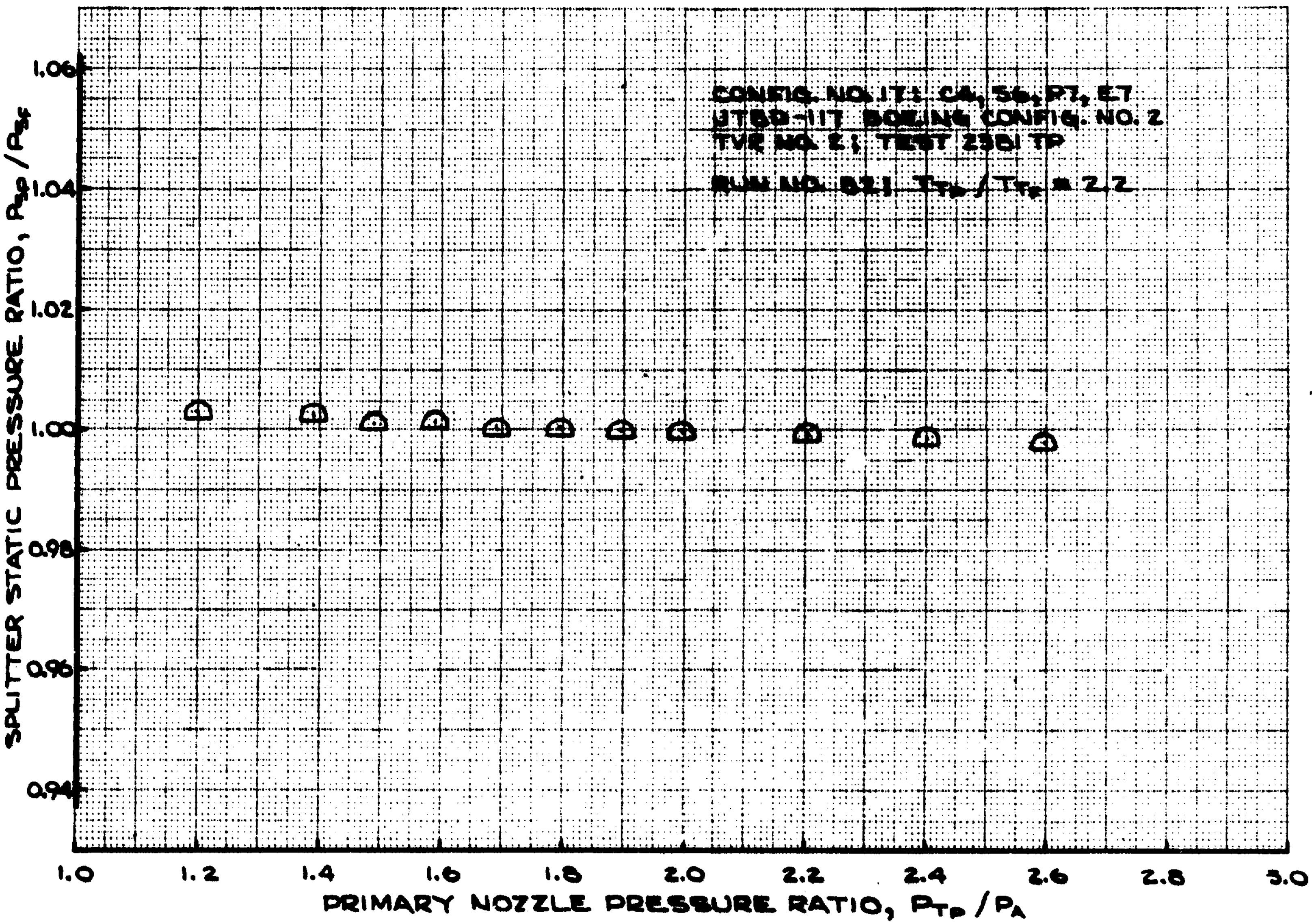

FIGURE 209 - SPLITTER STATIC PRESSURE RATIO
TEST CONFIG. NO. 17; RUN 82

7.2.18 TEST CONFIGURATION (T.C.) NO. 18

Configuration Description: Boeing Config. No. 2 design for JT8D-117.

Hardware Designations:

Outer Nozzle Wall	Splitter	Plug	Exit
C4	S7	P5-1	E7

Plotted Data:

Figure 210 - Velocity Coefficient; Runs 136-138, 143-145.

Figure 211 - Mixed Velocity Coefficient; Runs 136-138, 143-145.

Figure 212 - Flow Coefficient; Runs 136-138, 143-145.

Figure 213 - Mixed Flow Coefficient; Runs 136-138, 143-145.

Figure 214 - Fan/Primary Total Pressure Ratio; Runs 136-138, 143-145.

Figure 215 - Bypass Ratio; Runs 136-138, 143-145.

Figure 216 - Velocity Coefficient; Runs 141-142, 148-149.

Figure 217 - Mixed Velocity Coefficient; Runs 141-142, 148-149.

Figure 218 - Flow Coefficient; Runs 141-142, 148-149.

Figure 219 - Mixed Flow Coefficient; Runs 141-142, 148-149.

Figure 220 - Fan/Primary Total Pressure Ratio; Runs 141-142, 148-149.

Figure 221 - Bypass Ratio; Runs 141-142, 148-149.

Figure 222 - Velocity Coefficient; Runs 139-140, 146-147.

Figure 223 - Mixed Velocity Coefficient; Runs 139-140, 146-147.

Figure 224 - Flow Coefficient; Runs 139-140, 146-147.

Figure 225 - Mixed Flow Coefficient; Runs 139-140, 146-147.

Figure 226 - Fan/Primary Total Pressure Ratio; Runs 139-140, 146-147.

Figure 227 - Bypass Ratio; Runs 139-140, 146-147.

Figure 228 - Splitter Static Pressure Ratio; Runs 137, 139, 141.

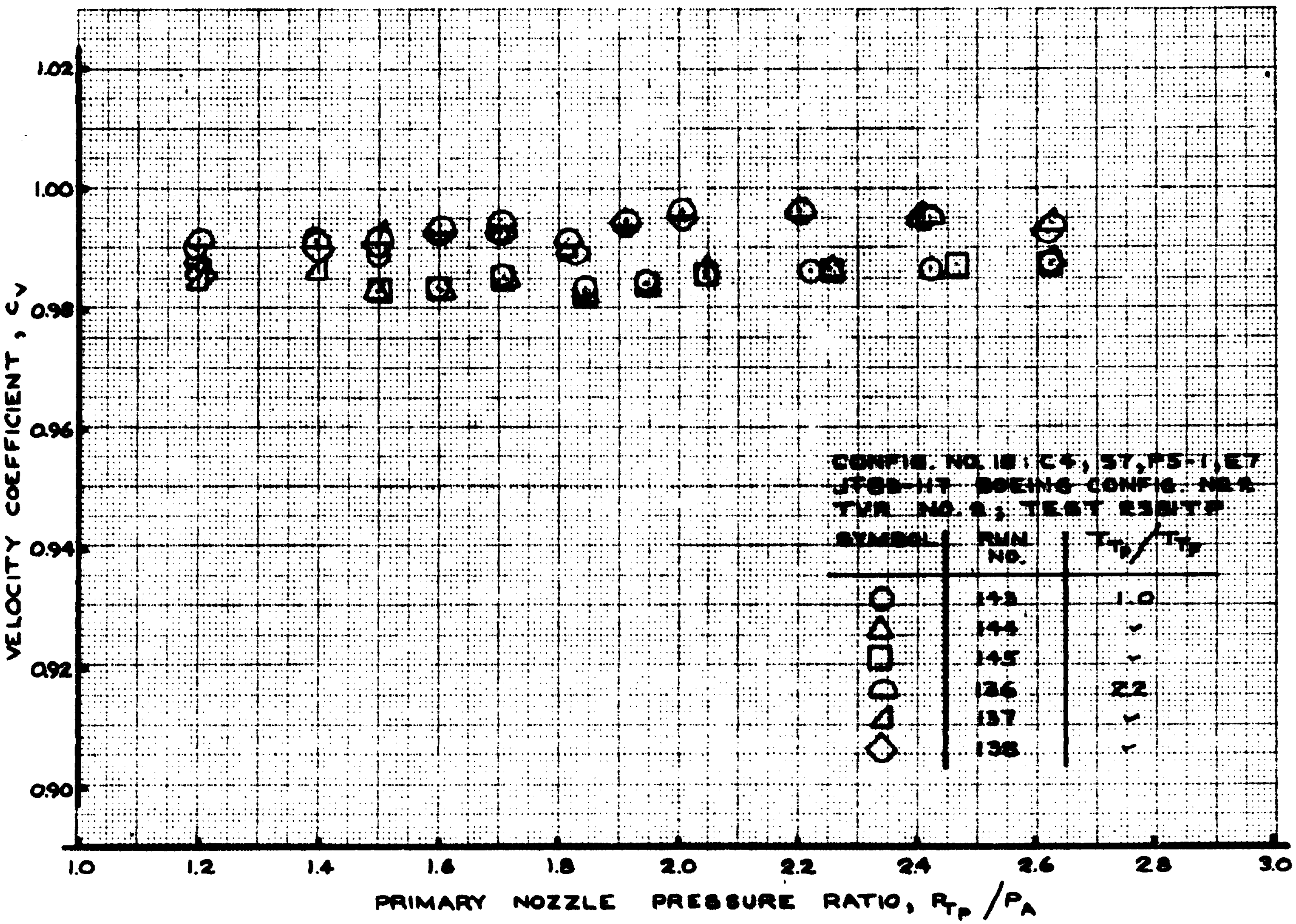

FIGURE 210- VELOCITY COEFFICIENT
TEST CONFIG. NO. 18; RUNS 136-138, 143-145

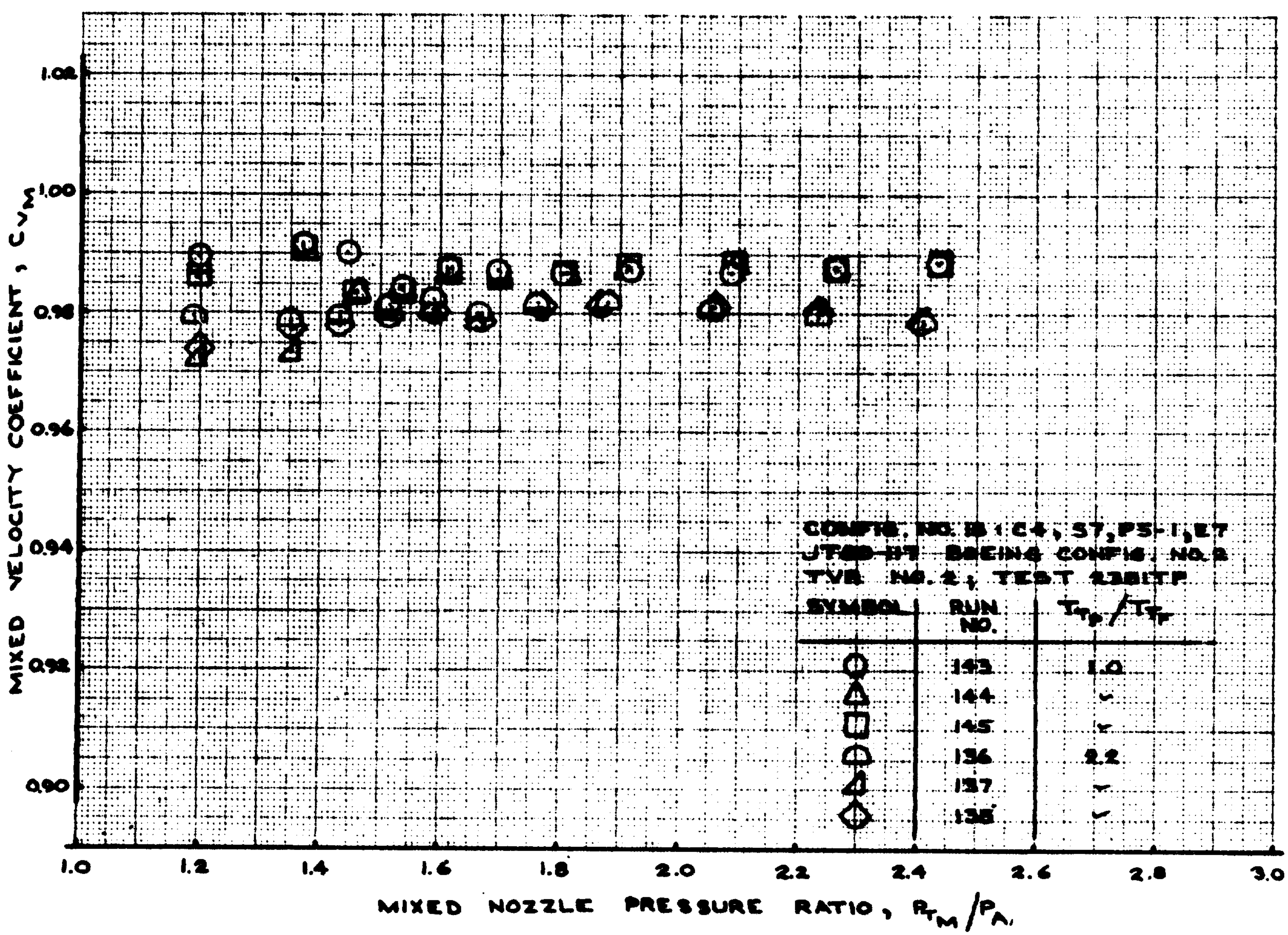

FIGURE 211- MIXED VELOCITY COEFFICIENT
TEST CONFIG. NO. 18; RUNS 136-138, 143-145

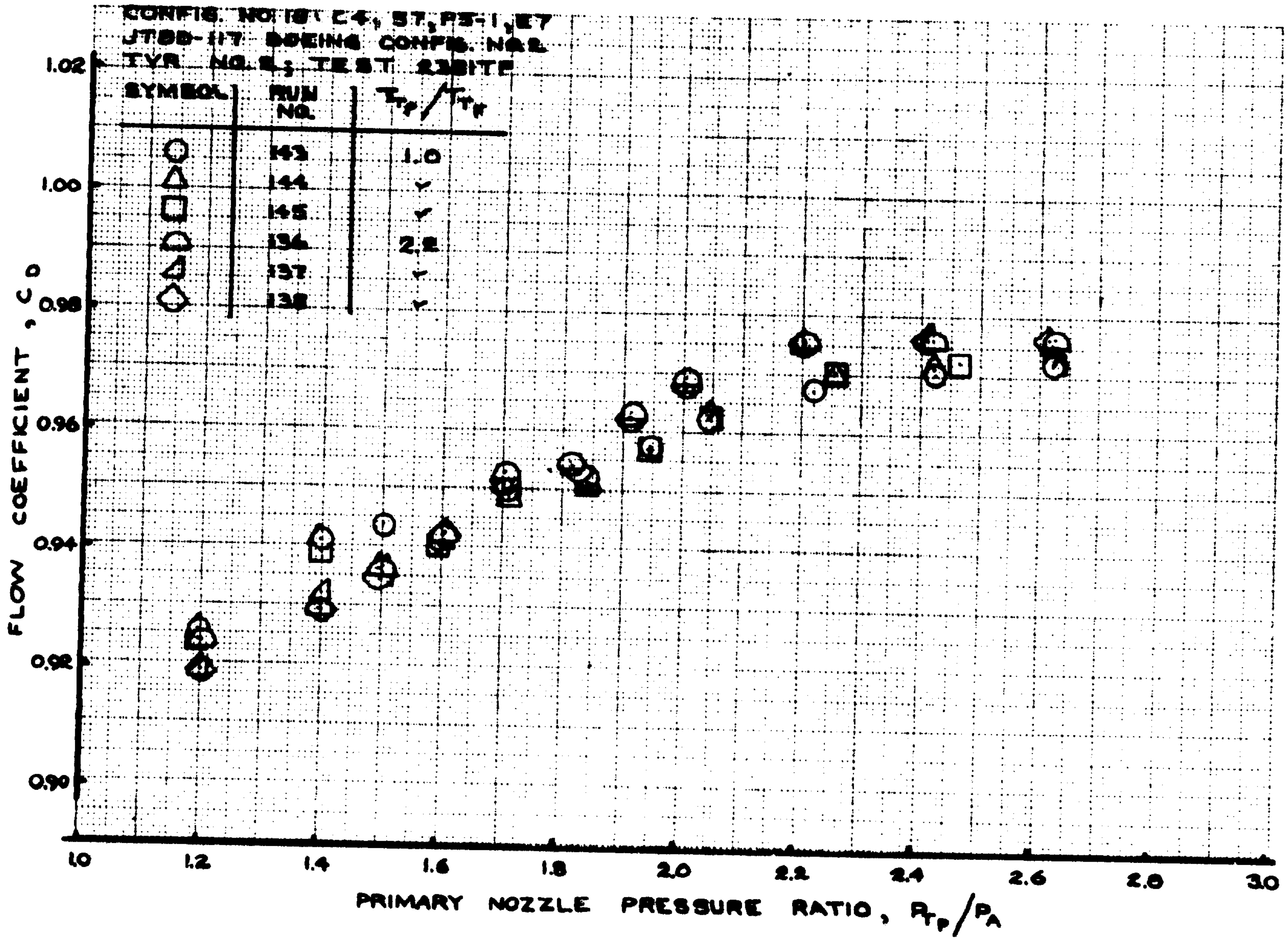

FIGURE 212- FLOW COEFFICIENT
TEST CONFIG. NO. 18; RUNS 136-138, 143-145

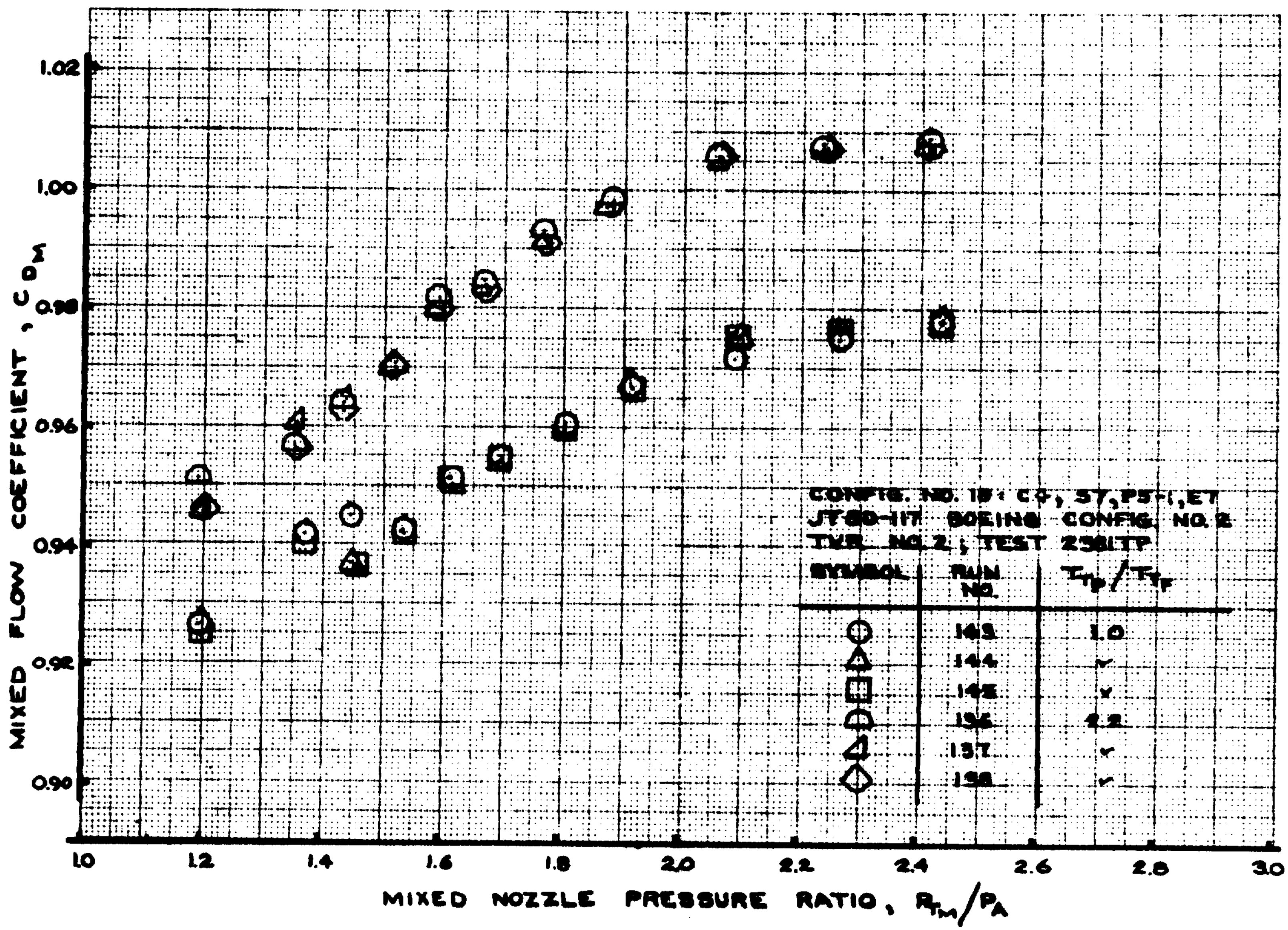

FIGURE 213- MIXED FLOW COEFFICIENT
TEST CONFIG. NO. 18; RUNS 136-138, 143-145

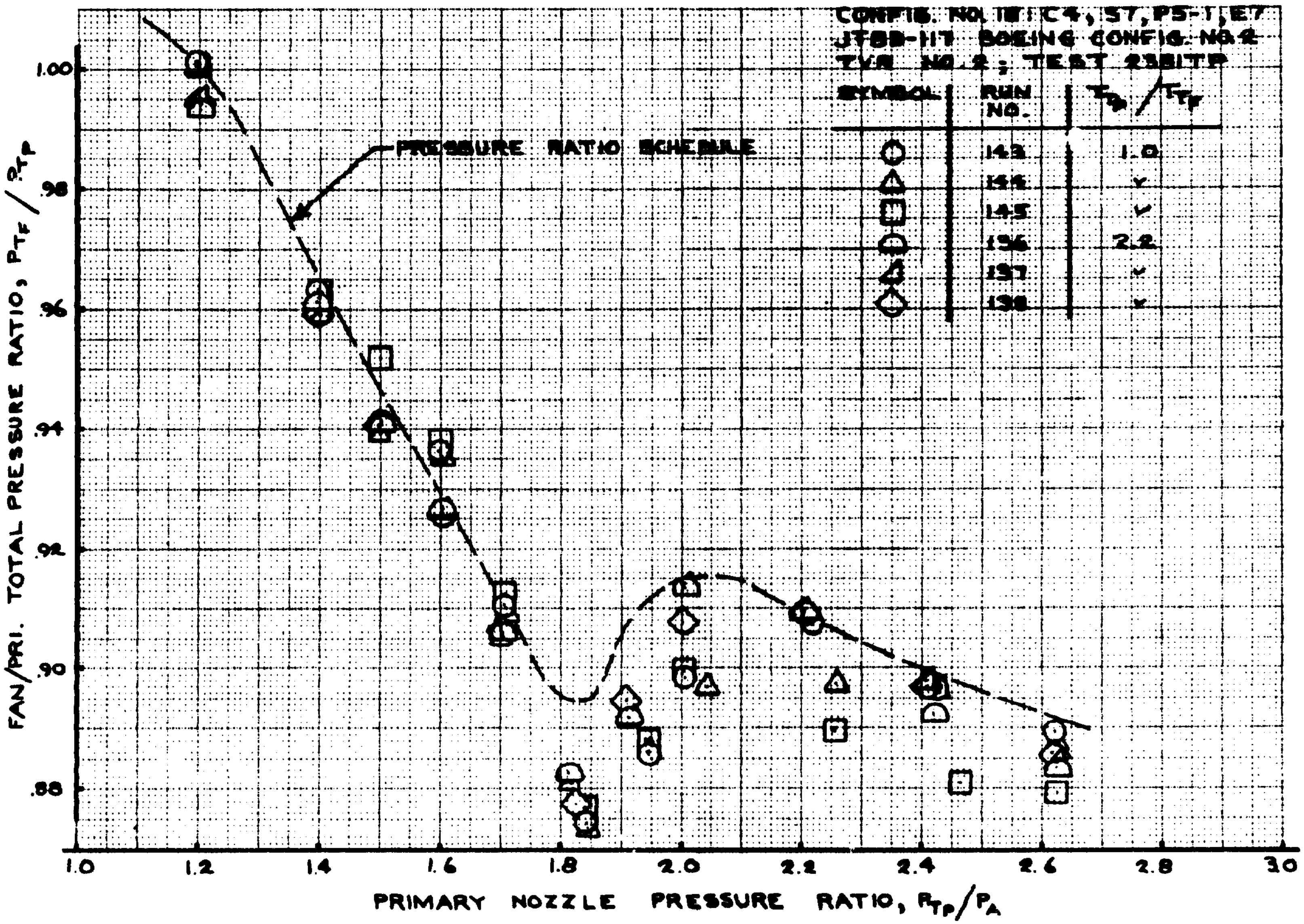

FIGURE 214- FAN/PRIMARY TOTAL PRESSURE RATIO
TEST CONFIG. NO. 18; RUNS 136-138, 143-145

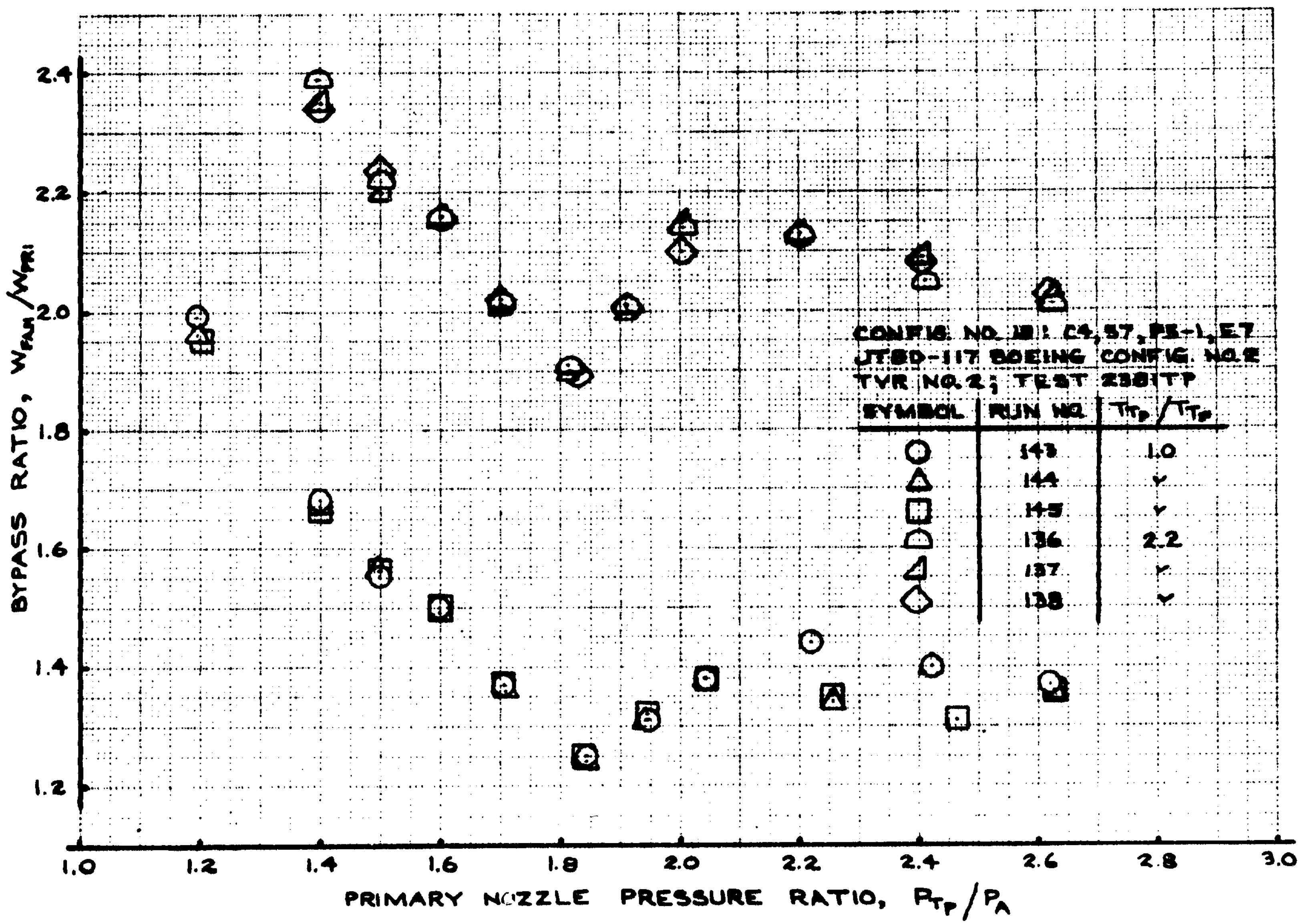

FIGURE 215- BYPASS RATIO
TEST CONFIG. NO. 18; RUNS 136-138, 143-145

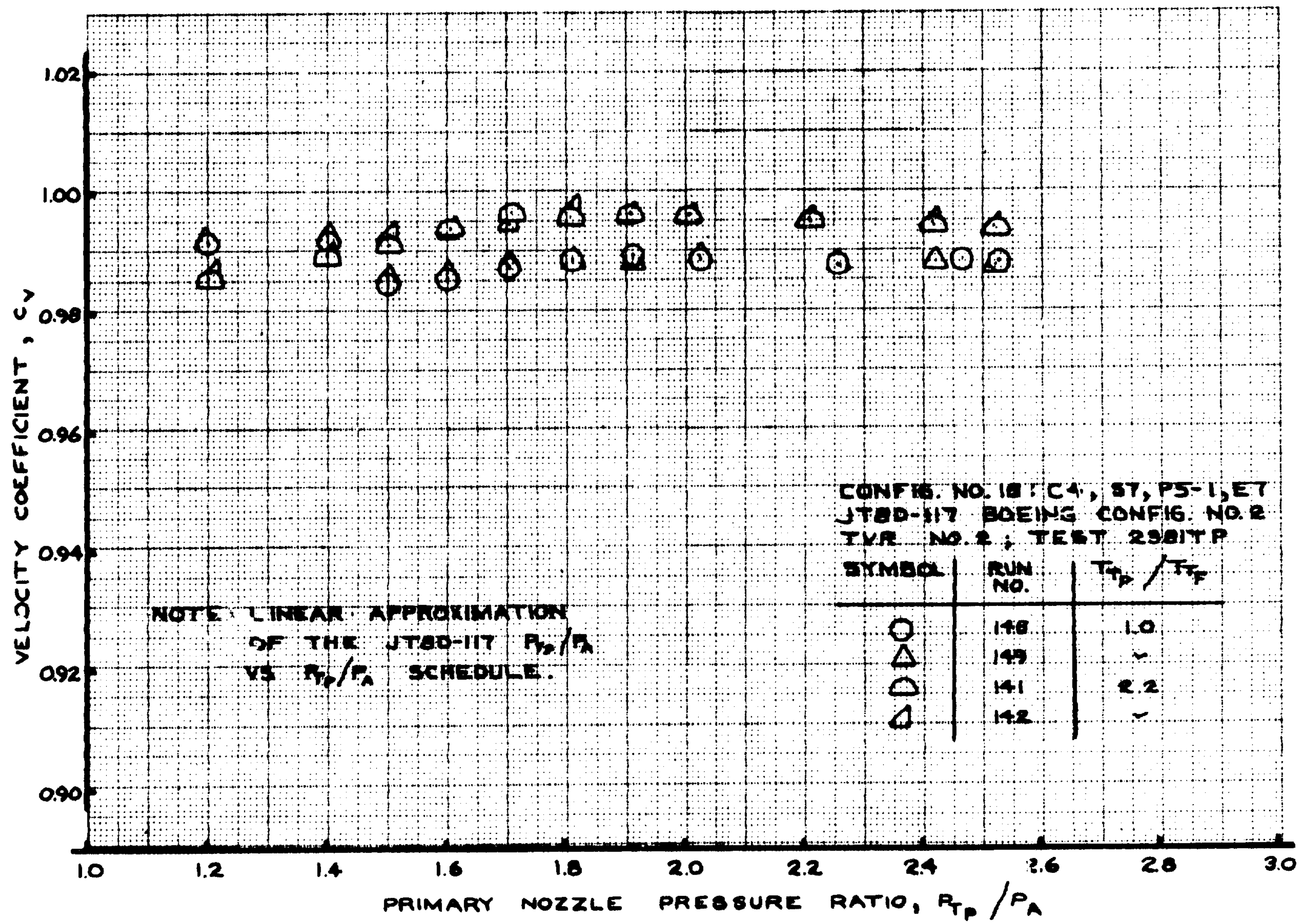

FIGURE 216- VELOCITY COEFFICIENT
TEST CONFIG. NO. 18; RUNS 141-142, 148-149

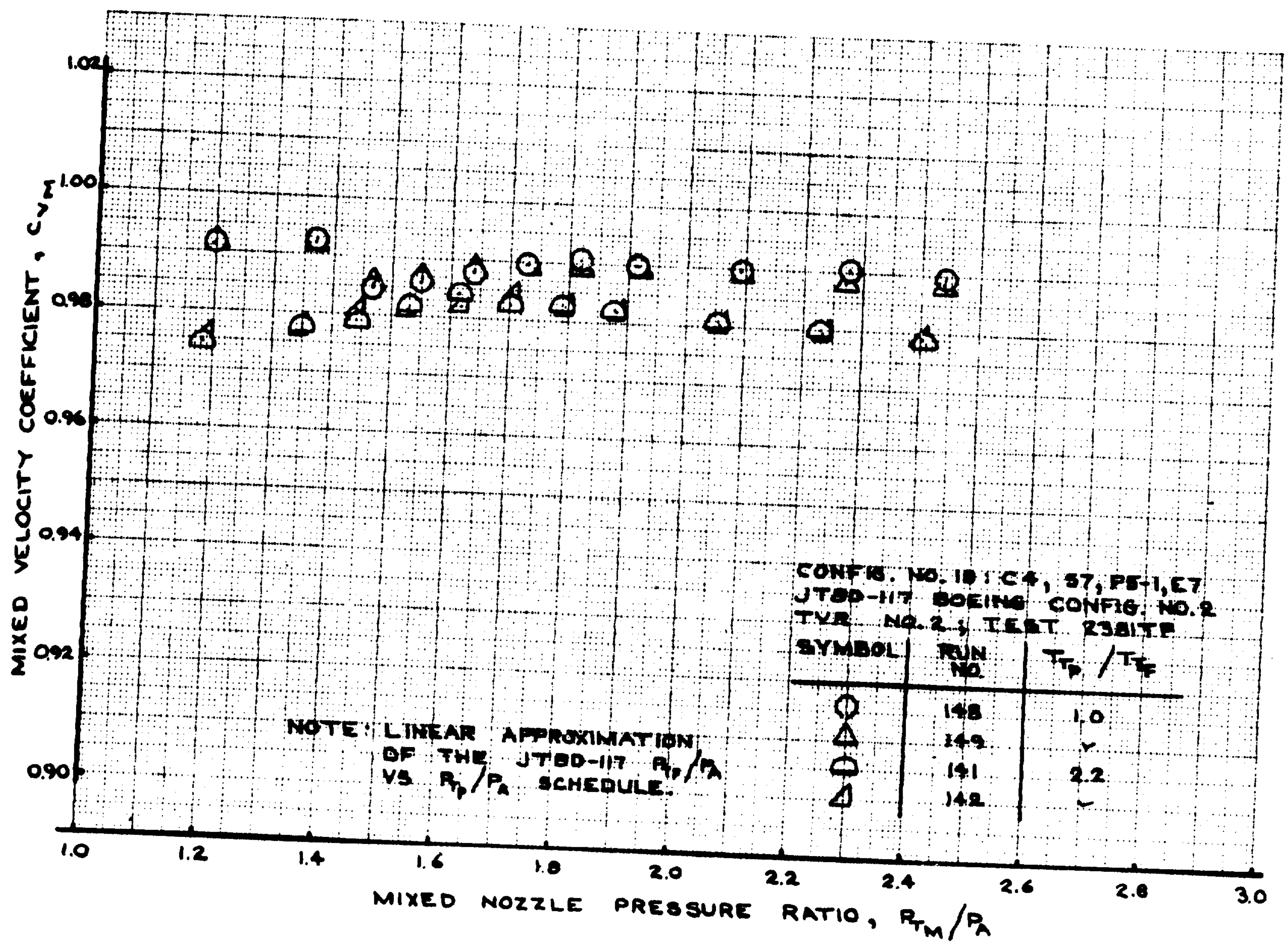

FIGURE 217- MIXED VELOCITY COEFFICIENT
TEST CONFIG. NO. 18; RUNS 141-142, 148-149

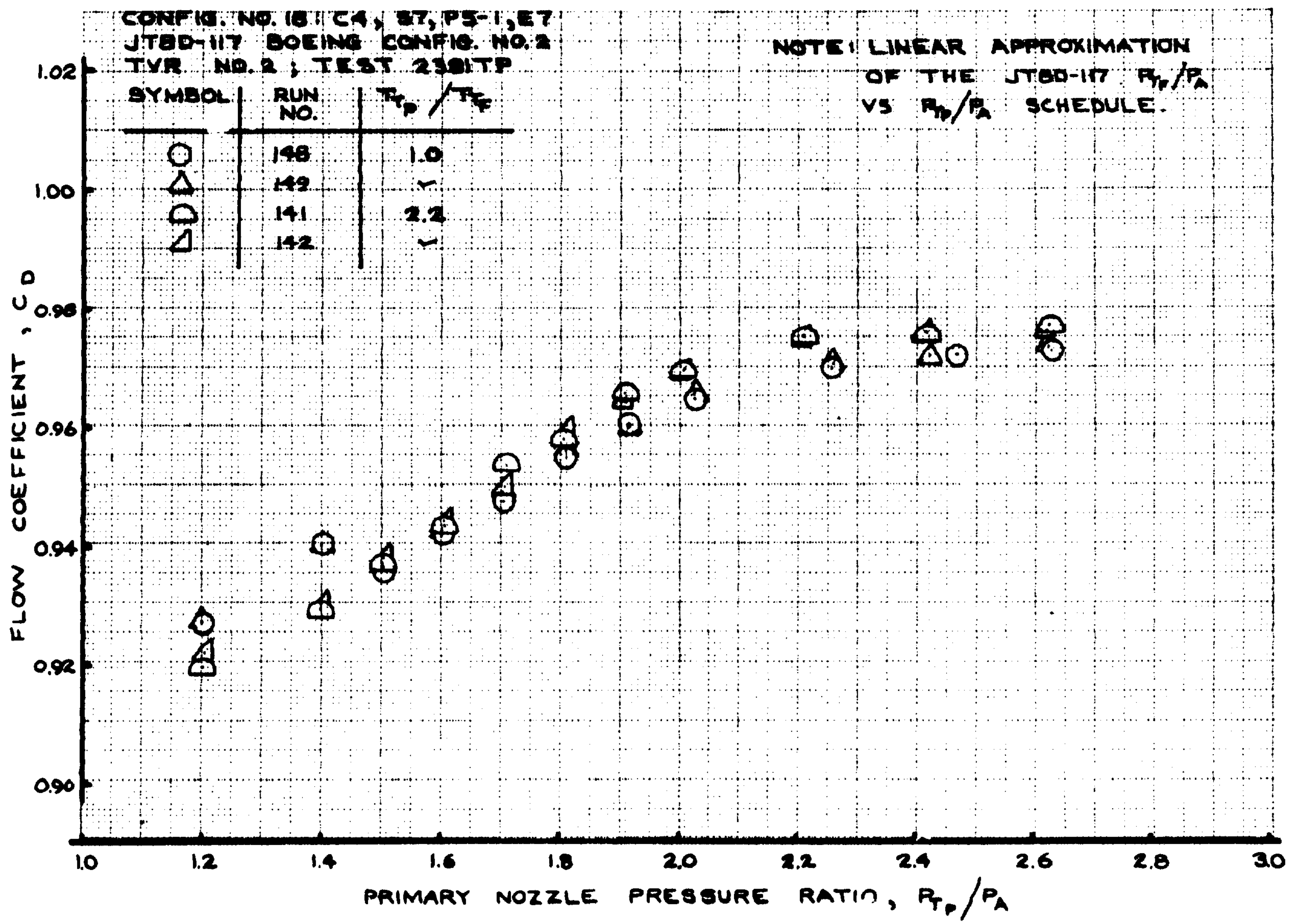

FIGURE 218- FLOW COEFFICIENT
TEST CONFIG. NO. 18; RUNS 141-142, 148-149

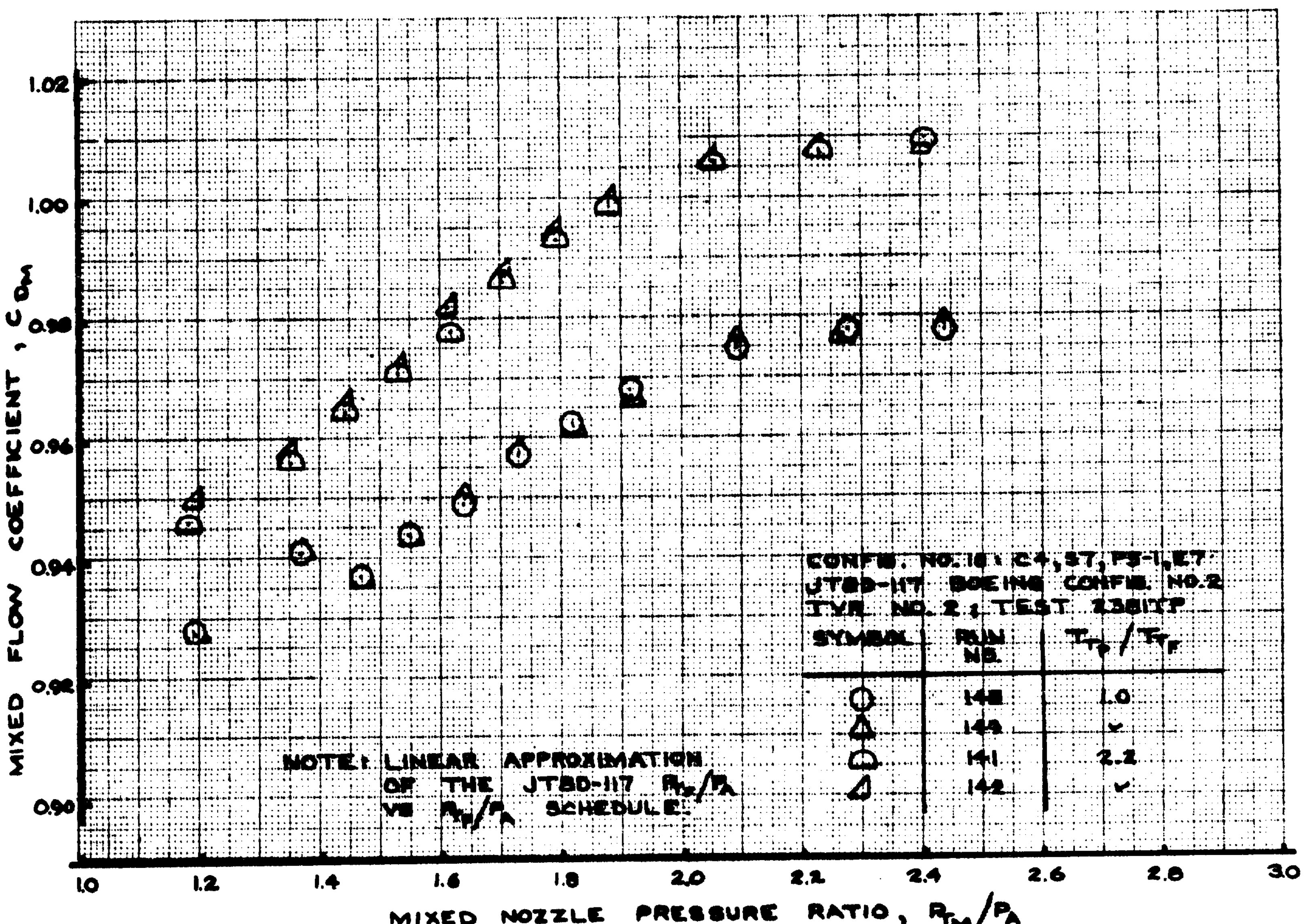

FIGURE 219- MIXED FLOW COEFFICIENT
TEST CONFIG. NO. 18; RUNS 141-142, 148-149

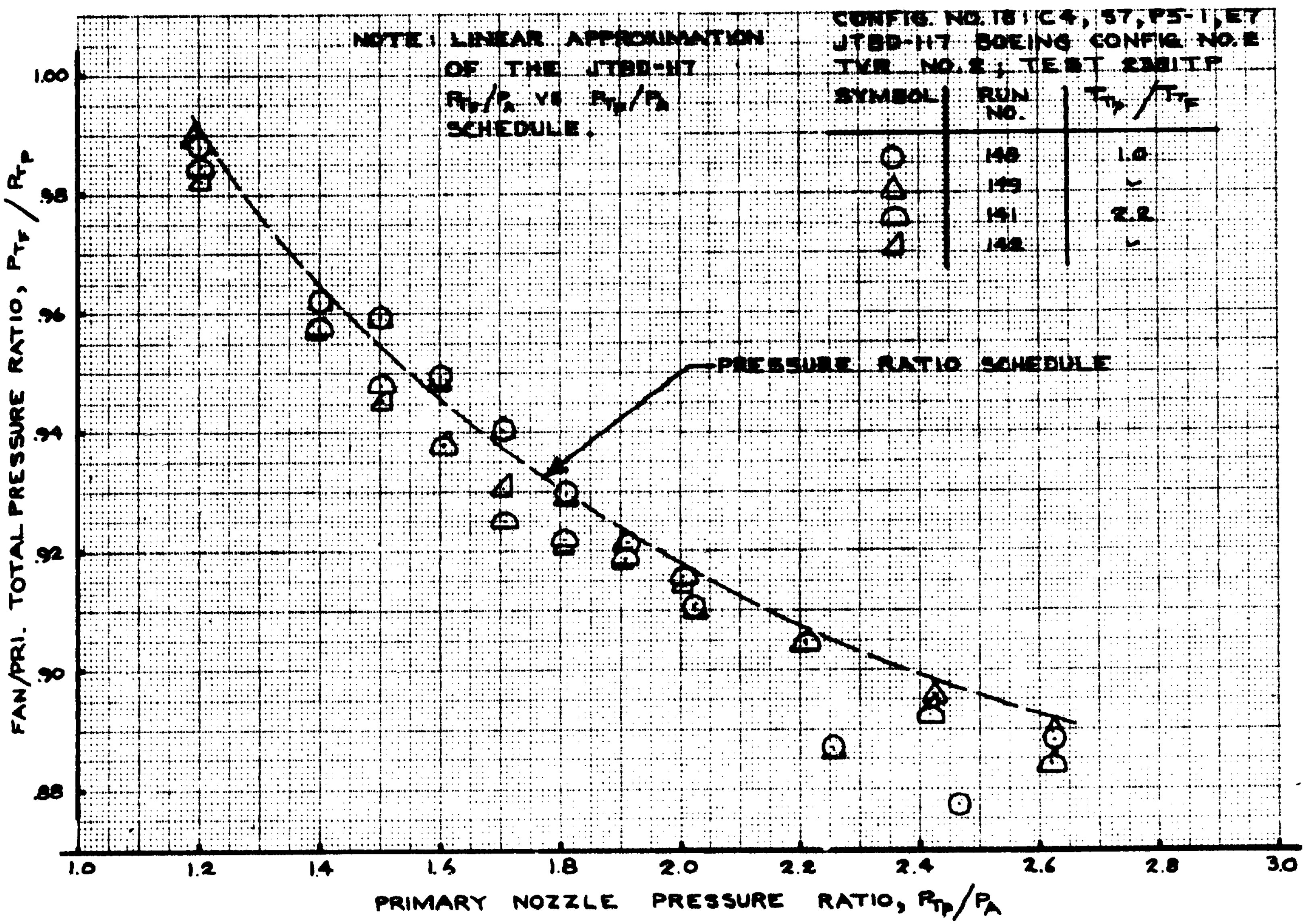

FIGURE 220- FAN/PRIMARY TOTAL PRESSURE RATIO
TEST CONFIG. NO. 18; RUNS 141-142, 148-149

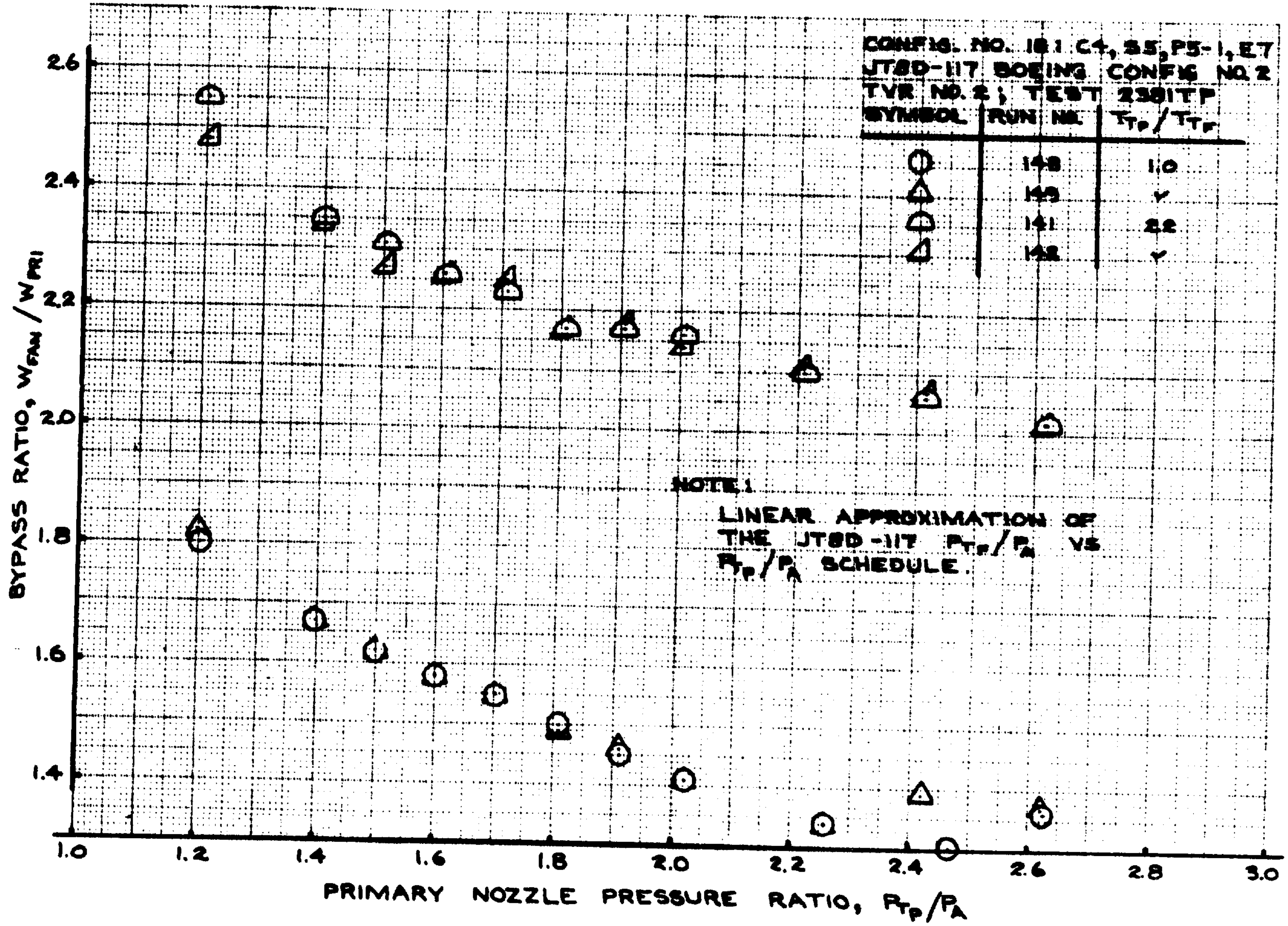

FIGURE 221 - BYPASS RATIO
TEST CONFIG. NO. 18; RUNS 141-142, 148-149

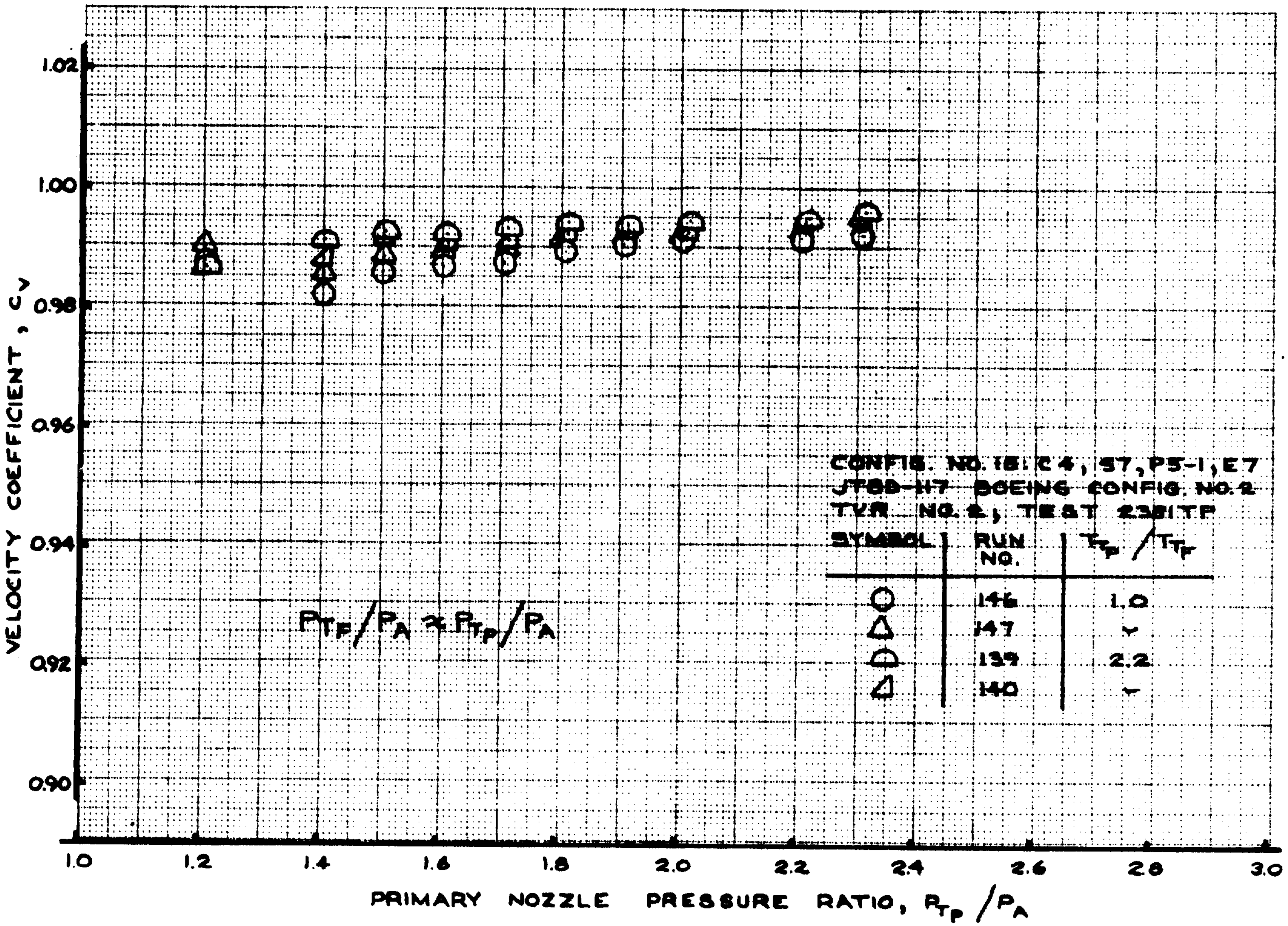

FIGURE 222 - VELOCITY COEFFICIENT
TEST CONFIG. NO. 18; RUNS 139-140, 146-147

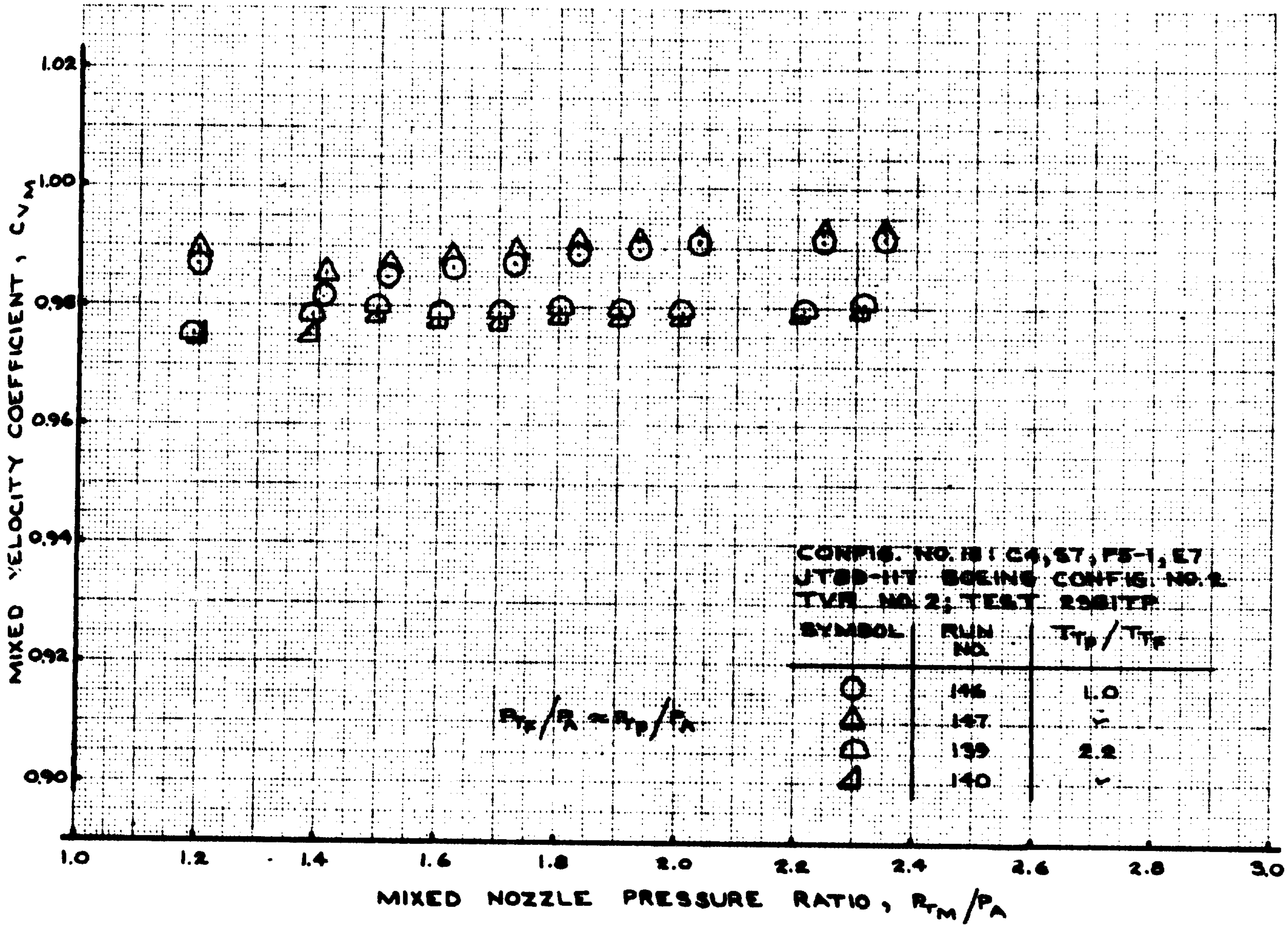

FIGURE 223 - MIXED VELOCITY COEFFICIENT
TEST CONFIG. NO. 18; RUNS 139-140, 146-147

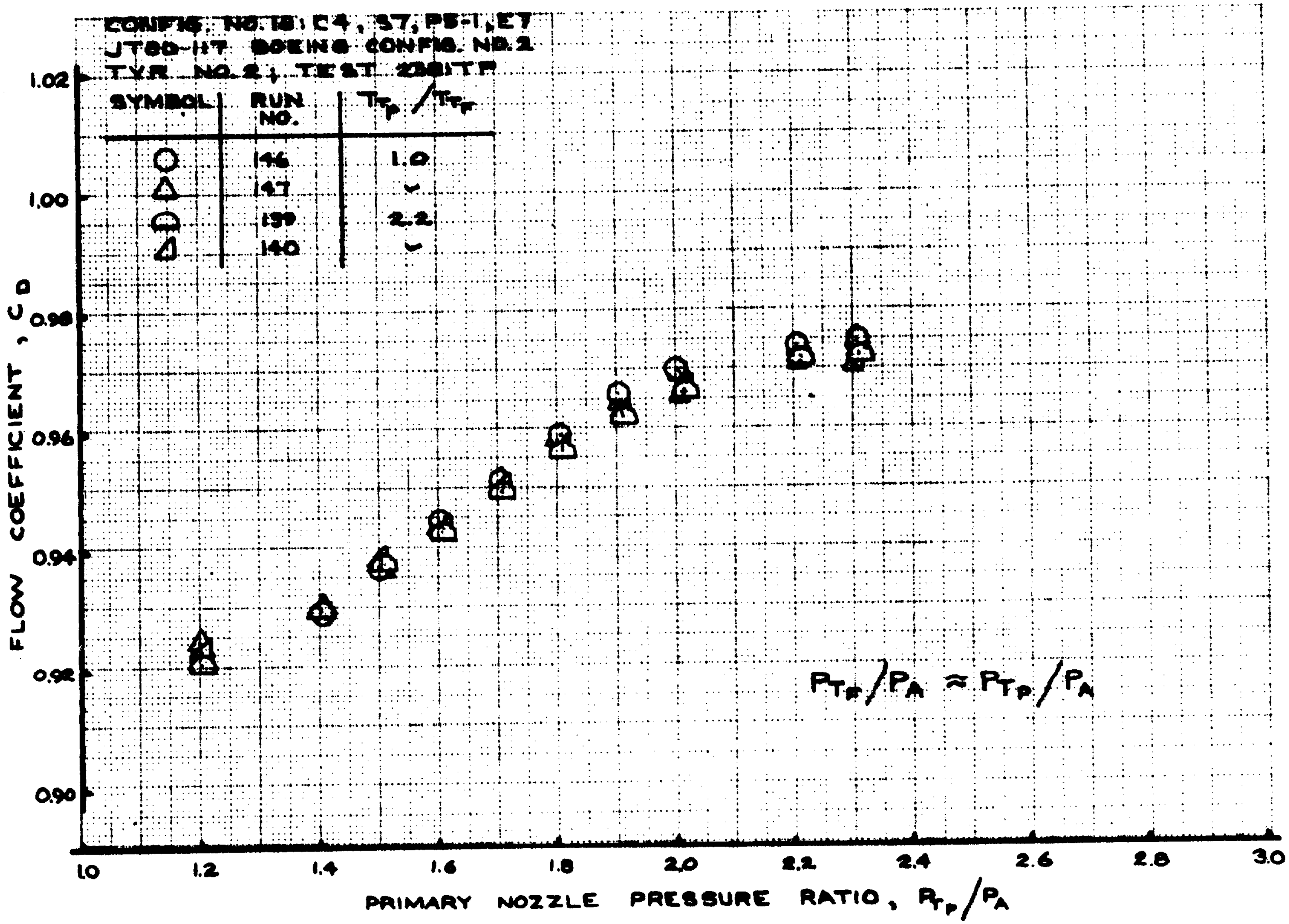

FIGURE 224 - FLOW COEFFICIENT
TEST CONFIG. NO. 18; RUNS 139-140, 146-147

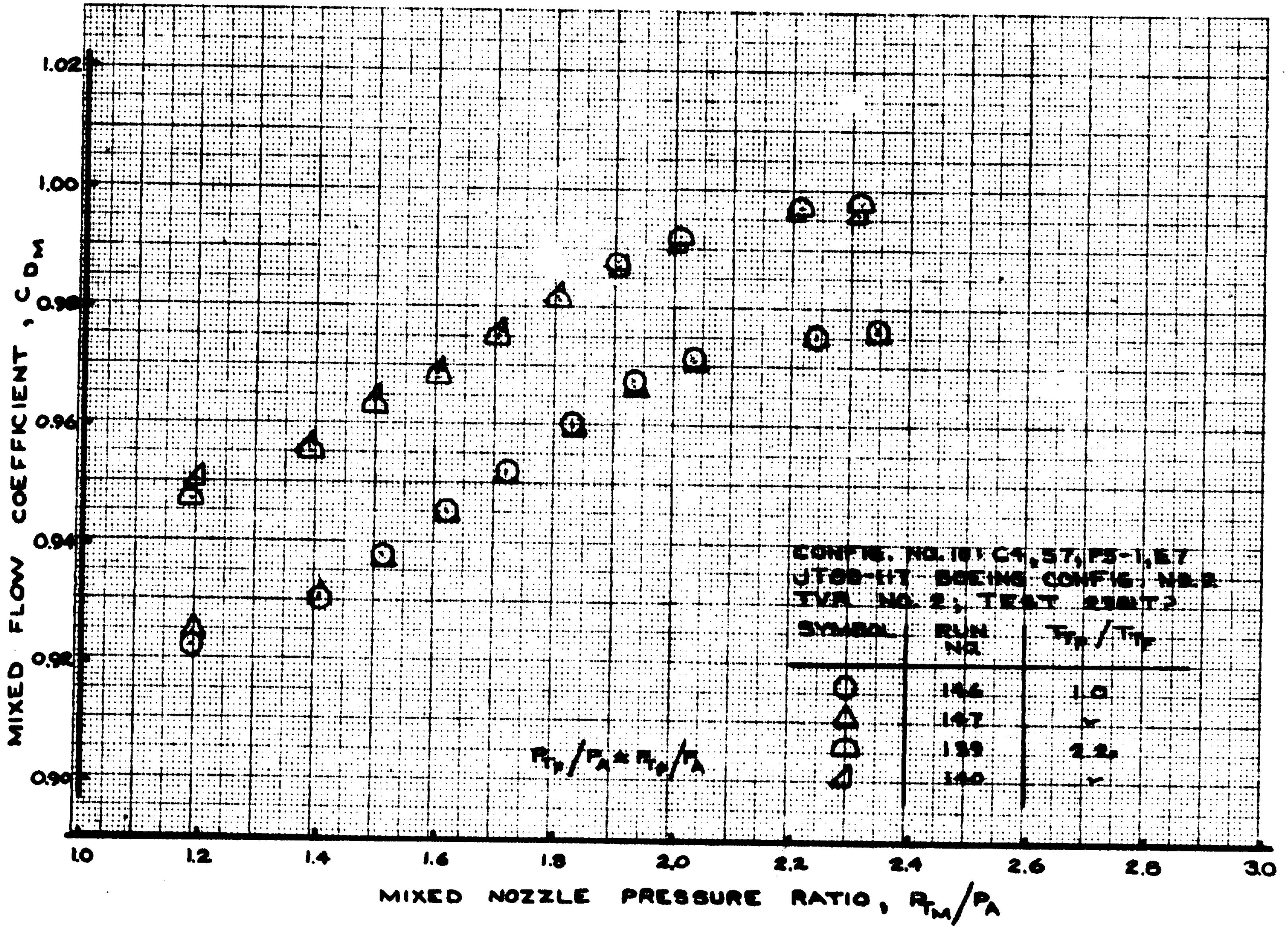

FIGURE 225 - MIXED FLOW COEFFICIENT
TEST CONFIG. NO. 18; RUNS 139-140, 146-147

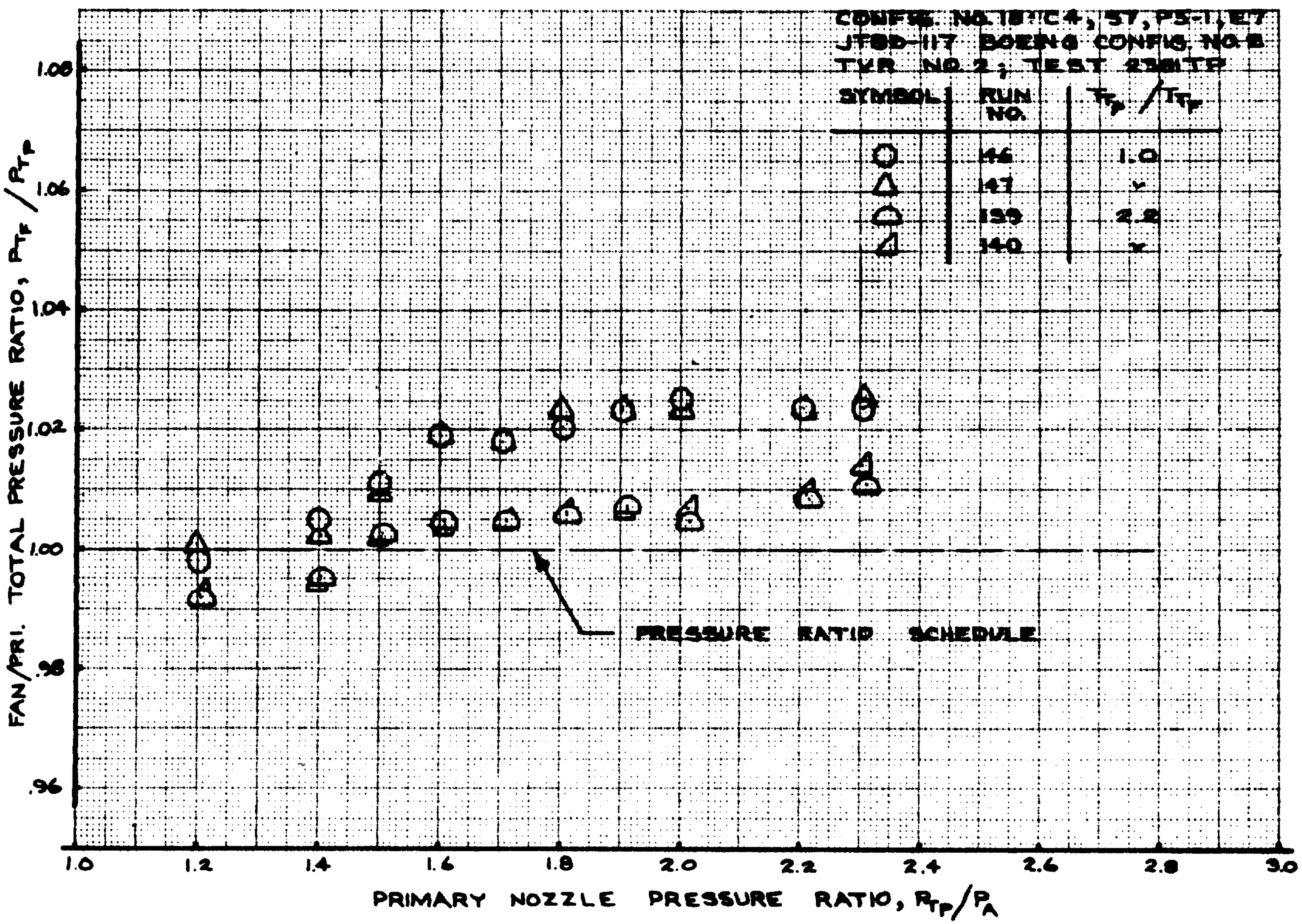

FIGURE 226 - FAN/PRIMARY TOTAL PRESSURE RATIO
TEST CONFIG. NO. 18; RUNS 139-140, 146-147

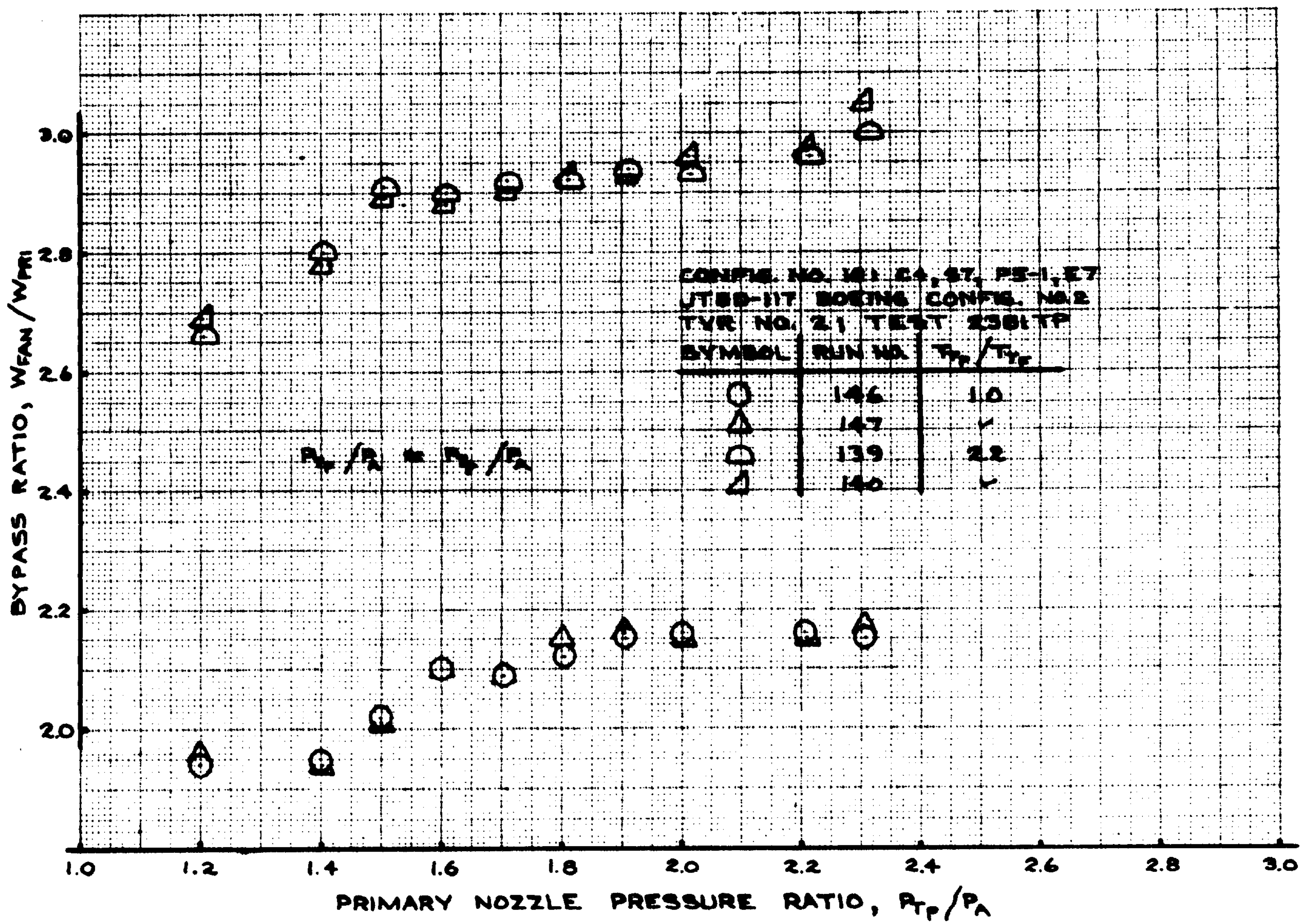

FIGURE 227 - BYPASS RATIO
TEST CONFIG. NO. 18; RUNS 139-140, 146-147

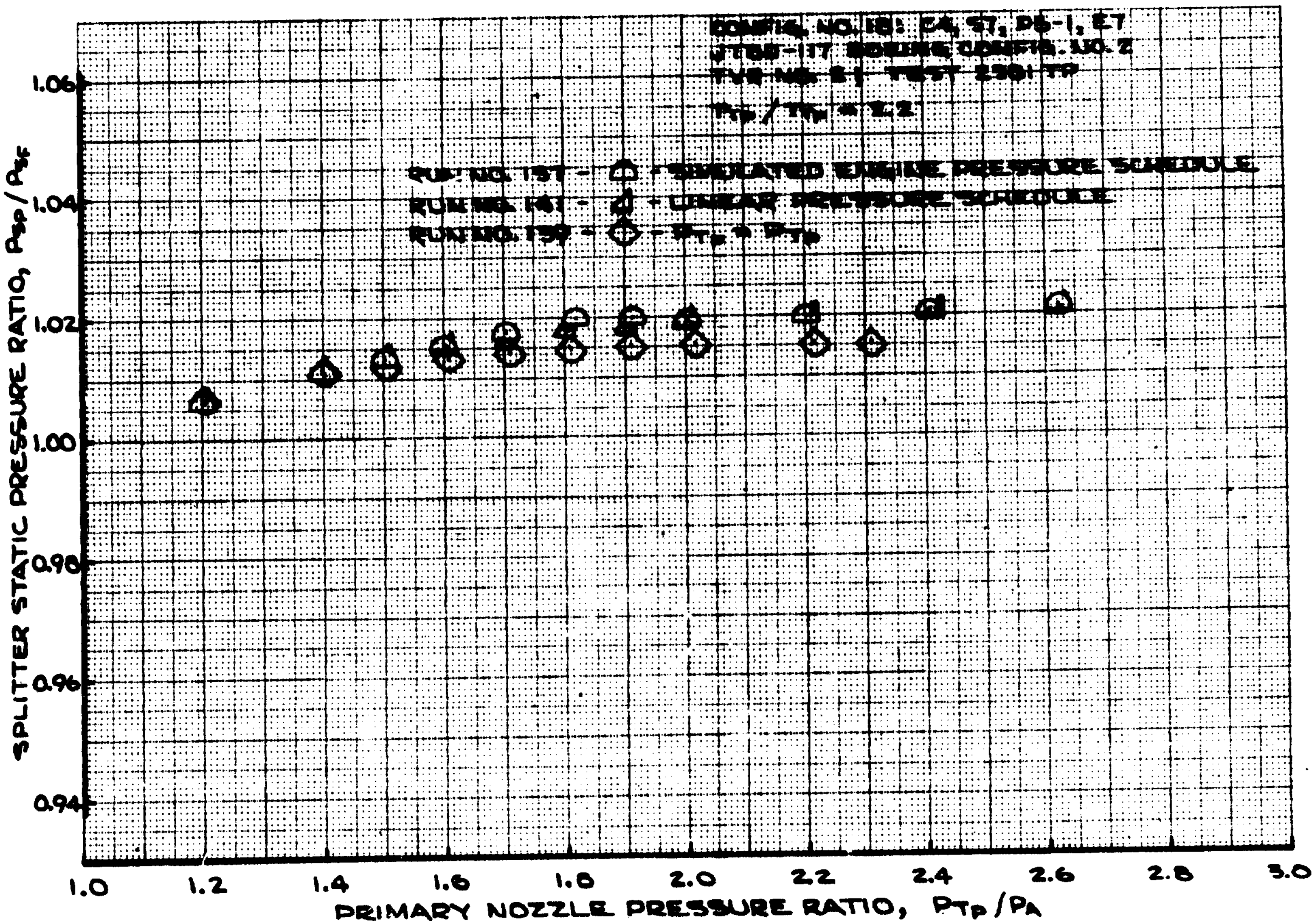

FIGURE 228 - SPLITTER STATIC PRESSURE RATIO
TEST CONFIG. NO.18; RUNS 137, 139, 141

7.2.19 TEST CONFIGURATION (T.C.) NO. 19

Configuration Description: Boeing Config. No. 2 design for JT8D-109 with primary swirl.

Hardware Designations:

Outer Nozzle Wall	Splitter	Plug	Exit
C4	S5	P5-1	E5

Plotted Data:

- Figure 229 - Velocity Coefficient; Runs 226-231.
- Figure 230 - Mixed Velocity Coefficient; Runs 226-231.
- Figure 231 - Flow Coefficient; Runs 226-231.
- Figure 232 - Mixed Flow Coefficient; Runs 226-231.
- Figure 233 - Fan/Primary Total Pressure Ratio; Runs 226-231.
- Figure 234 - Bypass Ratio; Runs 226-231.
- Figure 235 - Splitter Static Pressure Ratio; Run 227.

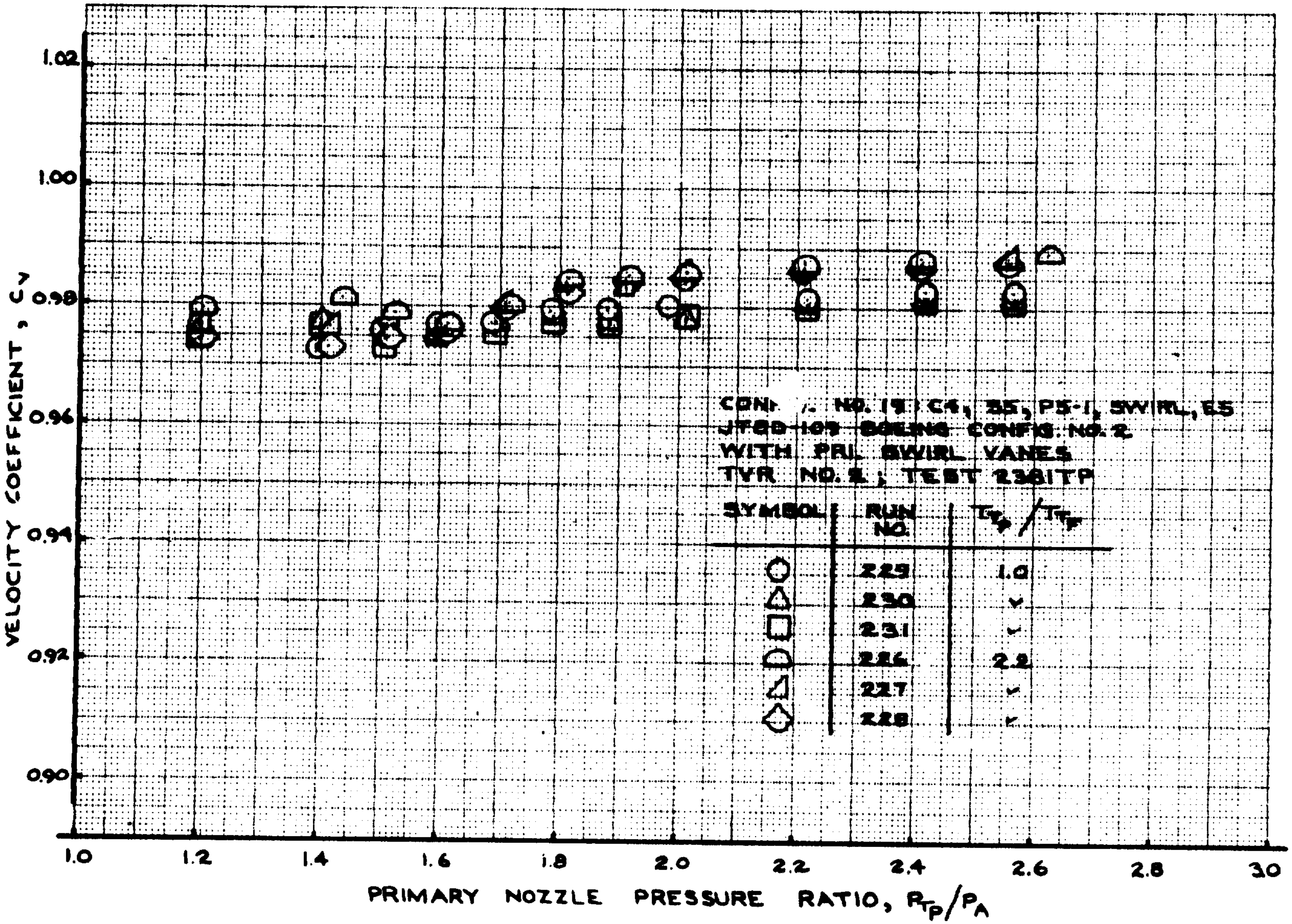

FIGURE 229- VELOCITY COEFFICIENT
TEST CONFIG. NO. 19; RUNS 226-231

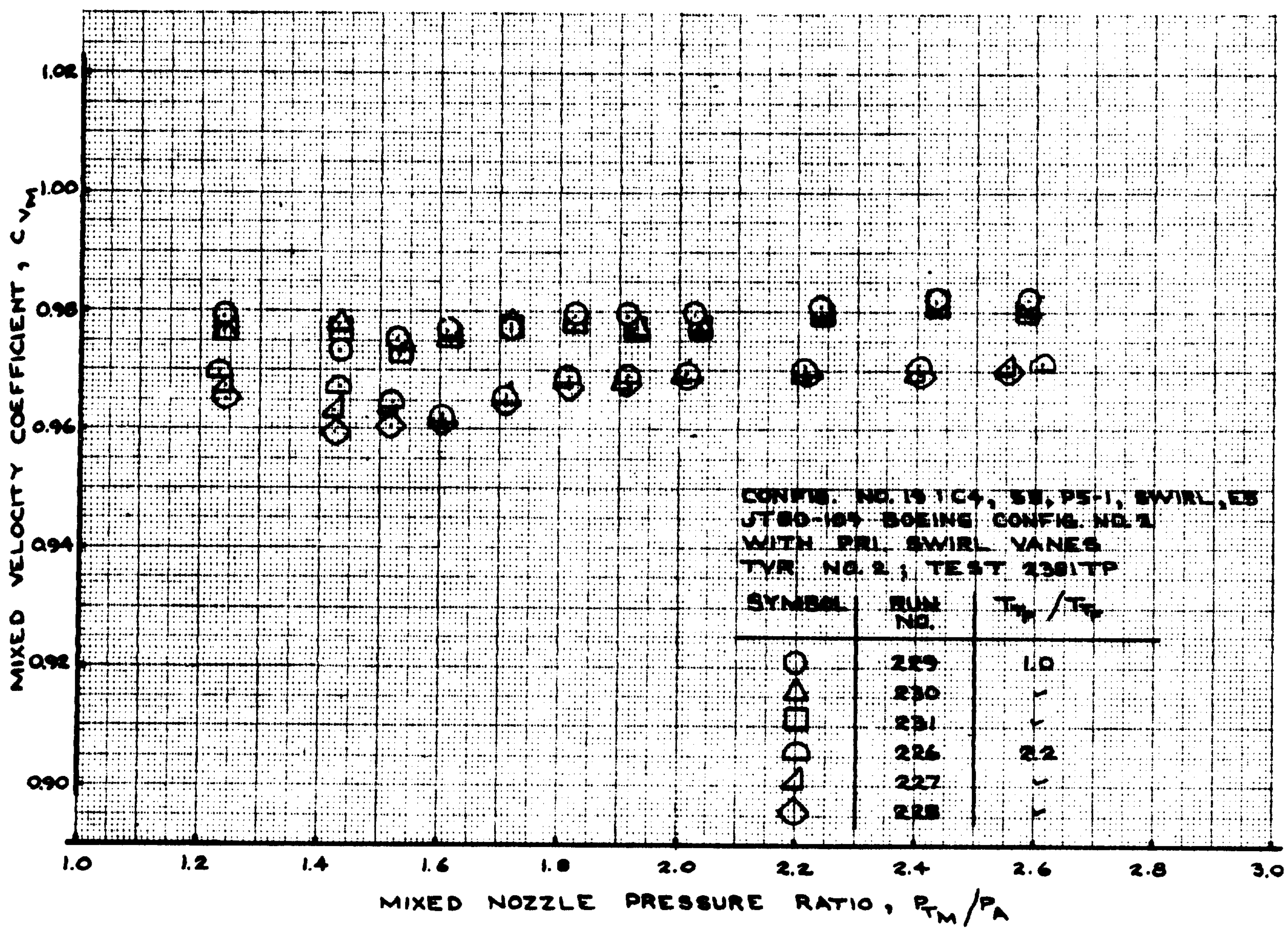

FIGURE 230- MIXED VELOCITY COEFFICIENT
TEST CONFIG. NO. 19; RUNS 226-231

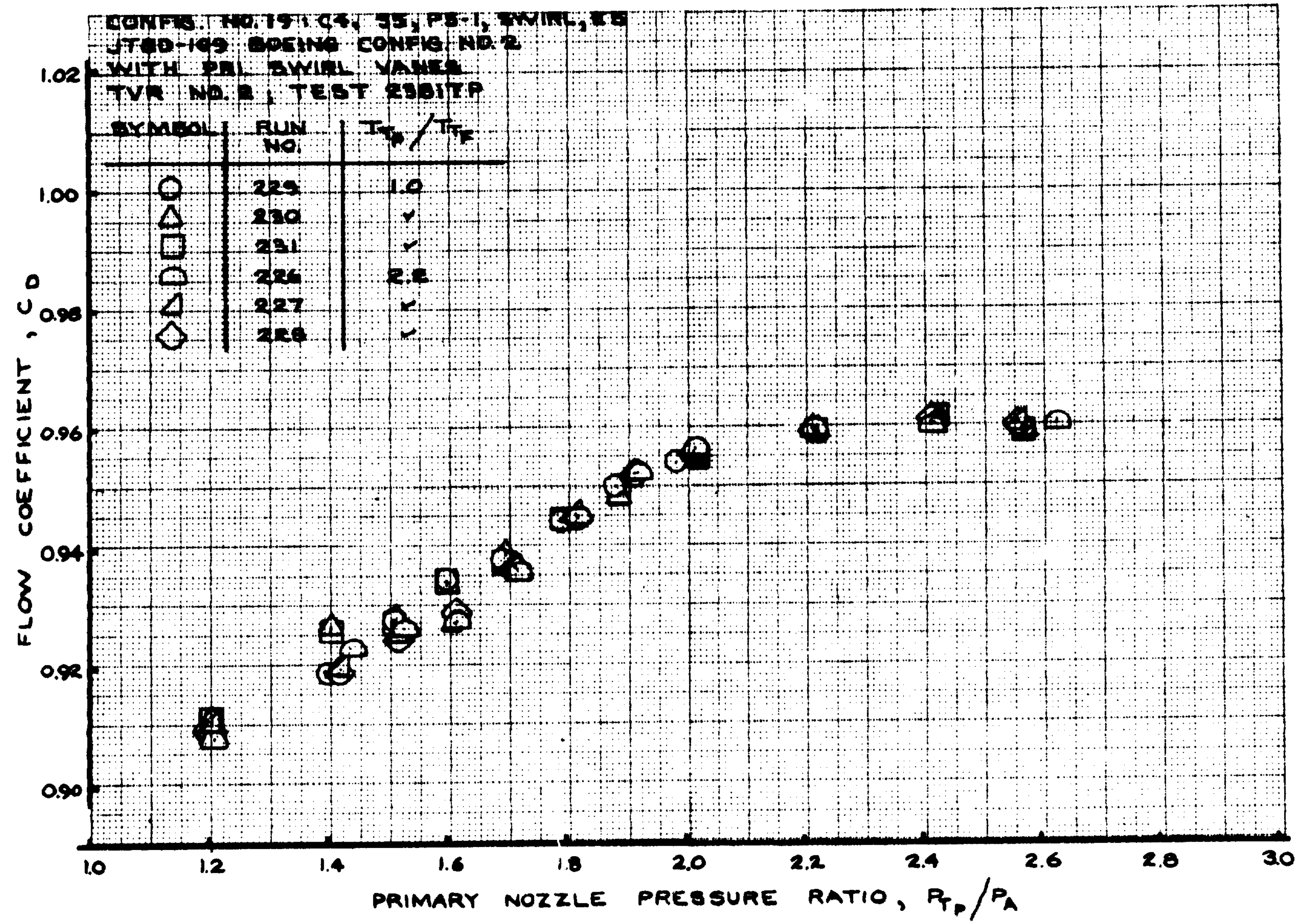

FIGURE 231- FLOW COEFFICIENT
TEST CONFIG. NO. 19; RUNS 226-231

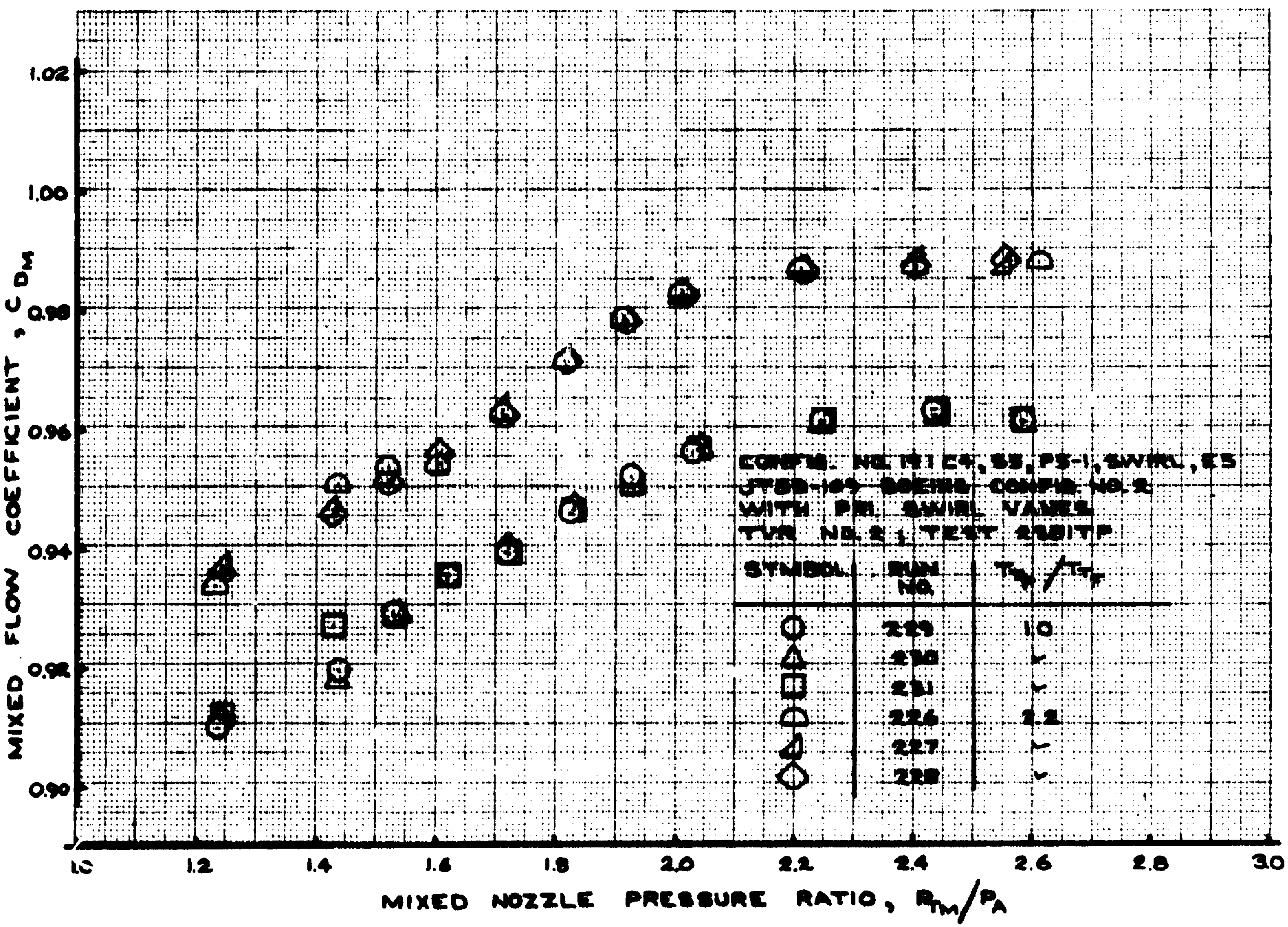

FIGURE 232- MIXED FLOW COEFFICIENT
TEST CONFIG. NO. 19; RUNS 226-231

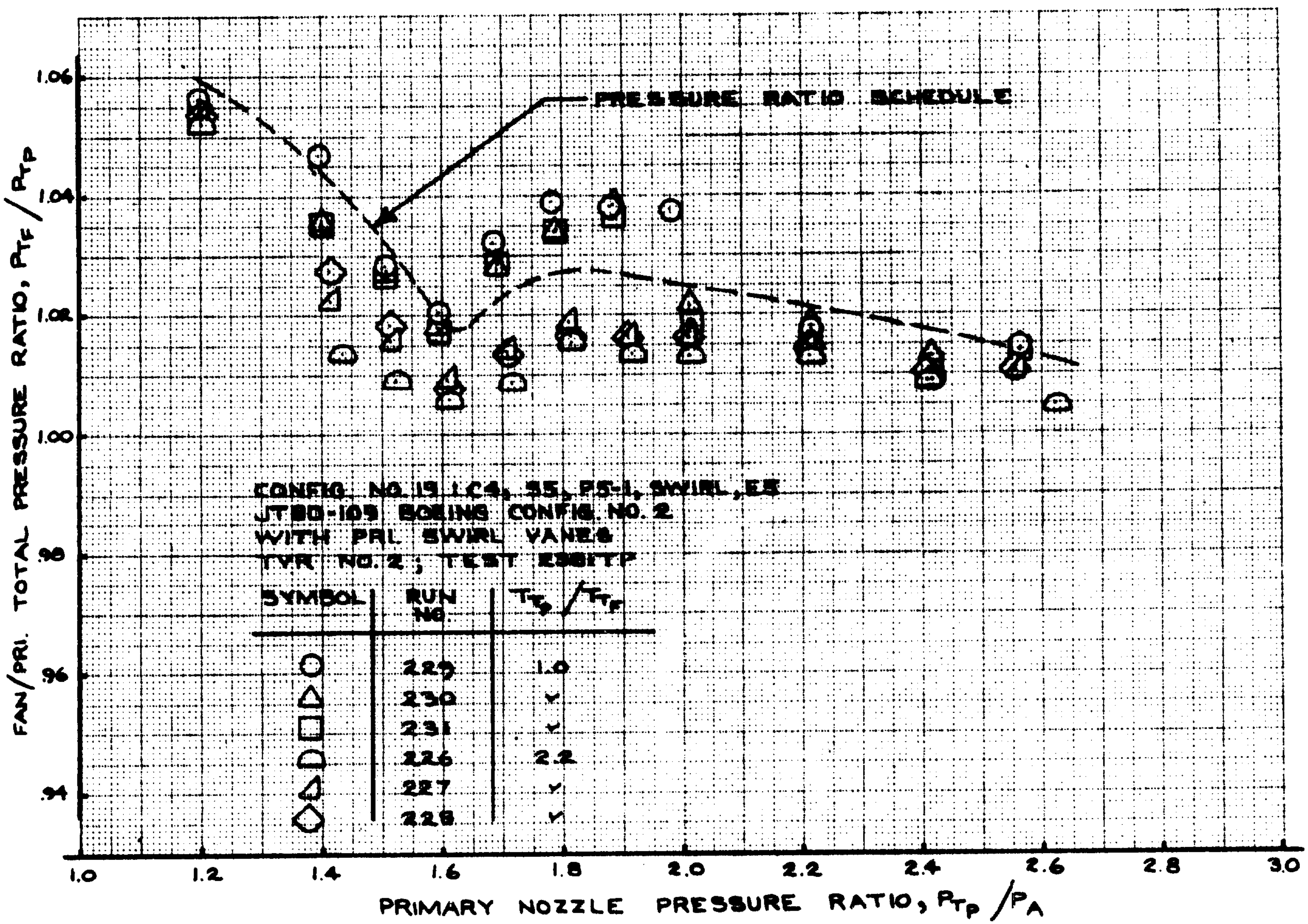

FIGURE 233- FAN/PRIMARY TOTAL PRESSURE RATIO
TEST CONFIG. NO. 19; RUNS 226-231

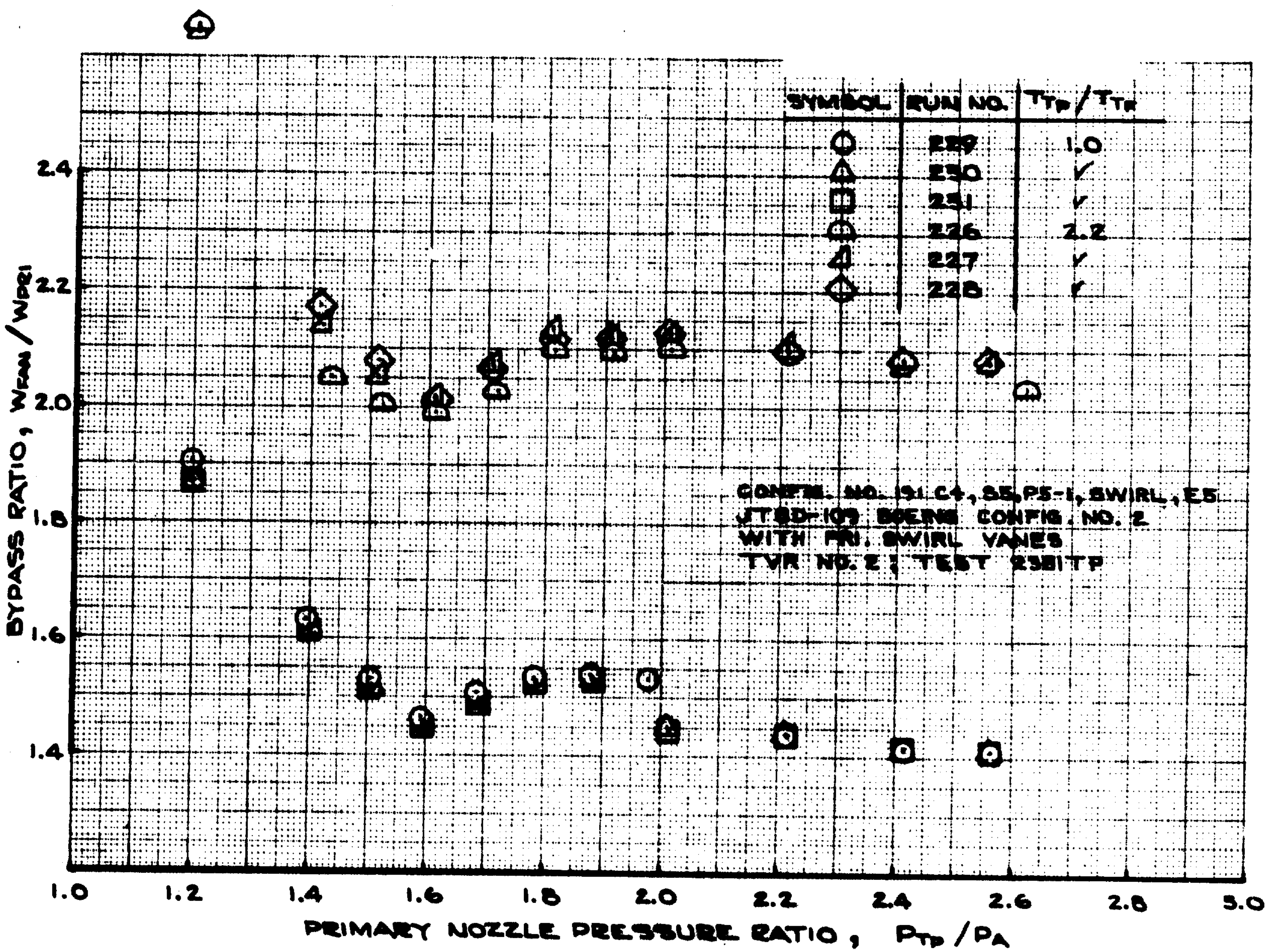

FIGURE 234- BYPASS RATIO
TEST CONFIG. NO. 19; RUNS 226-231

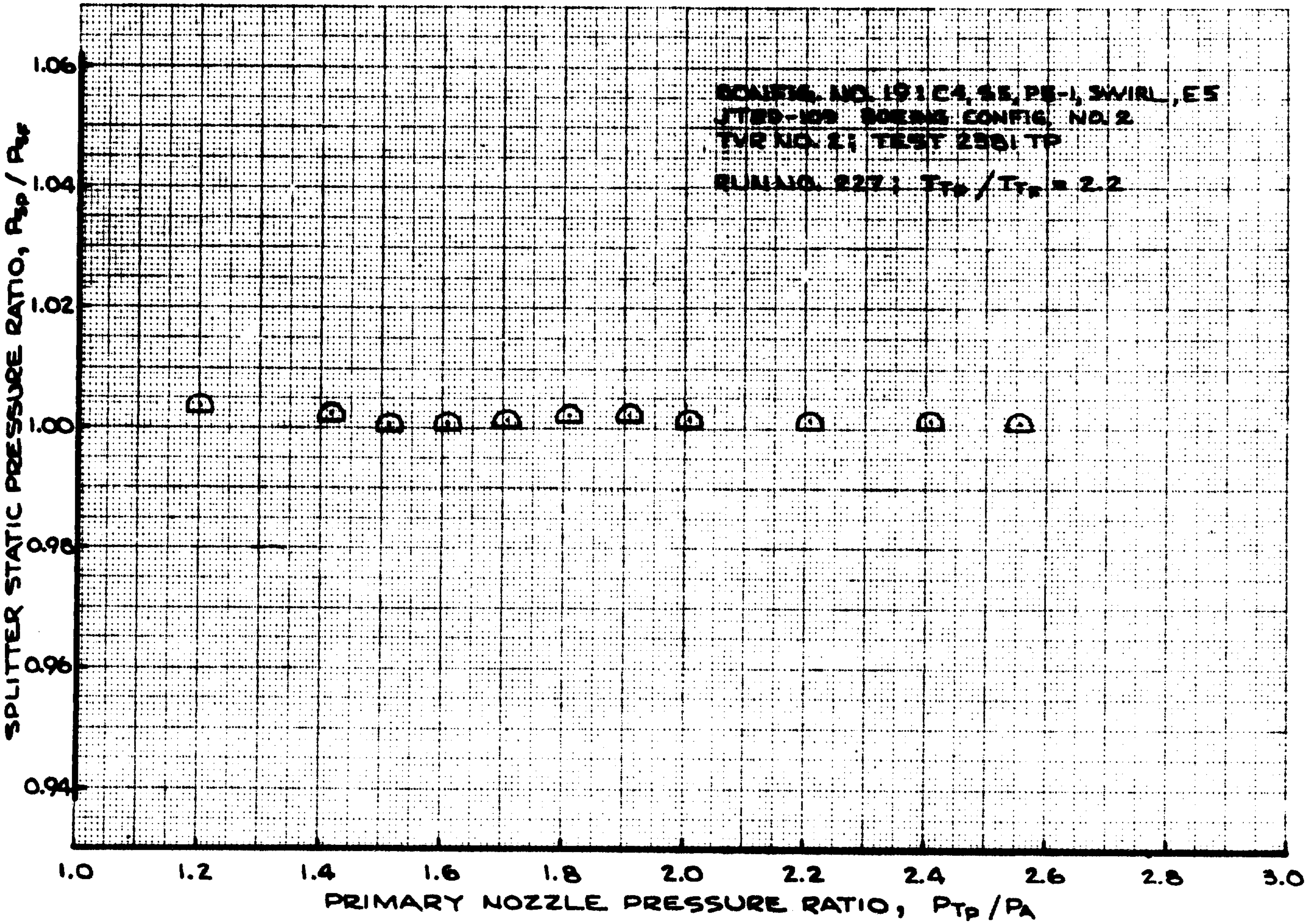

FIGURE 235 - SPLITTER STATIC PRESSURE RATIO
TEST CONFIG. NO. 19; RUN 227

7.3 MIXING PLANE AND EXIT PLANE DATA

7.3.1 MIXING PLANE DATA

A single 0.042-inch diameter total pressure probe was attached to an L. C. Smith, Model No. 2108 actuator. The actuator was mounted to the nozzle outer wall for the JT8D-9/727 production configuration and the P&WA Reference and Boeing configurations for the JT8D-100 engines such that the probe-tip was at an axial position just downstream of the splitter trailing edge. Mixing plane total pressure data were recorded at the following exhaust station planes:

JT8D-9/727 Production (T.C. 2)	EXH STA 1.1
P&WA JT8D-109 Reference (T.C. 3 & 4)	EXH STA 10.9
Boeing JT8D-109 & -115 Config. No. 2 (T.C. 7, 11 & 19)	EXH STA 21.0

Circumferential positioning was accomplished by rotating the nozzle outer wall and the traversing probe mechanism at the forward attach flange of the nozzle. Any angle could be set because of the O-ring seal and clamping flange design. Figure 307, Section 7.4, shows the installation of the L. C. Smith actuator with the total pressure probe at the mixing plane.

The pressure sensed by the total pressure probe was converted to an electrical signal by a gage pressure transducer. This electrical signal was amplified and recorded using an XY-plotter along with the position indication of the probe. Once the nozzle pressure conditions were set (with the fan and primary streams both at ambient temperature conditions), a continuous trace of the mixing plane total pressure was recorded from the outer nozzle wall to the nozzle centerline or plug surface.

Traversing rate of the pressure probe was set at four inches/ minute. Each trace of total pressure versus radius was digitized nearly every 0.09-inch to facilitate data processing by a digital computer to obtain total pressure and Mach number plots versus non-dimensional radial position; i.e., $(R-R_{PL})/(R_{OW}-R_{PL})$. Mach numbers along the radial traverse were calculated using the average static pressure near the splitter trailing edge. The splitter static pressure of the primary stream was used for Mach number calculations from the plug wall or centerline to the splitter radius while the splitter fan stream static pressure was used to calculate the Mach numbers from the splitter to the nozzle outer wall. Static pressure data was not obtained for the JT8D-9/727 configuration (T.C. 2) and, hence, the Mach number data could not be generated. The following is a tabulation of the mixing plane data obtained:

Test Config. & No.	P_T/P_A Figure No.	Mach No. Figure No.	Traversing Probe Location (Degrees measured clockwise from top - rear view)
2. JT8D-9/727 Production	236 237 238	N.A. N.A. N.A.	270 135 45
3. P&WA JT8D-109 Reference	239 241 243	240 242 244	270 150 30
7. Boeing JT8D-109 Config. No. 2	245 247 249	246 248 250	270 150 30
11. Boeing JT8D-115 Config. No. 2	251 253 255	252 254 256	270 150 30
4. P&WA JT8D-109 Reference with Pri. Swirl Vanes	257 259 261	258 260 262	270 150 30
19. Boeing JT8D-109 Config. No. 2 with Pri. Swirl Vanes	263 265 267	264 266 268	270 150 30

Summarizing the above figures, it can be stated that:

1. The measured splitter wake location matches the geometric splitter location within 4% of the distance from the nozzle wall to the plug surface, and it is not necessarily the same magnitude at each probe circumferential position. This may be due to non-concentricity of the model hardware, non-symmetry of the flows entering the instrumentation section, errors in determining true probe location or all three.

2. In general, the Mach numbers on the fan side of the splitter trailing edge do not decrease as much as the primary flow Mach numbers when the primary pressure ratio is decreased. This is due to the fan-to-primary pressure ratio schedule used to simulate the engine cycle.

3. The swirl vanes in the primary flow do not appreciably affect the location of the minimum total pressure in the wake of the splitter trailing edge. Mach numbers and total pressures near the plug or centerline are questionable as the swirl angles are too large for internally chamfered total pressure probes to record the true total pressure. Section 5.7 presents total pressure profiles which were recorded with the total probe aligned with the flow direction.

4. The wake profiles from the splitter do not match the geometric splitter location for the configurations listed, indicating the stream flows do not satisfy the Kutta condition at the trailing edge of the splitter. This supports the flow mismatch situation discussed in Section 5.6.

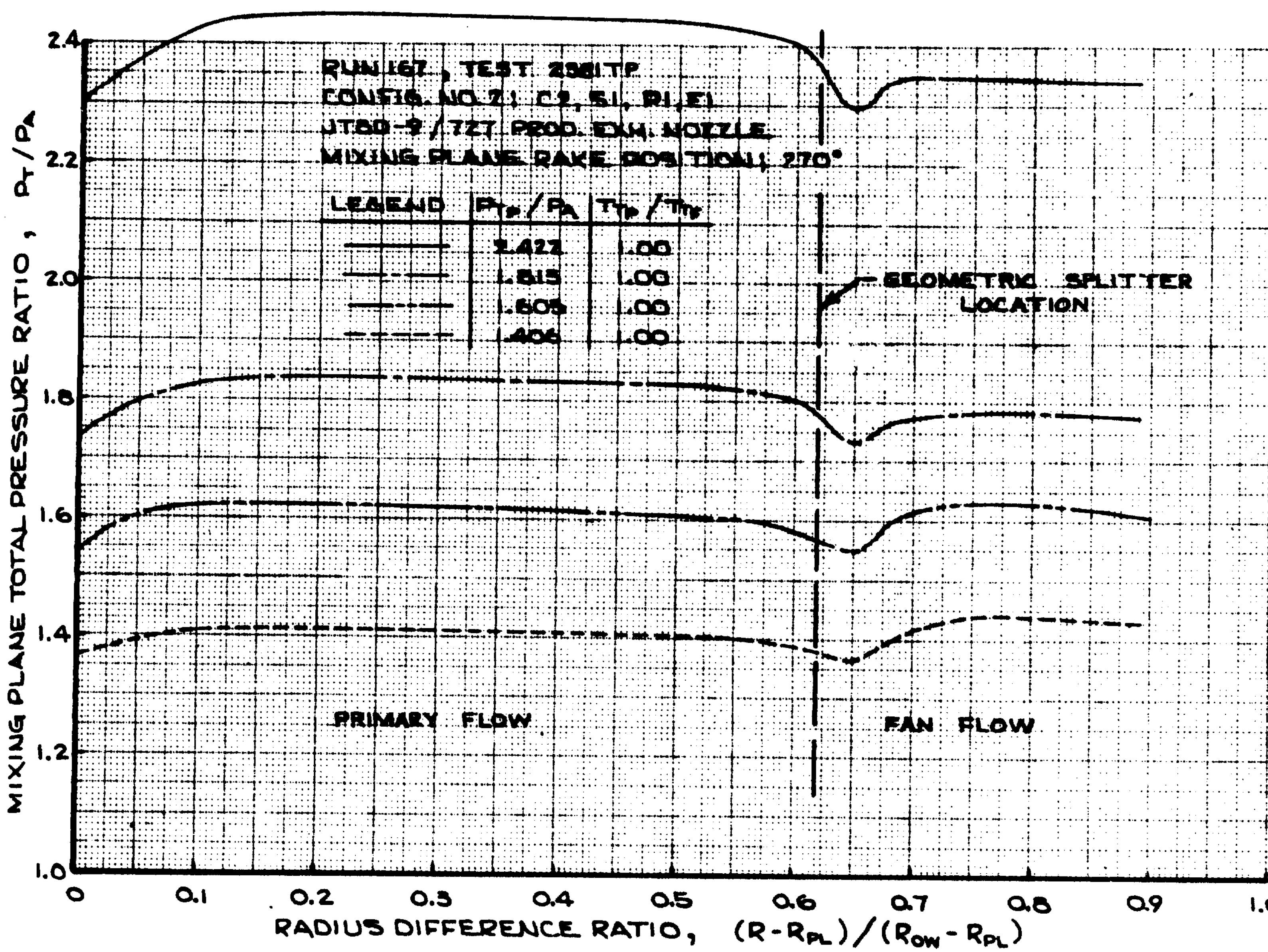

FIGURE 236- MIXING PLANE TOTAL PRESSURE RATIO PROFILES
TEST CONFIG. NO. 2; TRAVERSING PROBE LOCATION - 270 DEG.

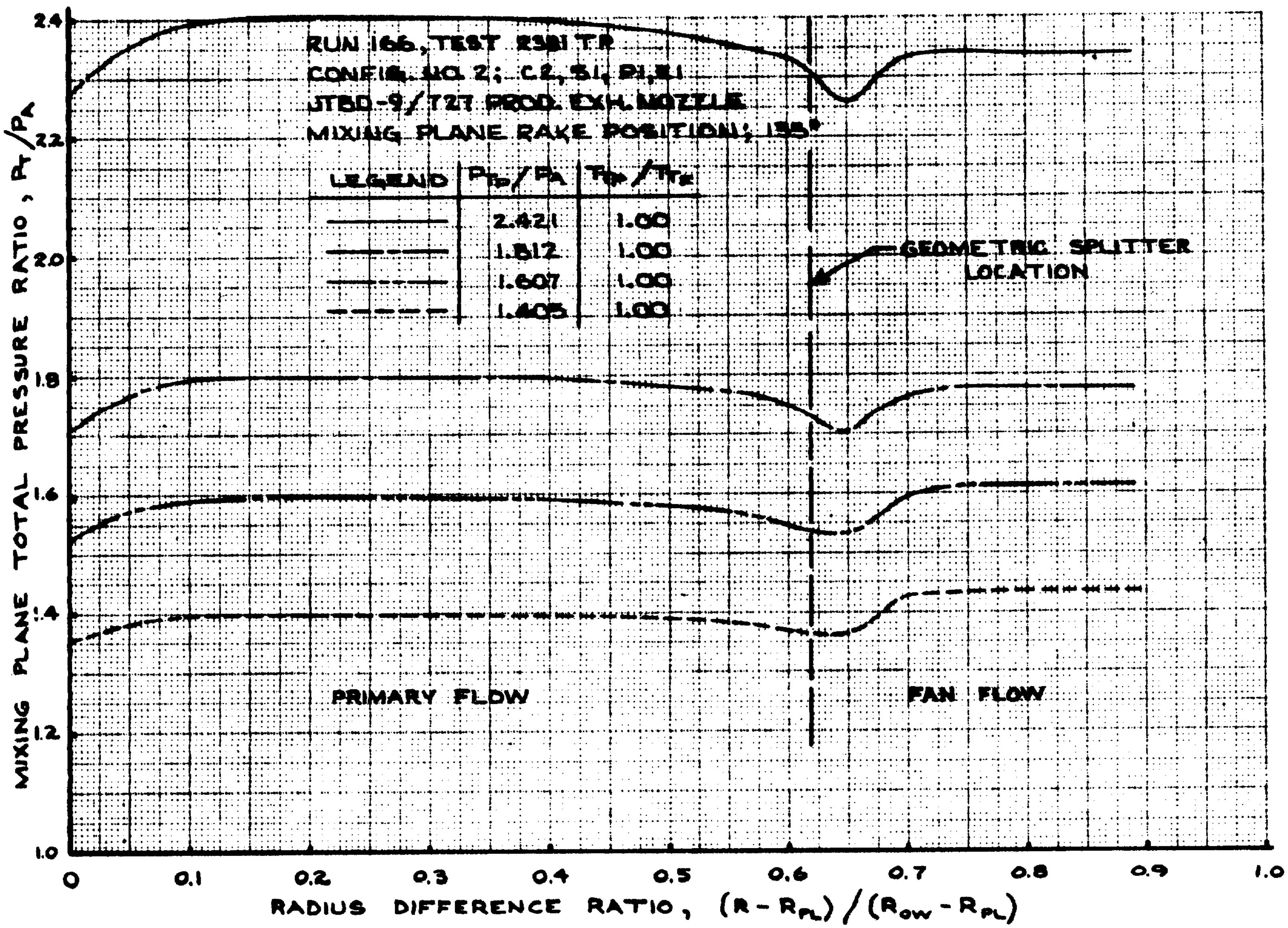

FIGURE 237- MIXING PLANE TOTAL PRESSURE RATIO PROFILES
TEST CONFIG. NO. 2; TRAVERSING PROBE LOCATION - 135 DEG.

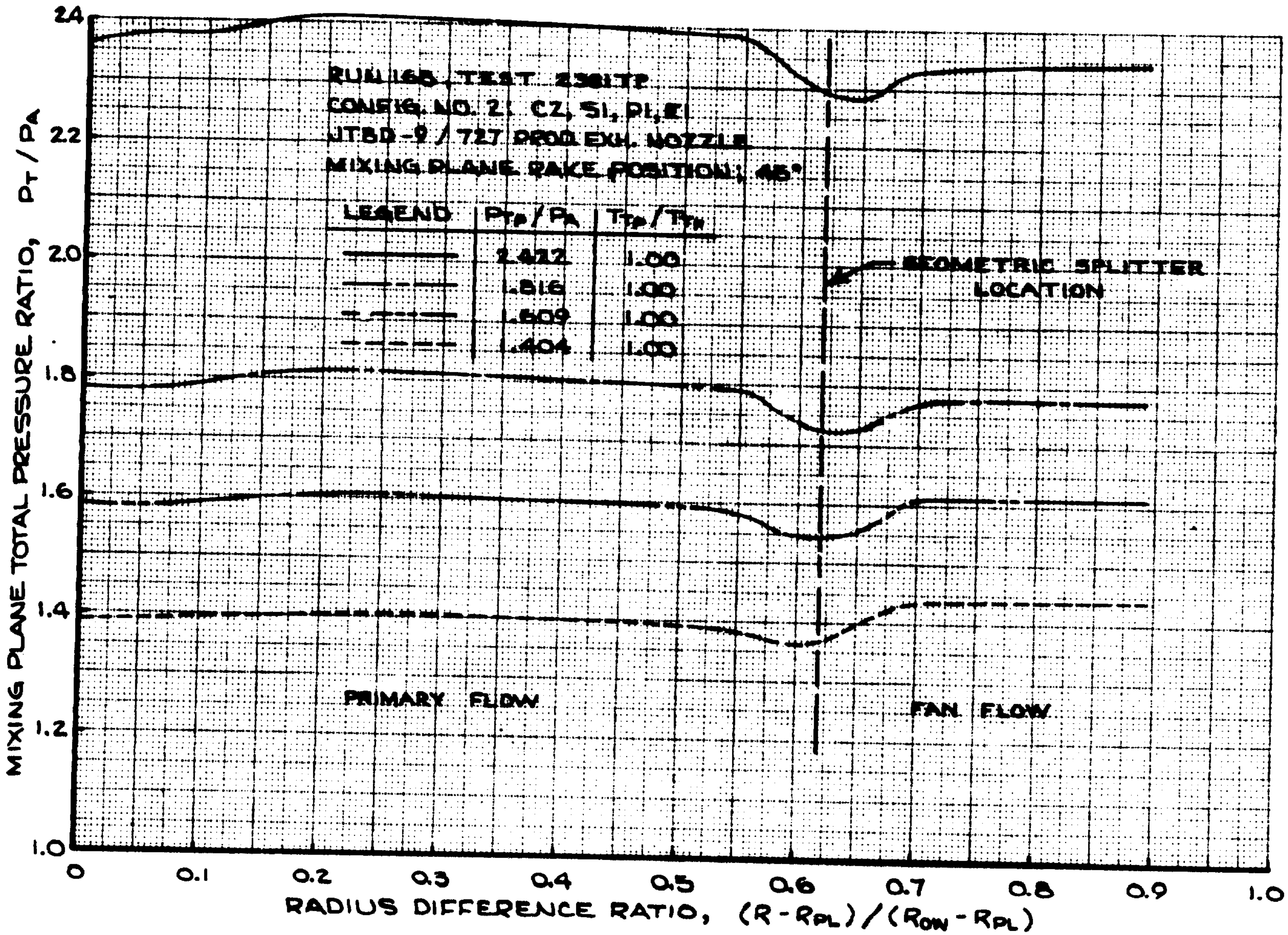

FIGURE 238- MIXING PLANE TOTAL PRESSURE RATIO PROFILES
TEST CONFIG. NO. 2; TRAVERSING PROBE LOCATION - 45 DEG.

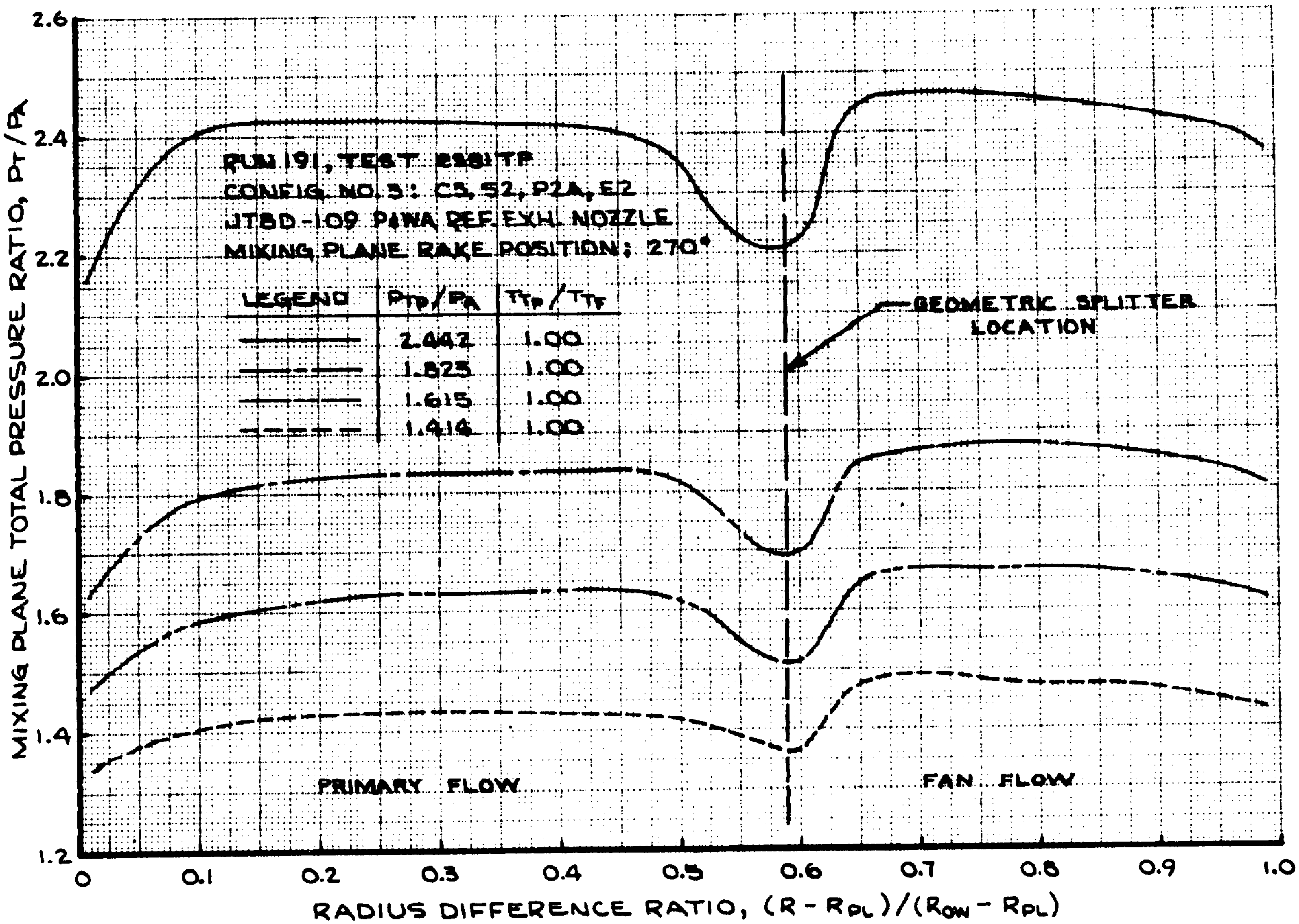

FIGURE 239- MIXING PLANE TOTAL PRESSURE RATIO PROFILES
TEST CONFIG. NO. 3; TRAVERSING PROBE LOCATION - 270 DEG.

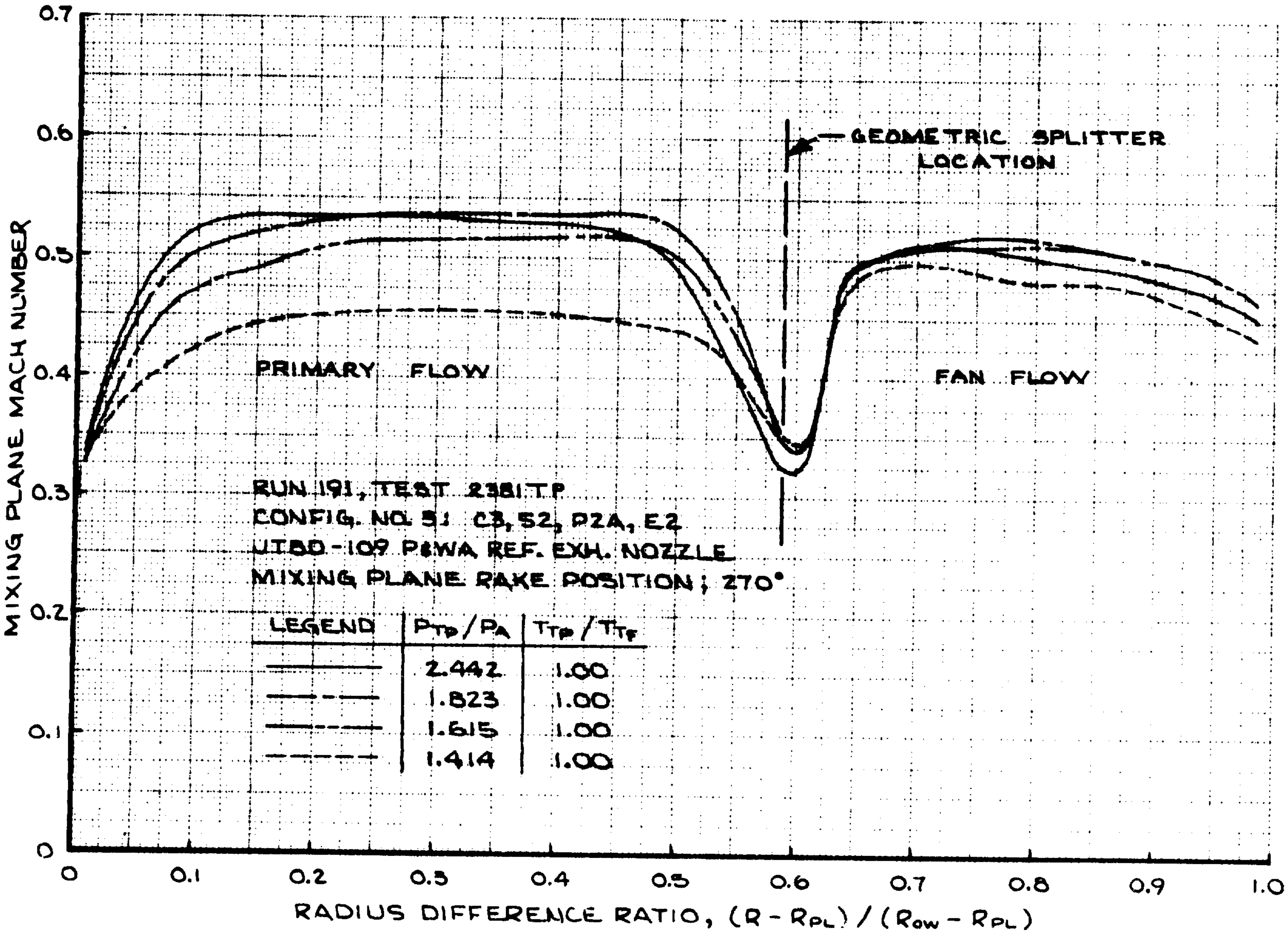

FIGURE 240- MIXING PLANE MACH NO. PROFILES
TEST CONFIG. NO. 3; TRAVERSING PROBE LOCATION - 270 DEG.

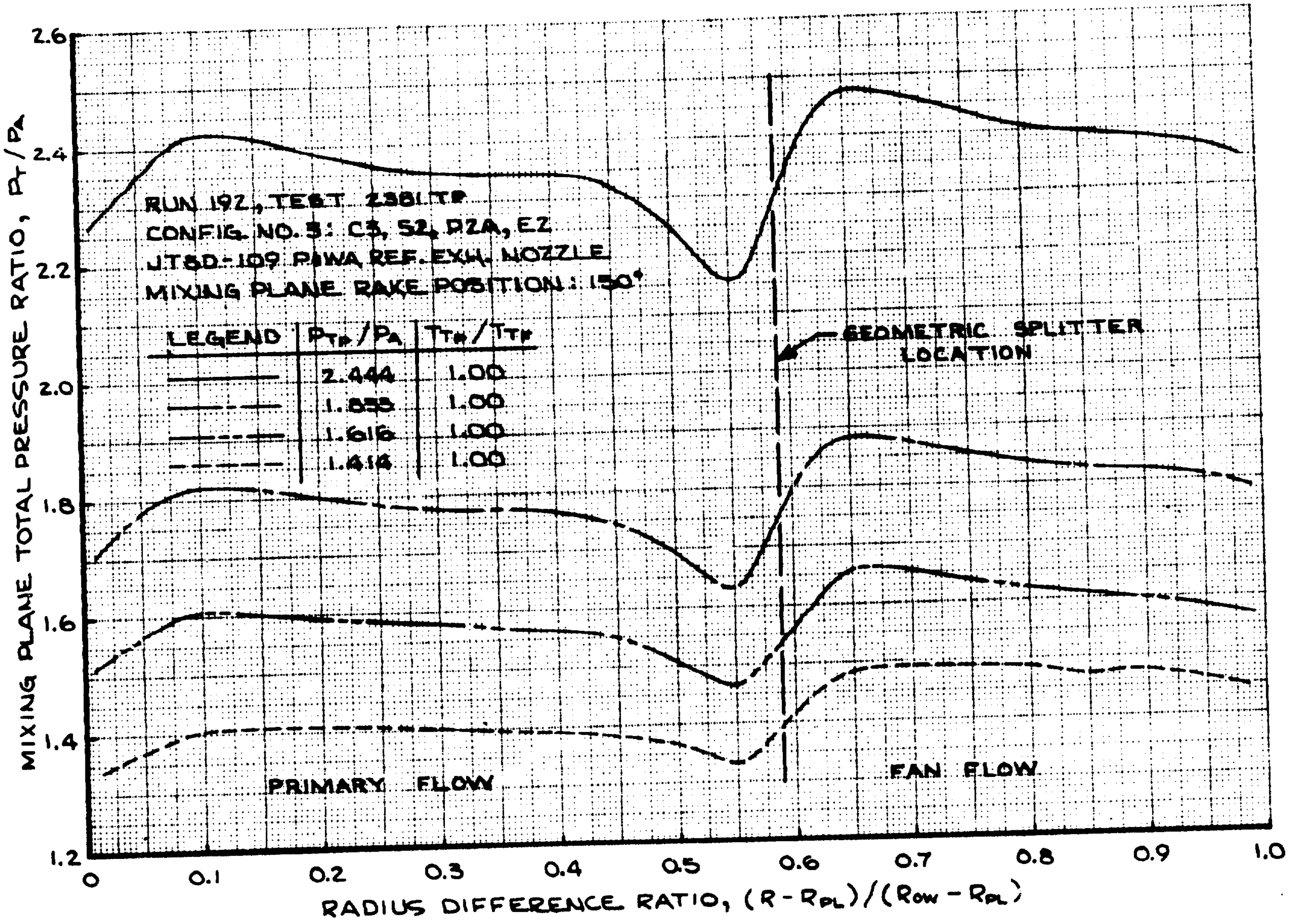

FIGURE 241- MIXING PLANE TOTAL PRESSURE RATIO PROFILES
TEST CONFIG. NO. 3: TRAVERSING PROBE LOCATION - 150 DEG.

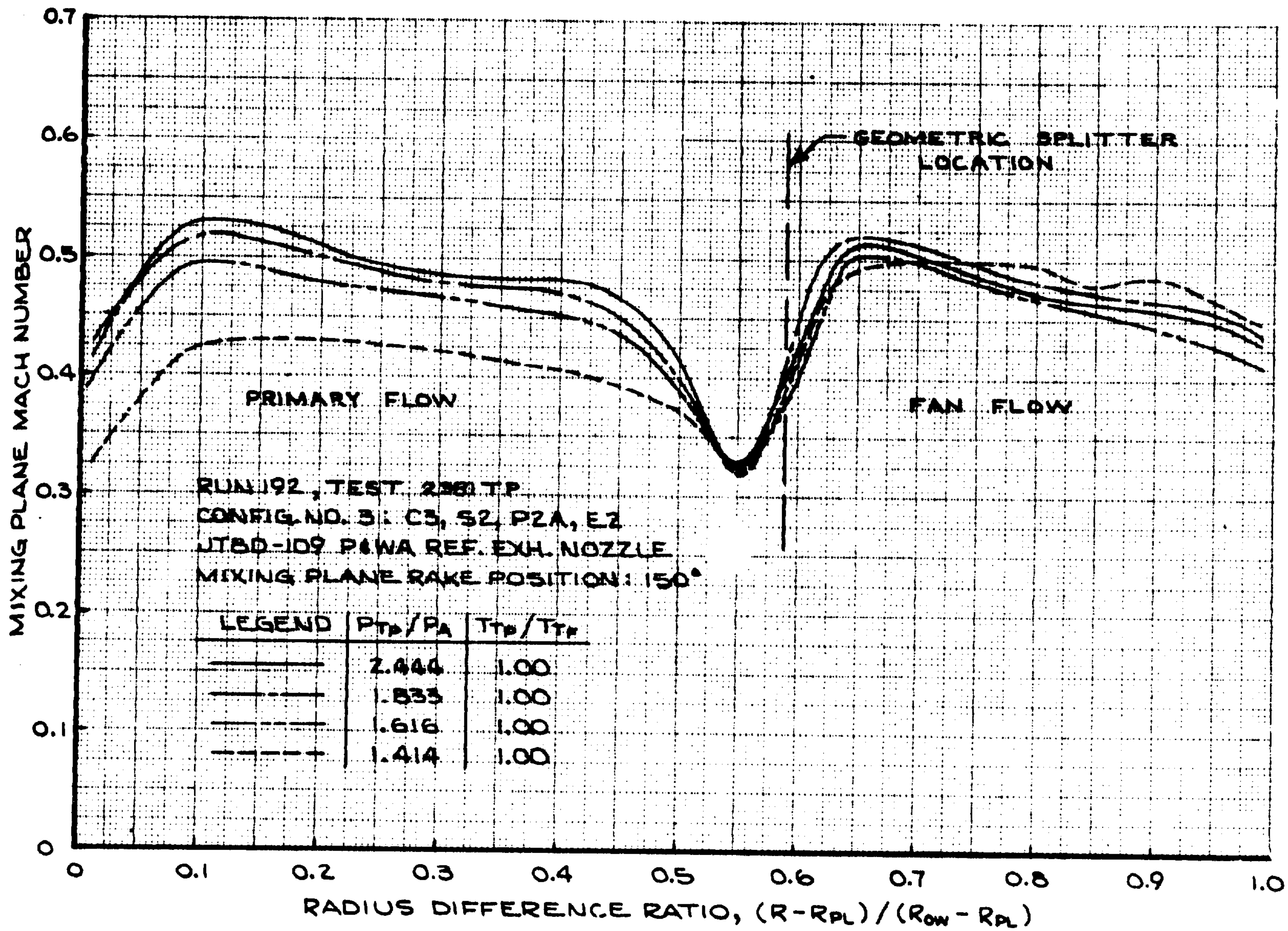

FIGURE 242- MIXING PLANE MACH NO. PROFILES
TEST CONFIG. NO. 3; TRAVERSING PROBE LOCATION - 150 DEG.

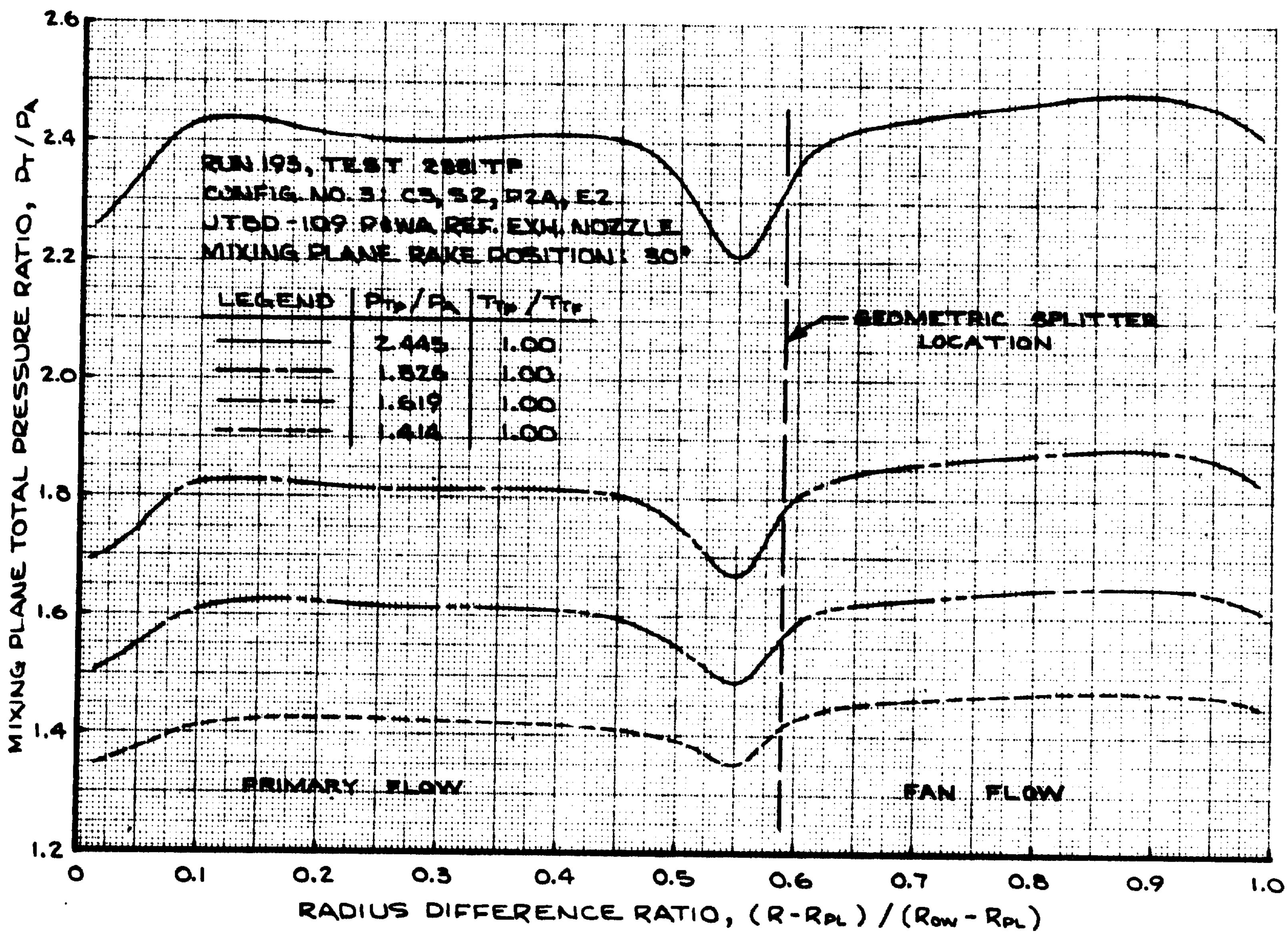

FIGURE 243. MIXING PLANE TOTAL PRESSURE RATIO PROFILES
TEST CONFIG. NO. 3; TRAVERSING PROBE LOCATION - 30 DEG.

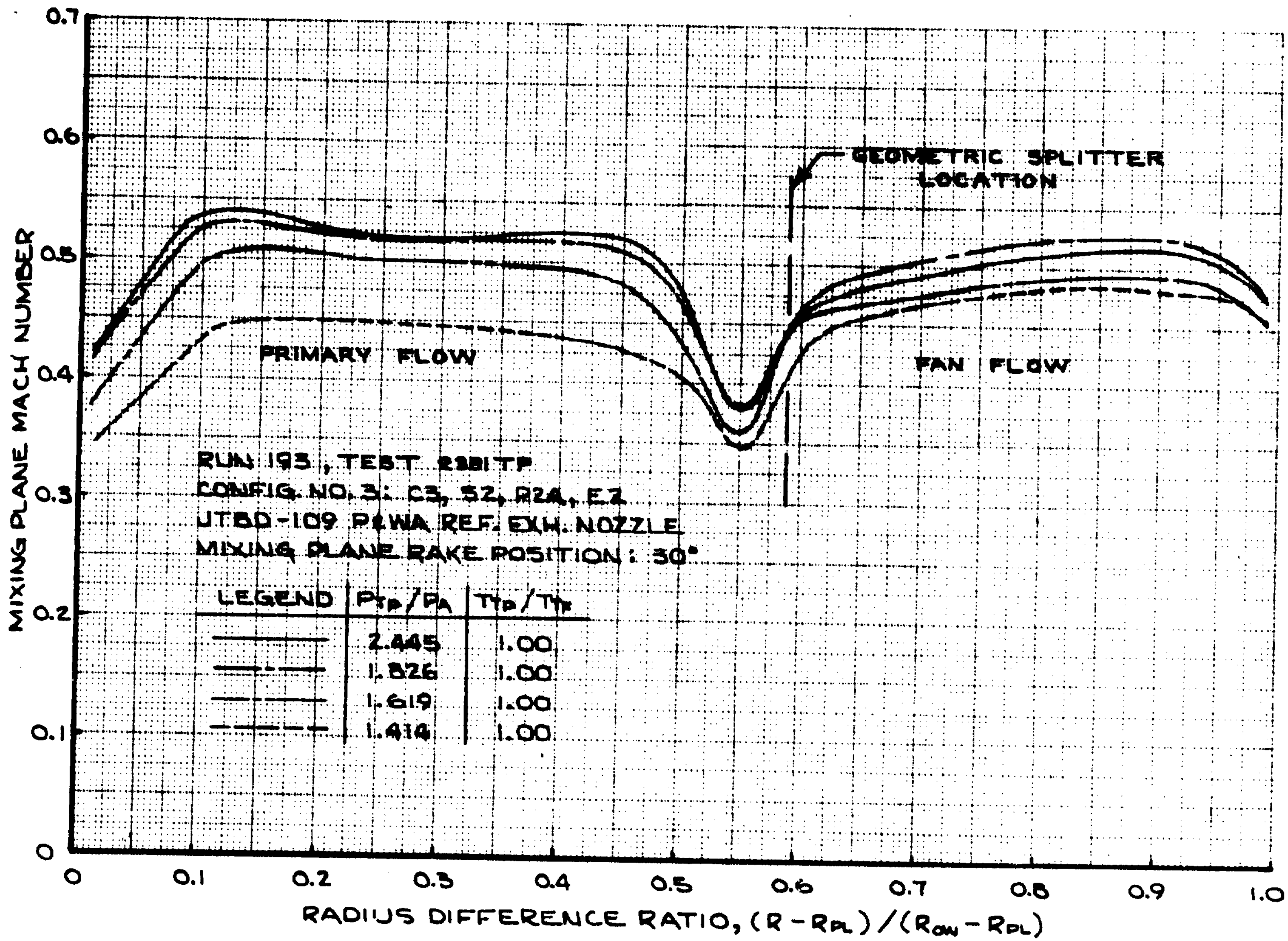

FIGURE 244- MIXING PLANE MACH NO. PROFILES
TEST CONFIG. NO. 3; TRAVERSING PROBE LOCATION - 30 DEG.

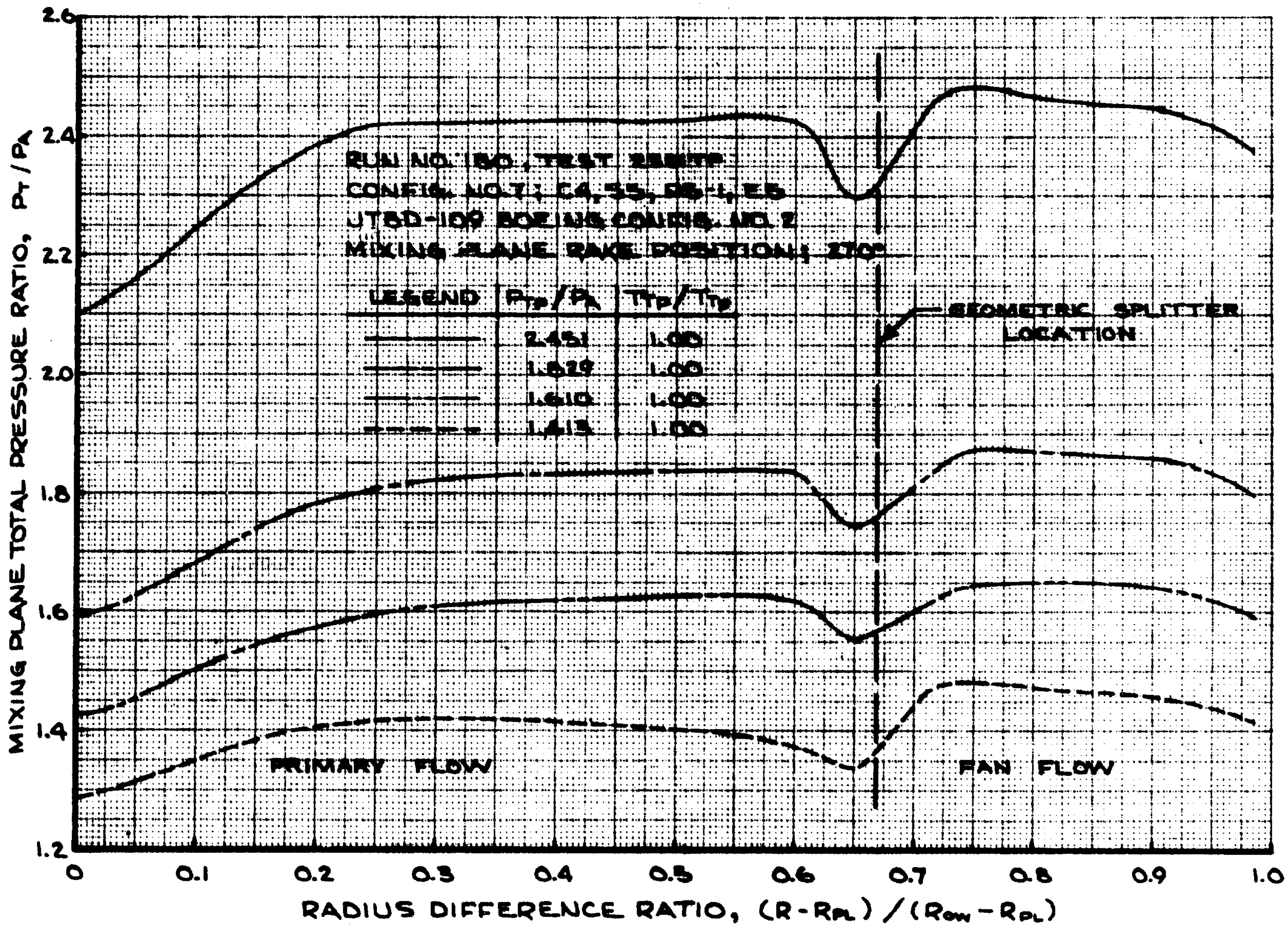

FIGURE 245- MIXING PLANE TOTAL PRESSURE RATIO PROFILES
TEST CONFIG. NO. 7; TRAVERSING PROBE LOCATION - 270 DEG.

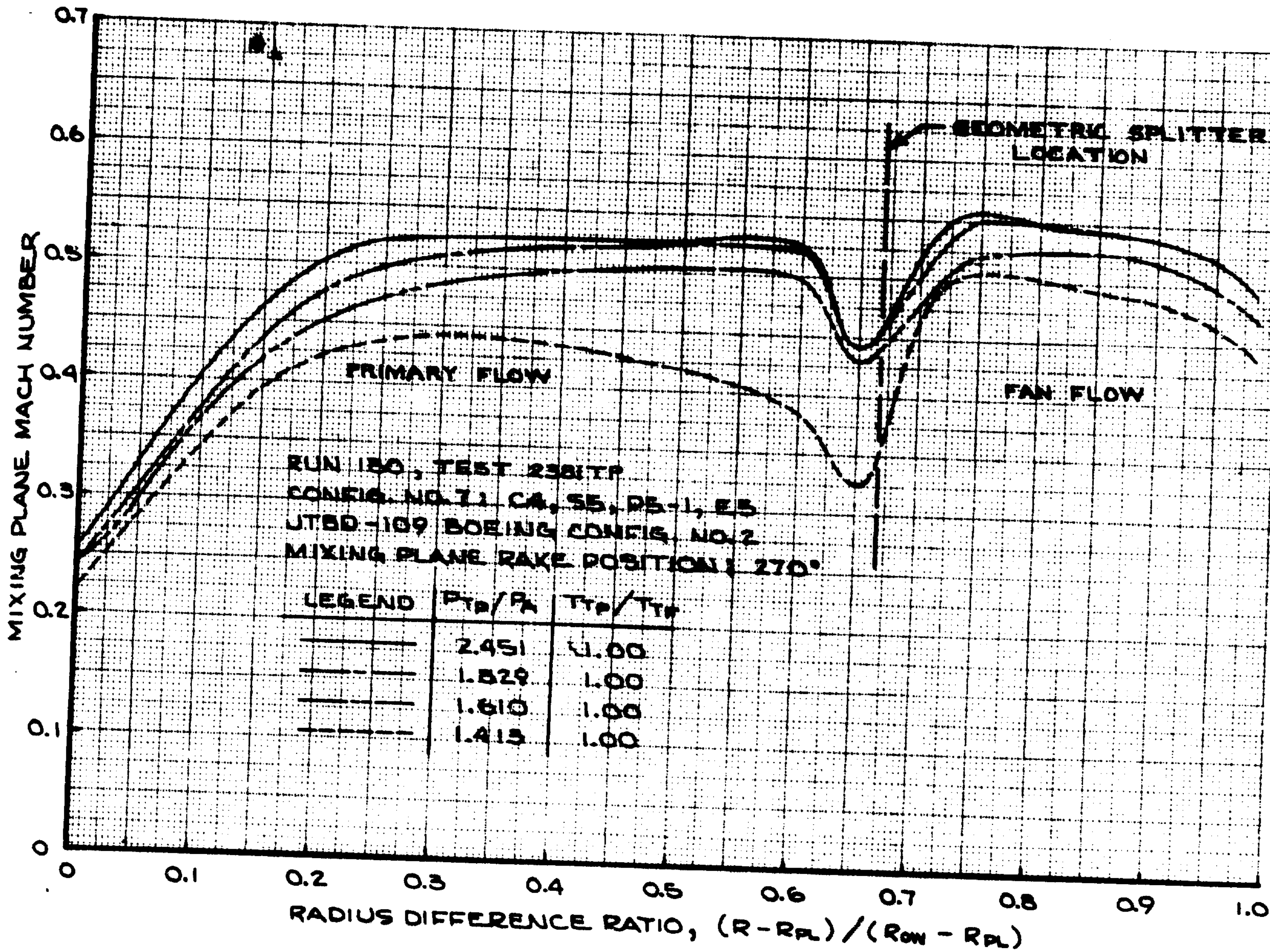

FIGURE 246- MIXING PLANE MACH NO. PROFILES
TEST CONFIG. NO. 7; TRAVERSING PROBE LOCATION - 270 DEG.

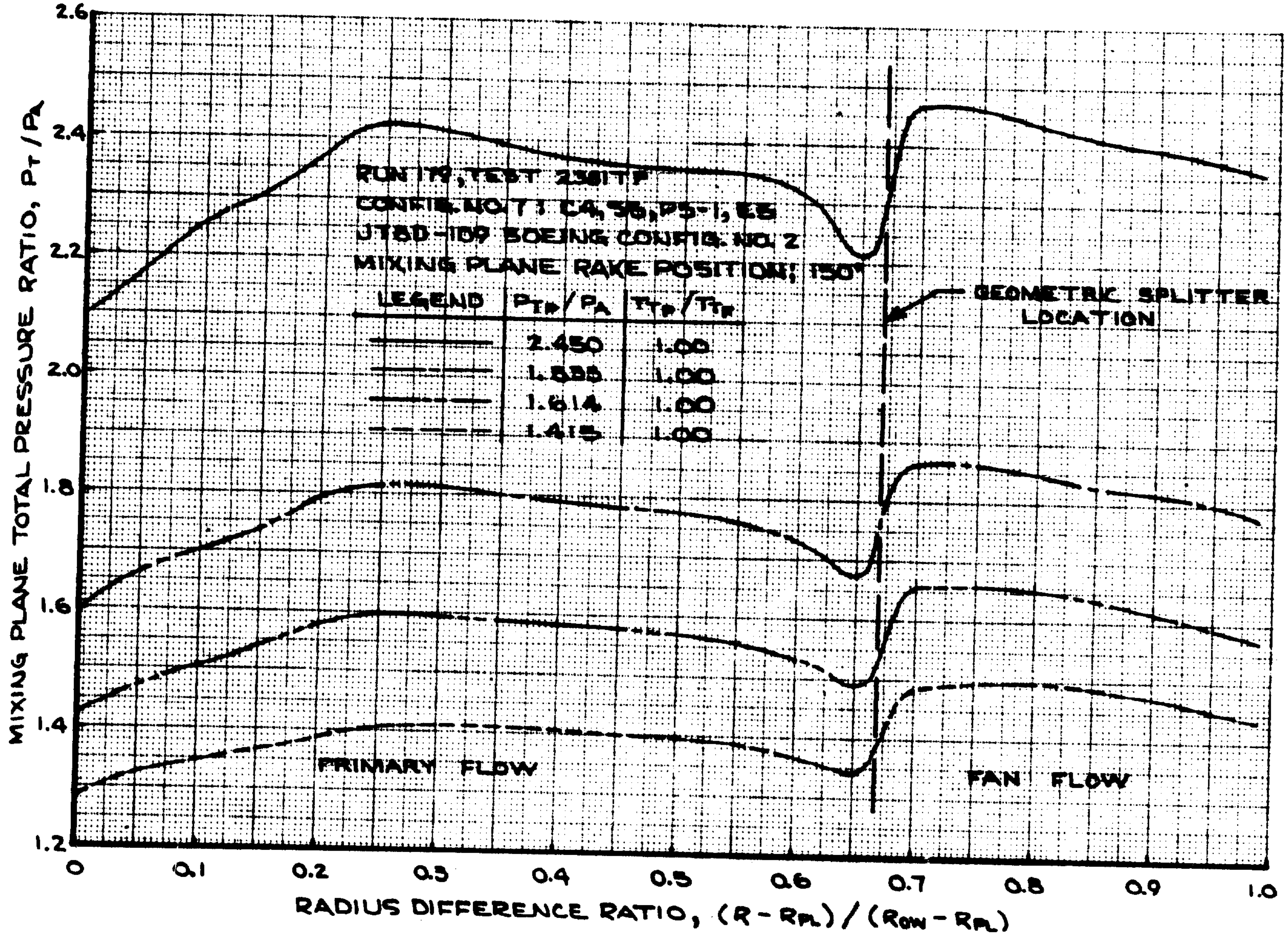

FIGURE 247- MIXING PLANE TOTAL PRESSURE RATIO PROFILES
TEST CONFIG. NO. 7; TRAVERSING PROBE LOCATION - 150 DEG.

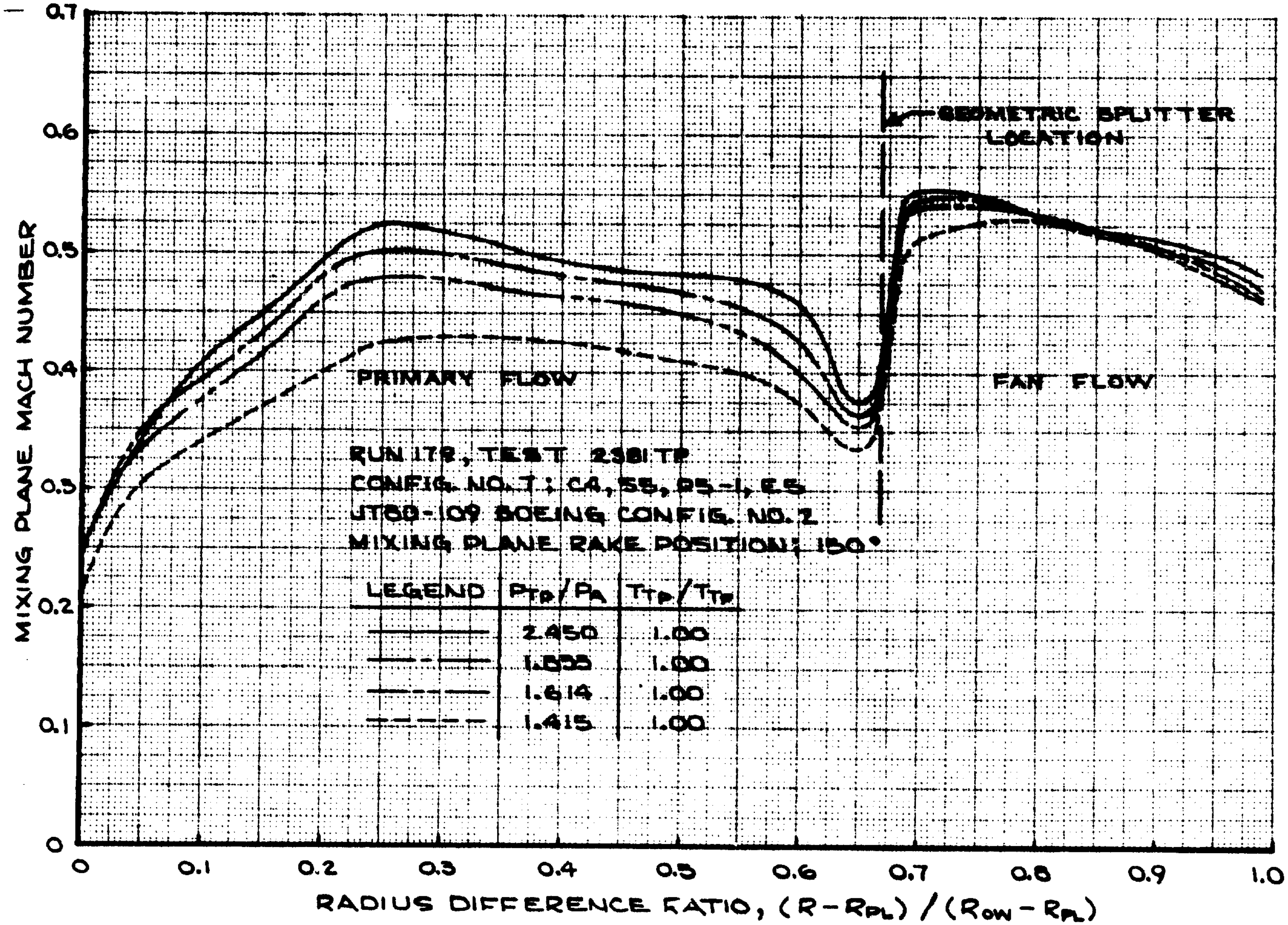

FIGURE 248- MIXING PLANE MACH NO. PROFILES
TEST CONFIG. NO. 7; TRAVERSING PROBE LOCATION - 150 DEG.

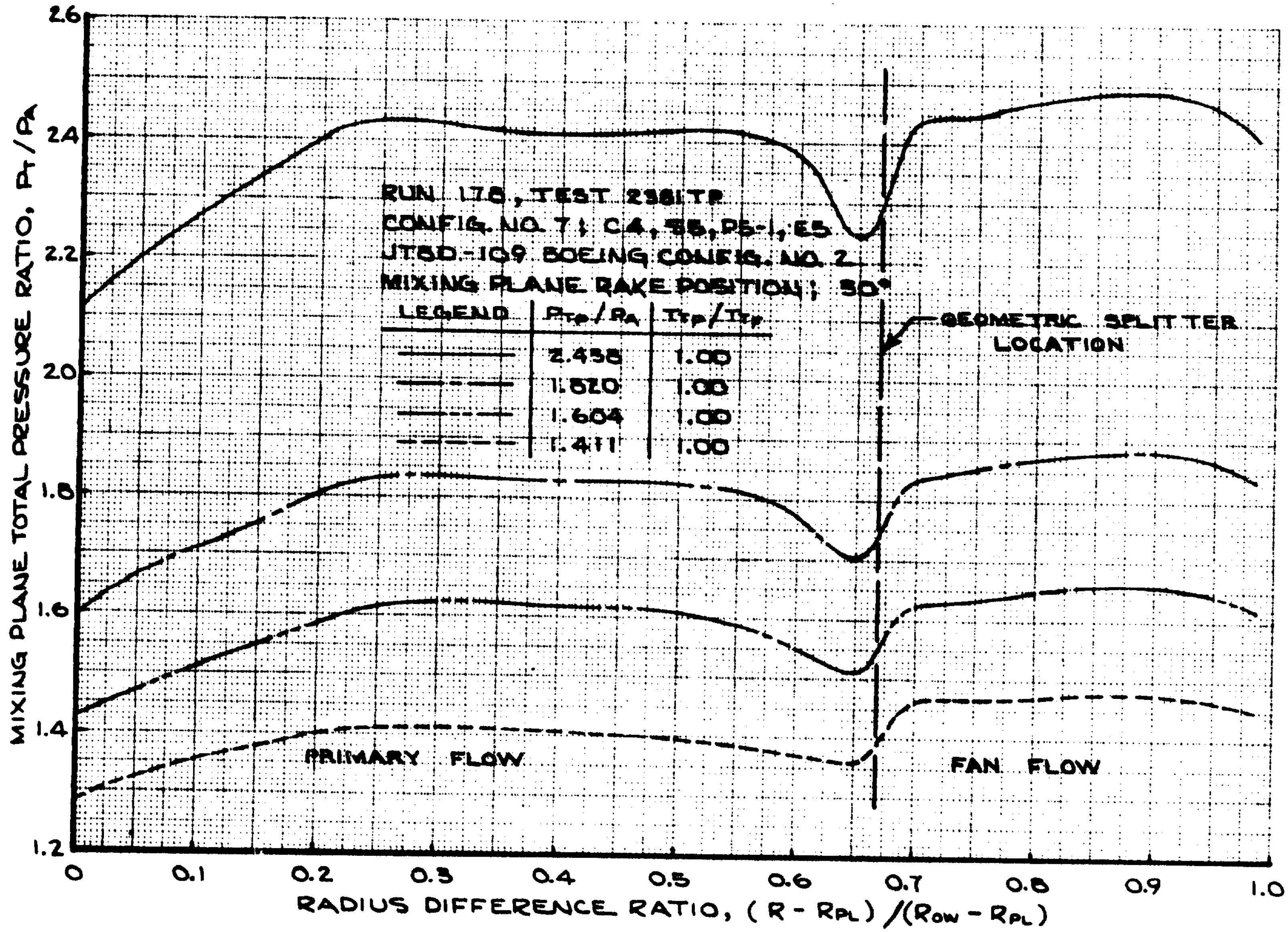

FIGURE 249- MIXING PLANE TOTAL PRESSURE RATIO PROFILES
TEST CONFIG. NO. 7; TRAVERSING PROBE LOCATION - 30 DEG.

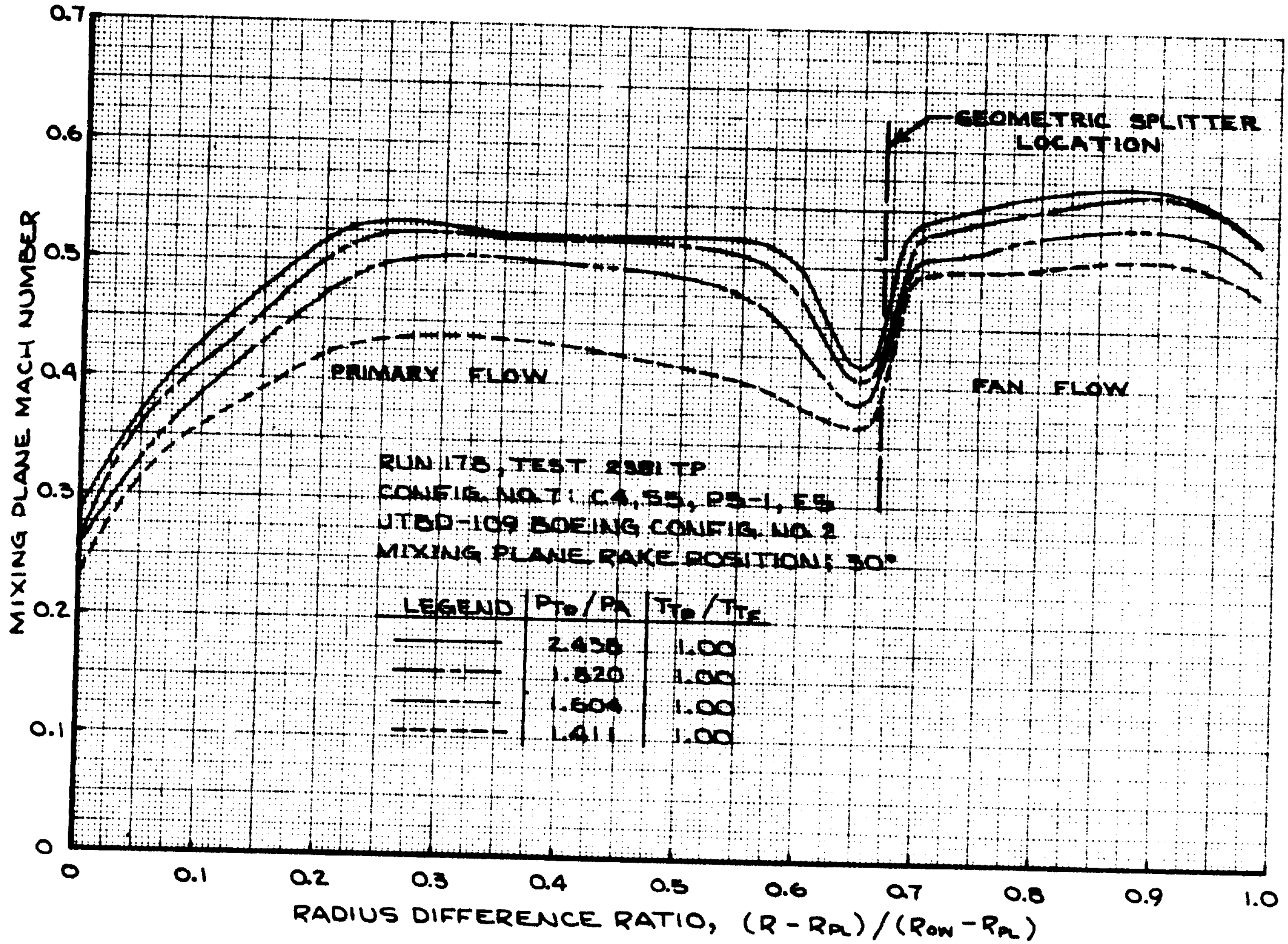

FIGURE 250- MIXING PLANE MACH NO. PROFILES
TEST CONFIG. NO. 7; TRAVERSING PROBE LOCATION - 30 DEG.

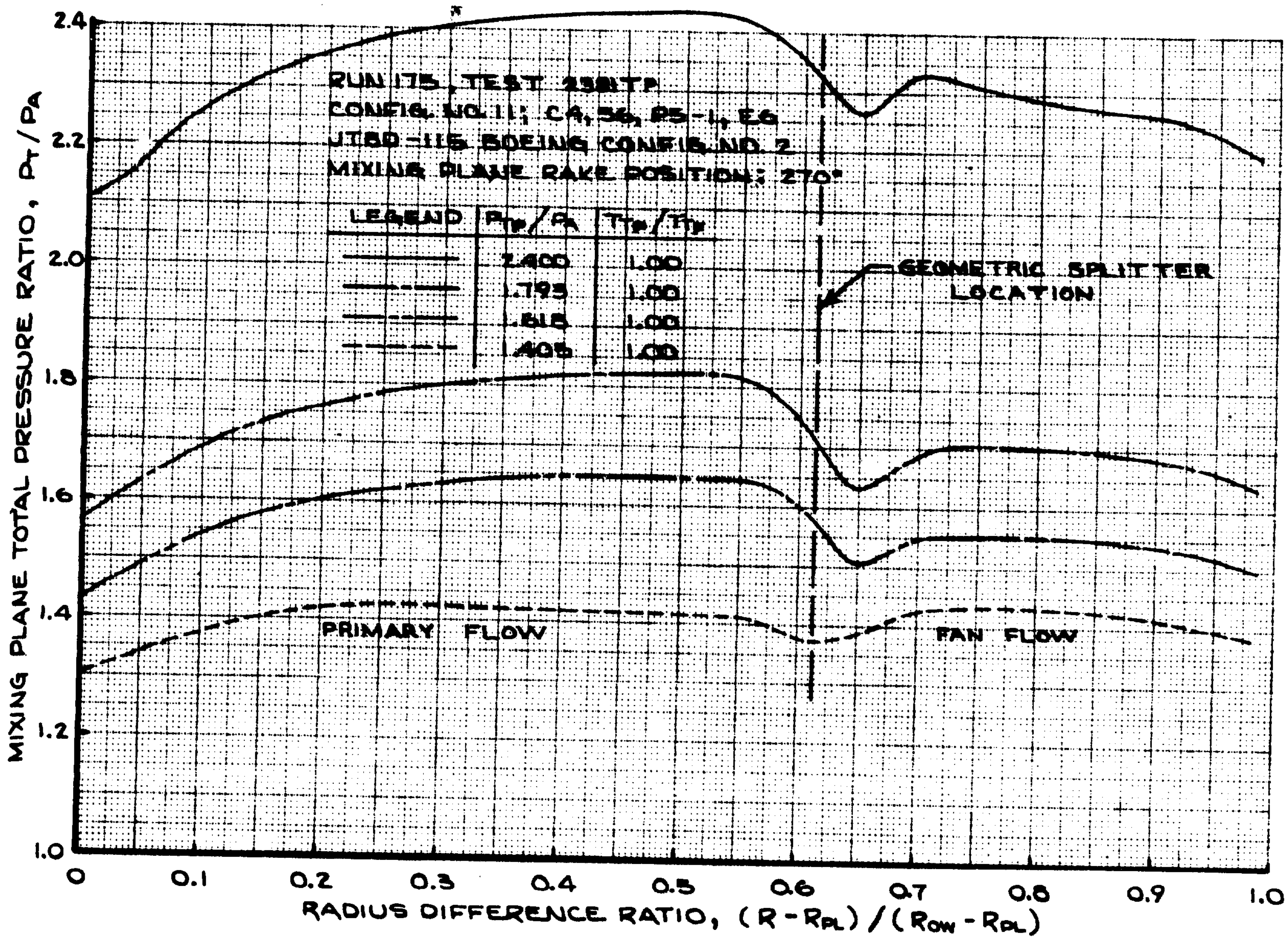

FIGURE 251- MIXING PLANE TOTAL PRESSURE RATIO PROFILES
TEST CONFIG. NO. 11; TRAVERSING PROBE LOCATIONS - 270 DEG.

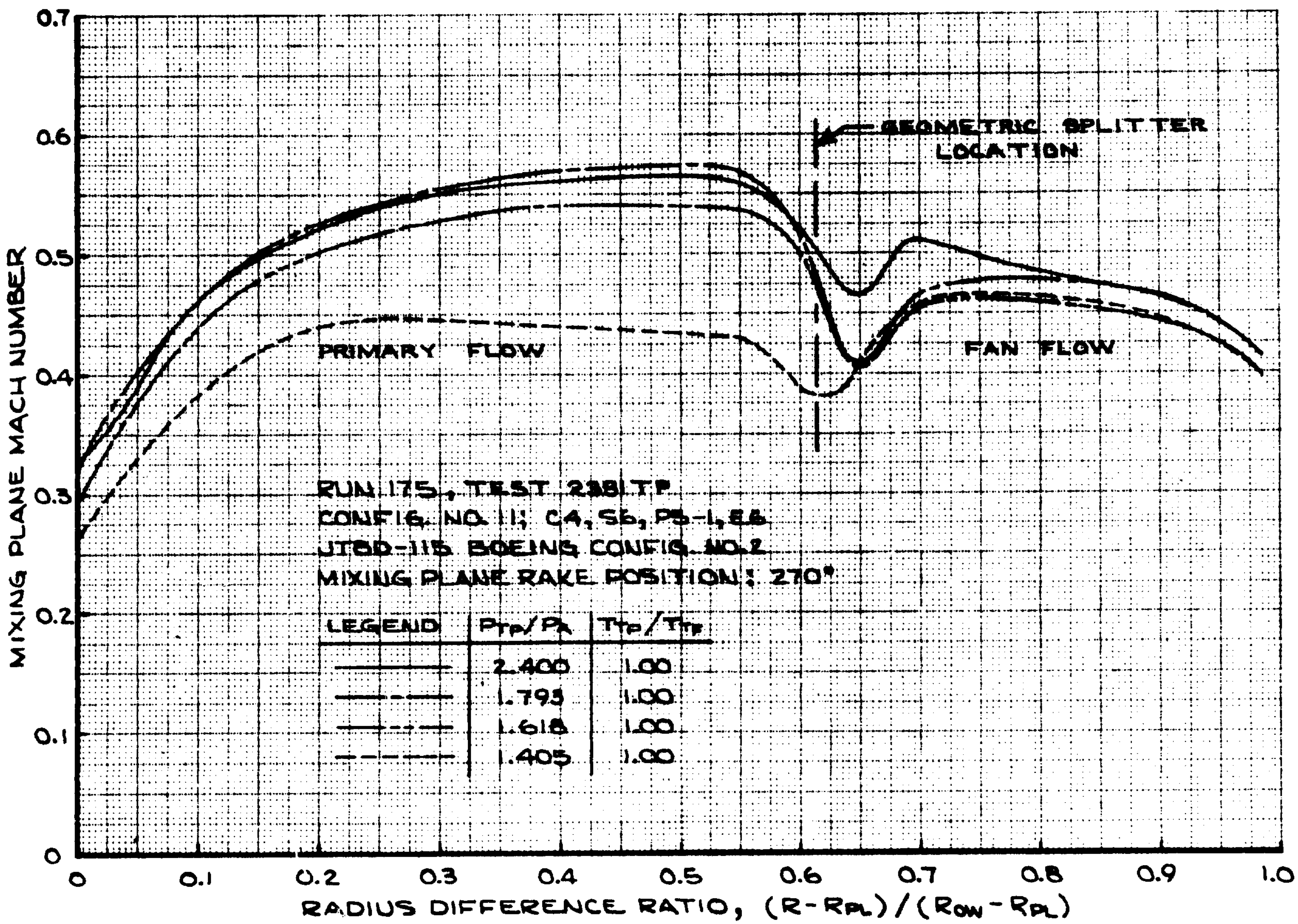

FIGURE 252- MIXING PLANE MACH NO. PROFILES
TEST CONFIG. NO. 11; TRAVERSING PROBE LOCATION - 270 DEG.

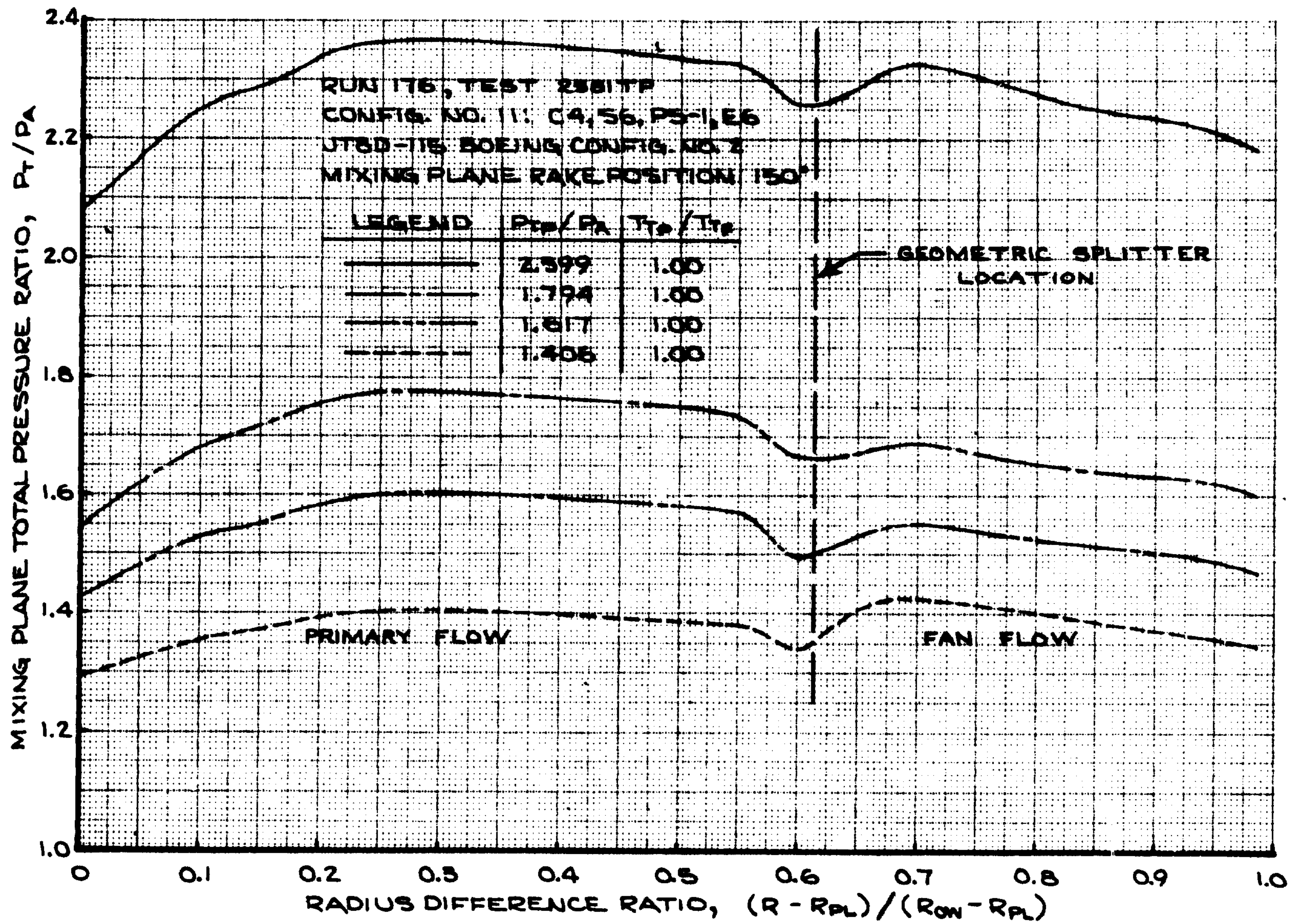

FIGURE 253- MIXING PLANE TOTAL PRESSURE RATIO PROFILES
TEST CONFIG. NO. 11; TRAVERSING PROBE LOCATION - 150 DEG.

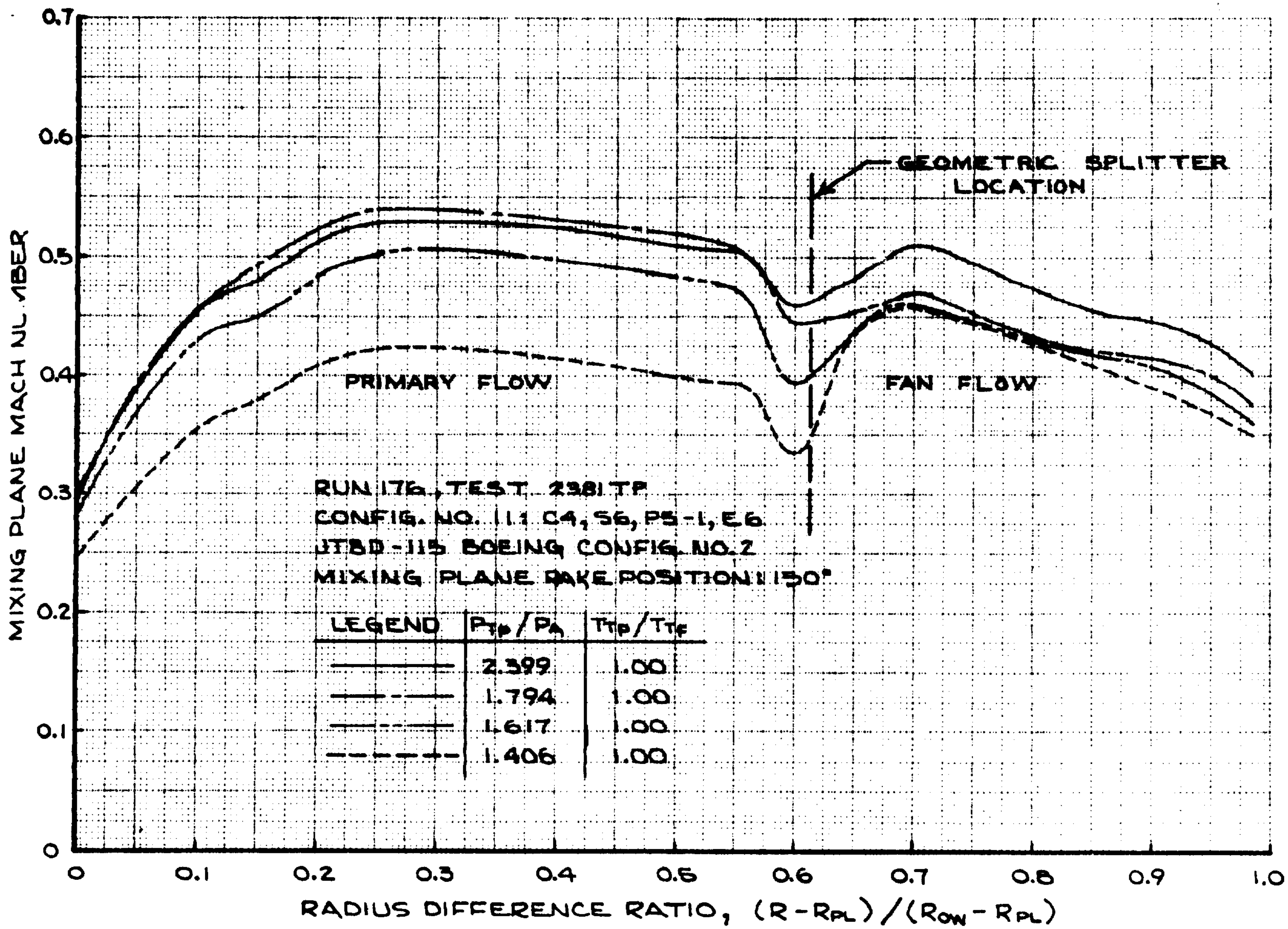

FIGURE 254- MIXING PLANE MACH NO. PROFILES
TEST CONFIG. NO. 11; TRAVERSING PROBE LOCATION - 150 DEG.

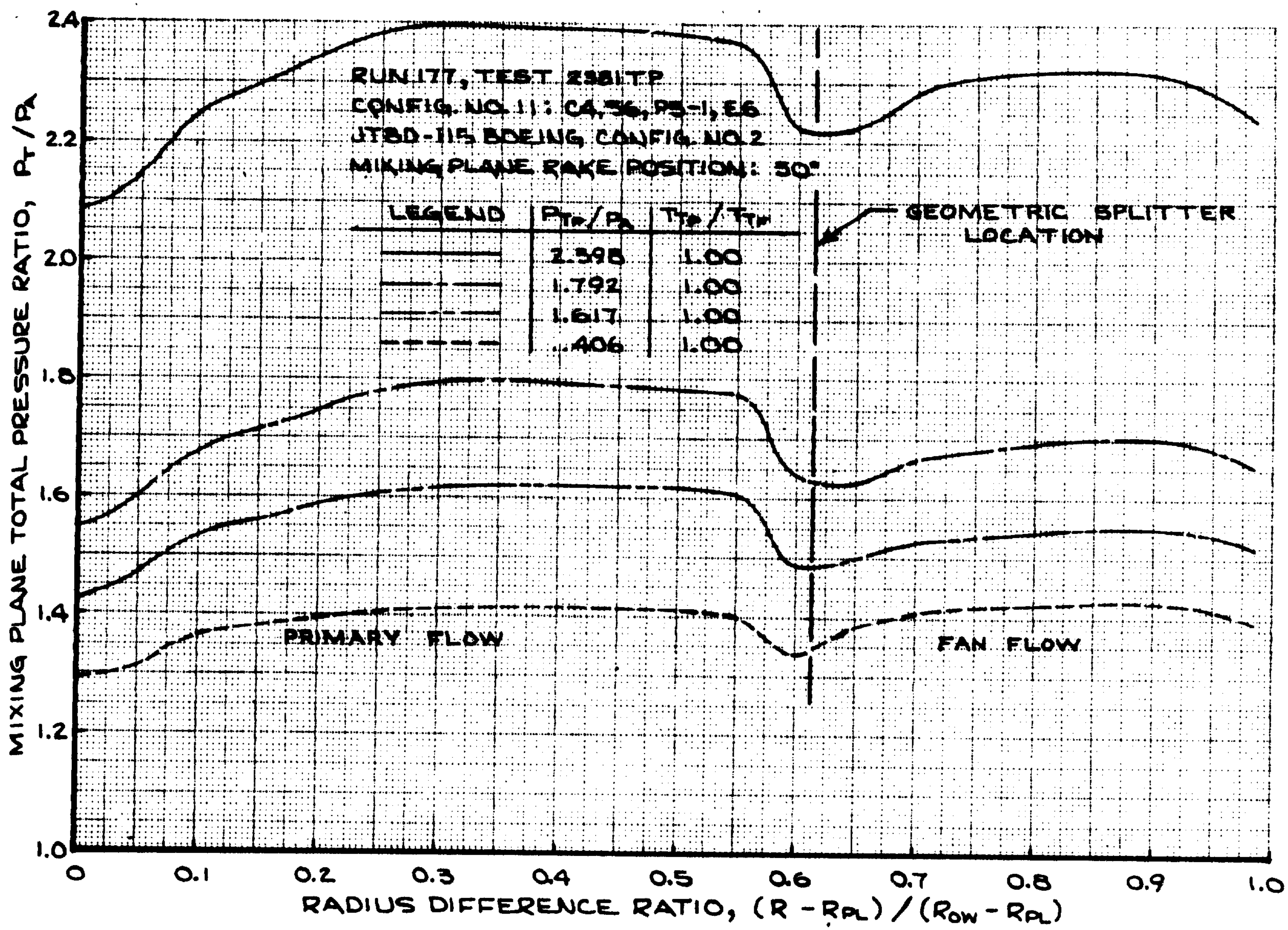

FIGURE 255- MIXING PLANE TOTAL PRESSURE RATIO PROFILES
TEST CONFIG. NO. 11; TRAVERSING PROBE LOCATION - 30 DEG.

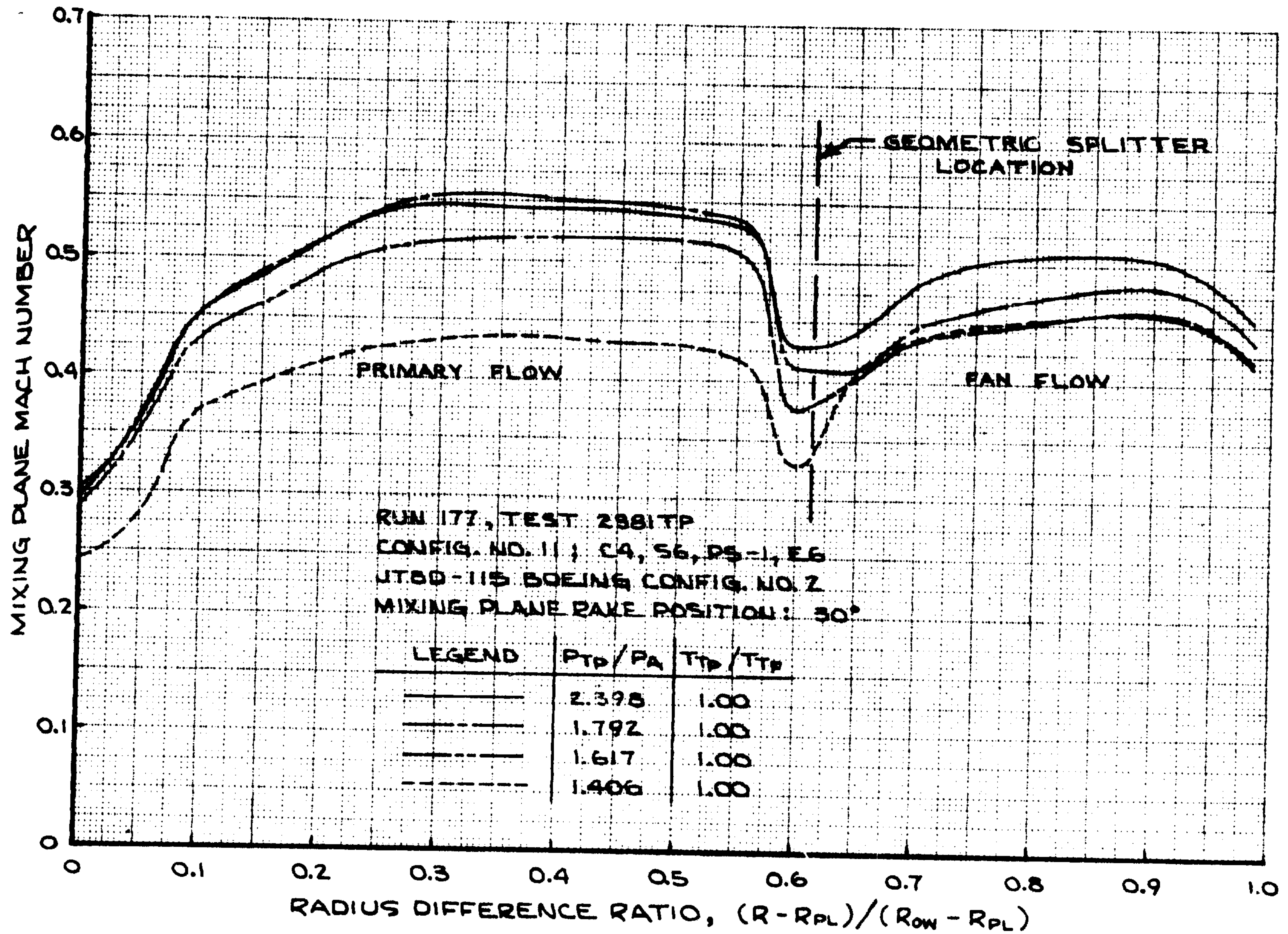

FIGURE 256- MIXING PLANE MACH NO. PROFILES
TEST CONFIG. NO. 11; TRAVERSING PROBE LOCATION - 30 DEG.

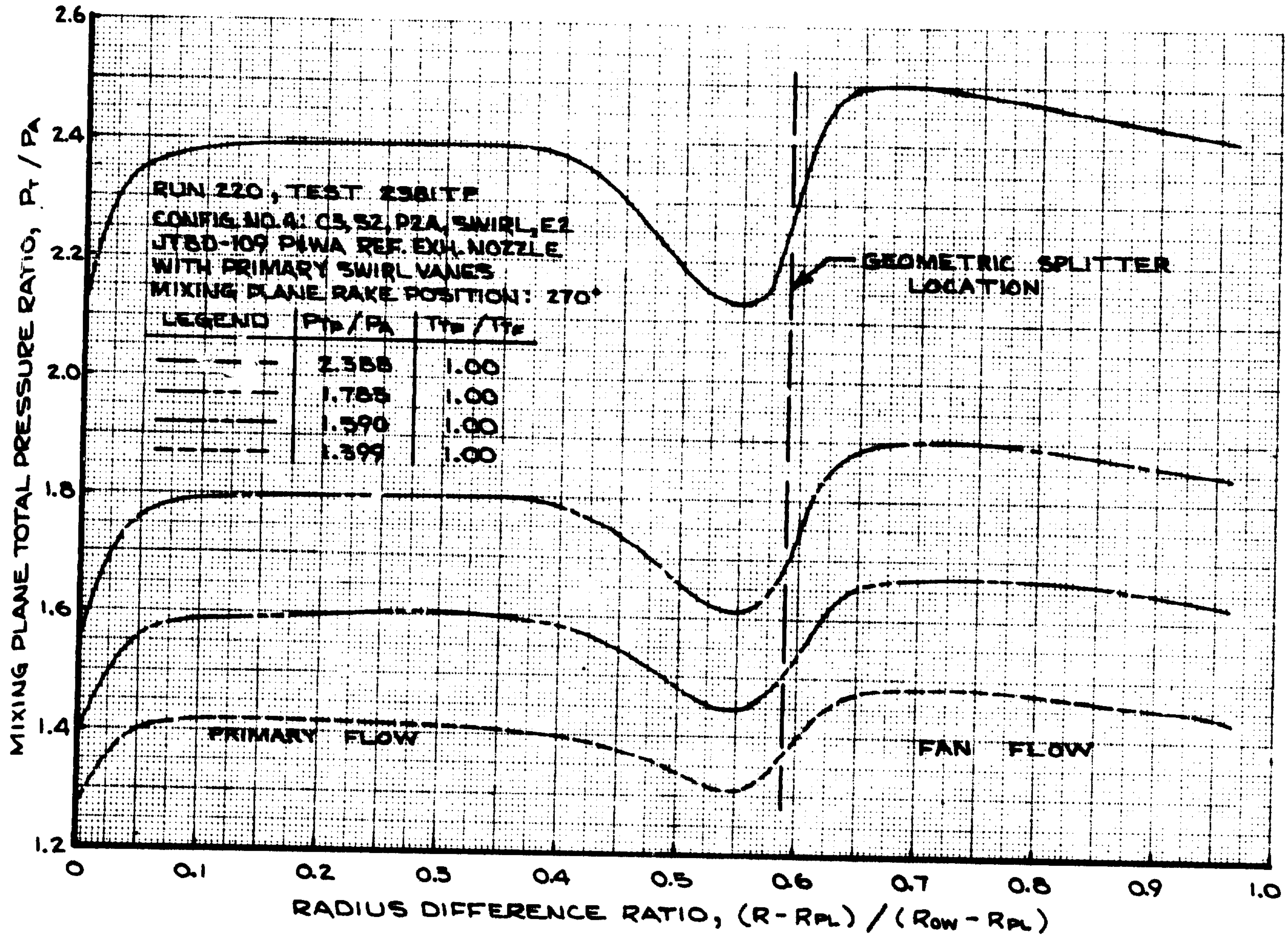

FIGURE 257- MIXING PLANE TOTAL PRESSURE RATIO PROFILES
TEST CONFIG. NO. 4; TRAVERSING PROBE LOCATION - 270 DEG.

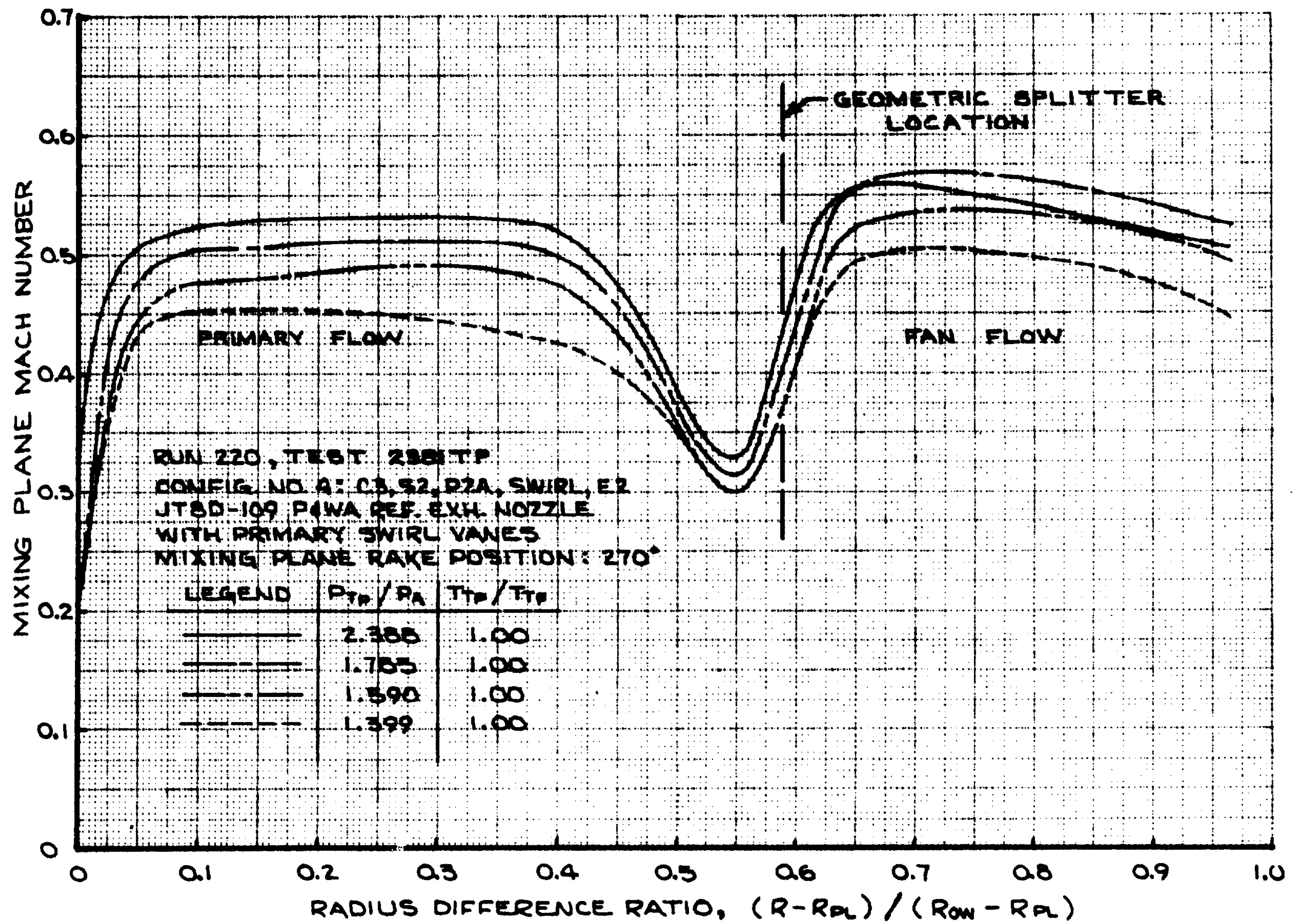

FIGURE 258- MIXING PLANE MACH NO. PROFILES
TEST CONFIG. NO. 4; TRAVERSING PROBE LOCATION - 270 DEG.

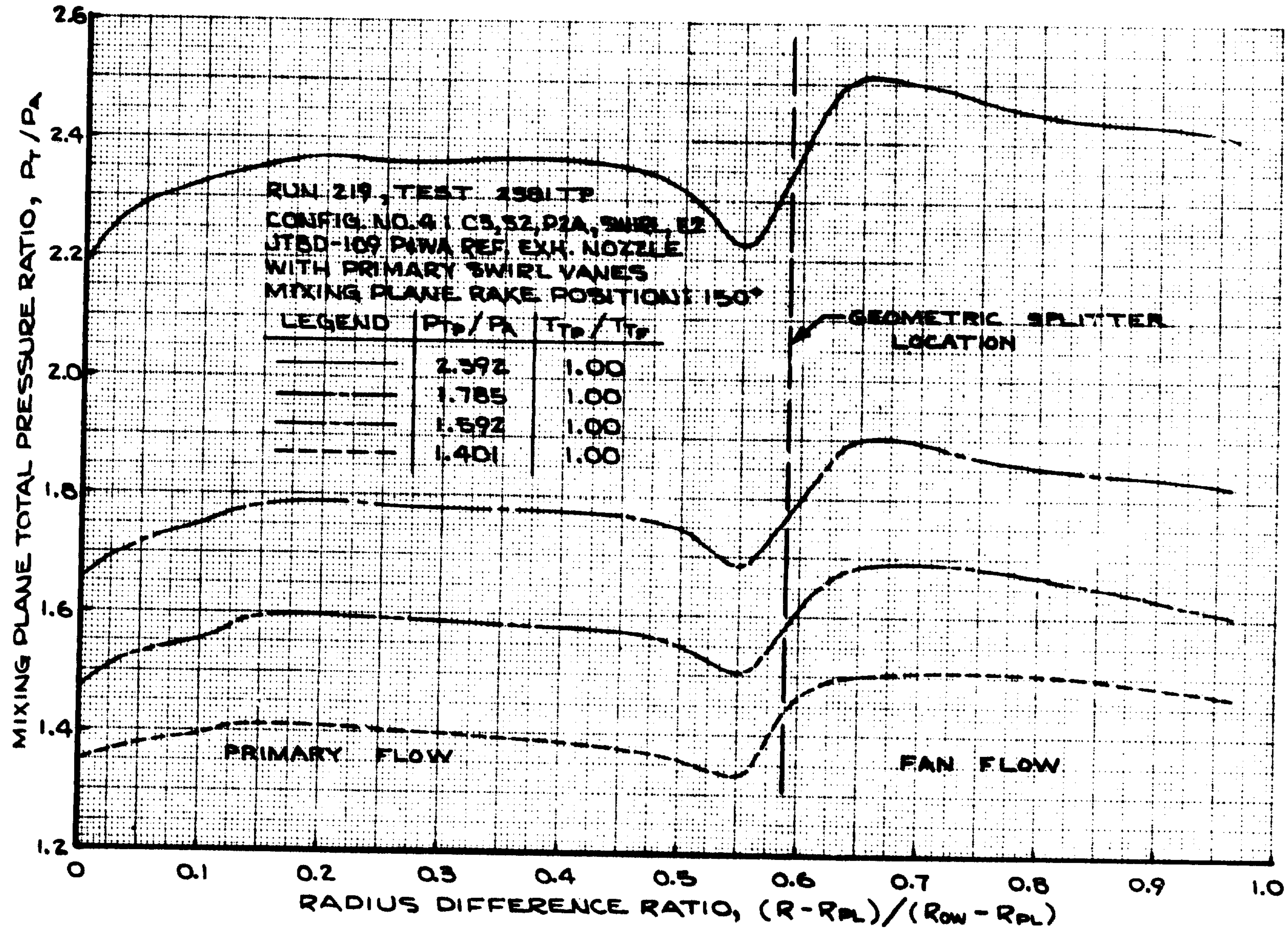

FIGURE 259. MIXING PLANE TOTAL PRESSURE RATIO PROFILES
TEST CONFIG. NO. 4; TRAVERSING PROBE LOCATION - 150 DEG.

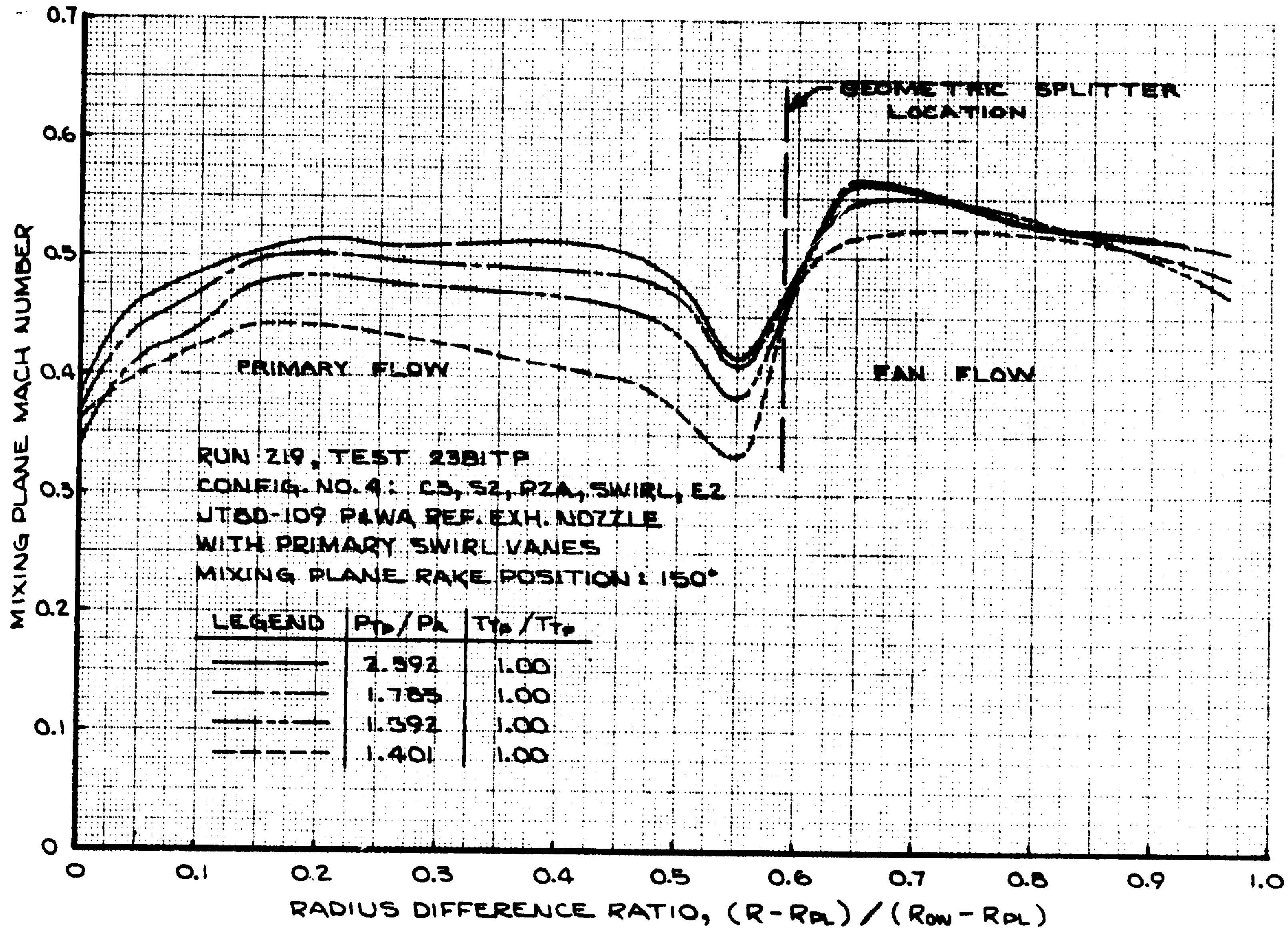

FIGURE 260- MIXING PLANE MACH NO. PROFILES
TEST CONFIG. NO. 4; TRAVERSING PROBE LOCATION - 150 DEG.

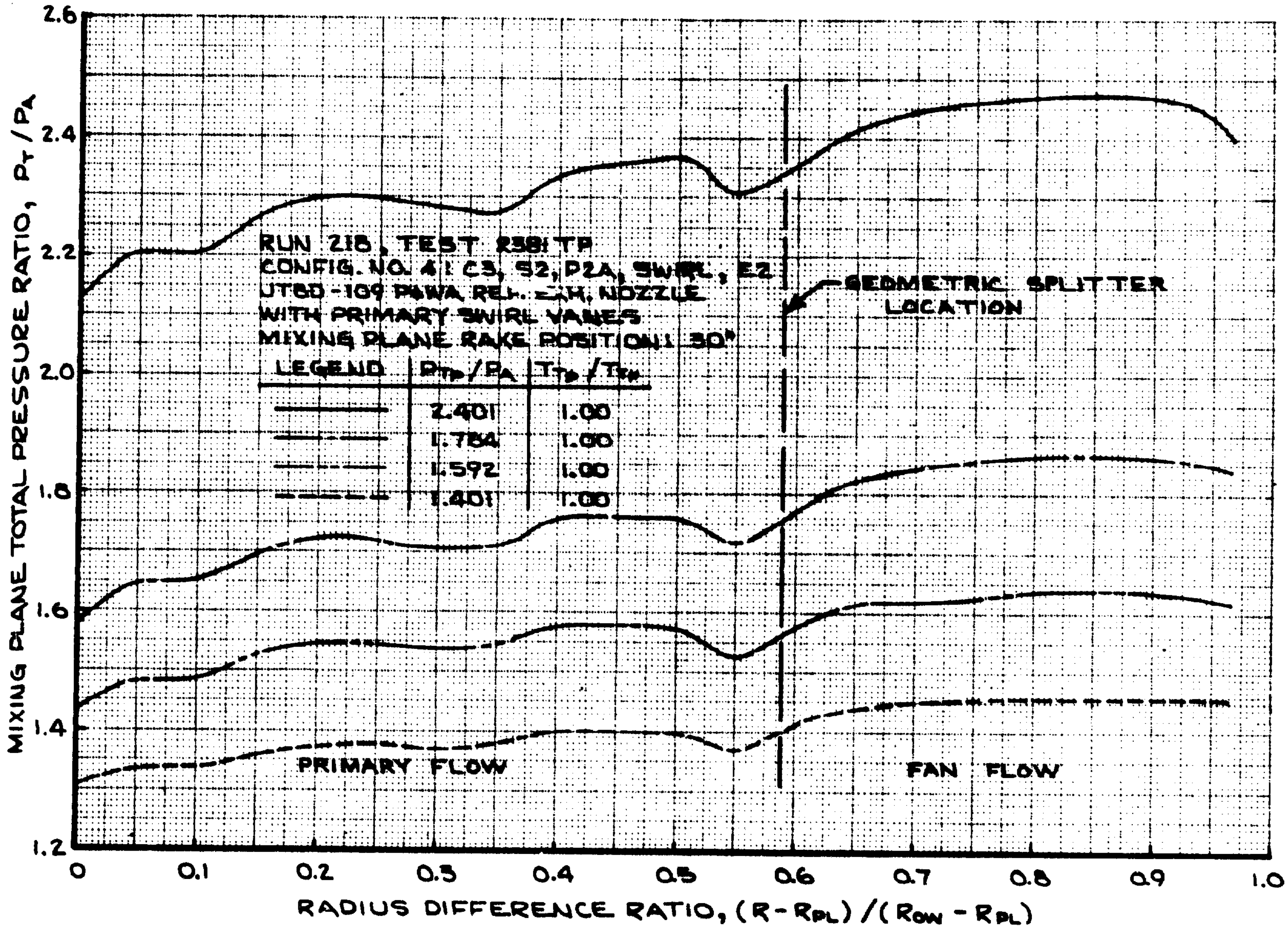

FIGURE 261- MIXING PLANE TOTAL PRESSURE RATIO PROFILES
TEST CONFIG. NO. 4; TRAVERSING PROBE LOCATION - 30 DEG.

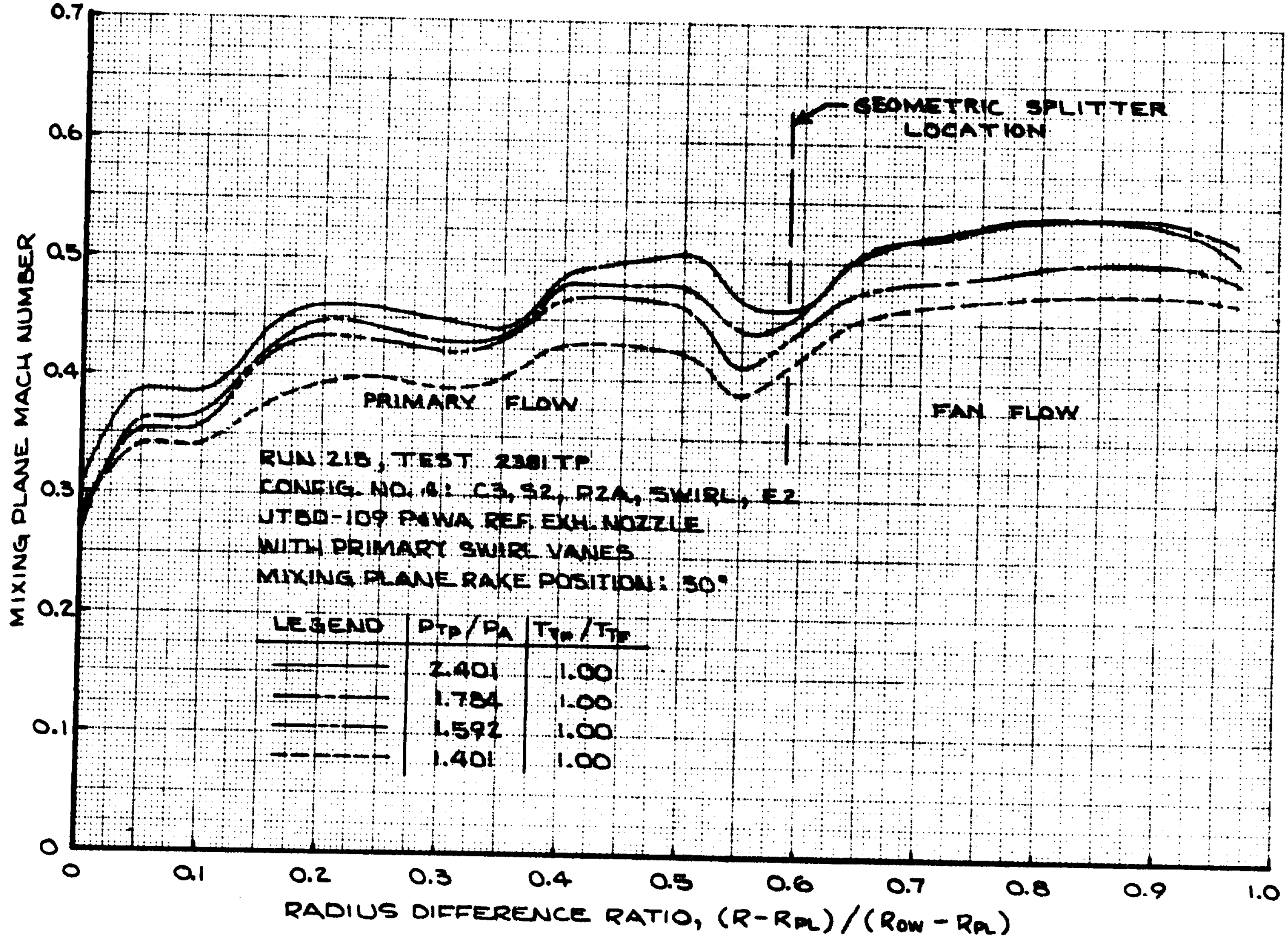

FIGURE 262- MIXING PLANE MACH NO. PROFILES
TEST CONFIG. NO. 4: TRAVERSING PROBE LOCATION - 30 DEG.

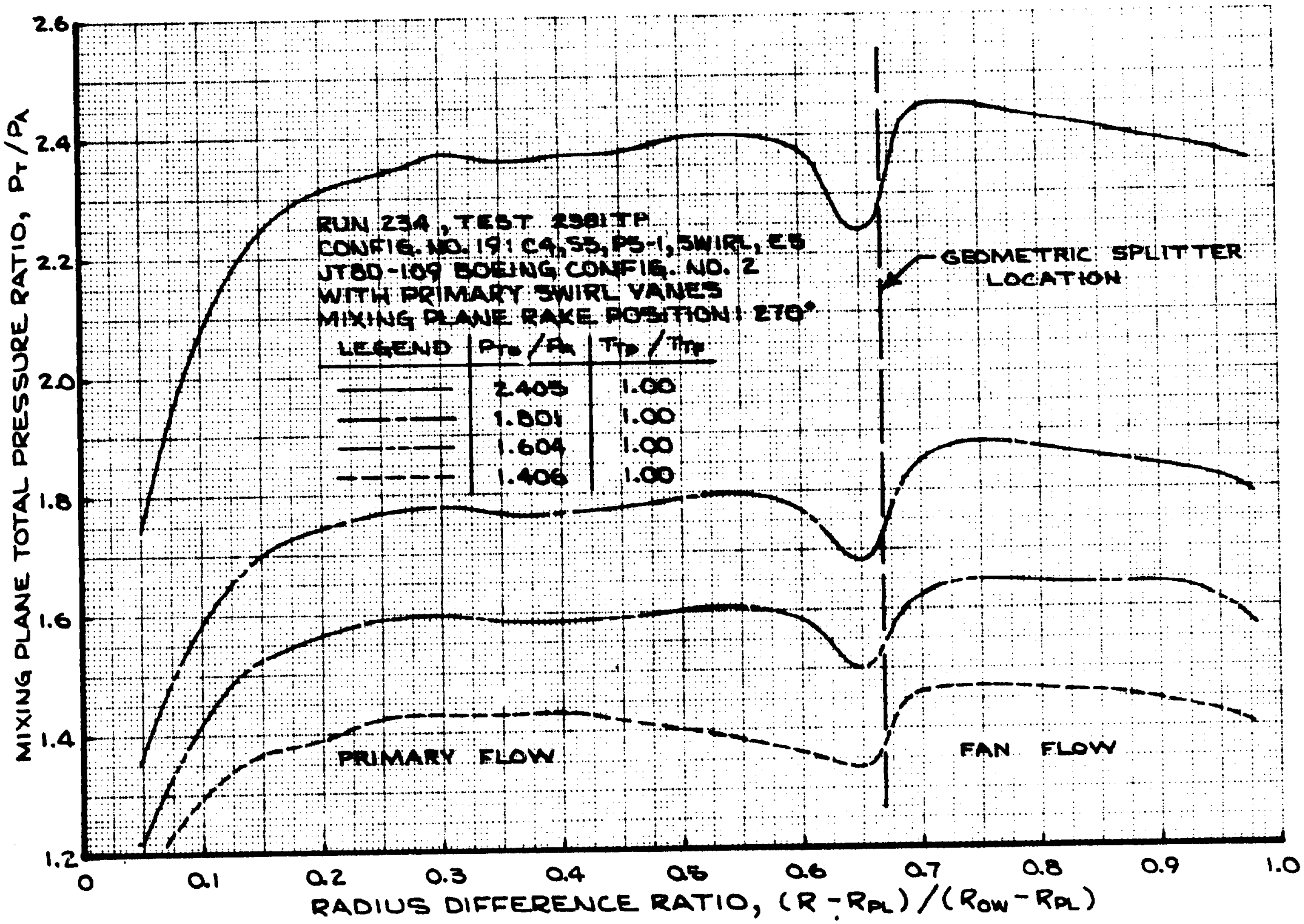

FIGURE 263- MIXING PLANE TOTAL PRESSURE RATIO PROFILES
TEST CONFIG. NO. 19; TRAVERSING PROBE LOCATION - 270 DEG.

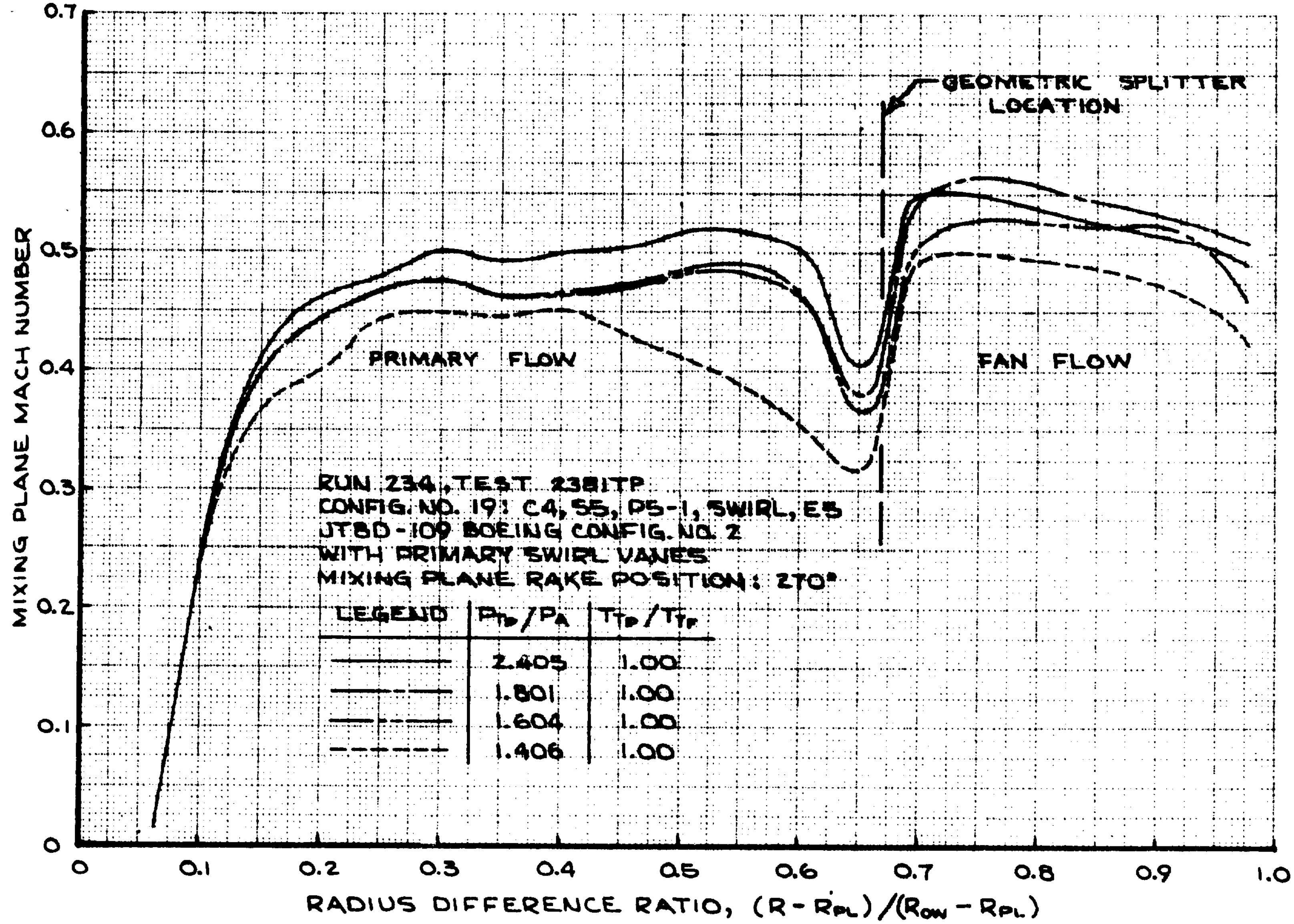

FIGURE 264- MIXING PLANE MACH NO. PROFILES
TEST CONFIG. NO. 19; TRAVERSING PROBE LOCATION - 270 DEG.

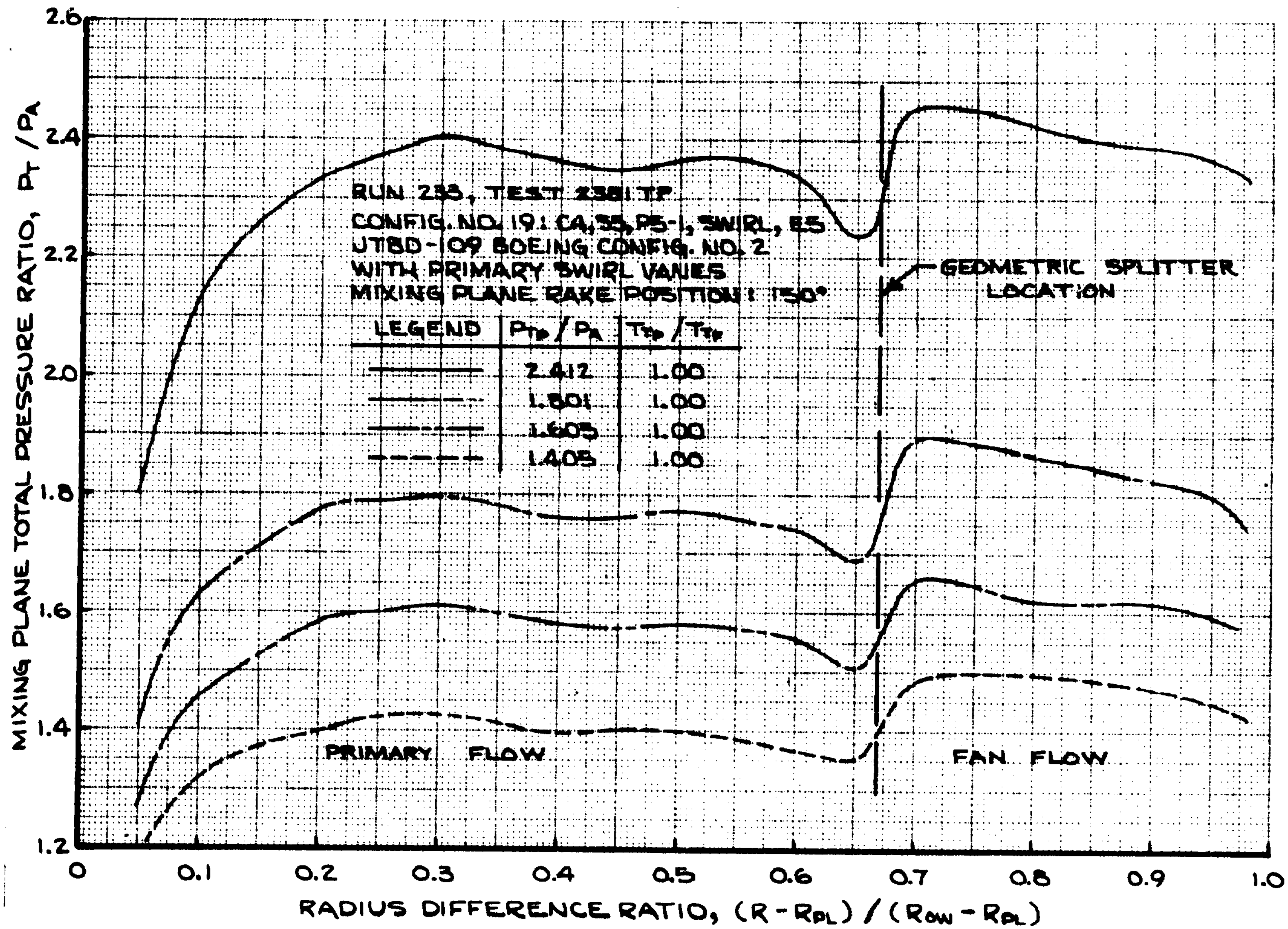

FIGURE 265- MIXING PLANE TOTAL PRESSURE RATIO PROFILES
TEST CONFIG. NO. 19; TRAVERSING PROBE LOCATION - 150 DEG.

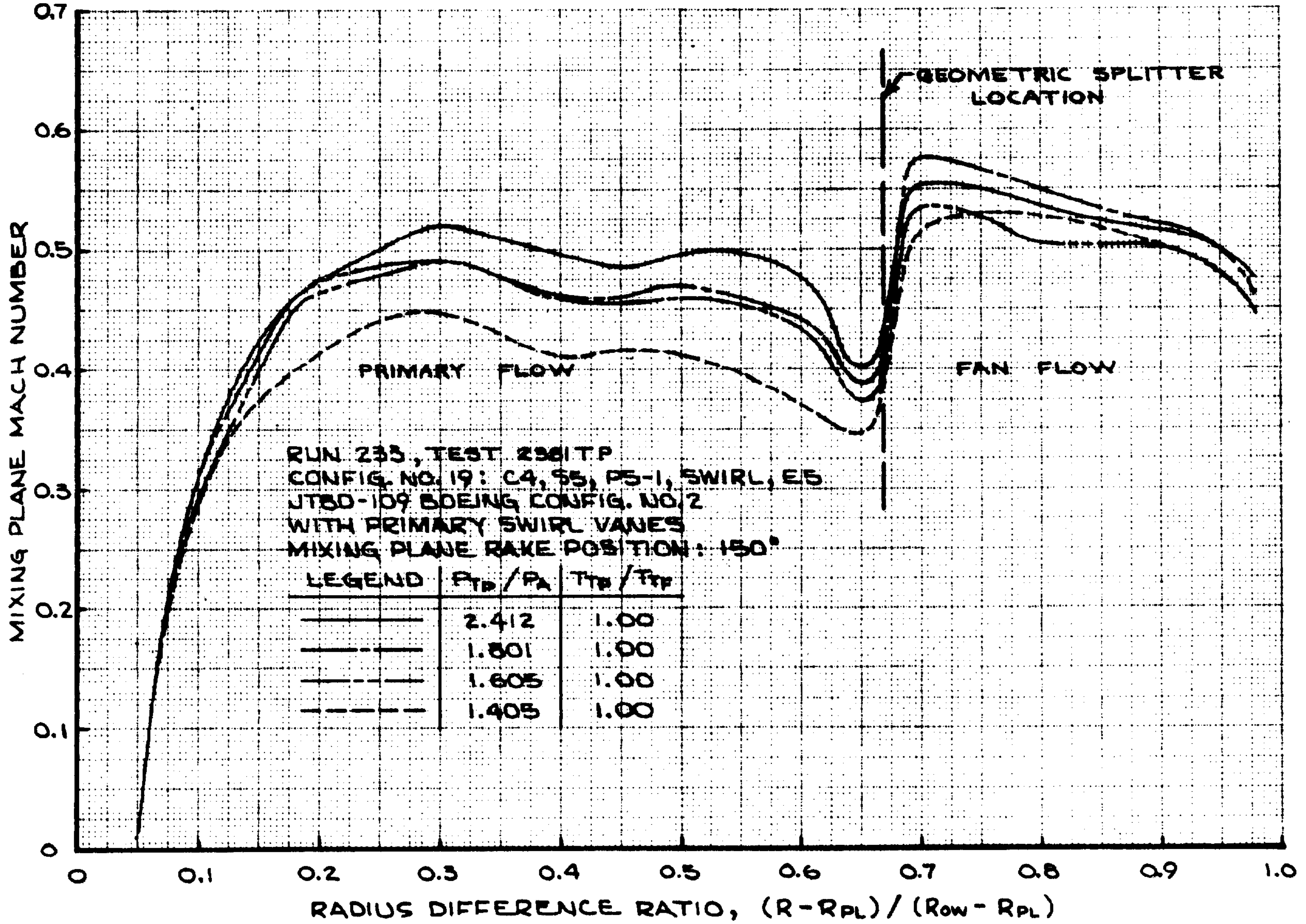

FIGURE 266- MIXING PLANE MACH NO. PROFILES
TEST CONFIG. NO. 19; TRAVERSING PROBE LOCATION - 150 DEG.

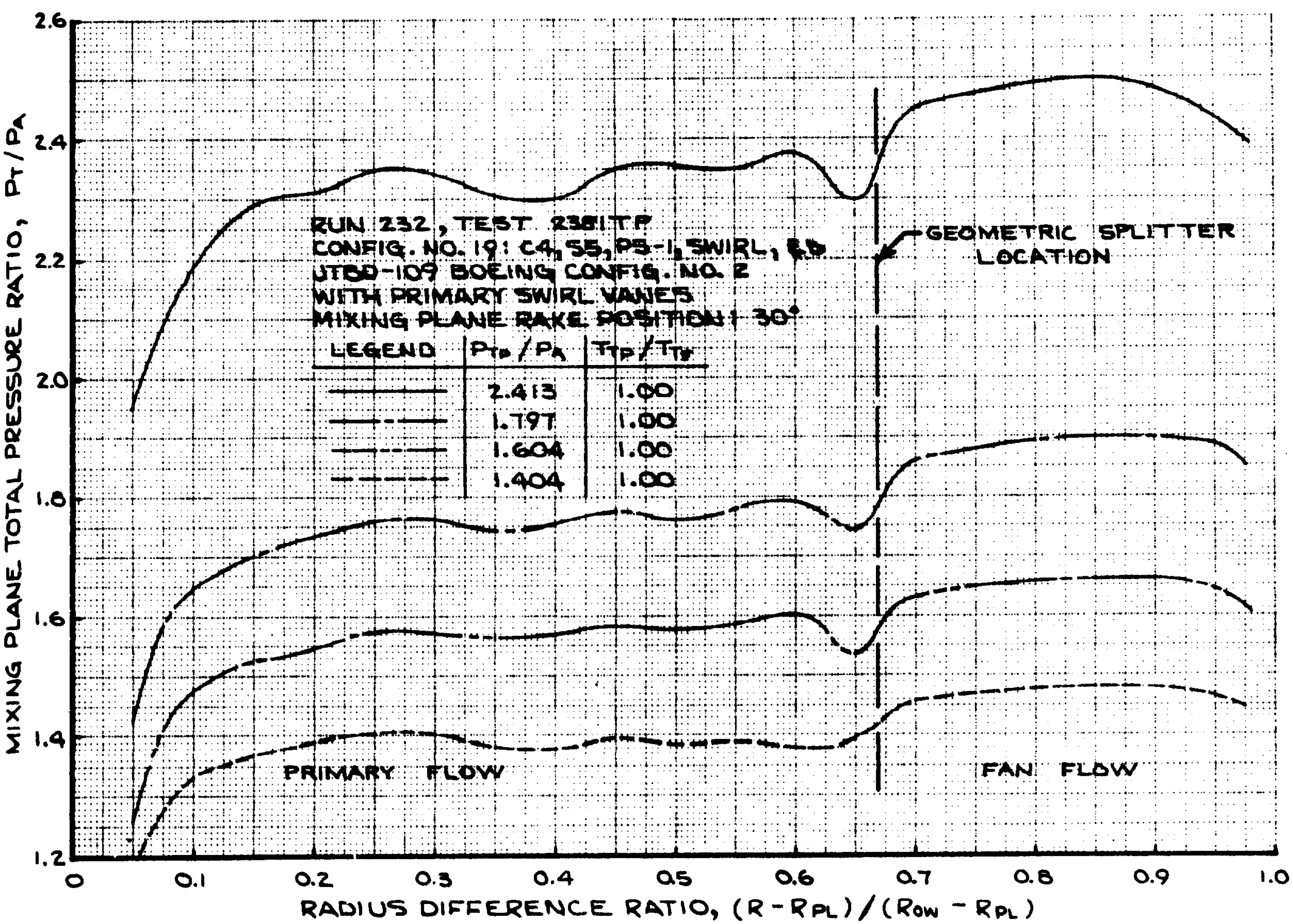

FIGURE 267- MIXING PLANE TOTAL PRESSURE RATIO PROFILES
TEST CONFIG. NO. 19; TRAVERSING PROBE LOCATION - 30 DEG.

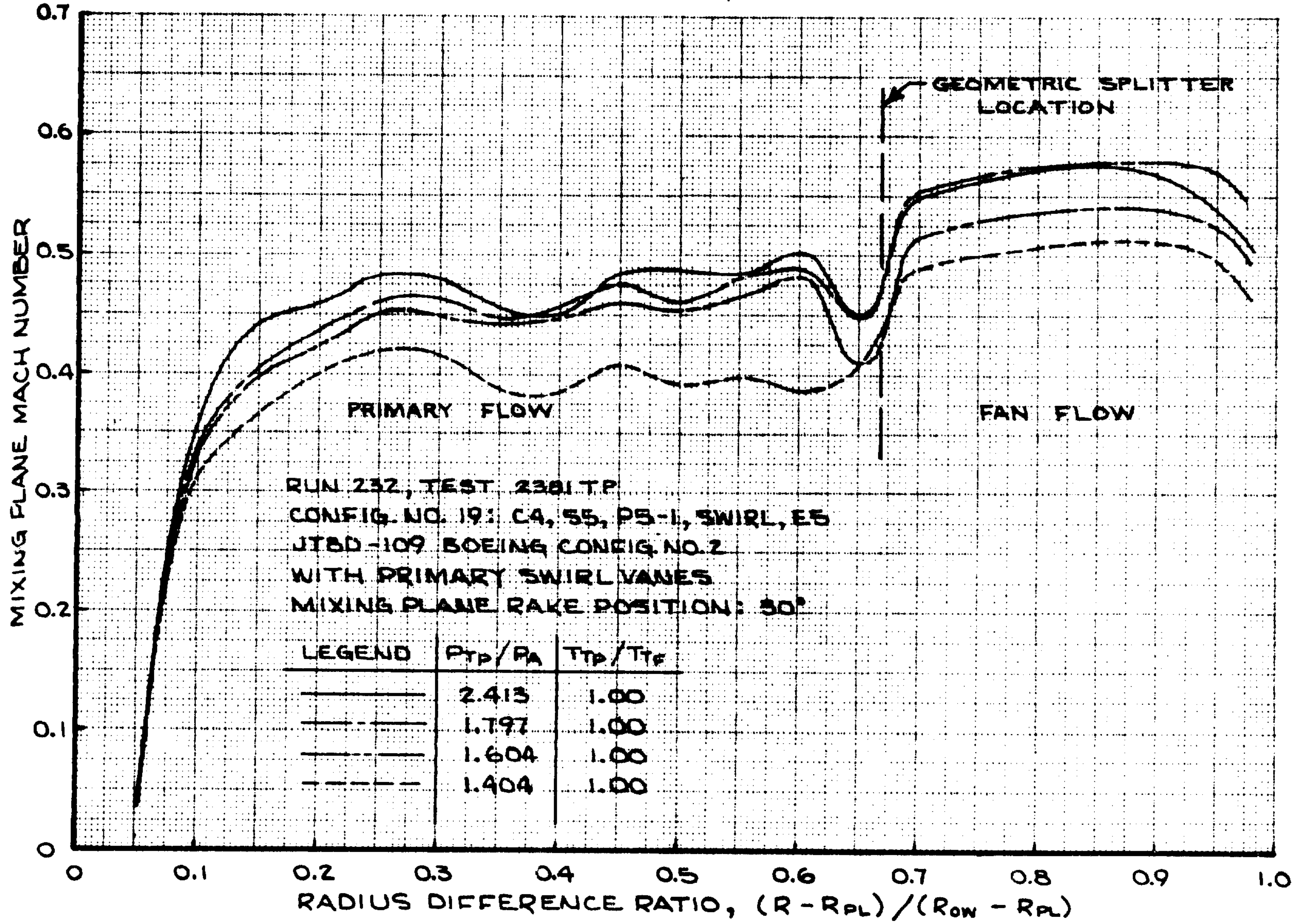

FIGURE 268- MIXING PLANE MACH NO. PROFILES
TEST CONFIG. NO. 19; TRAVERSING PROBE LOCATION - 30 DEG.

7.3.2 EXIT PLANE DATA

A total pressure and a total temperature probe were assembled in the L. C. Smith traversing actuator. The 0.042-inch diameter total pressure probe and the 0.093-inch diameter total temperature probe geometric relationship is shown in the following sketch:

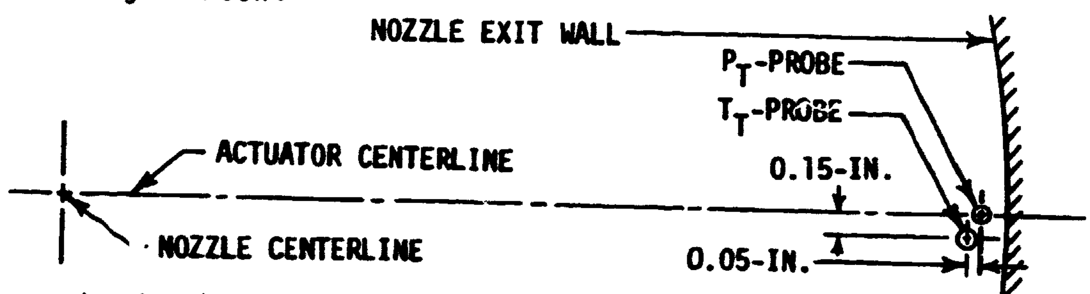

The actuator/probe assembly was mounted from a bracket which was cantilevered from the nozzle outer wall over the nozzle exit plane such that the P_T and T_T probe-tips would just clear the nozzle exit in the retracted position. Figures 18 and 19 show the locations of the nozzle exit planes for the JT8D-9/727 production, P&WA JT8D-100 Reference hardware, and the Boeing JT8D-100 Config. No. 2 hardware. Similar to the mixing plane actuator installation, the probe/actuator assembly could also be positioned to any circumferential location by rotating the nozzle outer wall at the forward mount flange. Figure 308 Section 7.4, shows the installation of the L. C. Smith actuator with the P_T and T_T probes at the nozzle exit plane.

The pressure and temperature sensed by the probes were recorded simultaneously on the same XY-plotter used for the mixing plane data. Surveys of the exit plane were conducted while simulating the engine cycle total pressure from the fan and primary streams at a total temperature ratio (T_{T_P}/T_{T_F}) of 2.2. Continuous traces of P_T and T_T were recorded from the nozzle exit wall to the nozzle centerline. Each trace was digitized in a similar manner as the mixing plane data. Data processing

by a digital computer calculated pressure ratio, temperature ratio, and fully expanded jet velocity.

The following is a tabulation of the exit plane data obtained:

Test Config. & No.	P_T/P_A & T_T/T_A Figure No.	Velocity Ratio Figure No.	Traversing Probe Location (Degrees measured clockwise from top-rear view)
2. JT8D-9/727 Production	269 271 273	270 272 274	270 135 45
3. P&WA JT8D-109 Reference	275 277 279	276 278 280	270 150 30
7. Boeing JT8D-109 Config. No. 2	281 283 285	282 284 286	270 150 30
11. Boeing JT8D-115 Config. No. 2	287 289 291	288 290 292	270 150 30
4. P&WA JT8D-109 Reference with Pri. Swirl Vanes	293 295	294 296	270 30
19. Boeing JT8D-109 Config. No. 2 with Pri. Swirl Vanes	297	298	270

For Test Configuration Nos. 2, 3, 7, and 11, velocity ratio was calculated by dividing the jet velocity at any given radius by the jet velocity on the nozzle centerline; i.e. $(V_{JET})/(V_{JET})_{℄}$.

This was done in order to compare with previously obtained JT8D full scale engine data. However, this ratio could not be used for the JT8D-100 nozzles when the swirl vanes were installed in test configuration numbers 4 and 19 as the velocity on the nozzle centerline was near zero or even possibly in the negative direction. The velocity ratio for these two configurations (No. 4

and No. 19) were calculated by dividing the jet velocity at any given radius by the maximum velocity obtained during the traverse from the nozzle exit radius to the centerline.

Summarizing the above figures, it can be stated that:

1. There is very good agreement with the JT8D full scale engine profiles.

2. Temperature profiles are not completely mixed at the exit plane for any of the tested configurations.

3. The wake from the splitter trailing edge can be seen more readily on the Boeing Config. No. 2 models than either the JT8D-9 production or the P&WA reference configurations. This is because the distance from the splitter trailing edge to the nozzle exit plane for Boeing Config. No. 2 is nominally 15 inches (full scale) shorter than that for the other configurations.

4. The velocity profiles, when non-dimensionalized, are not appreciably affected by the level of the simulated engine power setting. This was also found true for the full scale JT8D engine tests.

5. Swirl vanes affect only the inner 15% of the nozzle exit radius, where the flow velocity goes to zero or possibly becomes negative.

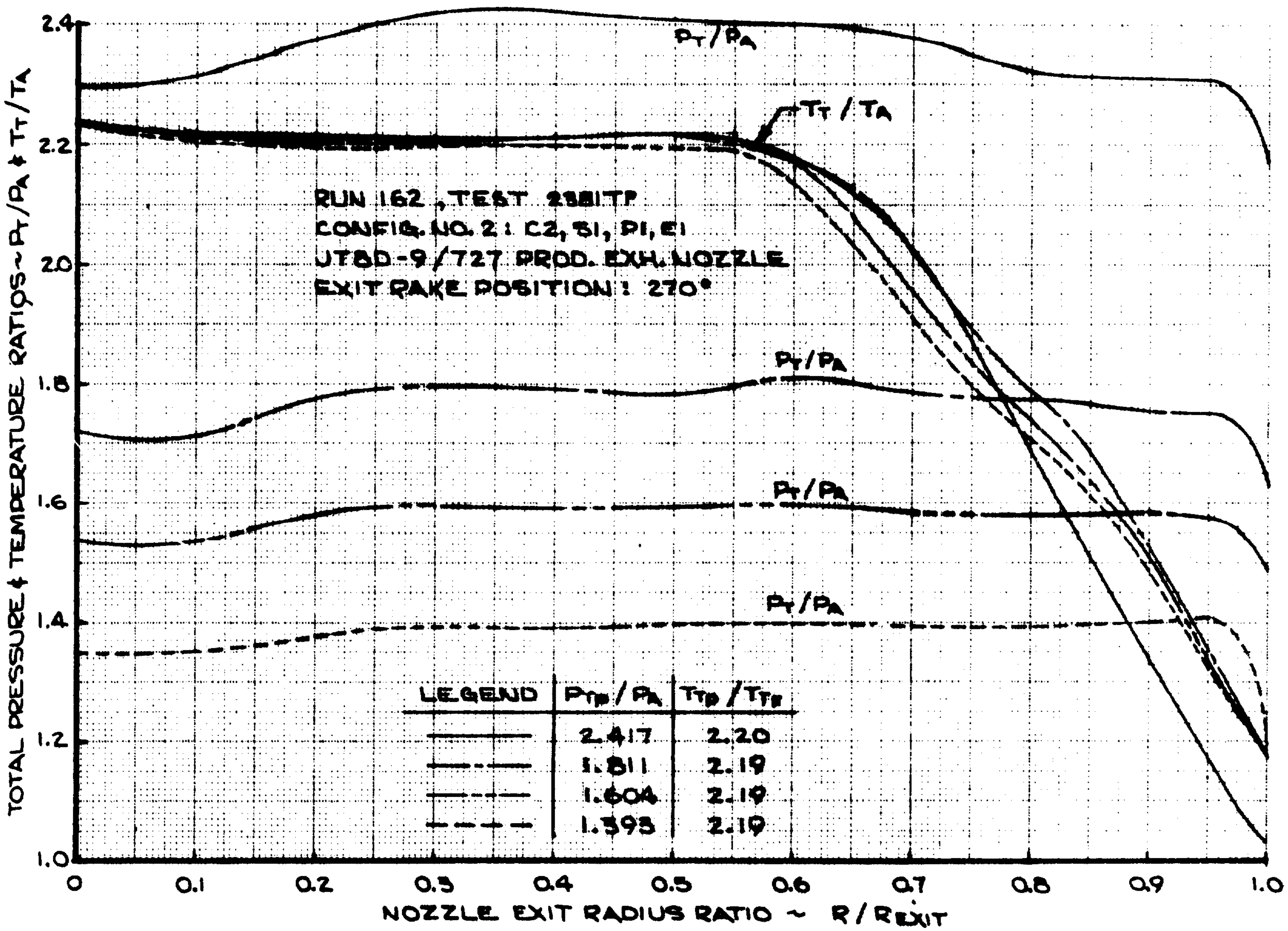

FIGURE 269- EXIT PLANE TOTAL PRESSURE & TEMPERATURE RATIO PROFILES
TEST CONFIG. NO. 2; TRAVERSING PROBE LOCATION - 270 DEG.

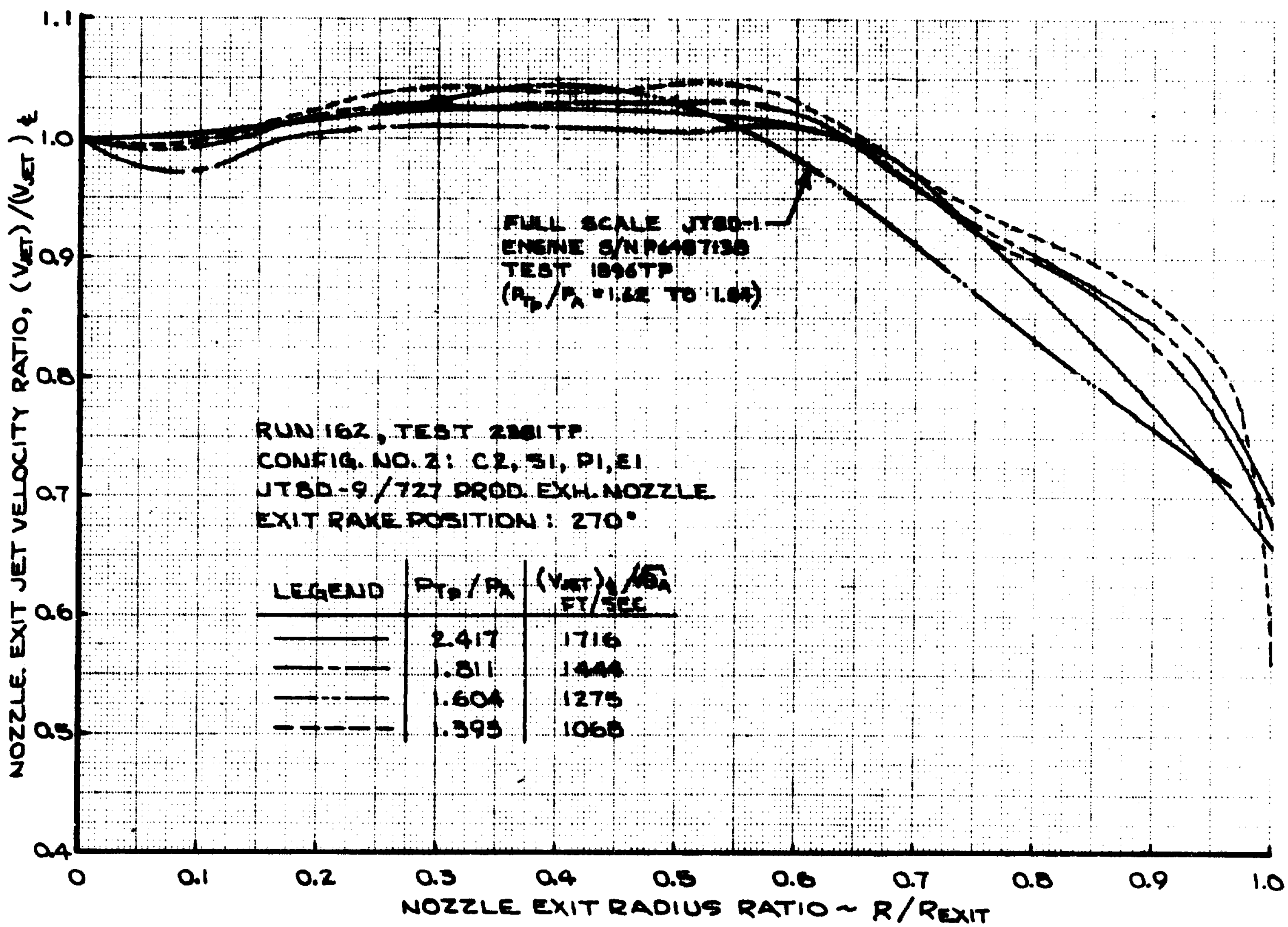

FIGURE 270- NOZZLE EXIT JET VELOCITY RATIO
TEST CONFIG. NO. 2; TRAVERSING PROBE LOCATION - 270 DEG.

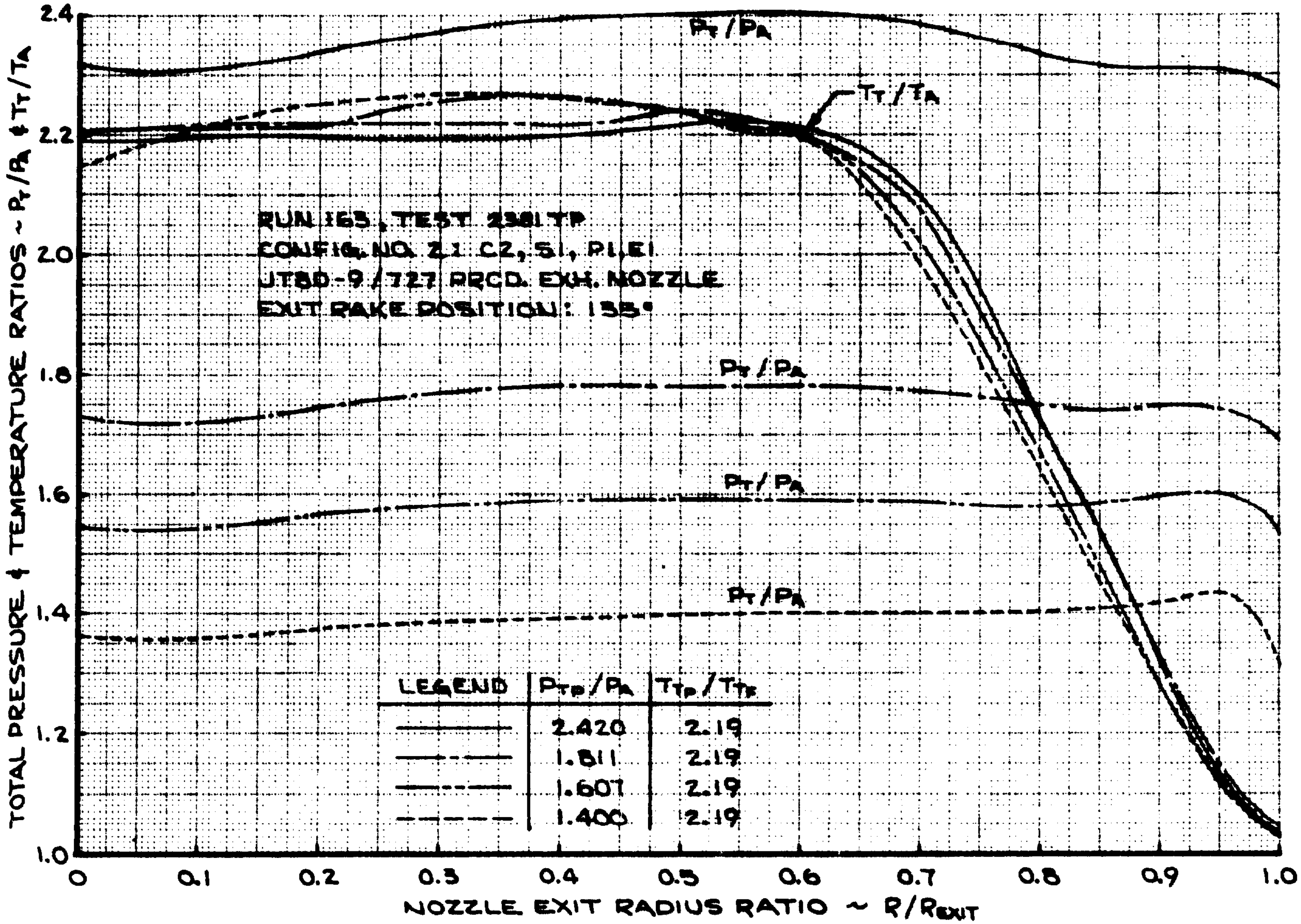

FIGURE 271- EXIT PLANE TOTAL PRESSURE & TEMPERATURE RATIO PROFILES
TEST CONFIG. NO. 2; TRAVERSING PROBE LOCATION - 135 DEG.

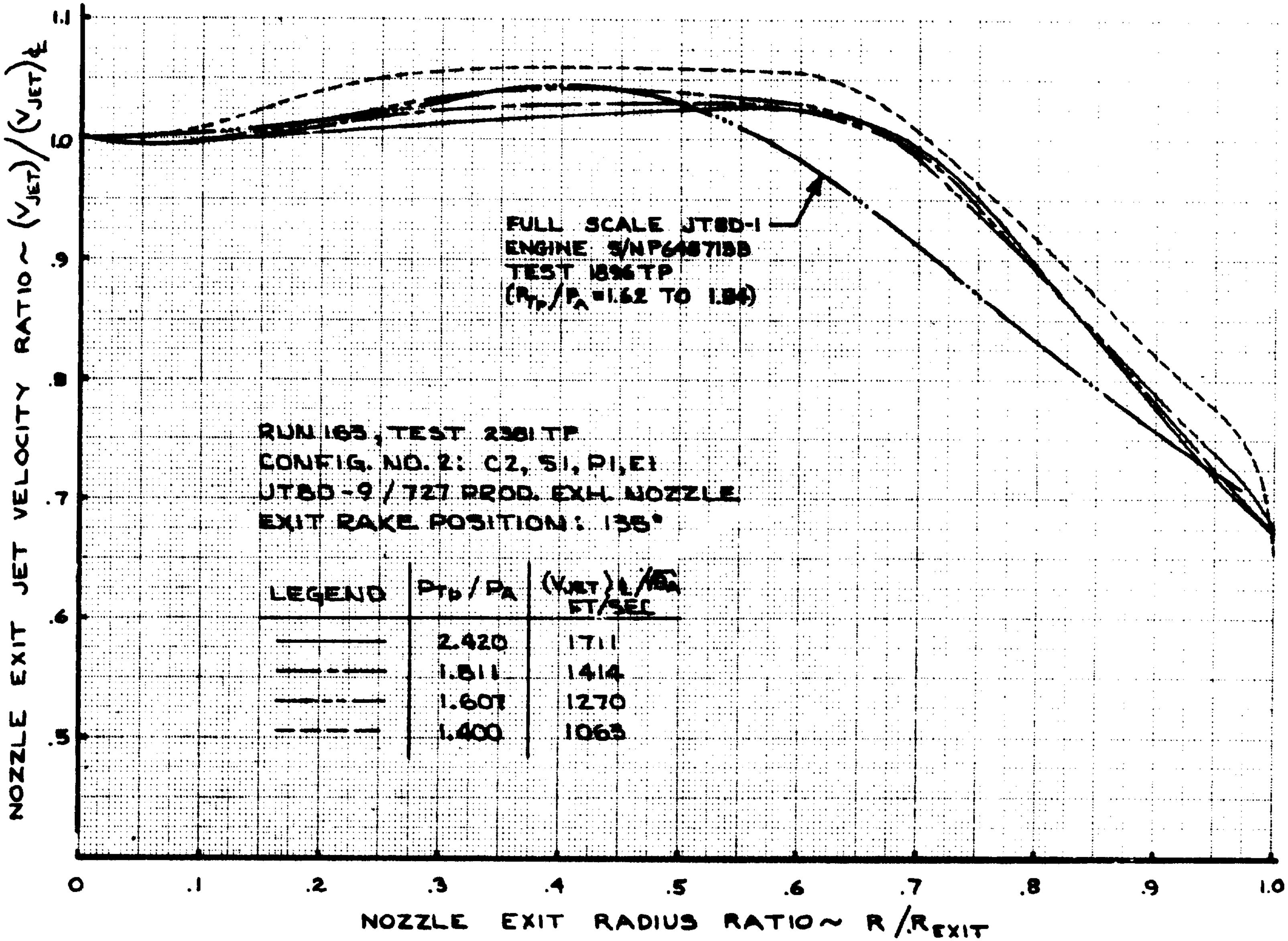

FIGURE 272- NOZZLE EXIT JET VELOCITY RATIO
TEST CONFIG. NO. 2; TRAVERSING PROBE LOCATION - 135 DEG.

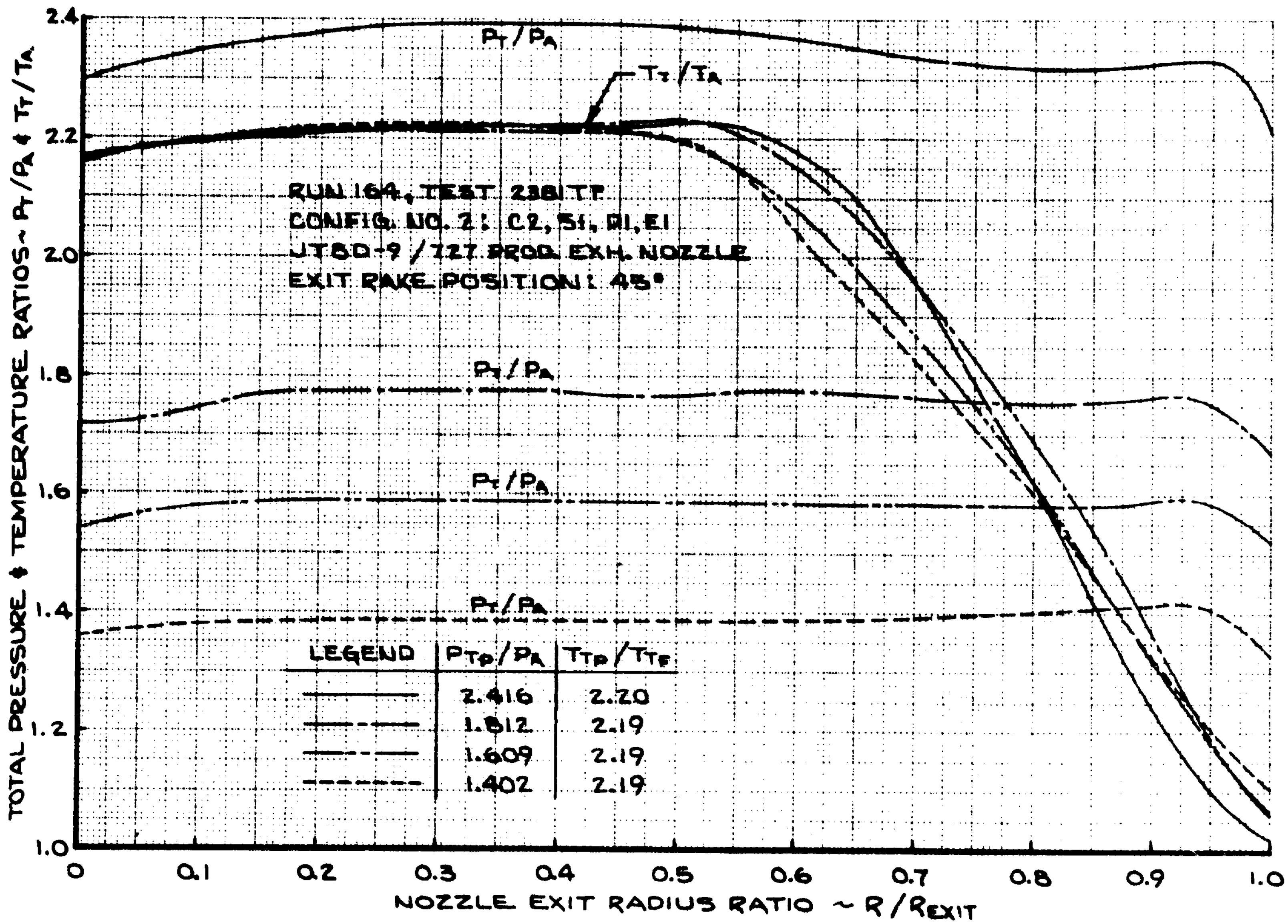

FIGURE 273- EXIT PLANE TOTAL PRESSURE & TEMPERATURE RATIO PROFILES
TEST CONFIG. NO. 2; TRAVERSING PROBE LOCATION - 45 DEG.

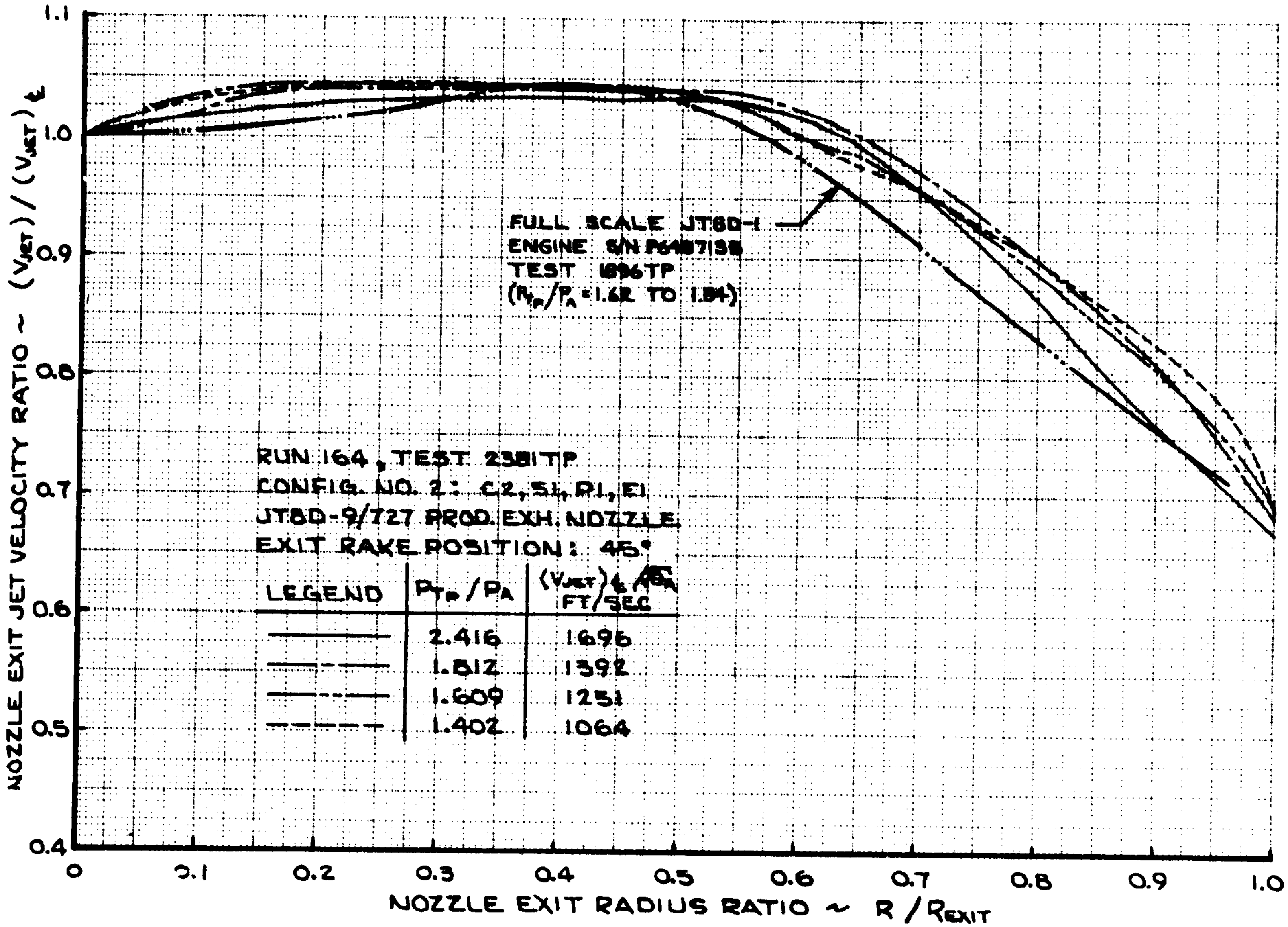

FIGURE 274- NOZZLE EXIT JET VELOCITY RATIO
TEST CONFIG. NO. 2; TRAVERSING PROBE LOCATION - 45 DEG.

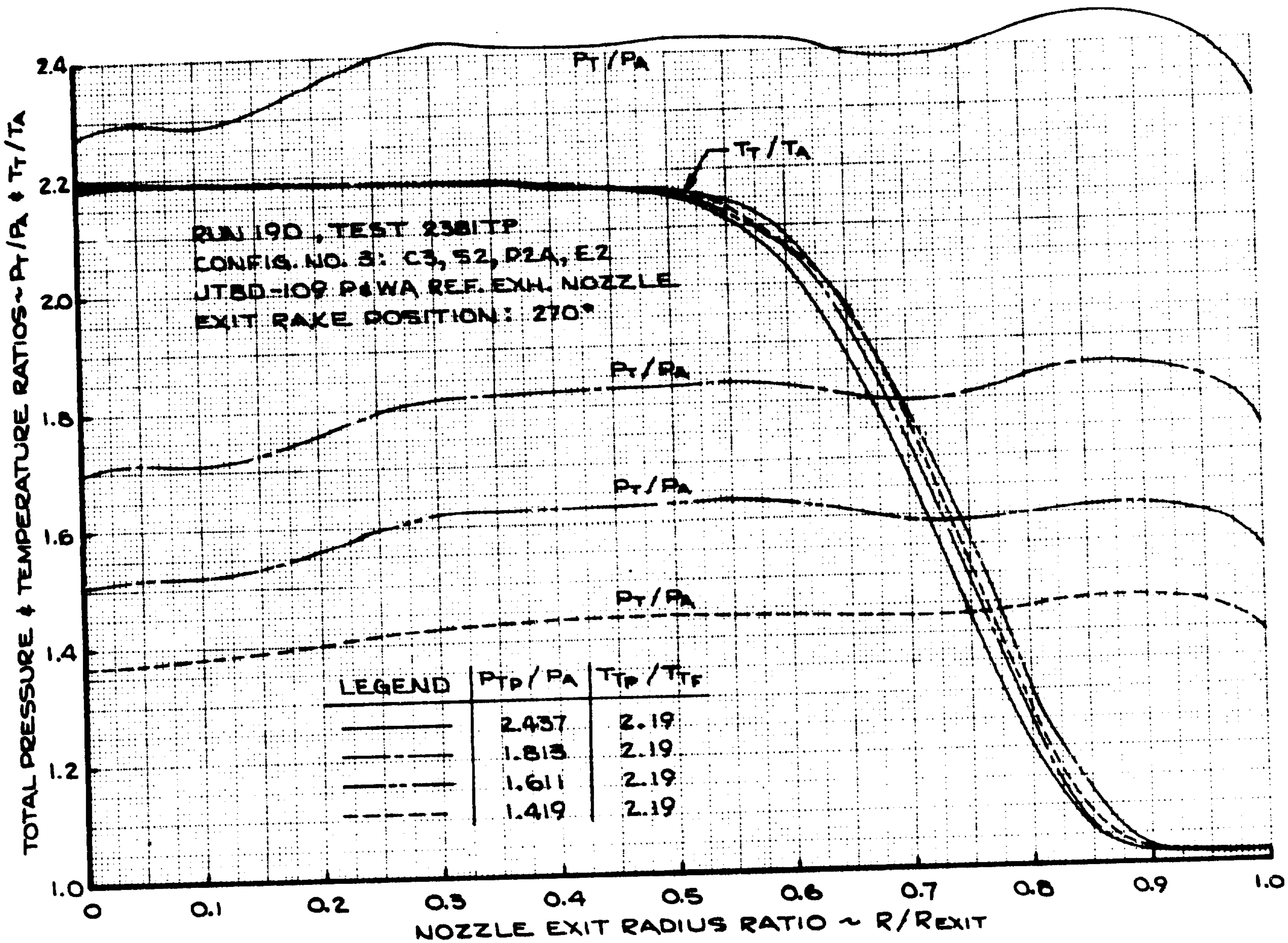

FIGURE 275- EXIT PLANE TOTAL PRESSURE & TEMPERATURE RATIO PROFILES
TEST CONFIG. NO. 3; TRAVERSING PROBE LOCATION - 270 DEG.

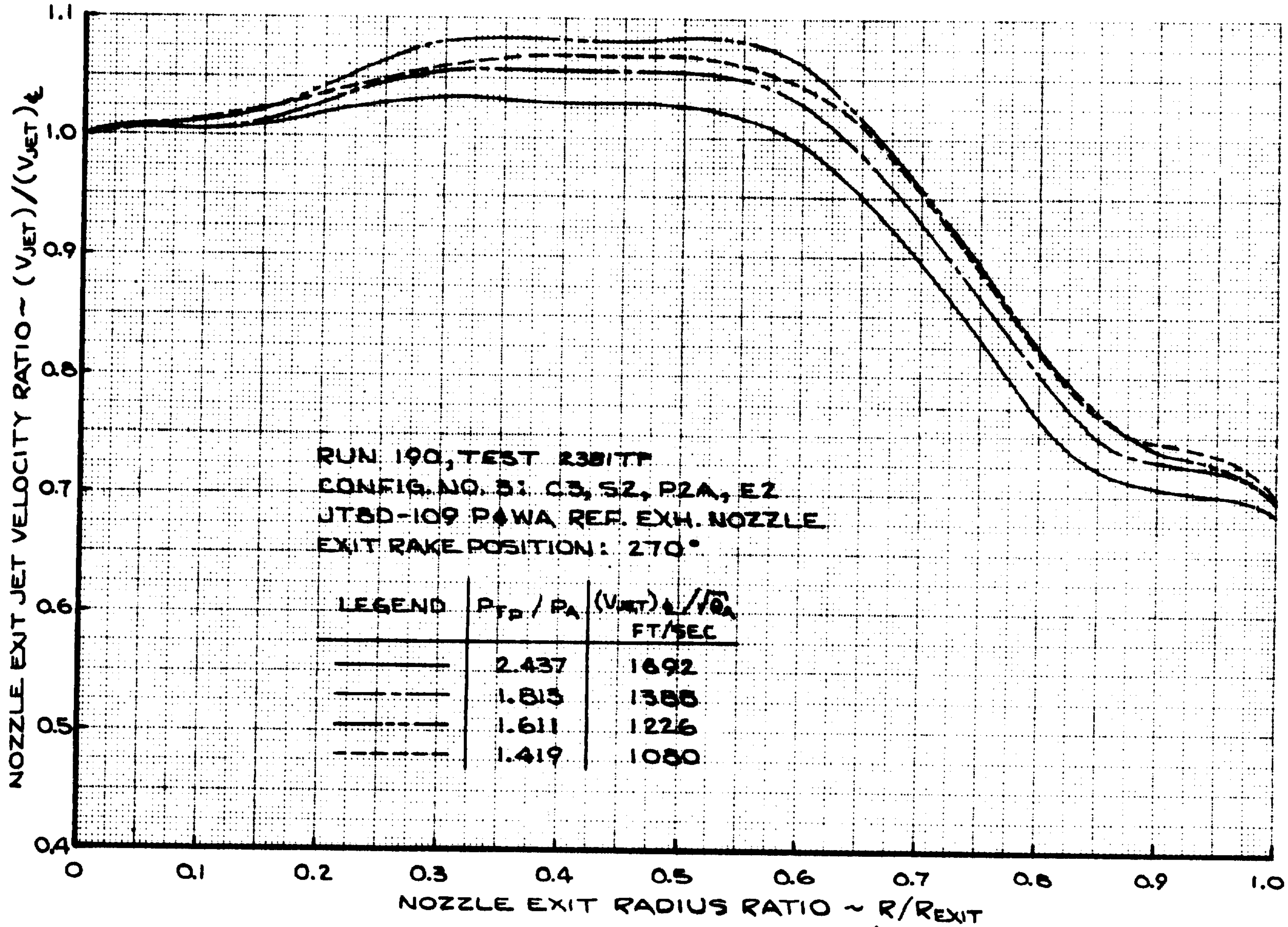

FIGURE 276- NOZZLE EXIT JET VELOCITY RATIO
TEST CONFIG. NO. 3; TRAVERSING PROBE LOCATION - 270 DEG.

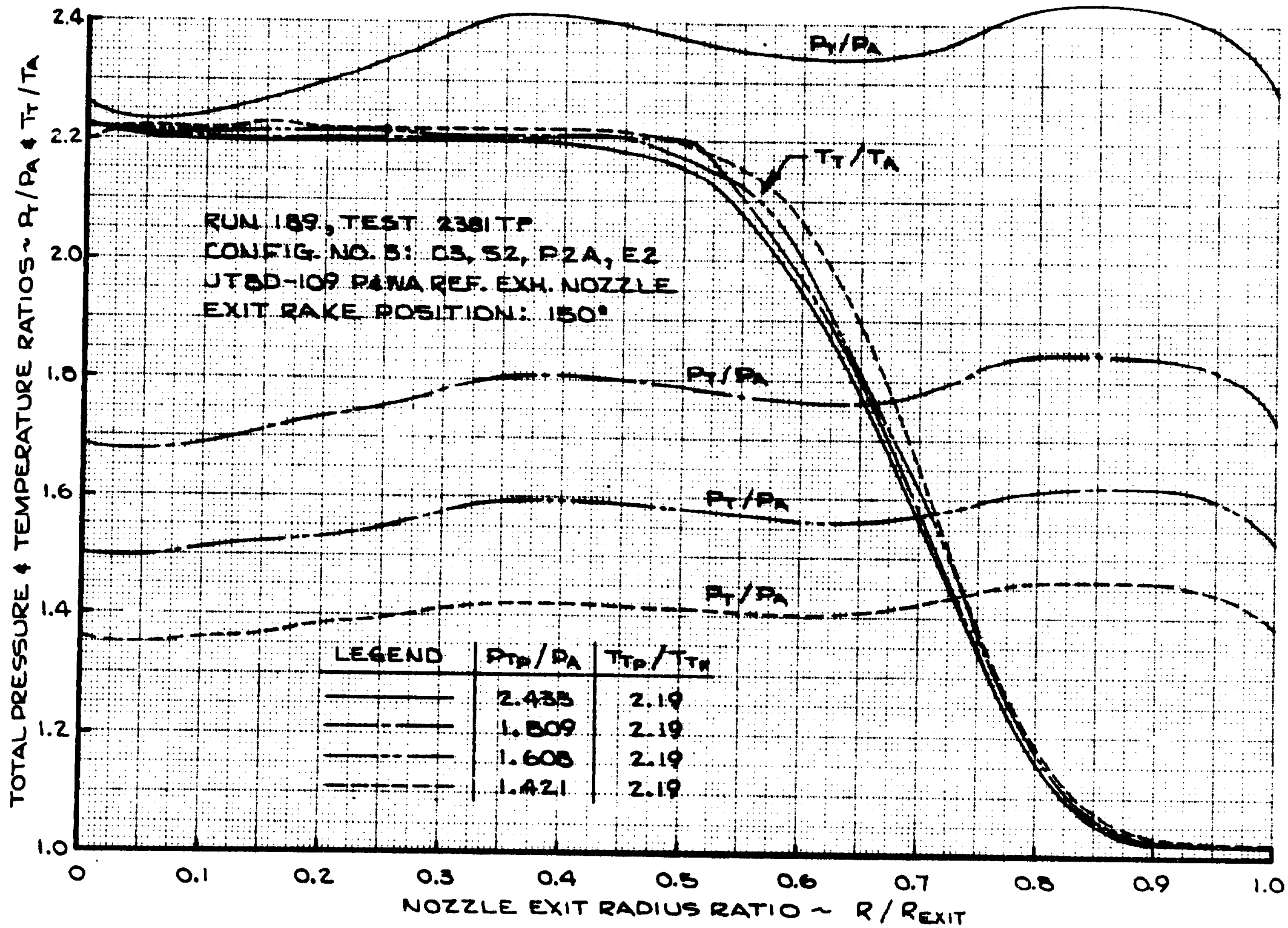

FIGURE 277- EXIT PLANE TOTAL PRESSURE & TEMPERATURE RATIO PROFILES
TEST CONFIG. NO. 3; TRAVERSING PROBE LOCATION - 150 DEG.

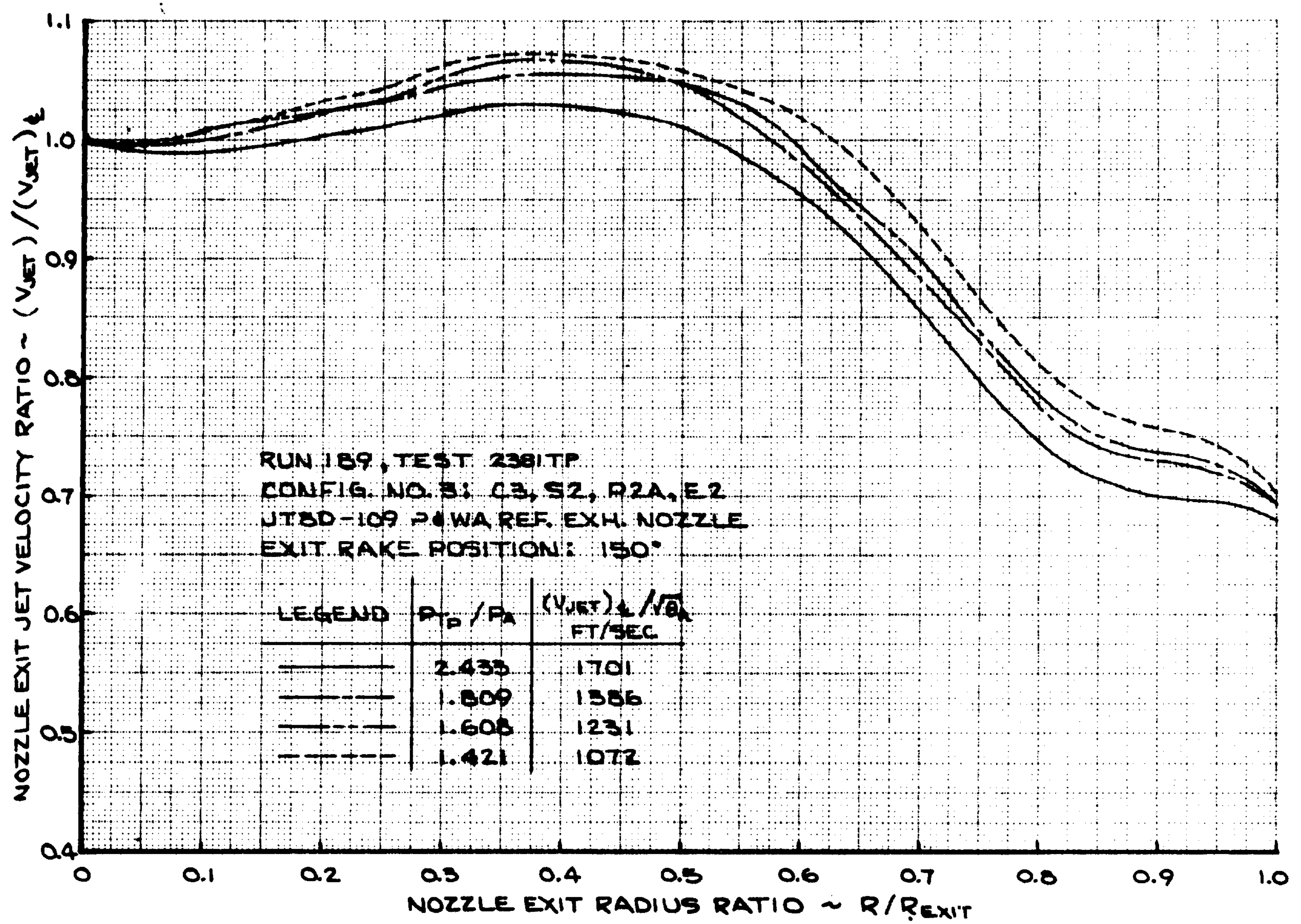

FIGURE 278- NOZZLE EXIT JET VELOCITY RATIO
TEST CONFIG. NO. 3; TRAVERSING PROBE LOCATION - 150 DEG.

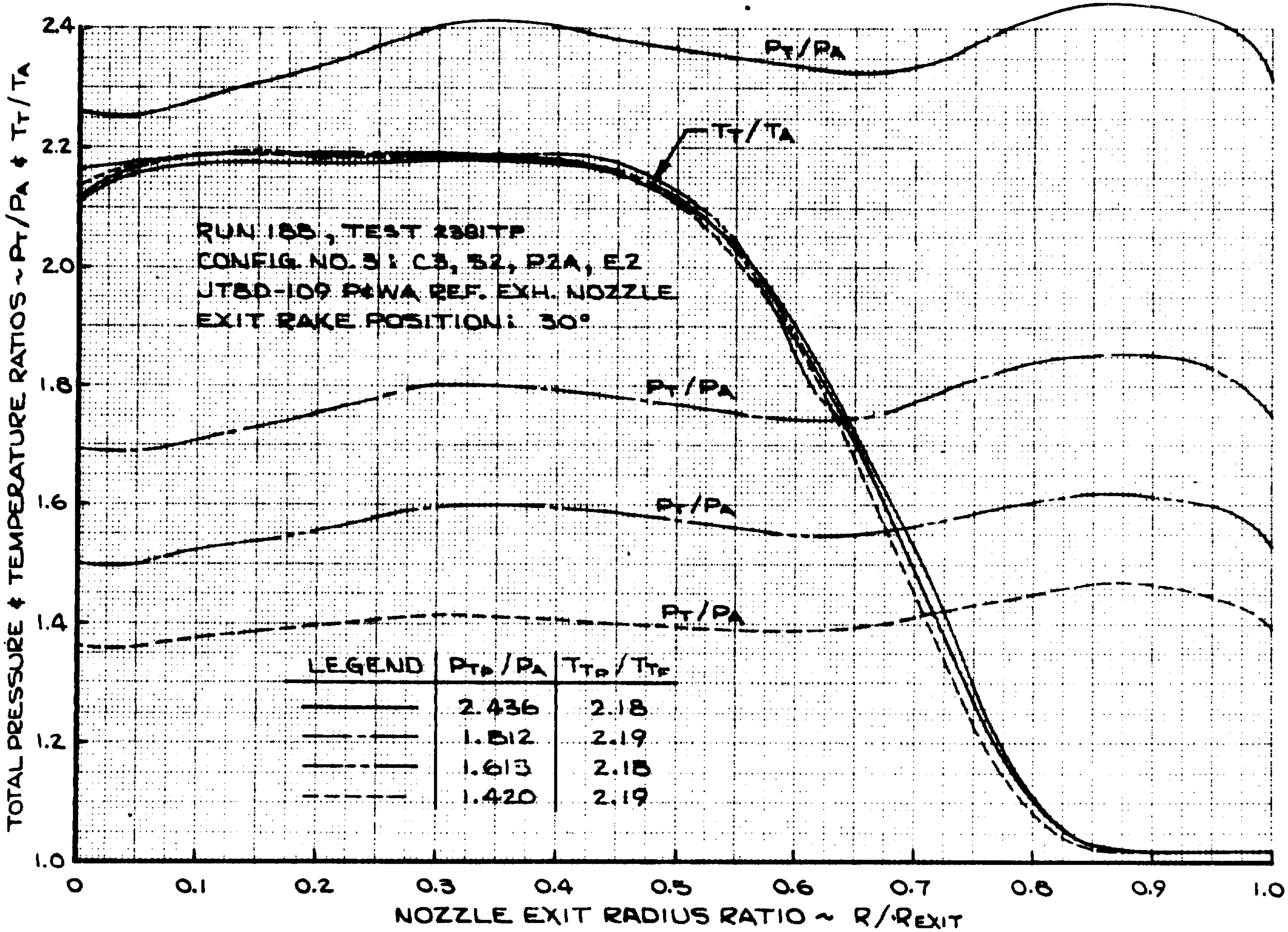

FIGURE 279- EXIT PLANE TOTAL PRESSURE & TEMPERATURE RATIO PROFILES
TEST CONFIG. NO. 3; TRAVERSING PROBE LOCATION - 30 DEG.

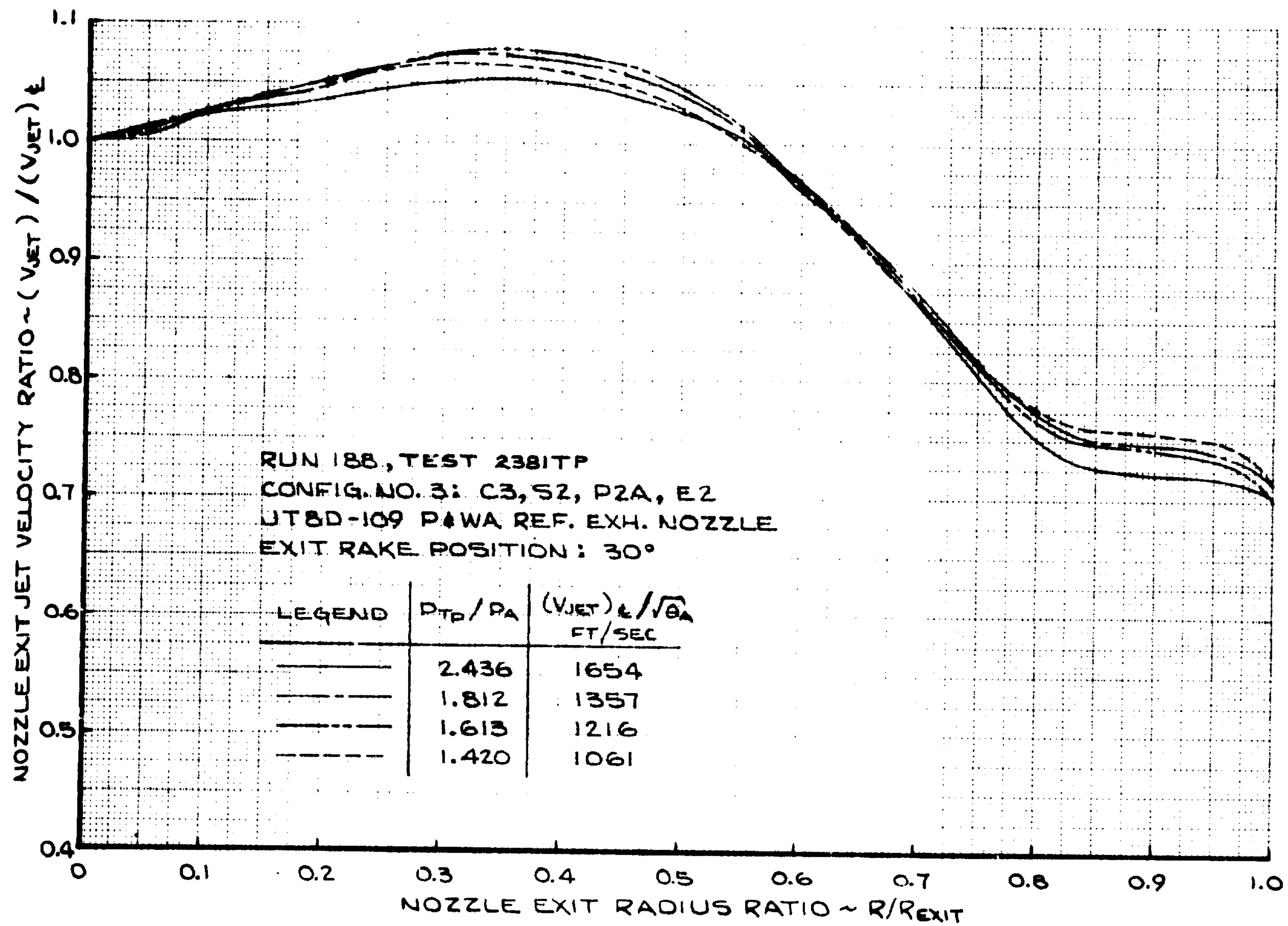

FIGURE 280- NOZZLE EXIT JET VELOCITY RATIO
TEST CONFIG. NO. 3; TRAVERSING PROBE LOCATION - 30 DEG.

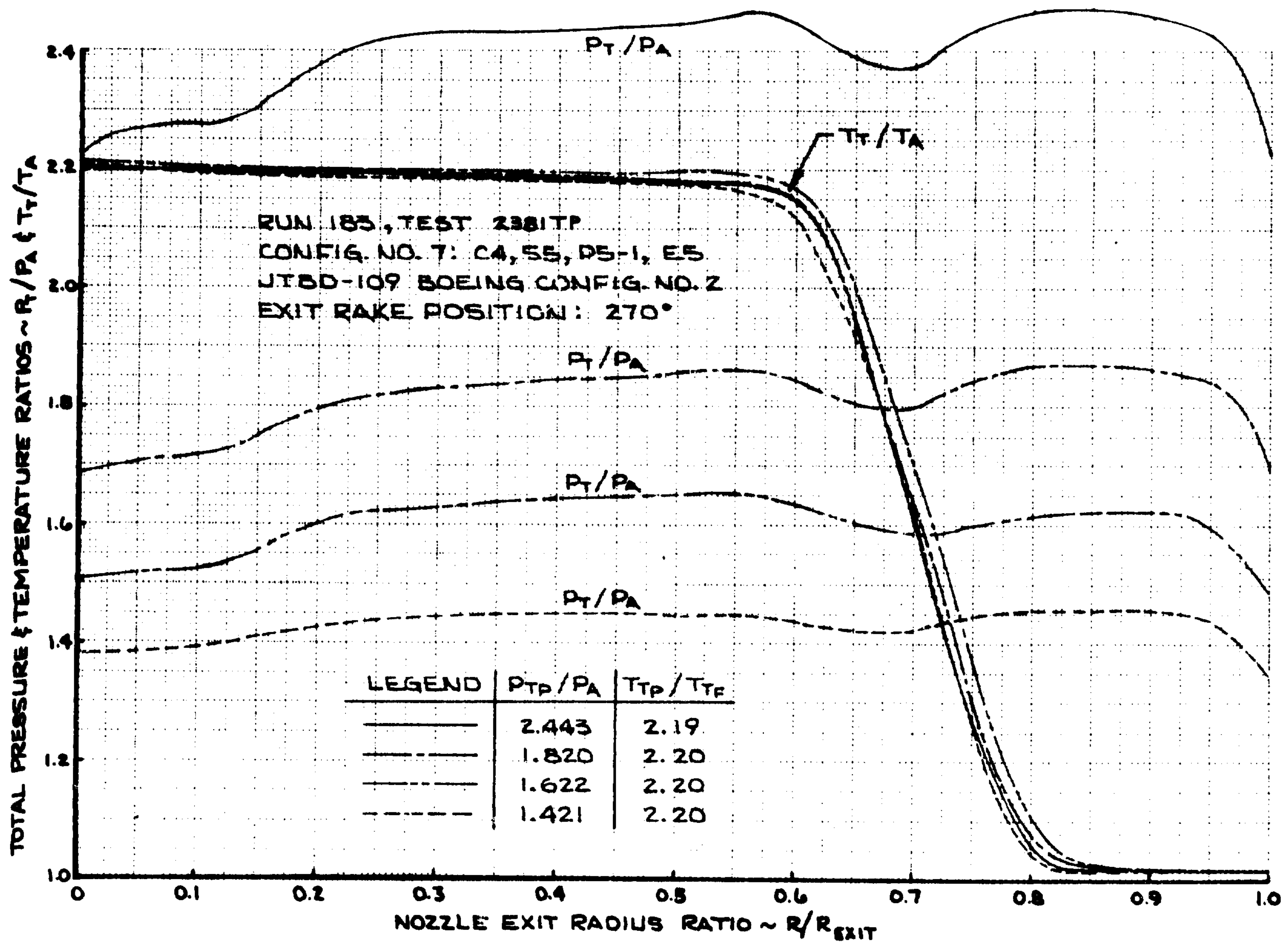

FIGURE 281- EXIT PLANE TOTAL PRESSURE & TEMPERATURE RATIO PROFILES
TEST CONFIG. NO. 7; TRAVERSING PROBE LOCATION - 270 DEG.

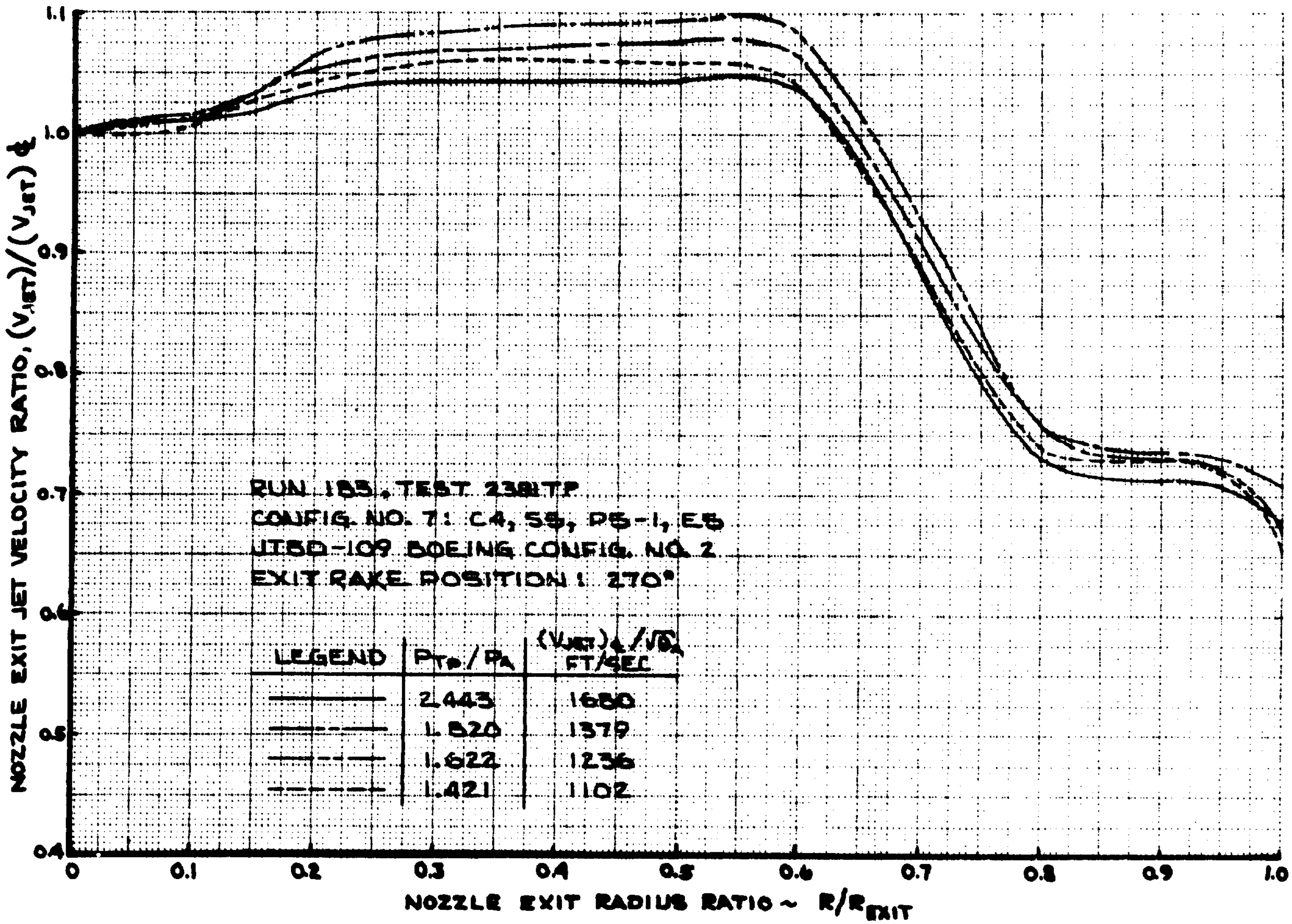

FIGURE 282- NOZZLE EXIT JET VELOCITY RATIO
TEST CONFIG. NO. 7; TRAVERSING PROBE LOCATION - 270 DEG.

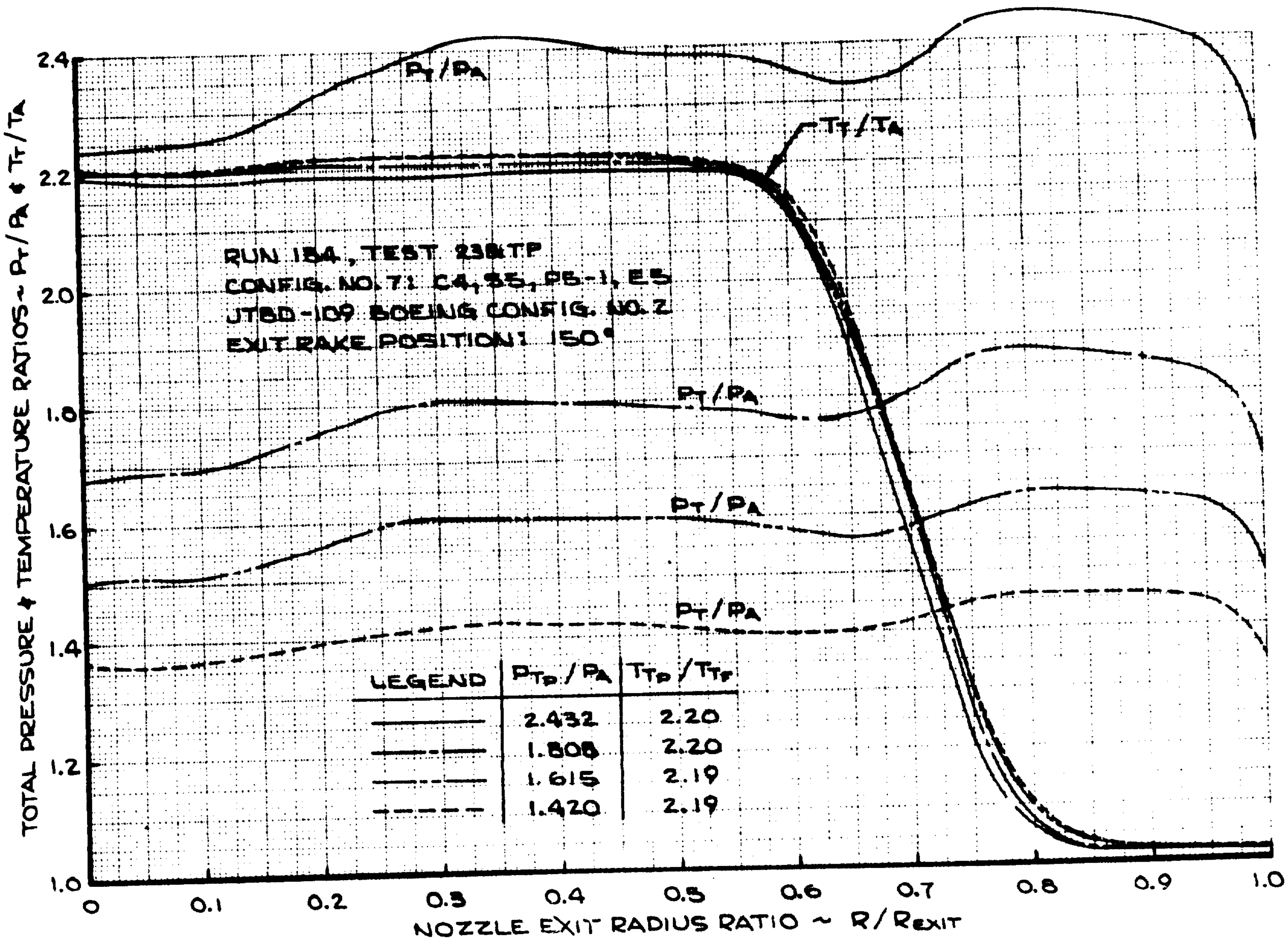

FIGURE 283- EXIT PLANE TOTAL PRESSURE & TEMPERATURE RATIO PROFILES
TEST CONFIG. NO. 7; TRAVERSING PROBE LOCATION - 150 DEG.

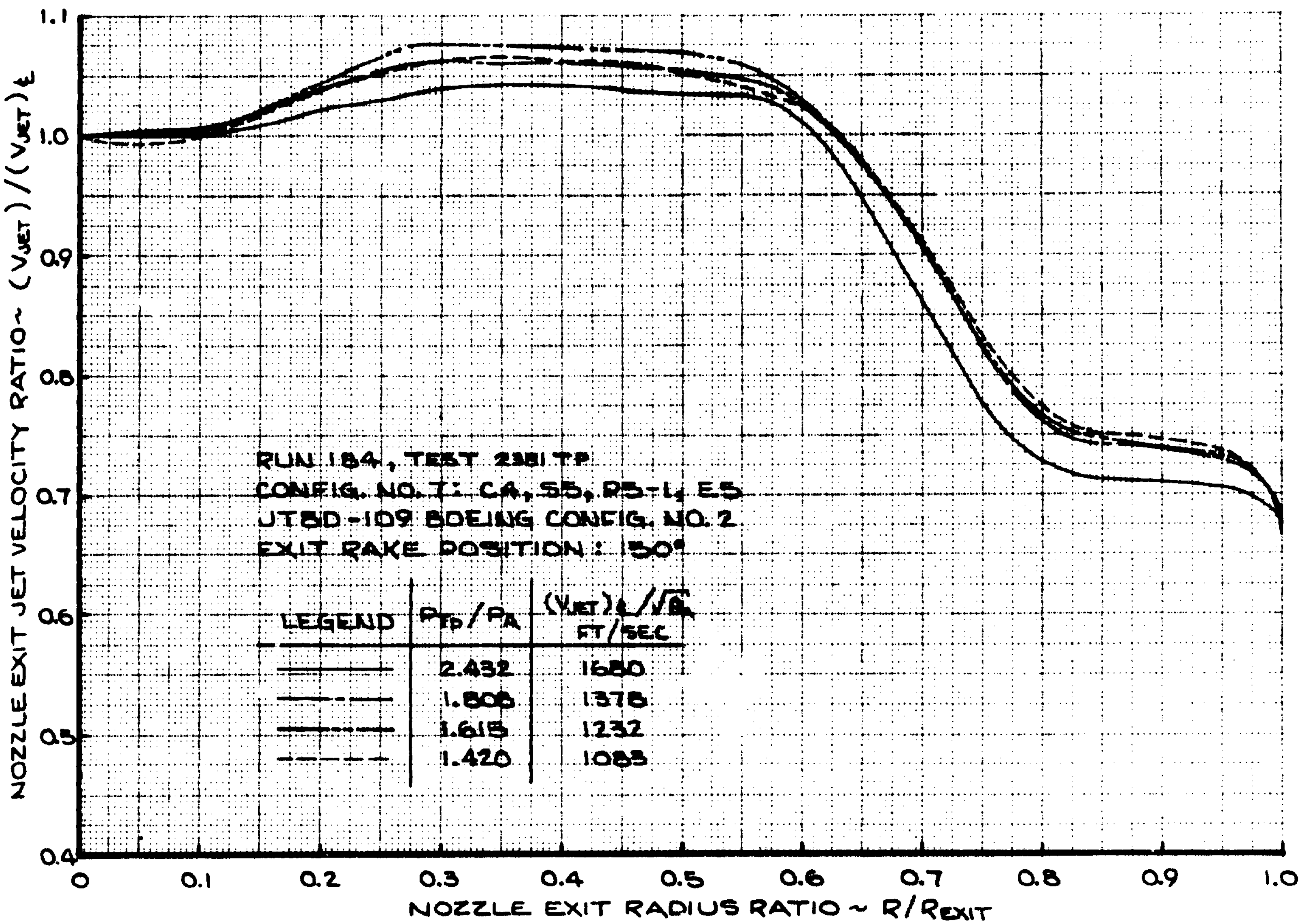

FIGURE 284- NOZZLE EXIT JET VELOCITY RATIO
TEST CONFIG. NO. 7; TRAVERSING PROBE LOCATION - 150 DEG.

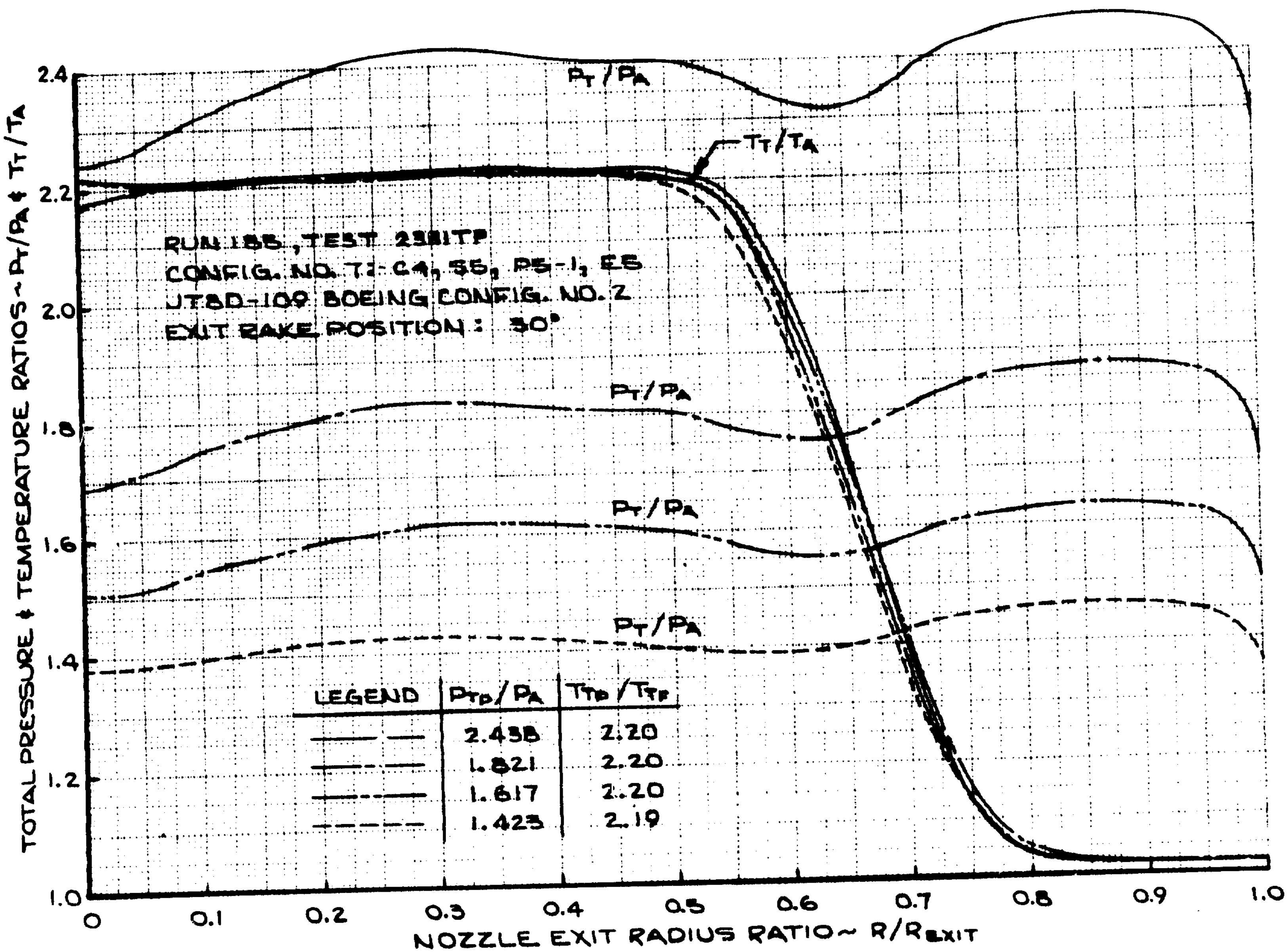

FIGURE 285- EXIT PLANE TOTAL PRESSURE & TEMPERATURE RATIO PROFILES
TEST CONFIG. NO. 7; TRAVERSING PROBE LOCATION - 30 DEG.

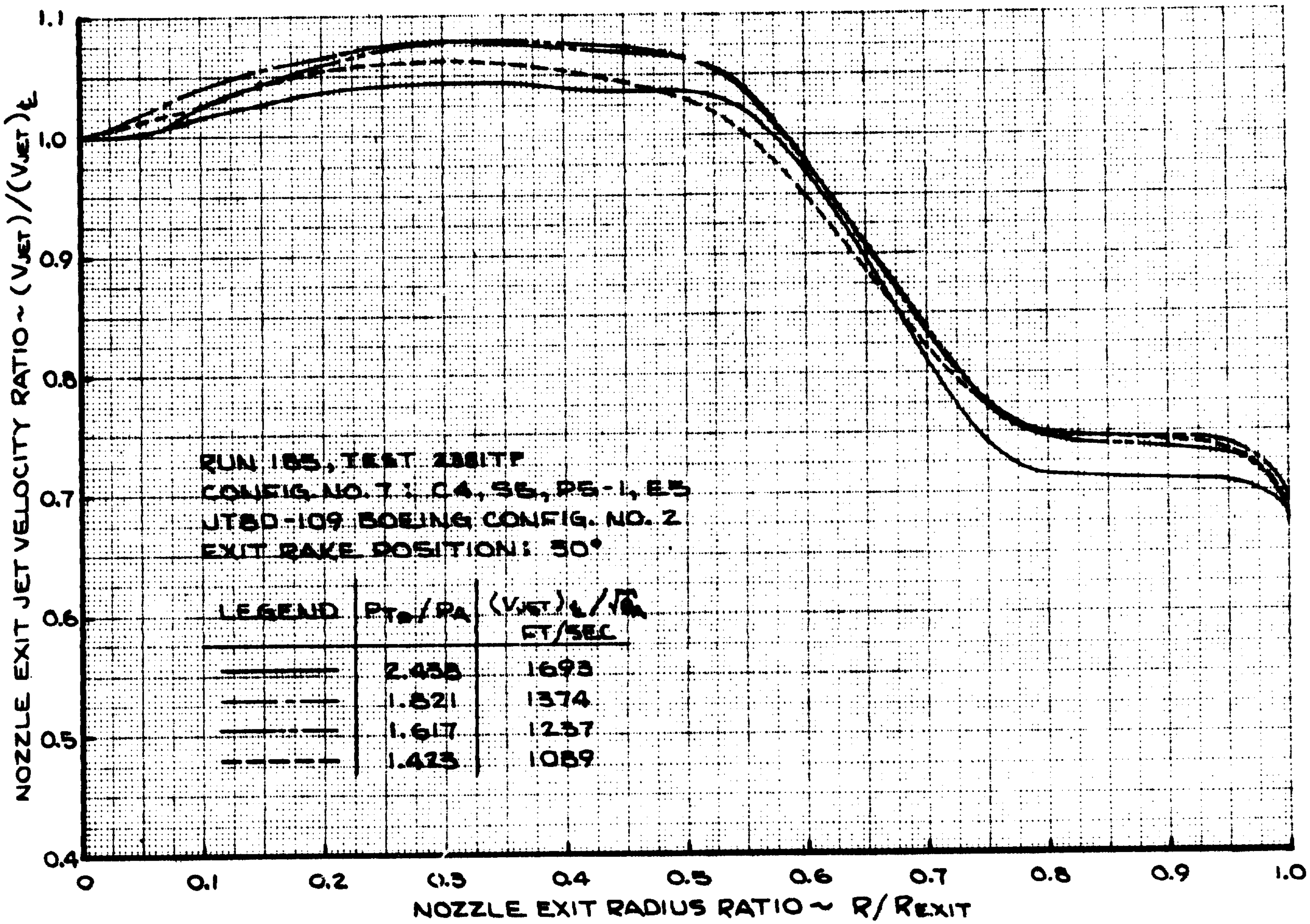

FIGURE 286- NOZZLE EXIT JET VELOCITY RATIO
TEST CONFIG. NO. 7; TRAVERSING PROBE LOCATION - 30 DEG.

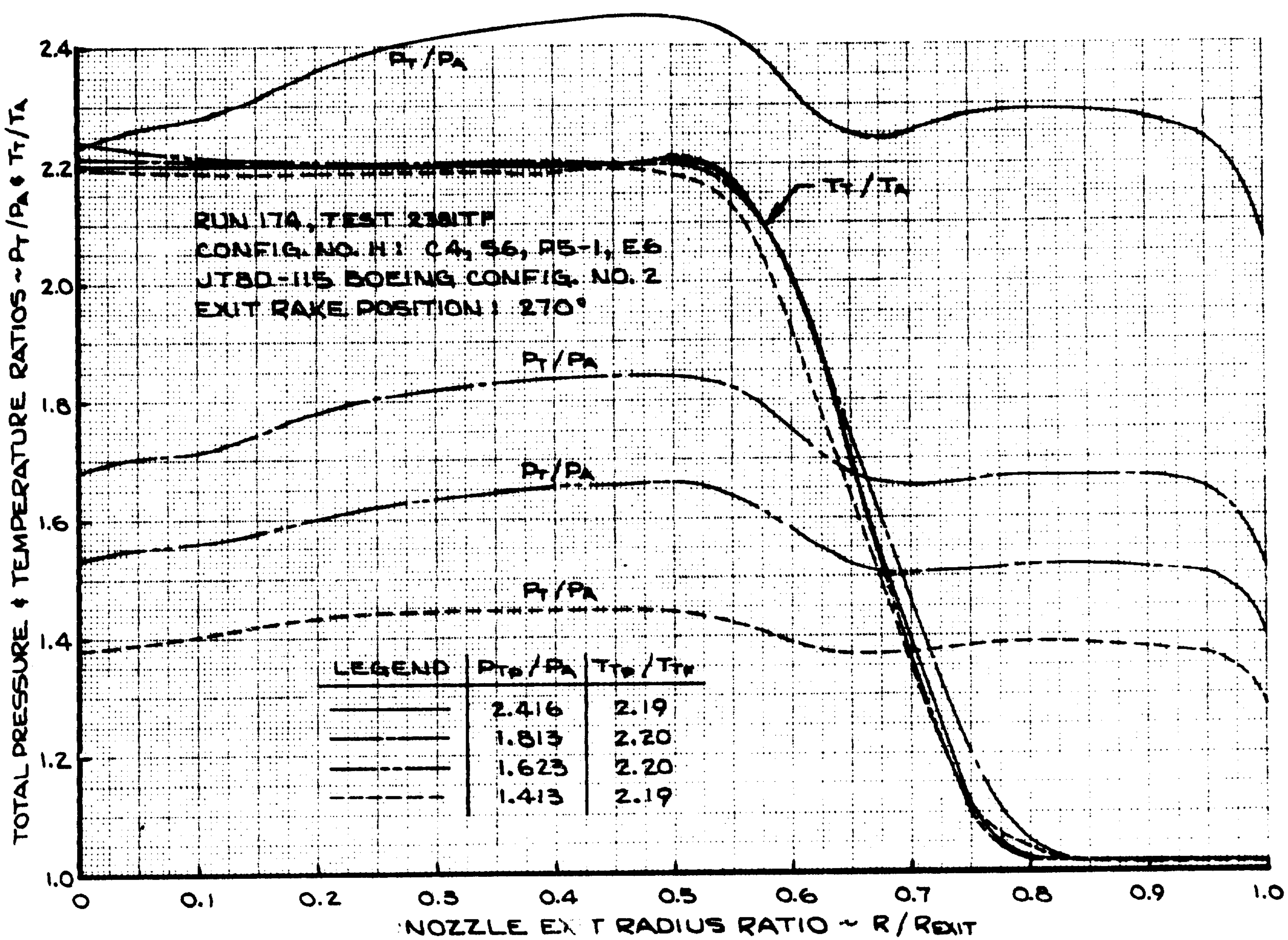

FIGURE 287- EXIT PLANE TOTAL PRESSURE & TEMPERATURE RATIO PROFILES
TEST CONFIG. NO. 11; TRAVERSING PROBE LOCATION - 270 DEG.

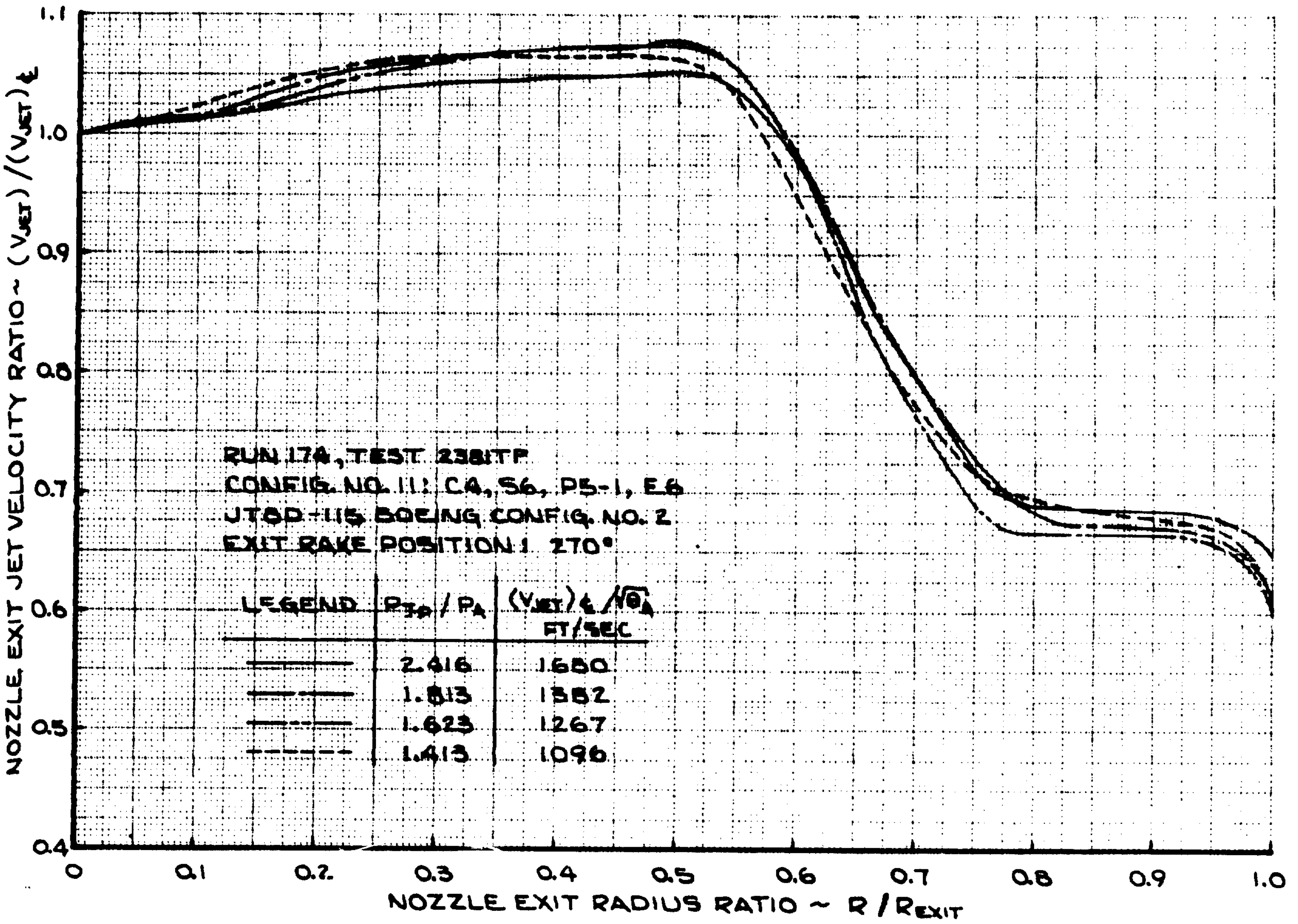

FIGURE 288- NOZZLE EXIT JET VELOCITY RATIO
TEST CONFIG. NO. 11; TRAVERSING PROBE LOCATION - 270 DEG.

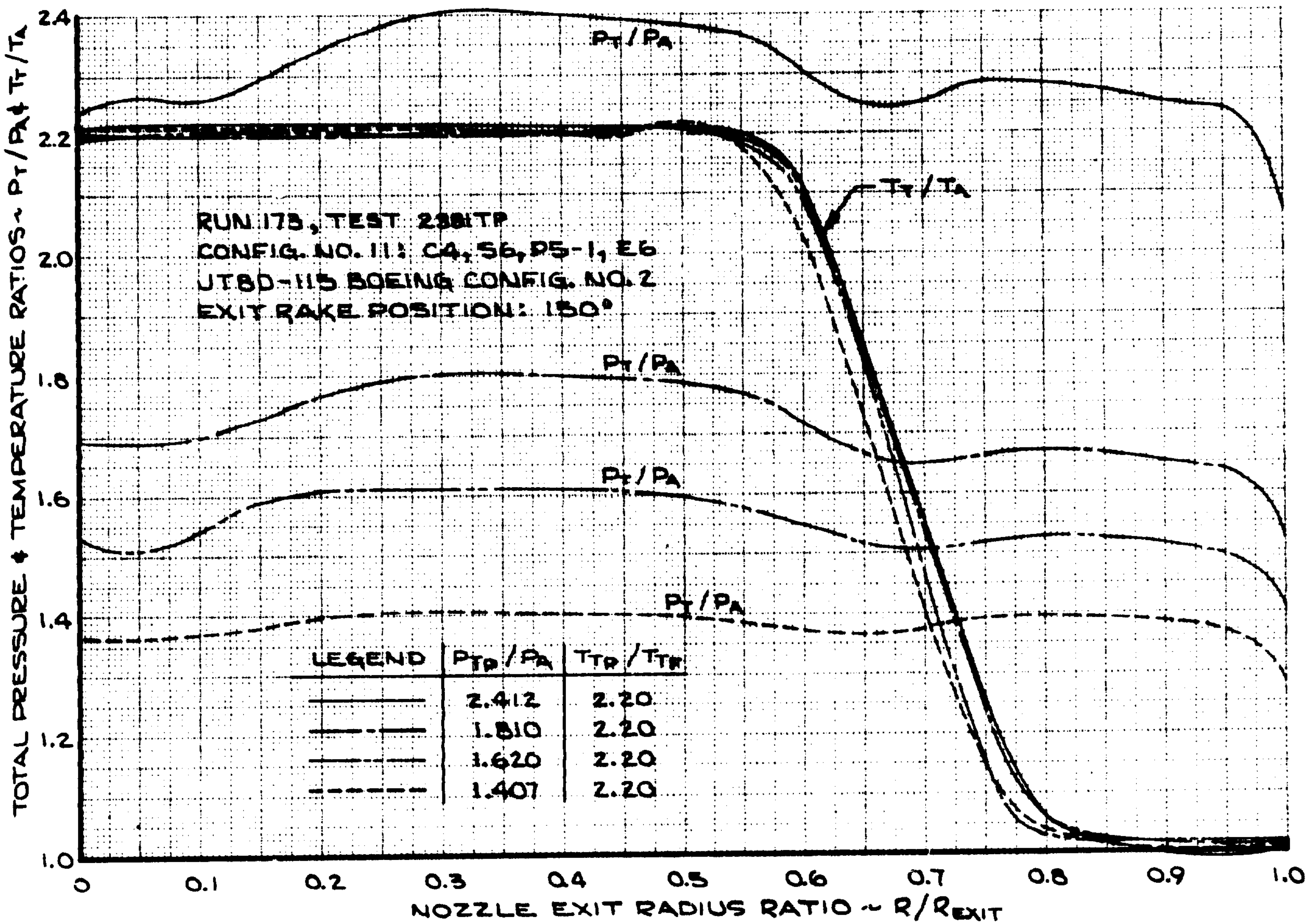

FIGURE 289- EXIT PLANE TOTAL PRESSURE & TEMPERATURE RATIO PROFILES
TEST CONFIG. NO. 11; TRAVERSING PROBE LOCATION - 150 DEG.

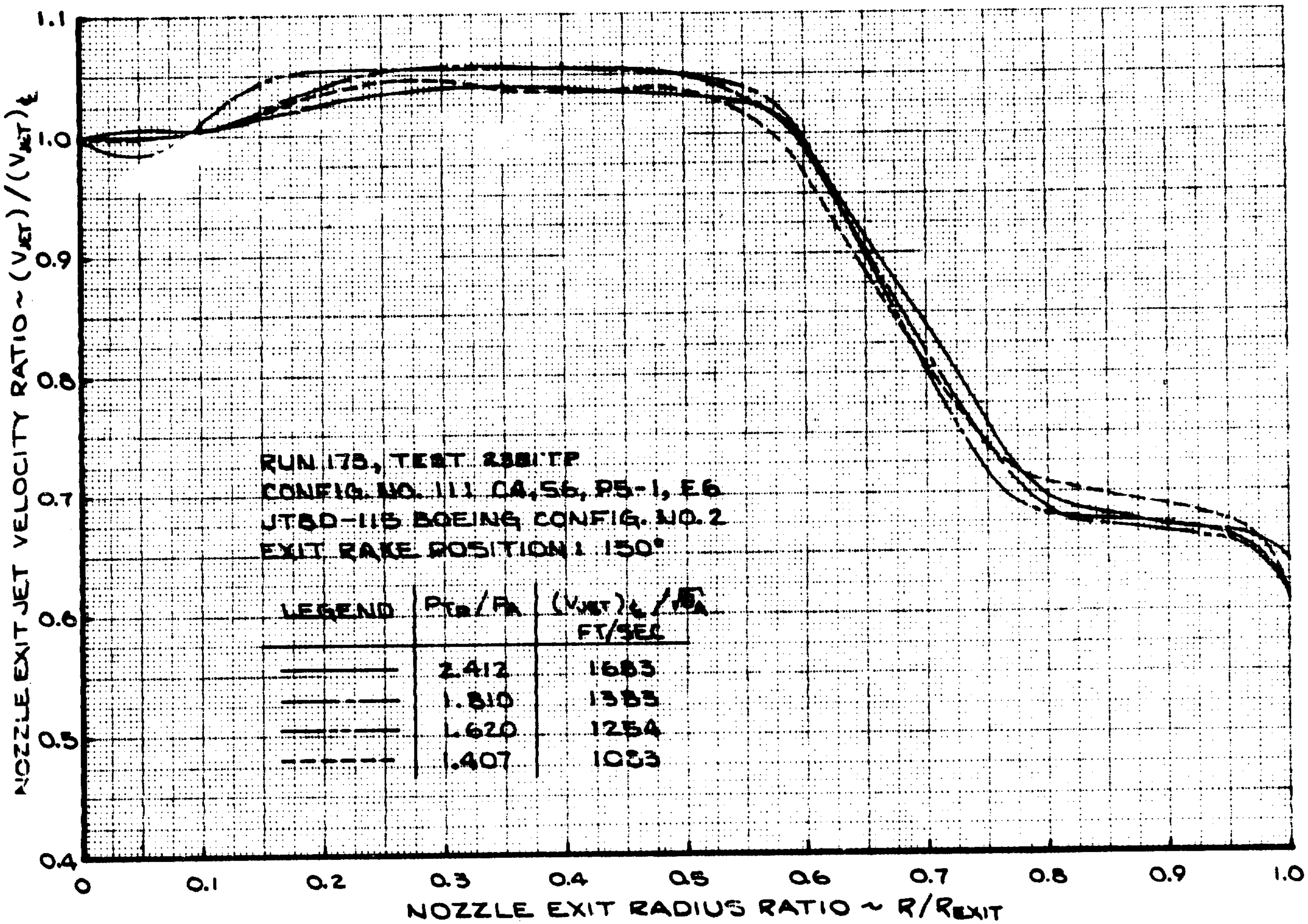

FIGURE 290- NOZZLE EXIT JET VELOCITY RATIO
TEST CONFIG. NO. 11; TRAVERSING PROBE LOCATION - 150 DEG.

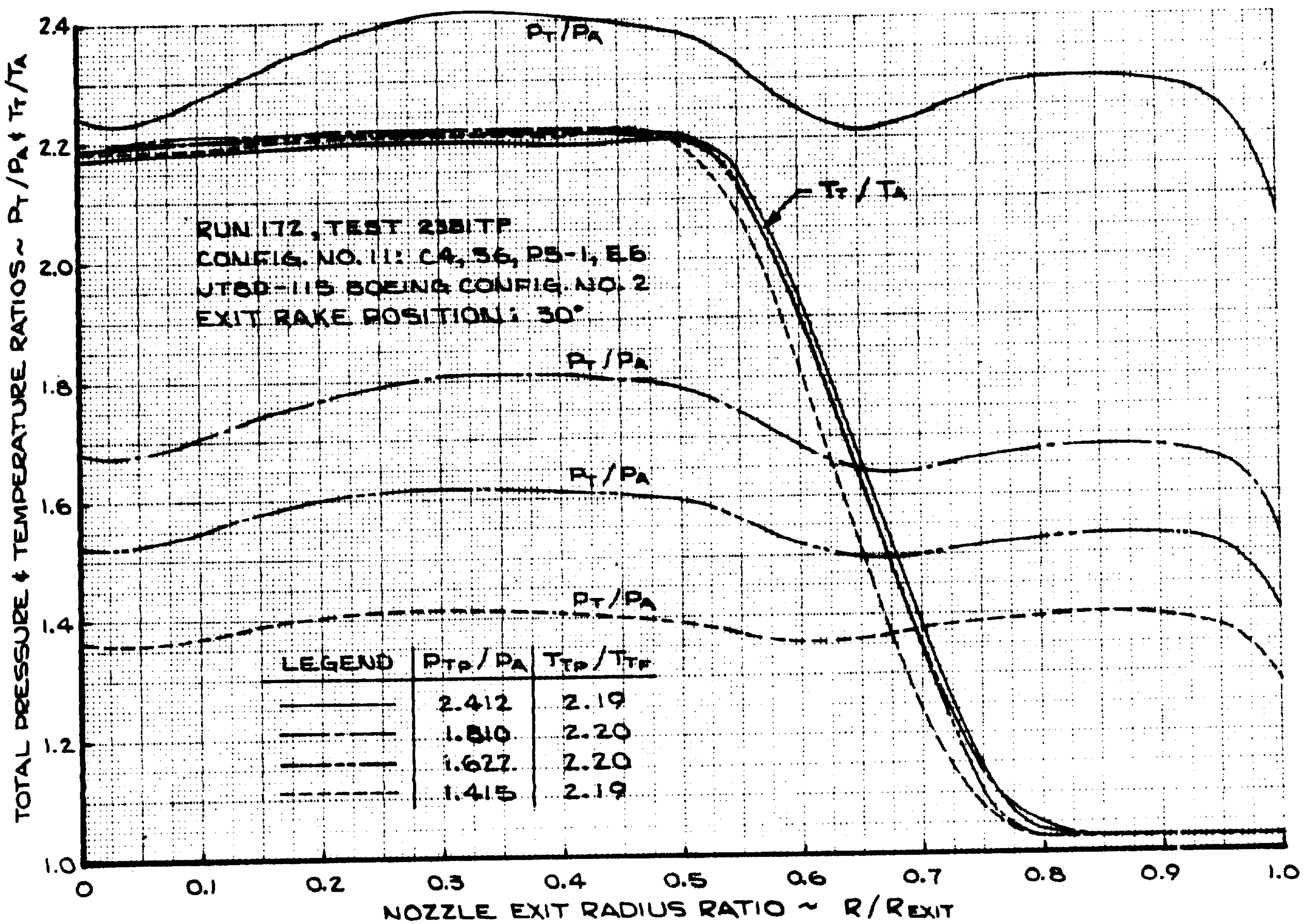

FIGURE 291- EXIT PLANE TOTAL PRESSURE & TEMPERATURE RATIO PROFILES
TEST CONFIG. NO. 11; TRAVERSING PROBE LOCATION - 30 DEG.

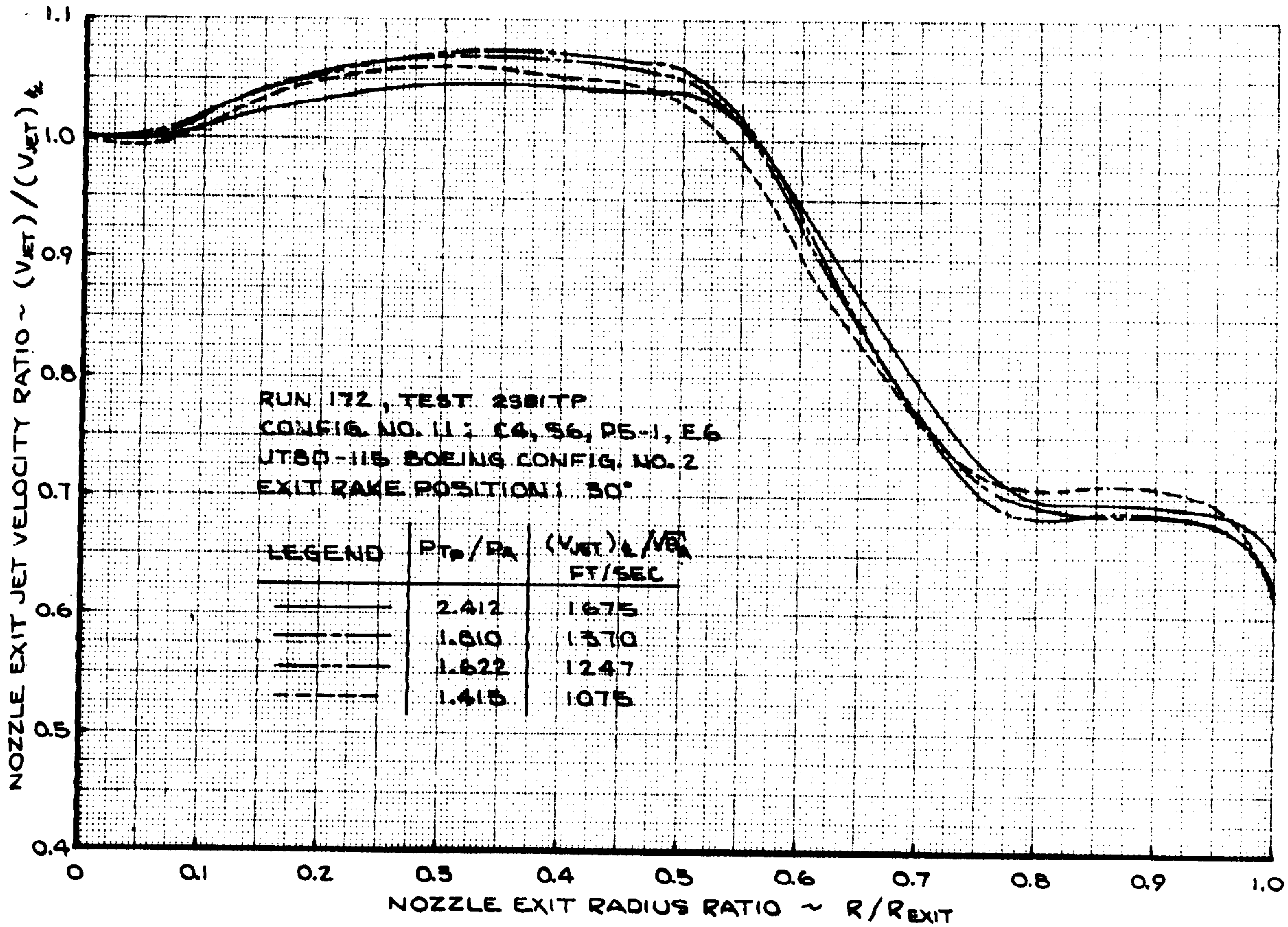

FIGURE 292- NOZZLE EXIT JET VELOCITY RATIO
TEST CONFIG. NO. 11; TRAVERSING PROBE LOCATION - 30 DEG.

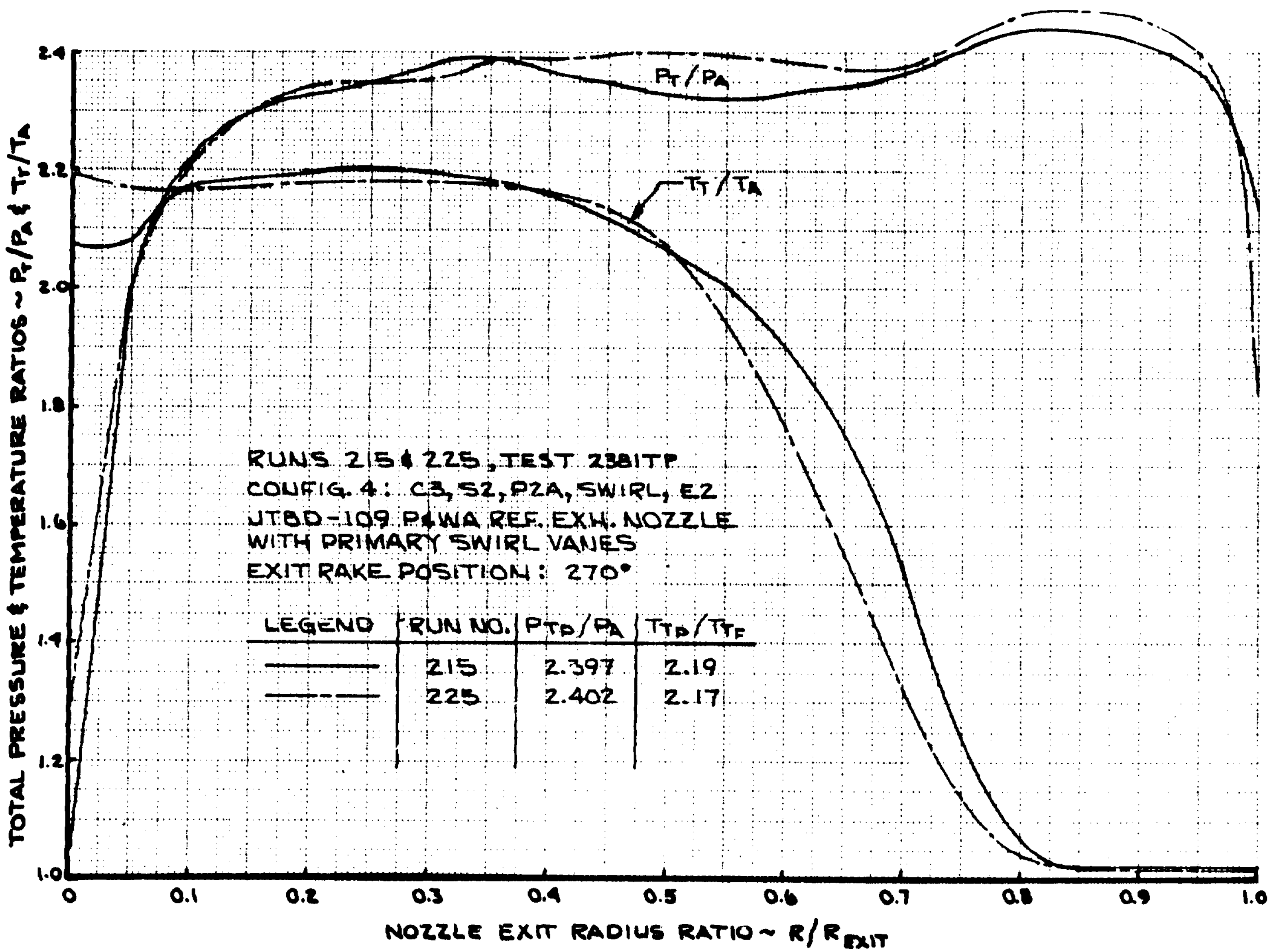

LEGEND	RUN NO.	P_{TP}/P_A	T_{TP}/T_{TF}
———	215	2.397	2.19
— — —	225	2.402	2.17

FIGURE 293- EXIT PLANE TOTAL PRESSURE & TEMPERATURE RATIO PROFILES
TEST CONFIG. NO. 4; TRAVERSING PROBE LOCATION - 270 DEG.

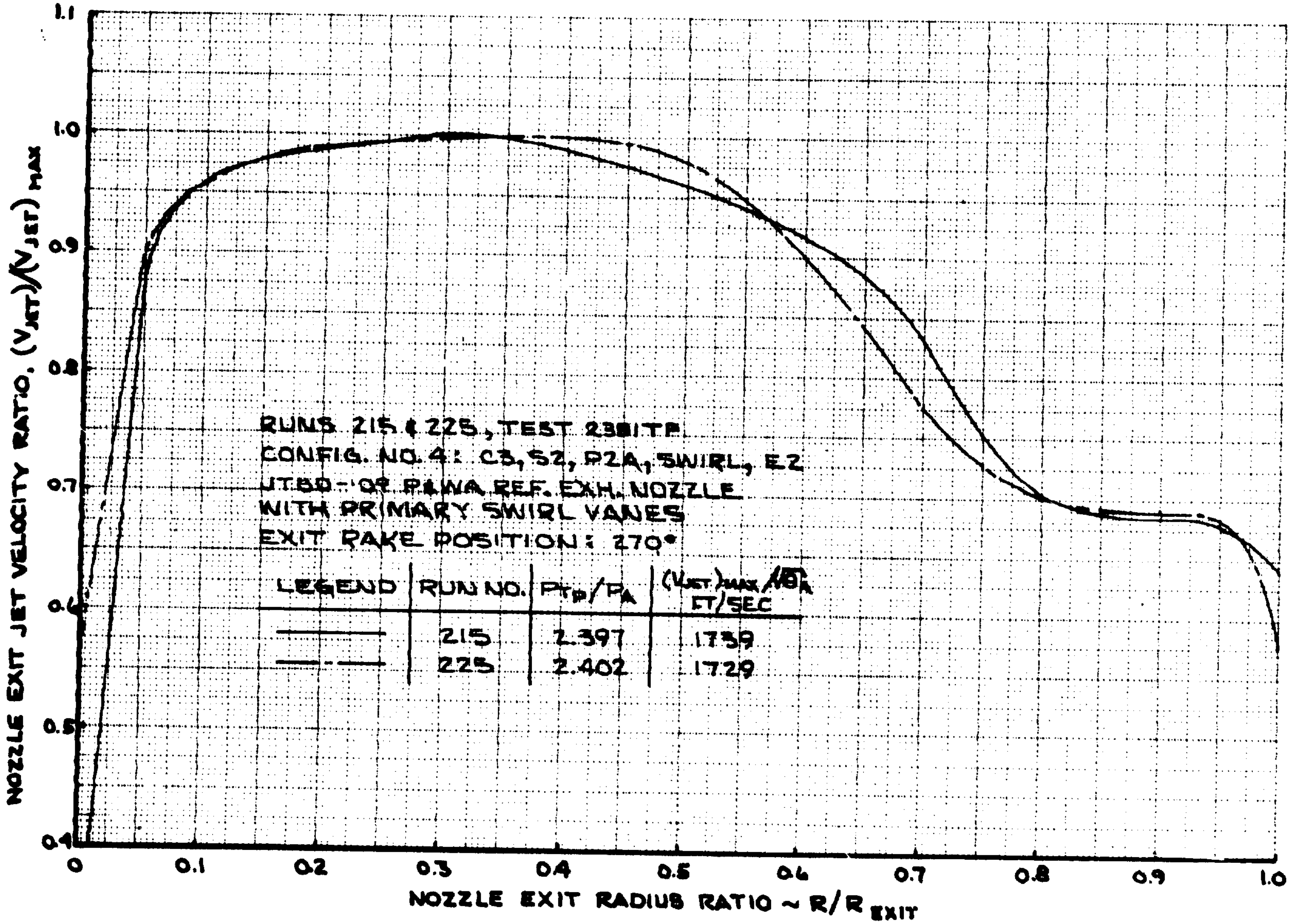

FIGURE 294- NOZZLE EXIT JET VELOCITY RATIO
TEST CONFIG. NO. 4; TRAVERSING PROBE LOCATION - 270 DEG.

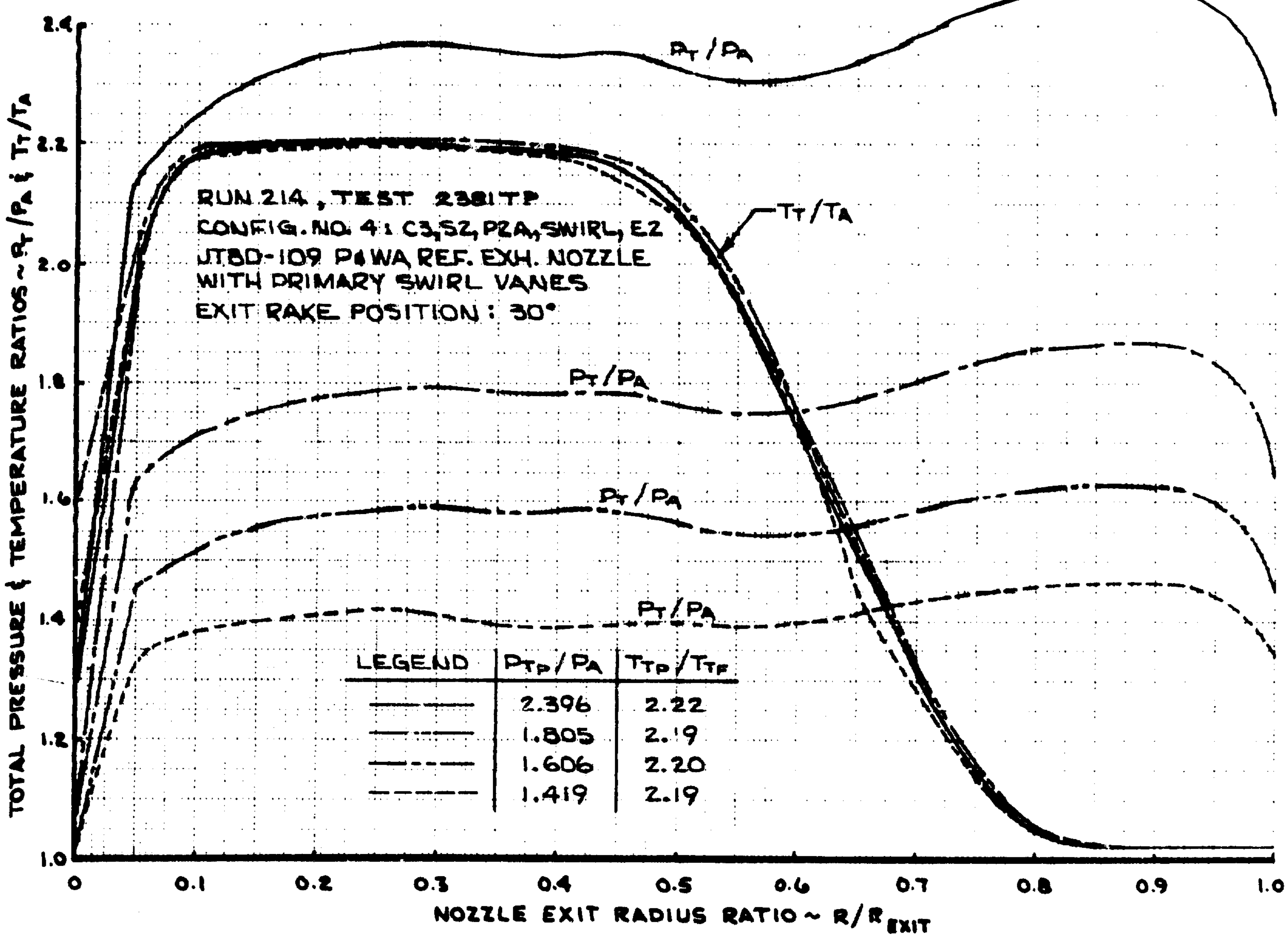

FIGURE 295- EXIT PLANE TOTAL PRESSURE & TEMPERATURE RATIO PROFILES
TEST CONFIG. NO. 4; TRAVERSING PROBE LOCATION - 30 DEG.

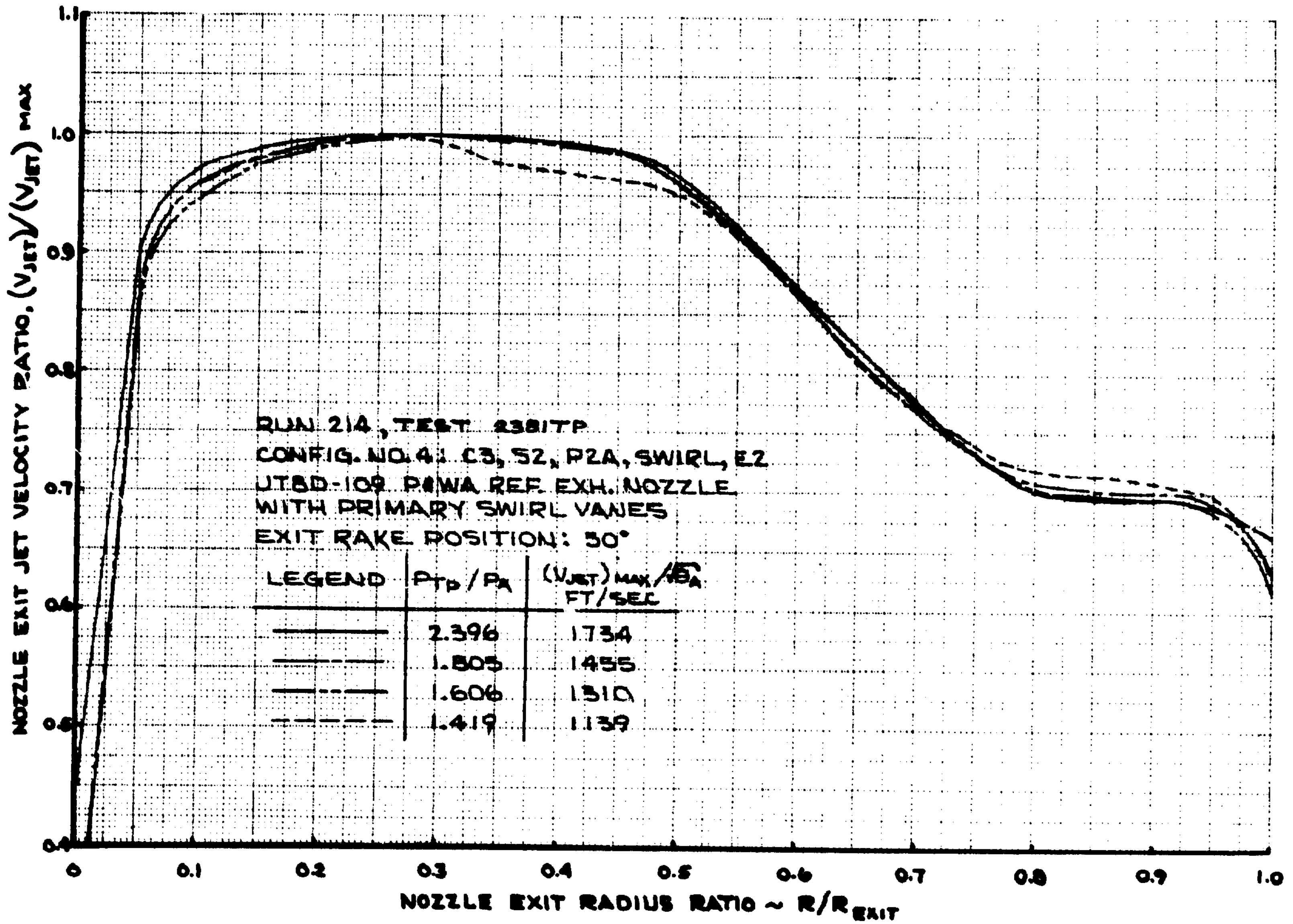

FIGURE 296- NOZZLE EXIT JET VELOCITY RATIO
TEST CONFIG. NO. 4; TRAVERSING PROBE LOCATION - 30 DEG.

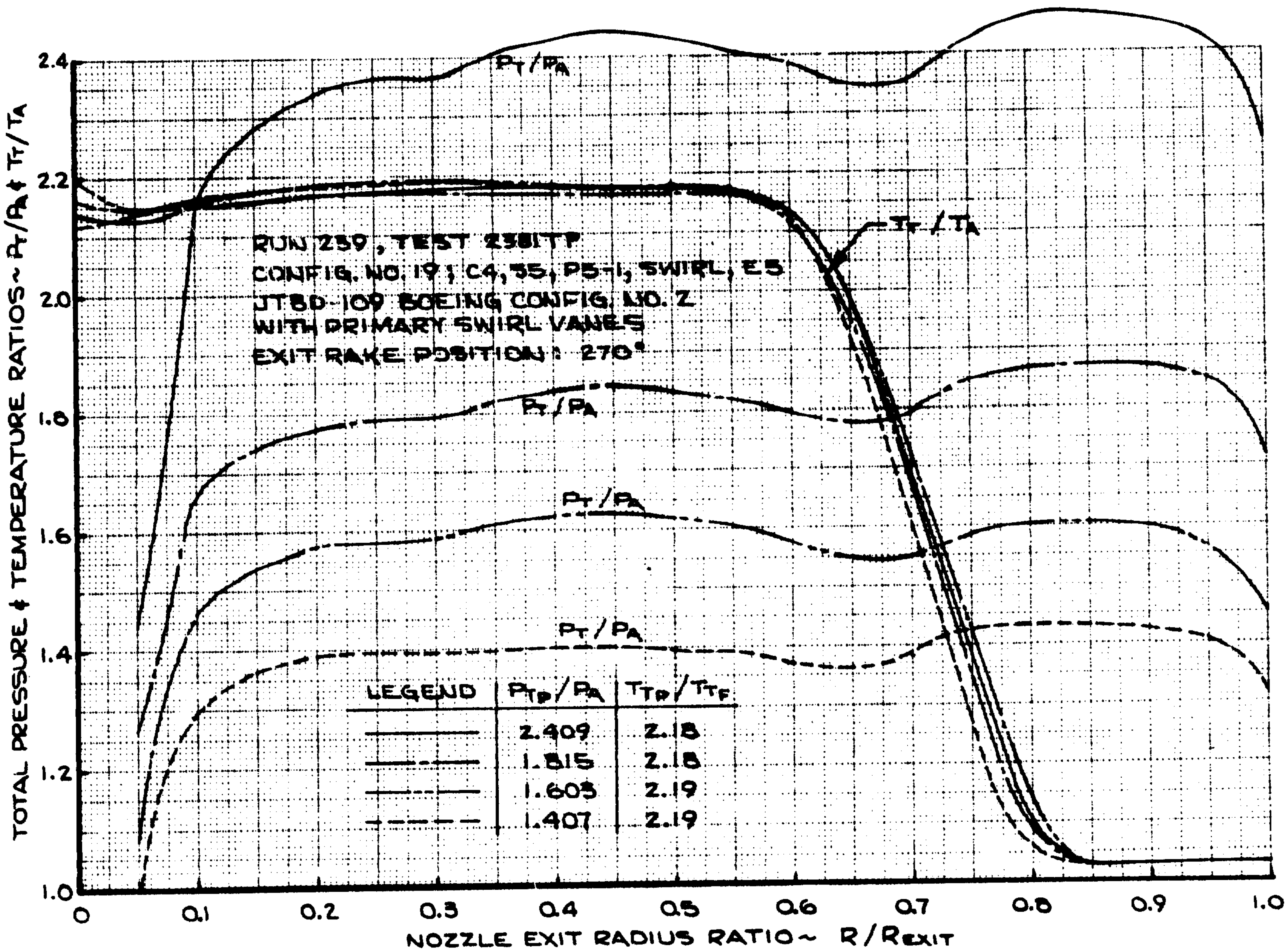

FIGURE 297- EXIT PLANE TOTAL PRESSURE & TEMPERATURE RATIO PROFILES
TEST CONFIG. NO. 19; TRAVERSING PROBE LOCATION - 270 DEG.

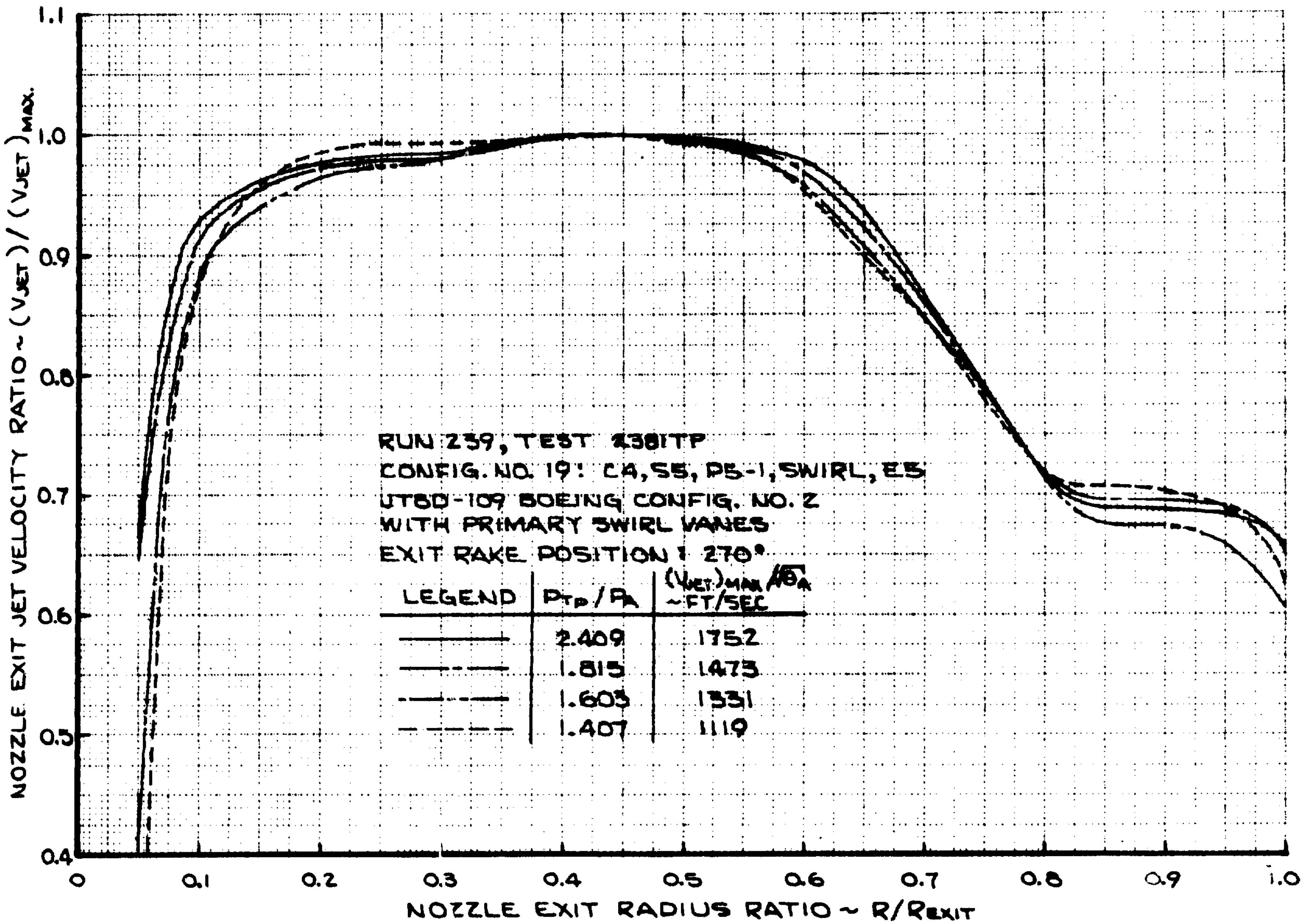

FIGURE 298- NOZZLE EXIT JET VELOCITY RATIO
TEST CONFIG. NO. 19; TRAVERSING PROBE LOCATION - 270 DEG.

7.4 FIGURES SHOWING MODEL TEST HARDWARE

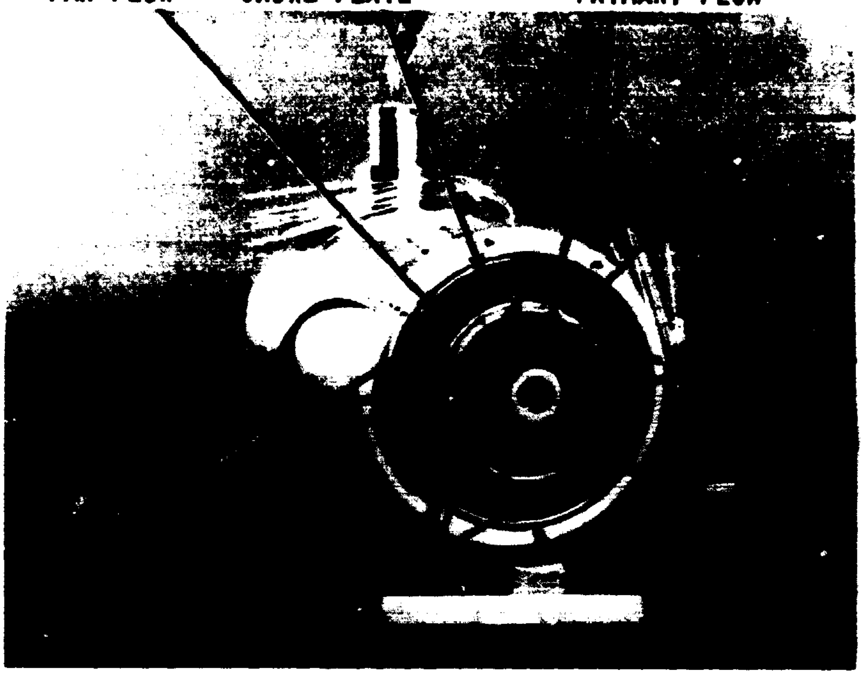

FIGURE 299. - INSTRUMENTATION SECTION

FIGURE 300. - TEST CONFIGURATION NO. 2: JT8D-9/727 PRODUCTION NOZZLE

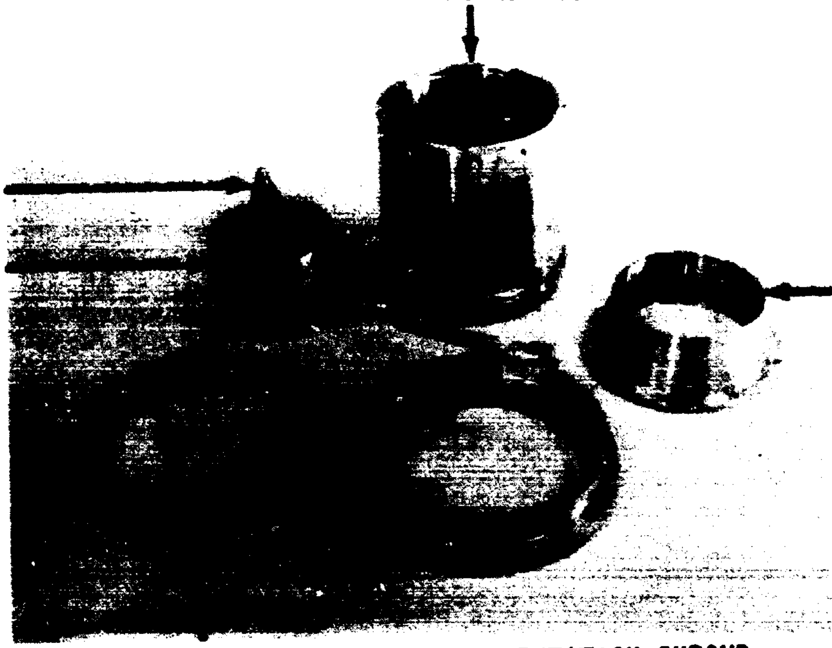

FIGURE 301. - TEST CONFIGURATION NO. 3: P&WA JT8D-109 REFERENCE HARDWARE

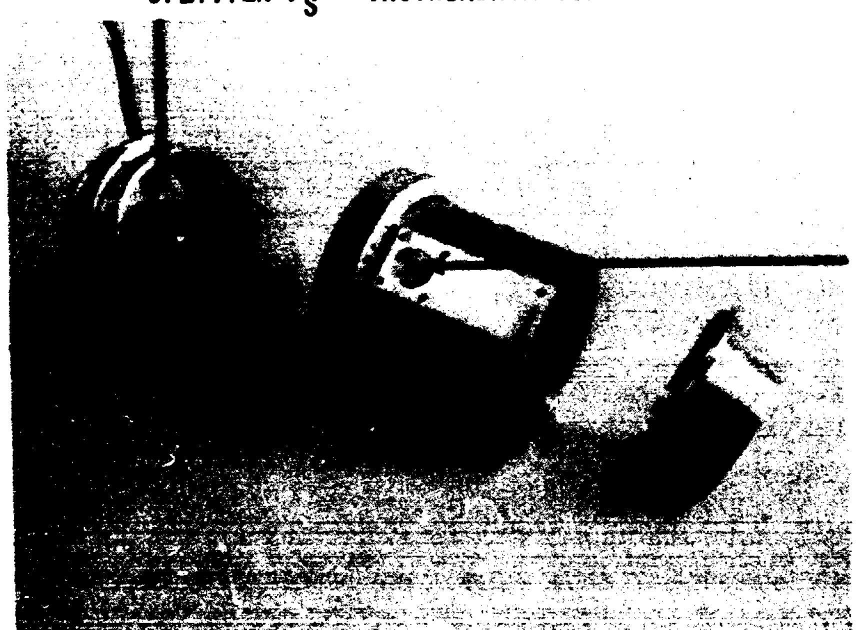

FIGURE 302. - TEST CONFIGURATION NO. 4: P&WA JT8D-109 REFERENCE HARDWARE WITH SWIRL VANES

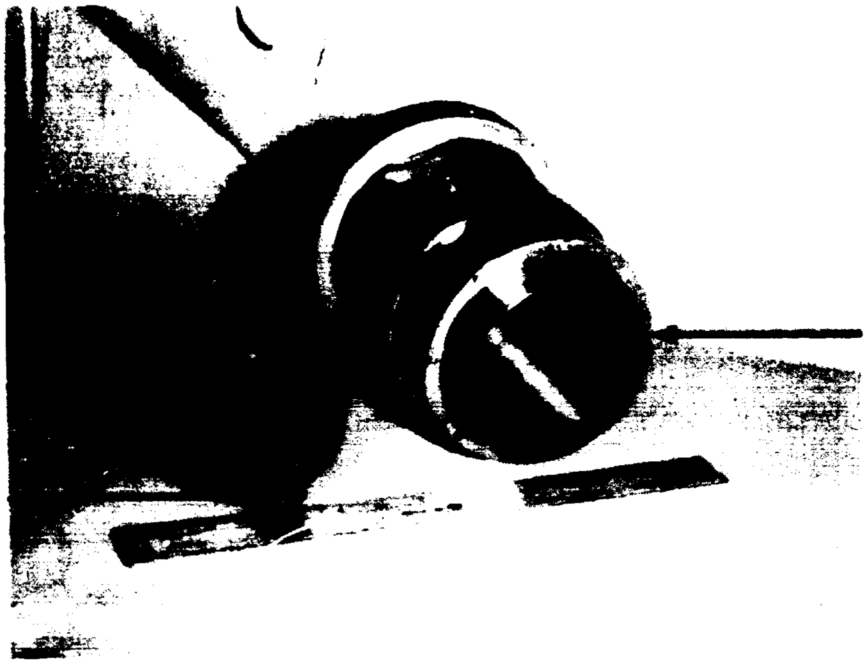

FIGURE 303. - TEST CONFIGURATION NO. 4: P&WA JT8D-109 REFERENCE HARDWARE WITH SWIRL VANES (ASSEMBLED)

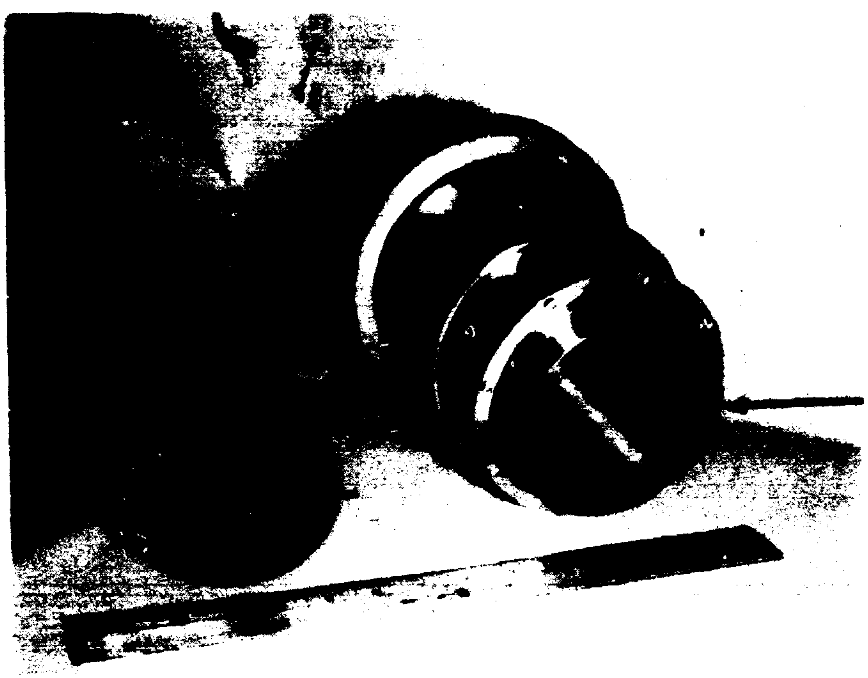

FIGURE 304. - TEST CONFIGURATION NO. 19: BOEING JT8D-109 HARDWARE WITH SWIRL VANES (ASSEMBLED)

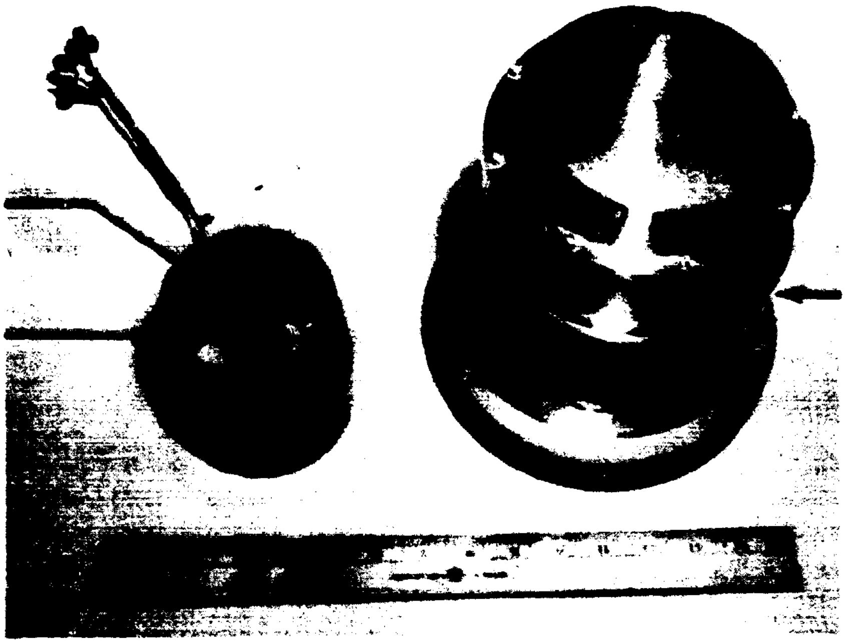

FIGURE 305. - TEST CONFIGURATION NO. 9: BOEING JT8D-115 HARDWARE WITH TRUNCATED PLUG (P5-1S)

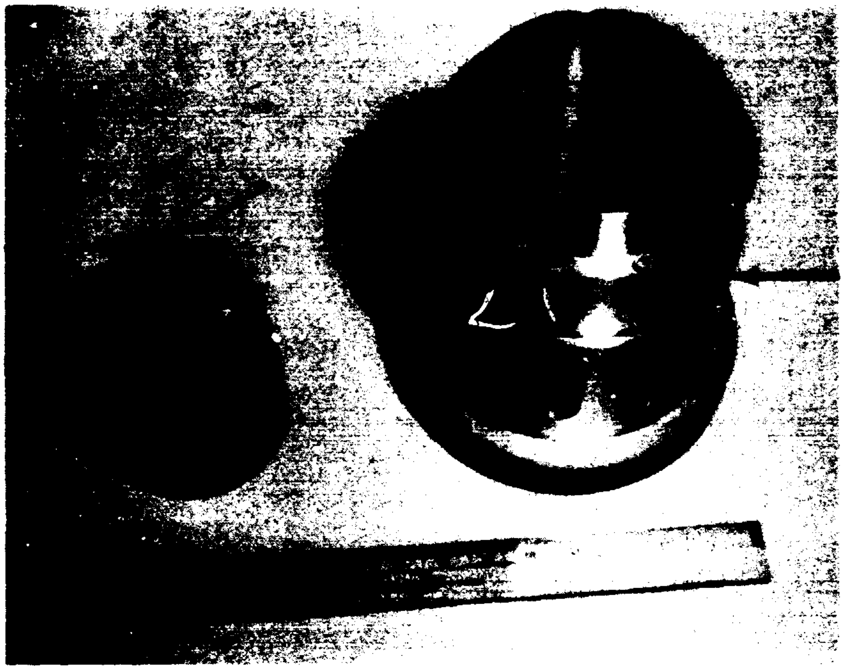

FIGURE 306. - TEST CONFIGURATION NO. 15: BOEING JT8D-117 HARDWARE WITH LONG PLUG (P5-3)

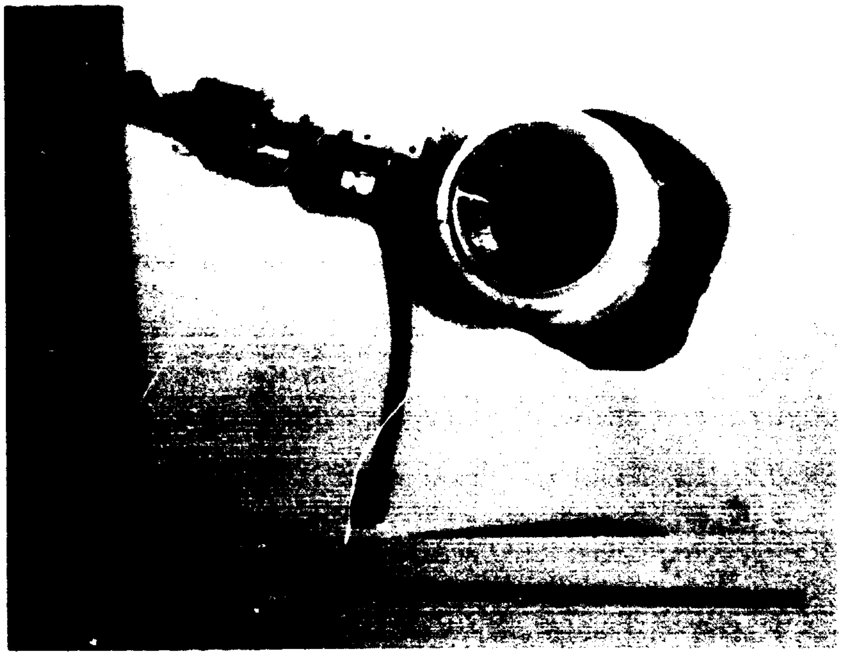

FIGURE 307. - MIXING PLANE P_T - PROBE AND TRAVERSING MECHANISM

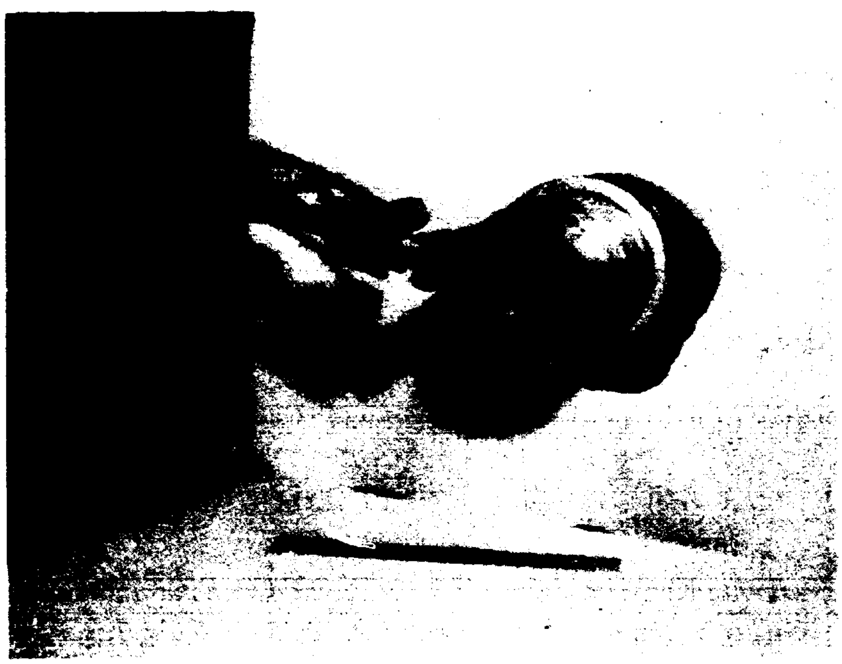

FIGURE 308 . - EXIT PLANE P_T - & T_T - PROBE AND TRAVERSING MECHANISM

APPENDIX

PRECEDING PAGE BLANK NOT FILMED

A. DATA REDUCTION RELATIONSHIPS

A.1 FLOW COEFFICIENT BASED ON SEPARATE FLOWS, C_D

$$C_D = \frac{A_{e_F} + A_{e_P}}{A_E}$$

where
$$A_{e_F} = \frac{W_{a_F}\sqrt{T_{T_F}}}{P_{T_F}\left\{\frac{2g\gamma}{R_c(\gamma-1)}\left[\left(\frac{P_{T_F}}{P_A}\right)^{-\frac{2}{\gamma}} - \left(\frac{P_{T_F}}{P_A}\right)^{-\left(\frac{\gamma+1}{\gamma}\right)}\right]\right\}^{1/2}}$$

if, $\frac{P_{T_F}}{P_A} > \left(\frac{\gamma+1}{2}\right)^{\frac{\gamma}{\gamma-1}}$; THEN $\frac{P_{T_F}}{P_A} = \left(\frac{\gamma+1}{2}\right)^{\frac{\gamma}{\gamma-1}}$

γ is based on fan stream properties.

$$A_{e_P} = \frac{W_{a_P}\sqrt{T_{T_P}}}{P_{T_P}\left\{\frac{2g\gamma}{R_c(\gamma-1)}\left[\left(\frac{P_{T_P}}{P_A}\right)^{-\frac{2}{\gamma}} - \left(\frac{P_{T_P}}{P_A}\right)^{-\left(\frac{\gamma+1}{\gamma}\right)}\right]\right\}^{1/2}}$$

if, $\frac{P_{T_P}}{P_A} > \left(\frac{\gamma+1}{2}\right)^{\frac{\gamma}{\gamma-1}}$; THEN $\frac{P_{T_P}}{P_A} = \left(\frac{\gamma+1}{2}\right)^{\frac{\gamma}{\gamma-1}}$

γ is based on primary stream properties.

and

A_E = Nozzle geometric area

PRECEDING PAGE BLANK NOT FILMED

A.2 FLOW COEFFICIENT BASED ON FULLY MIXED FLOW, C_{D_M}

$$C_{D_M} = \frac{W_{a_P} + W_{a_F}}{W_{a_M}}$$

$$W_{a_M} = \frac{A_E P_{T_M}}{\sqrt{T_{T_M}}} \left\{ \frac{2 g \gamma}{R_C(\gamma - 1)} \left[\left(\frac{P_{T_M}}{P_A} \right)^{-\frac{2}{\gamma}} - \left(\frac{P_{T_M}}{P_A} \right)^{-\left(\frac{\gamma+1}{\gamma}\right)} \right] \right\}^{1/2}$$

$$\text{if, } \frac{P_{T_M}}{P_A} > \left(\frac{\gamma+1}{2} \right)^{\frac{\gamma}{\gamma-1}} \text{ ; THEN } \frac{P_{T_M}}{P_A} = \left(\frac{\gamma+1}{2} \right)^{\frac{\gamma}{\gamma-1}}$$

γ is based on ideal 100% mixed stream properties.

A.3 VELOCITY COEFFICIENT BASED ON SEPARATE FLOWS, C_V

$$C_V = \frac{F_g}{\frac{W_{a_P}}{g} V_{i_P} + \frac{W_{a_F}}{g} V_{i_F}}$$

$$V_{i_P} = \left\{ 2 g R_C T_{T_P} \left(\frac{\gamma}{\gamma - 1} \right) \left[1 - \left(\frac{P_{T_P}}{P_A} \right)^{-\left(\frac{\gamma-1}{\gamma}\right)} \right] \right\}^{1/2}$$

where γ is based on primary stream properties and W_{a_p} is the measured primary stream mass flow.

$$V_{i_F} = \left\{ 2 g R_C T_{T_F} \left(\frac{\gamma}{\gamma - 1} \right) \left[1 - \left(\frac{P_{T_F}}{P_A} \right)^{-\left(\frac{\gamma-1}{\gamma}\right)} \right] \right\}^{1/2}$$

where γ is based on fan stream properties and W_{a_F} is the measured fan stream mass flow.

A.4 VELOCITY COEFFICIENT BASED ON FULLY MIXED FLOW, C_{V_M}

$$C_{V_M} = \frac{F_g}{\left(\frac{W_{a_P} + W_{a_F}}{g}\right) V_{i_M}}$$

$$V_{i_M} = \left\{ 2g\, R_C T_{T_M} \left(\frac{\gamma}{\gamma - 1}\right)\left[1 - \left(\frac{P_{T_M}}{P_A}\right)^{-\left(\frac{\gamma-1}{\gamma}\right)}\right]\right\}^{1/2}$$

where γ is based on ideal 100% mixed stream properties.

A.5 IDEAL 100%-MIXED TOTAL TEMPERATURE AND TOTAL PRESSURE RELATIONSHIPS

Mixing is assumed to be at constant area, with no heat loss and no loss due to friction

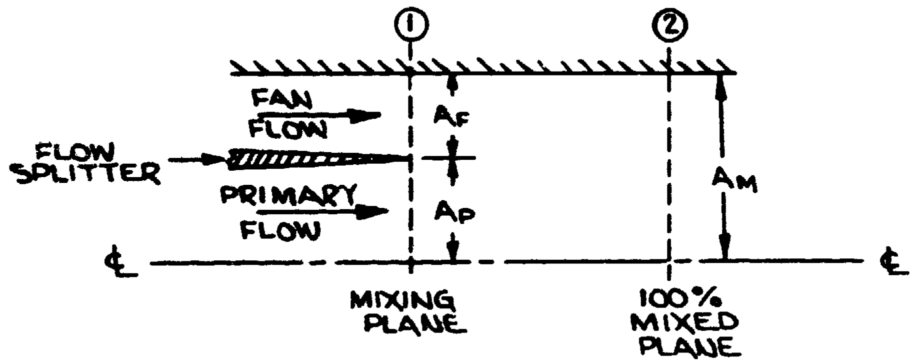

Quantities known at the mixing plane (Station ①)

W_{a_F}, P_{T_F}, T_{T_F}, γ_F, A_F

W_{a_p}, P_{T_p}, T_{T_p}, γ_p, A_p

$P_{S_F} = P_{S_p}$ (at the splitter trailing edge)

Quantities known at the 100%-mixed plane (Station ②)

$W_a = W_{a_F} + W_{a_p}$ (from the continuity equation)

$A_M = A_F + A_p$

The problem now is to determine the total temperature (T_{T_M}) and total pressure (P_{T_M}) for the 100%-mixed conditions.

Writing the energy equation between stations ① and ② allows the determination of the 100%-mixed total temperature, i.e.

$$T_{T_M} = \frac{C_{PR_F} W_{a_F} T_{T_F} + C_{PR_p} W_{a_p} T_{T_p}}{C_{PR_M} (W_{a_F} + W_{a_p})}$$

EQUATION A

C_{PR_F} and C_{PR_p}, the specific heats at constant pressure for the fan and primary, respectively, are determined from the individual flow stream properties given at the mixing plane. The specific heat for a mixture, C_{PR_M}, is determined as follows:

$$C_{PR_M} = \frac{C_{PR_F} W_{a_F} + C_{PR_p} W_{a_p}}{W_{a_F} + W_{a_p}}$$

EQUATION B

The continuity equation can be expanded, (in terms of total pressure, total temperature, $\mho$, Mach number, and area) to the following expression using also the fact that $P_{S_F} = P_{S_p}$:

$$\frac{P_{T_F}}{P_{T_P}}\sqrt{\frac{\gamma_F}{\gamma_P}\frac{T_{T_P}}{T_{T_F}}}\ \frac{A_F}{A_P}\ \frac{M_F}{\left(1+\frac{\gamma_F-1}{2}M_F^2\right)^{\frac{\gamma_F+1}{2(\gamma_F-1)}}}+\frac{M_P}{\left(1+\frac{\gamma_P-1}{2}M_P^2\right)^{\frac{\gamma_P+1}{2(\gamma_P-1)}}}$$

$$=\frac{P_{T_M}}{P_{T_P}}\sqrt{\frac{\gamma_M}{\gamma_P}\frac{T_{T_P}}{T_{T_M}}}\ \frac{A_M}{A_P}\ \frac{M_M}{\left(1+\frac{\gamma_M-1}{2}M_M^2\right)^{\frac{\gamma_M+1}{2(\gamma_M-1)}}}$$

EQUATION C

γ_M, ratio of specific heats, for the mixed flow conditions can be obtained from Equation B and the following thermodynamic relationship:

$$C_{PR_M} = R_C\left(\frac{\gamma_M}{\gamma_M-1}\right)$$

EQUATION D

The momentum equation between stations ① and ② (in terms of total pressure, total temperature, γ, Mach number, and area) is as follows:

$$\frac{A_F}{A_P}\frac{P_{T_F}}{P_{T_P}}\left(1+\frac{\gamma_F-1}{2}M_F^2\right)^{-\frac{\gamma_F}{\gamma_F-1}}\left(1-\gamma_F M_F^2\right)$$

$$+\left(1+\frac{\gamma_P-1}{2}M_P^2\right)^{-\frac{\gamma_P}{\gamma_P-1}}\left(1-\gamma_P M_P^2\right) =$$

$$\frac{A_M}{A_P}\frac{P_{T_M}}{P_{T_P}}\left(1+\frac{\gamma_M-1}{2}M_M^2\right)^{-\frac{\gamma_M}{\gamma_M-1}}\left(1-\gamma_M M_M^2\right)$$

$\boxed{\text{EQUATION E}}$

The unknowns in equations A, B, C, D, and E are P_{T_M}, T_{T_M}, M_M, γ_M, and C_{PR_M}; i.e., five equations with five unknowns. These equations are solved using a digital computer program for the 100%-mixed flow conditions at station 2 .